

Trinity College Dublin
Coláiste na Tríonóide, Baile Átha Cliath
The University of Dublin

Wastewater as a thermal resource: Exploitation strategies, design methodologies & prototype development

Jan Spriet

Thesis submitted for the fulfilment of the rquirements for the Degree of Doctorate of Philosophy in Engineering to the University of Dublin, Trinity College.

Date:
April 2020

Theme:
Wastewater heat recovery

Project:
Dwr-Uisce

Supervisor:
Prof. Aonghus McNabola, School of Engineering, the University of Dublin, Trinity College

Department:
Department of Civil, Structural and Environmental Engineering
The University of Dublin, Trinity College

Declaration

I declare that this thesis has not been submitted as an exercise for a degree at this or any other university and it is entirely my own work.

I agree to deposit this thesis in the University's open access institutional repository or allow the library to do so on my behalf, subject to Irish Copyright Legislation and Trinity College Library conditions of use and acknowledgement.

Date

March 28th 2020

Signed



Jan Spriet

Summary

The disruption of the climate was identified as one of nine planetary boundaries, and is one for which we are reaching the limits of safe operation on this planet. To that effect the European Commission launched the **European Green Deal**, aiming at transitioning the EU's economy towards increased sustainability. The research presented in this thesis subscribes to three of the main axes of this Green Deal:

- Increasing the EU's climate ambition.
- Supplying clean, affordable and secure energy.
- Building and renovating in an energy and resource efficient way.

In the EU, heating and cooling account for around 50% of the energy consumption. $15-30\%$ of thermal energy delivered to a building is still embedded in the wastewater when leaving the building, making it the largest source of energy loss in modern (passive and low–energy) buildings. For this reason, the EU, through a directive released in December 2018, officially recognised wastewater as a renewable source of energy.

The research presented in this thesis aims at recovering the embedded heat in wastewater, and, on the one hand, to use it to reduce fuel requirements of the conventional heating system, thus reducing related costs and greenhouse gas emissions. On the other hand, it aims to use this embedded heat as a heat source for heat pumps, providing low–carbon, renewable heat.

The research project focuses on three research questions (enumerated below), regarding the development and exploitation of recovering thermal energy from drain or waste water, called Drain Water Heat Recovery (DWHR).

1. *How can DWHR contribute to the current heating mix, and to reaching emission reduction and renewable heating targets?*
2. *How do different situations in different sectors affect the design of DWHR systems? How can DWHR be implemented?*
3. *How can the current set of commercially available DWHR system be complemented or extended?*

To answer these questions the project assessed three different aspects from heat recovery from drain– and wastewater:

1. The exploitation strategy: Where, within the water cycle, should heat be recovered from wastewater? (Chapters 5–6–7)
2. The design methodology: What are the differences in design for different sectors, different situations? (Chapters 8–9)
3. The prototype development: How can the current set of commercially available DWHR system be complemented and extended? (Chapter 10)

The sectoral potential, related to three exploitation strategies, was assessed for the domestic, residential sector (Chapter 5), the commercial food and hospitality sector (Chapter 6), and the sector of licensed wastewater treatment plants (municipal and industrial, see Chapter 7).

The starting point at the domestic, residential sector was selected because, in Europe, heating is mainly provided on an individual residence basis. A novel, proabilistic method was introduced, considering the temporal variations of both waste heat supply and heat demand. This analysis showed that 4.79 TWh of heat is flushed through the drain each year. This is equivalent to 1.24 $M\ tons\ C_e$ of GHG emissions. Recovering this heat has the potential to increase the share of renewable heat in the heating mix up to $17.4-18.4\%$, and reducing heating related GHG emissions for households by $7.6-22\%$. However, the drain

water heat recovery system was not able to meet all demand (ranging from 8 to 42%), and an additional heating system was required. This drain water heat recovery system thus entailed increased heating costs, ranging from 120 to 130%.

In order to counteract this, two approaches were considered. The first one, moving upstream, studied the potential for heat recovery in commercial kitchens in the hospitality and food services sector in the UK (Chapter 6). It showed a potential for direct drain water heat recovery systems, that was financially feasible for 88% of the total energy potential (1.24 TWh/yr), and an annual reduction of GHG emissions of 344 $k\ tons\ C_e/yr$. This can be achieved at a cost of 2.94 $p£/kg\ C_{e,saved}$, several orders of magnitude smaller than the cost of replacing current heating systems. However, the current systems have important space requirements and are not profitable for commercial kitchens with low water consumption. In the UK, this leaves approximately 160 GWh of potential untapped, equivalent to 44 $k\ tons\ C_e/yr$.

The second approach consisted of moving downstream, this showed a potential for heat recovery from the effluent of 40 (out of 479 in Ireland) wastewater treatment plants of 236.55 GWh/yr, through indirect heat recovery (Chapter 7). This indicates that wastewater heat recovery from the effluent of wastewater treatment plants, as the sole heat source for a district heating network, has only a limited market for financially profitable application. However, in the case of heating networks with multiple heat sources, they can provide an interesting interface between the electricity and heat networks. A novel, integrated spatio-temporal analysis was applied on the Tullamore wastewater treatment plant, identifying five potential zones for the consumption of the recovered heat. Investigations showed that the heat supply from the wastewater treatment plant was not always sufficient to meet demand in the zones. However, the net annual excess recovered heat was positive, meaning that on an annual basis, there is more heat available than consumed. This indicates that the effluent heat recovery system can be used to meet the baseload heat demand, but must be complemented by other sources.

Two demonstration sites showed the difference in design methodology for drain water heat recovery systems under different conditions. The pilot site at Penrhyn castle showed high temperatures, but low, and irregular flow. The design of a novel heat recovery system from the system drain was shown in Chapter 8. In this heat recovery system, three different configurations were included, using a heat exchanger to transfer the heat from the drain water to the incoming fresh water. Preheating the fresh water reduces the required energy, and thus the fuel consumption of the conventional heating system. This system is expected to reduce the heat consumption of the kitchen with over 2 000 kWh per year. Due to physical restrictions on site, only one configuration could be tested, reducing the heat consumption of the kitchen by 594 kWh per year. This is significantly lower than the predicted recovery, due to the lower water consumption of the kitchen during the operation period compared to the time of the feasibility study (293.05 l/day vs 652.5 l/day).

The pilot site at ABP food group, Cahir showed large wastewater flows, and a temperature that was only slightly higher than the temperature of the incoming fresh water. The design of an experimental set-up for heat recovery from the industrial wastewater treatment system of the meat processing facility was shown in Chapter 9. The designed system combined both direct heat recovery, and hybrid heat recovery, where the incoming fresh water was preheated, and then brought to the required temperature by a heat pump, using the wastewater as a heat source. The expected energy saving ranged from 80 to 140 MWh per year. The operation showed that at the inlet of the treatment system, the wastewater was heavily loaded in suspended solid matter to be pumped into the experimental unit. The submersible wastewater pump clogged after a few days of operation. The pump was then moved to the outlet of the DAF tank, where 120 to 140 kWh of heat could be recovered daily, through the proposed heat recovery system. There was no flow control on the incoming fresh water, this resulted in regular emergency shut downs of the heat pump in the hybrid heat recovery system. The longer term operation of this hybrid heat recovery system can thus not be reported in a conclusive manner.

The prototype, developed in Chapter 10, aims at complementing the set of commercially available drain water heat recovery systems for wastewater from kitchen drains. The system was integrated in a grease interceptor, and experimental results showed a heating power of up to 1.8 kW at an effectiveness of up to 58%. However, improvement of the design, and testing the design with actual fat, oil and grease emulsions, typical for kitchen wastewater, remains necessary before this idea can be converted to a market–ready product.

The research questions, answered through the three different types of studies described above were answered, as shown below:

1. *How can DWHR contribute to the current heating mix, and to reaching emission reduction and renewable heating targets?*

   DWHR can contribute to the reduction of emissions in two ways: (i) by reducing the fuel demand of traditional heating systems, (ii) by providing a high–temperature heat source for heat pumps, providing an additional renewable heating alternative, with low carbon–intensity (depending on the heating mix). The former can be achieved by direct heat recovery at locations where high temperature wastewater is available (such as kitchens, shower systems, lavatories, etc.), but where the wastewater flow is intermittent, and less predictable. This heat recovery method is characterised by a low capital investment, but requires an additional heating source. The total amount of recovered energy is low, however it is performed at low cost. This results in a limited impact on the total carbon budget of a nation, even when applied nation–wide, but provides the reduction in GHG emissions at a cost that is several orders of magnitude smaller than switching entire energy systems. The latter is usually performed through indirect and/or hybrid heat recovery, in places where a large, steady flow of wastewater is available. These are often found in large sewer collectors or wastewater treatment plants. They present the additional challenge of being often located at a distance from the consumer, and require a means of transporting the heat to the consumer. This can be achieved, for example through heating networks. Providing heat in this way can significantly change the energy landscape and mix of a region, and thus have a great effect on GHG reduction targets. This has the added benefit of providing an interface between the electric and heating energy system, through the use of a heat pump, and could thus also be used to attenuate electricity production peaks, caused by the intermittent character of renewable electricity sources such as solar and wind.

2. *How do different situations in different sectors affect the design of DWHR systems? How can DWHR be implemented?*

   As mentioned above, temperature and flow have an important impact on the selection and design of a DWHR system. High temperature, intermittent flow lends itself to direct heat recovery, whereas constant, large flow is more suited for indirect or hybrid heat recovery. The amount of pollutants in the wastewater also affects the design of DWHR systems. Wastewater with a high concentration of suspended solids may not be suited for DWHR systems, or be required to go through primary treatment before heat recovery can be attempted, because these solids clog heat exchangers and other auxiliary equipment. On the other end of the spectrum, fully treated wastewater can still be a valuable source of heat. Contradictory to the widespread belief that the wastewater looses all (or most) of its heat through the treatment process, the temperature of the wastewater leaving the treatment plant still has a significantly higher temperature than the ground or surrounding air during heating season. This was observed in the Tullamore municipal wastewater treatment plant, but also in the industrial wastewater treatment plants of ABP food and Pepsico. The effluent of wastewater treatment plants can be used directly in a water–source heat pump, eliminating the need for intermediary heat carriers. Indirect or hybrid DWHR from the inlet of wastewater treatment plants requires the use of an intermediary heat carrier, to transfer the heat from the wastewater to the heat pump, in order to fully separate the wastewater and heating system. This requires the use of an additional heat exchanger, and thus introduces an additional temperature drop. This added complexity and heat loss could offset the advantage of the higher temperature observed at the inlet of the treatment system, compared to the outlet.

3. *How can the current set of commercially available DWHR system be complemented or extended?*

   Current DWHR systems often require a significant vertical drop, as the effectiveness of the commonly used double-walled heat exchanger is much higher in vertical systems. In a society where space constraints become more and more of a factor, this could prove to be an important bottleneck. To counteract this, the research presented in this thesis looked at integrating the DWHR system in existing, often mandatory, equipment. This could reduce additional space constraints to a minimum, but also reduce installation costs, as qualified personnel can install both systems at once. This thesis focused on integrating DWHR systems into grease interceptors for kitchen wastewater, but the same thought process could also be applied to other equipment, such as septic tanks, DAF units, etc.

In short, heat recovery from drain and wastewater can find its place in the future energy landscape in three different ways, under three different operating conditions.

1. *As an energy efficiency measure.*
   This form represents the use of direct DWHR, to preheat the incoming wastewater, resulting in a reduced heat and fuel consumption of traditional heating systems. This form is particularly suited for locations with high temperatures, but with sporadic or small flow. It is characterised by a low investment cost, but also by relatively small amounts of recovered energy. This makes it particularly suitable for new installations (eg. in new buildings or commercial kitchens), where it can be installed at a minimal added cost, but less so for retrofitting, as these marginal gains may be deemed unworthy of the trouble.
2. *As an efficiency boost for individual heat pump systems.*
   This second form, represents the recovery of heat for individual residences, and could be particularly beneficial for systems in remote areas with low population density. It consists of using the wastewater as an additional heat source for a traditional (air–source or ground–source) heat pump system. As the wastewater has a higher temperature than these traditional sources during most of the heating season, but (for an individual residence), does not contain sufficient energy to meet all heating demand in this building, it could be used as a booster for the temperature of the heat carrier (often brine in ground source heat pumping systems). This boost in temperature would induce a boost in COP of the heat pump.
3. *As the heat source for heating networks.*
   This last form requires the availability of large volumes of wastewater, usually in centralized locations, such as large sewer collectors or wastewater treatment plants. It uses an indirect heat recovery system to provide heat to a network using heat pumps. For this form to be profitable, large quantities of wastewater are necessary to provide economies of scale. However, the centralized locations where these quantities are available are often located at a distance from consumers. Heating networks are thus required for the distribution of the heat to consumers. This can be under the form of district heating, but also the heating network in a factory or industrial plant.

   In addition to this, a wastewater source heat pump could provide for a highly efficient interface between the electric and the heating network. This provides the option for increased flexibility of both networks, required with the growing importance of intermittent renewable source, such as PV and wind, but also solar-thermal heat.

Acknowledgements

The work presented in this thesis was the result of the collaboration of a team of researchers, and would not have been possible without the support of family and friends. Therefore, I would like to thank Prof. Aonghus McNabola, for his trust, support, structure and guidance throughout this PhD project, his methodological approach, and structure have been a great added value to the research presented here. I would also like to thank Prof. Paul Coughlan, Prof. Prysor Williams and Dr. John Gallagher for their help and guidance with the research. I would also like to thank Prof. Biswajit Basu, Mr Ian Harris, Dr. David Styles and Dr. Sopan Patil, for their contribution to our research project, and questions and interest throughout the development of the research project.

During this PhD project, I had the opportunity to spend three months in Vienna, Austria at the Institute of Sanitary Engineering and Water Pollution Control (SIG) of the University of Natural Resources and Life Sciences, Vienna. Here I would specially like to thank Dr. Florian Kretschmer for his support and guidance, additionally, thanks go to Prof. Thomas Ertl, Dr. Gunther Langergraber, and Ms. Lena Simperler at SIG, and Dr. Georg Neugebauer, Prof. Gernot Stoeglehner and Mr. Peter Lichtenwoehrer at the Institute of Spatial Planning, Environmental Planning and Land Rearrangement (IRUB). I'd also like to mention Ms. Ulrike Piringer for facilitating and supporting the exchange.

A joyful and stimulating working atmosphere are essential for the production of quality work outputs. Therefore, I thank Djordje, Daniele, Miguel, Nilki, Isabel, Nathan, Richard, Himanshu, Szu–Hsin, Ana, Irene, David, Vanajah, Annum, Aisha and Andrew, for the laughs, the discussion and the complaining, about research and work, but especially about life. I would also like to mention a special thanks to all our colleagues in the civil engineering department at Trinity college.

I would also like to thank the technicians of the department of civil, structural and environmental engineering, and in particular Dave McAulay, Michael Grimes and Robert Fitzpatrick, for their help and support during this project.

This project included installing two pilot sites, integrating it in the operation of a tourist site and a meat processing plant. This process was only possible thanks to the cooperation and support of the people in those place. Therefore, I'd like to thank Elgan Roberts, Clive Parkinson and Keith Jones from the National Trust Wales, and John Durkan, Barry O'Donovan, Fergal McGuire and Mark McQuaid from ABP food group. In addition to this a special mention of thanks goes out to Fergus Halligan, the site manager of the wastewater treatment plant at ABP, Cahir, for his tireless help in adapting the experimental unit.

I would like to thank my friends, you know who you are, for the critical questions, and for reminding me that you do not truly understand something if you can not explain it simply, to someone without the technical background. My family, Cathy, Georges, Nico and Melissa for supporting me, even though they probably can not see the beauty in dirty wastewater.

Lastly, I would like to thank Leti, for being the spark of enthusiasm through these great times, and through the times in between.

List of publications

Publications as first author

Journal Publications

Spriet, J. & McNabola, A., 2019. **'Decentralized drain water heat recovery: A probabilistic method for prediction of wastewater and heating system interaction'**, *Energy and Buildings*, 183, pp. 684-696.

Spriet, J. & McNabola, A., 2019. **'Decentralized drain water heat recovery from commercial kitchens in the hospitality sector'**, *Energy and Buildings*, 194, pp. 247-259.

Spriet, J., McNabola, A., Neugebauer, G., Stoeglehner, G., Ertl, T. & Kretschmer, F. 2020. **'Spatial and temporal considerations in the performance of wastewater heat recovery systems'**, *Journal of Cleaner Production*, 247

Conference publications

Spriet, J. & McNabola, A., 2018. **'Decentralized Drain Water Heat Recovery: Interaction between Wastewater and Heating Flows on a Single Residence Scale.'** *3rd EWaS International Conference on Insights on the Water-Energy-Food Nexus, Lefkada Island, Greece*, 27-30 June 2018.

Spriet J. & McNabola A. 2019. **'Drain water heat recovery in commercial kitchens: Case of tourist attraction.'** *14th conference on sustainable development in energy, water and environment system 2019, Dubrovnik, Croatia*, 1st-6th October.

Conference presentations

Spriet, J. & McNabola, A. 2019. **'DWHR in commercial kitchens: Insights from the Dwr-Uisce project.'** *Future in Food Ireland, Cork, Ireland*, 28 November 2018.

Spriet, J., McNabola, A. & Kretschmer F. 2019. **'Integrated spatio-temporal analysis for effluent heat recovery.'** *European International Conference on Transforming Urban Systems, Strasbourg, France*, 26-28 June 2019.

Publications as contributing author

Journal Publications

Nagpal H., **Spriet, J.** & McNabola, A. **' Numerical Simulation Study on Improving Energy Efficiency of Residential Building using Wastewater assisted heat pump and Model Predictive Control.'**, *Journal of Building Engineering*, Under Review

Schestak I., **Spriet J.**, Williams, P. A. & Styles D. **'Environmental sustainability of heat recovery systems using drain water from commercial kitchens.'**, *Journal of Environmental Management*, Under Review

Conference publications

Schestak I., **Spriet J.** & Styles D. 2019. **'Life Cycle Assessment of an inline heat exchanger for heat recovery from drain water in a commercial kitchen.'** *14th conference on sustainable development in energy, water and environment system 2019, Dubrovnik, Croatia*, 1st-6th October.

Dreyer-Gibney, K., Coughlan, P., Wu, S-H., Bello-Dambatta, A., Dallison, R., Novara, D., Rafique, A., Schestak, I., **Spriet, J.** & Walker, N. 2020.**'Responding to the UN Sustainability Goals through network action learning.'** *20th annual conference of the European Academy of Management (EURAM), Dublin, Ireland*, 10th-12th June.

de Almeida Kumlien, A., Coughlan, P., **Spriet, J.** & McNabola, A. 2020.**'Accelerating innovation in the water sector through smart specialisation clusters.'** *20th annual conference of the European Academy of Management (EURAM), Dublin, Ireland*, 10th-12th June.

Publications outside of this PhD research

Journal Publications

Spriet, J. & Hendrick, P., 2017. **'Wastewater as a Heat Source for individual Residence Heating: A Techno-econoic Feasibility Study in the Brussels Capital Region'**, *Journal of Sustainable Development of Energy, Water and Environment Systems*, 5, pp. 289-308.

Morabito A., **Spriet J.** & Hendrick, P. **'Underground pumped storage hydropower case studies in Belgium: perspectives and challenges.'**, *Energies*, Under Review

Conference publications

Spriet J. & Hendrick, P. 2015. **'Heat recovery from wastewater in the Brussels Capital Region.'** *10th conference on sustainable development in energy, water and environment system 2015, Dubrovnik, Croatia*, 27th September - 02 October.

Nomenclature

Abbreviations

BER	Building Energy Rating
BM–WP	Biomass -wood pellets
CAD	Computer Aided Design
CAPEX	Capital expenses
Cat	Category
CIP	Clean in Place
CFD	Computational Fluid Dynamics
Co.	County
Ch	Chapter
CHP	Combined Heat and Power
COP	Coefficient of Performance
DAF	Dissolved Air Flotation
DEAP	Dwelling Energy Assessment Procedure
DHW	Domestic Hot Water
DN	Nominal Diameter
DNS	Direct Numerical Simulations
DWHR	Drain water heat recovery
Elec	Electricity
EM	Electric meter
EPA	Environmental Protection Agency
ESSCO	Company providing the heat interface unit
EU	European Union
FM	Flow meter
FOG	Fat, Oil and Grease
GHG	Greenhous gases
GWP	Global warming Potential
HEFO	Heavy Fuel Oil
HDD	Heating Degree Days
HM	Heat meter
HX	Heat exchanger
IHR	Indirect Heat Recovery
LCA	Life Cycle Analysis
LCOH	Levelised Cost of Heating
LCOE	Levelised Cost of Energy
LES	Large Eddy Simulation
LMTD	Logarithmic Mean Temperature Difference
OPEX	Operational expenses
NGas	Natural Gas
NPV	Net PResent Value
NT	National Trust
PE	Person Equivalent
PV	Photovoltaic

RANS	Reynolds Averaged Navier–Stokes Simulation
RES–H	Renewable Energy Sources – Heating
SA	Small area
SEAI	Sustainable Energy Authority of Ireland
SH	Space Heating
SLP	Synthetic Load Profile
SST	Shear Stress Transport
ST	Storage Tank
TEWI	Total Equivalent Warming Impact
TL	Temperature Lift
TRL	Technology Readiness Level
UK	United Kingdom
VAT	Value Added Tax
WWDA	Wastewwater Discharge Authorisation
WWTP	Wastewater Treatment plant
x–SHP	x–Source Heat Pump

Symbols

A_s	Heat exchange surface
C	Consumption
C_e	Carbon equivalent
C_p	Specific heat
D	Diameter
E	Energy
η	efficiency
η	effectiveness of the heat exchanger
f_D	Darcy Friction Factor
F	Correction factor (for LMTD method)
F_x	Fuel cost
g	gravitational constant
h	head
I	Investment cost
L	Leakage rate
L	Length
λ	Thermal conductivity
M	Maintenance sot
m	Mass
ν	Kinematic viscosity
NCF	Net Cash Flow
Q	heat
r	discount rate
T	Temperature
tod	time of day

U	Heat exchange coefficient
u_r	friction velocity
v	velocity
$\dot{V}$	Volumetric flow
$y+$	Dimensionless wall distance
W	Work

Subscripts

α_{recov}	recovery rate
avg	average
CW	Cold water
DW	Drain Water
$embedded$	Embedded
FW	Fresh water
HE	Heat Exchanger
HP	Heat Pump
l	losses
n	year n
out	out
PB	Peak Burner
ref	reference
$refr$	refrigerant
ρ	density
s	static
st	stored
WW	Wastewater

Contents

List of Figures **XVII**

List of Tables **XXV**

1. Introduction **1**
1.1. Research context . . . 1
1.2. Problem statement . . . 2
1.2.1. Lack of awareness about the technology and its potential. . . . 2
1.2.2. Lack of information regarding the total sectoral potential of DWHR. . . . 2
1.2.3. Off the shelf solution only exist for a limited number of applications. . . . 2
1.2.4. At low available energy volumes, DWHR technology might not be cost effective. . . . 3
1.3. Research project . . . 3
1.4. Research purpose . . . 4
1.4.1. Research aim and objectives . . . 4
1.4.2. Research questions . . . 4
1.4.3. Research contributions . . . 5
1.4.4. Contribution to other papers . . . 8
1.5. Lay-out of the thesis . . . 8

2. Climate, Energy and Wastewater **10**
2.1. Planetary boundaries . . . 10
2.2. Climate Change . . . 11
2.2.1. Energy and climate policy . . . 11
2.3. Thermal energy and greenhouse gas intensity of production . . . 15
2.3.1. Renewable heating sources . . . 16
2.3.2. Energy consumption in Buildings . . . 17
2.3.3. Energy loss through drain water in buildings . . . 18
2.3.4. District heating networks . . . 19
2.4. Water cycle efficiency . . . 20
2.4.1. Drain and Waste Water . . . 22
2.4.2. Drain and waste water collection and treatment . . . 22

3. Drain and Waste Water Heat Recovery **25**
3.1. Resource Assesment . . . 25
3.1.1. Temperature of drain and waste water . . . 25
3.1.2. Resource recovery from wastewater . . . 25
3.2. Technology . . . 27
3.2.1. Heat Recovery Systems . . . 27
3.2.2. Components of the system . . . 28
3.3. Matching heat recovery with consumption profile . . . 31
3.3.1. Temporal analysis . . . 31
3.3.2. Spatial analysis . . . 32
3.4. Drain- and wastewater heat recovery . . . 34
3.4.1. Direct Heat Recovery . . . 35
3.4.2. Wastewater source heat pumps for heating purposes . . . 40
3.4.3. Wastewater Source Heat Pumps for heating and cooling . . . 45
3.4.4. Multifunctional heat pumps . . . 49
3.4.5. Untreated Sewage Source Heat Pumps . . . 52
3.4.6. Temperature and wastewater treatment . . . 53

3.5. Case studies of existing systems . . . 54
3.5.1. Sports infrastructure in Basel(Ch) . . . 54
3.5.2. Public buildings in Binningen (Ch) . . . 54
3.5.3. Education center in Loewenberg (Ch) . . . 55
3.5.4. Appartments in Winterthur (Ch) . . . 55
3.5.5. Commercial buildings in Schaffhouse (Ch) . . . 55
3.5.6. Living area in Sandvika (No) . . . 55
3.5.7. Kakola heat pump plant (Fi) . . . 57
3.5.8. Swimming pool in Hasselt (Be) . . . 57
3.5.9. Inners project in Leuven (Be) . . . 57
3.5.10. Heat recovery scheme at Scottish Borders college campus in Galashiels (UK) . . . 57
3.5.11. The role of additional pilot plants . . . 57
3.6. Summary . . . 58

4. Research Methodology 59
4.1. Introduction and general outline . . . 59
4.2. Monitoring campaign . . . 60
4.2.1. Temperature Considerations . . . 61
4.2.2. Flow considerations . . . 61
4.3. Desk study on exploitation strategies . . . 62
4.3.1. General methodology for potential in a sector . . . 63
4.3.2. Spatio-Temporal Analysis for potential in a WWTP . . . 65
4.4. Demonstration sites . . . 66
4.4.1. Site selection . . . 66
4.4.2. Design of the heat recovery system . . . 67
4.4.3. Construction and installation of the systems . . . 67
4.4.4. Monitoring the system . . . 67
4.5. Prototype development . . . 69
4.5.1. Ideation phase: Translating desk studies into ideas . . . 71
4.5.2. Prototype phase: Construction and testing of the first prototype . . . 71
4.5.3. Testing phase: Numerical simulations . . . 71
4.6. Summary . . . 72

5. Exploitation Strategy: Decentralized drain water heat recovery in a domestic setting 73
5.1. Introduction . . . 73
5.2. Monitored Data . . . 74
5.2.1. Drain Water characteristics . . . 74
5.3. Potential of domestic drain water heat recovery in the Republic of Ireland . . . 76
5.3.1. Methods and materials . . . 76
5.3.2. Potential for energy recovery . . . 78
5.3.3. Considerations for cost effectiveness . . . 80
5.4. Drain water heat recovery in a domestic setting . . . 81
5.4.1. Methods and Analysis . . . 81
5.4.2. DWHR System set-up . . . 86
5.4.3. Financial and Environmental comparison methods . . . 89
5.4.4. Applying the model to the Irish Residential Market . . . 91
5.4.5. Results and Discussion . . . 92
5.5. Summary . . . 96

6. Exploitation Strategy: Decentralized drain water heat recovery in commercial kitchens 98
6.1. Introduction . . . 98
6.2. Drain water heat recovery from commercial kitchens in the hospitality sector . . . 99
6.2.1. Methods and analysis . . . 99
6.2.2. DWHR System set-up . . . 105
6.2.3. Assesment of the heat recovery potential in kitchens in the hospitality sector . . . 107
6.3. Conclusion and Summary . . . 115

7. Exploitation Strategy: Centralized drain water heat recovery at wastewater treatment plants 117
7.1. Introduction . . . 117
7.2. Heat recovery potential from WWTP effluent in Ireland: a spatial analysis . . . 118
7.2.1. Method . . . 118
7.2.2. Materials . . . 119
7.2.3. Results . . . 120
7.2.4. Discussion . . . 123
7.3. Integrated spatio-temporal analysis for wastewater heat recovery . . . 123
7.3.1. Methods and materials . . . 125
7.3.2. Results . . . 129
7.3.3. Discussion . . . 135
7.4. Environmental and financial aspects of effluent heat recovery . . . 137
7.4.1. Introduction . . . 137
7.4.2. Methods and Materials . . . 137
7.4.3. Results . . . 139
7.4.4. Discussion . . . 141
7.5. Summary . . . 142

8. Drainwater Heat Recovery in Commercial Kitchens: Demonstrator at Penrhyn Castle 144
8.1. Introduction . . . 144
8.2. Selection of the pilot site . . . 145
8.2.1. The kitchen and hospitality sector . . . 145
8.2.2. Penrhyn castle . . . 146
8.2.3. Selection of the pilot location at Penrhyn castle . . . 153
8.3. Methods and Materials . . . 154
8.3.1. Heat Recovery Methods . . . 154
8.3.2. Components . . . 154
8.3.3. Monitored data . . . 155
8.4. Design of the experimental unit . . . 157
8.4.1. Current heating system . . . 157
8.4.2. Drainwater heat recovery system . . . 158
8.4.3. Instrumentation . . . 159
8.5. Feasibility study . . . 160
8.5.1. Methodology . . . 160
8.5.2. Expected savings . . . 161
8.6. Installation procedure . . . 164
8.6.1. Physical installation of the components . . . 164
8.6.2. Commissioning . . . 165
8.7. Pilot site operation . . . 166
8.7.1. Heat recovery from the kitchen drain . . . 166
8.7.2. Energy efficiency of the kitchen's hot water . . . 167
8.7.3. Electric consumption in the recirculation loop . . . 168
8.7.4. Yearly savings and financial viability . . . 168
8.8. Summary . . . 170

9. Centralized drainwater Heat Recovery: Demonstrator in the meat processing industry 172
9.1. Introduction . . . 172
9.2. Selection of the pilot site . . . 173
9.2.1. Industrial wastewater treatment systems . . . 173
9.2.2. Selection of the pilot location at ABP Food Group, Co. Tipperary . . . 175
9.3. Methods and Materials . . . 175
9.3.1. Heat Recovery Methods . . . 175
9.3.2. Components . . . 176
9.3.3. Measured Data . . . 177
9.4. Design of the experimental unit . . . 179
9.4.1. The current heating system . . . 179
9.4.2. Working principle of the experimental unit . . . 179

9.4.3. Instrumentation . . . 180
9.5. Feasibility study . . . 181
9.5.1. Estimated cost of the experimental unit . . . 182
9.5.2. Energy savings . . . 182
9.5.3. Greenhouse gas emission savings . . . 182
9.5.4. Financial savings . . . 184
9.5.5. Comparing the direct and hybrid system . . . 186
9.5.6. Discussion . . . 187
9.6. Construction of the experimental unit . . . 188
9.6.1. Heat exchanger arrangement . . . 188
9.6.2. Hydraulic arrangement and rig construction . . . 189
9.6.3. Installation of the logging system . . . 190
9.7. Installation and commissioning of the experimental unit . . . 191
9.7.1. Installation . . . 191
9.7.2. Commissioning and verifying the operation . . . 191
9.8. Experimental Operation . . . 192
9.8.1. Operation at the inlet of the wastewater treatment system . . . 192
9.8.2. Operation at the outlet of the DAF unit . . . 196
9.8.3. Challenges regarding the experimental unit . . . 199
9.9. Effluent heat recovery . . . 201
9.9.1. Effluent temperature . . . 201
9.9.2. Comparison between the brine and effluent source system . . . 202
9.10. Yearly savings of the recommended DWHR system . . . 203
9.10.1. Recommended direct heat recovery system . . . 203
9.10.2. Recommended indirect heat recovery system . . . 204
9.10.3. Yearly savings and financial viability of the recommended system . . . 204
9.11. Summary . . . 207

10. Prototype development: Heat recovery from grease interceptors 209
10.1. Introduction . . . 209
10.2. Design thinking . . . 209
10.2.1. Empathize . . . 210
10.2.2. Define . . . 210
10.2.3. Ideate . . . 211
10.2.4. Prototype and Testing . . . 211
10.3. Methods and Materials . . . 211
10.3.1. Objectives . . . 211
10.3.2. Grease interceptors . . . 211
10.3.3. Experimental lab set-up . . . 214
10.3.4. Numerical simulations . . . 218
10.4. Experimental results . . . 222
10.5. Viability of the prototype . . . 223
10.5.1. The current prototype . . . 223
10.5.2. The commercialised prototype . . . 225
10.6. Validation of the numerical model . . . 227
10.6.1. Objectives of the numerical model . . . 227
10.6.2. Computational Fluid Dynamics . . . 227
10.6.3. Simulation results and discussion . . . 237
10.7. Design of the heat recovery unit . . . 241
10.7.1. FOG simulation . . . 241
10.7.2. Heat exchanger integrated in the baffle . . . 242
10.8. Summary . . . 244
10.8.1. Discussion . . . 244
10.8.2. Future work . . . 244

11. Discussion, conclusions and perspectives **246**
11.1. Discussion . . . 246
11.1.1. Exploitation Strategies . . . 246
11.1.2. Design methodologies: Demonstration sites . . . 248
11.1.3. Prototype development . . . 251
11.2. Future work and perspectives . . . 251
11.3. Research purpose . . . 252
11.4. Conclusion: The place of DWHR in the future heating landscape . . . 253

Appendix A. Data sheets of sensors **268**
A.1. TinyTag temperature logger . . . 268
A.2. Magnetic-inductive flow meter . . . 269
A.3. Temperature controller . . . 270

Appendix B. Non financial support scheme: Feasibility studies **271**
B.1. Druids Glen: Hotel and Leisure center . . . 271
B.2. Talbot Hotel Stillorgan . . . 284
B.3. Ashlawn Nursing Home . . . 292
B.4. ABP meat processing plant, Clones . . . 301
B.5. PEPSICO, Cork . . . 313

Appendix C. Appendices related to decentralized drain water heat recovery in a domestic setting (Chapter 5) **323**
C.1. List of heat pumps . . . 323

Appendix D. Appendices related to decentralized drain water heat recovery in commercial kitchens (Chapter 6) **324**
D.1. Commercial kitchens in the United Kingdom . . . 324

Appendix E. Appendices related to the spatio-temporal analysis (Chapter 7) **325**
E.1. Flow chart of the integrated method . . . 325

Appendix F. Appendices related to Penrhyn castle **326**
F.1. Poster of the Demonstrator at Penrhyn castle . . . 326
F.2. Sizing of the circulation pump at Penrhyn castle . . . 327
F.3. Data sheet of the circulation pump at Penrhyn castle . . . 328
F.4. Detailed schematic of the Demonstrator at Penrhyn castle . . . 348
F.5. Schematic of the heating system in the plant room . . . 349

Appendix G. Characterization of the experimental set-up **350**
G.1. Definition of the steady state condition . . . 350
G.2. Flow Control . . . 351
G.3. Temperature Equivalence of the fresh water flow control system . . . 352

Appendix H. Appendices related to ABP, Cahir **354**
H.1. Schematic of the ABP test rig . . . 354
H.2. Calibration of the temperature sensors . . . 355
H.3. Datasheet of the submersible pump . . . 356
H.4. Datasheet of the additional flow meter . . . 358

List of Figures

1.1. Thermal energy flows in Ireland in 2014 [Howley et al., 2015]. 1
1.2. Main disciplines and thematic areas in the Dwr-Uisce project. 3
1.3. Scale of the different investigative axes. 5

2.1. The current status of the control variables for the planetary boundaries 10
2.2. Global emissions abatement by technology and region in the 66% $2°C$ Scenario relative to the New Policies Scenario 13
2.3. Global total primary energy supply, 2015-2050 14
2.4. Main action points of the **European Green Deal** [European Commision, 2019]. 14
2.5. Headlines of Ireland's energy and emission targets [Scheer et al., 2016]. 15
2.6. Primary Energy for heating and cooling in the EU in 2012 16
2.7. Thermal Energy flows in Ireland in 2014 [Howley et al., 2015] 16
2.8. Heat output by renewable heating source in Ireland, in 2015 [SEAI, 2017*a*] 17
2.9. Final energy consumption of households by energy products in the EU in 2015 [Eurostat, 2017] 17
2.10. Heat demand by sector in the Ireland in 2012 [SEAI, 2017*a*] 18
2.11. Exergy embedded in wastewater [Meggers and Leibundgut, 2011]. 19
2.12. Progression of District Heating: 1st to 4th generation [Thorsen et al., 2018]. 20
2.13. Energy involved in different stages of the Urban Water Cycle [Elías-Maxil et al., 2014] . . . 21

3.1. Energy balance towards the carbon-neutral operation of the evaluated WWTP.[Hao et al., 2019] 26
3.2. Wastewater-based supply of electricity, thermal energy, and biogas.([Kretschmer et al., 2018]) 27
3.3. Direct Heat Recovery 27
3.4. Indirect Heat Recovery 27
3.5. Hybrid Heat Recovery 27
3.6. Double pipe heat exchangers.[Cengel Yunus, 2006] 29
3.7. Different configuration of shell-and-tube heat exchangers.[Cengel Yunus, 2006] 29
3.8. Schematic of a plate and frame heat exchanger.([Alfa Lavel, 2020]) 30
3.9. Summary schematic of a heat pump (Adapted from [Alter, 2010]) 30
3.10. General scheme of a heat recovery system from the sewer system. [Spriet and Hendrick, 2017] 31
3.11. Evolution of the observed sewer temperature over a day. [Spriet and Hendrick, 2017] 32
3.12. Example of a WWTP within the settlement area. [Neugebauer et al., 2015] 32
3.13. Representation of calculation methodology. [Kollmann et al., 2017] 33
3.14. The schematic of integrating heat pumps in district heating, with high and low renewable electricity production, respectively. [David et al., 2017] 34
3.15. Zones of wastewater treatment plants overlapping in the agglomeration of Budapestm Hungary. [Somogyi et al., 2018a] 34
3.16. A typical residential shower installation with a single-pass counter-flow heat exchanger [Wong et al., 2010] 35
3.17. Cross section of the proposed heat recovery unit [McNabola and Shields, 2013] 36
3.18. Schematic presentation of the Domestic Hot Water system. [Eslami-nejad and Bernier, 2009] 37
3.19. Diagram of the working of the system in the option 1. [Slyś and Kordana, 2014] 37
3.20. Diagram of the installation including DWHR [Stec and Kordana, 2015] 38
3.21. Diagram of a DWHR system. [Beentjes et al., 2014] 39
3.22. Schematic of the constructed prototype. [Ramadan et al., 2016] 39
3.23. Schematic diagram of the combined heat recovery and solar energy heating system [Baek et al., 2005] 40
3.24. Schematic diagram of the Heat Punp Shower Water Heating system. [Dong et al., 2015] . . 41

3.25. Schematic diagram of four-stage heat-pump operations used for MED [Li et al., 2011]. . . . 41
3.26. Schematic diagram of the combined heat recovery and gas boiler heating system [Li et al., 2013]. . . . 42
3.27. Schematic diagram of a freezing latent heat source heat pump [Qian et al., 2009] 43
3.28. Schematic design of introducing heat pump and heat exchangers to utilize waste heat in the aerated tank [Somogyi et al., 2018]. . . . 44
3.29. Station's diagram of the heating system [Ninikas et al., 2019] 44
3.30. Neutral wastewater source heat pump (Chen et al. [2006]) 46
3.31. Untreated wastewater source heat pump (Chen et al. [2006]) 46
3.32. Schematic diagram of the wastewater source heat pump in[Baek et al., 2005] 46
3.33. Exhaust heat recovery system using electric heat pump ([Liu et al., 2014]) 47
3.34. Exhaust heat recovery system using direct-fired absorption heat pump ([Liu et al., 2014]) . 47
3.35. Urban sewage source heat pump system [Zhao et al., 2010] 47
3.36. Half centralized operation mode in large projects [Chenghu et al., 2011] 48
3.37. Variation of the COP over the year [Oh et al., 2014] 48
3.38. Principal design of the localized energy-recovery system from residential wastewater [Ni et al., 2012] 49
3.39. Schematic diagram of the Multifunctional heat pump system. [Wang et al., 2013] 50
3.40. Schematic diagram of the prototype multi-functional heat pump system [Liu et al., 2013*b*] . 51
3.41. The avoiding-clogging equipment. [Liu et al., 2014a] 52
3.42. The heat exchanger described in [Spriet and Hendrick, 2017] 52
3.43. Construction system of the sewage-source heat pump heater unit dealing with large temperature difference [Ma et al., 2017] 53
3.44. Heat exchanger in the sewer in Zurich, Switzerland. [Leuenberger, 2006] 54
3.45. Schematic of the Sandvika DWHR system. [Leuenberger, 2006] 56

4.1. General outline of the principal investigative axes. 59
4.2. Scale of the different investigative axes and their contribution to the scientific literature. . . 60
4.3. The TinyTag temperature sensor. 61
4.4. Installation of tipping bucket distribution box: inlet effluent pipe (left), distribution box receiving effluent (middle), closing of the reed switch assembly (right)[Knappe, 2018]. 61
4.5. Schematic of Sewer Heat recovery adapted from [Müller and Schmid, 2005]. 63
4.6. Graphical summary of the key steps in the spatio-temporal analysis. 66
4.7. The modular single phase power meter. 68
4.8. PT100 temperature sensor. 68
4.9. Thermopocket for PT100 sensors. 68
4.10. The Itron CF Echo II heat meter. 68
4.11. Flow and temperature meters. 69
4.12. Datalogger connected to the flow meter. 69
4.13. The data logger and transmitter. 69
4.14. The online data platform. 69
4.15. The five phases in design thinking [Rodgers, 2017]. 70
4.16. The flow chart of the thought process for prototype development. 70
4.17. Five steps in the fluent workbench. 72

5.1. Decentralized heat recovery on a domestic scale. 73
5.2. Septic tank with temperature loggers at the different measuring locations. 74
5.3. Sample of the temperature measurements at the domestic residence in Crecora, co. Limerick. 75
5.4. Tipping bucket flow meters. 75
5.5. Sample of the flow measurement at the domestic residence in Crecora, co. Limerick. 75
5.6. Embedded energy evolution over a day at Crecora, co. Limerick. 76
5.7. Daily embedded energy compared to the daily wastewater flow. 77
5.8. Indirect Heat Recovery 78
5.9. Potential role of wastewater source heat pumps in Ireland's heating mix. 79
5.10. Evolution of the fuel cost with changing COP. 80
5.11. Evolution of the LCOH with varying daily wastewater flow. 81
5.12. Concept of the temporal mismatch between supply and demand. 82

5.13. Example of a daily DHW consumption profile. . . . 83
5.14. Example of a monthly DHW consumption profile. . . . 83
5.15. Hourly SLP profile for DHW demand. . . . 83
5.16. Monthly SLP profile for DHW demand. . . . 83
5.17. Monthly SLP profile for space heating demand. . . . 83
5.18. Distribution of the temperature profile during the month of April. . . . 84
5.19. Summary of the probabilistic method. . . . 85
5.20. Outline of the simulation. . . . 85
5.21. Principal design of the decentralized drain water heat recovery unit. . . . 86
5.22. Flow chart representing the time series of the energy balance in the hot water storage tank. 87
5.23. Regression of the COP vs the required Temperature Lift. . . . 88
5.24. Regression of the price per kW vs the rated power of the heat pump. . . . 89
5.25. Average Daily DHW demand in Ireland. . . . 91
5.26. Average Daily SH demand in Ireland. . . . 91
5.27. Heat demand met by the different heat sources. . . . 92
5.28. Distribution of the heat delivered by DWHR, with a 200l reservoir . . . 92
5.29. Distribution of the amount of unused recovered heat, with a 200l reservoir. . . . 92
5.30. Evolution of the heat delivered by DWHR. . . . 93
5.31. Evolution of the unused recovered heat. . . . 93
5.32. Evolution of the LCOE. . . . 93
5.33. Evolution of the TEWI. . . . 94
5.34. LCOE of the method compared to the average value analysis. . . . 94
5.35. TEWI of the method compared to the average value analysis. . . . 94
5.36. Impact of the COP uncertainty on LCOE at 200l. . . . 95
5.37. Impact of the COP uncertainty on TEWI at 200l. . . . 95
5.38. Impact of the price uncertainty on the LCOE for a reservoir of 200l. . . . 96

6.1. Decentralized heat recovery on a kitchen scale. . . . 98
6.2. Hourly SLP profile for water demand. . . . 100
6.3. Share of hot water consumption in the kitchen. . . . 100
6.4. Hourly SLP profile for drain water flow. . . . 101
6.5. Druids Glen hotel and resort. . . . 101
6.6. Manholes leading to the grease trap at the Talbot hotel, Stillorgan, Dublin. . . . 102
6.7. Temperature at the Grease interceptor, Talbot Hotel, Stillorgan, Dublin. . . . 102
6.8. Temperature evolution in the grease interceptor at Ashlawn nursing home. . . . 102
6.9. Temperature profile for a random kitchen. . . . 103
6.10. Fresh water temperature in Dublin, 2012. . . . 103
6.11. Boxplot of the NPV for a drain water heat recovery installation with water consumption of 4000 l, compared to Heavy Fuel Oil (HeFO). . . . 105
6.12. The ShowerSave Q-Blue 1 heat exchanger. . . . 106
6.13. Single heat exchanger. . . . 106
6.14. Combined heat exchanger system. . . . 106
6.15. Effectiveness of the heat exchanger. . . . 107
6.16. Evolution of the NPV compared to different heating fuels. . . . 108
6.17. Evolution of the carbon- NPV compared to different heating fuels. . . . 108
6.18. Evolution of the NPV compared to electricity (9.78 $p£/kWh$). . . . 109
6.19. Evolution of the NPV compared to electricity (15.72 $p£/kWh$). . . . 109
6.20. Evolution of the NPV compared to electricity (26.68 $p£/kWh$). . . . 109
6.21. Yearly heat recovery potential in the UK. . . . 110
6.22. Yearly GHG savings potential in the UK. . . . 110
6.23. Heat recovery potential per outlet type. . . . 112
6.24. GHG savings potential per outlet type. . . . 113
6.25. Yearly heat recovery potential in the UK, with varying discount rate. . . . 114
6.26. Yearly GHG savings potential in the UK, with varying discount rate. . . . 114
6.27. Sensitivity of the financial NPV with varying heat exchanger effectiveness. . . . 114
6.28. Sensitivity of the environmental (Carbon) NPV with varying heat exchanger effectiveness. . 115

7.1. Centralized heat recovery from the effluent of wastewater treatment plants. 117
7.2. Schematic of Sewer Heat recovery adapted from [Müller and Schmid, 2005]. 118
7.3. Summary of the WWTP ranking method. 119
7.4. Heat demand per small area in Dublin. 120
7.5. Deliverable energy from all wastewater treatment plants in Ireland. 121
7.6. Deliverable energy from suitable wastewater treatment plants in Ireland. 122
7.7. Heat recovery from the suitable WWTPs in the Republic of Ireland. 123
7.8. Graphical abstract of the integrated three-step methodology. 124
7.9. Evolution of the COP of a water source heat pump (based on Daikin Europe NV [n.d.]). . . 126
7.10. Schematic of the Tullamore WWTP. 128
7.11. Schematic of the system set-up. 129
7.12. Small areas complying with the heat density criteria in the Tullamore region. 130
7.13. Evolution of total heat demand in the different zones. 131
7.14. Evolution of the heat demand per sector in zone E. 132
7.15. Evolution of the effluent flow at the Tullamore WWTP in 2018. 132
7.16. Evolution of the effluent temperature at the Tullamore WWTP in 2018. 132
7.17. Exploitable heat for an effluent heat recovery system at the Tullamore WWTP. 133
7.18. Summary of Excess available energy at the wastewater treatment plant. 133
7.19. Yearly recovered Energy at the Tullamore WWTP. 134
7.20. Evolution of the excess available heat in Zone E. 134
7.21. Levelized Cost of Heating for the different zones at the Tullamore Wastewater treatment plants. 140
7.22. Total Equivalent Warming Impact for the different zones at the Tullamore Wastewater treatment plants. 141

8.1. Penrhyn castle, Bangor, Wales, UK (taken by author). 145
8.2. LCOE for different heating technologies at the grease trap in Druids Glen. 146
8.3. Map of the Penrhyn grounds. 147
8.4. Monitoring campaign at Penryhn Castle, Wales. 148
8.5. The vertical drop in the kitchen drain, as seen from the coal yard at Penrhyn castle. 149
8.6. Boxplot of the drain water temperature at the kitchen in Penrhyn castle. 149
8.7. Boxplot of the fresh water consumption at the kitchen in Penrhyn castle. 150
8.8. Schematic of a Klargester settlement tank. 150
8.9. Overflow protection of the settlement tanks at Pernhyn castle, Wales. 150
8.10. Temperature profile in the first settlement tank at Penrhyn Castle, Wales. 151
8.11. Temperature profile in the second settlement tank at Penrhyn Castle, Wales. 152
8.12. Temperature profile in the third settlement tank at Penrhyn Castle, Wales. 152
8.13. Temperature profile at the inlet of the third settlement tank at Penrhyn Castle, Wales on March 30th and 31st. 153
8.14. Direct Drain Water Heat Recovery System. 154
8.15. The ShowerSave Q-Blue 1 heat exchanger. 155
8.16. The Grundfoss Alpha 2L circulation pump. 155
8.17. Feed water temperature in Dublin, 2012. 156
8.18. Effectiveness of the heat exchanger. 156
8.19. Simplified schematic of the heating system in the plant room at Penrhyn Castle. 157
8.20. Configuration 1 of the drain water heat recovery system at Penrhyn Castle, Wales. 158
8.21. Configuration 2 of the drain water heat recovery system at Penrhyn Castle, Wales. 159
8.22. Configuration 3 of the drain water heat recovery system at Penrhyn Castle, Wales. 159
8.23. Metering of the drain water heat recovery system at Penrhyn Castle, Wales. 160
8.24. Savings related to the DWHR system on the kitchen drain at Penrhyn castle, Wales. 164
8.25. Heat exchangers installed at the sewer drain in Pernhyn castle, Wales. 165
8.26. Buffer tank installed at the sewer drain in Pernhyn castle, Wales. 165
8.27. Evolution of the fresh water temp at Penrhyn castle, Wales. 166
8.28. Energy efficiency metric for hot water consumption of the kitchen at Penrhyn castle, Wales. 167
8.29. Energy consumption of the kitchen at Penrhyn castle, Wales. 169
8.30. Yearly savings of the corrected operation of configuration 2 at Penrhyn Castle, Wales. . . . 170

9.1. CIP drain at the Pepsico facility in Cork. . . . 173
9.2. Direct Drain Water Heat Recovery System. . . . 175
9.3. Hybrid Drain Water Heat Recovery System. . . . 176
9.4. Co Flo heat exchanger. . . . 177
9.5. Schematic of the WWTS at ABP, Cahir. . . . 178
9.6. Average temperature profile at the WWTS of ABP, Cahir. . . . 179
9.7. Principle scheme of the test rig. . . . 180
9.8. Schematic of the experimental unit at ABP, Cahir. . . . 181
9.9. Energetic savings for the different locations at the ABP plant in Cahir. . . . 182
9.10. GHG reduction at the inlet. . . . 183
9.11. GHG reduction at the condensate. . . . 183
9.12. GHG reduction at the effluent. . . . 184
9.13. OPEX reduction at the inlet. . . . 184
9.14. OPEX reduction at the Condensate, ABP, Cahir. . . . 185
9.15. OPEX reduction at the Effluent, ABP, Cahir. . . . 186
9.16. Heat exchanger arrangement. . . . 189
9.17. Distributor of the heat exchanger arrangement, ABP, Cahir. . . . 189
9.18. Connection of the heat pump to the test rig. . . . 189
9.19. Stairs on the experimental unit. . . . 189
9.20. The experimental test rig, with extended drain pipe. . . . 190
9.21. The data logger and transmitter. . . . 190
9.22. The online data platform. . . . 190
9.23. Experimental set-up, placed on a platform at the effluent of the WWTP at ABP, Cahir. . . . 191
9.24. Submersible pump placed in the effluent flow at ABP, Cahir. . . . 191
9.25. The experimental unit, set up at the inlet sump. . . . 193
9.26. Operation of the direct heat recovery system at the inlet. . . . 193
9.27. The temperature limiter alarm of the heat pump. . . . 194
9.28. The decreasing flow velocity at the inlet on January 18th 2020. . . . 195
9.29. Clogging of the Savy 300 pump at the inlet at ABP, Cahir. . . . 195
9.30. Clogging of the GOVOX 204 pump at the inlet at ABP, Cahir. . . . 195
9.31. Submersible pump, placed at the outlet wedge of the DAF unit, ABP, Cahir. . . . 196
9.32. Power supply of the submersible pump, connected to the power switch of the DAF unit, ABP, Cahir. . . . 196
9.33. Operation of the direct heat recovery system at the DAF unit. . . . 197
9.34. Lid of the experimental unit, secured with additional screws, at ABP, Cahir. . . . 197
9.35. Disconnected pipe of a single heat exchanger. . . . 198
9.36. Disconnected wastewater collector. . . . 198
9.37. Feedback loop introduced by the experimental set-up at the DAF at ABP, Cahir. . . . 199
9.38. In-line DWHR set-up at the DAF at ABP, Cahir. . . . 200
9.39. Moving from a brine to an effluent source heat pump. . . . 201
9.40. Comparison of the brine and effluent temperature at ABP, Cahir. . . . 202
9.41. Comparison of the brine and effluent system COP at ABP, Cahir. . . . 202
9.42. Evolution of the NPV over time for the recommended direct heat recovery unit. . . . 205
9.43. Evolution of the NPV over time for the recommended indirect heat recovery unit. . . . 206
9.44. Evolution of the NPV over time for a 248 kW indirect heat recovery unit. . . . 207

10.1. The five phases in design thinking [Rodgers, 2017]. . . . 210
10.2. Example of a passive grease interceptor [Dempsey and Rowe, n.d.]. . . . 212
10.3. Example of a mechanical grease interceptor [British Water, 2014]. . . . 213
10.4. Example of a bacteria dosing system [British Water, 2014]. . . . 213
10.5. Drawing of the grease trap with prototype DWHR device. . . . 214
10.6. Picture of the prototype DWHR device. . . . 214
10.7. Boxplot of the temperature profile at the observed kitchens. . . . 215
10.8. Schematic of the experimental set-up. . . . 215
10.9. Picture of the experimental set-up. . . . 216
10.10Schematic of the measuring grid in the grease trap. . . . 216
10.11Picture of the measuring grid in the grease trap. . . . 216

10.12Calibration curve of the flow meter. . . . 217
10.13Verification of the flow meter calibration. . . . 217
10.14Five steps in the fluent workbench. . . . 218
10.15A preview of the Autodesk Inventor software. . . . 219
10.16A preview of the ANSYS meshing software. . . . 219
10.17A preview of the ANSYS Fluent solver. . . . 220
10.18Example of residual evolution over the different iteration. . . . 220
10.19Overview of the Pressure-Based Solution Methods [ANSYS, 2019]. . . . 221
10.20A preview of the ANSYS CFD-Post application. . . . 221
10.21Effectiveness of the heat exchanger at $40°C$ drain water. . . . 222
10.22Effectiveness of the heat exchanger at $30°C$ drain water. . . . 222
10.23Recovered heating power of the heat exchanger at $40°C$ drain water. . . . 222
10.24Recovered heating power of the heat exchanger at $30°C$ drain water. . . . 222
10.25Temperature in the center plane of the grease trap. . . . 223
10.26Evolution of the NPV over 5 years for the current prototype. . . . 224
10.27Evolution of the NPV over 10 years for the current prototype. . . . 224
10.28Evolution of the NPV over 5 years for the commercialised prototype. . . . 226
10.29Evolution of the NPV over 10 years for the commercialised prototype. . . . 226
10.30Sliced geometry for the CFD simulation. . . . 228
10.31The employed mesh for the CFD simulations of the full geometry. . . . 228
10.32Example of an inflation layer. . . . 229
10.33Summary of the flow conditions in the different flow bodies. . . . 230
10.34The law of the wall [Simscale, 2018]. . . . 231
10.35Viscous sublayer resolving approach used to resolve boundary layer[ANSYS, 2019]. . . . 232
10.36The coupled walls for the heat exchanger fluid-solid interfaces. . . . 235
10.37Location of the verification control lines. . . . 236
10.38Location of the verification control lines in the sliced geometry. . . . 237
10.39Dimensionless wall distance at the wall of the fresh water, for a fresh water flow rate of 6 l/min. 237
10.40GCI for the fine mesh. . . . 238
10.41GCI for the coarser mesh. . . . 238
10.42GCI in the wastewater body. . . . 239
10.43GCI at the heat exchanger outlet. . . . 239
10.44Comparison of simulated results for the full and sliced geometry for a wastewater flow at $40°C$. 240
10.45Comparison of simulated results for the full and sliced geometry for a wastewater flow at $30°C$. 240
10.46Comparison of simulated and experimental results for a wastewater flow at $40°C$. . . . 240
10.47Comparison of simulated and experimental results for a wastewater flow at $30°C$. . . . 240
10.48Approximate linear relationship between the experimental and simulated outlet temperature of the heat exchanger. . . . 241
10.49Comparison between the outlet temperature of the heat exchanger for clean water, and the FOG emulation fluid at $40°C$. . . . 242
10.50Comparison between the outlet temperature of the heat exchanger for clean water, and the FOG emulation fluid at $30°C$. . . . 242
10.51Rendering of the heat exchanger, integrated into the baffle of the grease interceptor. . . . 243
10.52Technical drawing of the heat exchanger, integrated into the baffle of the grease interceptor. 243
10.53Comparison between the outlet temperature of the heat exchanger for the initial, and improved design at $40°C$. . . . 243
10.54Comparison between the outlet temperature of the heat exchanger for the initial, and improved design at $30°C$. . . . 243

E.1. Flow chart of the spatial analysis in the integrated methodology. . . . 325
E.2. Flow chart of the temporal analysis in the integrated methodology. . . . 325

G.1. Effluent temperature and fit in steady state. . . . 350
G.2. Histogram of the observed recovered heat during steady state. . . . 351
G.3. Probability plot f the observed recovered heat during steady state. . . . 351
G.4. Histogram of the treated recovered heat during steady state. . . . 351
G.5. Probability plot of the treated recovered heat during steady state. . . . 351

G.6. Schematic of the experimental set-up. 352
G.7. Schematic of the overflow system. 352
G.8. Simulated drain water flow in steady state. 352
G.9. Heat exchanger flow in steady state. 352
G.10.Boxplot of the feed water temperature for both configurations. 353

List of Tables

3.1. Waste water temperature of different domestic appliances [Cunniffe and McNabola, 2014]. . 25
3.2. Sewage water temperature variation in different cities 25
3.3. General parameters of the heating network in Binningen 54
3.4. General parameters of the heating network in Loewenberg 55
3.5. General parameters of the heating network in Winterthur 55
3.6. General parameters of the heating network in Schaffhouse 56
3.7. General parameters of the heating network in Sandvika 56
3.8. General parameters of the heating network in Hasselt 57

4.1. Water consumption per meal served in different types of food outlets. 62
4.2. Parameter for LCOH calculation 65

5.1. Monitoring matrix for the drain water temperature monitoring in Ireland. 75
5.2. Wastewater Discharge Authorisation Licenses 77
5.3. Estimated wastewater flow in local treatment systems 78
5.4. Unexploited embedded energy in domestic wastewater 78
5.5. Indirect Heat recovery in Ireland's heating energy mix. 79

6.1. Fuel prices and carbon conversion factors in the UK. 104
6.2. Fuel prices and carbon conversion factors in the UK. 107
6.3. Consumption levels. 110
6.4. Daily water consumption for the different categories. 111
6.5. Summary of results based on the financial criterion.. 111

7.1. Heat recovery from the three suitable WWTPs with a potential larger than 100 GWh/yr . 122
7.2. Parameters of the five identified zones. 131
7.3. Commercial Fuel Cost in the Republic of Ireland in 2019. 138
7.4. Characteristics used for TEWI calculation. 139
7.5. Piping characteristic for the five identified zones. 139
7.6. Investment costs, in €, for the different zones at the Tullamore Wastewater treatment plants. 140
7.7. Fuel costs, for the different zones at the Tullamore Wastewater treatment plants. 140
7.8. Financial and environmental savings, for the different zones at the Tullamore Wastewater treatment plants. 141

8.1. Payback period and emission reduction at a hotel in Dublin, Ireland. 146
8.2. Payback period and emission reduction at a nursing home in Tipperary, Ireland. 146
8.3. Summary table of monitoring programme at Penrhyn Castle, Wales. 148
8.4. Hydraulic characteristics of the heating system at the plant room of Penrhyn castle. 157
8.5. Daily energy consumption related to the kitchen at Penrhyn castle, Wales. 162
8.6. Emission parameters related to the kitchen at Penrhyn castle, Wales. 162
8.7. Summary of the estimated capital investment at Penrhyn castle, Wales. 163
8.8. OPEX and payback period at Penrhyn castle, Wales. 163
8.9. Fuel prices and carbon conversion factors for the National Trust property at Penrhyn castle. 163
8.10. Fuel prices and carbon conversion factors in the UK. 164
8.11. Measurements of the heat recovery from the kitchen drain water at Penrhyn castle, Wales. . 166
8.12. Measurements of heat consumption for hot water at Penrhyn castle, Wales. 167
8.13. Measurements of electric consumption of the pumps at Penrhyn castle, Wales. 168

9.1. Results of the feasibility study at PEPSICO, Cork. 174
9.2. Results of the feasibility study at the DAF unit at ABP, Monaghan. 174

9.3. Results of the feasibility study at the outlet at ABP, Monaghan. 174
9.4. NIBE F1145 output data, according to EN 14511 at 0/45. 177
9.5. Test rig design, clean fluid flows, ABP, Cahir. 180
9.6. Financial and Environmental parameters. 181
9.7. Cost Estimate for the experimental unit. 182
9.8. Financial results for DWHR at the inlet screen, ABP, Cahir. 185
9.9. Financial results for DWHR at the Condensate, ABP, Cahir. 185
9.10. Financial results for DWHR at the Effluent, ABP, Cahir. 186
9.11. Comparison of heat recovery systems at the inlet screen, ABP, Cahir. 186
9.12. Comparison of heat recovery systems at the condensate, ABP, Cahir. 187
9.13. Comparison of heat recovery systems at the effluent, ABP, Cahir. 187
9.14. Commissioning of the experimental set-up, ABP, Cahir. 192
9.15. Operation of the direct heat recovery system at the inlet, ABP, Cahir. 194
9.16. Operation of the direct heat recovery system at the DAF, ABP, Cahir. 197
9.17. Comparison of the capital investment for both systems. 203
9.18. Comparison of the operational parameters for both systems. 203
9.19. Cost Estimate for the recommended direct heat recovery unit. 205
9.20. Reduction in yearly GHG emissions for the recommended direct heat recovery unit. 205
9.21. Reduction in yearly GHG emissions for the recommended indirect heat recovery unit. . . . 206
9.22. Reduction in yearly GHG emissions for a 248 kW indirect heat recovery unit. 207

10.1. Approximate settings of the experimental runs, simulated during the validation process. . . 218
10.2. Breakdown of the construction costs of the prototype DWHR device. 224
10.3. NPV for the current prototype. 225
10.4. Potential customers for the current prototype. 225
10.5. NPV for the commercialised prototype. 226
10.6. Potential customers for the commercialised prototype. 226
10.7. Main characteristics of the employed mesh. 229
10.8. Main characteristics of the employed mesh for the sliced geometry. 229
10.9. Specific set points of the simulation runs, during the validation process. 233
10.10Specific set points of the simulation runs, during the validation process, using the sliced geometry. 234
10.11The heat exchange characteristics of the specific materials of the outer walls of the heat exchanger. 234
10.12Thermal characteristics of the fluids. 242

C.1. List of heat pumps 323

1. Introduction

1.1. Research context

In northern developed countries, thermal energy, in the form of process heat, space heating or hot water represents a large part of the energy consumption. Along with cooling, it represents 50% of the final energy consumption in the EU, and about 32% of the primary energy consumption in Ireland. This thermal energy is still mainly produced by fossil fuels, the share of fossil fuels in the heating mix is 75% in the EU (compared to 18% heat from renewable sources), and 87% in Ireland (6.6% from renewable sources), as can be seen in Figure 1.1 Commision [2016]; Howley et al. [2015]. This important share of fossil fuels, results in a share of 31% of the Ireland's greenhouse gas (GHG) emissions.

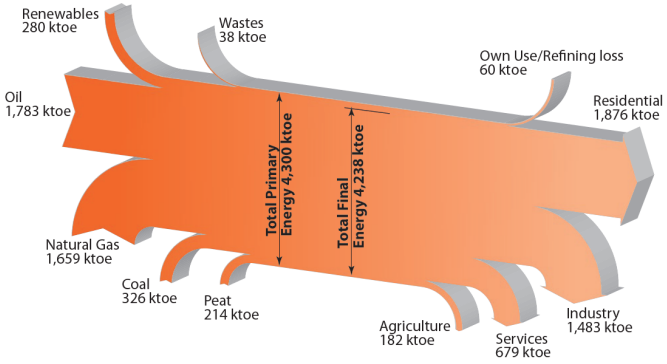


Figure 1.1.: Thermal energy flows in Ireland in 2014 [Howley et al., 2015].

The agreements made by the conference of the parties (COP) of the United Nations Climate Change Conference (UNCCC) (Kyoto 1992 and Paris 2015) have prompted the EU to impose the '20−20−20'targets for 2020, aiming at improving the energy efficieny by 20%, reducing the GHG emissions by 20% and reaching a share of 20% renewable energy sources in the energy mix EU2015.LV [2015]. For 2030 these targets are 32.5%, 40% and 32% respectively [European Council, 2014]. The European Green Deal intends an even higher emission reduction target, aiming at 50 and even towards 55% European Commision [2019]. These targets are to be reached by the Nationally Determined Contributions (NDC) of each of the member states. For Ireland the emission reduction target for 2020 is 20%, and the target share of renewable heat is 12%, and especially for the latter Ireland is currently falling short [Clancy, 2015]. Failing to reach these targets would require to purchase renewable energy compliance from other member states [SEAI, 2017*a*]. For the renewable energy target, penalties are expected to reach 100-150 M€per missing percentage [Donnelly, 2018]. For 2030, no specific Irish targets have been set at the moment, but the EU target of 40% is taken as a starting point [SEAI, 2020].

Since the 1980's a lot of progress has been made in the installation of buildings. The consumption of thermal energy by buildings has been reduced by $10-30\%$, thanks to, amongst others, improved insulation, and thus lower transmission losses through windows and walls. However still a large part (around 15%) of the thermal energy delivered to a building is lost via the drain and sewer system (for low-energy consuming buildings this can go up to 30%). Today drain water is the largest source of heat leakage in buildings [Schmid, 2008]. Research within this project has shown that an estimated 15% of heat consumed by Irish families is still embedded in the wastewater, leaving the building through the drain, corresponding to yearly emission of 1.24 $Mton\ CO_{2,eq}$, and a fuel expense of 0.23 €/$person\ day$.

Similarly heat is lost in industrial installations, it is not uncommon for the wastewater to be cooled before discharge, without exploiting the heating potential of this wastewater.

Recovering the heat enables, depending on the employed technology, to ensure higher utilisation rate of the produced heat, and thus increases energy efficiency. Through reduced energy consumption in a carbon intensive sector it reduces GHG emissions, and provides an additional renewable heat source, to be used in combination with heat pumps [Scheer et al., 2016]. Integrating and correlating the (waste) water and heating energy network is an aspect of the Water-Energy nexus. Energy and water are strongly interconnected in terms of resource uses, and such links are referred to as the Water-Energy Nexus (WEN). The WEN definition is also sometimes broadened to include Food production and consumption, acquiring the name of Water-Energy-Food Nexus. The extent of such links reveals itself on multiple scales and is a matter of growing concern given the predicted worldwide increase of energy, water and food demand expected as higher than 50% by 2050 [IEA and IRENA, 2017].

1.2. Problem statement

Although recovering heat from wastewater is environmentally, energetically, and, in a lot of cases, financially beneficial, its application is not common. After investigation of literature, and discussions with professionals in the field, the following points have been identified as bottlenecks or challenges for the implementation of Drain Water Heat Recovery (DWHR) technology. The contributions mentioned in Section 1.4.3 aim to provide answers for the challenges these bottlenecks provide.

1.2.1. Lack of awareness about the technology and its potential.

Very few consumers have considered DWHR technology in their plant or installation, the linearity of considering this wastewater as a waste stream without value must give way to a new way of thinking, considering the wastewater stream as a resource. This transition is well under way with regards to recovering biogas, reusing the sludge as fertilizer, etc. However, the thermal reuse is lagging.

Through the demonstrators, and the corresponding design methodologies, this research contributes to improving the awareness and visibility of this technology. This is done through published journal papers, conference papers and presentations, workshops, invited lectures, and by installing two demonstration sites.

1.2.2. Lack of information regarding the total sectoral potential of DWHR.

Because of this lack of awareness, there is no information on how significant the contribution of this technology can be to reduce the GHG intensity of the heating mix. Therefore, it is difficult to determine what measure of support, promotion and regulation should be set-up for this technology, and how important it can be in future pathways towards decarbonisation.

The sectoral potential, on a national level, is studied in this project through the different exploitation strategies (Chapters 5, 6 and 7). These chapters are (partly) published in different journal papers (Spriet and McNabola [2019*a*], Spriet and McNabola [2019*b*], Spriet et al. [2020]), and give an indication of this potential, and provide decision- and policy-makers with a support tool. Furthermore, it provides support in the planning of regional district heating systems. This technology collectivises heat provision, in a similar way that it is done for electricity and water provision, which can improve the financial cost-effectiveness of DWHR technology .

1.2.3. Off the shelf solution only exist for a limited number of applications.

Off the shelf heat recovery solutions exist for showers, dishwashers, and sewers, however, there are other applications showing potential. These applications currently require a specific study, using generalised heat exchange solutions, which are often time- and space consuming.

The developed prototype aims at designing a DWHR solution for the specific case of grease traps for industrial kitchens. In Ireland, it is mandatory for industrial and large-scale kitchens to install grease traps to cut down on the problem of fatberg formation. The research proposes an integrated solution, which could be further developed in an inherent feature of grease traps. This developed prototype, if this proves to be attractive, can extend the set of off the shelf systems.

1.2.4. At low available energy volumes, DWHR technology might not be cost effective.

The main bottleneck for financial profitability of DWHR projects is the increased investment they entail, when compared to classic heating systems. In cases where heat consumption, and thus available heat in drain- or wastewater is small, the benefit of reduced fuel consumption might not outweigh the additional investment cost. This is particularly a problem in domestic, home heating. Because this is generally provided individually for each residence, it might not be cost effective to recover the heat on a single residence scale.

A possible solution is the use of collective heating systems, such as a district heating system, but also a central heating system for an apartment block. Another option is to diversify the heat supply, such using hybrid heat pumps.

1.3. Research project

This Ph.D. position is part of the multidisciplinary Dwr-Uisce ('Distributing our Water Resources: utilizing Integrated, Smart and low- Carbon Energy ') research program involving Trinity College Dublin and Bangor University. Its main target is to improve the long-term sustainability of water resources in Ireland and Wales from economic, environmental and social perspectives. Main steps involved are:

- Benchmark assessment of water sector in Wales and Ireland;
- Development of new technological platforms for electricity and heat recovery from water supply systems including prototyping, business plan assessment and installation of pilot schemes;
- Development of a cross-border smart specialization cluster in the field of water-energy challenges;
- Investigation on climate change impacts and resilience of water industry in Ireland and Wales.

The Dwr-Uisce project is by birth a multidisciplinary one, including many different research areas as summed up in Figure 1.2.

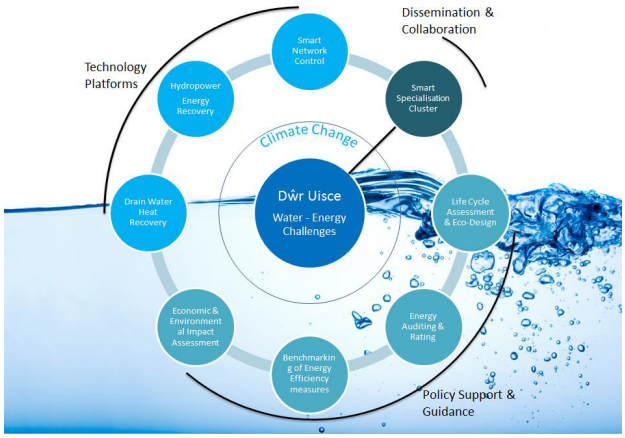


Figure 1.2.: Main disciplines and thematic areas in the Dwr-Uisce project.

Drain- and wastewater heat recovery (DWHR) forms the 2nd work package of the research project, the work is described in the following four subcategories.

- Desk studies of the potential impact of DWHR technology in Ireland and Wales.
- Lab-scale development of a DWHR unit for a whole building (Commercial).
- Field demonstration of DWHR in the hospitality sector.
- Field demonstration of DWHR in the industrial sector.

The deliverables include resource and market assessments, lab-scale prototypes and field demonstrations.

1.4. Research purpose

1.4.1. Research aim and objectives

The aim of the research is to provide a balanced response to the research questions below, showing the potential, impact and technologies of DWHR. This results in an assessment of the contribution of this technology towards, GHG emission reduction and renewable heating targets.

This aim is formulated in different objectives, containing the following aspects:

- A resource assessment of the embedded energy in wastewater in the region.
- Design guidelines for DWHR systems, through the experience in this project.
- Laboratory campaign studying a novel heat recovery system in grease traps.
- Design and construction of full-scale demonstration sites.

1.4.2. Research questions

This research aims to address three research questions (enumerated below), regarding the development and exploitation of recovering thermal energy from drain or waste water, called Drain Water Heat Recovery (DWHR).

1. How can DWHR contribute to the current heating mix, and to reaching emission reduction and renewable heating targets?
2. How do different situations in different sectors affect the design of DWHR systems? How can DWHR be implemented?
3. How can the current set of commercially available DWHR system be complemented or extended?

One can observe that these questions are interconnected, as, for example, the design of the DWHR system has an impact on the recovered energy, and thus impacts the contribution to the current heating mix. Another example is that the study of potential contribution of existing DWHR systems to the current heating mix, can highlight gaps in the market, where unexploited potential is available, and the current set of DWHR systems can be complemented.

How can DWHR contribute to the current heating mix, and to reaching emission reduction and renewable heating targets?

A complete and balanced answer to this question includes following aspects:

- What is the current untapped potential in the studied region, and how does this potential relate to the greater picture of heat consumption in the sector (domestic, commercial kitchen, wastewater treatment plants), on a national level?
- What would be the cost be of recovering or utilising this potential? The cost will include a technical-operational cost, changing the temperature will change the behaviour of different wastewater related system. This cost also includes the environmental, and financial cost of recovering the heat. How much additional energy, and/or material is required to exploit this untapped potential?
- How do these costs compare to the current cost, both environmental and financial, of thermal energy?

How do varying conditions in different sectors affect the design of DWHR systems? How can DWHR be implemented?

Different sectors are characterized by different conditions of the wastewater, for example the hospitality sector, and more specifically its kitchens, will be characterized be small flows at high temperatures, whereas certain industries might be characterized by very large flows at lower temperatures. To assist with these design choices, following aspects will be studied:

- What are the minimal required flow and temperatures for a feasible DWHR project of a certain technology? How can we make a trade-off between high temperatures, high flows, and proximity to heat consumers?
- How can DWHR systems be implemented with a minimal impact on current infrastructure and available space?
- What are the main steps and bottlenecks in implementing a DWHR project, could this be simplified and/or facilitated?

How can the current set of commercially available DWHR system be complemented or extended?

The study of the regional potential in commercial kitchens in the UK (see Chapter 6) showed a significant amount of energy embedded in the drain water flow of small kitchens, representing a significant potential for the reduction of greenhouse gas emissions, which is currently not recoverable in a financially profitable way. Furthermore, the installation of grease traps is mandatory for all commercial kitchens, regardless of their size. The possibility to add a heat recovery system, that is integrated in the grease trap, to the market is also studied in this thesis. To assess the potential of this system, following points were addressed:

- What is the market for this type of systems?
- What is the optimal design for such a system? And what is its heat recovery potential?
- What are the additional costs related to integrating a heat recovery system into the grease trap?

1.4.3. Research contributions

The research will contribute to existing literature and knowledge on different scales. On the one hand the sectoral potential will be documented, but studies will investigate the interactions between heat recovery and the operation and function of systems and buildings. And lastly the operation and design of a specific DWHR application.

The different scales are represented in Figure 1.3, and further described in this section.

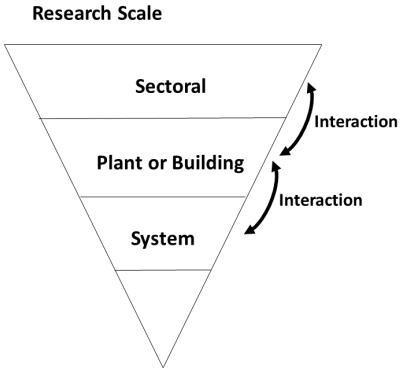


Figure 1.3.: Scale of the different investigative axes.

National scale

The study of the potential of drain water heat recovery, on a national scale, is divided into three sectors, the residential (or domestic) sector, the commercial sector (here represented through commercial kitchens) and the industrial sector, which is represented in this thesis as wastewater treatment plants, both municipal and from industrial plants.

The potential for heat recovery in the domestic sector in Ireland is estimated in Chapter 5, and its financial and environmental feasibility was studied on a system scale (see next Section). The potential for heat recovery from commercial kitchens in the hospitality sector, in the UK, is estimated in Chapter 6, these results were published in the journal *Energy and Buildings*. The regional potential from licensed wastewater treatment plants in Ireland is discussed in chapter 7, the financial and environmental benefits are discussed for a particular case in the Tullamore wastewater treatment plant, in co. Offaly, Ireland.

- **Journal Paper: Decentralized drain water heat recovery from commercial kitchens in the hospitality sector**

Spriet, J. & McNabola, A., 2019. **'Decentralized drain water heat recovery from commercial kitchens in the hospitality sector'**, *Energy and Buildings*, 194, pp. 247-259.

This paper assesses the impact of introducing direct drain water heat recovery systems in commercial kitchens in the UK, based on a commercially available heat exchangers. The recoverable heat from these kitchens was estimated using Monte Carlo simulation, sector consumption data, and data measured in the field. This analysis resulted in a total financially feasible potential for drain water heat recovery in the hospitality and food service sector in the UK of approximately 1.24 TWh/yr, leading to a reduction in GHG emissions of 344 $ktons\ C_e/yr$. This could be achieved at a cost of approximately 2.94 $p£/kg\ C_{e,\ saved}$, over a 10-year lifetime, which was several orders of magnitude smaller than traditional renewable heat sources such as heat pumps. Commercially available drain water heat recovery systems could, when installed, exploit around 88% of current potential in drain water heat in commercial kitchens (1.40 TWh/yr) in a manner that is financially profitable.

Plant or Building scale

The feasibility of heat recovery systems for single residences is discussed in Chapter 5, and was presented at the *3rd EWaS International Conference on Insights on the Water-Energy-Food Nexus*, and published in the journal *Energy and Buildings*.

The integration of drain water heat recovery systems was investigated through a **demonstration site**, at Penrhyn castle in Wales. The concept of this demonstrator was presented at the *14th conference on sustainable development in energy, water and environment system*. The target being the publication of an extended version of this conference paper, including returns from the real world implementation in *Applied Thermal Engineering*.

The integration of heat recovery systems from wastewater treatment plants a **demonstration site** at the ABP meat processing plant in Cahir, co. Tipperary, Ireland, and through a theoretical study on the Tullamore wastewater treatment plant in co. Offaly, Ireland. A paper describing the results of the former is planned to be submitted to the journal *Applied Thermal Engineering*. The results of the latter study were published in the *Journal of Cleaner Production.*

- **Conference Paper: Decentralized Drain Water Heat Recovery: Interaction between Wastewater and Heating Flows on a Single Residence Scale.**

Spriet, J. & McNabola, A., 2018. **'Decentralized Drain Water Heat Recovery: Interaction between Wastewater and Heating Flows on a Single Residence Scale.'** *3rd EWaS International Conference on Insights on the Water-Energy-Food Nexus, Lefkada Island, Greece*, 27-30 June 2018.

- **Journal Paper: Decentralized drain water heat recovery: A probabilistic method for prediction of wastewater and heating system interaction**

Spriet, J. & McNabola, A., 2019. **'Decentralized drain water heat recovery: A probabilistic method for prediction of wastewater and heating system interaction'**, *Energy and Buildings*, 183, pp. 684-696.

These papers describe a probabilistic method using observations from 113 residences to predict daily and monthly consumption profiles, using monthly consumption as a starting point. These profiles were then used to study the operation of a drain water heat recovery system, but can also be used to assess the operation of other heating methods where the supply is not controlled, such as solar thermal. The operation of the drain water heat recovery systems was predicted based on a monitoring campaign at 3 residences, measuring wastewater temperature and flow at 5-minute intervals, for over a 1-year period. The method was applied to a theoretical average Irish residence, obtained through a Monte Carlo analysis on just under 700 000 Irish residences. The method highlighted the potential for a reduction in heating related greenhouse gas emissions by 7.6% to 22%. However, this increased heating costs by 120% to 130%.

- **Conference Paper: Drain water heat recovery in commercial kitchens: Case of tourist attraction.**

Spriet J. & McNabola A. 2019. **'Drain water heat recovery in commercial kitchens: Case of tourist attraction.'** *14th conference on sustainable development in energy, water and environment system 2019, Dubrovnik, Croatia*, 1st-6th October.

This paper discusses a monitoring campaign, which ran for over a year, measuring the hot and cold water consumption and the drain water temperature of a commercial kitchen at Penrhyn castle. This kitchen serves a tea room, and a small restaurant, with approximately 100 000 visitors each year, in addition to 32 to 45 personnel working on an expansive site. Based on these observations, the value of the embedded energy and the related heat recovery potential were estimated. This paper discusses the predicted energy recovery and related energy savings based on the precursor monitoring campaign. This resulted in predicted thermal savings ranging between 1 675 and 2 267.5 kWh per year, which represents 28 to 38% of the kitchens heat demand, and yearly electric savings ranging between 22.5 and 50 kWh.

- **Journal Paper: Spatial and temporal considerations in the performance of wastewater heat recovery systems**

Spriet, J., McNabola, A., Neugebauer, G., Stoeglehner, G., Ertl, T. & Kretschmer, F. 2020. **'Spatial and temporal considerations in the performance of wastewater heat recovery systems'**, *Journal of Cleaner Production*, 247

This paper proposes a three-step methodology, including an energetic analysis at the wastewater treatment plant, a spatio-temporal analysis of supply and demand in potential supply areas, and an integrated analysis, overlaying the supply and demand profiles. This allows to account for both the proximity of consumers and potential temporal mismatches between supply and demand. The methodology was applied on a case study in Ireland, being able to clearly identify potentials and pitfalls for laying out grids and dimensioning the energy generation systems. It can be concluded, that wastewater energy is a well-suited source of energy to supply baseloads, but the spatio-temporal patterns reveal that both periods of excess wastewater heat potentials as well as additional heating in bivalent systems is required.

System scale

The operation of drain water heat recovery on a system scale, is studied by the experimental testing, and the development of a lab-scale prototype. This prototype studies the integration of a heat recovery system in the grease trap of a commercial kitchen. Grease traps are mandatory in commercial kitchens, and one of their main inconveniences is the high temperature of the wastewater. Recovering heat from these grease traps would not only be beneficial from an energetic point of view, but also improve the Fat, Oil and Grease (FOG) removal efficiency of the system. A prototype was developed and tested in the lab, these experimental results were then used to validate a computer model of the system, in order to be able to simulate different designs using Computational Fluid Dynamics (CFD). The aim is to publish the results of this study in the journal *Energy Conversion and Management.*

1.4.4. Contribution to other papers

The research presented in this thesis also contributed to other papers, listed in this section.

Conference papers

- **Conference Paper: Life Cycle Assessment of an inline heat exchanger for heat recovery from drain water in a commercial kitchen.**

Schestak I., Spriet J. & Styles D. 2019. **'Life Cycle Assessment of an inline heat exchanger for heat recovery from drain water in a commercial kitchen.'** *14th conference on sustainable development in energy, water and environment system 2019, Dubrovnik, Croatia*, 1st-6th October.

This study assesses the environmental sustainability of heat recovery systems for recovering heat from drain water applying the Life Cycle Assessment (LCA) methodology. For the first time, a heat recovery system from copper is compared to one including the innovative polymer-graphite composite; and for the first time environmental burdens related to their life cycle is set into context with the energy and environmental savings when installed in the drainpipe of a commercial kitchen. The results show an environmental payback for most of the assessed emissions within the 10-year lifetime for the copper system and full payback for the polymer-graphite system, even when compared to renewable energies. Extrapolation of the findings to UK level proves that environmental savings can be achieved for all addressed impact categories and hence, application of this technology can be recommended for the food and drink service sector.

1.5. Lay-out of the thesis

The research presented in this thesis includes desk studies on exploitation strategies, using newly designed assessment methods, the design and installation of demonstration sites, and the development of a lab-scale prototype, as well as the modelling and optimisation of this prototype. In this section the reader will find a brief outline of the contents of each of the chapters.

Chapter 2 - Climate, Energy and Wastewater

This chapter discusses literature and policy on the link between the climate, energy production and consumption, and the wastewater cycle. It describes the current European, Irish and UK energy and climate policy, and is giving background on the concepts used further on in this thesis.

Chapter 3 - Literature review: Drain and Waste Water Heat Recovery

Chapter 3 discusses previous scientific literature on the recovery of heat from drain and waste water. The different experimental and methodological approaches are discussed, and existing installations are discussed. From this literature study, some gaps in the literature, that this research thesis aims to address, are identified.

Chapter 4 - Research Methodology

In Chapter 4 the thought process behind the different assessments is discussed, along with a brief overview of the employed methodology and the motivation for using this methodology. The employed methodologies are described in more details in the individual chapters where they are applied.

Chapter 5 - Exploitation Strategy: Decentralized drain water heat recovery in a domestic setting

This chapter presents the methodology and results for the first of three exploitation strategies. It looks into the possibility of recovering heat on an individual residence scale, and discusses the availability of this thermal resource in the Republic of Ireland. The majority of thermal energy in Ireland is delivered on an individual residence basis, generally under the form of gas or fuel oil being burnt in a boiler. Later, the

financial feasibility, and potential emission savings are discussed on a single residence basis. The employed methodology focuses on the importance of the temporal aspect in this assessment.

Chapter 6 - Exploitation Strategy: Decentralized drain water heat recovery in commercial kitchens

Chapter 6 describes the second exploitation strategy, discussed in this thesis. It proposes heat recovery from a more upstream location, where temperatures are higher, and the effectiveness of heat recovery is higher. It proposes heat recovery from commercial kitchens as the monitoring campaign identified kitchen wastewater as having a large energy density. Commercial kitchens are expected to have a relatively large discharge of wastewater, increasing the volume of energy that can be recovered. The chapter studies the potential for deploying a particular drain water heat recovery system in the UK, taking into account the temporal variations of supply and demand. This Chapter highlights the promise of DWHR from commercial kitchens as a low-cost way to reduce the fuel consumption and carbon intensity of the heating consumption in the sector.

Chapter 7 - Exploitation Strategy: Centralized drain water heat recovery at wastewater treatment plants

In Chapter 7 the heat recovery at a downstream location, the effluent of the wastewater treatment plant is studied, and shows an estimation of the potential in Ireland. Here, both the spatial aspects, proximity of the consumer to the heat recovery location, and the temporal aspects are important. The chapter proposes a method for urban and energy planners to keep both these aspects into consideration when designing a project. This method is then applied to the wastewater treatment plant in Tullamore, Ireland, showing the importance of temporal mismatches in the feasibility of such systems. The financial and environmental cost-benefit analysis is also made in this chapter, for this particular case study.

Chapter 8 - Drainwater Heat Recovery in Commercial Kitchens: Demonstrator at Penrhyn Castle

Chapter 8 discusses the feasibility assessment, design and installation of a demonstration heat recovery system, in the kitchen of a tourist attraction, at Penrhyn castle, Wales. It discusses the monitoring campaign, providing the data for the feasibility assessment, the subsequent design of the system, and the installation procedure. Data, performance indicators, and information on the operation of the system are also provided.

Chapter 9 - Centralized drainwater Heat Recovery at Wastewater treatment plantss: Demonstrator in the meat processing industry

In Chapter 9 the demonstrator at the facilities of ABP food group is described. Similar to the other demonstration site it discusses the feasibility assessment, design and installation of the heat recovery unit. The chapter also focuses on the particular challenges of heat recovery system in combination with the highly loaded wastewater from a meat processing factory.

Chapter 10 - Prototype development: Heat recovery from grease traps

Finally a prototype is developed, aiming at supplementing the range of existing, commercially available heat recovery systems. Chapter 10 describes the reasoning behind the concept, the design and testing of an early prototype, and the development of a validated model, used to optimize the design of this system.

Chapter 11 - Discussion, conclusions and perspectives

Chapter 11 summarizes and discusses the different results, and reflects on how they answer the research questions. The position of different drain water heat recovery techniques in the future energy landscape is discussed, and a pathway of different future research possibilities is presented.

2. Climate, Energy and Wastewater

2.1. Planetary boundaries

Modern industry, energy production and modern lifestyle have increased the anthropogenic pressures on the planet's system up to such levels that abrupt global environmental change cannot be excluded. In [Rockström et al., 2009], nine planetary boundaries are suggested in a new global sustainability approach, the idea being that humanity can operate safely when staying within these boundaries. In the article seven have been quantified:

- Climate change: The CO_2 concentration in the atmosphere must remain below 350 ppm, and the change in radiative forcing can be no greater than $1W/m^2$.
- Ocean acidification: The mean aragonite surface seawater saturation state must remain above 80% of the pre-industrial levels.
- Stratospheric ozone: The reduction in ozone (O_3) concentration from pre-industrial level (290 $Dobson\ units$) must not be greater than 5%.
- Biogeochemical nitrogen and Phosphorus cycle: The limit of industrial and agricultural N_2 is fixed at $35Tg\ N/yr$, and the annual P inflow to the oceans must remain below 10 times the natural background weathering of P.
- Global fresh water use: The consumption of runoff resources must remain below 4000 km^3/yr.
- Land system change: Less than 15% of the ice-free land surface can be under cropland.
- Biological diversity loss: The annual rate must be below 10 extinctions per million species.

For the two remaining planetary boundaries the limits have not yet been quantified, they are:

- Atmospheric aerosol loading.
- Chemical pollution and the introduction of novel entities.

In Figure 2.1, an estimation of the recent (2015) status of the control variables for the planetary boundaries can be found, as described in Steffen et al. [2015].

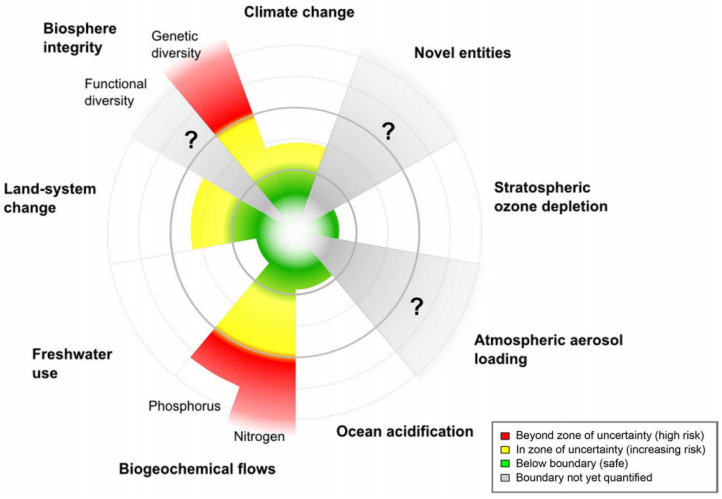


Figure 2.1.: The current status of the control variables for the planetary boundaries

In this Figure, one can observe that the limits for at least two (Biological diversity and Biochemical flows) out of nine boundaries are already being surpassed, with two others (Land-system change and Climate change) being in the uncertainty zone. The interaction among the different planetary boundaries might shift the safe level, for example, the water boundary will be highly sensitive to land-use and climate-change boundaries.

2.2. Climate Change

Climate disruption, being one of the planetary boundaries is reported and documented in a wide array of reports and publications, but the leading report is written by the Intergovernmental Panel on Climate Change (IPCC). In Pachauri et al. [2015] it is stated that human influence on climate change is clear, and that current anthropogenic emissions of greenhouse gases are the highest in history. In the period between 2000 and 2010 a yearly increase in greenhouse gas emissions of 2.2% has been observed, 78% of this increase is related to CO_2 emissions from fossil fuel combustion and industrial processes.

Changing precipitation, melting snow and ice, due to climate change, are altering hydrological systems, and are affecting the water resources. Along with changing temperature conditions, this is one of the factors causing many species to shift their geographic ranges, seasonal activities and migration patterns. Climate change, and the subsequent altered hydrological system also have a negative impact on crop yields. Furthermore it has a strong influence on extreme weather events, it causes the occurrence of warm temperature extremes, extremely high sea levels, and heavy precipitation events to increase.

Climate change increases the likelihood of severe, pervasive and irreversible impacts for people and ecosystems. A large fraction of species faces increased extinction risks, due to their inability to adapt sufficiently fast to a rapidly changing climate, food security is undermined, and the impact on human health is negative as well.

Pachauri et al. [2015] recognizes cumulative CO_2 emissions as one of the key drivers for climate change, limiting climate change would thus require substantial and sustained reduction of greenhouse gas emissions. The report states that adaptation and mitigation are complementary for reducing and managing climate change risks. The mitigation pathways require substantial (near-zero by 2100) reduction in CO_2 emissions, in order to reduce climate risks and to increase the prospects for effective adaptation. This would reduce long term costs and challenges as well. The cost effectiveness of mitigation improves when using an integrated approach combining the reduction of energy use and the greenhouse gas intensity of end-use sectors, decarbonizing the energy supply, reducing the net emissions and increasing the carbon sinks.

The main greenhouse gases, contributing to climate change are:

- Water vapour (H_2O)
- Carbon Dioxide (CO_2)
- Methane (CH_4)
- Nitrous Oxide (N_2O)
- Ozone (O_3)

2.2.1. Energy and climate policy

In reaction to the threat climate change poses, the United Nations (UN) negotiated an environmental treaty, the United Nations Framework Convention on Climate Change (UNFCCC), at the 'Rio Earth Summit' in Rio de Janeiro, Brazil in 1992. The ultimate objective of the Convention was to stabilize greenhouse gas concentrations 'at a level that would prevent dangerous anthropogenic (human induced) interference with the climate system.' It states that "such a level should be achieved within a time-frame sufficient to allow ecosystems to adapt naturally to climate change, to ensure that food production is not threatened, and to enable economic development to proceed in a sustainable manner." [UNFCCC, 2016]

Following this UNFCCC, the Kyoto Protocol was adopted in 1997 in Kyoto, Japan, entering into force in 2005. This protocol contained mandatory targets on greenhouse-gas emissions for the parties which ratified the convention. Stating an overall 5% reduction target below 1990 emission levels in the period $2008 - 2012$,

with different parties committing to different percentage targets. The agreement offered flexibility in how the different parties can meet the targets. Three main mechanisms can be distinguished:

- International Emissions Trading: This trading allows parties, with emission units to spare, to sell this capacity to parties which are exceeding their targets.
- Clean Development Mechanism: This mechanism allows a party with an emission-reduction or -limitation commitment (Annex B party) to implement an emission-reduction project in developing countries. These projects can obtain saleable (under the International Emissions Trading) certified emission reduction (CER) credits, which can be factored in meeting the targets.
- Joint Implementation: This mechanism allows an Annex B party to implement an emission-reduction project to benefit from emission reduction units (ERU), obtained from an emission-reduction or emission-removal project in another Annex B party. [UNFCCC, 2016]

An annual Convention of the Parties (COP) is organized, the United Nations Climate Change Conference (UNCCC), serving as the formal meeting of UNFCCC parties. Since 2005 these meetings have also served as the Conference of the Parties serving as the Meeting of Parties to the Kyoto protocol (CMP). In Paris, France, in 2015, the 21st COP was organized, reaching an agreement between all nations for the first time. The agreement entered into force in 2016, and future COP meetings will also serve as the Meeting of the Parties to the Paris Agreement (CMA). The agreement and commitments are summarized in the following section.

The United Nations Climate Change Conference in Paris (2015)

The 21st COP (COP21) took place in Paris, France in 2015, and entered into force in 2016. The essential points of the agreement that was reached are summarized below,as described in UNFCCC [2016]:

- Keeping the global temperature rise well below $2°C$ above pre-industrial levels, pursuing efforts to keep it below $1.5°C$.
- Reaching global peaking of greenhouse-gas emissions as soon as possible, and subsequentially reaching a balance between anthropogenic emission by sources and removal by sinks by the 2nd half of the 21st century.
- The agreement contains a commitment from the parties to prepare, communicate and maintain Nationally Determined Contributions (NDC) and pursue domestic measures to achieve them.
- Conserve and enhance greenhouse-gas sinks and reservoirs.
- The agreement recognizes the possibility of voluntary cooperation amongst parties to allow for higher ambitions. Such cooperation can involve the international transfer of mitigation outcomes. It outlines mechanisms to contribute to mitigation of greenhouse-gase emissions and support Sustainable Development.
- The agreement aims at enhancing adaptive capacity, strengthening resilience and reducing of vulnerability to climate change, through support and international cooperation.
- An obligation of developed countries to support the efforts of developing countries to build clean climate-resilient futures, is included as well. As is an objective of achieving a balance between adaptation and mitigation.

The latest COP on climate change, COP25 in Madrid, yielded a small commitment from members to increase their targets with regards to climate change.

European targets and policy

The responsibility of the means used to reach the global temperature and global peaking targets lies largely with the parties which have ratified the convention, through their proposed NDC's, and the measures the employ to achieve them. The intended NDC for the European Union (EU) and its member states (including the United Kingdom) was delivered in October 2016 [EU2015.LV, 2015]. It commits to a binding target of a 40% reduction in greenhouse gas emission with respect to the 1990 level by 2030, this includes a renewable energy target of at least 27% [European Council, 2014]. This builds upon the 20% emission reduction

commitment by 2020, and fits within the EU's target to reduce the EU emissions by $80 - 95\%$ by 2050. The green new deal, presented by the European Commission, presents a reduction in the EU's greenhouse gas emission by $50 - 55\%$ (compared to the 1990 level) for 2030 [European Commision, 2019].

Based on the international framework provided by the Paris agreement, the International Energy Agency (IEA) and the International Renewable Energy Agency (IRENA) published a report, commissioned by the German Government, on the essential elements of an energy sector transition. [IEA and IRENA, 2017]

This report estimates the remaining carbon budget for the energy sector at 790 $GtCO_{2,equivalent}$ until 2050, in order to stay below the projected $2°C$ temperature rise in the Paris agreement, with a 66% probability. Current NDC's would emits 1 260 Gt in that same time period. The report is divided into two possible scenarios. One developed by IEA, which is technology neutral, and on by IRENA, putting energy efficiency and renewable energy sources forward.

In the IEA scenario the energy related $CO_{2,equivalent}$ emissions peak should occur before 2020, and fall by more than 70% by 2050, as is shown in Figure 2.2. The share of fossil fuels in primary energy demand should be divided by two between 2014 and 2050. The improvements in energy and material efficiency should allow for the energy intensity of the global economy to decrease by 2.5% each year. In this scenario fossil fuels will remain important, however coal and oil shares in the energy mix will significantly reduce, and natural will mainly play a role in transitioning towards cleaner technologies across several sectors.

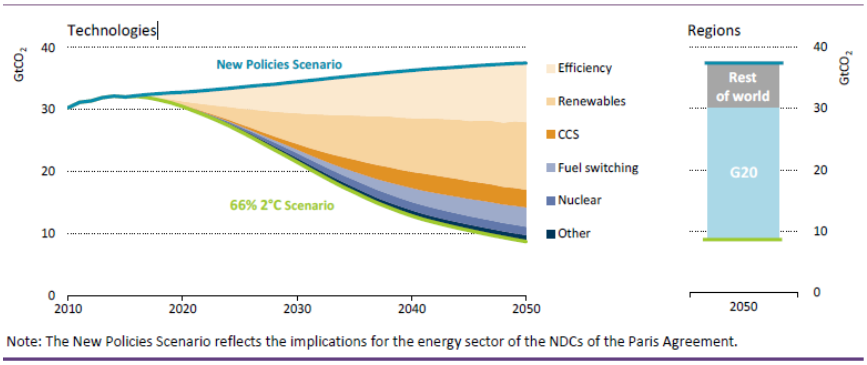


Figure 2.2.: Global emissions abatement by technology and region in the 66% $2°C$ Scenario relative to the New Policies Scenario

In the IRENA scenario 90% of emission reduction needs would be met by energy efficiency and renewable energy sources by 2050, the remaining 10% would be obtained through shifting of the fossil fuels and CCS. The energy intensity improvement must double each year to around 2.5% by 2030, and continue at this level until 2050. Energy demand in 2050 would be at the same level as today, thanks to energy efficiency and intensity improvements, as can be seen in Figure 2.3.

Developing integrated management of water and energy resources to ensure the functioning of the energy system without affecting agriculture and water supply, is one of the key recommendations of the *Water-Energy Nexus in Europe* report from the European Commission [González Hidalgo et al., 2019]. Waste heat recovery, and the optimisation of Wastewater Treatment Plants operation are identified as important technology options.

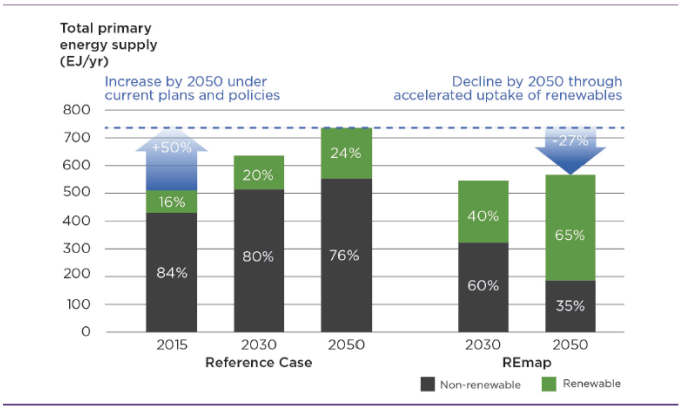


Figure 2.3.: Global total primary energy supply, 2015-2050

In December 2019, the European Commission launched the **European Green Deal**, a roadmap for creating a sustainable economy in the EU. The Green Deal focuses on:

- Boosting the efficient use of resources by moving to a clean, circular economy.
- Restoring biodiversity and cutting pollution.

The main action points are summarized in Figure 2.4 [European Commision, 2019].

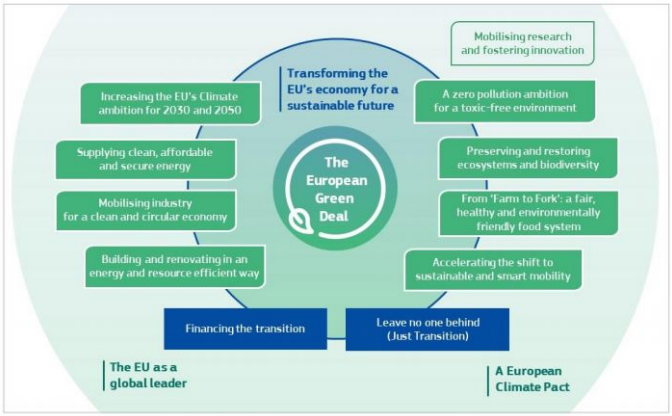


Figure 2.4.: Main action points of the **European Green Deal** [European Commision, 2019].

Energy efficiency and the reduction of the greenhouse-gas intensity of the energy mix is essential in both scenarios. The PhD research presented in this report will discuss a technology and strategy aiming at both improving the energy efficiency of thermal energy in buildings and reducing the greenhouse-gas intensity of thermal energy production. This is done by integrating the water cycle with the thermal energy sector, through heat exchange.

Energy and Climate Policy in Ireland and the United Kingdom

Both the Irish and British energy and climate policy are derived from the EU policies. The national targets to reach Europe's 2030 targets haven't been published yet for Ireland and the United Kingdom. This section focuses on the national targets that have been established for 2020.

Ireland's energy and climate targets for 2020 are summarized in Figure 2.5. The targets are a reduction in energy consumption, through energy efficiency measures of 20% compared to 2005 (a reduction of 31 925 GWh), a renewable energy share of 16% of the total energy mix, and 12% in the heating sector, and a reduction in non-ETS emissions of 20%, compared to the level of 2005.

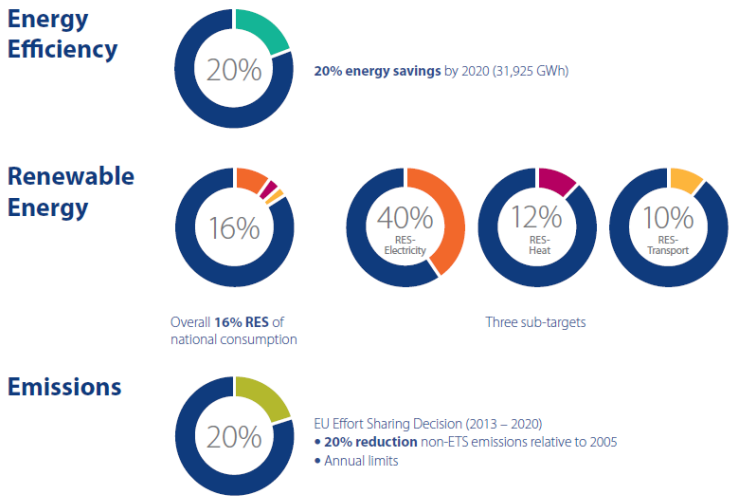


Figure 2.5.: Headlines of Ireland's energy and emission targets [Scheer et al., 2016].

In 2014 Ireland's reduction in energy consumption is 16 000 GWh, and the share of renewable energy in the final energy mix is 8.6% (and 6.6% in the heating mix). At current rates it's expected that the renewable heat targets will not be reached by 2020 [Clancy, 2015], depending on the forecast scenario, the shortage is estimated between 1 and 5%. A shortfall of the targets would force Ireland to purchase renewable energy compliance from EU member states which are exceeding their targets [SEAI, 2017a]. For 2030, no specific Irish targets have been set at the moment, but the former EU target of 40% is currently taken as a starting point [SEAI, 2020], one can expect that, like the european objectives, this number will be revised and increased in the future [European Commision, 2019].

The non-ETS emissions have been reduced from 45 $MtCO_{2,eq}$ in 2005 to 36.3 $MtCO_{2,eq}$ in 2013, the target for 2020 is 30.9 $MtCO_{2,eq}$. Modelling by SEAI shows that, in the absence of additional emissions reduction measures, the annual reduction targets will not be met, resulting of a possible gap of 12 $MtCO_{2,eq}$ by 2020, Brennan and Cagney [2015] expresses the concern that the gap between the Irish situation and the targets put forward by the European council might increase up to 16 $MtCO_{2,eq}$ in case Ireland's national target is set to 40%.

For 2020 **Wales**' targets were set at a reduction of 40% compared to the 1990 levels, and a reduction of at least 3% per year after 2011, compared to the average year in the period $2006 - 2010$. In 2016, Wales achieved a total reduction of carbon emissions of 14%, compared to 1990 [BEIS, 2019]. For 2050, the UK's draft National Energy and Climate Plan (NECP) [BEIS, 2019] states a target of 80% reduction of carbon emissions compared to the 1990 level, along with additional intermediate targets to be set. The Welsh Government has accepted the Committee on Climate Change (CCC) recommendation for a 95% reduction in greenhouse gas emissions [Welsh Government, 2019]. In terms of renewable energy, the UK is aiming for 70% of renewable energy in the mix by 2030, the renewable heat share in 2017 was 7.7%. The UK aims at increasing this number by means of the Renewable Heating Incentive (RHI), planning to incest 4.5 Bn £in the period $2016 - 2021$. Another important axes for renewable heat in the action plan are district heating networks [BEIS, 2019].

2.3. Thermal energy and greenhouse gas intensity of production

One of the targeted energy sectors in the different policies is the thermal energy sector, both residential and industrial.

In 2012, heating and cooling was responsible for 50% (546 *MTOE*) of the final energy consumption in the **EU**. Where renewable energy sources accounted for 18% of the production, and around 75% was produced by fossil fuels, as is summarized in Figure 2.6. [Commision, 2016]

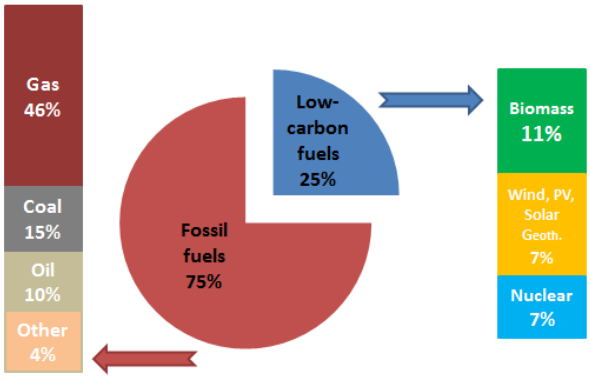


Figure 2.6.: Primary Energy for heating and cooling in the EU in 2012

In **Ireland**, thermal energy was responsible for 32% of total primary energy consumption in 2014, and for 31% of total emissions. In 2014 the share of heat provided by renewables was 6.6%, over 87% was provided by oil, gas and coal, as can be seen in Figure 2.7 [Howley et al., 2015]. In 2018, the heat demand increased by 6.4%, and the share of heat provided by renewables dropped very slightly to 6.5% [SEAI, 2019*c*].

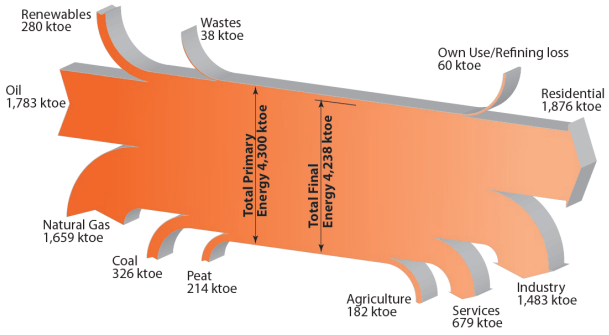


Figure 2.7.: Thermal Energy flows in Ireland in 2014 [Howley et al., 2015]

2.3.1. Renewable heating sources

The International Energy Agency (IEA) states that 'good potential' exists globally for renewable heat, but is largely unexploited. The IEA states that the growth in renewable heat would have to increase 32% between 2014 and 2025, requiring an annual deployment rate of more than twice the current level [IEA, 2017].

In order to reduce the greenhouse gas intensity of the thermal energy mix, a target for heat from renewable heating sources is set in Ireland at 12%, by the year 2020 [Scheer et al., 2016]. The heating technologies considered to be renewable are 'Solar thermal', 'Biomass', 'Biogas', 'Geothermal' and 'Heat pumps'. In addition to this, the EU recognised wastewater as a renewable source of energy, by a directive published in October 2018 [European Parliament; Council of the European Union, 2018]. The current distribution of these renewable heating technologies is shown in Figure 2.8.

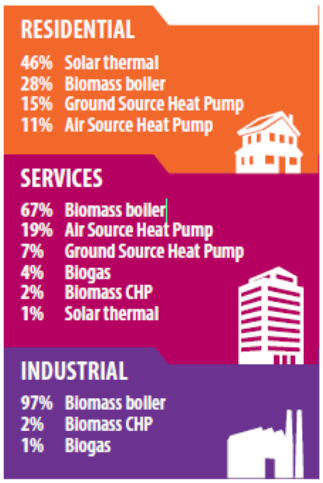


Figure 2.8.: Heat output by renewable heating source in Ireland, in 2015 [SEAI, 2017*a*]

2.3.2. Energy consumption in Buildings

Residential buildings and households are responsible for around 25% of final energy consumption in the EU [Eurostat, 2017]. In Figure 2.9, one can observe that the energy is still largely supplied by fossil fuels, and electricity which still have a significant greenhouse gas intensity.

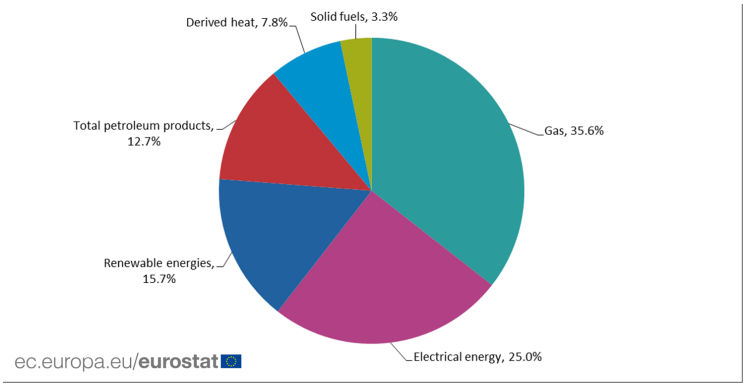


Figure 2.9.: Final energy consumption of households by energy products in the EU in 2015 [Eurostat, 2017]

Heating of space and water accounts for 78.6% of household energy consumption [Eurostat, 2017]. This results in a residential share in greenhouse gas emissions of around 10% [Commision, 2016]. With improved insulation and air tightness the heat losses in buildings have decreased over the years, passive houses reaching a space heating demand of less than 15 $kWh/(m^2\ yr)$ [Barbier, 2015]. However domestic hot water demand does not follow this trend, and remains around 50 $kWh/(m^2\ yr)$ [Meggers and Leibundgut, 2011]

In terms of heat demand this translates in a share of 45% for the domestic sector, and 17% for services, as shown in Figure 2.10.

The heat sector has seen much less activity to support renewable energy when compared to transport and electricity sectors, this is due to the fragmented nature of the heating market, difficulties related to retrofitting these technologies in buildings, the complexities of biomass fuel supply, and administrative challenges of implementing policy support [Clancy, 2015].

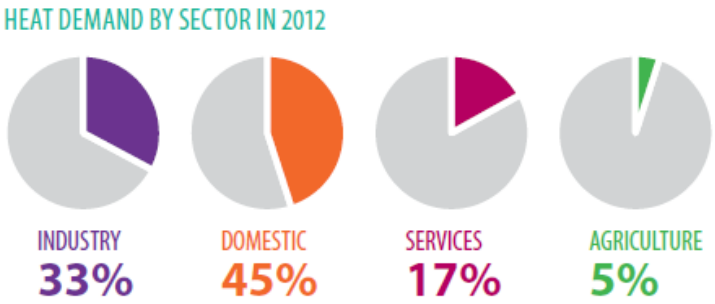


Figure 2.10.: Heat demand by sector in the Ireland in 2012 [SEAI, 2017*a*]

In addition the large share of heat consumed in the residential sector results in a large number of relatively small consumers, compared to industrial players. For these small consumers the importance of fuel cost (usually advantageous for renewable heating sources), compared to the capital investment (usually advantageous for traditional sources), is small, reducing the competitiveness of renewable heating sources. Furthermore, tenants and landlords might have divergent motivations, where the landlord, typically the decision maker, is more concerned with capital investment costs [Clancy, 2015].

Improving the energy efficiency of buildings, designing buildings in line with the circular economy, and improving the energy performance of buildings are some of the main pillars of the building and renovating section of the European Green Deal, as presented by the European Commission [European Commision, 2019]. Boosting energy efficiency, and interconnecting energy systems are important pillars in the clean energy section of this report.

2.3.3. Energy loss through drain water in buildings

In Schmid [2008] the evolution of thermal energy consumption in buildings is described, showing that efforts to reduce this thermal energy consumption, and thus increase the energy efficiency, have been going on since the 1980's, resulting in a reduction of consumption by $10 - 30\%$. However, still a large part of the thermal energy (around 15%) is lost through the drain and sewer system (up to 30% in low-energy buildings). In modern times, the heat lost through the drain represents the largest source of heat loss in buildings. In a modern house the heat losses through wastewater imply a CO_2 emission of over 450 kg per year, as stated in van der Hoek [2011]. Furthermore, a comfort temperature of the room of $20°C$ is not very high, and when classical radiator systems are used, a large amount of energy is needed to generate high-temperature water for heating. The temperature drop of this water is low, and water with a high energetic and exergetic value is simply flushed out of the building [Meggers and Leibundgut, 2011; Meggers, 2008].

In Figure 2.11, the exergy embedded in wastewater is depicted. The exergy is a measure of energy, including the quality of the available energy (hence embedded heat at higher temperature will have a higher exergetic value). The Figure also shows that with improved water efficiency the exergetic value will increase, as most water efficiency measures relate to cold water consumption [Meggers and Leibundgut, 2011].

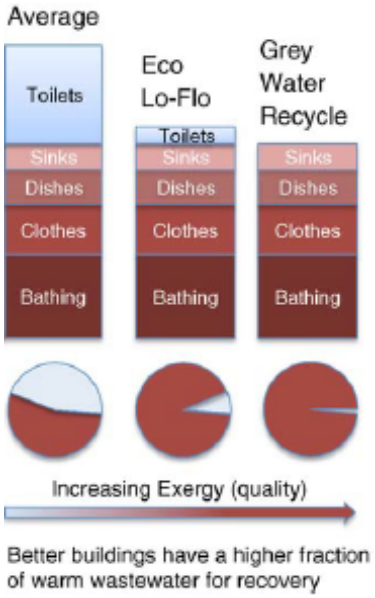


Figure 2.11.: Exergy embedded in wastewater [Meggers and Leibundgut, 2011].

2.3.4. District heating networks

In addition to the increasing population, a shift in the spatial distribution of the population is occurring [Erker et al., 2019], The United Nations predict that 68% of the population will live in cities by 2050 [United Nations, 2018]. With this shift in population distribution comes also a related shift in the spatial distribution of thermal energy demand. More densely populated areas results in an increased amount of regions where heat demand density could be sufficient to justify district heating networks [Gartland and Bruton, 2016].

District heating networks deliver heat to buildings in the form of hot water, through a network of insulated pipes. The difference with the current system of gas networks that the thermal energy (heat) is delivered to the buildings, rather than the fuel (gas). Every building would require a heat exchanger to withdraw heat from the network, rather than an individual burner or boiler, with the heat being delivered for both space heating and domestic hot water [Gartland and Bruton, 2016]. In the European Union, around 13% of heat is delivered through district heating (8% worldwide) [Erker et al., 2019].

Over the years, as the efficiency and insulation of district heating systems improved, the required temperature decreased, as can be seen in Figure 2.12 [Thorsen et al., 2018]. Another evolution in time was the evolution from a single, centralised plant delivering the heat for the network, to networks distributing heat from a multitude of different sources, including from by-products of human activities, such as waste heat from electricity production and large industries, but also biogas from wastewater treatment, etc. [Gartland and Bruton, 2016] District heating networks are identified as key players in the road towards energy systems with a large share of renewable energy. Both for the support of renewable energy sources, like geothermal, biomass, biogas, waste heat, etc. [Lund et al., 2017b], [Di Lucia and Ericsson, 2014], and for its energy storage capacity, through thermal storage [Romanchenko et al., 2018]

The importance of interconnecting different energy systems was also recognised in the European Green Deal, as presented by the European Commision [2019]. Heat pumps are one way of interconnecting the heating energy system and the electric grid, providing the heat for this heat pump by heat recovered from wastewater improves the efficiency (Coefficient of performance, see Chapter 3), and includes an interconnection with the wastewater system.

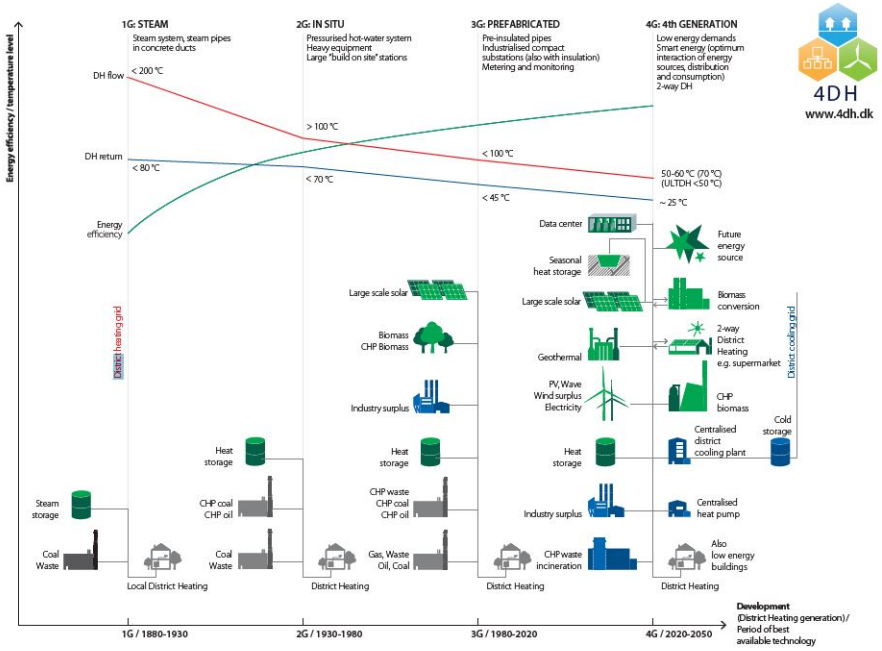


Figure 2.12.: Progression of District Heating: 1st to 4th generation [Thorsen et al., 2018].

2.4. Water cycle efficiency

The water cycle contains multiple points of energy consumption, summarized in Figure 2.13. Energy is consumed in all stages of the cycle, being the raw water treatment, the water use and the wastewater treatment. The energy costs of water utilities represents 5 to 30% of their operating costs [Chae and Kang, 2013]. In California 5% of the total electricity consumption is used for water supply, the bulk of which is used for transportation. Additionally 14% of California's electricity consumption is used for water heating [Elías-Maxil et al., 2014]. However the water cycle provides multiple opportunities to recover energy as well, being it using small scale hydro-power, thermal-, or chemical energy recovery. The following papers describe efforts to use these energy recovery opportunities, to offset the energy consumption in the water cycle, in other words to make the water cycle carbon and/or energy neutral.

The environmental impact of the *Waternet* network, the manager of the entire water network of Amsterdam, the Netherlands, is estimated at 53 000 $t\ CO_{2,eq}/yr$ in van der Hoek [2011]. Their ambition is to operate in a climate neutral way by 2020, and in order to achieve this objective, energy recovery from wastewater is considered. The authors suggest both chemical recovery, by using the anaerobic sludge digestion and anaerobic treatment to extract bio-gas to be used in combined heat and power plants, or to be upgraded to greengas, and thermal energy recovery, via heat exchangers and heat pumps. It is estimated that 54% of drinking water is heated and leaves the house at an average temperature of $27°C$, resulting in a waste of energy equivalent to the yearly emission of around 450 $kg\ CO_{2,eq}/(house\ yr)$. van der Hoek [2011] proposes to recover energy at a housing estate level with a heat exchanger in the sewer. The potential emission savings using both techniques are estimated at 148 000 $t\ CO_{2,eq}/yr$, thus far exceeding the required savings, however the challenge consists of choosing robust combinations of energy provision methods, in order to meet energy demand at all times.

The idea of wastewater as an energy carrier is further developed in Frijns et al. [2013]. They estimate the actual maximal yearly energy recovery potential from wastewater in the Netherlands at 12.67 TWh, of which 70% is thermal energy recovery. Recovering 25% would represent the total energy consumption of the water industry sector in the Netherlands.

In Elías-Maxil et al. [2014], the water cycle, and its energy consumption is described as in Figure 2.13. The authors report that the balance shows that 80% of the primary energy demand is consumed during water heating. The authors propose the prevention of energy use, the use of renewable energy sources, and efficient use of fossil fuels as ways to reduce the environmental impact of the water cycle. The paper presents the possibility of direct heat recovery (see Section 3.2) at the place of consumption, and indirect heat recovery (see Section 3.2) in the sewage network. It claims that, due to heat loss to the environment, the wastewater will reach soil temperature after 10 km of transport in the main sewer. Recovering heat will decrease the wastewater temperature, and thus bacterial activity during the nitrification process [Wanner et al., 2005]. The proposed solution for this issue is to adjust the hydraulic retention time.

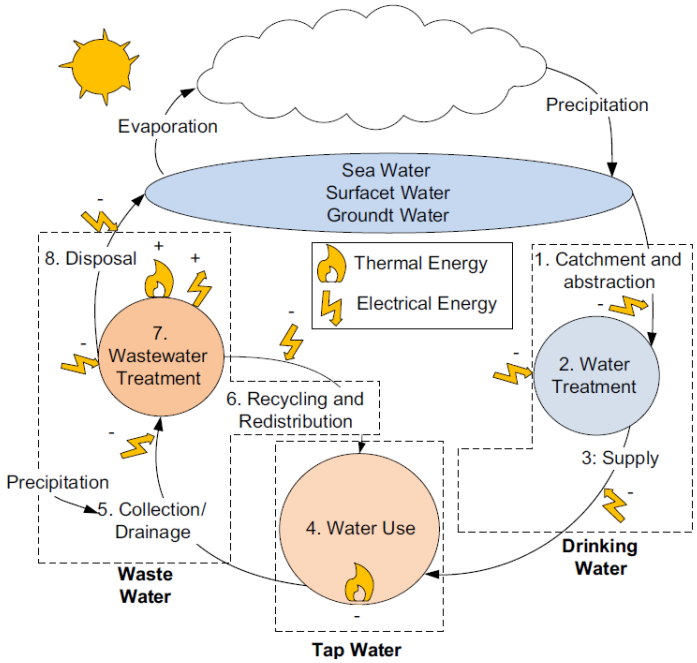


Figure 2.13.: Energy involved in different stages of the Urban Water Cycle [Elías-Maxil et al., 2014]

In order to predict the temperature decrease of wastewater in sewer systems, in case of heat recovery, Dürrenmatt and Wanner [2014] presents a mathematical model. The authors claim that it's required in the planning process, because in the County of Zurich, Switzerland, regulation states that the temperature of the wastewater must remain above $10°C$. The example shown for Rümlang, Switzerland shows a temperature decrease of no more than $1°C$, over a length of 1845 m with incoming water temperature and flow at $12°C$ and 0.03 m^3/s, respectively.

On a smaller scale, Chae and Kang [2013] investigates steps towards energy independance of a municipal wastewater treatment plant using renewable resources. The authors propose 100 kWp of Photovoltaics, 10 kW of small hydropower and an effluent heat recovery system with 25 heat pumps. It is estimated that a 6.5% self-sufficiency is achievable.

Mo and Zhang [2013] state three different ways of energy recovery in wastewater treatment plants: water reuse, nutrient recycling and energy generation. The energy generation contains the incineration of biogas and biosoolids, on site wind and solar installations, effluent hydropower, bioelectrochimical systems and thermal energy recovery. The major challenges for these technologies are the large capital cost, and the specific requirement regarding climate conditions and locations. The authors state that, although different studies have been performed on economic parameters, there is a lack of studies investigating the environmental perspective. Examples of self-sufficient wastewater treatment plants are given in Gu et al. [2017], they contain plants in Tampa, Florida and Oakland, California, both in the USA. The considered possibilities for energy recovery are biogas, hydroelectric generators in case a natural elevation difference occurs, photovoltaic panels and thermal energy recovery. The paper states that the recoverable heat exceeds the heat consumption of the wastewater treatment plants, and could be used as a heating source for district heating, or other consumers.

2.4.1. Drain and Waste Water

Residential buildings and households are responsible for around 25% of final energy consumption in the EU [Eurostat, 2017]. Over the years efforts have been made to reduce the energy consumption in buildings (between 10 and 30% since the 1980' s) through improved insulation of the building envelope, amongst others. However a large quantity of energy ($15 - 30\%$) leaves the building through the drain as hot waste water, making this the largest source of energy loss in modern buildings [Schmid, 2008]. Furthermore, domestic hot water represents $17 - 50\%$ of the total thermal energy consumption in buildings [Meggers and Leibundgut, 2011].

2.4.2. Drain and waste water collection and treatment

Wastewater treatment can be defined as a combination of unit processes, designed to reduce contaminant levels in the water to acceptable levels. Generally, it consists of five stages, preliminary, primary, secondary, tertiary and sludge treatment. [Templeton and Butler, 2011]

Preliminary treatment

In the preliminary treatment, large and heavy debris is removed from the water, to avoid this debris from interfering with the procedures in the wastewater treatment system. This is mainly done by screening and grit removal steps. Screening generally remove large floating debris. Grit includes heavy inorganic particles such as sand, gravel and other heavy particulate matter. Grit removal is generally performed by the grit chambers, where flow velocity of the water is reduced, and the grid settles at the bottom of this chamber.

Primary treatment

Primary treatment consist of removing suspended organic and inorganic particles. The wastewater is passed through sedimentation tanks such that fine solids settle out of suspension by gravity, forming sludge at the base of the tank (primary sludge). The removal of suspended solids is performed by simultaneous physical processes, flocculation, adsorption and sedimentation.

Primary sedimentation clarifies the (sewage) wastewater by flotation and settlement. Suspended matter, which is less dense than water, such as fat, oil and grease (FOG), floats on the surface as scum, and can be skimmed of using skimmer blades. [Gray, 2017] At lower temperatures, this process is accelerated, which can be an added benefit of drain water heat recovery.

Secondary treatment

During the secondary treatment phase, a biological conversion of dissolved organics to bio-mass occurs. This biomass is then removed through sedimentation. Alternatively, chemical treatment using coagulants can be used, but this option requires continuous chemical addition and has the problem of disposing of chemical sludge, which can make this option unattractive. Although secondary treatment is mainly an aerobic process, anaerobic and anoxic reactors are also used [Gray, 2017].

The micro organisms break down the organic matter by two different processes:

- Biological oxidation: This results in the formation of mineralized products which remains in solution and are discharged with the effluent.
- Biosynthesis: converts the dissolved organics to bio-mass, which are them removed by settlement.

One of these biological treatment processes is nitrification where the bacterial activity, and thus the nitrification rate, is temperature dependant. Recovering heat, and effectively reducing the temperature of the wastewater would decrease the nitrification rate, and thus has an impact on the treatment process [Wanner et al., 2005].

Tertiary treatment

In the tertiary treatment phase suspended solids and nutrients are removed further, and disinfectation is performed before the water is discharged into a natural water stream. This treatment is only performed in case the effluent exceeds the required legal limits. Main tertiary treatment methods include:

- Prolonged settlement (eg. in Lagoons).
- Irrigation into grasslands or percolation areas.
- Straining through a fine mesh.
- Filtration.

Disinfectation is used where patogens form a problem [Gray, 2017].

Sludge treatment

Throughout the process, mainly in the primary and secondary stages sludge is accumulated and collected, the physical, chemical and biological treatment of this sludge is the fifth phase of the wastewater treatment process. When sludge is collected, the water content of sludge generally exceeds 90% and the sludge acts as a liquid, therefore the water content of sludge needs to be reduced, thus reducing the volume, before disposing of it. Generally, sludge is first thickened, before it is dewatered, and then ultimately disposed of. Before dewatering, sludge is often stabilized by anaerobic digestion, which also permits the conversion of some of the organic content to bio-gas (methane). Methane being a greenhouse gas with a global warming potential $28 - 36$ times the one of CO_2, utilizing this biogas not only has energetic, but also environmental benefits.

Ultimately, the sludge disposal is performed through land spreading, landfill, sea disposal or incineration [Gray, 2017].

Centralized wastewater treatment

In centralized wastewater treatment systems, wastewater is collected through a sewer system, and the transported to the wastewater treatment plant, where it is treated. Two basic types of wastewater collection system exist:

- **Combined system:** In a combined system the wastewater and storm (rain) water is collected through a same piping network. This is thus characterized by an increased flow, but generally lower temperatures [Spriet and Hendrick, 2017].
- **Separate system:** In a separate system waste- and rainwater are separated.

The selection of the unit processes, required to achieve the different treatment stages mentioned above, depends on the nature of the wastewater, the discharge requirements, environmental impact, land availability, the projected operation time and the cost. [Gray, 2017] Based on the selected unit processes, rough calculations can be made to estimate the size of the components.

An important factor for selecting the location of the plant is proximity to receiving water bodies, and possibilities for expansion. This results in the fact that wastewater treatment plants are often located outside of urban areas, and thus at a relative distance from heat consumers. Other factors considered for selecting the plant's location are the potential for flooding, foundation stability, groundwater intrusion,... [Davis, 2011]

Domestic on-site wastewater treatment

Another possibility for the treatment of wastewater, especially for buildings which are not connected to the sewer system, but also in cases where water is intended for reuse, eg. for irrigation, is the use of an on-site treatment system, such as septic tanks, rotating biological contactors (RBC), cesspools, constructed wetlands or small wastewater treatment systems. In conventional on-site wastewater treatment systems, most of the treatment takes place in the soil [Gray, 2017; Jantrania and Gross, 2006].

There are two broad categories of on-site wastewater treatment systems [Amador and Loomis, 2019]:

- **Conventional systems:** Conventional systems generally consist of a septic tank, followed by a distribution box, connected to a soil treatment area. The sewage to be treated is collected in the septic tank, where wastewater is clarified as solids and particles, settling to the bottom, forming a sludge layer, or floating as a scum layer (primary treatment, see above). The clarified effluent is then dispersed through the soil treatment area, where the soil provides additional treatment. Generally, the sludge is collected and treated in specialized facilities.
- **Advanced systems:** Advance systems ad secondary treatment to remove specific contaminants, before discharging to the soil treatment area.

Industrial on-site wastewater treatment

Industrial facilities can have a wide range of treatment systems on their sites, ranging from small scales systems, similar to the domestic ones, up to systems equivalent or larger than municipal wastewater treatment plants. The design of these plants is dependant on the size of the industrial facility, their activities, and the related pollutants in the wastewater. In Ireland, wastewater treatment plants larger than 40 persons equivalent (PE) have to apply for a wastewater discharge authorisation, submit an annual environmental report, and be open to inspection by the Environmental Protection Agency (EPA) [Environmental Protection Agency, 2018].

3. Drain and Waste Water Heat Recovery

3.1. Resource Assesment

3.1.1. Temperature of drain and waste water

Waste water availability is closely linked to human activity, both domestic and non-domestic, it is thus available close to the consumer, and can be collected and treated in two different ways, either locally, via individual collection and treatment systems, or through the municipal sewer system.

It's expected that the waste water temperatures in the former are higher than those in the latter, as the waste water will have travelled a shorter distance from it's heat source (the application), however few temperature measurements are available in literature. The waste and drain water temperatures of different applications is described in [McNabola and Shields, 2013; Cunniffe and McNabola, 2014], and summarized in Table 3.1, however they're measured directly at application level, and not at the outlet of the building. This results in lower flow and thus less embedded energy. The embedded energy is estimated, for reference based on a lower temperature of $10°C$, the flow rates and durations as mentioned by Cunniffe and McNabola [2014].

Appliance	Temperature	Flow	Embedded energy
Washing machine	$35 - 40°C$	$42\ l$	$1.22 - 1.46\ kWh$
Bathing water	$20 - 38°C$	$80\ l$	$0.93 - 2.60\ kWh$
Shower water	$30 - 38°C$	$60\ l$	$1.39 - 1.95\ kWh$
Sink	$20 - 40°C$	$15\ l$	$0.17 - 0.52\ kWh$
Dishwasher	$20 - 35°C$	$12\ l$	$0.14 - 0.35\ kWh$
Toilet	$10 - 16°C$	$6\ l$	$0 - 0.04\ kWh$

Table 3.1.: Waste water temperature of different domestic appliances [Cunniffe and McNabola, 2014].

Multiple studies have been performed measuring sewage water temperature in cities, the observed temperatures are summarized in Table 3.2. In Beijing, the temperature in winter is about $20°C$ higher than the average outdoor circumstances [Xiao-Yan and Hai-Tao, 2005], which suggests that heat extraction from waste water could be more effective than from outside air, as confirmed in Spriet and Hendrick [2017].

Bejing, China	$13.5 - 25°C$	[Xiao-Yan and Hai-Tao, 2005]
Bologna, Italy	$10 - 22°C$	[Cipolla and Maglionico, 2013]
Sala, Sweden	$8 - 16°C$	[Lindstrom, 1985]
Zurich, Switzerland	$10 - 22°C$	[Schmid, 2008]
Brussels, Belgium	$8 - 16°C$	[Spriet and Hendrick, 2017]

Table 3.2.: Sewage water temperature variation in different cities

3.1.2. Resource recovery from wastewater

Chemical energy, generally under the form of biogas (largely methane), has traditionally been perceived as the dominant form of renewable energy, recoverable from wastewater. This is described in this section. However, Hao et al. [2019] demonstrated that the potential for thermal energy (90% recovery from wastewater) is much higher than for chemical energy (10% recovery from the Chemical Oxygen Demand, COD). The

carrier of chemical energy (COD) has a high exergy value which should, from a sustainability point of view, be utilized to the greatest extent possible. Thermal energy could be utilized for district heating/cooling, agricultural greenhouses, and even for drying dewatered sludge. In this way, thermal energy can indirectly offset the energy demand for wastewater treatment. The limitations in utilizing thermal energy are not generally based on technical difficulties; in fact, they can be mainly attributed to supply distances and governmental policies. It would, therefore, be greatly beneficial if municipal authorities work together to jointly plan utilization of this thermal energy. Hao et al. [2019] also indicates that the chemical energy content of wastewater amounts to about 1.54 kWh/m^3, whereas thermal energy was estimated at about 4.64 kWh/m^3m or threefold of the chemical energy, as shown in Figure 3.1.

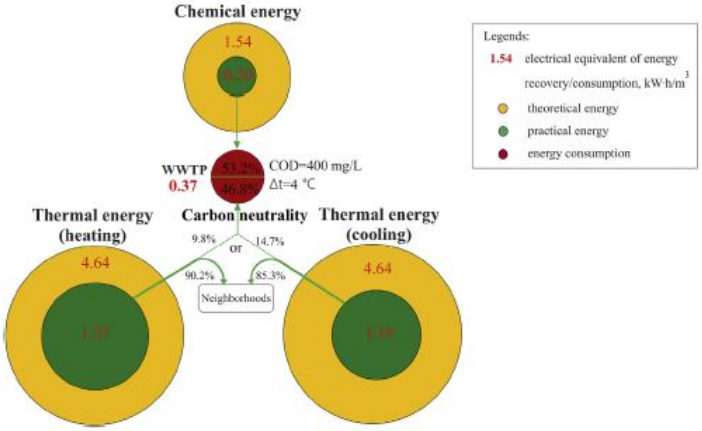


Figure 3.1.: Energy balance towards the carbon-neutral operation of the evaluated WWTP.[Hao et al., 2019]

Strategies to recover resources from the wastewater of the city of Amsterdam are described in van der Hoek et al. [2016]. The authors identify the lack of a planning and design methodology to identify and deploy the most sustainable solutions in a given context as the main bottleneck, rather than the availability of technology. A development process of dynamic adaptive policy pathways was used to determine alternative strategies regarding resource recovery from Amsterdam's wastewater cycle. In the first phase a material flow analysis was made for the wastewater cycle and analyzed for water, organic matter and phosphorus. In the second phase, measures were identified and characterized. For the Amsterdam case recovered products concerned alginic acid, bioplastic, cellulose, phosphorus and biogas. In the third phase the measures were combined into strategies, which are combinations of measures that focus on a specific goal of resource recovery. This resulted in four strategies: a strategy focusing on production of alginic acid, a strategy focusing on production of bioplastics, a strategy focusing on recovery of cellulose, and a strategy focusing on recovery of phosphorus.

The potential for chemical energy recovery at anaerobic digestion in the United States of America was estimated by Stillwell et al. [2010] at 628 to 4 940 *million kWh* annually in the United States. In Texas, anaerobic digestion could save 40.2 to 460 *million kWh* annually and biosolids incineration could save 51.9 to 1 030 *million kWh* annually.

Fox et al. [2019] investigated the hydrothermal conversion of underutilized waste streams for biomass feedstock. This work blended municipal sewage sludge solids, poultry dissolved air flotation solids, and used cooking oil to form a waste slurry that was thermally converted to renewable fuel products. Prior to processing, the blended waste slurry contained 8 490 kJ/kg. Following processing, the recovered gas products contained 38 747 kJ/kg and 42% methane. The recovered renewable oil contained 40 468 kJ/kg. These streams were determined to be marketable products, (partially) replacing crop-based bio-fuels.

In Fernández-Arévalo et al. [2017], a simulation model of a wastewater treatment facility, with integrated resource recovery facilities was described, and compared to a conventional plant, and an upgraded/retro-fitted plant. In the conventional plant, the COD used to produce biogas was around 29%, in the upgraded plant it was around 36%, and 34% in the plant with integrated resource recovery facilities. With regard to the self-sufficiency of plants, achieving self-sufficiency was deemed impossible in the conventional plant, in

the upgraded plant it was dependant on the influent Carbon/Nitrogen ratio, and in the plant with integrated resource recovery facilities, self-sufficiency was deemed feasible for almost all influents, especially at high COD concentrations.

Kretschmer et al. [2018] showed the different possibilities to utilize wastewater as a resource (see Figure 3.2), and highlighted the importance of social aspects in the development of such projects. To support a broader awareness and acceptance of energy from wastewater, the authors proposed targeted participation of stakeholders from different professional fields as a crucial point. Involvement in the planning process facilitates knowledge-building and increase of awareness which, in turn, can be considered key aspects for a better recognition of energetic use of wastewater as an option for local energy supply beyond the premises of the wastewater infrastructure. Finally, participation fosters the building of ownership leading to solutions of broadest support.

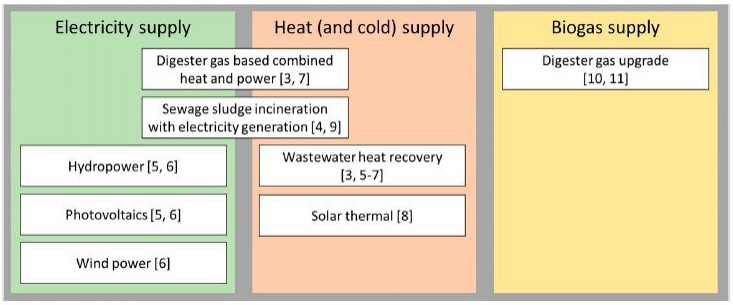


Figure 3.2.: Wastewater-based supply of electricity, thermal energy, and biogas.([Kretschmer et al., 2018])

3.2. Technology

3.2.1. Heat Recovery Systems

Two different heat recovery techniques from drain and waste water can be distinguished. At high source (waste or drain water) temperatures, the heat can be recovered directly, through a heat exchanger. At lower source temperatures the heat is recovered indirectly, using a heat pump. A combination of both systems can also be feasible, this will further be denominated as hybrid heat recovery. The different heat recovery techniques are summarized in Figures 3.3, 3.4 and 3.5.

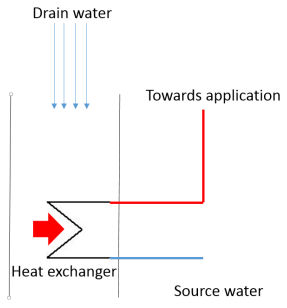


Figure 3.3.: Direct Heat Recovery

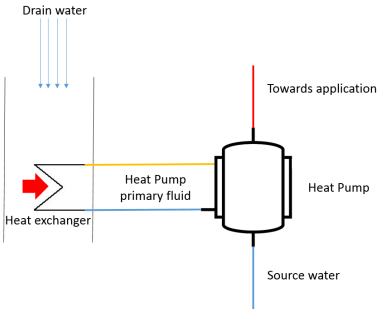


Figure 3.4.: Indirect Heat Recovery

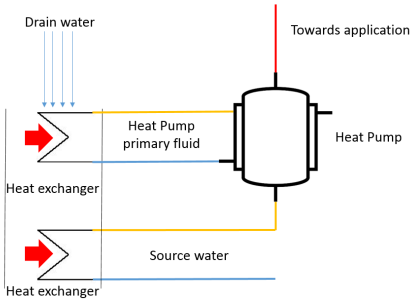


Figure 3.5.: Hybrid Heat Recovery

Direct heat recovery

Direct heat recovery can be employed when the drain or waste water's temperature is higher than the temperature required for the application. In this case the heat can be recovered from the waste water

through a heat exchanger, in a natural manner. The exchanged heat is given by Equation 3.1. Where WW stands for the waste water and FW stands for feed water. In this equation, $\dot{m}$ is the mass flow rate, C_p is the specific heat capacity, and T is temperature.

$$\dot{Q}_{HE} \;=\; \left\{\; \dot{m}\; Cp\; (T_{in} - T_{out}) \;\right\}_{WW} \;=\; \left\{\; \dot{m}\; Cp\; (T_{out} - T_{in}) \;\right\}_{FW} \tag{3.1}$$

A heat exchanger is used in order to facilitate the heat exchange between both fluids, without mixing. The operation of heat exchangers is described in Section 3.2.2 .

Indirect heat recovery

When the temperature of the waste water is lower than the required operation temperature of the application's working fluid, direct heat recovery is insufficient to reach the application temperature. In this case one can employ an indirect heat recovery method, using an intermediary heat carrier. This intermediary heat carrier, or working fluid of the heat pump, can be a brine, or glycolated water for *brine-to-water heat pumps*, or water for *water-to-water heat pumps*. The advantage of using a brine is the lower crystallization point, depending on the application a type of heat pump can be selected.

The heat is transferred to the primary fluid using a heat exchanger, in the same way as described above, the difference is that the temperature is still too low to employ in the application. The primary fluid will then serve as the low-temperature heat source in a heat pump cycle, as described in Figure 3.9. The oepration of heat pumps is described in Section 3.2.2.

3.2.2. Components of the system

Heat Exchanger

Heat exchangers are devices that facilitate the transfer of heat between two fluids, while avoiding mixing between those two fluids. Even though the heat exchange is done through two physical phenomenons, *conduction* and *convection*, a heat exchanger is characterised by a single *heat transfer coefficient, U*, as can be seen in Equation 3.2.

This Equation represents the *logarithmic mean temperature difference method*, where F is a correction factor, depending on the type of heat exchanger, A_s the heat exchange surface and ΔT_{LMTD} the logarithmic mean temperature difference [Cengel Yunus, 2006]. Because the temperature difference between both fluids varies along the heat exchanger, the logarithmic mean temperature difference is used.

$$\dot{Q}_{HE} \;=\; F\; U\; A_s\; \Delta T_{LMTD} \tag{3.2}$$

Another possibility to analyse the operation and performance of the heat exchanger is the *effectiveness - NTU method*, where NTU stands for Number of Transfer Units. This method is useful when the type and size of the heat exchanger are fixed, and the mass flow rates and the inlet temperatures are known. The method is based on a dimensionless parameter, the *heat transfer effectiveness* ϵ (see Equation 3.3). Where $\dot{Q}$ is the actual heat transfer, and $\dot{Q}_{max}$ the maximal heat transfer. [Cengel Yunus, 2006]

$$\epsilon \;=\; \frac{\dot{Q}}{\dot{Q}_{max}} \tag{3.3}$$

The actual heat transfer rate is given in Equation 3.4. Where $\dot{m}$ is the mass flow rate, C_p is the specific heat capacity, and T is temperature.

$$\dot{Q} \;=\; [\dot{m}\; C_p\; (T_{out} - T_{in})]_{cold} \;=\; [\dot{m}\; C_p\; (T_{in} - T_{out})]_{hot} \tag{3.4}$$

The maximal heat transfer ($\dot{Q}_{max}$) can be found through Equation 3.5.

$$\dot{Q}_{max} \;=\; [\dot{m}\; C_p]_{min}\; (T_{hot} - T_{cold})_{in} \tag{3.5}$$

Heat exchangers can broadly be categorised in four main types:

- Double-pipe parallel flow
- Double-pipe counter flow
- Shell-and-tube
- Plate and frame

The difference between both double pipe heat exchangers is the relative flow direction between both fluids, as shown in Figure 3.6. The advantages of double piped systems are their simplicity and flexibility. They are generally found in space heating, refrigeration, air conditioning, power plants, chemical plants, and sewage treatment.



Figure 3.6.: Double pipe heat exchangers.[Cengel Yunus, 2006]

Shell-and-tube heat exchangers contain a large number of pipes packed in a shell with parallel axes. Heat transfer occurs between the fluid in the pipes, and another fluid outside the pipes through the shell. Baffles can be placed to enhance heat transfer. Different configurations are shown in Figure 3.7. These heat exchanger are generally less compatible with waste and sewage water, because they are prone to fouling. They are often used for the removal of process heat, turbine and compressor cooling, etc. Generally shell and tube heat exchanger have an increase area for convective heat transfer, improving the effectiveness of the heat exchanger.

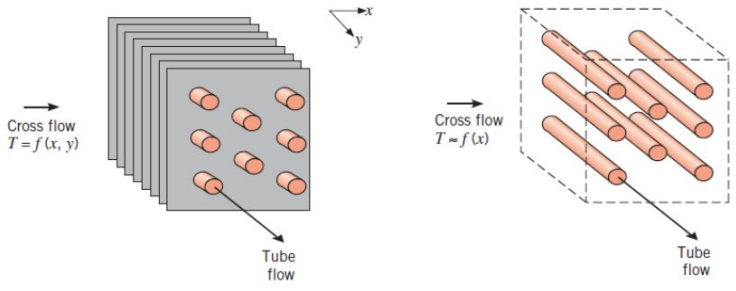


Figure 3.7.: Different configuration of shell-and-tube heat exchangers.[Cengel Yunus, 2006]

A plate and frame heat exchanger consists of a series of flat flow passages, the hot and cold fluids flow in alternating passages. Such that each cold stream is surrounded by two hot streams, and vice-versa. A schematic is shown in Figure 3.8. [Cengel Yunus, 2006]

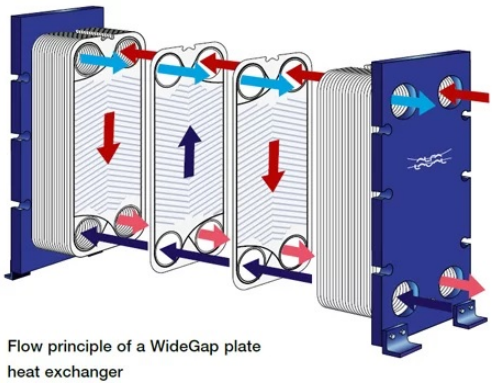


Figure 3.8.: Schematic of a plate and frame heat exchanger.([Alfa Lavel, 2020])

Heat Pump

In a heat pump system, energy is moved from a low-temperature source, to a higher temperature sink. [McQuiston et al., 2005]

The heat is transferred from the primary fluid to the heat pump's refrigerant, in vapour state, which is in turn, compressed, and yields it's heat to the application in the condensor, the refrigerant, in a liquid state. It is then expanded through a valve and the cycle is completed [Yunus and Boles, 2007].

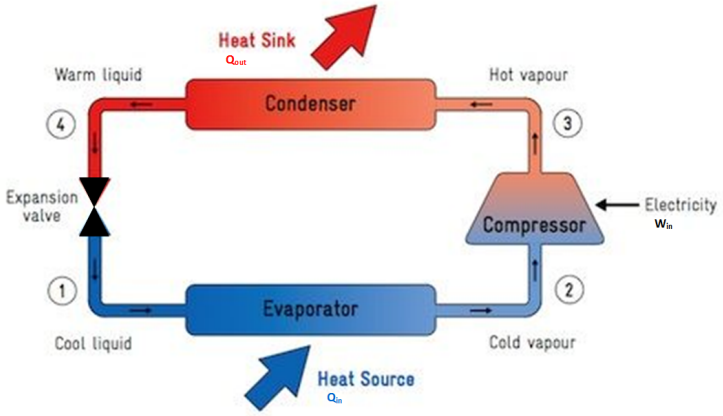


Figure 3.9.: Summary schematic of a heat pump (Adapted from [Alter, 2010])

A heat pump is used to transfer heat from a lower temperature environment, to an application at a higher temperature. This is not the natural, reversible sense in which heat is transferred, and the addition of work, through the operation of a compressors, is required to make this cycle operational. In Figure 3.9 one can observe that the principle of energy conservation (the 1st law of thermodynamics), states that $W_{in} = Q_{out} - Q_{in}$.

The efficiency of a heat pump is expressed using the **Coefficient of Performance (COP)**, as described in Equation 3.6. In order to represent the performance over a certain period of time, in different operating conditions the **Seasonal COP (SCOP)** is often used, averaging the COP over a longer period of time. [Yunus and Boles, 2007]

$$COP = \frac{Desired\ output}{Required\ input} = \frac{Q_{out}}{W_{in}} \tag{3.6}$$

Heat pump types are generally categorised by their source and sink, common examples are [McQuiston et al., 2005]:

- Air-to-Air heat pumps
- Air-to-water heat pumps
- Water-to-Air heat pumps
- Water-to-Water heat pumps
- Brine-to-water heat pumps

The water and brine source heat pumps are the types generally applicable in drain and wastewater heat recovery. Water source heat pumps are used with clean effluent. Brine source heat pumps are used when the heat is recovered from untreated wastewater. An intermediary heat carrier is then used to transfer the heat from the wastewater to the heat pump, ensuring separation between the heating system and the wastewater system. An example of this can be found in Spriet and Hendrick [2017], and is shown in Figure 3.42.

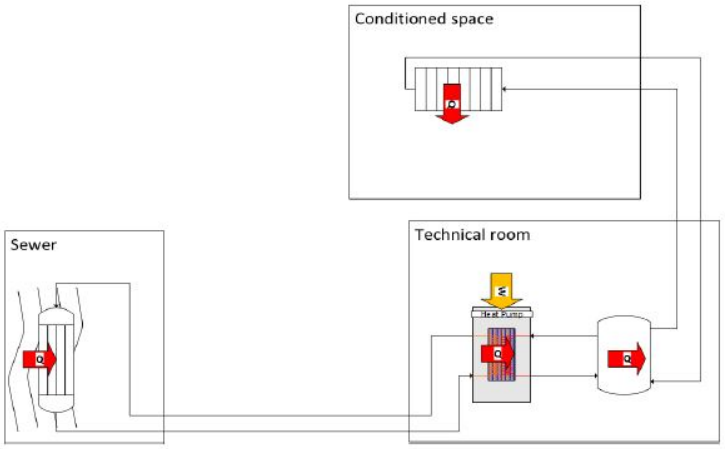


Figure 3.10.: General scheme of a heat recovery system from the sewer system. [Spriet and Hendrick, 2017]

3.3. Matching heat recovery with consumption profile

3.3.1. Temporal analysis

Wallin and Claesson [2014] investigates how the intermittent behaviour of drain water, and the sizing of the system, influence the performance of an in-line heat exchanger with heat pump. The study is based on the measured consumption profile of a multi-family building, containing 110 apartments, in Sweden. The authors claim that a large portion of the available heat is recoverable, if the system has been sized to match the drain profile, both sizing of the heat pump and the hot water storage tank are important in this regard. The authors state that more knowledge on log term fouling effects, and drain water flow characteristics and profiles is required.

The temporal variations of available heat in a sewer system over a day, was described in Spriet and Hendrick [2017]. The authors recorded the variation in wastewater temperature and flow for an installation installed in the sewer in Brussels, Belgium. This showed temperature peaks in the morning (around 9 AM) and evening (around 8 PM), these peaks also introduced peaks in the available heat (Figure 3.11). However, these variations were not correlated with the consumption pattern.

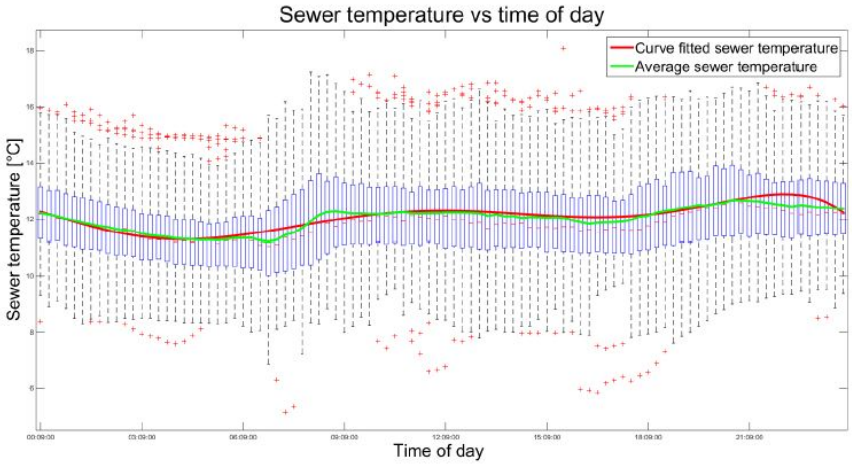


Figure 3.11.: Evolution of the observed sewer temperature over a day. [Spriet and Hendrick, 2017]

3.3.2. Spatial analysis

The concept of using wastewaster treatment utilities not only for water quality control purposes, but also as an energy source was also introduced in Kretschmer et al. [2016a]. The paper focuses on integrating wastewater treatment plants in local energy supply systems. The authors showed that different resources (Electricity, heat, sewage sludge,...) can be recovered and used, either locally inside the wastewater treatment system, or externally using the treatment plant as a regional energy cell. In Kretschmer et al. [2015] the authors add that the energetic performance of a wastewater treatment plant can be optimised if consumption is minimised and production is maximised. The reuse of produced energy can help to increase energetic self-sufficiency of a wastewater treatment plant, if a wastewater treatment plant could produce surplus energy, it should be integrated into regional energy supply concepts and serve as a regional energy cell. The authors claim that wastewater and sewage sludge should not be considered as waste anymore, but need to be considered as resources.

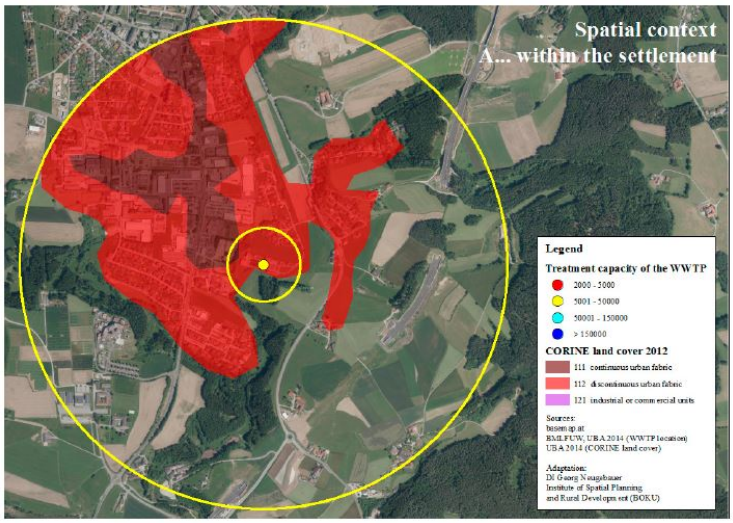


Figure 3.12.: Example of a WWTP within the settlement area. [Neugebauer et al., 2015]

In Neugebauer et al. [2015], the authors expand on this concept of regional energy cells, by overlapping the location of the wastewater treatment plant, and a radius of 1 km with the CORINE land cover database, as a proxy for heat consumption in the area. This is shown in Figure 3.12. CORINE is a land cover database of the European Commissionm covering consistent localized geographical information on the land cover for most areas of Europe, in 44 land cover classes. Three of these were considered a potential heat consumers:

- Continuous urban fabric
- Discontinuous urban fabric
- Industrial or commercial units

This resulted in 173 plants, in Austria, with potential for sensible utilization of the recovered heat, yielding about 3.1 TWh/yr and reducing the greenhouse gas emissions for room heating with 17%.

Kollmann et al. [2017] focuses on a case study where the surplus energy is intended for a public distribution system (district heating) to supply other consumers. Different tools are applied to support optimised integration and to analyse existing and future energy demands of different spatial units. Optimisation is also performed on an economical level. The Sustainable Process Index is used to assess the ecological footprint of the regarded technologies. The methodology is summarized in Figure 3.13

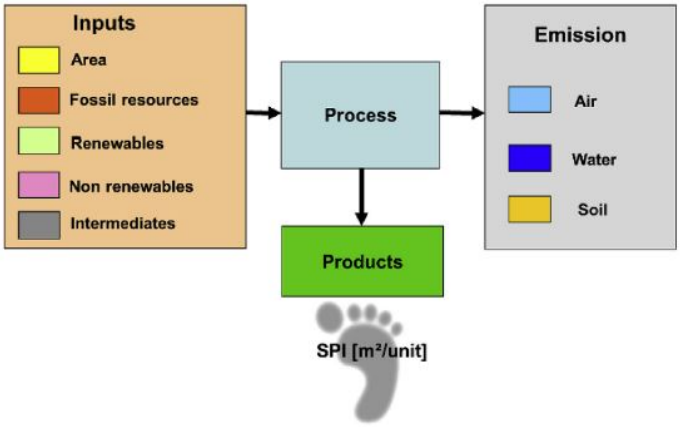


Figure 3.13.: Representation of calculation methodology. [Kollmann et al., 2017]

The integration of heat pumps in district heating was discussed in David et al. [2017]. The authors claim a target of increasing the district heating (DH) share to 50% of the entire heat demand by 2050, with approximately $25 - 30\%$ of this heat being supplied by large-scale electric heat pumps. The lay out of such a system is shown in Figure 3.14. The paper presents a database and the status of the technology and its ability of expansion to other European locations by reviewing experiences aimed at further research or application in the heating industry. This is based on a survey of the existing capacity of electric large-scale heat pumps. The study concluded that the technical level of the existing heat pumps is mature enough for replication in other locations in Europe.

In Hawley and Fenner [2012], the authors propose to use the recovered heat at four different wastewater treatment plants in three different ways:

- District heating
- Sludge drying
- Thermophilic heating in anaerobic sludge digestion

The authors report a carbon emission reduction of up to 110.7kgC_e/yr per capita, and a financial saving of up to 438 331£per annum. However, it is to be noted that not all options were environmentally and/or financially beneficial in all studied cases.

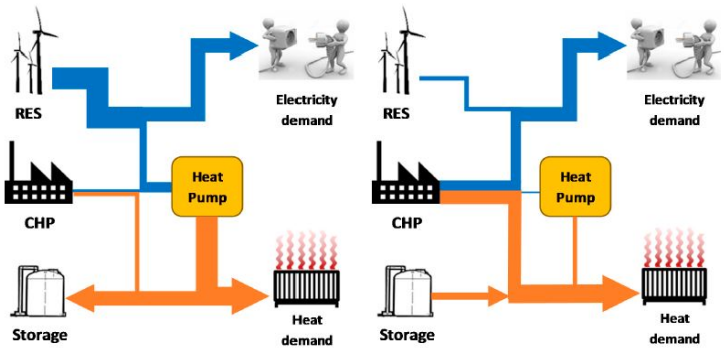


Figure 3.14.: The schematic of integrating heat pumps in district heating, with high and low renewable electricity production, respectively. [David et al., 2017]

Somogyi et al. [2018a] addresses the options for using the wastewater excess heat in district heating systems in Hungary. The distance between heat sources and areas with district heating was determined to show where the excess heat could be used. Five scenarios were created as a function of distance in which the reclaimed heat would be transported to an already existing district heating station (see Figure 3.15). The major factors of return were the distances from the district heating station and the expenditures of the heat pump and pipelines. Under the chosen circumstances only a fraction of the investments (40% for the best scenario) showed return in less than 10 years. The situation may be improved by increasing the amount of reclaimed heat or in case of higher natural gas prices.

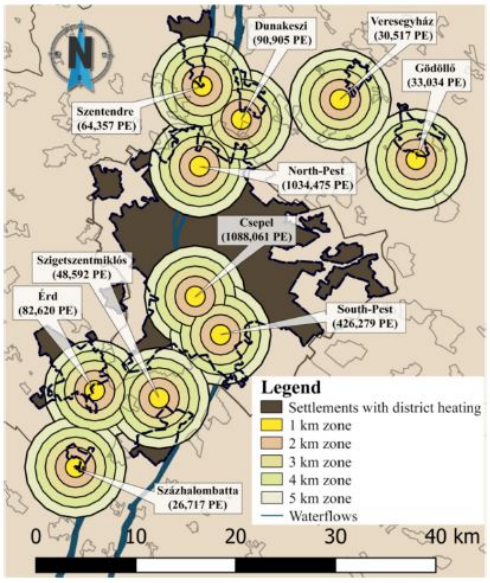


Figure 3.15.: Zones of wastewater treatment plants overlapping in the agglomeration of Budapestm Hungary. [Somogyi et al., 2018a]

3.4. Drain- and wastewater heat recovery

This sections reviews the existing systems, as described in literature. Because heat pumps can also be used for cooling, indirect and hybrid heat recovery systems are referred to as wastewater source heat pumps. This section is divided into direct heat recovery systems, wastewater source heat pumps for the sole purpose of heating, wastewater source heat pumps used for both cooling and heating, multifunctional heat pumps,

used for both space heating and - cooling, and for domestic hot water heating, and wastewater source heat pumps utilizing the embedded energy in untreated waste water.

Indirect heat recovery entails the utilization of a heat pump, which can, in a reversed cycle be used as a refrigeration device. Hence it is often denominated as wastewater source heat pump ($WWSHP$). Wastewater temperature is about $20°C$ higher than ambient temperature in winter, and about $10°C$ lower than ambient temperature in summer, giving it good properties as both a heat source in winter and a heat sink in summer [Xiao-Yan and Hai-Tao, 2005]. Literature proposing reversible heat pumps, providing both space heating and cooling are given in Section 3.4.3.

Heat pumps can be utilized to provide space heating and- cooling, but can provide the required heat, or part of it, for domestic hot water heating, as well. Heat pump systems providing these functionalities simultaneously over a certain period of time are denoted as multifunctional heat pumps. An overview on the literature on the subject is given in Section 3.4.4.

Utilizing raw, untreated wastewater as a heat sources brings about the issue of fouling of heat exchangers. The literature proposing solutions to this problem is discussed in Section 3.4.5.

3.4.1. Direct Heat Recovery

The idea of using direct heat recovery from wastewater from showers, bathrooms, swimming pools,... in a spa center to complement a low temperature geothermal heat source is introduced in González et al. [2001], however it is not technically developed by the author. The authors of Zaloum et al. [2007] propose a standard test set up to measure energy recovery and performance of drain water heat recovery units, and to determine the flow vs loss curves. They also report an optimal balance between performance and size of the heat recovery unit, as the marginal improvement in performance will stagnate at a certain unit size.

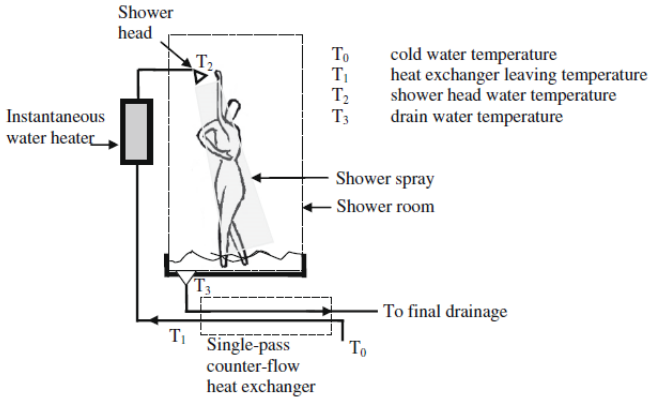


Figure 3.16.: A typical residential shower installation with a single-pass counter-flow heat exchanger [Wong et al., 2010]

Direct heat recovery systems from showers have been described in literature in McNabola and Shields [2013]; Slyś and Kordana [2014]; Wong et al. [2010], they propose to preheat source water before the classical heating system, as is shown in Figure 3.16. Wong et al. [2010] argues that $4-15\%$ of the embedded energy in shower drain water can be recovered with a single pass counter flow heat exchanger, resulting in a heat recovery from an apartment block containing 800 showers with an occupant load of 3 486 people of 104 to 406 MWh/yr.

A horizontal heat recovery system from showers is proposed in [McNabola and Shields, 2013], as shown in Figure 3.17, improving the efficiency to 23%. This results in yearly energy saving of 577 kWh for a three people household, corresponding to 103.8€per year. Implementing this system in all Irish homes would result in 808 GWh of energy savings in the country.

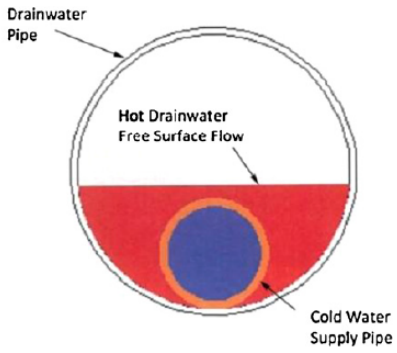


Figure 3.17.: Cross section of the proposed heat recovery unit [McNabola and Shields, 2013]

Slyś and Kordana [2014] presents a financial analysis of the implementation of such heat recovery units, and with shower lengths ranging from 5 to 12 minutes, the authors report a discount payback period ranging from 3.5 to 10 years. The viability of such units is reported to depend on shower time with improved profitability for longer shower times.

Ip et al. [2018] studied the life-cycle impacts of installing shower heat recovery at a university shower facility. The authors investigated the environmental and financial sustainability of a vertical waste heat recovery device, over a life cycle of 50 years, with comparison to the normal use of a PVC-u pipe. The results indicated that the seasonal thermal effectiveness was over 50%, enabling significant energy savings through heat recovery that led to a carbon payback time below 2 years compensating for the additional greenhouse gas emissions associated with the construction and installation of the heat exchangers. The life-cycle cost of the heat exchanger is much higher than using a PVC pipe, even with significant heat recovered under heavy usage, highlighting the need to adopt more economic configurations, such as combining waste water through fewer units, in order to maximize the return on investment and improve the financial viability.

De Paepe et al. [2003] describes a direct heat recovery system which is internal to dishwashers, similar to other direct heat recovery systems, the heat recovery rate is offset by a limited operation time, resulting in a payback period which is around 13 years.

On a larger scale Hua [2005] proposes an unconventional thermosyphon heat exchanger, in order to recover the heat from a dishwasher, discharging 2 500 l/day at $35 - 55°C$. Following the author's simulation, 27.8 kWh_{th}/day could be recovered directly. This system has the advantages of a simple construction, low maintenance and an ability to recover heat outside of hot water usage periods.

Zhi-Feng [2011], proposes the use of plastic heat exchangers, polytetrafluoroethylene($PTFE$) pipes in this case, for heat recovery from domestic sewage. They have the advantage of being cheap, and have good anti-corrosion and ant-fouling properties.

A system recovering the heat from the grey water going through the shower drain, used to preheat all hot water consumed in a household is described in Eslami-nejad and Bernier [2009]. The paper focuses on the impact that drain water heat recovery systems have on peak electrical demand from electric domestic hot water (DHW) tanks, and studied this by simulation. The system is summarized in Figure 3.18. The authors reported an impact on the peak electrical demand with reductions of 119.4 W (10.4% reduction) at 8 : 00 and 184.0 W (21.5% reduction) at 22 : 00. On an annual basis, the energy required for DHW heating is 4 501 and 5 299 kWh with and without a DWHR, respectively.

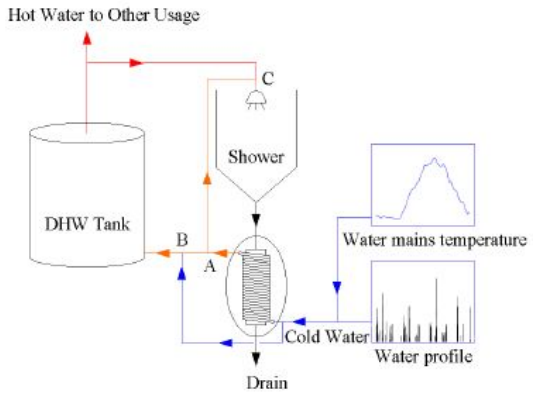


Figure 3.18.: Schematic presentation of the Domestic Hot Water system. [Eslami-nejad and Bernier, 2009]

The aim of the use of Drain Water Heat Recovery units is thermal energy recovery from warm drainwater and transferring it to incoming cold water. Slyś and Kordana [2014] presents a calculation model that allows the estimation of the financial efficiency of the project involving the construction of a shower drainwater heat recovery system in a single-family dwelling house. The presented method of investment risk assessment is intended for decision making by individual users, designers and others. From investors point of view the most beneficial option of heat recovery system installation is a system where preheated water is fed to both the hot water heater and the shower mixing valve. The obtained financial results are also affected by showering time and water consumption. DWHR units were deemed beneficial to apply in case of swimming pools, sports facilities or fitness clubs, where high turnover of users is observed. The authors investigated three options, the option with highest financial returns is shown in Figure 3.19.

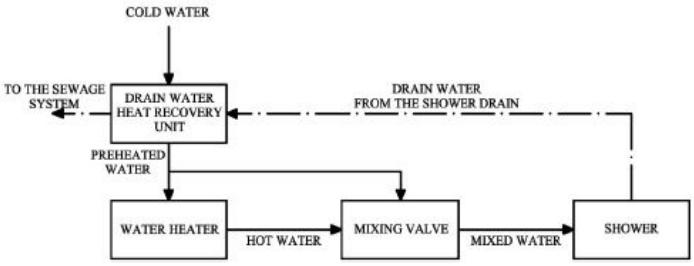


Figure 3.19.: Diagram of the working of the system in the option 1. [Slyś and Kordana, 2014]

Torras et al. [2016] studied the recovery of the waste heat from domestic warm drain water, and transferring it to cold water entering the house. The authors are using both numerical and experimental tools to design and study the performance of this device, focusing on the analysis of a specific drain water heat recovery storage-type based on a cylindrical tank with an internal coiled pipe. The DWHR storage had the capacity to recover from 34% to 60% of the energy available in the drain water for the investigated flow rates. A 50% reduction in stored energy is observed at 24 h, which reveals its limitations for long-term storage applicability.

Stec and Kordana [2015] presented a financial analysis with an application of the Life Cycle Cost methodology for a multi-family residential building for seven different variants of installation of water and sewage, which assumed the use of different solutions: grey water harvesting system, rainwater harvesting system and drain water heat recovery units. The analysis of the authors showed that the use of these systems in the tested building is financially viable, despite the fact that their implementation is associated with incurring higher investment cost than in the base case. This was compared through a method of total life cycle cost. The variant of the system, including drain water heat recovery is shown in Figure 3.20.

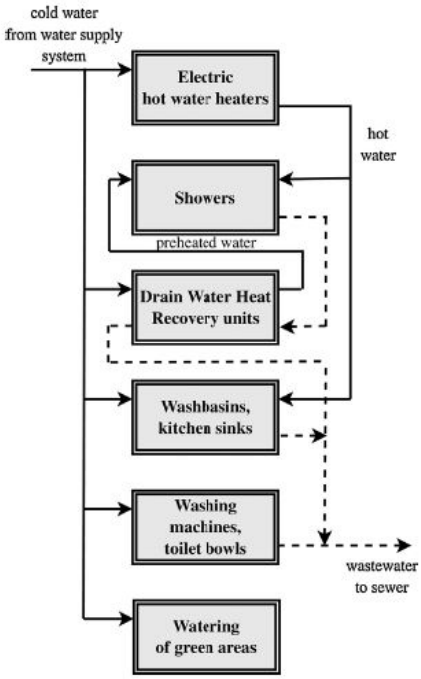


Figure 3.20.: Diagram of the installation including DWHR [Stec and Kordana, 2015]

A comparative study, applying the system in two occupied houses was performed in Tanha et al. [2015]. The DWHR units and water heater systems were installed side-by-side at the Archetype Sustainable Twin Houses at Kortright Center, Vaughan, Ontario, in combination with Solar Domestic Water Heaters (SDWH). The first system in House A consists of a flat plate solar thermal collector in conjunction with a gas boiler and a DWHR unit. The second SDHW system in House B consists of an evacuated tube solar collector, an electric tank, and a DWHR unit. The extrapolated results based on the experimental study showed that the DWHR unit is capable of an annual heat recovery of 789 kWh and an overall effectiveness of about 50%. The flat plate and evacuated tubes collectors based SDWH systems produce an annual thermal energy output of 2 038 kWh and 1 383 kWh, respectively.

The effect of drain-side wetting on the performance of falling film drain water heat recovery systems (see Figure 3.21) was studied in Beentjes et al. [2014]. It describes the experimental set up for testing the effectiveness of DWHR systems. The authors showed that as the flow rate increases, the effectiveness of the DWHR pipe decreases. They also indicated that there is a Critical Flow Rate (CFR) below which the performance of a DWHR pipe cannot be extrapolated. The inability to extrapolate is deemed to be due to the incoming drain water not repeatedly wetting the same amount of area on the pipe's interior wall.

Manouchehri and Collins [2016] investigates the impact of mains-side and drain-side water temperatures on the effectiveness of falling film drain water heat recovery (DWHR) systems, through experiments. The proposed system uses heat exchangers that recover energy from a building's greywater, and uses it to preheat incoming mains water. Four DWHR systems of varying diameter and length are tested at inlet temperatures of 25, 30, 35, 40 and 45°C on the drain-side, and 5, 10, 15, 20, and 30°C on the mains-side. Experiments show that heat exchanger effectiveness is strongly linked to fluid inlet temperatures, and that increases in either of these temperatures would lead to an increase in effectiveness, even if the temperature difference between the inlets is kept constant.

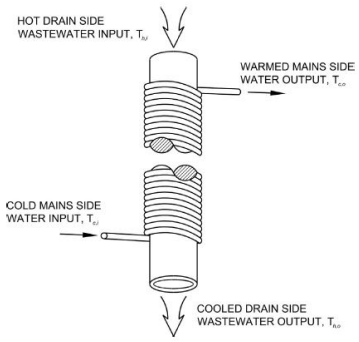


Figure 3.21.: Diagram of a DWHR system. [Beentjes et al., 2014]

A calculation procedure that can be applied to different drain water heat recovery systems and can be used as a calculation tool to evaluate and analyze drain water heat recovery systems or as an optimization technique for existing systems is described in Ramadan et al. [2016]. A parametric experimental analysis was performed using the an experimental setup. These experiments showed the temperature of the cold supply water can be increased significantly. The tested prototype setup is shown in Figure 3.22.

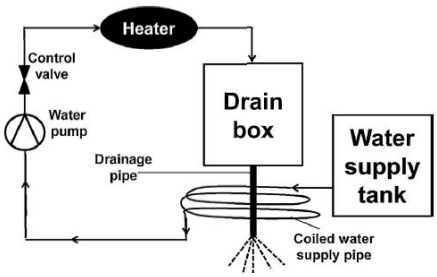


Figure 3.22.: Schematic of the constructed prototype. [Ramadan et al., 2016]

In order to recover heat at higher temperature direct heat recovery systems are generally installed close to the heat source, in this case the appliances consuming the heat. This results in the drain- and wastewater flows being small, and having an intermittent character. This has an adverse character on the available embedded energy. Furthermore, because of the strong localised character of these direct heat recovery systems, it requires the heat being reused in the same appliance, whereas situations might occur where heat reuse in another application might be desirable.

In order to recover the heat from multiple appliances most of the proposed technologies would require multiple local heat exchanger, resulting in multiple investments, and multiple material use for relatively small embedded recoverable energy, which might be financially and environmentally inefficient. The possibility of centralized Direct Heat Recovery is seldom investigated. Temperature of wastewater is expected to be lower in this centralized location, but this could be offset by larger flows, and the possibility of reusing the heat in other appliances. It remains to be investigated if such a system is competitive with the local systems, and what its possible significance in relation to the entire household energy consumption is. A centralized direct heat recovery system could provide additional benefits to indirect heat recovery systems (see Section 3.4.2).

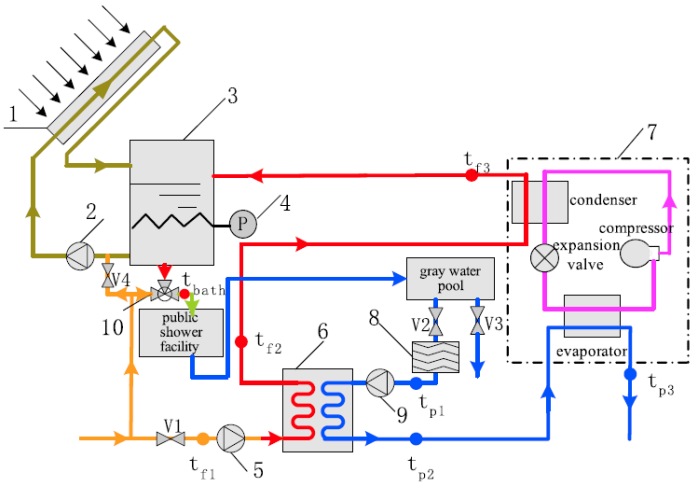
The applications of direct drain water heat recovery, mainly focus on showers, spa centres and swimming pools. Other than heat recovery inside the dish washing appliance, studies of heat recovery from kitchens are lacking. As kitchen water is required to be heated up to 60° because of legionella legislation [HSE/HPSC, 2009], temperature of kitchen wastewater is expected to be high.

3.4.2. Wastewater source heat pumps for heating purposes

Wastewater source heat pumps being utilized for heating purposes are generally installed in places where a significant, year-round hot water consumption is observed, such as spa- and leisure centres, bathing houses,... Often, the waste water temperature is high, but intermittent flow can reduce the system's COP.

Chao et al. [2012] describes an experimental set-up, recovering the heat from the wastewater discharged from a common bathroom in a spa center. The authors propose the use of a dry-expansion evaporator with defouling function, however the COP of the system decreased from 3.09 to 2.50, and after the cleaning the COP reached a value of 3.04. Similarly the authors in Chao et al. [2013] describe an experimental set-up, recovering the heat from the wastewater discharged from a common bathroom in a spa center. The COP of the system decreased from 3.80 to 2.87 after 5 months of operation due to bio fouling build-up. The wastewater temperature was estimated between 31 and 34$°C$, resulting in an operation cost which is lower than the competing systems.

Liu et al. [2010] describes the recovery of exhaust heat from public shower facilities in order to provide the heat for domestic hot water heating, in combination with solar energy collection, the system schematic is shown in Figure 3.23. The heat pump's COP reached a value of 3.55, and the system's operational costs were found to be lower than its competitors, on the contrary, the initial investment for the heat recovery system was higher than the ones of the competitors.



1-solar collector; 2-pump for collector; 3-heat storage tank; 4-electric heater; 5-water pump;6-water-water heat exchanger; 7-water-water heat pump; 8-filter; 9-wastewater pump; 10-tee joint mixing valve;

Figure 3.23.: Schematic diagram of the combined heat recovery and solar energy heating system [Baek et al., 2005]

In Meggers and Leibundgut [2011] the authors propose to recover the embedded heat in the wastewater of different household appliances locally, proposing the installation of multiple heat pumps within a home. Although this leads to a high COP of 6.7, the installation of multiple heat pumps doesn't seem feasible, due to increased investment costs and space constraints.

This concept was also studied in Alnahhal and Spremberg [2016]. The study was conducted inside student hostels in Berlin, in which water supply, wastewater, and room temperatures variations were observed during winter for one month. It showed a negligible effect of the incoming clean water temperature on the performance of the system. The authors illustrated that by selecting a suitable combination of heat exchanger and heat pump, about 40 kWh/h (917 kWh/day) average inhouse wastewater thermal heat can be recovered and about 230 €/day saved . This can contribute to reduction of energy needed for hot water provision by about 30% in the targeted hostels.

Specifically looking at shower drain water, Dong et al. [2015] discusses a heat pump water heater assisted with shower drain water for small single family, which could effectively recover the energy in domestic shower drain water (Shown in Figure 3.24). A shower waste heat extraction device with water pre-heated loops was proposed. A prototype of that system was set up, and the system performances under different conditions were studied experimentally. The experimental results showed an energy saving of approximately 70% compared to a traditional electric water heater. Furthermore, the COP of the system improved when using water pre-heated loops. The implementation of this novel heat pump water heater was capable of reducing energy usage and CO_2 emissions significantly.

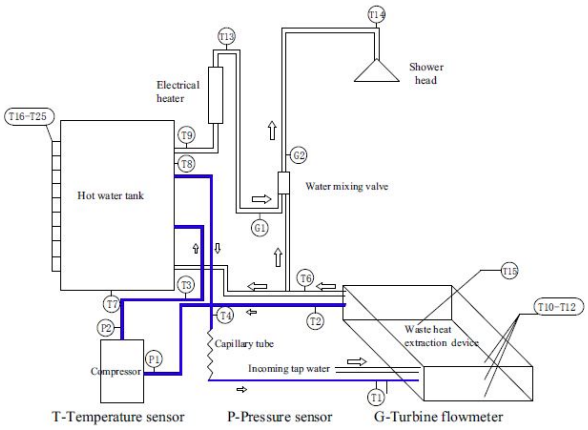


Figure 3.24.: Schematic diagram of the Heat Pump Shower Water Heating system. [Dong et al., 2015]

Li et al. [2011] propose to recover heat in thermal desalination plants through multi-stage heat pumps, to use in multiple effect desalination (MED). The COP of individual stages ranged from 3 to 11, the source temperature decreased gradually from 90 to 27°C, and provided hot water at 75°C, as can be seen in Figure 3.25. The authors claim an energy saving of 80%, compared to the traditional reverse osmosis technology, resulting in a payback period of around 2 $years$, at the studied location in Sheffield, UK.

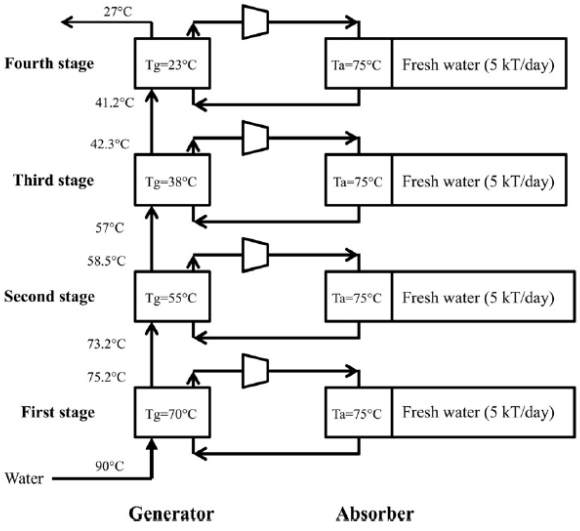


Figure 3.25.: Schematic diagram of four-stage heat-pump operations used for MED [Li et al., 2011].

Different studies have been performed in order to investigate the impact of control parameters and operational strategy. Kahraman and Celebi [2009] and Coskun et al. [2012] modelled the performance of the system experimentally. The former looks at the performance at different wastewater temperatures, resulting in COP values of 3.36, 3.43 and 3.69 at wastewater tempertures of 20,30 and $40°C$, respectively. The latter investigates the effect of compressor speed$(22.5-50\ Hz)$, wastewater temperature$(23.3-52°C)$, and wastewater flow$(60-135\ l/h)$, showing a COP ranging from 4.36 to 6.94.

Li et al. [2013] investigates the optimal operation strategy for a combined system with a wastewater source heat pump, and a gas boiler, in a community in Xi'an, China with a mix of residential and public buildings, as is shown in Figure 3.26. The desired supply water temperature $(57.9°C)$ is higher than the maximal capacity of the heat pump $(51°C)$, hence the use of the gas boiler. The result is an annual decrease of energy consumption of 45.2% and a decrease in operation cost of 13.5% compared with a conventional coal-fired boiler, thanks to a COP varying between 3.95 and 5.72.

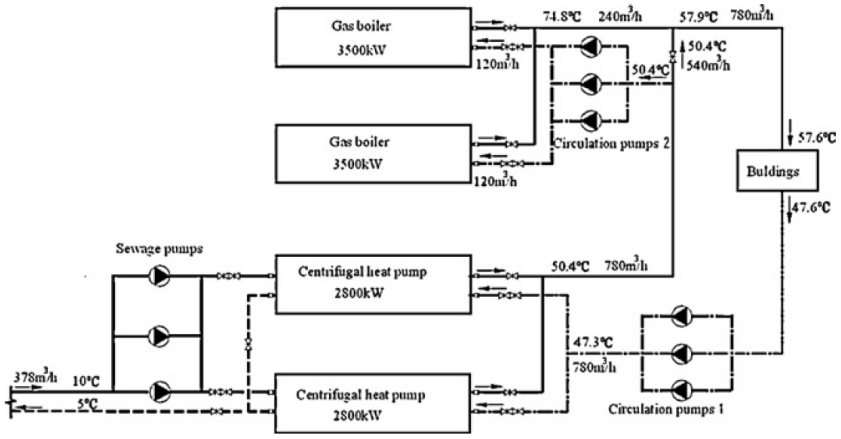
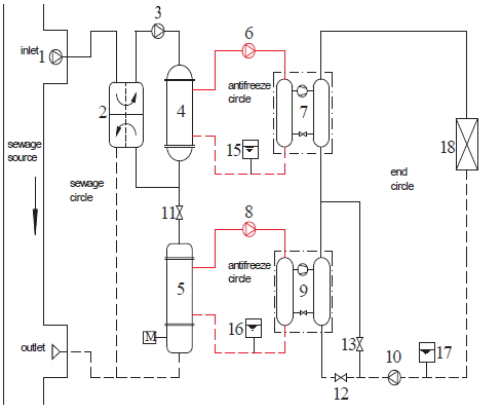


Figure 3.26.: Schematic diagram of the combined heat recovery and gas boiler heating system [Li et al., 2013].

A complete prototype plant in a residential setting was described in Postrioti et al. [2016]. The characteristics and performance of heat recovery from civil wastewater was assessed. This heat was used as ancillary thermal supply to a heat pump heating system; during the experimental analysis, the wastewater discharge cycles were estimated from data derived by the most common buildings typologies. Although the enthalpy content of sewage water was generally low, its storage in a properly dimensioned tank could bring a contribution to the COP improvement of around 12% (3.72 vs 3.32). The considered additional costs related to the wastewater exploitation, was estimated at a few thousand of Euros, and the energy saving led to an acceptable payback period of the investment.

Bertrand et al. [2017] studied the detailed impact of waste water heat recovery at a city scale by aggregating building data. A method to quantify the building-specific energy cost and energy saving potentials, at the urban scale of in-building waste water heat recovery systems was discussed. A complementary method was also developed, used for spatial allocation and characterisation of the grey water streams with respect to thermal load and temperature levels in function of the building specificities. These methods were applied on two case studies, resulting in the finding that grey water heat recovery would reduce the residential fuel consumption of the city by 6.3%. An integrated approach combining grey water heat recovery for hot water preheating and a heat pump yields up to 28% and 41% electricity savings for passive single family houses and multifamily buildings, respectively.

In certain very low-temperature regions the wastewater flux can be insufficient to provide heating peak loads. In Qian et al. [2009], the idea of a heat pump collecting the latent heat of wastewater freezing is introduced. The proposed system has two stages, and thus two heat pumps, as shown in Figure 3.27, and the heat pump using latent freezing heat as a heat source is only used in case the conventional system is inadequate. The proposed design heat load is 1 MW, and the authors claim a large applicability thanks to the fact that the heat pump will only operate at peak load during a small portion of time, and only a small amount of freezing latent heat is required. In Qian [2011] the system is optimized, using an annual cost evaluation as the objective function. The system would operate at 1 300 kW for 4 200 hrs at COP's of 3.41 and 3.31 for both stages respectively. The author claims that the profitability for the system is superior to that of a traditional water chiller and heating system.



1, 3. Sewage pump; 2. counter-washing device; 4. Sewage heat exchanger; 5. Freezing latent heat exchanger; 6, 8. Antifreeze solution pump; 7. First-stage heat pump unit; 9. Second-stage heat pump unit; 10. End pump; 11~14. valves; 15~17. Expansion tanks, 18.Fan-coil

Figure 3.27.: Schematic diagram of a freezing latent heat source heat pump [Qian et al., 2009]

In Song et al. [2006] a system recovering heat from effluent wastewater to heat up raw sewage to the optimal operating temperature for biological treatment ($25 - 30°C$). The performance of a three stage evaporator is simulated, showing a seasonal COP of 4.18, raising the temperature of the raw sewage to $29.57°C$, by delivering 714.36 kW of heat. The simulations also show that an increase in heat exchange surface of $73 - 83\%$ is required to compensate for the additional heat exchange resistance due to fouling.

Alekseiko et al. [2014] presented an analysis of the effectiveness of the heat pumps installed in the wastewater treatment plants of Vladivostok. Reporting that:

- The treatment plant is a valuable source of heat. This heat can be efficiently utilised by heat pumps.
- The heat received from the community sewage plants could be sold to consumers to great advantage.
- A Heat Pump Project on urban wastewater treatment plants is beneficial to investors.
- Heat pumps at wastewater treatment plants reduce the emissions of heat into the environment.

A system utilizing the heat embedded in the effluent leaving the wastewater treatment plant is described in Somogyi et al. [2018]. It outlines the possibility for DWHR in a wastewater treatment facility with a daily hydraulic loading of about 2 300 $^3/day$ and a wintertime temperature of $10 - 14°C$. This wintertime temperature reduced the nitrification rate in the plant, and the recovered heat was used to increase the temperature of the aeration tank in order to enhance the microbiological activity and thus the efficiency of pollutant removal. Increasing the temperature by $6°C$ in the aerated tank, ammonium removal improved by 61%. The system is shown in Figure 3.28.

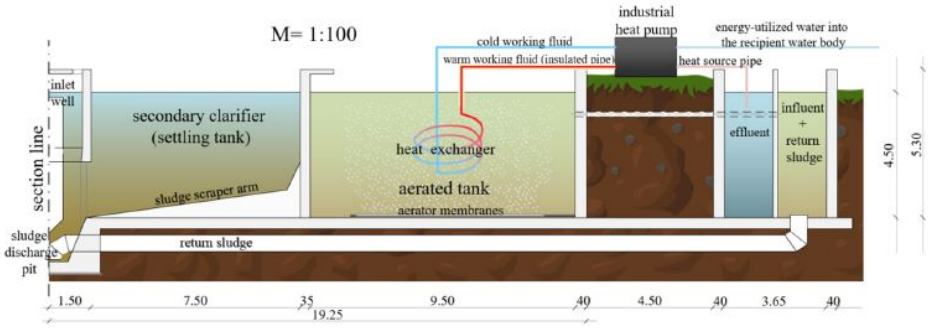


Figure 3.28.: Schematic design of introducing heat pump and heat exchangers to utilize waste heat in the aerated tank [Somogyi et al., 2018].

Ninikas et al. [2019] describes an installation of a wastewater source heat pump in the Glasgow underground system. This system uses subsurface wastewater ingress to heat the office at St. George's Cross station. The system is represented schematically in Figure 3.29, and is characterised by a COP of 2.5 and a 60 % reduction in required energy input. The COP is lower than in the previously described systems because the ingress water was not previously heated and/or used for human activities, it is water flooding the underground system due to its position relative to the water table. Fifteen cities across Europe have been identified, where such a heating system may be applied.

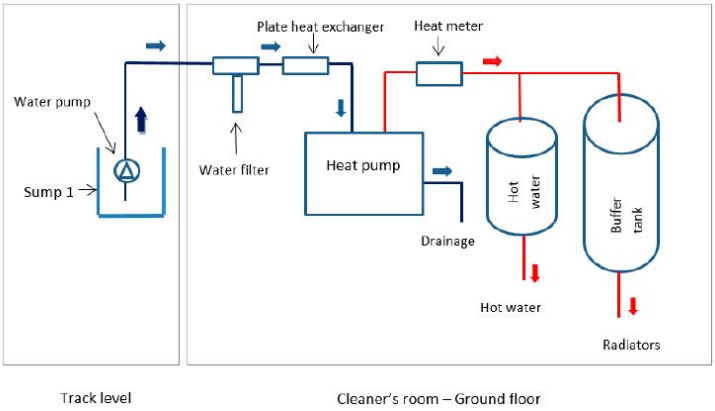


Figure 3.29.: Station's diagram of the heating system [Ninikas et al., 2019]

In Słyś et al. [2020], possible solutions for installations enabling heat recovery from wastewater to supply agri-breeding farms with hot water were studied. Four variants of cooperation between a heat pump and an exchanger were considered:

- Waste heat used in the process of heating water used to clean stands and prepare feed.
- Waste heat taking part in heating the water used for watering plants.
- Waste heat used in the process of drying cereals.
- Waste heat supporting the preparation of utility hot water for the breeder's residential building.

The study showed the legitimacy of using thermal energy from liquid manure as a waste heat source on farms and farming. This is mainly due to the short payback period, which can be within $2-4$ years. In turn, the analysis of pollution reduction associated with the recovery of waste energy showed that the use of heat pumps allowed a significant reduction in the emission of harmful compounds to the atmosphere, in particular carbon dioxide.

The literature presented in this section consists of specific studies, applied to specific locations. However, the broader scope, which is the potential place of WWSHP in the heating and energy landscape, is generally not addressed. The contribution of wastewater source heat pumps towards renewable heating deployment, and towards energy- or carbon neutrality in the water cycle (see Section 2.4) has not yet been reported on. There's thus no basis for policy makers to decide which policies and/or incentives should be provided in order to stimulate this technology. There's an information gap between the potential carbon and energy neutrality in the water cycle (discussed in section 2.4), and the impact of the technology discussed in this section.

Because all presented studies are applied to specific situations, the proposed solutions are tailor-made, and a very large range in COPs can be observed. There's a lack of general design guidelines, indicating measures which would lead to an optimized COP and thus improved profitability. Individual, tailor-made engineering is time and cost consuming, in order to counteract this the possibility of a modular, scalable system could simplify the process, and reduce engineering time and costs.

In Section 3.3 the importance of both spatial and temporal aspects in the operation of drain- and wastewater heat recovery systems is emphasized, however studies integrating both aspects in the investigation of feasibility and/or operation are lacking.

3.4.3. Wastewater Source Heat Pumps for heating and cooling

Given the relatively stable and favourable conditions of wastewater, being about $20°C$ higher than ambient temperature in winter, and about $10°C$ lower than ambient temperature in summer, Zhou and Li [2004] proposes the practical application of sewage source heat pumps in the Republic of China, for both heating and cooling applications. The authors discuss the example of the Qinhuangdao Haigang District sewage treatment plant, and compare the costs to a system using electric chillers and an oil boiler. The estimated investment and operation cost of the sewage source heat pump are smaller than those of the reference system, and the heating COP is estimated to be $3.5-4.5$. The system contains an auto-rinsing strainer, which is a self-cleaning filter, to counter fouling.

Qu et al. [2011] studied the growth regulation of fouling on the surface of a PE pipe in untreated sewage and the maximum thickness of fouling growth was found through biological electron microscopy. The studied case was the wastewater treatment station in Shandong Jianzhu University, China. The authors propose that the fouling accumulated slowly in the first two weeks, and started to accumulate faster after the third week. The thickness of the fouling reached its maximum in the sixth week (around $0.03-0.035\ mm$. And the fouling started to decrease from the seventh week onwards, afterwards the thickness gradually stabilized.

In the same operating conditions Chen et al. [2006] describes two possible styles of wastewater source heat pumps, as summarized in Figures 3.30 and 3.31. Figure 3.30 describes the case the wastewater is sufficiently clean to introduce it to the evaporator heat exchanger of the heat pump. Figure 3.31 describes the case where too much pollutants are found in the wastewater to introduce it to the evaporator directly, in this case an intermediary heat exchanger and intermediary heat carrier (also denoted as the heat pump's primary fluid) is used to transfer the heat to the evaporator. In this case the estimated investment and operation cost of the sewage source heat pump are smaller than those of the reference system as well, and the payback period varies from 2.6 to 7.8 years.

The economic feasibility of a wastewater source heat pump under the same conditions as described in Zhou and Li [2004]; Chen et al. [2006] is investigated in Xiao-Yan and Tao [2005], using the annual expenditure method. The authors state that the initial investments for the wastewater source heat pump is more important than those for traditional heating systems, but the operational costs are lower, except for coal boilers, the authors claim a payback period of less than one year.

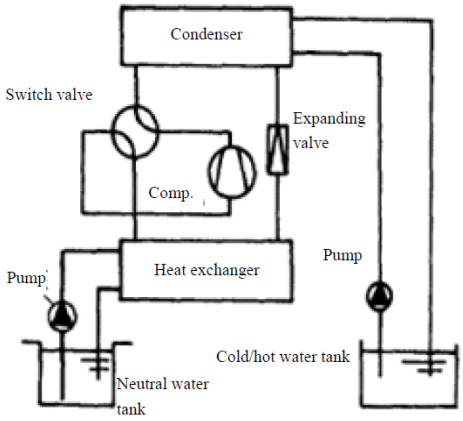


Figure 3.30.: Neutral wastewater source heat pump (Chen et al. [2006])

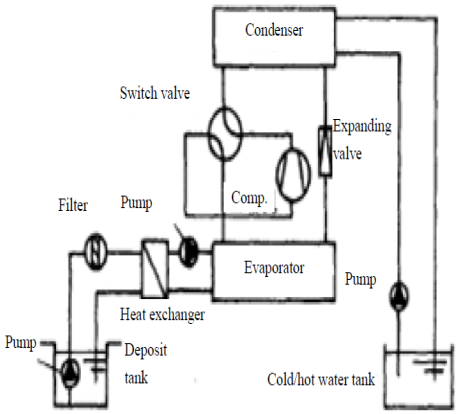


Figure 3.31.: Untreated wastewater source heat pump (Chen et al. [2006])

In Yaxiu et al. [2011], the feasibility of such a system at five wastewater treatment plants in Xi'an, China is discussed. The effluent temperature from the treatment plants varies between 20 and 26°C in summer and between 10 and 18°C in winter. For plant 4, the considered hot water temperature in winter is 50°C, with a heating load of 10 989 − 16 389 kW. The cooling load is estimated at 9 720 kW. The air conditioning supply water in summer is considered to have a temperature of 7°C. The authors predict a reduction in energy consumption compared to fossil fuel systems, without mentioning specific numbers.

Baek et al. [2005] proposes to use wastewater from a hotel with a sauna as a heat source and heat sink for a heat pump. The heat is recovered at night, during off-peak hours, with off-peak electricity prices. The forecasted COP of the heat pump is 4.8 and it is forecasted to deliver 100% of heating requirements during the winter season, except for the weekends. The wastewater temperature is 18°C and the hot water temperature 50°C. A schematic of the system is shown in Figure 3.32. The wastewater passes through a filter and is sent to the wastewater storage tank, where its temperature is lowered through the heat exchanger, providing the heat for the evaporator of the heat pump. The heat pump provides its heat to water stored in a hot water storage tank, which is used as the hot water supply for the building.

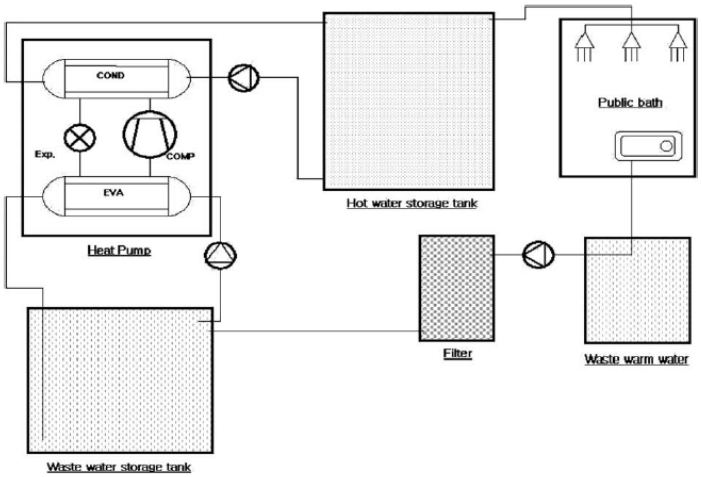


Figure 3.32.: Schematic diagram of the wastewater source heat pump in[Baek et al., 2005]

A drain water source heat pump from shower facilities utilizing a hybrid heat recovery system using two different kinds of heat pumps is discussed in Liu et al. [2014]. The wastewater is drained through a pipe to a grey water holding tank, where at first heat is recover directly to heat the mains supply water from 12 to 25°C, and the wastewater dropping from 30 to 17°C. Thereafter the wastewater is led to the evaporator of the heat pump. Two different types of heat pumps are considered, an electric heat pump, with a heating capacity of 410 kW and a cooling capacity of 528 kW, and a direct fired absorption heat pump, with a heating capacity of 410 kW. They are summarized in Figures 3.33 and 3.34. The payback period for both systems are 2.6 and 2.1 years respectively. Considering a COP between 2 and 5.5 the potential reduction in greenhouse gas emissions is around 10 000 $t\ CO_{2,eq}$.

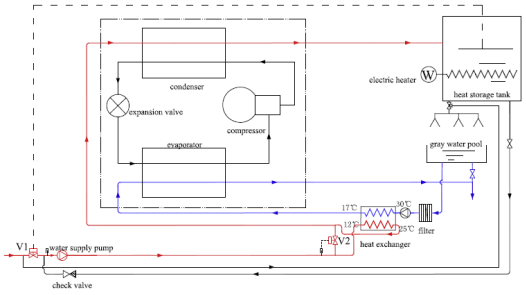


Figure 3.33.: Exhaust heat recovery system using electric heat pump ([Liu et al., 2014])

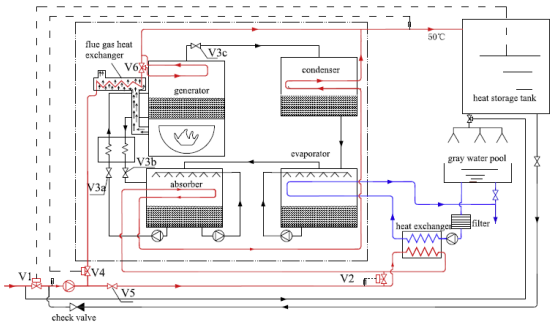


Figure 3.34.: Exhaust heat recovery system using direct-fired absorption heat pump ([Liu et al., 2014])

The experimental observation of the operation of an urban sewage source heat pump is described in Zhao et al. [2010], observing a COP in heating mode of 4.3 and 3.5 in cooling mode. The proposed system is shown in Figure 3.35, where a filth block device is used to avoid larger pollutants from entering the system. In heating mode, valves $1-4$ are opened, and valves $5-8$ are closed, resulting in the evaporator withdrawing its heat indirectly from the wastewater, and the condensor of the heat pump delivering the heat to the heating system. During the cooling season, valves $1-4$ are closed and valves $5-8$ are opened. Such that the heat withdrawn from the conditioned space is delivered in the evaporator, and the wastewater is indirectly used as a heat sink for the condensor.

Zhang et al. [2010] compares three cold and heat source programs, one being the sewage source heat pump ($P1$), the second one being a fuel boiler in combination with a water chiller system ($P2$), and the third one where a fuel boiler is combined with the sewage source heat pump ($P3$), for an office building in Shanghai, China. The considered heating and cooling loads were 668.16 kW and 973.77 kW. The analysis shows that from an energy, environmental and economic point of view $P1$ delivered the best results, followed by $P3$.

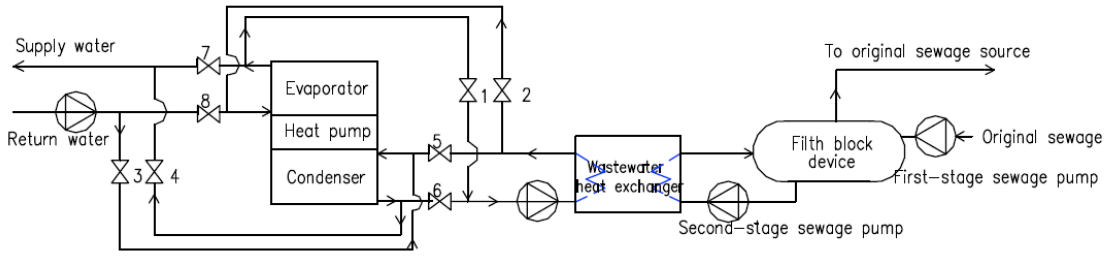


Figure 3.35.: Urban sewage source heat pump system [Zhao et al., 2010]

The design, construction and operation of four large sewage source heat pumps in Harbin and Beijing, China is discussed in Chenghu et al. [2011], the authors propose a half-centralized operation mode, where a large centralized heat exchanger recovers the heat from the wastewater, which is then distributed to multiple, decentralized heat pumps, as can be seen in Figure 3.36.

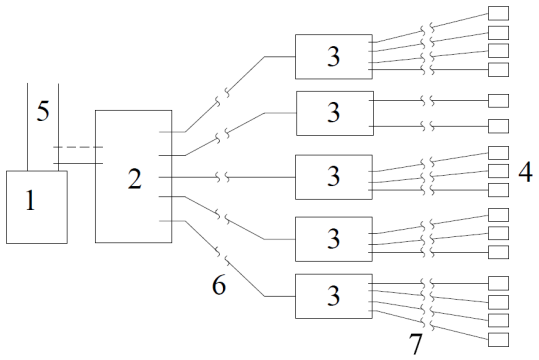


Figure 3.36.: Half centralized operation mode in large projects [Chenghu et al., 2011]

As discussed in Section 2.4, Chae and Kang [2013] proposed an effluent source heat pump at a municipal wastewater treatment plant. Effluent flow temperatures vary between 12 and 28°C, resulting in a cooling COP between 4.48 and 5.35, with a capacity ranging from 103 to 107 kW, and a heating COP between 3.53 and 4.06, with a capacity ranging from 106 to 130 kW. The total yearly energy production from the heat pump systems is 276 MWh/yr resulting in an equivalent greenhouse gas emissions decrease of 130 $t\ CO_{2,eq}/yr$.

A similar system from raw water is described in Oh et al. [2014], showing an average, simulated COP of 4.79 for cooling and 3.76 for heating for a single heat pump system, and of 4.92 and 3.68 for a two-heat pump system, the yearly predicted COP variation can be seen in Figure 3.37.

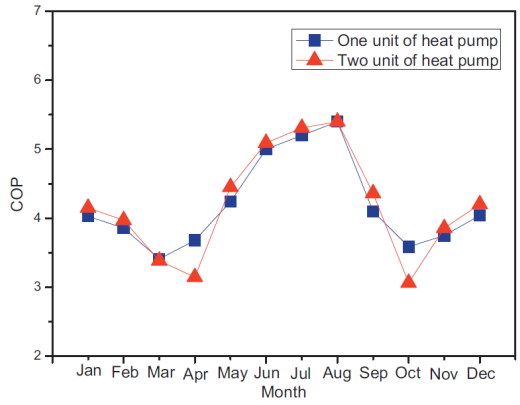


Figure 3.37.: Variation of the COP over the year [Oh et al., 2014]

Similar to the literature in the previous section, the papers discussed in this section focus on specific applications, but no applicable criteria have been identified on when a wastewater source heat pump is suitable for both heating and cooling, and when the addition of the reversibility of the heat pump is not feasible. Guidelines on when reversibility has a potential benefit to the system are lacking, and the potential benefit in the broader context of the energy mix remains to be investigated. In this PhD thesis, the total sectoral potential, on a national level, is discussed for three different sectors:

- Individual residence.
- Commercial kitchens.
- Municipal wastewater treatment plants.

Thermal use of the wastewater (neither for heating nor cooling) of industrial plants was, up until now, not reported. Depending on the industrial applications, high temperature wastewater can be available in large volumes. Furthermore, they provide a location, where these large volumes are assembled, close to the consumer (the industrial facility). Additionally, hybrid heat recovery, the combination of direct and indirect heat recovery, is also rarely studied. In this PhD thesis, a hybrid heat recovery was installed and studied in the wastewater treatment system of meat processing plant.

3.4.4. Multifunctional heat pumps

The idea of a multi-function heat pump, combining domestic water heating, and space-heating and -cooling was introduced in Ni et al. [2012]. The proposed system uses residential grey wastewater as a heat source. The system is summarized in Figure 3.38.

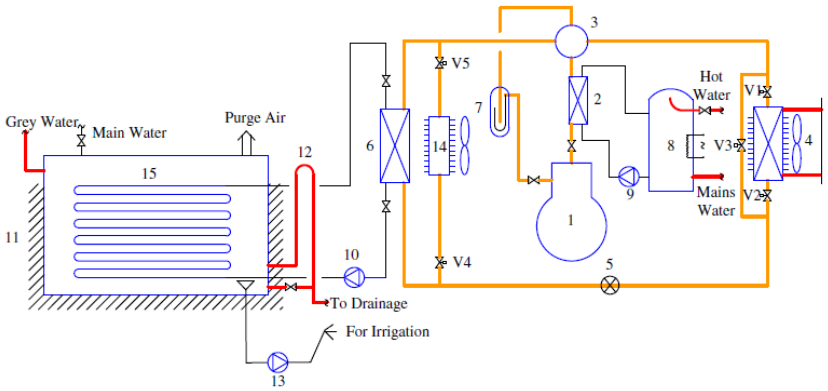


Fig. 1. Principal design of the localized energy-recovery system from residential wastewater assisted by outdoor air heat exchanger. Labels: 1 = compressor; 2 = plate heat exchanger for service water; 3 = four-way reversing valve; 4 = indoor coil; 5 = bi-flow expansion valve; 6 = wastewater heat exchanger; 7 = suction accumulator; 8 = hot water storage tank; 9, 10 = circulation pumps; 11 = wastewater tank; 12 = overflow pipe; 13 = pump for irrigation; 14 = outdoor coil; 15 = submerged-pipe coil; V1-V9 = solenoid valves.

Figure 3.38.: Principal design of the localized energy-recovery system from residential wastewater [Ni et al., 2012]

The authors describe a numerical model, investigating the annual energy and water consumption of the proposed heat recovery, and comparing it to a conventional system with gas furnace space heating, package air-conditioning and electricity water heater. The analysis is based on a case study for a four-member, three-bedroom residence in New York, USA. The analysis considers 1 300 l/day of fresh water consumption, resulting in 800 l/day of wastewater, the indoor air temperature was kept at 24°C, and the hot water supply at 49°C. Thanks to an average COP of 4.03, the authors claim a reduction in potable water consumption of around 27%, and a decrease in overall source energy consumption of around 33%, when the study was reiterated for 15 different cities in the US the savings varied between 15 and 34% and between 17 and 59%, respectively.

The experimental analysis of the performance of such a multifunctional heat pump was described in Wang et al. [2013], the set-up used shower drain water ($11 - 36°C$) as the heat source to supply artificial springs, sauna rooms, and domestic and commercial facilities. The experiments have been completed in Shenzhen, Republic of China. As is shown in Figure 3.39, the heat pump is used to heat the supply city water from its initial temperature (15°C on average) to above 40°C in the water-to-water heat exchanger ($WWHE$), and to provide space heating in the air source evaporator(AE). The reported COP varies between 3.69 and 5.70, resulting in an estimated payback period of 5.5 years.

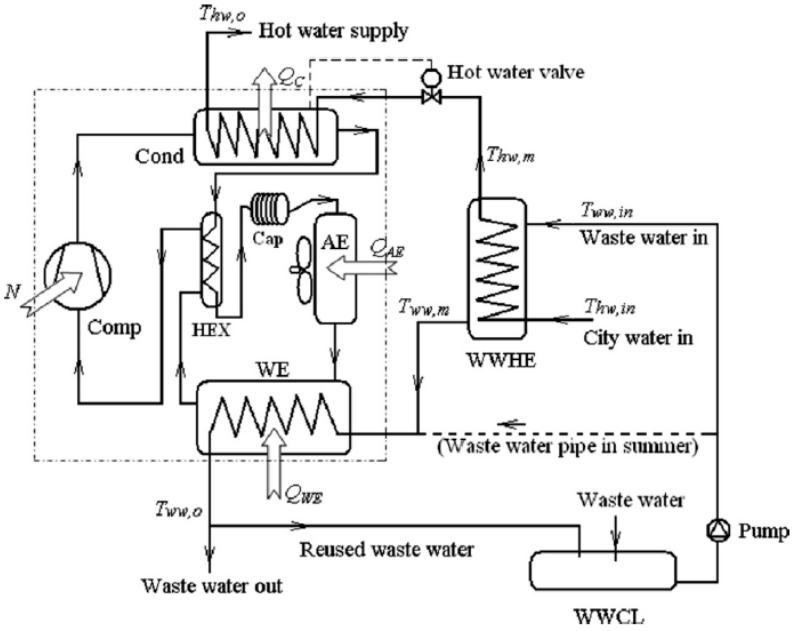


Figure 3.39.: Schematic diagram of the Multifunctional heat pump system. [Wang et al., 2013]

In Liu et al. [2013*b*,*a*, 2014b] a similar grey water heat recovery system is proposed and tested in a laboratory setting in different operating conditions. The heat pump utilizes four different heat source settings, to provide domestic hot water, and space-heating and -cooling. The domestic hot water is heated from 30 to 48.9°C. The four proposed settings are:

- Air source heat pump
- Wastewater source heat pump
- Both systems in parallel
- Both systems in series

The air temperature is set at 1.1, 8.3 and 15.6°C, the wastewater temperature is considered to be 21.1°C. The set-up is described in Figure 3.40.

Liu et al. [2013*b*] describes the operation of this system in heating mode (indoor temperature 21.1°C). The COP of the wastewater source only is lower than the air source in case the outside temperature is 15.6°C, in other situations it's higher. Generally the parallel system has the highest COP, it varies between 3.8 and 6, depending on the outside air temperature. The authors further claim that the lower-bound performance estimate of the multifunctional heat pump is superior to the performance of classical air heat pump systems.

The operation in cooling mode of the same system is described in Liu et al. [2013*a*], at outdoor temperatures of 29.4, 35 and 40.5°C, and an indoor temperature of 26.7°C. The tested grey water temperature are 23.9, 29.4 and 35°C. Again the performance of the parallel system is generally superior to the other systems, with a COP varying around 4. The authors further claim that the lower-bound performance estimate of the multifunctional heat pump is superior to the performance of classical air heat pump systems.

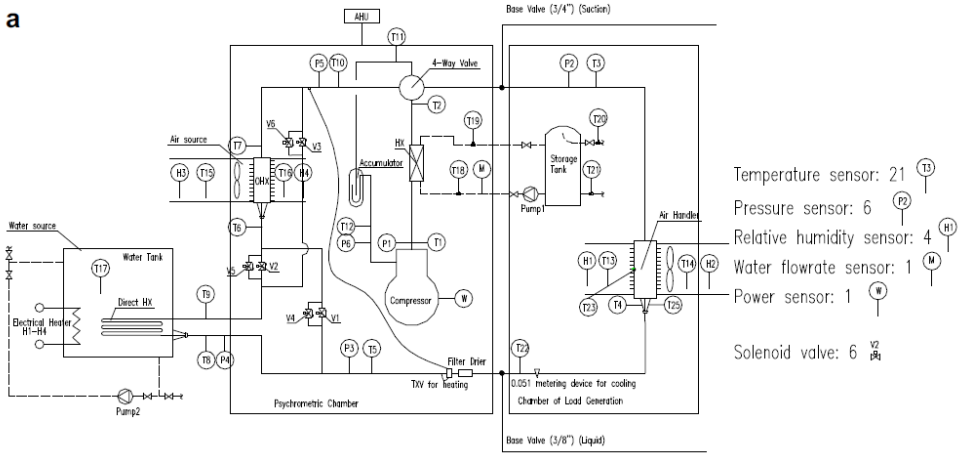


Figure 3.40.: Schematic diagram of the prototype multi-functional heat pump system [Liu et al., 2013*b*]

In Liu et al. [2014b] the authors discuss three problems occurring in the prototype as designed in Liu et al. [2013*b*,*a*]:

- Heating and cooling modes require different amounts of refrigerant.
- The COP of the singular hot water supply mode is low.
- The outdoor air temperature has a large influence on system performance, even in wastewater source operating mode.

In order to counter these problems the authors propose four adjustments:

- Installing a liquid receiver in order to balance the difference in required refrigerant in different modes (cooling and heating). This allows for the regulation of the amount of refrigerant when using different heat sources as well.
- An extra plate heat exchanger is installed in the hot water supply system in order to improve its performance.
- A thermal expansion valve is installed.
- A ball valve is installed at the air source heat exchanger in order to limit the effect of outside temperature on operating performance.

In a combined space heating and and domestic hot water mode these modifications lead to an increase in COP of 22.89, 24.55, 19.61 and 27.77% for the different heat source respectively, but the performance of parallel systems remains superior to other heating sources.

The theoretical study for a multi-source heat pump with heat source air and wastewater, or ground and wastewater, could provide a solution for individual residence heating, where the base of the heat is delivered by the air or ground, and the wastewater can be used to increase the temperature in the evaporator, thus reducing the temperature lift and improving the COP of the heat pump (see Section 5.4.2).

In addition to the multifunctional, multi-source heat pumping systems described here, the potential of direct heat recovery as a subsystem of multifunctional heat pumps would provide a contribution to current scientific literature. In the literature described above the system is considered as a single package, but the system could be viewed as a combination of different modules, which begs the question under which conditions the different modules should be added or activated. Research on the optimal conditions for activating different functions of the multifunctional heat pumps, and when each of these functions is cost-effective.

3.4.5. Untreated Sewage Source Heat Pumps

Recognizing the problem of fouling in untreated sewage source heat pumps, amongst others described in Song et al. [2006], a system with auto-cleansing equipment is proposed in Liu et al. [2014a], this equipment's operating principle is shown in Figure 3.41. The characteristics of a heat pump using this system are tested under typical operating conditions. The results indicate that 80% of the thermal resistance is made up by the convective resistance and the fouling resistance. The observed COP of the heat pump unit and the total system respectively are 4.3 and 3.6, with a heating capacity of 500 kW. In cooling mode the COP is 5.5 with a capacity of 700 kW.

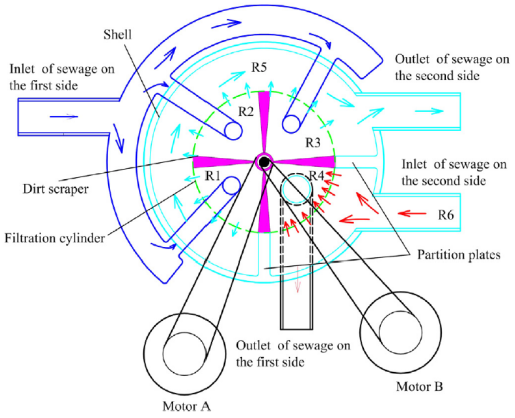


Figure 3.41.: The avoiding-clogging equipment. [Liu et al., 2014a]

In Shen et al. [2014] a novel Dry-Expansion Shell-and-Tube Evaporator with a de-fouling function was developed, in order to tackle the same fouling problem. Experimental results presented show an improvement in COP with increased flow rate. A steady state model estimated the heating capacity of the system to be between 13.8 and 15.5 kW. The authors claim that fouling resistance should remain below $2.5E{-}4\ m^2K/W$.

In Spriet and Hendrick [2017] a run of the sewer heat exchanger is proposed, to provide the heat for the evaporator indirectly (see Figure 3.42). The fouling build-up is neglected in the analysis, following the claim of the local sewer manager that such problems will not occur when the auto-rinsing flow speed of 0.6 m/s is reached. An average simulated heating capacity varying between 6.5 and 6.8 kW was reported, with a simulated COP of 3.5. The authors state that profitability increases with increased amount of heat recovered, and thus with increased operation time. However favourable electricity tariffs are required, in order to be profitable compared to gas systems.



Figure 3.42.: The heat exchanger described in [Spriet and Hendrick, 2017]

In most papers the heat recovery systems are evaluated on the basis of an energetic or financial analysis, however Li and Li [2010] proposes the use of exergy, also known as energetic quality, as the considered unit. Based on the 2nd law of thermodynamics, in a heating system exergy is lost when the temperature is decreasing. The authors state that the exergetic performance of a wastewater heat pump is superior to the one of a ground source heat pump. The calculated exergy loss in winter is smaller than in summer, and the (energetic) COP in the proposed system varies from 3.34 in summer to 3.80 in winter.

Ma et al. [2017] describes two staged series of heat pump water heater dealing with large temperature differences, the system is shown in Figure 3.43. The authors simulate the performance factor of the system to find the optimum middle operating point. This method ensures a pattern operating in large temperature difference but in small flow at both the hot and cold sides. It also avoids the lasting elevation of condensing temperature and the constant reduction of temperature in evaporation, which helps to facilitate the stability and optimal performance of the operating unit. The observed COP reached values of up to 5.4

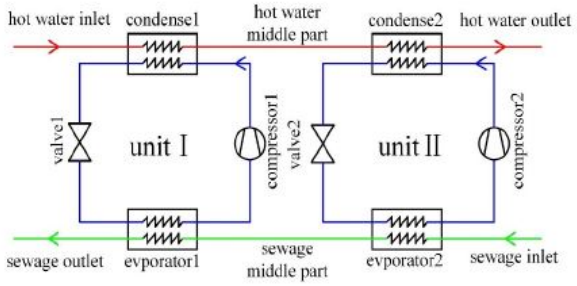


Figure 3.43.: Construction system of the sewage-source heat pump heater unit dealing with large temperature difference [Ma et al., 2017]

3.4.6. Temperature and wastewater treatment

Certain treatment processes in wastewater treatment plants are temperature-sensitive, namely nitrification. From the perspective of water quality it is important to ensure that heat recovery does not adversely affect the operation of the wastewater treatment system. Wanner et al. [2005] reported a study on the wastewater treatment plant of Zurich, Switzerland. The study showed that during the cold season, the effluent temperature is about 0.7° higher than the influent temperature and that nitrification is not affected by a decrease of the influent wastewater temperature lasting for a couple of hours only, but is significantly affected by a longer lasting temperature decrease.

In Simperler [2015], the wastewater temperature and its development in the sewer is analysed. The evaluation of the data, measured from 18 measuring points in one sewer main over a period of five months, revealed even though wastewater enters the sewer with an average of $19.5°C$ it decreases to a certain level in the main sewer. This wastewater temperature level increases by around $2°C$ every month between March and July. The temperature increase over time was mainly driven by changes in soil temperature.

Kretschmer et al. [2016b] introduced a methodological framework to evaluate the suitability of a potential heat recovery site integrating both the energy supply and water quality control requirements. It includes decision support criteria and planning principles for energy planners and water authorities.

3.5. Case studies of existing systems

In this section existing, functioning projects, recovering heat from wastewater, are discussed, most of them are located in Switzerland (Ch), but projects also exist in Norway (No). All of the discussed projects are indirect heat recovery schemes, systems providing solely heating or both heating and cooling can be found. An example of the in-sewer heat exchanger is shown in Figure 3.44.



Figure 3.44.: Heat exchanger in the sewer in Zurich, Switzerland. [Leuenberger, 2006]

3.5.1. Sports infrastructure in Basel(Ch)

In Basel, Switzerland, residual heat from wastewater is used to heat the locker rooms, for a sports centre, using floor heating, and to heat the water for the showers. This system was installed in 1982. The sport infrastructure consists of several football (soccer) fields, and an athletics track. The fields are heavily used in summer when wastewater temperature is higher, and less so in winter when the temperature of the wastewater is lower. This results in a very large COP of around 7. ([Schmid, 2008])

In 2001 the heat pump was replaced, and the heat exchanger inspected thoroughly. The conclusion for the heat exchanger was that it could still operate for the next 20 years.([Leuenberger, 2006])

3.5.2. Public buildings in Binningen (Ch)

In Binningen, close to Basel, Switzerland a heat recuperation system was installed on the wastewater circuit in 2001. A network of 3.5 km provides the heating for 70 buildings, including public buildings and residential houses (600 apartments), the specific demands are given in table 3.3. The electricity for the heat pumps is delivered by a cogeneration system, three peak burners are used to dampen consumption peaks.

Heat consumption	4800 kW
Heat output from the heat pumps	$2 * 380$ kW
Amount of heat delivered from wastewater	14%
Length of the heat exchanger	140 m
Heat exchanging capacity of the heat exchanger	330 kW

Table 3.3.: General parameters of the heating network in Binningen

Yearly the heat exchanger delivers 2.4 $Million$ kWh of heat to the system for water and space heating, the specifics for the heat exchanger are given in table 3.3. Around 30 000 people are connected to this network. Up until 2006 no break downs were recorded, and no cleaning was needed for the heat exchanger.([Leuenberger, 2006])

3.5.3. Education center in Loewenberg (Ch)

In 1983, a six-building education center was built in Loewenberg, Switzerland. Here the wastewater is both used for heating and refrigerating. On one hand it's used to heat the buildings and heat sanitary hot water, the other use of the connected heat pump is to cool down iced water.

The electrical power input of the heat pump is delivered by cogeneration, and the heat is recuperated at the exit of a nearby purification plant. The general characteristics are given in table 3.4.([Leuenberger, 2006])

Yearly heat consumption		870 000 kWh
Yearly refrigeration consumption		320 000 kWh
Heat pump	**Heating power**	$2 * 390$ kW $COP = 4.1$
	Cooling power	$2 * 370$ kW $COP = 4.9$
Amount delivered from wastewater		48 %
Power by cogeneration	**Work**	190 kW
	Heat	256 kW

Table 3.4.: General parameters of the heating network in Loewenberg

3.5.4. Appartments in Winterthur (Ch)

In Winterthur, Switzerland, the wastewater from over 150 000 inhabitants to heat around 400 appartments. According to a study ordered by the city council of Winterthur, the use of wastewater as a heat source represents 12% savings with respect to the use of natural gas to heat the apartments.

The heat exchanger is installed on a by-pass of the general sewer system. The advantage of this approach is that the amount of water entering this by-pass channel can be controlled, the heat exchanger can thus operate at it's optimal design point at all times. Another advantage is that the installation of this system didn't effect the wastewater flow.

The general characteristics are given in table 3.5.([Leuenberger, 2006])

Number of appartments	400
Length of the network	200 m
Required heating power	1150 kW
Heat pump power	850 kW
Amount delivered from wastewater	70%

Table 3.5.: General parameters of the heating network in Winterthur

3.5.5. Commercial buildings in Schaffhouse (Ch)

In Schaffhouse the wastewater is used to heat and condition some 2000 apartments. The system was installed at the same time as the construction of new buildings. The project started in 2001. General information on the project is given in table 3.6.([Leuenberger, 2006])

3.5.6. Living area in Sandvika (No)

Due to the growth of Oslo in the 1980's a new city center of 300 000 m^2 was built, using collective heating and conditioning of the buildings. A study comparing different heating and refrigerating options showed that the combination of wastewater and a heat pump was the most viable option, both economically and ecologically., thanks to the combination of heating and refrigerating. In order to be able to achieve simultaneous heating and refrigerating two parallel networks are installed.

Volume of the heated rooms		21 000 m^3
Required heating power		600 kW
Required conditioning power		400 kW
Heat pump power		370 kW
Power of the refrigerating machine	**In winter**	242 kW
	In summer	324 kW
Amount delivered from wastewater		25%

Table 3.6.: General parameters of the heating network in Schaffhouse

The heat recovery system is installed on a sewer with a flow of 3000 l/s, due to this large flow, the heat exchanger that would be needed to extract the heat would be very large, and this space is not available. Therefore the wastewater serves directly as a heat source for the heat pump, after filtration. The schematic of the plant is shown in Figure 3.45.

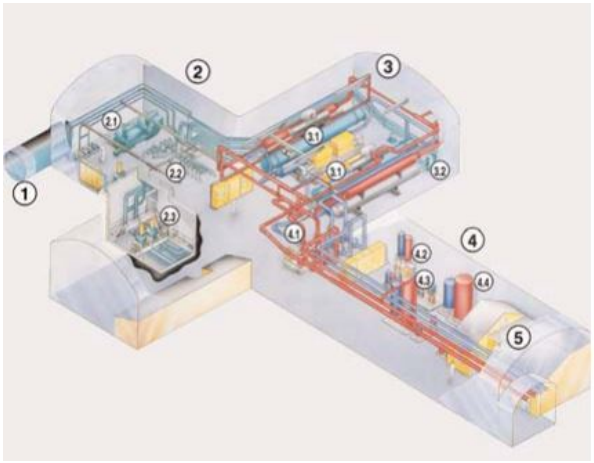


Figure 3.45.: Schematic of the Sandvika DWHR system. [Leuenberger, 2006]

The energy production is realized by 3 plants:

- One plant for the base load, consisting of the heat pumps. This plant is installed directly on the sewer system.
- The second plant consists of three oil burners, used to dampen consumption peaks.
- The third plant consists of a refrigerating machine.

The excess heat of the wastewater system can also be used to defreeze frozen boardwalks, however this is not permitted in every country. General information on the project is given in table 3.7.([Leuenberger, 2006; Friotherm, 2005])

Number of buildings	**Heating**	56
	Conditioning	18
Length of the network	**Heating**	10 km
	Conditioning	4 km
Required Power	**Heating**	22 000 kW
	Conditioning	10 000 kW
Output Power	**Heat pump**	2 $*$ 6500 kW
	Refrigerating machine	2 $*$ 4500 kW
Amount delivered from wastewater		50%

Table 3.7.: General parameters of the heating network in Sandvika

3.5.7. Kakola heat pump plant (Fi)

In the city of Turku, Finland, a municipal scheme, using wastewater from a wastewater treatment plant, serving 10 000 users was reclaimed in the beginning of 2009. The plant fits in Turku Energia Environment's target of 50% renewable energy by 2020. The heat pump plant in Kakola will cover approximately 80% of the yearly cooling needs and 10% of the yearly heating needs. The estimated annual reduction in greenhouse gas emissions is 45 000 $-$ 50 000 $t\ CO_{2,eq}$.

The heat pump plant is used as a heating source for the district heating network, which operates at $90°C$, adjacent to the heat pump plant a 17 000 m^3 water accumulator is installed, used to balance the daily fluctuations in the district cooling network. The heating output is 19.5 MW, providing 170 GWh_{th} in 2010, and the cooling output 13.0 MW providing 70 GWh_{th}. The average COP in 2010 was 3.3 Niemela and Saarela [2014].

3.5.8. Swimming pool in Hasselt (Be)

In this project in Hasselt, Belgium, the water flowing out of the Intercommunale WaterMaatschappij (IWM) is used as a heat source. IWM produces drinkable water and provides it to the residences in Hasselt. The heat recovered in the wastewater from IWM is used to heat a swimming pool, using a heat pump. This project started in 2013. General information on the project is given in table 3.8. ([Dumas, 2014])

Heated building	Swimming pool
Length of the network	180 m
Heat exchange surface	35 m^2
Temperature of the wastewater	$15°C$
Heat pump power	433 kW
Amount delivered from wastewater	$95 - 100\%$

Table 3.8.: General parameters of the heating network in Hasselt

3.5.9. Inners project in Leuven (Be)

In 2014, a project was inaugurated using a wastewater source heat pump to heat 92 social residences in Leuven, Belgium. The temperature of the heating network is $45°C$, (30 upon return), and the heating power of the heat pump is 250 kW. The wastewater temperature decreases from 15 to $10.5°C$ on average, and the overall system COP is 3.2. The heat recovery system delivers around 60% of the total annual heat demand, the rest is delivered by gas boilers. [SMET, 2016]

3.5.10. Heat recovery scheme at Scottish Borders college campus in Galashiels (UK)

At the Scottish Borders college campus in Galashiels, United Kingdom, a wastewater source heat pump scheme provides up to 95% of the heating requirements of the campus. Scottish water is planning on expanding this heat recovery projext, and deploying wastewater source heat pumps over its entire network, collaborating with SHARC Energy Systems. Scottish Water [2017]

3.5.11. The role of additional pilot plants

Although multiple examples of drain water heat recovery projects exist, they mainly focus on repeating a same, proven technology. Current indirect heat recovery systems often focus on sewage heat recovery, or effluent heat recovery for wastewater treatment plants, and on shower heat recovery for direct heat recovery systems. Heat recovery from industrial wastewater, and from the kitchen sector, has largely been ignored so far. Hybrid heat recovery was not applied as of yet (to the knowledge of the author), and centralized direct drain water heat recovery was not applied either. The research presented in this thesis aims at addressing these gaps, through demonstration sites, and prototyped development.

3.6. Summary

Resource recovery from wastewater has traditionally focused on chemical energy, through the form of biogas. However the density of thermal energy in wastewater is threefold the chemical energy density, for a given wastewater flow the recoverable thermal energy is thus three times the potential recoverable chemical energy. To recover this embedded thermal energy, three different heat recovery systems, direct, indirect and hybrid heat recovery were described. The choice between those three types of systems depends on the characteristics of the wastewater flow.

Two important aspects regarding the operation and analysis of drain- and wastewater were identified, temporal aspects, and spatial aspects. The temporal aspect, found in literature is mainly approached from a heat availability perspective, a methodology for temporal matching of supply and demand is not described in literature. Chapters 5 and 6 describe and apply such a methodology.

The spatial aspect is extensively reported in literature, where the emphasis lies on the use of wastewater treatment plants as regional energy cells, and integrating them in local energy distribution networks, such as district heating. However, a combination of both the spatial and temporal aspects for this type of heat recovery has not yet been reported, this is described in Chapter 7.

Direct heat recovery is mainly described in literature for wastewater leaving houses, or for shower drains. Other than internal heat recovery in dishwashers, another high temperature water consumer, the kitchen, is largely left unresearched and unexploited. Chapters 6, researches the potential of heat recovery from commercial kitchens and 8 describes the design and operation of such a heat recovery system. Chapter 10, describes the development of a prototype for direct heat recovery from kitchen drains. Furthermore, centralized direct heat recovery, for example in industrial wastewater treatment plants is not discussed in literature. In Chapter 9 this is designed and studied as part of a demonstration site in a meat processing plant.

Indirect heat recovery from wastewater, both for heating and for cooling purposes is extensively studied in literature, both from the effluent of wastewater treatment plants, and from raw sewage (using and intermediary heat carrier). However, the application of hybrid heat recovery, the combination of direct and indirect heat recovery, is not often studied. Chapter 9 looks at addressing this gap for the meat processing sector.

This results in a comprehensive study of three potential exploitation strategies (Chapters 5, 6 and 7), a demonstration of the difference in design methodology for different scenarios (Chapters 8, and 9) and the development of a prototype to complement existing heat recovery technology and fill a gap in the market.

4. Research Methodology

4.1. Introduction and general outline

This research aims to address three research questions (enumerated below), regarding the development and exploitation of recovering thermal energy from drain or waste water, called Drain Water Heat Recovery (DWHR), as discussed in Section 1.4.2.

1. How can DWHR contribute to the current heating mix, and to reaching emission reduction and renewable heating targets?
2. How do varying conditions in different sectors affect the design of DWHR systems? How can DWHR be implemented?
3. How can the current set of commercially available DWHR system be complemented or extended?

One can observe that these questions are interconnected, as, for example, the design of the DWHR system has an impact on the recovered energy, and thus impacts the contribution to the current heating mix. Another example is that the study of potential contribution of existing DWHR systems to the current heating mix, can highlight gaps in the market, where unexploited potential is available, and the current set of DWHR systems can be complemented.

These research questions provided the background for the main investigative axes used in this research thesis, which are summarized in Figure 4.1. The potential for the contribution of DWHR to heating mix (research question 1), was studied by considering the exploitation strategy (Section 4.3). The impact of different conditions on the design (research question 2) was put forward in the design of the demonstration sites (Section 4.4), and the prototype design (Section 4.5). The extension of the set of available DWHR systems (research question 3), was considered by development of a prototype heat recovery system (Section 4.5). The data for all three of these investigative axes was delivered by an extensive monitoring campaign (Section 4.2).

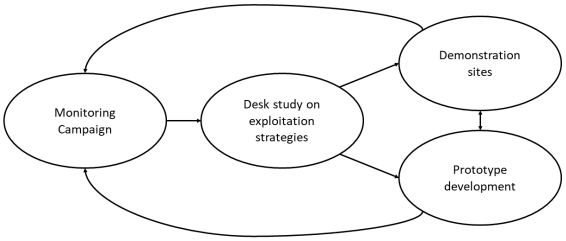


Figure 4.1.: General outline of the principal investigative axes.

These investigative axes deal with a different scale of investigation into DWHR system (see Figure 4.2), the exploitation strategies (research question 1), deal with the potential and impact of DWHR on a regional scale. The demonstration sites (research question 2) highlight the importance of local conditions, and look into the integration of DWHR system on a building or plant scale. Thirdly, the prototype development (research question 3), acts on a system scale, as it aims at developing and design a novel DWHR system. All these scales interact with each other, as the integration in a building or plant has an impact on the regional potential, and the detailed design of a DWHR system impacts, in turn, the integration in the building or plant.

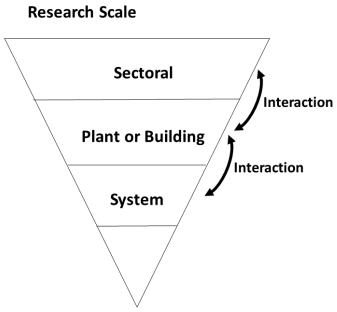


Figure 4.2.: Scale of the different investigative axes and their contribution to the scientific literature.

This chapter discuss the methodological approach, and underlying reasoning for each of the principal investigative axes.

4.2. Monitoring campaign

Wastewater and its characteristics are often not monitored in processes and buildings, as they are not billed. Generally, daily flow values are available for wastewater treatment plants, with a rare few wastewater treatment plant measuring temperatures. For buildings, processes and industries the flow was estimated through a proxy, which can be the clean water consumption, the amount of meals consumed, or others. This section describes the materials used to measure and/or estimate the wastewater flows and temperatures.

The monitoring campaign started on an individual, domestic residence level, as heating is generally provided on an individual customer level (see Chapter 5). A monitoring campaign of up to a year long was held at four different residences. Literature mentioned the importance of the wastewater flow rate, when considering the financial feasibility for indirect heat recovery systems, and the importance of high temperatures and proximity to the consuming appliances for direct heat recovery systems. For this reason the continuation of this monitoring campaign focused on two different sectors; commercial, large-scale kitchens, and industrial, on-site wastewater treatment systems. One multi-residence (10 residences) wastewater treatment system was also considered (see Appendix B).

Commercial kitchens have the advantage, compared to domestic wastewater, of a higher temperature of the wastewater. Commercial kitchens were selected, as they are characterized by larger flows (than domestic ones), and have a mandatory installed grease trap, which provides a suitable locations for temperature monitoring. A monitoring campaing of three weeks, up to a year was performed at four different commercial kitchens (see Chapter 6). A pilot system was installed and tested at one of these sites (see Chapter 8), and a prototype heat recovery system was developed (see Chapter 10).

Industrial on-site wastewater treatment systems, for example at large industrial factories, have the advantage of the availability of large wastewater volumes, at locations close to the consumer (the industrial facility). Three different industrial wastewater treatment systems were monitored (see Appendix B), for at least three weeks. And a pilot system was installed and tested at one of them (see Chapter 9).

Process data from 540 municipal wastewater treatment plants in the Republic of Ireland was also collected, and a study on the heat recovery potential was performed (see Chapter 7)

In case no process data was available at the studied location (for example from a SCADA system), Feasibility studies were based on a monitoring campaign of the temperature, and estimations of the drain water flow. These methods are outlined below.

4.2.1. Temperature Considerations

The temperature was generally measured using TinyTag temperature sensors, shown in Figure 4.3. These sensors have a programmable logging interval, and operate independently with an internal logger and battery. The data can be downloaded using an inductive pad. The operating interval is -40 to $70°C$, its datasheet can be found in Appendix A. The temperature was monitored in campaigns during a period ranging from minimum 3 weeks, to a full year.



Figure 4.3.: The TinyTag temperature sensor.

4.2.2. Flow considerations

The flow was estimated using one of four ways:

- Measured using tipping buckets.
- Estimated based on the clean water flow.
- Estimated based on daily averages made public for authorisation procedures.
- Data received from SCADA systems.

Depending on the scale, the available and the sector, one of these ways was employed to estimate the wastewater flow. This is detailed below for different sectors.

Domestic wastewater

The domestic wastewater flow was measured using tipping buckets, which were installed on site in the framework of the research project presented in Knappe [2018]. In this research the wastewater flow was measured using tipping buckets, the readings were monitored using reed switches. With each tip a normal-open reed switch was closed by a magnet attached to the tipping bucket. The counts were then converted to a wastewater flow value by calibrations, performed in situ. For more details, the reader is referred to Knappe [2018]; Knappe et al. [2020]. The installation of the tipping bucket distribution box is shown in Figure 4.4).



Figure 4.4.: Installation of tipping bucket distribution box: inlet effluent pipe (left), distribution box receiving effluent (middle), closing of the reed switch assembly (right)[Knappe, 2018].

At these locations the soil temperature (and the volumetric water content and electrical conductivity) was also measured in the aforementioned project, using two different types of soil sensors, type EC5 (a capacitive sensor) and type GS3, where the temperature was measured using a thermistor. [Knappe, 2018]

Wastewater from commercial kitchens

The wastewater discharged through the kitchen drain is estimated as 90% of the kitchens clean water consumption, which is a slightly more conservative estimate than the one described in Butler and Davies [2010]. The clean water consumption was either measured or estimated based on a proxy, the amount of meals consumed. This strategy, originally proposed in Bromley-Challenor et al. [2013], associates a certain water consumption which each meal served, which depends on the type of food outlet which is considered. This is summarized in Table 4.1.

	Water consumption ($l/meal$)
Restaurant	25
Quick Service Restaurants (QSR)	12
Pubs	12
Leisure	20
Staff catering	18.5
Health care	25
Eductation	18.5
Services	25

Table 4.1.: Water consumption per meal served in different types of food outlets.

Municipal and industrial wastewater treatment plants

The wastewater flow in wastewater treatment plants is either measured by their SCADA system, or estimated based on the information on hydraulic loading, which each wastewater treatment plant is required to provide in the annual environmental reports, as a part of the procedure for their wastewater discharge authorisation [Environmental Protection Agency, 2018].

4.3. Desk study on exploitation strategies

The desk studies aim at providing an overview of the realistic potential for heat recovery from wastewater, at different locations in the water cycle. As can be seen in Figure 4.5, heat can be recovered at different locations in the water cycle, these desk studies investigate the potential at three of such locations:

- At the exit of an individual residence (domestic) (see Chapter 5).
- At the kitchen drain (see Chapter 6).
- At the effluent of wastewater treatment plants (see Chapter 7).

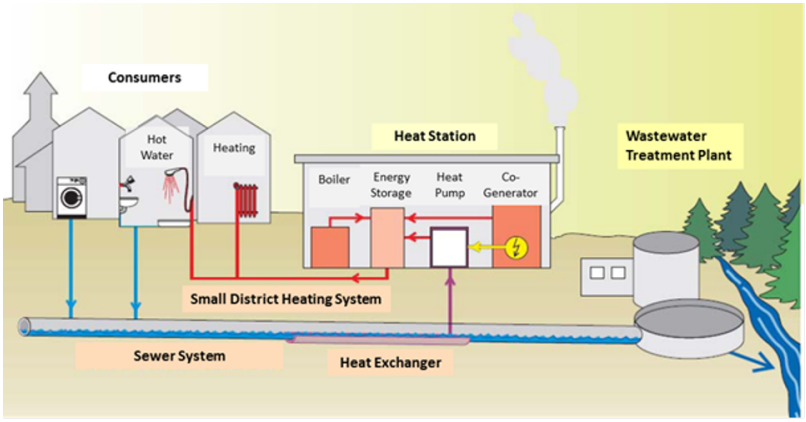


Figure 4.5.: Schematic of Sewer Heat recovery adapted from [Müller and Schmid, 2005].

In these desk studies, the potential for the full sector (domestic residences, commercial kitchens, and wastewater treatment plants) was studied. The domestic sector and the sector of commercial kitchens was studied using a probabilistic method, based on Monte Carlo simulations (see Section 4.3.1). This method accounted for the temporal variations of both heat supply and demand. In the domestic sector, the method was also applied to a generalized, Irish residence.

In the sector of wastewater treatment plants, a spatial method was applied on all licensed wastewater treatment plants (WWTPs) in the Republic of Ireland. This method assessed the potential in the sector (See Section 7.2), taking the spatial proximity of consumers to the WWTP into account. After that a specific, newly developed, spatio-temporal analysis was performed on the Tullamore wastewater treatment plant, adding the temporal variation of supply and demand to the spatial analysis. This method is described in Section 4.3.2.

The key methodologies for these desk studies are described in this section.

4.3.1. General methodology for potential in a sector

The potential for heat recovery from domestic, single-residence buildings (see Chapter 5), and from commercial kitchens (see Chapter 6), was estimated, considering variation in heat availability and consumption in time. The general steps in the employed methodology are described in this section, whereas the details are explained in the respective chapters. Spatial proximity between the heat recovery location and the heat consumer was not a factor in these studies, as the consumer and wastewater source are the same in these two cases.

System set-up

The system set-up is an important consideration in these desk studies, as it will significantly affect the amount of heat that can be recovered, and the temperature at which the heat is available. The three considered options, as described in Section 3.2.1, Chapter 3 are listed below:

- Direct Drain Water Heat Recovery.
- Indirect Drain Water Heat Recovery.
- Hybrid Drain Water Heat Recovery.

Temporal analysis

Variation in time in both the available thermal energy in the wastewater, and the heat consumption were considered in estimating the total potential for recovery of heat from the wastewater. Mismatches in time reduce the amount of exploitable energy, recovered from the wastewater, when no suitable thermal storage systems are available. The desk studies investigating heat recovery from domestic residences consider variations over the 24 hours in a day, but also over the whole year. The heat recovery from commercial kitchens is investigated, considering the variation over the 24 hours in a day, as this is within a building the impact of external variations such as the seasonal ones is considered negligible, this is confirmed by the commercial hot water consumption profiles in Ramboll [2019].

To account for this temporal variation, in the case of the wastewater flow, and the thermal energy consumption synthetic load profiles (SLP) were used. Thes SLPs show how the consumption at a certain point in time, relates to the mean value. The details are shown in the respective chapters Pillai et al. [2014].

Monte Carlo simulations

The Monte Carlo method is a probabilistic method, based on repeated random sampling of the parameters. This method is often used for simulating systems with coupled degrees of freedom, and uncertainties on the inputs. Both of which are present in the problem of estimating the recoverable heat from wastewater, and its interaction with the heating system(s). For example, the domestic hot water consumption and wastewater flow are directly coupled, and uncertainties exist on the drain water temperature, and the predicted hot water consumption. The underlying principle is to solve problems using the distributions of the input parameters, rather than solving them in a deterministic way.

The key steps in the Monte Carlo Method are as follows:

- Defining the domain and the probability function of the input variables.
- Generating a fixed amount of random sets of the input variables, based on their probability distribution.
- Performing a deterministic calculation for each of these sets of inputs.
- Describing the results as a statistical distribution.

The results can thus be represented as a statistical distribution of their own, with a related confidence interval, rather than as a single value. This simulation method was used for the sectoral analysis of both domestic residences and commercial kitchens (Chapters 5 and 6, in order to create a generalized profile, based on a monitored sample of residences or kitchens. Rather than sampling straight from the observations, the observations were used to create a statistical distribution, from which the parameters were then sampled. This was done in this way because these distributions form an approximation of the situation in the respective populations, whereas sampling from the observed data would only be representative for the sample (ie. the residences and kitchens which were part of the monitoring campaign). The drawback of this method is that the distribution could be strongly influenced by an anomalous representative in the sample (ie. a kitchen or residence with a significantly different usage pattern than the population average).

Financial comparison method: Levelized cost of Energy

Investment in drain- and wastewater heat recovery system are generally paired with an additional investment cost, and reduced operation costs. In order to make a trade off between reduced fuel costs, and increased capital investment, the Levelized Cost of Heating Method (LCOH) is employed, represented by Equation 4.1.

$$LCOH = \frac{\sum_{n=1}^{lifetime} \frac{I_n + M_n + F_n}{(1+r)^n}}{\sum_{n=1}^{lifetime} \frac{E_n}{(1+r)^n}} \tag{4.1}$$

Table 4.2.: Parameter for LCOH calculation

Investment cost	I_1
Maintenance cost	M_n
Fuel cost	F_n
Yearly consumed heat	E_n
Discount rate	r

The parameters of Equation 4.1 are described in Table 4.2.

Financial comparison method: The Net Present Value method

The NPV method is an economic valuation technique discounting future net cash flows (NCF), resulting from a current investment, with a given discount rate (r), and summing them together. The optimal investment is considered to be the one creating the largest economic value, hence the largest NPV-value, over the targeted period [Žižlavský, 2014]. The employed formula is given in Equation 4.2.

$$NPV \;=\; \sum_{t=0}^{n} \frac{NCF_t}{(1+r)^t} \tag{4.2}$$

Environmental comparison method: Total Equivalent Warming impact

To estimate the environmental impact of the different heating systems, the Total Equivalent Warming Impact (TEWI), divided by the produced heat was considered. The TEWI, is based on the emissions related to the functioning of the heating devices, the emissions related to construction and decomposition of these devices were considered to be negligible compared to the emissions related to the fuel [Zottl et al., 2011]. The formula for heat pumps is given in Equation 4.3, where GWP_{refr} is the global warming potential of the refrigerant, L the leakage rate, n the lifetime, α_{recov} the refrigerant recovery rate, E_{cons} the electricity consumption and K the carbon intensity [SEAI, 2017*b*].

$$TEWI \;=\; GWP_{refr}\; L\; n \;+\; GWP_{refr}\; m_{refr}\; (1-\alpha_{recov}) \;+\; E_{cons}\; K_{el}\; n \tag{4.3}$$

Similarly, the formula for fossil fuel boiler systems is given by Equation 4.4, where $Cons_{fuel}$ is the fuel consumption.

$$TEWI \;=\; Cons_{fuel}\; K_{fuel}\; n \tag{4.4}$$

The advantage of using the TEWI method, compared to simply reporting on the reduced greenhouse gas emissions, is that the global warming potential of the refrigerant leakage is also included.

4.3.2. Spatio-Temporal Analysis for potential in a WWTP

In the case of heat recovery from wastewater treatment plant, the location of the consumer of the recovered heat, and the proximity of that consumer to the treatment plant is not as straight forward as with smaller scale heat recovery systems. That is why a spatial component was added when studying heat recovery at the level of wastewater treatment plants.

Three main steps were followed in the analysis of heat recovery from effluent in wastewater treatment plants:

- Energetic analysis.
- Spatio-Temporal analysis.
- Integrated analysis.
- Describing the results as a statistical distribution.

The energetic analysis studies the amount of recoverable heat at the level of the wastewater treatment plant, and looks at the consumption at the same level. This leaves an excess of energy, the spatio-temporal analysis studies how this excess energy can be distributed over space and time. Looking into potential consumers in proximity to the treatment plant, and temporal profiles of supply and demand. The integrated analysis overlaps these profiles for the selected areas, looking into the need for additional heating sources, and for additional heat sinks in case of excess energy. The method is summarized graphically in Figure 4.6.

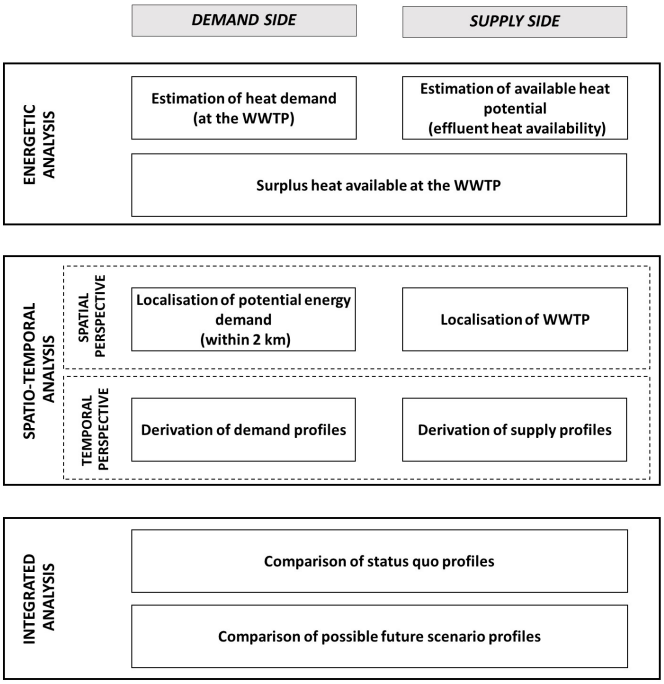


Figure 4.6.: Graphical summary of the key steps in the spatio-temporal analysis.

4.4. Demonstration sites

Based on the desk studies, two sectors were selected, commercial kitchens, and an industrial, full-scale wastewater treatment plant, for the development of a demonstration site, demonstrating the operation and viability of different heat recovery techniques.

4.4.1. Site selection

The site selection included different criteria:

- The heat recovery potential.
- The proximity of the wastewater drain or treatment works to the heating system.
- The possibility for visits to the demonstration sites.
- The opportunity for testing experimental, innovative methods.

4.4.2. Design of the heat recovery system

The concept of both heat recovery systems is to combine commercially available, off the shelf components, and integrate them in a novel way, taking into account the following characteristics:

- Characteristics of the wastewater.
- Conditions and positioning of the heat recovery site in the lay-out of the plant or building.
- Requests of the plant owner or manager.
- Uncertainties in the feasibility study.

This resulted in two very different systems in the demonstration site:

- A fixed, direct heat recovery system at Penrhyn castle, Wales (see Chapter 8).
- A moveable heat recovery system, combining direct and hybrid heat recovery at the meat processing factor of ABP food group in Cahir, co. Tipperary, Ireland (see Chapter 9).

The approach of using existing, available components drives down capital costs, and allows for a relative ease in maintaining the system. As spare parts are commercially available, and contractors have experience with these components.

4.4.3. Construction and installation of the systems

The approach for the construction of the system was the same for both demonstrators. The concept of both demonstration site is to combine existing, off the shelf components, and to assemble and integrate them in a novel way, in order to achieve heat recovery at the selected sites.

The installation of the system was performed differently in both cases. Penrhyn castle, being a historic, protected site, requires specific certifications for the contractors operating on site, limiting the choice of contractors. Here, the installation was performed by an external contractor, also delivering the plumbing and piping components to the system.

One requirement for the demonstrator at the ABP meat processing plant, was to be moveable. This moveable test rig was assembled in house, at Trinity College, and then transported to the ABP facilities. The advantage being close supervision, and early identification and resolving of faults in the system.

4.4.4. Monitoring the system

The monitoring of the experimental, demonstration set-ups consists of both the metering of the characteristics of interest, and subsequently the logging (storing) of the metered values. The approach for both these steps is detailed below.

Data metering

The parameters measured are the electric consumption, the temperature, the volumetric flow and the thermal energy recovered. Each of these systems is metered using a different device, and transmits the information in different ways.

The **electric consumption** is measured by modular single phase power meter, as shown in Figure 4.7. The power meter measures the electric energy transmitted through the metering unit, and the consumption is transmitted through the form of a voltage pulse.



Figure 4.7.: The modular single phase power meter.

The **temperature sensors** used in this experimental set-up are PT 100 resistance sensors, meaning that the resistance of the sensor changes with temperature. When an excitation voltage is applied, one can thus observe a change in output voltage, a temperature transmitter converts this to a standard output parameter, a signal ranging from 4 to 20 mA in this case (see Section 4.4.4). Before use, the sensor-transmitter pairs were calibrated, this is shown in Appendix H.2. The temperature sensors used in this set-up were PT 100 sensors (shown in Figure 4.8), meaning that the material is platinum, and that their resistance at $0°C$ is 100Ω. They were placed in pockets, shown in Figure 4.9.



Figure 4.8.: PT100 temperature sensor.



Figure 4.9.: Thermopocket for PT100 sensors.

The **clean water flow and recovered energy** is measured using a heat meter, which measures the flow through the device, and the in and output temperature, and calculates the energy. The energy and volume are transmitted through pulse repetition. The device is shown in Figure 4.10.



Figure 4.10.: The Itron CF Echo II heat meter.

A combined meter measuring both wastewater flow and wastewater temperature was used, measuring the wastewater flow through the pipe, and the temperature when it leaves the set-up. This was done with a MCERTS Multi Sensor Flow Meter (see Figure 4.11), this meter is intended for open water flow. As can be seen in Figure 4.12, the meter is battery powered, and has a connected data logger. It measures flow depth and velocity, and has a built-in temperature sensor.

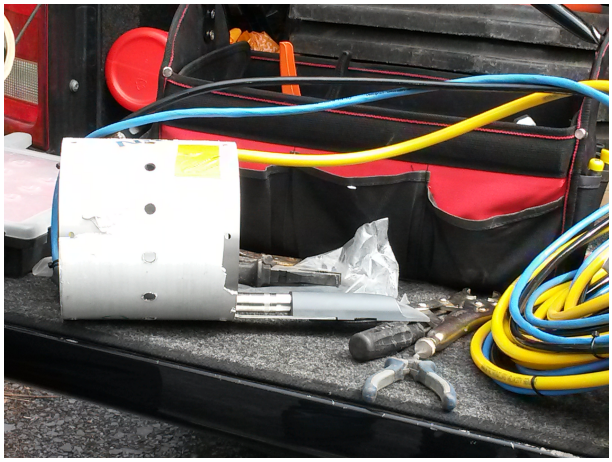


Figure 4.11.: Flow and temperature meters.



Figure 4.12.: Datalogger connected to the flow meter.

Data logging

After measurement the data is recorded (logged) and made available on an online platform. Pulses, representing the electric or thermal energy, or the volumetric flow, are counted during the logging interval (15 minutes in the cases represented in this thesis), and the temperature signal is measured at the end of each interval, by the data logger (the square box on Figure 4.13). These recorded values are then sent to the online platform (see Figure 4.14) by the transmitter (the cylinder on Figure 4.13), and converted to the physical units.



Figure 4.13.: The data logger and transmitter.

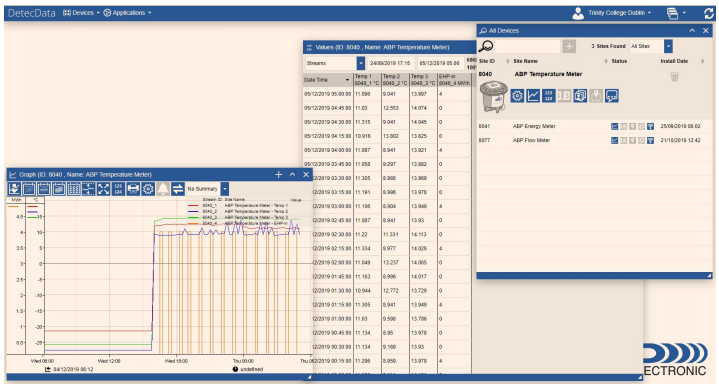


Figure 4.14.: The online data platform.

4.5. Prototype development

Rodgers [2017] describes five phases in the design thinking process for innovation, as shown in Figure 4.15. In the case of this research project, the first two steps, **Empathizing** and **Defining the problem statement** are performed in the definition of the project, and described in Chapter 1. The different phases are described below, and their implications for the project is briefly discussed.

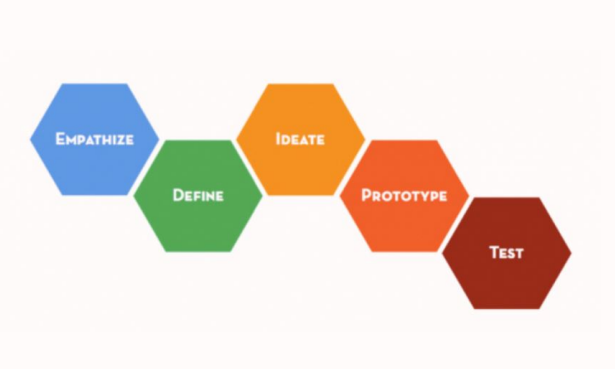


Figure 4.15.: The five phases in design thinking [Rodgers, 2017].

- **Empathize:**

Empathizing is described as observing behaviour in order to gain insight in the wants and needs of potential consumers. In our case the considered consumer are people or the part of society which are concerned about the effects of our energy consumption (and subsequently its production) on our habitat and environment. The concern is translated to the energy (in this case heat) related greenhouse gas emissions.

- **Defining the problem statement:**

Based on the concerns of this part of society, a broader problem statement was determined, and summarized in three research questions (see Section 4.1). The innovative prototype, described in Chapter 10, focuses on research question 3, but also affects the answer for both other research questions.

This thesis describes two phases of the design thinking process, the **Ideation** phase, and the **prototype** phase, and adds some lab-scale testing and simulation, which are the initial steps of the **Testing** phase. The overall flow chart of this process is shown in Figure 4.16, and the three phases, along with their implication for the project are described below.

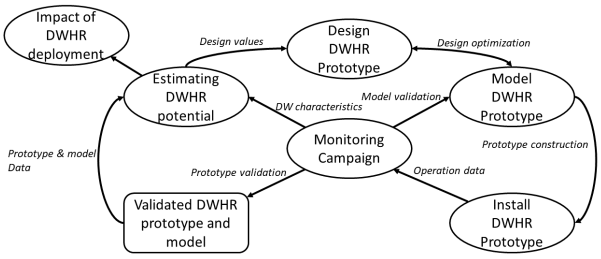


Figure 4.16.: The flow chart of the thought process for prototype development.

- **Ideate:**

Ideation is described as transitioning from identifying problems to creating solutions. In the case of this project, the monitoring campaign, along with the estimation of the Drain Water heat recovery potential, uncovered a currently untapped potential, which forms the targeted market of the prototype.

- **Prototype:**

The prototyping phase is described as the first built of the product, keeping the user in mind. In this project, a prototype was designed, built and lab tested, it served as a first proof of concept to start the conversation, but also to validate a computer model, which can be used to test improved designs.

- **Test:**

The testing phase is defined as refining the prototype and solutions. In this project, a validated computer model was used to test different design ideas and improvements. The operation in real world conditions is a logical continuation of this process.

4.5.1. Ideation phase: Translating desk studies into ideas

The idea for the prototype developed in Chapter 10 of this research thesis was developed based on four different factors.

1. The results of the studies on the different exploitation strategies.
2. Observations made during the monitoring campaign.
3. Legislation regarding the management and treatment of the particular type of wastewater.
4. Discussion with actors in the sector.

The exploitation strategy for heat recovery from commercial kitchen drains (item 1.), discussed in Chapter 6, revealed a gap in the market, where environmental and energetic savings could be made, which are currently not viable. A possible reason, identified in the exploitation study, was the lack of commercially available, specialized equipment. In this case, heat exchangers, designed for heat recovery from shower systems, were employed for heat recovery from kitchen drain water. The underlying idea was thus that equipment which was adapted for use in kitchen environments could (partially) fill this gap in the market.

Furthermore, the monitoring campaign (see Section 4.2) identified a location in the waste water cycle (the grease trap in this case), where a relatively large body of water was forced into nearly stagnant conditions. This allowed for ease of access, and available space for the fitting of a heat recovery device. In addition, regulations regarding the management and treatment of kitchen wastewater (item 3.) mandate the presence of the identified location, resulting in a large amount of potential consumers.

Lastly, different actors in the sector were contacted and these discussions revealed a general interest in reducing the temperature of the kitchen drain water in grease traps. This was part of the project framework, as feasibility studies for different enterprises were performed as part of the 'Non-FinancialSupport'-scheme (NFS).

4.5.2. Prototype phase: Construction and testing of the first prototype

The first prototype, for heat recovery from grease traps, was developed in-house, by the lab technicians of the Department of Civil, Structural and Environmental Engineering at Trinity College, Dublin. It was assembled and combined with existing commercial material, and placed in a lab environment where several system parameters could be controlled.

The prototype was then tested for its thermal characteristics, using clean water as the medium. The flow conditions were controlled, and the temperature evolution was monitored at several places in the system. All tests were performed under steady-state conditions (see Appendix G.1), meaning that no transient behaviour was tested at this stage of the project.

4.5.3. Testing phase: Numerical simulations

The results of these lab-controlled steady state tests were then used to validate a numerical model of the prototype. This numerical model, being a Computational Fluid Dynamics (CFD) model was simulated using the ANSYS Fluent software. As can be seen in Figure 10.14, this numerical simulation consists of four steps, described below.

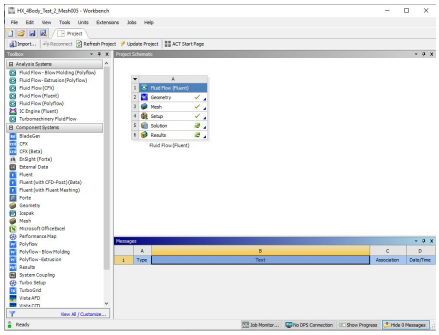


Figure 4.17.: Five steps in the fluent workbench.

- Building the geometry.
- Meshing (Discretizing) the geeometry.
- Setting-up and solving the simulation.
- Analysing the simulation results.

these steps are described in more detail in Section 10.3.4.

4.6. Summary

The overall structure of the research presented in this thesis can thus be summarized as follows. Characteristics of drain and wastewater were monitored and collected through a monitoring campaign, performed at different locations,different sort of buildings and industries over Ireland and the United Kingdom.

The potential impact of applying existing, understood heat recovery methods for drain and wastewater was studied by means of studying different exploitation strategies, in three different locations in the (waste)water cycle:

- On an individual residence scale.
- At the drain of commercial kitchens.
- On the effluent of the wastewater treatment plant.

These desk studies regarding the exploitation studies showed an undervalued potential, possibly due to the lack of general awareness regarding the possibilities for drain water heat recovery systems. To address this challenge, two demonstration sites were design, installed and tested, showing the required design steps, the energy recovery potential, and the operating principles of such systems. The results, observed at these demonstration sites, feed back into the monitoring campaign.

The combination of the monitoring campaign, discussions with different actors in the sector and the desk studies mentioned above, revealed a possibility for the development of a new, innovative prototype to complement the existing market of heat recovery devices. The development, construction and testing of such a prototype aims at tackling this gap in the market.

As a whole the research presented in this thesis aims to:

- Quantify the heat recovery potential at different locations in the water cycle.
- Identify the particular changes in characteristics and design, at different locations in the (waste)water cycle.
- Provide methodologies allowing to (more) accurately predict the operation and yield of drain water heat recovery (DWHR) systems.
- Demonstrate the operating principles of such DWHR systems, in different situations and industries.
- Set the wheels in motion to bring a new DWHR unit to the market, complementing the existing set, rather than competing with it, through the development of a new prototype.

5. Exploitation Strategy: Decentralized drain water heat recovery in a domestic setting

5.1. Introduction

Heating and cooling account for around half of the energy consumed in the EU, and around 75% of this energy is produced by fossil fuels. In that framework the European Comission has developed a strategy, aimed at making heating and cooling more sustainable and more efficient. On the one hand to reach the envisioned reduction in the emission of greenhouse gases, on the other hand to reduce energy imports, and the EU's dependency on these imports [European Commission, 2016]. In light of promoting the use of energy from renewable sources, the European Parliament and Council of the EU, have issued a directive, listing wastewater as a renewable energy source. [European Parliament; Council of the European Union, 2018]

But, what is the best suited strategy for heat recovery, where in the water cycle should heat be recovered to optimize it's environmental and financial benefits? In Chapters 5, 6 and 7 of this thesis, the heat recovery potential is assessed at three different locations (exploitation strategies) in the (waste)water cycle:

- At the wastewater or sewer drain of an individual domestic residence. (Chapter 5)
- At the drain of commercial kitchens. (Chapter 6)
- At the effluent of a wastewater treatment plant. (Chapter 7)

The objective being to highlight advantage and drawbacks of each of these exploitation strategies, and to discuss the relevant technologies. Space and water heating is generally delivered on an individual residence basis (91% in Europe [Gartland and Bruton, 2016]). The first studied exploitation strategy, described in Chapter 5 focuses on replacing and/or supplementing traditional heating systems for individual domestic residences, as shown in Figure 5.1.

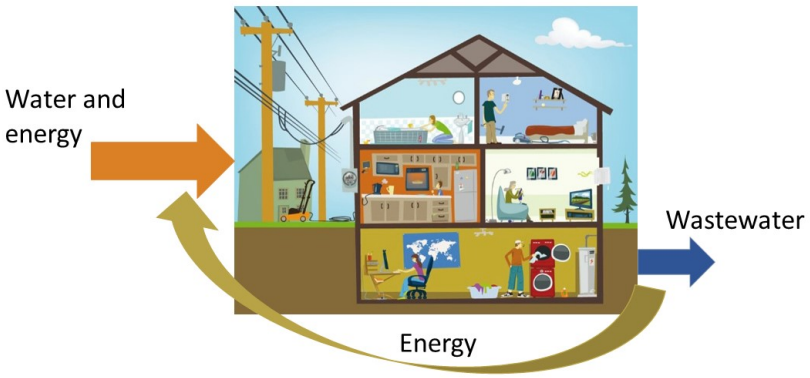


Figure 5.1.: Decentralized heat recovery on a domestic scale.

The costs related to these heat recovery on a domestic scale, are larger than current heating costs using conventional systems, such as gas and fuel oil. Two methods are considered for increasing the profitability of DWHR systems. The first one is moving upstream, represented by heat recovery from kitchens in this thesis, and, secondly, moving downstream, which is represented by heat recovery from the effluent of wastewater treatment plants in this thesis.

Chapter 6 studies heat recovery at a location upstream of the building's drain, ie. the kitchen. This exploitation strategy deals with a lower volume of wastewater, but a higher temperature and thus a higher energy density, also referred to as higher grade heat, or greater exergy. The volume of recovered energy proved to be lower, however, investment costs were significantly lower as well. The chapter focuses on commercial kitchens to have a regular flow, which is larger than for single households.

Chapter 7 studies heat recovery at a downstream location, i.e. the effluent of the wastewater treatment plant. This exploitation strategy has the advantage of very large flows and thus the availability of a large quantity of energy. However, it can be located at a large distance from the heat consumers, and is characterised by lower temperatures (lower grade energy). The proposed methodology was applied to the wastewater treatment plant in Tullamore, co. Offaly in Ireland.

5.2. Monitored Data

5.2.1. Drain Water characteristics

Drain water temperature, even average temperatures are generally unknown. For this reason, this parameter was measured at different residences in Ireland. The drain water temperature from single residences was measured at three different houses, all in Ireland. Temperature sensors were placed, depending on the accessibility, at three different locations in the sewer system. The outflow temperature of the drainage system of the house into a septic tank (which served as the wastewater holding tank, see Section 5.4.2) was measured using a TinyTag TG4105 temperature logger, selected for its faster response time than the TG4100 model. The first chamber (Ch1) of the septic tank, and the second chamber of the septic tank (Ch2) were measured using TinyTag TG4100 temperature loggers (see Figure 5.2).

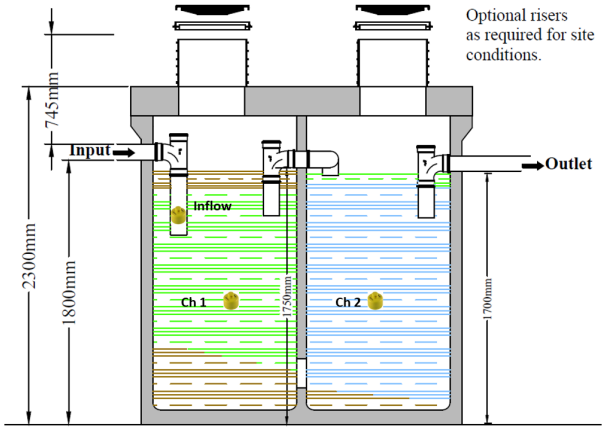


Figure 5.2.: Septic tank with temperature loggers at the different measuring locations.

Table 5.1 shows the position of monitoring points across the three locations. This table also shows the number of inhabitants of the residence, the monitoring interval, and the time over which observations took place. One can observe that the outflow was monitored in just one location, this is the reason why, in the method, the waste water outflow is estimated based on the domestic hot water consumption, as is its SLP profile (see earlier this Section), rather than the monitored data.

Table 5.1.: Monitoring matrix for the drain water temperature monitoring in Ireland.

		Monitoring location			Monitoring characteristics	
Residence	**# residents**	**Input**	**Ch1**	**Ch2**	**Interval**	**Period**
Crecora, co. Limerick	5	x	x	x	$1/5min$	April 2017 – May 2018
Kilmallock, co. Limerick	4		x	x	$1/5min$	May 2017 – August 2017
Louth, co. Louth	3		x		$1/5min$	3 months

As can be seen in Figure 5.3, the average temperature in the second chamber is slightly lower (on average about $1°C$) than in the first chamber. The temperature changes due to the inflow of wastewater are heavily dampened in the second chamber, such that the temperature remains relatively stable. Temperature fluctuations in the first chamber are more important, due to the effect of inflowing waste water.

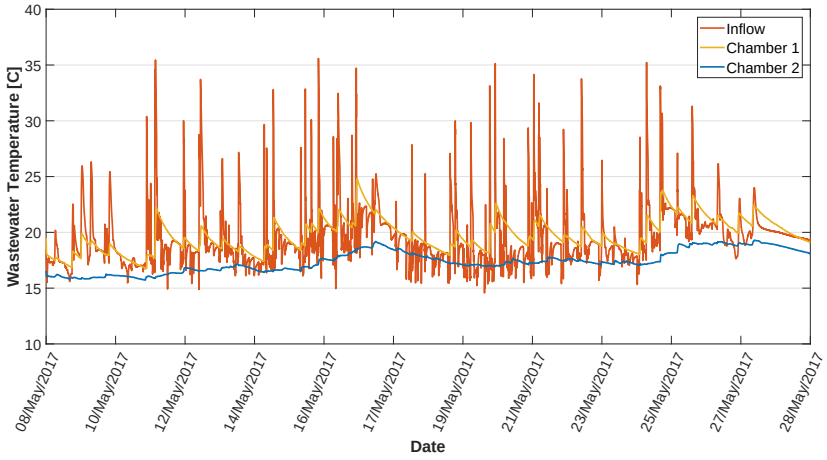


Figure 5.3.: Sample of the temperature measurements at the domestic residence in Crecora, co. Limerick.

The flow is measured using a tipping bucket system at the outlet (see Figure 5.4). As can be seen in Figure 5.5, the spread (difference between largest and smallest) flow is large, but daily and weekly patterns emerge.



Figure 5.4.: Tipping bucket flow meters.

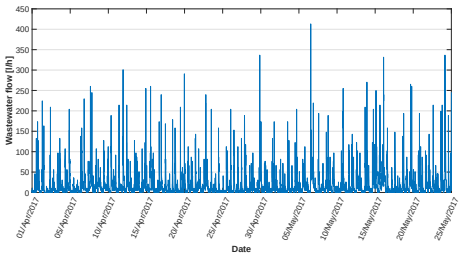


Figure 5.5.: Sample of the flow measurement at the domestic residence in Crecora, co. Limerick.

5.3. Potential of domestic drain water heat recovery in the Republic of Ireland

In order to estimate the unexploited energy potential from wastewater in the Republic of Ireland, the embedded energy, contained in the wastewater when exiting the residence is estimated using the results observed during an on-site monitoring campaign. This information is then combined with available data on domestic wastewater flow in wastewater treatment plants, and an estimation of wastewater flows in local treatment systems. Finally, the resulting unexploited heat potential is put in the context of Ireland's total thermal energy consumption.

5.3.1. Methods and materials

Embedded energy in domestic wastewater

The embedded energy is estimated based on measurements of the wastewater temperature, when exiting the home, in Crecora, county Limerick. The formula is given in Equation 5.1.

$$E_{embedded} = m_{WW}\, Cp_{WW}\, (T_{WW,out} - T_{ref}) \tag{5.1}$$

The reference temperature (T_{ref}) chosen is the soil temperature measured on the same location. The variation over a day, as observed in Crecora is shown in Figure 5.6.

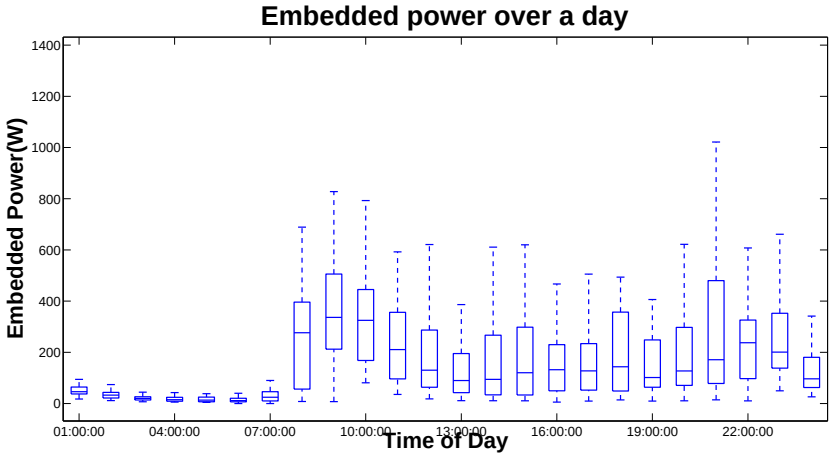


Figure 5.6.: Embedded energy evolution over a day at Crecora, co. Limerick.

In Figure 5.1 one can clearly observe that the embedded energy is close to 0 during the night time, and that peaks occur arround 9 AM and 9 PM, coinciding with morning showers, and evening showers, dish- and clothes washing,... This results in a daily embedded energy, depending on the daily flow as shown in Figure 5.7. The black line represents the curve fit, with it's 95%-confidence interval in gray.

The relationship between the embedded energy and the daily wastewater flow (see Equation 5.2) is used to estimate the energy potential in wastewater at the source(ie. the domestic residence).

$$E_{embedded} = 9.2 kWh/m^3\, \dot{V}_{WW} \tag{5.2}$$

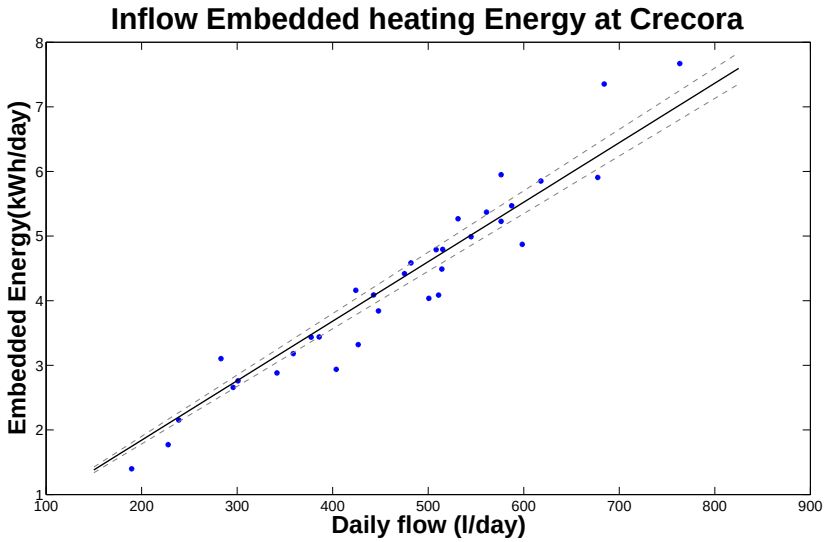


Figure 5.7.: Daily embedded energy compared to the daily wastewater flow.

Domestic wastewater flow

The estimation of the daily wastewater flow is estimated using two sources, the domestic wastewater being collected in the wastewater treatment plants, and the domestic wastewater treated in local treatment systems, such as septic tanks.

The average daily waste water flow at wastewater treatment plants is listed in the 'WasteWater Discharge Authorisation Licenses'. Such a license, delivered by the Irish Environmental Protection Agency (EPA), is required when a treatment plant has a hydraulic loading exceeding 500 Person Equivalent. The EPA has granted 509 such licenses, however 40 of them did not contain the information regarding the average daily hydraulic loading.

Most of these treatment plants treat both domestic and non-domestic wastewater, in some of the license documents the distribution between these two types of wastewater is given. For wastewater treatment plants where this distribution isn't given, it's assumed that 80% of the total flow is domestic wastewater, this assumption is made by the EPA for the design guidelines of flood spillways. [Environmental Protection Agency, 2018]

The data extracted from these 'WasteWater Discharge Authorisation Licenses' are summarized in Table 5.2.

Table 5.2.: Wastewater Discharge Authorisation Licenses

Licenses	509	
Licenses with source distribution	469	92.14%
Total hydraulic loading	1.38 $M\ m^3/day$	
Total domestic hydraulic loading	1.1 $M\ m^3/day$	80.36%
Total non-domestic hydraulic loading	0.27 $M\ m^3/day$	19.64%

In order to estimate the daily wastewater flow in local treatment plants and septic tanks a daily hydraulic loading per person of 0.2055 m^3/day is assumed [Gill, 2015]. Furthermore, an estimated 33% of inhabitants of Ireland are connected to a local treatment system [Gill et al., 2015]. Given Ireland's population in 2016, this results in the estimated wastewater flow given in Table 5.3.

Table 5.3.: Estimated wastewater flow in local treatment systems

Irish Population in 2016	4.71 M	
People connected to a local treatment system	1.55 M	33%
Related domestic hydraulic loading	0.32 $M\ m^3/day$	

Total unexploited embedded energy

Combining both sources of wastewater, this results in an embedded energy, currently being lost of $13.12E6\ kWh/day$, which is 9.72% of total produced thermal energy in the Republic of Ireland, literally being flushed through the drain [SEAI, 2015*b*]. Taking into account the carbon intensities from SEAI [2017*b*], and the distribution of heating sources as recorded in the Building Energy Rating database [SEAI, 2014], it also signifies 3.4 $E6\ kg, CO_{2,eq}/day$ of Green house gas emissions , or 10.80% of all Irish emissions related to thermal Energy [SEAI, 2015*b*]. Given the fuel prices in Ireland [SEAI, 2019*a*], this results in a daily spending of 1.09 $M€/day$, or $0.23€/citizen\ day$.

The results are summarized in Table 5.4.

Table 5.4.: Unexploited embedded energy in domestic wastewater

		% of Total	% of Thermal
Total yearly primary energy consumption	125.99 TWh		
Total related yearly emissions	37 $M\ tons\ CO_{2,eq}$		
Yearly thermal energy consumption	49.29 TWh	39.12%	
Thermal related yearly emissions	11.5 $M\ tons\ CO_{2,eq}$	31.08%	
Yearly embedded energy in wastewater	4.79 TWh	3.80%	9.72%
Related yearly emissions	1.24 $M\ tons CO_{2,eq}$	3.36%	10.80%
Related yearly fuel cost	397 $M€$		

5.3.2. Potential for energy recovery

Heat recovery system

Because the observed wastewater temperature (see Section 5.2.1) is significantly lower than the intended $50°C$ of the hot water in the heating network, indirect heat recovery was considered. The schematic diagram is shown in Figure 5.8.

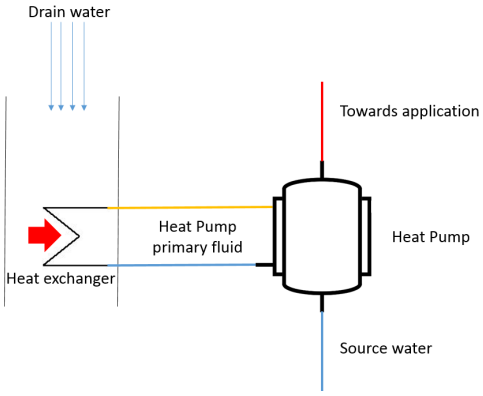


Figure 5.8.: Indirect Heat Recovery

The potential assessment in this section had as objective to estimate the potential of the whole sector. A more detailed design of the system is introduced in Section 5.4.2, when the feasibility at the outlet of individual, domestic residences is assessed.

Potential for indirect heat recovery

In this section the impact of exploiting the entirety of the wastewater embedded energy, using indirect heat recovery, on Ireland's renewable heat target, and Ireland's Greenhouse Gas Emission reduction targets. The analysis is based on the assumption that the primary fluid is heated up to $13°C$. This temperature is based on the observations during the monitoring campaign in Louth, co. Louth, and Crecora and Kilmallock, both in county Limerick, Ireland, where an average temperature of $18°C$ was observed. A temperature difference between the hot and the cold fluid of $5°C$ was considered over the heat exchanger. The temperature of the hot water in the heating network is considered to be $50°C$.

This results in a daily produced heat from wastewater source heat pumps between 16.56 GWh/day and 17.97 GWh/day at a greenhouse gas intensity between 0.1028 kg/kWh and 0.1336 kg/kWh. This is estimated based on the expected COP given the wastewater temperatures as measured, see Section 5.2.1, and the embedded energy (See Section 5.3.1). This results in the yearly values given in Table 5.5. The total consumed thermal energy, the related emissions and the share of renewable heat were obtained from SEAI [2015*a*] and SEAI [2019*b*].

Table 5.5.: Indirect Heat recovery in Ireland's heating energy mix.

				% of Thermal
Yearly thermal energy consumption	49.29 TWh			
Thermal related yearly emissions	11.5 $M\ tons\ CO_{2,eq}$			
Yearly heat produced RES-H (2015)	2.51 TWh		5.10%	
	Min	**Max**	**Min**	**Max**
Yearly heat produced IHR	6.05 TWh	6.56 TWh	12.26%	13.31%
Yearly heat produced RES-H (new mix)	8.56 TWh	9.07 TWh	17.36%	18.41%
			Reduction	
Thermal related yearly emissions	10.71 $M\ tons\ CO_{2,eq}$	10.85 $M\ tons\ CO_{2,eq}$	6.87%	5.70%

The unexploited, embedded energy has the potential to increase the share of renewable heat in the heating mix to around 18%, which exceeds Ireland target for 2020 which is 12%, as is shown in Figure 5.9.

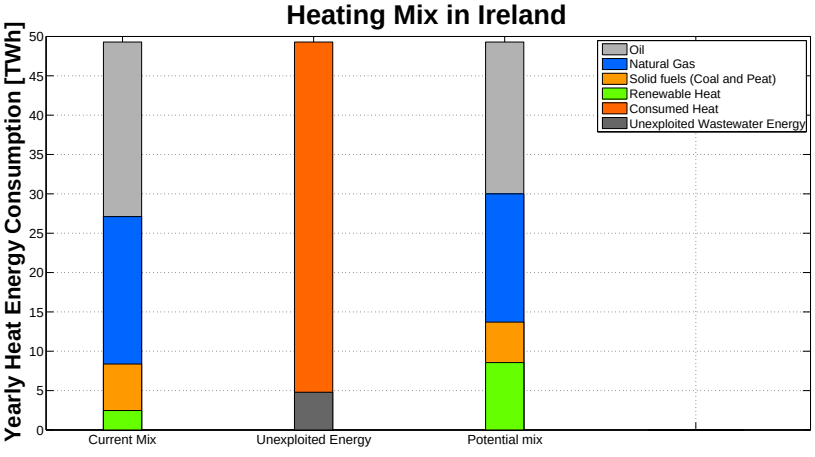


Figure 5.9.: Potential role of wastewater source heat pumps in Ireland's heating mix.

The potential depicted in this Figure represents the maximum share obtainable for domestic wastewater source heat pumps, however only a part of this will be technically and financially feasible. Section 5.4 a method is described to estimate the technically and financially feasible potential for this technology.

5.3.3. Considerations for cost effectiveness

The indirect heat recovery method, proposed above, requires the replacement of certain existing heating systems with wastewater source heat pumps. In this paper, a gradual replacement is proposed. Clancy [2015] states that 108 000 electric, gas and oil boilers are replaced in Ireland every year, however the cost of heating remains an important decision factor when replacing a boiler.

Even though fuel costs are expected to be cheaper, as can be seen in Figure 5.10, the capital investment of a wastewater source heat pump is higher than the investment for traditional heating system. In order to make a trade off between reduced fuel costs, and increased capital investment, the Levelized Cost of Heating Method (LCOH) is employed, described in section 4.3.1.

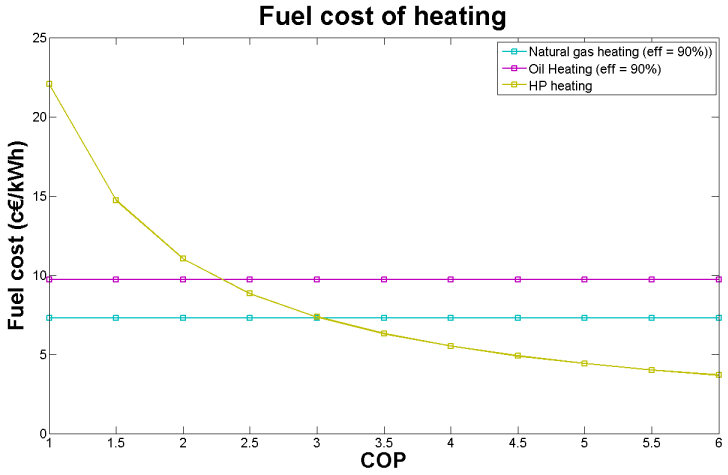


Figure 5.10.: Evolution of the fuel cost with changing COP.

For the wastewater source heat pump to be cost effective the higher initial investment must be offset by the cheaper fuel cost, compared to traditional systems. In order to achieve this a significant amount of embedded energy must be available in the wastewater, and be consumed relatively close to the point of extraction, in other words the wastewater flow must be significant. Figure 5.11 shows the evolution of the LCOH, with respect to the daily wastewater flow, and compares it to the LCOH of traditional heating systems, as given in Wang [2017].

The COP of the wastewater heat pump is based on the assumption that the primary fluid is heated up to $13°C$, which is based on the observations during the monitoring campaign in Crecora and Kilmallock, both in county Limerick, Ireland. In Figure 5.11, one can observe that a flow of at least 4.8 m^3/day is required for the wastewater source heat pump to provide a cheaper heating solution than a mains gas heating system. Using the earlier assumption of 0.2055 $m^3/person\ day$ this amounts to wastewater equivalent of 24 people.

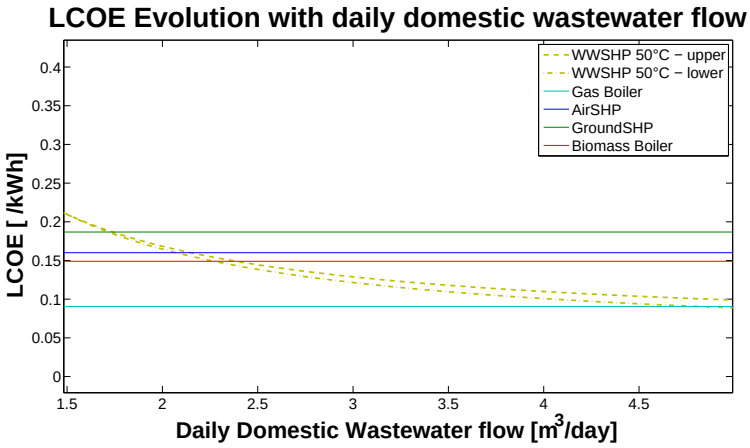


Figure 5.11.: Evolution of the LCOH with varying daily wastewater flow.

5.4. Drain water heat recovery in a domestic setting

To investigate whether the wastewater flow is sufficient to be considered for a financially attractive DWHR system, this section proposes a method taking into account the temporal aspects related to both the heat recovery system and the heat demand in a residence. The proposed method is then applied to the average Irish residence. [1] This section describes:

1. The probabilistic method, used for the feasibility study of indirect heat recovery from domestic residences.
2. The indirect heat recovery system for domestic residences.
3. The price and environmental parameters used, to compare the indirect heat recovery system to conventional heating systems.
4. The application of the model on the Irish residential market.

5.4.1. Methods and Analysis

Objectives of the method

Heat consumption, and the availability of heat in wastewater depend strongly on the time of day and the time of year. This profile also depends on the habits and hot-water usage time of the inhabitants. For most residences, this profile is unknown, as a lot of residences do not have a building management system, and the only available information is the cumulative consumption (often monthly, or even yearly). Yet, when drain water heat recovery systems, and also other systems with a non-controlled heat supply are considered, the temporal concurrence of heat recovery and heat demand is an essential factor in their feasibility analysis [Wallin and Claesson, 2014]. A conceptual diagram is shown in Figure 5.12.

The current method aims at using available data, be it monthly, yearly or daily averages, to predict seasonal/monthly or daily profiles for heat consumption, based on the statistical distribution of known consumption profiles. The availability of heat in the wastewater, and how the heating system and the drain water heat recovery system would interact, can be derived from this data as well. This method indicates: i) when back-up heating systems are necessary to meet peak demands; ii) the share of heat that can be delivered by the heat recovery system; and iii) provides an indication of the environmental and financial costs and benefits.

[1] The research presented in this section was published as a journal paper in the journal *Energy and Buildings* [Spriet and McNabola, 2019*a*]

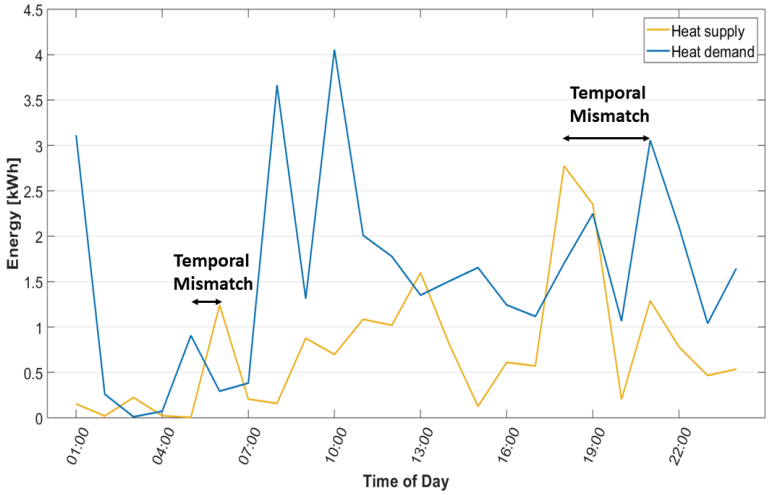


Figure 5.12.: Concept of the temporal mismatch between supply and demand.

Because these profiles are case-dependent, the results are given as a statistical distribution, generated by observed statistical distributions on these profiles.

Data

In order to account for daily and seasonal variations in domestic hot water (DHW) consumption, space heating (SH) consumption, and in wastewater flow and temperature, synthetic load profiles (SLP) were generated. Using Monte Carlo simulation, synthetic load profiles were generated [Pillai et al., 2014] to show how the consumption at a certain point in time, relates to the mean value. In this probabilistic method, two different load profiles were considered, one for the daily variation, and one for the monthly variation. The actual consumption or flow is then given by multiplying the average daily value with the value of the synthetic load profile for the particular time of day, and the value for the particular month (see Equation 5.3) where C is consumption and *tod* is time of day).

$$C(tod,\ month) = C_{avg,\ daily}\ SLP_{daily}(tod)\ SLP_{monthly}(month) \tag{5.3}$$

In practice, these synthetic load profiles are residence specific, e.g. a person who starts working at 6am will have a peak morning consumption earlier than someone who starts at 9am. This variation is taken into account by considering the statistical variation on the SLP values. Each Monte Carlo iteration generates SLP values for each time of day and each month following their respective statistical distributions.

The data used to fit the distributions and generate the random samples at each of the Monte Carlo iterations, was taken from different sources, in order to approximate actual consumption profiles as closely as possible. Some of the data was measured, other data was collected through official instances, or other research projects. The data sources are described in this section.

- **Domestic Hot Water consumption**

The synthetic load profiles for DHW consumption were generated based on the raw data from the Energy Monitoring Company and Energy Savings Trust [2011]. This data shows the daily and monthly variation in DHW consumption for 113 dwellings in the United Kingdom, monitoring at 10-minute intervals, brought back to 1-hour intervals. An example of a daily (Figure 5.13), and a monthly DHW consumption profile (Figure 5.14) is shown below.

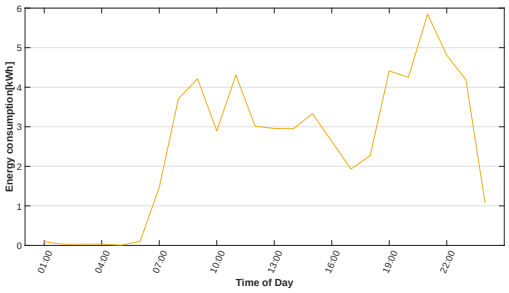


Figure 5.13.: Example of a daily DHW consumption profile.

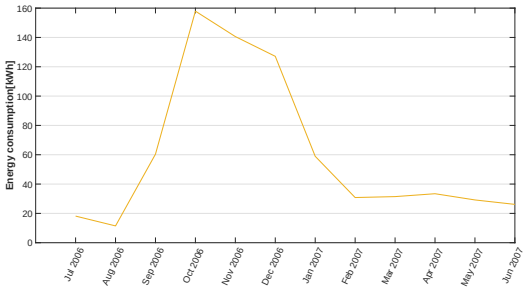


Figure 5.14.: Example of a monthly DHW consumption profile.

The synthetic load profiles were defined as the value of a particular time of day, or for a particular month divided by the daily average. Their distributions are given in Figures 5.15 and 5.16. Given the similarities in climate between the UK, and Ireland, these profiles were considered to be representative for Ireland as well

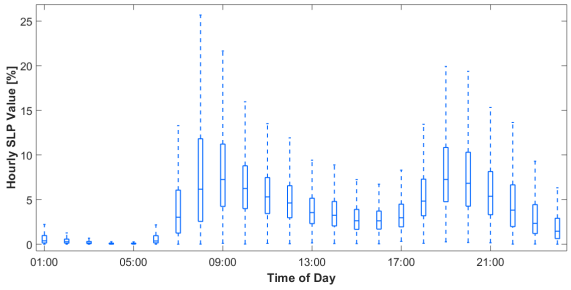


Figure 5.15.: Hourly SLP profile for DHW demand.

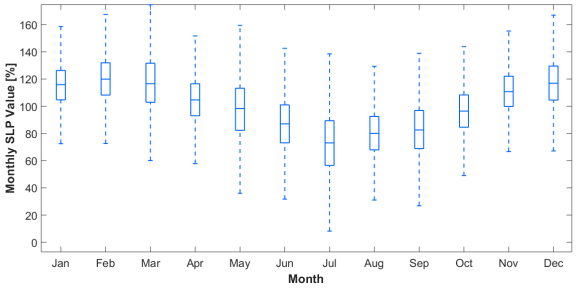


Figure 5.16.: Monthly SLP profile for DHW demand.

- **Space heating consumption**

The synthetic load profiles, and their distributions were estimated based on the heating degree day (HDD) information, as given by MET Eireann [2019]. Heating degree days are a proxy for SH energy demand. They are derived from comparing outside air temperature to a certain reference temperature (in the case of this analysis $18°C$) [Europeam Environmental Agency, 2018]. The monthly SLP profile for HDD is given in Figure 5.17, as expected, one can observe larger values during winter time. The hourly SLP profile for space heating demand cannot be obtained in this way, as the HDD values were only given on a daily basis, it was therefore assumed that the hourly space heating SLP was the same as the hourly SLP for DHW demand (Figure 5.15).

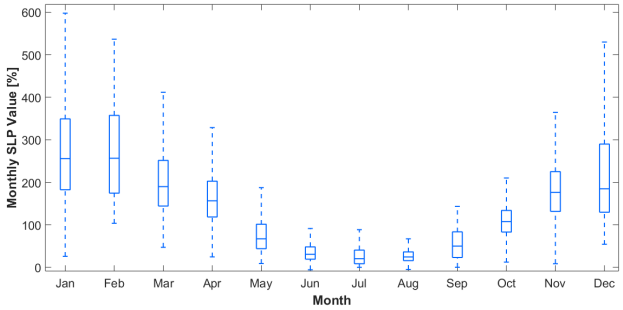


Figure 5.17.: Monthly SLP profile for space heating demand.

- **Drain Water Profile**

The drain water flow is closely related to the DHW consumption, as this is the main source of hot drain water, therefore the analysis assumes the same hourly SLP for drain water and DHW consumption. It was assumed that no domestic appliance has a holding time of more than one hour, hence the water leaves the residence within an hour after entering it. Some of the hot water (estimated at 20%) is evaporated, or spilled during the consumption, this is taken into account when the average daily hot water consumption is used to estimate wastewater flow.

- **Drain Water Temperature**

The drain water temperature is not predicted using an SLP, because drain water temperature, even average temperatures are generally unknown. For this reason, the daily and monthly distributions are generated based the measured values at different residences in Ireland. This distribution will also account for potential deviations from the hourly average, within the considered hour. An example of such a distribution, for the month of April, is shown in Figure 5.18. In case the actual local temperatures are available, these values can replace the ones used in this paper.

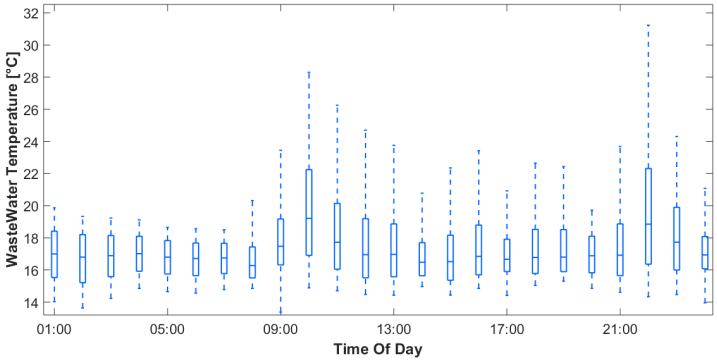


Figure 5.18.: Distribution of the temperature profile during the month of April.

Monte Carlo Simulations

The Monte Carlo simulation method was used for the sectoral analysis, in order to create a generalized profile, based on a monitored sample of residences or kitchens. The four key steps, as described in Section 4.3.1, are enumerated below:

- The domain and the probability functions of the input variables (drain water flow and drain water temperature) were defined based on the data described above.
- A random set of $N = 10\ 000$ iterations was generated, this number was determined based on a trade-off between computation time, and a negligible change in the distribution of the results. The probabilistic method is described below.
- The calculation method is described below, in Sections 5.4.2 and 5.4.3.
- The resulting distributions are described in Section 5.4.5.

Probabilistic method

The input variables for the model were the average daily space heating and hot water consumption, the method consisted of n iterations (10 000 in this case). The amount of iterations was determined by refining (increasing the amount of iterations, until the distribution of the results remained unchanged with further refining. In each of these iterations a daily SLP was generated based on the distributions mentioned above: different SLP s are generated for domestic hot water and space heating consumption, and for drain water flow. This SLP was adjusted for the different months of the year, resulting in 12 different SLPs for each of the studied parameters (DHW, SH consumption and drain water temperature) at each iteration. The

temperature of the drain water was directly generated based on the distribution of observed temperatures (see above). Combining the obtained SLPs with the input variables leads to space heating and domestic hot water consumption profile, and to a profile of the embedded energy in the wastewater. This is summarized in Figure 5.19.

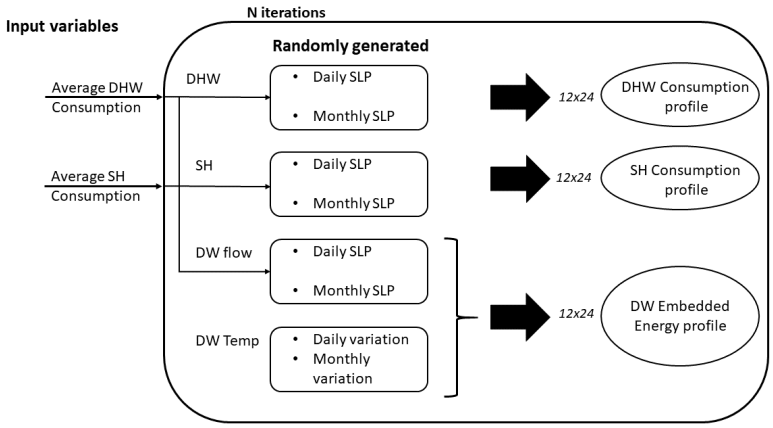


Figure 5.19.: Summary of the probabilistic method.

Each of the iterations thus generated profiles for these three parameters, and for each parameter 12 profiles (1 per month), of 24 points (1 per hour of the day) were generated, resulting in 10 $000x12x24$ calculation points. At each of these points the recovered heat was calculated and compared to the consumption. The temporal concurrence of recovered heat and heat consumption was thus assessed at each of these calculation points, and thus on an hourly basis. This means that the concurrence was verified within this one-hour timestep. Mismatches on a smaller timescale were not detected. However the analysis could be repeated using smaller timesteps for individual buildings showing promising results, to obtain a higher degree of detail and confidence. The data required to generate these profiles on a smaller time-scale was not available. In case of excess, recovered heat can be stored if a reservoir is present. In case the recovered heat is insufficient, a back-up heating system needs to be used. The delivered amount of recovered and back-up heat allows for the calculation of the levelized cost of energy (LCOE, see Section 5.4.3) and total equivalent warming impact (TEWI, Section 5.4.3) of the heat consumed (and recovered) in the residence. This approach is summarized in Figure 5.20.

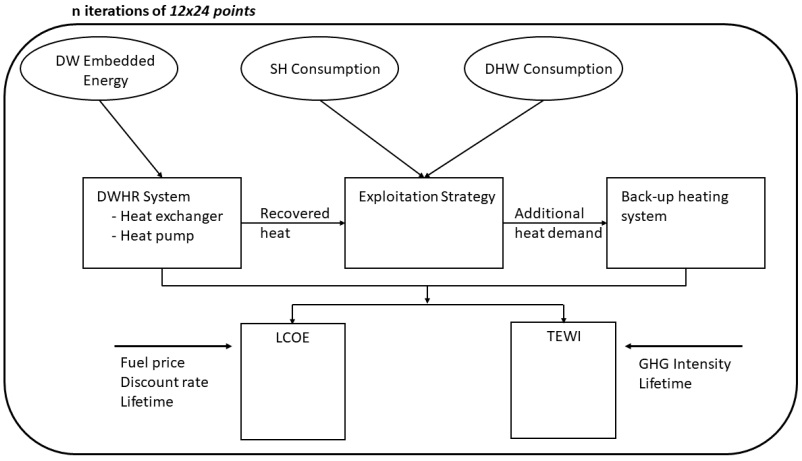


Figure 5.20.: Outline of the simulation.

5.4.2. DWHR System set-up

DWHR System description

The proposed system enables the recovery of heat from the drain water and raw sewage in a holding tank, allowing for this tank to serve as a buffer to attenuate potential mismatches between the heat consumption and the flow of drain water. The heat contained in this holding tank is recovered through a heat exchanger, heating the primary fluid of a heat pump, which serves as the low temperature heat source for this heat pump. The heat pump is primarily used for space heating, but in case excess heat is available, it is used to heat up the feed water from the water supply to the desired temperature. The hot water is stored in the domestic hot water storage tank (DHWST), and this way the heat pump can be operated continuously over a given time period, improving the performance of the heat pump, and increasing its profitability [Spriet and Hendrick, 2017]. The consumed DHW is then pumped from the DHWST to match DHW demand. In case there is not enough heat available in the holding tank to provide all the space heating and DHW demand, a backup system is provided. The principal design of the system is shown in Figure 5.22. The design, and variation of the operation parameters of the components is described further this section.

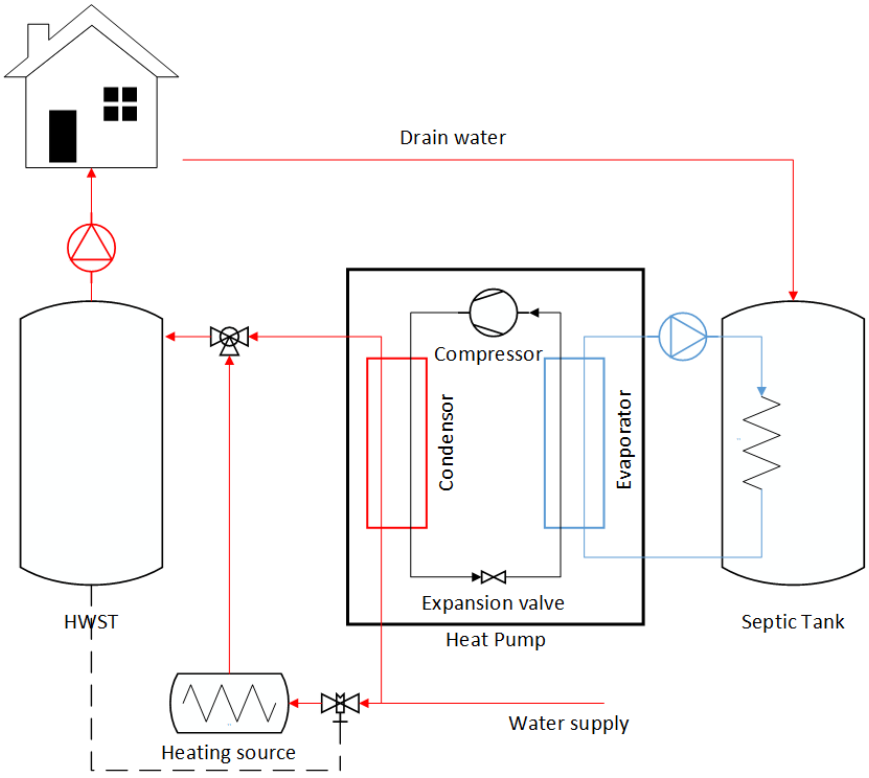


Figure 5.21.: Principal design of the decentralized drain water heat recovery unit.

The backup heating system is considered to have the same cost and carbon intensity as the overall thermal energy mix in Ireland, as given in Howley et al. [2015].

Local exploitation strategy

The recovered heat was assumed to be primarily used to meet space heating demand. If the available energy exceeds this demand, the remaining heat was then used to meet domestic hot water demand. In case excess heat was still available this heat was used to fill the domestic hot water storage tank (the size of this storage tank was varied in this study). Once this tank was filled to capacity the remaining heat was dumped, and thus wasted. The remaining storage capacity is characterized by a mass balance, which is converted to an energy balance in this case (assuming a fixed fresh water temperature of $15°C$, a target temperature of $60°C$, and neglecting losses from the hot water storage tank). This means that a time series of the energy

balance of the domestic hot water storage tank is generated, in order to determine the stored heat, wasted heat, and additional required peak heating, on an hourly basis. The thought process is repeated for each calculation point and is represented by the flow chart shown in Figure 5.22. However, from a programming point of view the stored and wasted heat, and the heat provided by the peak burner are given by the set of Equations 5.4. In these equations the iteration and month index were omitted to simplify the notation. In this set of equations, Q signifies the heat, and the subscripts st, HP, SH and DHW, stand for the heat in the storage tank, delivered by the heat pump, consumed for space heating and consumed for domestic hot water, respectively. $Q_{st,max}$ stands for the maximal amount of heat that can be stored in the storage tank, this depends on the reservoir volume.

$$\begin{cases} Q_{st}(tod) = max[0, min(Q_{st,max}, Q_{st}(tod-1) + Q_{HP}(tod) - Q_{SH}(tod) - Q_{DHW}(tod))] \\ Q_{wasted(tod)} = max[0, Q_{st}(tod-1) + Q_{HP}(tod) - Q_{SH}(tod) - Q_{DHW}(tod) - Q_{st,max}] \\ Q_{PB}(tod) = max[0, Q_{SH}(tod) + Q_{DHW}(tod) - Q_{HP}(tod) - Q_{st}(tod-1)] \end{cases} \quad (5.4)$$

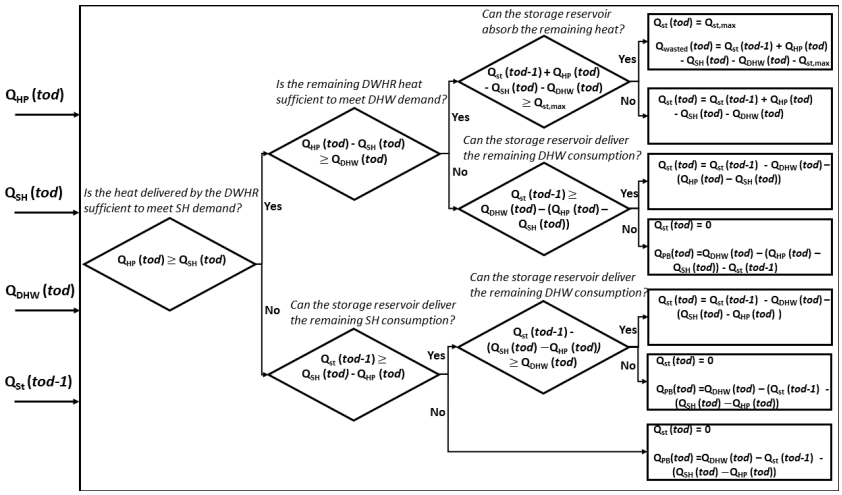


Figure 5.22.: Flow chart representing the time series of the energy balance in the hot water storage tank.

Heat Exchanger

To estimate the recovery of the heat embedded in the wastewater the performance of a heat exchanger placed in the wastewater holding tank was evaluated. In this analysis a copper heat exchanger was considered. This device was required to ensure the physical separation between the wastewater and heating - and hot water network.

- **Heat exchange surface**

The heat exchange surface was determined using the log mean temperature difference method, as shown in Equation 5.5. Where F is a correction factor based on the heat exchanger type, A_s the exchange surface and U the heat transfer coefficient of the heat exchanger [Yunus and Boles, 2007].

$$\dot{Q}_{HE} = F\ A_s\ U\ \Delta T_{LMTD} \quad (5.5)$$

The heat exchanger was designed for the average conditions of that particular operation, and the operation was then calculated using Equation 5.5, for all operation points of the iteration (12x24 points for each iteration). In contrast with the effectiviness method described in Section 3.2.2, the effectiveness of the heat exchanger is not explicitely used, but is implicitly incorporated in the heat exchange surface and the heat transfer coefficient of the heat exchanger, along with the correction factor.

The limitation of this method is that fouling and reduced operational performance over time was not considered. A single, average heat transfer coefficient was used, assumed constant over the lifetime of the heat exchanger. Potential variations in this coefficient, for example due to increased fouling during certain periods of the day or certain months of the year were not included in this research.

- **Heat exchanger price**

The price of the heat exchanger (E_C in €) was determined using the Vatavuk method, shown in Equation 5.6, and described in Taal et al. [2003].

$$E_c \ = \ 885 \ * A_s^{0.432} \tag{5.6}$$

Heat pump

A heat pump is commonly used to convert low grade heat (at low temperature), to high grade heat, this process does not happen spontaneously, the input of mechanical work is required.

- **Heat pump performance**

The performance of a heat pump is described as the ratio of the produced heat and the electric input. This ratio is called the Coefficient of Performance (COP, Equation 5.7).

$$COP \ = \ \frac{Q_{out}}{W_{in}} \tag{5.7}$$

The higher this ratio, the lower the required work input, and thus fuel consumption, to produce a certain amount of heat. This performance was calculated using a regression on the relationship between the required temperature lift (TL, temperature difference between the low temperature heat source and the high temperature heat sink, in $°C$ or K), and the COP, obtained through the analysis of the datasheets of 26 different heat pumps, with a rated power below 7 kW. The regression formula is given in Equation 5.8 ($R^2 \ = 90.94\%$).

$$log_{10} \ COP(TL) \ = \ 1.012 \ - \ 0.01052 \ TL \tag{5.8}$$

The regression used to obtain Equation 5.8, is shown in Figure 5.23. The datapoints are obtained from the datasheets of 26 different heat pumps with rated power below 7 kW. The list of heat pumps is given in Appendix C.1. The regression line, and the goodness of fit characteristics are shown in Figure 5.23, an adjusted R^2 value of over 90% is obtained.

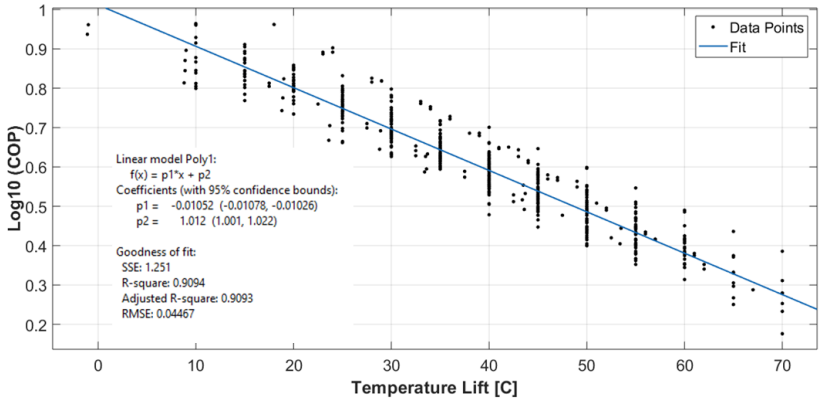


Figure 5.23.: Regression of the COP vs the required Temperature Lift.

- **Heat pump price**

The price of the heat pump (in €) was determined by regression on the catalogue price of 26 heat pumps, with a rated power below 9 kW. The regression formula is given in Equation 5.9 ($R^2 = 77.10\%$).

$$Price_{HP} = 8831\ Q_{out,rated}^{-1.09}\ Q_(out, rated) \tag{5.9}$$

Equation 5.9 was obtained through regression on a subgroup of these 26 heat pump models, for which the catalogue price was available. The regression line, and the goodness of fit characteristics are shown in Figure 5.24, an adjusted R^2 value of over 75% is obtained.

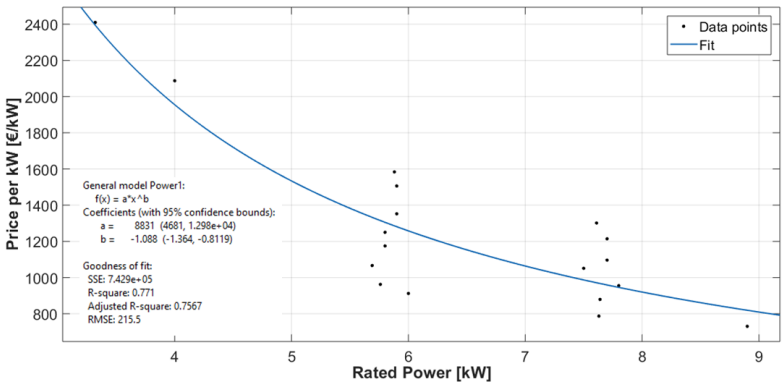


Figure 5.24.: Regression of the price per kW vs the rated power of the heat pump.

5.4.3. Financial and Environmental comparison methods

Operation of the DWHR System

The operation of the DWHR system, and its interaction with the peak burner, is represented schematically in Figure 5.20. This section describes the underlying equations and thought processes. This process was executed for each of the 40 000 iterations (10 000) of the Monte Carlo method.

- **Recovered heat**

The recovered heat was determined for a representative day of each month (i), and for each hour of the day (j). This was conducted by solving the set of equations described in Equation 5.10, for the recovered heat in the heat exchanger Q_{HE}, the upper value of the temperature of the primary fluid of the heat pump, $T_{high,PF}$ and the lower temperature of the wastewater $T_{low,WW}$.

$$\begin{cases} Q_{HE}(i,j) = F\ As\ U\ \Delta T_{LMTD} \\ Q_{HE}(i,j) = [\dot{m}\ Cp\ (T_{high}(i,j) - T_{low}(i,j))]_{PF} \\ Q_{HE}(i,j) = [\dot{m}(i,j)\ Cp\ (T_{high}(i,j) - T_{low}(i,j))]_{WW} \end{cases} \tag{5.10}$$

On these equations, the constraints described in Equation 5.11 were applied. The first constraint is related to the operation of the heat pump, for which a temperature drop over the primary fluid ranging from 3 to 8°C was recommended in data sheets. The second constraint related to the effectiveness of the drain water treatment. The nitrogen removal in the wastewater treatment process is affected by reduced temperature [Wanner et al., 2005], and Swiss legislation recommends a lower limit of 10°C [Schmid, 2008]. Nitrogen removal is not part of the treatment process performed by a septic tank, however it is for large-scale treatment systems. This limit was thus taken to ensure a generalized approach.

$$\begin{cases} 3°C \ \leq \ (T_{high}(i,j) - T_{low}(i,j))_P F \ \leq \ 8°C \\ 10°C \ \leq \ T_{low,WW}(i,j)) \end{cases} \tag{5.11}$$

Using the solution from the set of Equations 5.10, the temperature lift can be determined using Equation 5.12. This temperature lift was then used to estimate the heat pump performance, as described in Equation 5.8.

$$TL \ = \ T_{high,PF}(i,j) \ - \ T_{req} \tag{5.12}$$

Once the COP was known, the heat output by the heat pump, and the electric consumption of the heat pump were determined, using the set of Equations 5.13.

$$\begin{cases} Q_{HP}(i,j) \ = \ \frac{COP(TL)}{(COP(TL) \ - \ 1)} \ Q_{HE}(i,j) \\ \\ W_{HP}(i,j) \ = \ \frac{Q_{HP}(i,j)}{COP(TL)} \end{cases} \tag{5.13}$$

- **Utilization of the recovered heat**

As explained in Section 5.4.2 the total heat produced by the heat pump could be split in two different categories, heat that is used within the DWHR system (consumed or stored), and heat that cannot be used or stored and was thus wasted, as shown in Equation 5.14.

$$Q_{HP}(i,j) \ \rightarrow \ \begin{cases} \mathrm{Q}_{HP,used}(i,j) \\ \mathrm{Q}_{HP,wasted}(i,j) \end{cases} \tag{5.14}$$

The consumed electric power remains the total value. These values were then employed to estimate the total yearly (for year n) values, for each of the iterations. This was carried out by solving Equation 5.15, where DiM are the days in the month.

$$E_{HP,n} \ = \ \sum_{1=1}^{12} DiM(i) \ (\sum_{1=1}^{24} Q_{HP,used}(i,j)) \tag{5.15}$$

The total yearly values for electric consumption (Equation 5.16) and the heat produced by the peak burners (subscript PB, Equation 5.17) were found using similar equations.

$$W_{HP,n} \ = \ \sum_{1=1}^{12} DiM(i) \ (\sum_{1=1}^{24} W_{HP,used}(i,j)) \tag{5.16}$$

$$Q_{PB,n} \ = \ \sum_{1=1}^{12} DiM(i) \ (\sum_{1=1}^{24} Q_{PB,used}(i,j)) \tag{5.17}$$

Levelized Cost of Energy

In order to estimate the economic potential of decentralized heat recovery systems, the Levelized Cost of Energy was used (see Section 4.3.1)

The investment cost consists of the heat exchanger, heat pump and installation cost. The yearly maintenance cost was estimated at 2% of the investment cost, whereas the fuel costs were the average prices in Ireland, as described in SEAI [2017*a*]. The LCOE was then compared to the LCOE for classic heating systems, as given in Wang [2017]. The advantage of using LCOE, rather than payback periods is that it allows to compare systems, including their investment, maintenance and operation costs, at the time of investment, rather than investigating the scenario where one system replaces or complements the other.

Total Equivalent Warming Impact

To estimate the environmental impact of the different heating systems, the Total Equivalent Warming Impact (TEWI, discussed in Section 4.3.1), divided by the produced heat was considered.

The operational parameters were as described in Zottl et al. [2011], the carbon intensity of the fuels for the Republic of Ireland was taken from SEAI [2017*b*].

5.4.4. Applying the model to the Irish Residential Market

In order to demonstrate the operation of the method, and the output that can be produced, the model was applied to the Irish domestic/residential market.

Input Data: Building Energy Rating Certificate

Since 2007 a Building Energy Rating (BER) [SEAI, 2014] certificate is required for all new dwellings in Ireland. All existing buildings offered for sale or letting after 2009 require this certificate as well. The BER is calculated using the Dwelling Energy Assessment Procedure (DEAP), as issued by the Sustainable Energy Authority of Ireland (SEAI) [SEAI, 2018]. This procedure estimates, amongst other information, the input variables (average yearly SH and DHW consumption) used in the method described in Section 5.4.1. At the moment of the analysis the BER database contained the information of 697 984 domestic residences. This data was also used to estimate the size of hot water storage tank, in this research 4 different cases were considered:

- No hot water reservoir.
- 100 l hot water reservoir.
- 200 l hot water reservoir.
- 300 l hot water reservoir.

Average Irish Building

In the case of this project, the method was not applied to a specific residence, rather the method is applied to a virtual, average Irish domestic building. In order to obtain the values for this average residence, another Monte Carlo simulation (see Section 5.4.1) was applied for the average annual SH and DHW consumption, based on the data available in the BER database. The analysis doesn't take potential pre-warming in the heating space into account, this can occur when the water is first collected in a storage tank, as is often the case in Irish residences. This data is summarized in Figures 5.25 and 5.26. For all 10 000 of the iterations, the average annual SH and DHW consumption were generated based on the distribution of data in the BER database.

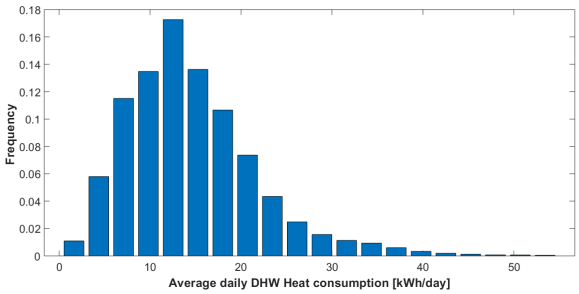


Figure 5.25.: Average Daily DHW demand in Ireland.

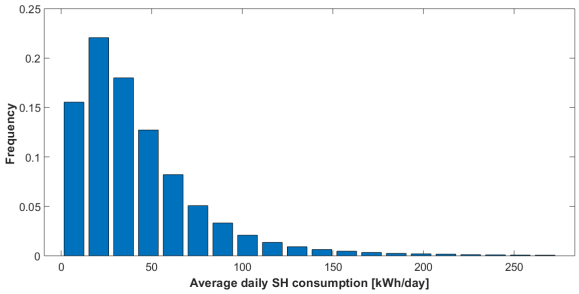


Figure 5.26.: Average Daily SH demand in Ireland.

5.4.5. Results and Discussion

DWHR vs Classic Back-up System

As a result of the conservation of energy principle, the DWHR system cannot provide all the heat demand to the dwelling. As described in Sections 5.4.1 and 5.4.2, a back-up heating system is required to meet all of the heat demand. Figure 5.27 shows that the need for the back-up heating system is greatest right after the demand peaks (10 AM and 8 PM), lagging the points of high production from the DWHR system, and the points of high demand. This shows that the consumption peaks will deplete the reserve of recovered heat, resulting in the need for back-up heating straight after these peaks. During the periods of low demand (3-4 PM), peak burner activity is often not required.

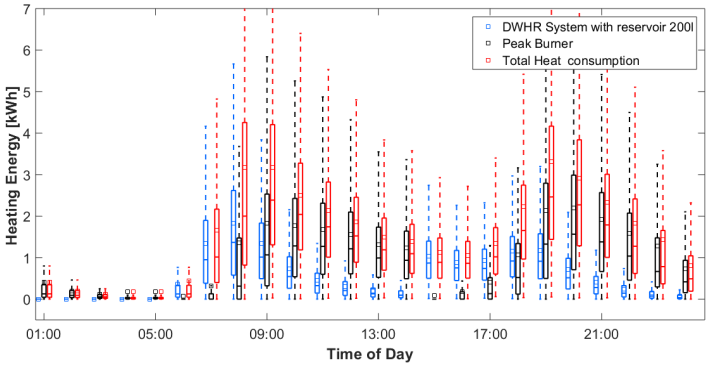


Figure 5.27.: Heat demand met by the different heat sources.

In Figure 5.28, one can observe the distribution over the 10 000 iterations of the percentage of the yearly heat consumption (see Equation 5.15) of an average Irish residence that is provided by the DWHR system. In Figure 5.29, one can observe that a small amount of recovered heat, remains unused. This is due to the mismatch between the availability of heat in the drain water, and the heat demand.

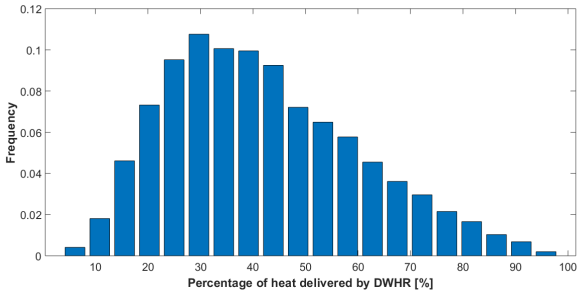


Figure 5.28.: Distribution of the heat delivered by DWHR, with a 200l reservoir

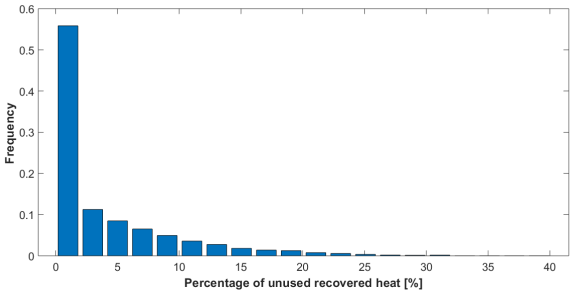


Figure 5.29.: Distribution of the amount of unused recovered heat, with a 200l reservoir.

To counteract this mismatch, the size of the hot water reservoir can be changed, and the effect of varying this size is summarized in Figures 5.30 and 5.31. Due to mismatching between heat recovery and heat consumption, the average share of heat demand met by the DWHR system without a hot water reservoir is an average yearly value of 8.2% over the 10 000 iterations. Adding a hot water reservoir of 300l to the system, this can be increased up to 42.4%. This is due to the fact that the amount of unused recovered heat can be decreased from around 75% to below 1% by increasing the volume of the storage reservoir to 300l.

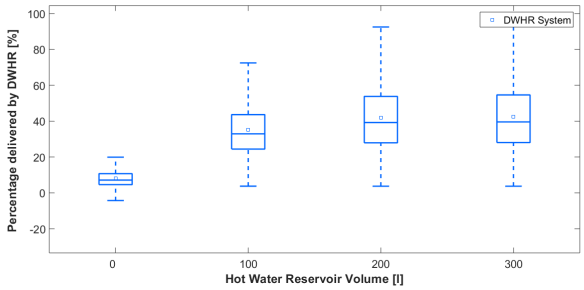


Figure 5.30.: Evolution of the heat delivered by DWHR.

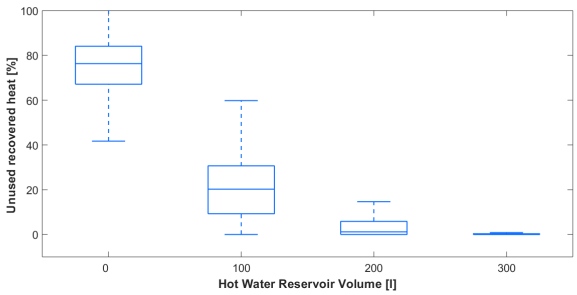


Figure 5.31.: Evolution of the unused recovered heat.

Levelized Cost of Energy

Due to the high capital costs of the DWHR system, the LCOE remains significantly higher than the average value in the current thermal energy mix, as can be seen in Figure 5.32. Implementing this heat recovery method would result in a yearly increased cost of heating ranging between 630€and 680€.

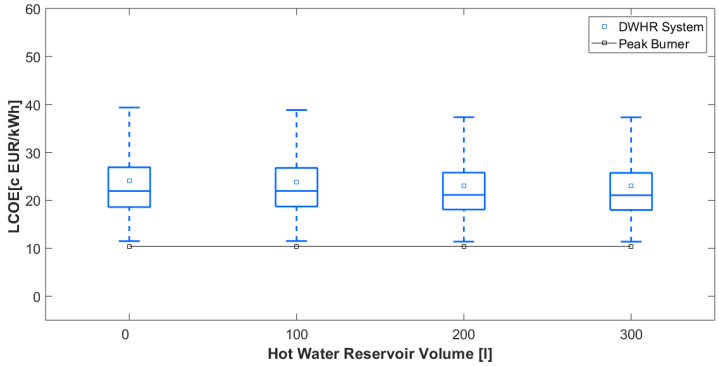


Figure 5.32.: Evolution of the LCOE.

The feasibility can be increased, by increasing the amount of recovered heat for a similar capital cost. Hence, the system needs to turn more hours per day. This increase can be achieved by considering domestic residences with a large occupancy, or by considering collective housing systems, such as apartment buildings, student dorms, etc. Alternatively, one can move downstream, where larger volumes of wastewater are available (see Chapter 7), or upstream where higher temperatures are available (see Chapter 6).

Total Equivalent Warming Impact

In contrast, Figure 5.33 shows a decrease in TEWI per kWh of heat from the DWHR system, with increased hot water reservoir volume, as compared to the TEWI of the average thermal energy mix. This results in an average reduction in $CO_{2,eq}$ emissions varying between 109.25 $kg\ CO_{2,eq}$ and 315.82 $kg\ CO_{2,eq}$ per year for an average residence.

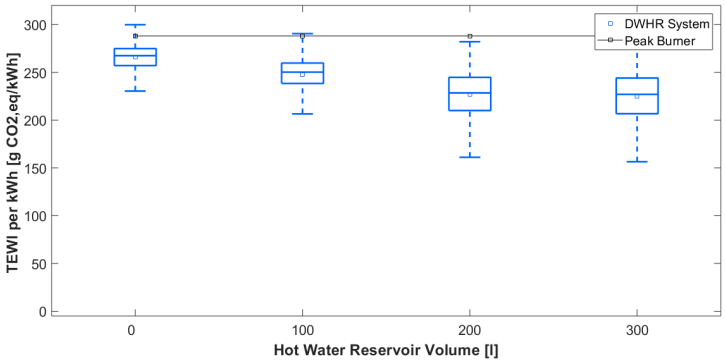


Figure 5.33.: Evolution of the TEWI.

Significance of the method

This method can be considered significant if the temporal component has a significant impact on the outputs, when compared to the regular analysis, which is based on average values. In order to investigate this, the method was applied to a fictional home, with a domestic hot water consumption of 11.21 kWh/day, and a space heating consumption of 25.74 kWh/day (average values of the Building Energy Rating database, see Section 5.4.4).

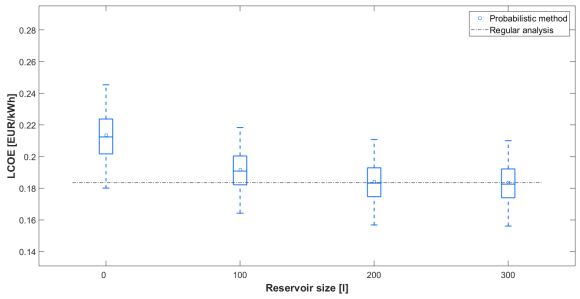


Figure 5.34.: LCOE of the method compared to the average value analysis.

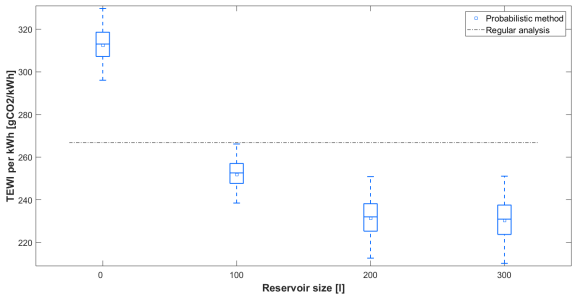


Figure 5.35.: TEWI of the method compared to the average value analysis.

Figure 5.34 shows that taking the temporal component into consideration did not affect the LCOE, as the LCOE obtained by the analysis based on average values falls within the confidence interval of the LCOE calculated with the probabilistic method. However, Figure 5.35 shows that the effect on the TEWI was significant. This is due to the fact that the LCOE is largely determined by the large capital cost, and the operational cost has a smaller impact. For the TEWI the fixed impact was less significant compared to the overall value, and this shows that the temporal component has a significant impact on the obtained result. These figures show that the TEWI is underestimated when no effort is made to mitigate temporal mismatches. This is due to the fact that part of the recovered energy is unused due to temporal mismatches (see earlier this Section). The TEWI is overestimated when efforts to counteract temporal mismatches are present, this can be achieved thanks to the system being able to operate at an improved efficiency (Coefficient of Performance, see Section 5.4.2) when the temperature exceeds the average temperature.

Impact of COP and Heat Pump Price uncertainties

As shown in Section 5.4.2, there are additional uncertainties related to the regressions used to predict the COP and the price of the heat pump. In order to investigate whether or not these uncertainties significantly impact the results of the simulation, the simulation is performed using a reservoir size of 200l, at the boundaries of the confidence interval given in Section 5.4.2. Similar to the previous Section, the simulation was performed for a fictional home, with a domestic hot water consumption of 11.21 kWh/day, and a space heating consumption of 25.74 kWh/day.

- **Impact of the COP uncertainty**

The resulting LCOE and TEWI of the simulation, using a 200l reservoir, for the predicted COP regression, and the boundaries of the confidence interval, are shown in Figure 5.36 and Figure 5.37. This shows that the impact of the COP uncertainty on the LCOE and TEWI is not significant, both show a spread between the predicted value at the lower and upper boundary of the COP of around 1% compared to the value at the predicted COP.

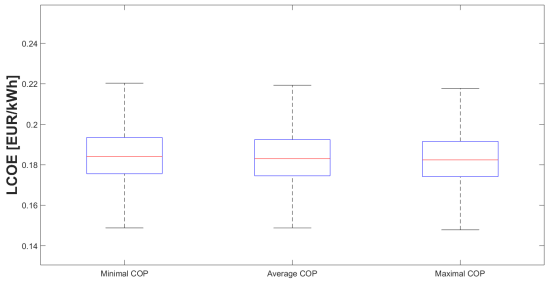


Figure 5.36.: Impact of the COP uncertainty on LCOE at 200l.

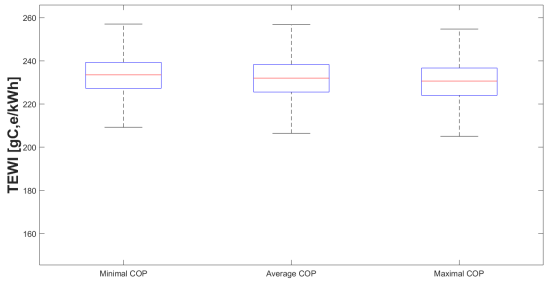


Figure 5.37.: Impact of the COP uncertainty on TEWI at 200l.

- **Impact of the heat pump price uncertainty**

The resulting LCOE of a simulation, using a 200l reservoir, for the predicted price regression, and the boundaries of the confidence interval, are shown in Figure 5.38. The heat pump price did not have an impact on the TEWI. However the impact of the price uncertainty on the resulting LCOE was significant, shown by the fact that the expected value for the minimal and maximal price do not fall within each other's 95%-confidence interval. The spread between the expected LCOE at the lower boundary of the heat pump price (12.88 $c€/kWh$), and the LCOE at the higher boundary (29.30 $c€/kWh$) is 89% of the LCOE at the predicted heat pump price (18.41 $c€/kWh$). On the one hand, this large spread is due to the goodness of fit of the regression on the heat pump price, which, at 75%, is lower than the one for the COP. On the other hand, a large variation remains on the price of the heat pump, one can often find different prices for the same heat pump model, depending on the supplier. A more precise estimation of the price is thus necessary, in further planning stages of the project.

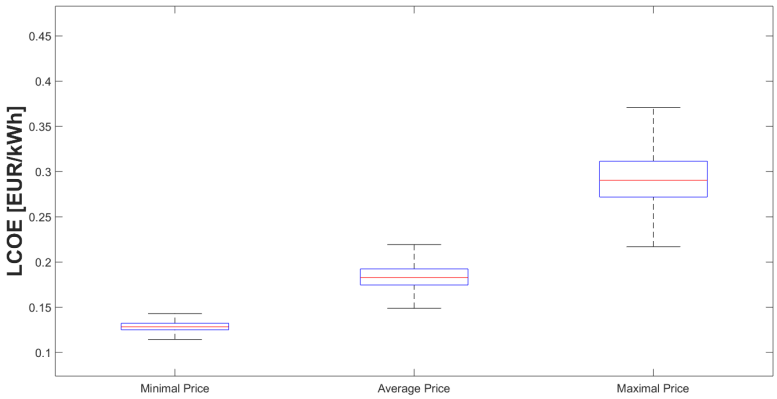


Figure 5.38.: Impact of the price uncertainty on the LCOE for a reservoir of 200l.

5.5. Summary

Currently, space and water heating is generally (91% in Europe [Gartland and Bruton, 2016]) delivered on an individual residence basis. Furthermore domestic wastewater accounts for a flow of about 1.42 $N\ m^3/day$, yearly this accounts for about 4.79 TWH of embedded energy being flushed through the drain. This corresponds to about 1.24 $M\ tons C_e$ emissions, and a cost of 397 $M€$. In addition to this, recovering (all) this heat would increase the share of renewable heat in Ireland's thermal energy mix to $17.4 - 18.4\%$, well above the 12% target for 2020. This chapter described a probabilistic method, for studying the interaction of this heat recovery with the wastewater system.

Temporal mismatches between heat provided by a drain water heat recovery system, and heat consumption are, although often disregarded in literature, a crucial factor in assessing the feasibility of the former. Generally, the only available information for residences is the average monthly consumption. This chapter described a probabilistic method to assess the temporal, daily evolution of DHW and SH demand, and the availability of waste heat in domestic drain water, using observations from 113 residences in the UK. The DHW and SH consumption of a residence is generally only known in terms of average monthly or yearly values, through energy bills or Building Energy Ratings. This method uses the observed distribution of the evolution of these demands during a day, and over the year, to create Synthetic Load Profiles. These SLPs were then used to generate distributions for the daily profiles of the demands and the availability of waste heat in drain water. The operation of the drain water heat recovery systems was predicted based on a monitoring campaign at three residences, measuring wastewater temperature and flow at 5-minute intervals, for over a 1-year period. The performance of this system was assessed using the performance data of 26 commercially available heat pumps, with rated power below 7 kW. This temporal, daily profile is important to assess the concurrence between the availability of waste heat in drain water, and the heat demand.

This impacts the financial viability, and related emission reductions of such systems. Similarly, the method can be used for other heating methods where the supply is not controlled, such as solar thermal. The paper shows a significant difference in the results obtained through this method, when compared to previously published analysis based on average values, in the case of the TEWI. For the LCOE the difference is not significant, this is mainly due to the large share of the capital investment in the final value of the LCOE. Where the temporal mismatch between heat demand and recovered heat availability is counteracted using a reservoir, the TEWI is reduced. This is because the system can be operated at times when the temperature exceeds the average temperature, and can thus increase its COP.

The method was applied to assess the feasibility of having drain water source heat pumps, as a means to indirectly recover the waste heat in drain water, for a hypothetical average Irish residence, obtained through a Monte Carlo analysis on just under 700 000 Irish residences. When using a drain water heat recovery system, a back-up heating system remains necessary. It is generally required right after the consumption peaks, when the accumulated recovered heat is depleted to meet the peak in demand. The share of heat demand that can be met by the DWHR system varies between 8% and 42%. Due to a mismatch between the availability of waste water heat and the heat demand, recovered heat could be wasted. In order to avoid this a hot water reservoir can be used to store the recovered heat. Using a hot water reservoir of $300l$ can reduce the amount of recovered heat that is unused from 75% without a reservoir to less than 1%, with a reservoir. This shows a mismatch between heat demand and the availability of heat in the wastewater.

Using the DWHR system greenhouse gas emissions related to domestic hot water- and space heating can be reduced by 7.6% to 22%. However, this increases heating costs by a factor ranging from 120% to 130%. At current traditional heating prices, the DWHR system for a single residence is not financially competitive with traditional systems, due to its high capital investment. Combining waste water streams from different residences would provide a larger flow, and potentially a high recoverable energy volume. However, heat would be lost between the residence and the collection point, reducing the energy density of the waste water. In turn this could lead to an increased GHG intensity of the recovered heat. An optimal collection point should be found, considering the trade-off between increased energy volume and reduced energy density.

In addition, policy makers should consider the financial incentivization of domestic DWHR systems to enable the GHG savings of up to 22% to be achieved. Financial incentives which could cover the additional 630€to 680€per year in heating costs, could be an attractive government level investment in GHG reductions, depending on the eventual cost of exceeding reduction targets.

Furthermore, applying this method to combined waste water streams, such as large apartment buildings for example, could also show a significant difference in the LCOE obtained through the averages-based analysis, and the method described in this paper. This remains to be investigated. Policy makers should also consider incentivizing DWHR to improve its financial competitiveness and help achieve the above GHG emissions savings.

Different choices in exploitation strategy exist, and could counteract this increased cost:

- Moving upstream, where temperatures (and thus energy density) are higher. The drawback here is that flow is smaller, and that the total energy volume is smaller. This is studied in Chapter 6.
- Move downstream, where a larger volume is available, however temperatures will be lower. This is studied in Chapter 7.
- Using hybrid heat pumps, with multiple sources. This means that a traditional air- or ground source heat pump is complemented with a heat recovery from drain- or wastewater, to boost the performance. This is not described in this thesis, but the author of this thesis participated in a research paper (under review), investigating this possibility.

6. Exploitation Strategy: Decentralized drain water heat recovery in commercial kitchens

6.1. Introduction

Chapter 5 showed the potential for heat recovery from wastewater streams of individual residences, and the related reduction in greenhouse gas intensity of the provided heat. However, this chapter also highlighted the increase in heating related costs, compared to conventional heating fuels. One of the methods considered for increasing the profitability of DWHR systems, was moving upstream where temperatures are higher. In a domestic setting, moving upstream implies low and infrequent flow, these aren't favourable conditions for improving the profitability. To counteract this, heat recovery upstream in a commercial setting was studied, where water intensive business activities allow for greater energy densities and volumes, and thus improve the viability of such projects. This chapter describes the potential from kitchen drain water (see Figure 6.1), in the hospitality and food services sector. Hot water – intensive outlets include hotels, restaurants, pubs, cafes, leisure centers, hair salons, etc. Commercial kitchens are common to many of these establishments, explaining the vantage point of this chapter.



Figure 6.1.: Decentralized heat recovery on a kitchen scale.

In 2013, the food and drink industry in the United Kingdom had an energy consumption of approximately 37 TWh/yr, and a water consumption varying between 347.3 and 366.4 Mm^3/yr, of which 153.7-158.8 Mm^3/yr was consumed in the hospitality and food services [Bromley-Challenor et al., 2013]. Over 80% of the energy provided to heat hot water in these sectors is delivered by fossil fuels [Goodright, 2014]. This is in strong contrast with the UKs ambitions in reducing greenhouse gas emissions. The UK aims for a 51% reduction by 2025, compared to 1990 levels, and a reduction of 80% by 2050 [CCC, 2018]. To achieve this target a legally binding carbon budget is fixed, estimated at 3 519 $ktons\ Ce$ for the period 2018 â 2025 [CCC, n.d.].

Furthermore, the monitoring campaign (see Section 4.2) showed drain water temperatures of kitchens ranging up to 55°C, as can be seen in the feasibility studies in Appendix B.

This research aims at defining the critical factors for feasibility of drain water heat recovery systems in commercial kitchens. Commercial kitchens in the hospitality and food sector represent a large user of both water and heat, and are thus a significant target for drain water heat recovery. This paper also aims at estimating the total potential for drain water heat recovery, through direct heat exchange, for the total hospitality and food services sector in the UK. [1]

6.2. Drain water heat recovery from commercial kitchens in the hospitality sector

6.2.1. Methods and analysis

Objectives of the method

During their peak occupancy, commercial kitchens can be large hot water consumers. Heat consumption, through hot water usage, and the availability of waste heat in drain water are strongly correlated and time dependent [Spriet and McNabola, 2019*a*; Wallin and Claesson, 2014]. The variation is largely due to the kitchens activity schedule, and the number of customers typically served.

The objective of this method is to predict daily profiles for heat consumption, based on the statistical distribution of the seprate consumption of both hot and cold water in monitored commercial kitchens (see later this Section). Based on these profiles, the availability of waste heat in commercial kitchen drain water was assessed. This information was used to size and simulate the operation of a direct drain water heat recovery system (DWHR), using commercially available heat exchangers. To avoid unrealistic draw profiles, and to account for non-random temporal effects, a different distribution of heat consumption was used for each hour of the day. These distributions are based on the measured data within each hour of the day, as described in this chapter.

The method aims to compare the optimal design from a financial and environmental point of view, and to extrapolate the results in order to estimate the potential market for this technology at a national scale (the UK). The related greenhouse gas emission savings potential was also estimated.

Data

The methodology applied here was adopted from Spriet and McNabola [2019*a*]. Synthetic load profiles (SLP) were generated to account for the daily variation in hot- and cold water consumption, and thus drain water flow, in commercial kitchens. These SLPs were generated using Monte Carlo simulation, showing the consumption at a certain point in time, as a percentage of the mean daily value. The actual consumption or flow was then given by multiplying the average daily value with the value of the synthetic load profile for the particular time of day (see Equation 6.1). For each time of day, a particular distribution for the SLP is determined based on the data described in this section. In each iteration, an SLP value is generated for each time of day, depending on these respective distributions.

$$\dot{V}(tod) \;=\; V_{FW,daily}\; SLP_{daily}(tod) \tag{6.1}$$

Where $\dot{V}$ is the hourly flow, V is the daily flow and tod is time of day, the subscript FW stands for fresh water.

The SLPs vary from kitchen to kitchen, depending on the activity schedule, amount of meals served, size of the dishwashers, etc. This variation is accounted for by considering the statistical variation on the SLP values. Each iteration of the Monte Carlo simulation randomly generates a different SLP profile, based on the statistical distributions of observed values.

The data used to fit the statistical distributions, which form the starting point to generate the random sample in each of the Monte Carlo iterations, was measured at four commercial kitchens, over a number of different monitoring periods.

[1] The research presented in this chapter was published as a journal paper in the journal *Energy and Buildings* [Spriet and McNabola, 2019*b*]

- **Kitchen water consumption**

Kitchen water consumption was measured at a café /restaurant in a tourist attraction in the UK (the tea rooms of Penrhyn castle, Bangor, North Wales). The café /restaurant and tourist attraction experienced annual visitor numbers of 100 000. Visitor numbers and hence kitchen water consumption also varied across the year according to the tourist season. The hot water and cold-water volumetric flow was measured, logging at a pulse for every liter consumed, between August 2017 and July 2018. The daily variation is shown in Figure 8.7, in Chapter 8. Based on this data, a distribution for the hourly SLP was generated for both hot water $SLP_{HW,flow}$,compared to mean hot water flow) and cold water $SLP_{CW,flow}$,compared to mean cold water flow), as shown in Figure 6.2. A distribution representing the share of hot water (α_{HW}) from the total water consumption is shown in Figure 6.3.

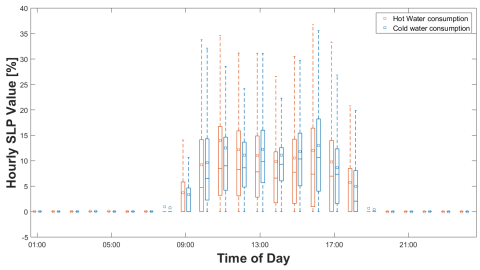


Figure 6.2.: Hourly SLP profile for water demand.

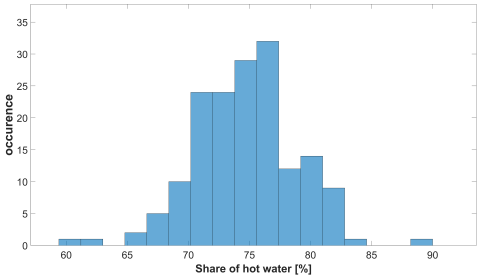


Figure 6.3.: Share of hot water consumption in the kitchen.

For each iteration (it), Equation 6.1 could then be split into hot and cold water flow, as shown in the set of Equations 6.2.

$$\begin{cases} \dot{V}_{FW,hot}(it,\ tod) \ = \ \alpha_{HW}(it)\ V_{daily}(it)\ SLP_{HW\ \ flow}(it,tod) \\ \dot{V}_{FW,cold}(it,\ tod) \ = \ (1-\alpha_{HW}(it))\ V_{daily}(it)\ SLP_{CW\ \ flow}(it,tod) \end{cases} \tag{6.2}$$

- **Kitchen drain water flow**

Butler and Davies [2010] estimate a return factor (link between water consumption and drain water flow) for the UK at 95%. In this paper, a more conservative figure was used, the drain water return flow was considered to be 90% ($\alpha_{todrain}$) of the total water consumption of the kitchen. The remaining 10% was assumed to have evaporated, been dried with towels, or left the kitchen through routes other than the drain. It was also assumed that none of the kitchen appliances had a water retention time of more than one hour, resulting in the drain water exiting the kitchen within the hour after it entered. This results in an SLP for the drain water ($SL_{DW\ \ flow}$) as shown in Figure 6.4. The value for a given iteration at a given time of the day is given by Equation 6.3.

$$\dot{V}_{DW}(it,tod) \ = \ \alpha_{todrain}\ V_{FW,daily}(it)\ SLP_{DW\ \ flow}(it,tod) \tag{6.3}$$

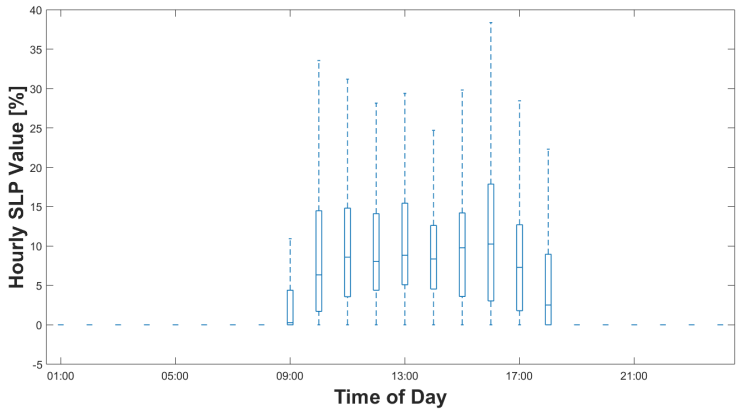


Figure 6.4.: Hourly SLP profile for drain water flow.

- **Kitchen drain water temperature**

The temperature of the drain water was predicted in a direct way, not using an SLP. The profiles were generated based on measurements performed in four different, large-scale or commercial kitchens:

- The kitchen of the tea rooms of a tourist attraction, welcoming 100 000 visitors a year, in Wales. The details regarding this tourist attraction and the commercial kitchen, are detailed in Chapter 8, as this establishment was used for a pilot study.

- The kitchen of a 145-bedroom hotel and resort, in county Wicklow, Ireland.

  At this luxury resort, spread over 360 acres, a monitoring campaign of about three weeks (18/08/2017 − − 09/09/2017) was performed, measuring the temperature of the grease trap, of the kitchen (location 2), and the drain of the showers of the swimming pool (location 1), as shown in Figure 6.5. Details are shown in Appendix B.1.

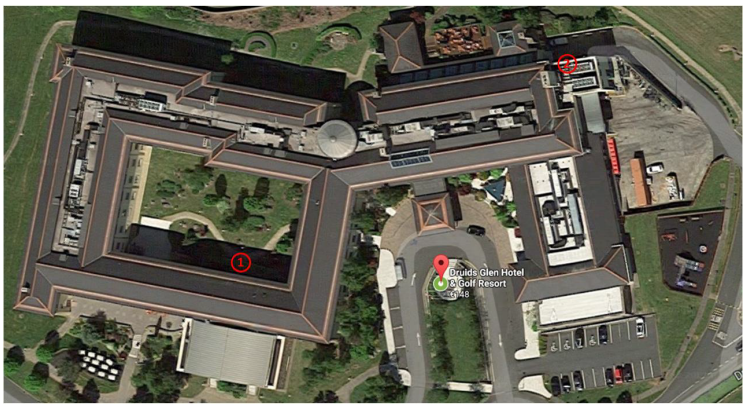


Figure 6.5.: Druids Glen hotel and resort.

- The kitchen of a 150-bedroom hotel in Dublin, Ireland.

  At this hotel, the grease interceptor is located under the parking lot, and is accessible through three manholes, one for the inlet, one for the first and one for the second chamber, as shown in Figure 6.6. The temperature in the first chamber, measured between 23/02/2018 and 12/03/2018, was relatively stable, around 25 to 30°C. When the temperature sensor was moved to the inlet manhole, the temperature was observed to be significantly higher, but showed more variation as can be observed in Figure 6.7. More details can be found in Appendix B.2.



Figure 6.6.: Manholes leading to the grease trap at the Talbot hotel, Stillorgan, Dublin.

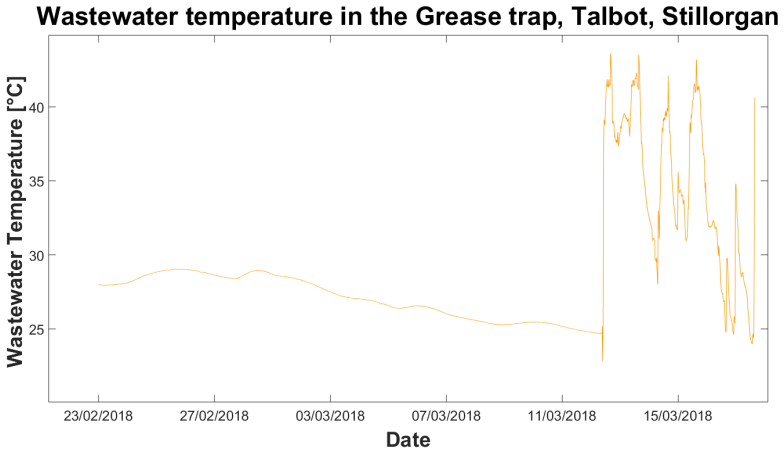


Figure 6.7.: Temperature at the Grease interceptor, Talbot Hotel, Stillorgan, Dublin.

- The kitchen of a retirement home, with 52 residents, in county Tipperary, Ireland.

  At the retirement home, in co. Tipperary, the temperature was monitored at two locations. The first one being the septic tank treating all the wastewater of the retirement home, and secondly the grease trap, placed under a courtyard on the premises. The temperature at the grease interceptor showed peaks up to 45°C, and a high temperature variability, as shown in Figure 6.8. The temperature was monitored from April 9th 2018 to May 1st 2018.

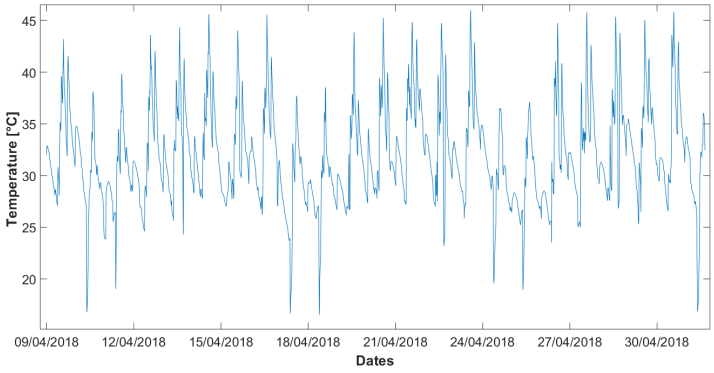


Figure 6.8.: Temperature evolution in the grease interceptor at Ashlawn nursing home.

The data was measured at these locations for a period varying between three weeks and one year, at a measuring interval of once per minute to once per five minutes. The temperatures were measured and logged using TinyTag TG4100 temperature loggers. A distribution for the temperature at each time of day was generated based on the combined data set, in order to approach a randomized hypothetical kitchen which is representative of a wider range of commercial kitchens. The resulting profile can be found in Figure 6.9.

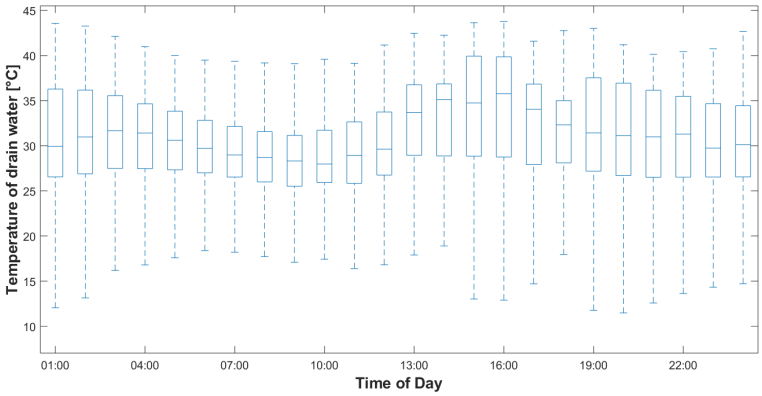


Figure 6.9.: Temperature profile for a random kitchen.

- **Fresh water temperature**

The fresh water temperature was measured, on a daily basis, for one year in a residence in Dublin in 2011-2012 [Gill et al., 2016]. For a simulation of the operation over a whole year, these measured temperatures (Figure 6.10) were used.

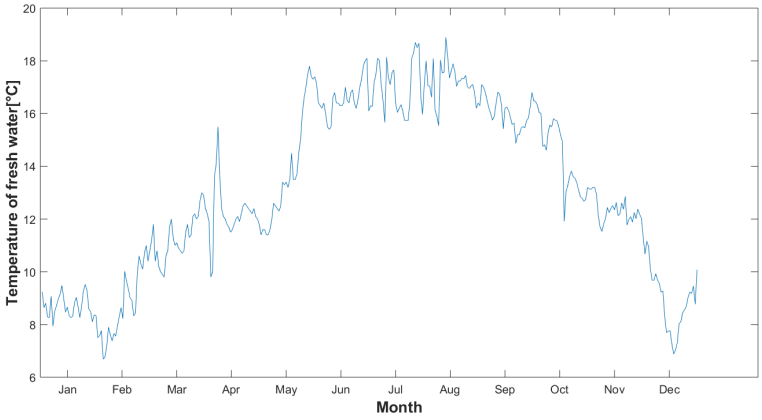


Figure 6.10.: Fresh water temperature in Dublin, 2012.

- **Water consumption in the food and hospitality sector**

Data on over 258 000 hospital and food outlets was assessed and divided into nine different outlet types. Each of these outlet types is characterized by a certain water intensity for the meals served at these outlets. Data on 9.59 *million* meals served in the UK in 2017 was obtained from Backman [2018], this data can be found in Appendix D.1. The outlets were categorized into four categories, each with a representative value of number of meals served in the UK (see section 6.2.3). The water intensity for each of the outlet types was then used to estimate the kitchens water consumption [Bromley-Challenor et al., 2013]. The number of outlets for each of these outlet type-category combinations in the UK in 2017 was also obtained from Backman [2018].

- **Carbon intensity**

The carbon intensity of the different heating fuels, used in the analysis were obtained from the UK Government GHG Conversion Factors for Company reporting [Department for Business Energy & Industrial Strategy, 2018*a*]. The conversion factors used are summarized in Table 6.1. The fuel prices are found in Department for Business Energy & Industrial Strategy [2018*b*].

Table 6.1.: Fuel prices and carbon conversion factors in the UK.

Fuel	**Abbreviation**	**Price**(p£$/kWh$)	**C intensity** ($kg\ C_e/kWh$)
Heavy Fuel Oil	HeFO	4.88	0.28544
Electricity	Elec	15.72	0.28307
Natural Gas	NGas	4.32	0.20437
Coal	Coal	4.98	0.36288
Bio Mass (Wood Pellets)	BMWP	4.50	0.01506

- **Carbon emissions related to production of the heat recovery system**

The carbon footprint of the heat exchanger was assumed to be 56 $kg\ Ce$ with copper requirements of 25 kg per device, adopted from the findings of Ip et al. [2018]. The system boundaries comprised the whole life cycle, while use phase was considered not to create any impacts. With the different scenarios for the amount of recovered heat, a carbon payback time of half a year to 10 $years$ is proposed [Ip et al., 2018].

Monte Carlo simulations

The Monte Carlo simulation method was used for the analysis, in order to create a generalized profile, based on a monitored sample of residences or kitchens. The four key steps, as described in Section 4.3.1, are enumerated below:

- The domain and the probability functions of the input variables (drain water flow and drain water temperature) were defined based on the data described above. In the case of this project, this distribution was used to randomly sample the share of the water consumption which is hot water, the SLP for the daily profile of hot and cold-water consumption, and wastewater generation at each hour of the day. This was done to allow for potential variations and differences in between the kitchens in the sector and for deviations in these kitchens from the behaviour observed in the monitored kitchens.
- A random set of $N = 10\ 000$ iterations was generated, this number was determined based on a trade-off between computation time, and a negligible change in the distribution of the results. The probabilistic method is described below.
- The calculation method is described below, in Section 6.2.2.
- The resulting distributions are described in Section 6.2.3.

Methods of comparison

A sensitivity analysis was performed on the total daily water consumption of the kitchen, and the method was applied for each total daily water consumption. Based on the results of each of the simulations an optimal design was determined selecting the number of commercial heat exchangers (see Section 6.2.2) required. The optimal design could be designated, both from an environmental point of view, and from a financial one, for each of the total daily water consumptions assessed. The optimal financial design point was selected based on maximizing the Net Present Value over 10 $years$. The environmental optimal point was defined as the design with the maximal Carbon-NPV value, calculated based on the Carbon payback of the Carbon emissions required for the production of the heat recovery system. Both methods are described in this section.

- **Financial Comparison: The Net Present Value method**(See section 4.3.1)

The net cash flow at year 0 was considered to be the initial investment, and thus negative. The cash flow during each year was the reduced operating expenses minus the maintenance cost, which was considered to be 1% of the investment. This number resulted from discussions with the manufacturer of the heat exchanger (see Section 6.2.2). The discount rate (r) was considered, first to be 7% in accordance with previous investigations on this topic and in line with US guidance [Spriet and McNabola, 2019*a*; Wang, 2017; Rushing et al., 2013]. The considered period over which NPV was calculated was 10 $years$ (n), and this was significantly shorter than the lifetime of the heat exchanger, which is expected to exceed 20 $years$. This discount rate and period is a compromise between the expected lifetime of the system and short-term business interests of commercial kitchens. An example of the evolution of the NPV of a system using one heat exchanger, over a 10 $year$ period is given in Figure 6.11, for a daily water consumption of 4000 l, and compared to heavy fuel oil as the heating fuel. Figure 6.11 shows that the NPV is expected to rise above 0 after 4 $years$, and that it can be said with 75% certainty that the true mean of the NPV will rise above 0 after 5 $years$. An NPV value above 0 means that the investment has been paid back, and profit is made.

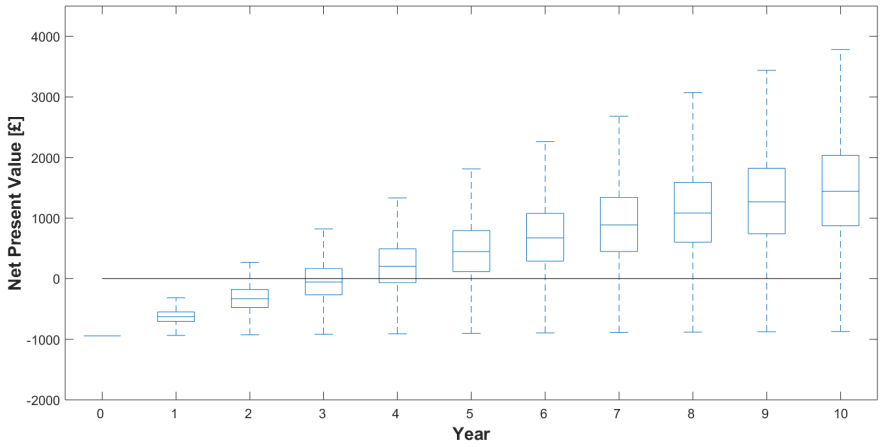


Figure 6.11.: Boxplot of the NPV for a drain water heat recovery installation with water consumption of 4000 l, compared to Heavy Fuel Oil (HeFO).

- **Environmental comparison: Carbon-NPV method**

The Net Present Value method is again employed, using the same parameters, but with carbon data as the input values. In this case the optimal use of carbon emissions, emitted in the present for production of the heat recovery system, is considered to be the one creating the largest amount of Carbon emission savings, over the targeted period. The formula is the same as in Equation 4.2. However, the considered 'Net Cash Flow', are the yearly carbon emission savings, and the cash flow at year 0, are the emissions related to the production of the system.

6.2.2. DWHR System set-up

DWHR System description

The direct DWHR system considered in this paper is a commercially available heat exchanger, consisting of 2 concentric pipes. The middle pipe contained the drain water flow, whereas the outer pipe contained clean fluid flow, circumscribing the inner pipe. The heat exchanger is shown in Figure 6.12



Figure 6.12.: The ShowerSave Q-Blue 1 heat exchanger.

The system requires a vertical orientation and a vertical drop in the drain pipe of 2.1 m, to be installed [Kimmels, 2011]. The direct DWHR system is used to preheat the fresh water, thus reducing the heat consumption of the regular heating system (see Figure 6.13). In case of multiple installed heat exchangers, they are considered to be installed in parallel, as can be seen in Figure 6.14.

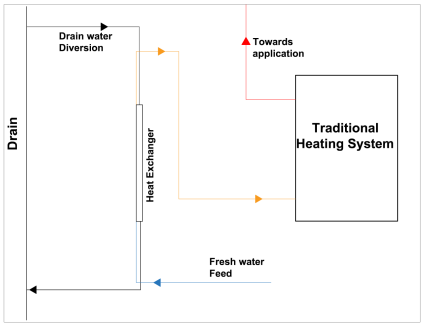


Figure 6.13.: Single heat exchanger.

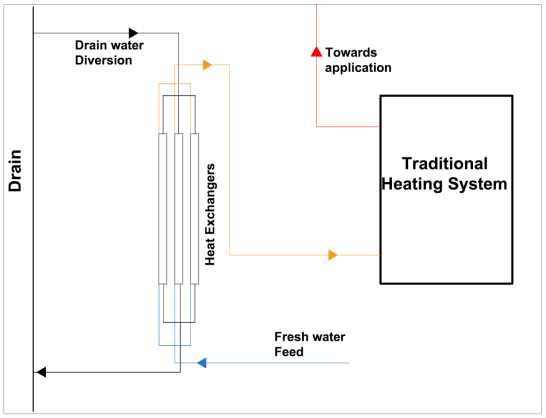


Figure 6.14.: Combined heat exchanger system.

Heat Exchanger

The heat exchanger that was considered comprised 168 cm long concentric pipes. Each pipe had a capacity of 50 l/min of drain water. In this analysis, the effectiveness of the heat exchanger was estimated at 58%. The variation of the effectiveness of the heat exchanger, with varying flows was shared by the manufacturer, and is shown in Figure 6.15. The estimated effectiveness here is a weighted average of the expected effectiveness, based on the manufacturer's information, and the flows observed in the drain of the kitchen at the tourist attraction in Wales (see Section 6.2.1).

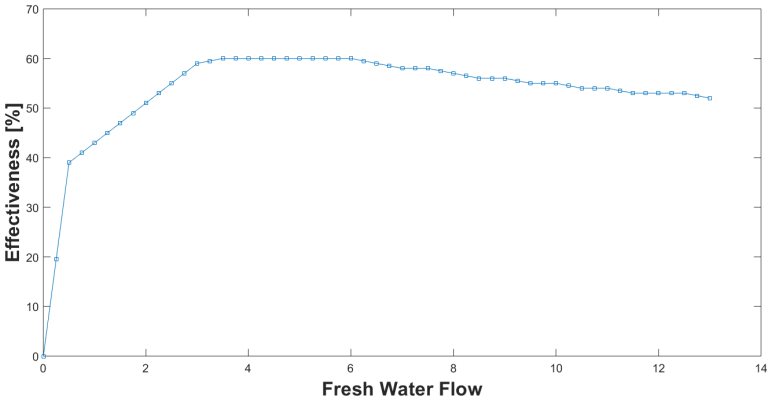


Figure 6.15.: Effectiveness of the heat exchanger.

The capital investment for the heat exchanger, and its installation is broken down in Table 6.2. The prices are obtained through quotations and actual purchasing costs from operators experienced in the installation heat recovery systems.

Table 6.2.: Fuel prices and carbon conversion factors in the UK.

	Unit cost (£/*unit*)	**# Units**	**Total cost (£)**
Labour	35	10	350
Material and fittings	100	1	100
Heat exchanger	496	*variable*	*variable*
Total			*variable*

6.2.3. Assesment of the heat recovery potential in kitchens in the hospitality sector

Optimal design

A sensitivity analysis was performed on the total daily water consumption of the hypothetical, generalized kitchen, selecting the design with the highest average NPV, and Carbon-NPV after 10 years. Over 100 000 Monte Carlo simulations were conducted. The solution varied depending on the type of current heating fuel in place for the studied kitchen, as shown in Figures 6.16 and 6.17.

- **Financial criterium**

Figure 6.16 shows the evolution of the expected NPV values with varying daily water consumption, the corresponding Carbon-NPV value, and the corresponding number of heat exchangers in the optimal solution, based on the financial criterion. The solution is shown for different fuel types. One can observe that the threshold for deciding to add an additional heat exchange pipe in parallel is different for each fuel type, ranging from 3 250 l/day for electric water heating to 5 500 l/day for natural gas and wood pellets. The daily flow threshold, required for profitability (when the NPV is larger than zero), also varies with different fuels, ranging from 500 l/day compared to electric heating, to 1 750 l/day for natural gas.

In Figure 6.16, one can observe that the heat recovery systems at kitchens with a relatively small water consumption, have a Carbon-NPV (in green) which is larger than 0. This means that even though the system is not considered financially viable, it would still provide a reduction in GHG emissions. Strictly applying the financial criterion would thus result in unexploited potential for GHG emission reduction. The importance of this share of unexploited potential for the UK is discussed in Section 6.2.3.

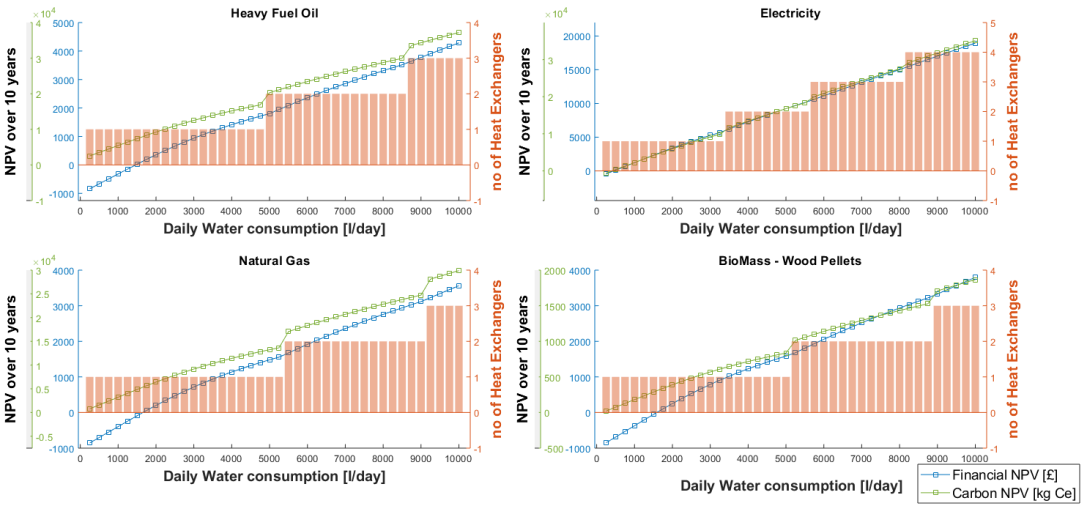


Figure 6.16.: Evolution of the NPV compared to different heating fuels.

- **Environmental criterion**

Figure 6.17 shows the evolution of the expected Carbon-NPV values, and the related financial NPV values, with varying daily water consumption, and the corresponding number of heat exchangers in the optimal solution. The solution is again shown for different fuel types. One can observe that the threshold for deciding to add an additional heat exchanger is different for each fuel, and falls at a lower flow rate than for the financial criterion.

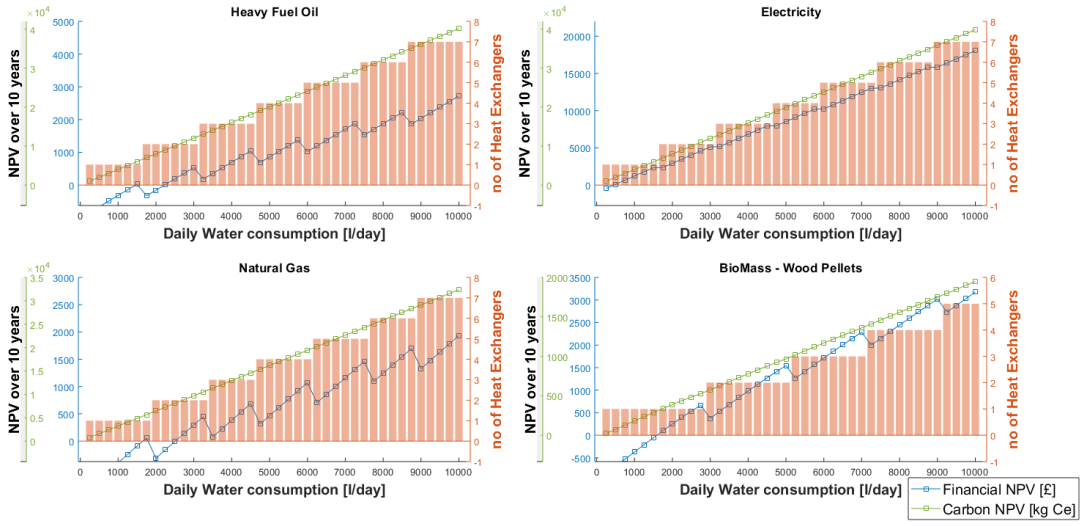


Figure 6.17.: Evolution of the carbon- NPV compared to different heating fuels.

In Figure 6.17, one can observe that when the environmental criterion is used, the selected system could not be financially viable (water consumption below 2 500 l/day), or the financial NPV can be smaller than the optimal solution determined in the prevvious Section. The number of heat exchanger pipes in the environmentally optimal solution is significantly higher than in the financially optimal solution.

- **Impact of fuel pricing and taxation**

Fuel prices and taxes are likely to change over time, and between countries. A sensitivity analysis, studying three fuel prices was performed, using electric heating for comparison. The three electricity prices which were studied are 9.78 $p£/kWh$ (the average industrial electricity price in the UK), 15.72 $p£/kWh$ (the average domestic electricity price in the UK) and 26.68 $p£/kWh$ (the average domestic electricity price in Germany in 2017, which was the highest in the EU) [Department for Business Energy & Industrial Strategy, 2018*b*]. In this analysis, taxes are considered as a part of the fuel price. The evolution of the NPV, at different electricity prices are shown in Figures 6.18, 6.19.

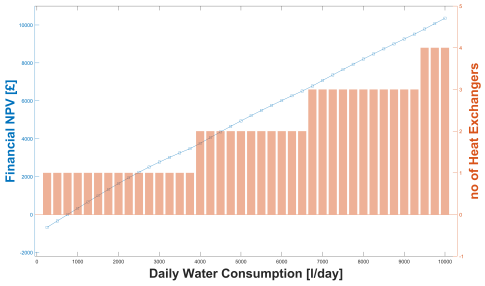


Figure 6.18.: Evolution of the NPV compared to electricity (9.78 $p£/kWh$).

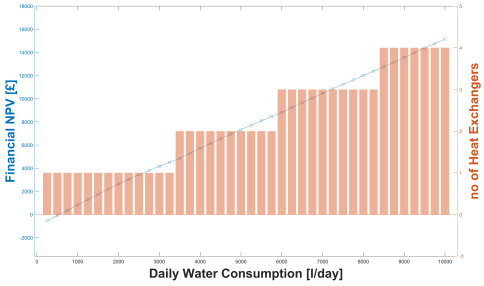


Figure 6.19.: Evolution of the NPV compared to electricity (15.72 $p£/kWh$).

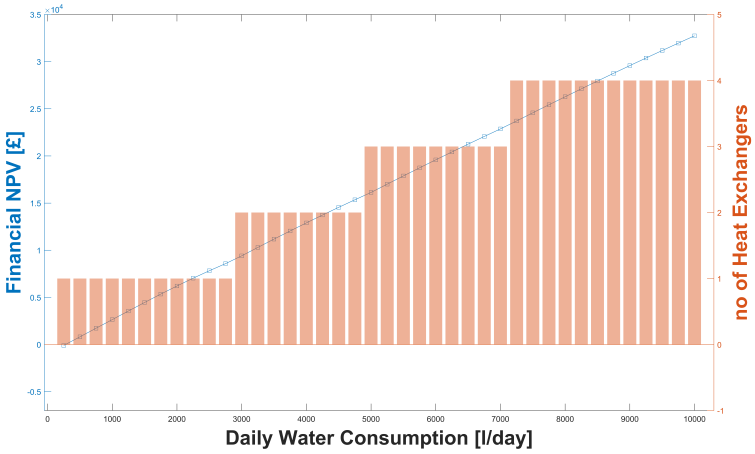


Figure 6.20.: Evolution of the NPV compared to electricity (26.68 $p£/kWh$).

One can observe that the profitability threshold is reached at lower daily water consumption, when the fuel price was increased. Similarly, for some cases, this resulted in a larger number of heat exchangers being installed at the financial optimum. Higher fuel prices, either through increased pricing or taxation, increase the profitability of the discussed DWHR system. A similar sensitivity analysis can be made for the discount ratio, where a reduced discount ratio, results in an increase in profitability, and thus lower threshold values, and a larger number of heat exchangers, in particular cases. The impact of a different choice in discount ratio, on the total recoverable heat in the sector in the UK is shown this Section.

Potential for the deployment of this technology in the UK

The total water consumption of the hospitality and food service sector in the UK varied between 153.7M and 158.8M $m^3/year$, in 2013 [Bromley-Challenor et al., 2013]. The number of meals served in 2017, in over 258 000 outlets in the UK, divided in nine different outlet types, each with their own water intensity per meal were. This assessment revealed a consumption of about 170.3M $m^3/year$, using the same assumptions of water consumption per meal as in Bromley-Challenor et al. [2013] (see Table 6.4) for approximately 9.59 *million* meals. Applying the same Monte Carlo analysis on the total flow in the sector shows an expected heat recovery potential for the UK of 1.40 $TWh/year$ (Figure 6.21). Assuming the carbon intensity of the energy mix for hot water heating [Goodright, 2014] at 0.2773 $kg\ C_e/kWh$, results in expected potential carbon emissions savings of approximately 388 $k\ tons\ C_e/yr$ (Figure 6.22).

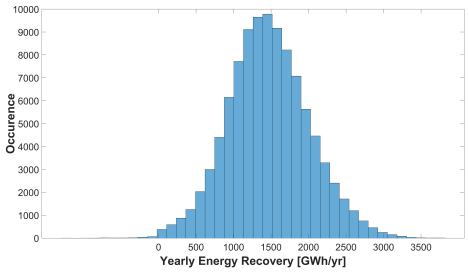


Figure 6.21.: Yearly heat recovery potential in the UK.

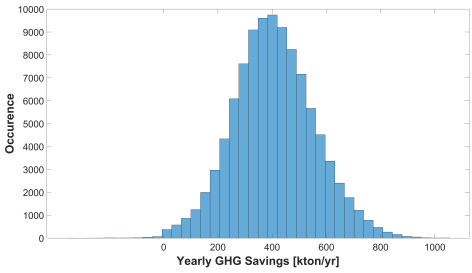


Figure 6.22.: Yearly GHG savings potential in the UK.

Not all of this available heat recovery potential can be recovered in a financially profitable way. Therefore, the distribution of the water consumption over the different consumers was examined, assessing which type of consumers can recover heat from their drain water in an economically viable fashion (selecting the maximum positive NPV, see Section 6.2.1), and how much heat they will recover in this case.

Distribution of hot water consumption in the food and services sector

Using the data mentioned in the previous Section, the commercial kitchens in the hospitality and food services sector can be split into four categories of consumption, with a fixed assumed value for each consumption category, as shown in Table 6.3.

Table 6.3.: Consumption levels.

	Cat I	**Cat II**	**Cat III**	**Cat IV**
Consumption ($meals/yr$)	$<$ 10 000	10 000-29 000	30 000-100 000	$>$ 100 000
Assumed value ($meals/yr$)	7 500	20 000	65 000	125 000

To estimate the water consumption in these categories of consumption, they were subdivided across nine different outlet types, with different characteristics regarding their water consumption per meal served. The resulting daily water consumption of each of these outlet types is summarized in Table 6.4.

Table 6.4.: Daily water consumption for the different categories.

	Water/meal ($l/meal$)	**Cat I** (l/day)	**Cat II** (l/day)	**Cat III** (l/day)	**Cat IV** (l/day)
Restaurants	25	750	2 000	6 500	12 500
Quick Service Restaurants	12	360	960	3 120	6 000
Pubs	12	360	960	3 120	6 000
Hotels	20	600	1 600	5 200	10 000
Leisure	12	360	960	3 120	6 000
Staff Catering	18.5	555	1 480	4 810	9 250
Health Care	25	750	2 000	6 500	12 500
Education	18.5	555	1 480	4 810	9 250
Services	25	750	2 000	6 500	12 500

The distribution of the different commercial kitchens over these categories and outlet types is given by Backman [2018] and can be found in Appendix D.1.

Results and Discussion

The total potential for heat recovery and the financial feasibility was then estimated, using the data from Table 6.4 as input values for the Monte Carlo simulation. They are compared using the financial criterion (the environmental criterion resulted a positive Carbon-NPV for all categories and outlet types). The potential for energetic savings and carbon equivalent emission reduction are discussed below. The price of the general fuel mix (6.13 $p£/kWh$) was used as the fuel price of comparison [Goodright, 2014].

- **Financial criterion**

The financial criterion, described in Section 6.2.1, was used to determine which of the different categories and outlet-type combinations could recover wastewater heat in a financially profitable way. As discussed earlier, a drain water heat recovery system was considered profitable if the NPV over 10 $years$ was larger than 0. The results are summarized in Table 6.5, where $C\ NPV$ is the Carbon NPV over 10 $years$ (see Section 6.2.1).

Table 6.5.: Summary of results based on the financial criterion..

	Cat I ***NPV***		**Cat II** ***NPV***		**Cat III** ***NPV***		**Cat IV** ***NPV***	
	(£)	($kg\ C_e$)	(£)	($kg\ C_e$)	(£)	($kg\ C_e$)	(£)	($kg\ C_e$)
Restaurants	−356.68	2 886.9	707.71	7 701.9	3 628.8	23 491.7	7 526.9	45 542
QSR	−695.20	1 355.6	−174.41	3 710.9	1 518.8	11 370.9	3 360.3	22 033
Pubs	−695.20	1 355.6	−174.41	3 710.9	1 518.8	11 370.9	3 360.3	22 033
Hotels	−486.88	2 298.5	377.58	6 208.5.9	2 808.1	19 534.7	5 919.7	35 942
Leisure	−695.20	1 355.6	−174.41	3 710.9	1 518.8	11 370.9	3 360.3	22 033
Staff Catering	−525.94	2 147.4	275.39	5 746.2	2 522.5	18 241.7	5 444.3	33 791
Health Care	−356.68	2 886.9	707.71	7 701.9	3 628.8	23 491.7	7 526.9	45 542
Education	−525.94	2 147.4	275.39	5 746.2	2 522.5	18 241.7	5 444.3	33 791
Services	−356.68	2 886.9	707.71	7 701.9	3 628.8	23 491.7	7 526.9	45 542

In Table 6.4, one can observe that all category and outlet-type combinations resulted in a positive Carbon NPV, meaning that they are profitable from a carbon emission point of view. However, for all outlet types in category I, along with Pubs, QSRs and Leisure in category II, the financial NPV is negative meaning that the DWHR system is not financially profitable. Heat recovery is thus unlikely to be implemented in these cases, leaving some unexploited potential for the reduction of carbon related emissions in the sector. Currently available DWHR systems are not financially attractive at low flow values, leaving a gap in the market for inexpensive DWHR devices, to fill this void.

- **Energy Savings**

Applying the Monte Carlo simulation on all outlets in the UK showed a certain potential for heat recovery, and thus energy savings in the sector. Applying the financial criterion showed which share of this can be expected to be implemented in a financially profitable way under the current conditions. It is expected that these systems can be implemented without additional financial support, and the fact that they are not can be partly explained by a lack of interest and/or awareness for the technology, and the fact that, in several cases, water heating represents only a small part of the operational budget of the outlet. However, technical difficulties such as the distance between the kitchen water drain and the heating system, and the availability of space to install such a system can impact the practical penetration of these systems in the market. The results, separated by outlet-type, are shown in Figure 6.23.

Figure 6.23 shows a very large potential among Health Care outlets (335 GWh/yr), mainly due to their large size, and thus large water consumption in most of the UK outlets. This results in a large share of the potential which can be exploited in a profitable manner. This assumes that the required space for installation of the heat exchanger is available, namely a $2m$ vertical drop in the drain, and that the kitchen drain is located within a reasonable distance of the heating system. A criterion for the distance could be that the kitchen drain passes through the technical room where the heating system resides, or an adjacent one. On another level one could represent this distance criterion as follows: the distance between the heat exchanger and the heating system should be transferrable using mains pressure only, so no additional pumping is required. This information is particular to each individual outlet, and was not available. Given these assumptions, 1.24 TWh of heat is estimated to be recoverable on a yearly basis, in a financially profitable way, over the entire sector. As a comparison, Neugebauer et al. [2015] estimated a potential from all wastewater entering wastewater treatment plants from all sectors in Austria at 2.32 TWh.

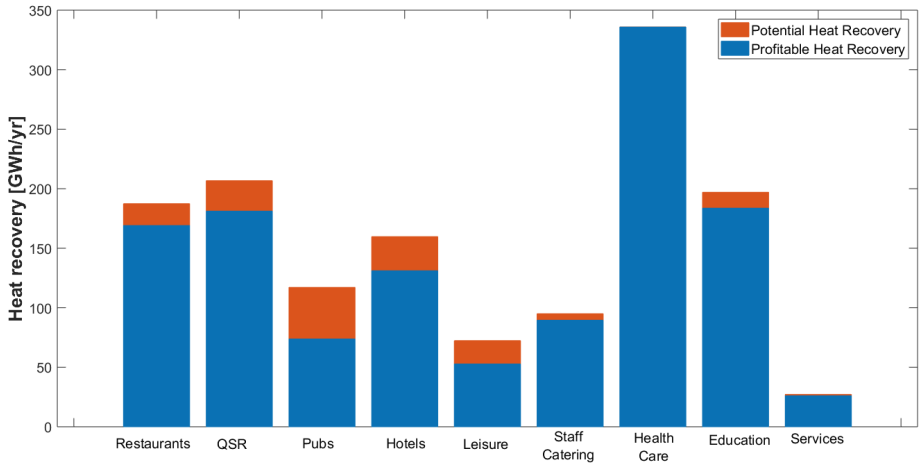


Figure 6.23.: Heat recovery potential per outlet type.

Around 11% of the assessed potential here would be untapped, when using the financial criterion and the current heat recovery system. This untapped potential was mainly found in category I outlets, at commercial kitchens with low water consumption.

- **Carbon emission reduction**

This heat recovery potential results in a potential for greenhouse gas emissions reduction, both total and profitable, as shown in Figure 6.24.

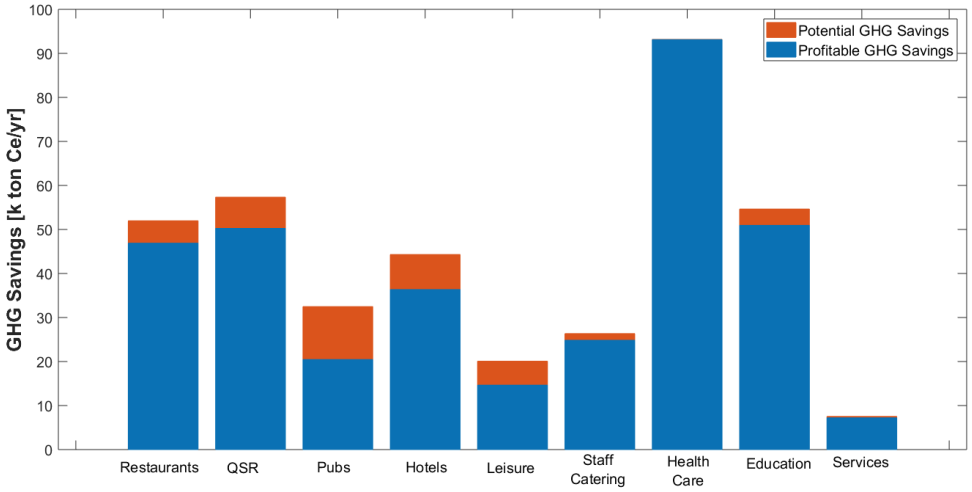


Figure 6.24.: GHG savings potential per outlet type.

The total potential for the reduction of Carbon equivalent emissions is around 388 $k\ tons\ C_e/yr$, of which 344 $k\ tons\ C_e/yr$ could be obtained in a financially profitable manner. The UK has an emission reduction target of 80% (compared to the 1990 level) by 2050, and an intermediary goal of a 51% reduction by 2025 [CCC, 2018]. This results in a legally binding carbon budget for the period 2018-2025 of 3 519 $k\ tons\ C_e$ [CCC, n.d.]. The reductions estimated here that could be obtained in a financially profitable manner, over the period 2018-2025, represent 0.07% of the carbon budget for that same period.

However, the profitable systems would require a total investment, over the whole sector, of around 101.02 $M£$. Assuming a 10 $year$ lifetime of the system, this represents an investment of 2.94 $p£/kg\ C_{e,saved}$. As a comparison, using the Levelized Cost of Energy as given by Spriet and McNabola [2019*a*] and Wang [2017], wastewater source, ground source, and air source heat pumps, for single residence domestic heating require an approximate cost of 1.9, 2.3 and 1.9 $£/kg\ C_{e,saved}$, several orders of magnitude larger. This heat recovery system in commercial kitchens can thus be considered as 'low-hanging fruit', as mentioned by the Climate Change Committee [CCC, 2018].

- **Impact of the discount rate on Energy and Carbon savings**

The acceptable discount rate for an investor (in this case the owner of the considered kitchens), is highly dependent on the investors preferences such as: is the investor risk adverse, or not?; what the rate of return of other investments is? The determination of the acceptable discount rates is thus a strategic decision, determined by the investors [Žižlavský, 2014]. In the analysis described above the discount rate was set at 7%, however more risk adverse investors might require a higher discount rate, or a lower one to allow more risk. The heat recovery potential in the UK was assessed with different discount rates (3, 7 and 10%), but the total profitable heat recovery potential proved insensitive to this parameter, meaning that no statistically significant difference in heat recovery potential was observed. Although individual NPV-values differed for varying discount rate, the changes in the number of heat exchangers in the optimal solution, and the profitability threshold were statistically insignificant, as is shown in Figure 6.25 and Figure 6.26.

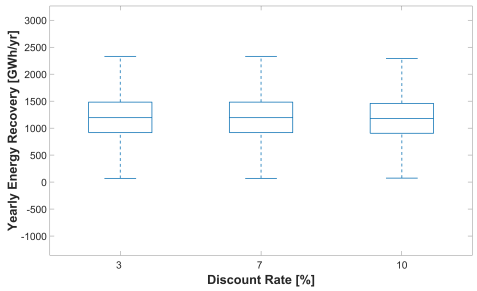


Figure 6.25.: Yearly heat recovery potential in the UK, with varying discount rate.

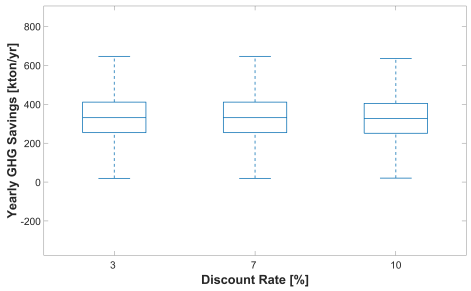


Figure 6.26.: Yearly GHG savings potential in the UK, with varying discount rate.

- **Sensitivity of the heat exchanger effectiveness**

The discussed heat exchanger (Section 6.2.2) requires an available head of just over 2 m, which is not always available. In case no head is available, horizontal heat exchangers can be considered, however the effectiveness of horizontal heat exchangers can be expected to be lower than vertical ones [McNabola and Shields, 2013]. Effectiveness could also lower over time due to fouling. To investigate the impact of changes to the effectiveness, a sensitivity analysis was performed. In this case a flow of 2000 l/day was considered, as was the weighted average flow, 5094.87 l/day. The lowest considered efficiency was 10%, the highest one 70%. The impact on the NPV of the system that is optimal from a financial point of view, is shown in Figure 6.27.

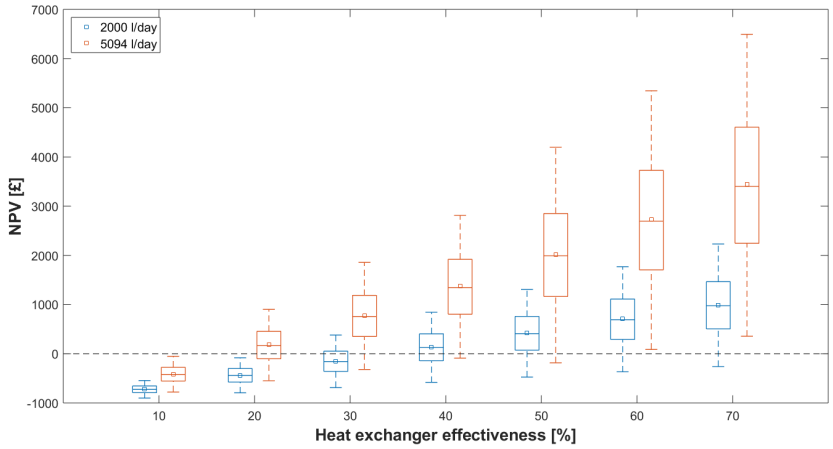


Figure 6.27.: Sensitivity of the financial NPV with varying heat exchanger effectiveness.

As expected, NPV increased with increasing effectiveness. In Figure 6.27 one can observe that the expected value of the NPV remains positive, once the effectiveness is larger than 20%, for a water consumption of 5 094 l/day, and once the effectiveness exceeds 40% for 2 000 l/day, meaning that the system is expected to be profitable. However, for the lower spectrum of effectiveness ($10 - 20\%$, even 30% for the lower water consumption), the NPV drops below 0. This means that the system is not profitable once considerable loss of efficiency occurs, for example due to extreme fouling, or due to the use of the (vertical) heat exchanger in a horizontal position. In case the required head space is not available, a specifically designed heat exchanger would be necessary, changing the capital investment, and thus these NPV considerations. One can also observe that the uncertainty increases for a water consumption of 5 094 l/day, starting at 30% and once again at 50% effectiveness. This is due to the fact that the financially optimal design switches from one heat exchanger to two heat exchangers at that value.

Figure 6.28 shows the evolution of the Carbon NPV with varying effectiveness. One can observe that the 5^{th}- percentile remains positive, showing that the solutions remain attractive from an environmental point of view. Loss of efficiency, for example due to fouling, or non-optimal use of the heat exchanger reduces the environmental benefits, but does not neutralize them.

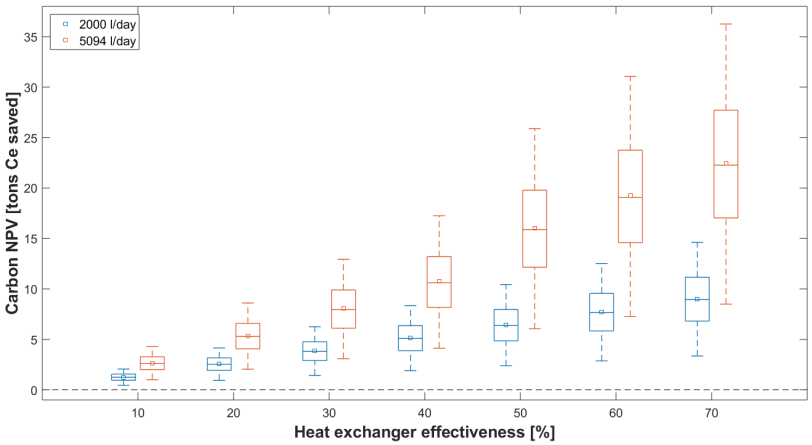


Figure 6.28.: Sensitivity of the environmental (Carbon) NPV with varying heat exchanger effectiveness.

6.3. Conclusion and Summary

In order to meet ambitious greenhouse gas reduction targets, the reduction of fuel consumption in the heating sector is necessary. This paper assesses the impact of introducing direct drain water heat recovery systems in commercial kitchens in the UK, based on a commercially available heat exchangers. The recoverable heat from these kitchens was estimated using Monte Carlo simulation, sector consumption data, and data measured in the field.

This chapter introduced a direct drain water heat recovery system for commercial kitchens, based on a commercially available heat exchanger. The recoverable heat from these kitchens was estimated using a probabilistic method. This recoverable heat was then used to study the financial feasibility, compared to different heating fuels used to provide hot water to the commercial kitchen, and the daily water consumption of the kitchen.

The feasibility was assessed based on financial and environmental criteria, both are a NPV calculated over 10 $years$. The financial criterion showed feasibility threshold values for the water consumption, varying with the heating fuel used in the kitchen. The environmental criterion yielded a feasible solution in all studied cases.

The financial criterion was then applied to estimate the total profitable potential for drain water heat recovery in the hospitality and food service sector in the UK. The fuel price was assumed as the price of the heating mix for hot water heating (6.13 $p£/kWh$) the same method was used for the carbon conversion factor (0.2773 $kg\ C_e/kWh$). Using the aforementioned Monte Carlo method, the study showed a financially attractive drain water heat recovery potential of around 1.24 TWh/yr which could result in a reduction in the global warming potential of the sector of 344 $k\ tons\ C_e/yr$. The outlet type with highest recovery potential was found in kitchens in the Health Care sector. However, in kitchens with low water consumption, unexploited heat recovery potential remains, which should be recovered by other methods.

A sensitivity analysis showed a significant influence of the heat exchanger effectiveness on the financial criterion. Special care must thus be taken when selecting the heat exchanger in actual projects. A heat exchanger which is not suited for the application could have adverse effects on financial profitability.

The installation of the proposed system in all financially feasible outlets in the sector would require an estimated investment of around 101.2 $M£$, which results in an investment cost of around 2.94 $p£/kg\ C_{e,saved}$ over a 10 $year$ lifetime. This ratio is several orders of magnitude smaller than the cost of replacing all current heating systems by heat pumps, it can thus be considered low hanging fruit on the pathway to a less-carbon intensive hot water production in the sector.

A sensitivity analysis showed that loss of efficiency of the heat exchanger (below 30% at a water consumption of 2 000 l/day, and below 20% at 5 094 l/day), leads to a drop below the feasibility threshold, meaning that the system would not be financially feasible anymore. It remains feasible using the environmental criterion however, although the environmental benefits are reduced.

Commercially available drain water heat recovery systems could, when installed, exploit around 88% of current potential in drain water heat in commercial kitchens (1.40 TWh/yr) in a manner that is financially profitable. However, this paper assumes the availability of a 2 m vertical drop in the kitchen drain, required to install the heat exchanger, and thus achieve optimal effectiveness. In case this head is not available, the heat recovery potential would be untapped, as in approximately 160 GWh, in kitchens where the hot water consumption is too small for financial profitability. This corresponds to a reduction in GHG emissions of 44 $k\ tons\ C_e/yr$ and leaves a gap in the market for inexpensive DWHR devices, which could exploit this potential at lower efficiencies. The development of a prototype of such a device, is described in Chapter 10.

7. Exploitation Strategy: Centralized drain water heat recovery at wastewater treatment plants

7.1. Introduction

Another possibility for increasing the profitability of DWHR systems, described in Chapter 5, was moving downstream, where wastewater volumes, and thus energy volumes are larger. In this chapter, the chosen downstream location is the effluent of the wastewater treatment plants, as shown in Figure 7.1.

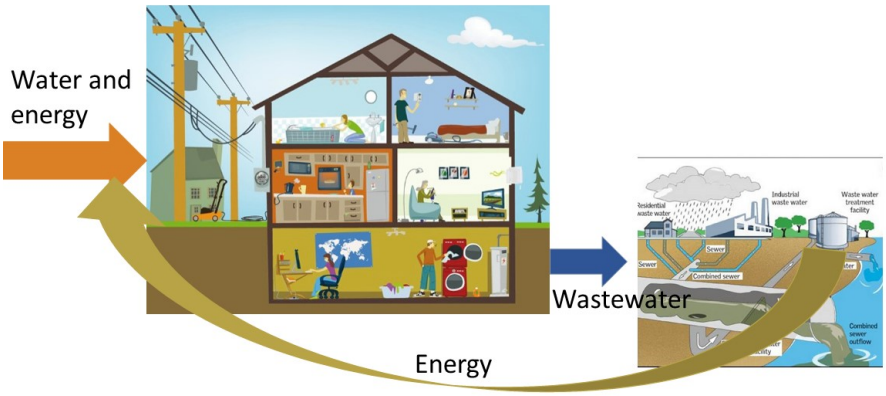


Figure 7.1.: Centralized heat recovery from the effluent of wastewater treatment plants.

Centralized drain water heat recovery has the advantage of large quantities of energy being available at a single location. However, as wastewater treatment is generally performed outside of town centres and living areas, this location can be at a distance of heat consumption. This can be done in large sewer collectors, or at the level of wastewater treatment plants. The sewers have the advantage of proximity to consumers, but also a shorter travel time of the wastewater, which results in a higher temperature, and thus a higher energy density of the wastewater. The disadvantage is that the wastewater hasen't received any type of treatment, and thus remains highly loaded with pollutants. This requires the use of an additional intermediary heat carrier, as described by Spriet and Hendrick [2017], to avoid complications with the heat pump system, this is shown in Figure 7.2. A second disadvantage is the concern it may raise with treatment plant operators, as a reduced wastewater temperature reduce the nitrification rate of the biological treatment process [Wanner et al., 2005].

Wastewater treatment plants provide the advantage of large volumes of wastewater, and the possibility to recover the heat directly from the clean effluent, without the need for an intermediate heat carrier. Their disadvantage is the distance to potential consumers. In this chapter, different aspects of heat recovery from wastewater treatment plants are discussed. This includes the proximity to demand, but also the temporal variation in both demand and supply, environmental aspects, etc.

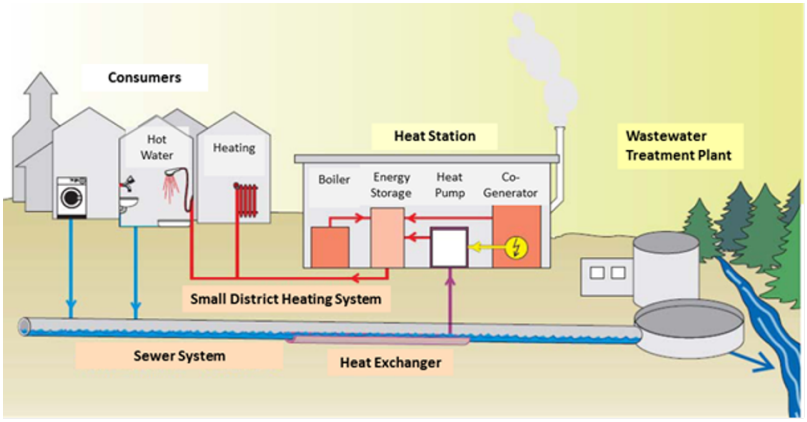


Figure 7.2.: Schematic of Sewer Heat recovery adapted from [Müller and Schmid, 2005].

Wastewater treatment plants have different ways to reach climate neutral operation, ranging from on-site renewable electricity generation through hydropower, photovoltaic panels or wind energy [Chae and Kang, 2013], use of energy from ground and drinking water [van der Hoek, 2011] to chemical and thermal energy recovery from the wastewater itself [Elías-Maxil et al., 2014]. Although the chemical energy is generally perceived as the main source of energy in wastewater, the potential for thermal energy recovery is 6-8 times larger [Hao et al., 2019]. However geographic proximity to heat demand and temporal mismatches impact the amount of energy that can be used in a sensible manner [Neugebauer et al., 2015; Spriet and McNabola, 2019*a*]. In this chapter the spatial proximity to heat demand is studied, for all wastewater treatment plants in Ireland (Section 7.2), and an integrated spatio-temporal method is applied to a case study on the treatment plant in Tullamore, Co. Offaly (Section 7.3). The environmental and financial aspects of this case study are discussed in (Section 7.4).

7.2. Heat recovery potential from WWTP effluent in Ireland: a spatial analysis

7.2.1. Method

The objective of the method is to establish a ranking of wastewater treatment plants in the Republic of Ireland, which should be considered for wastewater heat recovery, and to exclude treatment plants where heat recovery is not feasible or not desirable. In order to do this, different criteria must be taken into account, they are enumerated and described below.

- Heat demand density

For district heating, Danish heat planning uses a general rule of thumb requiring a yearly heat demand density of at least 40 kWh/m^2 for competitiveness of district heating. This is assuming that no established and competitive district heating exists in the network (which is not expected in Ireland), in which case lower heat density can be feasible [Gartland and Bruton, 2016]. In this analysis, the heat demand in small areas (see Section 7.2.2), was available, and thus the heat demand density was calculated per small area.

- Proximity to heat demand

The maximal distance between a heat source and heat consumer, for profitable systems is considered to be 2 km [Sandvall et al., 2016], however Hao et al. [2019]. mention distances from $3 - 5$ km, specifically for thermal energy recovery from effluent in WWTPs. In this analysis, the more conservative option was chosen, only wastewater treatment plants which lie within 2 km of a small area with a heat density of more than 40 kWh/m^2 are considered, and only the heat demand of small areas with the required heat density are taken into account.

The ranking method used here consists of selecting the small areas with sufficient heat demand density, within a distance of 2 km from the WWTP, and is summarized in Figure 7.3.

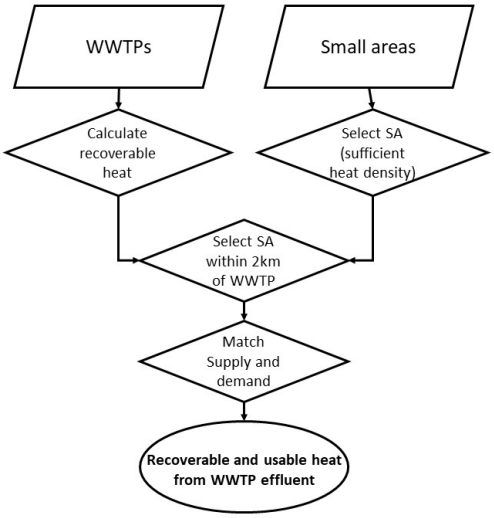


Figure 7.3.: Summary of the WWTP ranking method.

7.2.2. Materials

WWTPs in Ireland

The wastewater treatment plants, and their location are available from the Environmental Protection Agency of Ireland. In Ireland, all wastewater treatment plants, with a design population equivalent larger than 40 PE are required to apply for a wastewater discharge authorisation. Obtaining this authorisation requires producing a yearly environmental report, containing the hydraulic loading (in m^3/day).

In order to calculate the embedded energy in the wastewater, the allowable temperature is required, along with the hydraulic flow (given in the yearly environmental report). To calculate the temperature drop, the minimal temperature (T_{min})is set to $8°C$, the higher value is set based on the effuent temperature measured at the wastewater treatment plant in Tullamore, co. Offaly, where the average yearly temperature (T_{avg}), in 2018 was $15.8°C$. The embedded energy ($Q_{embedded}$) can then be calculated as in Equation 7.1, where $\dot{V}$is the volumetric flow, ρ is the density of the effluent, and c_p is the specific heat of the effluent.

$$Q_{embedded} = \dot{V}\ \rho\ c_p\ (T_{avg} - T_{min}) \tag{7.1}$$

The considered heat recovery system consists of using the effluent as a heat source for a heat pump. At the measured effluent temperature, the Coefficient of Performance (COP) of the heat pump is estimated at 4.2 [Spriet and McNabola, 2019*a*], meaning that per unit of electricity input, 4.2 heat units are produced. The delivered heat ($Q_{delivered}$), and the required electricity input (W_{el}) were calculated using Equations 7.2 and 7.3, respectively.

$$Q_{delivered} = Q_{embedded}\ \frac{COP}{COP - 1} \tag{7.2}$$

$$W_{el} = \frac{Q_{delivered}}{COP} \tag{7.3}$$

Heat demand in small areas in Ireland

In Ireland, census data is represented by small areas of $80 - 100$ households. This has the advantage of having more small areas, and thus increased precision in densely populated areas. The Sustainable Energy Authority of Ireland, used these same small areas to represent the distribution of heat demand over Ireland, as shown for Dublin in Figure 7.4. The heat density was then calculated based on the small area.

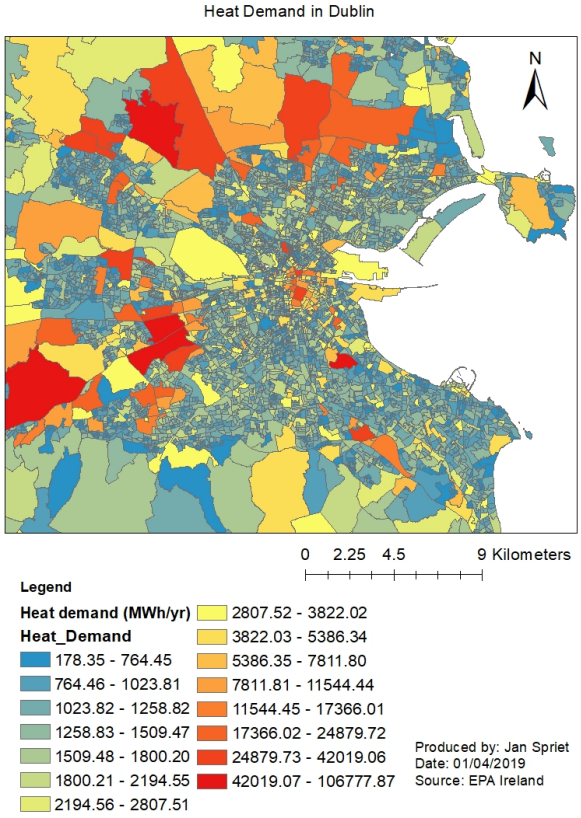


Figure 7.4.: Heat demand per small area in Dublin.

7.2.3. Results

Available energy at WWTPs in Ireland

The total deliverable energy from all 479 potential wastewater treatment plants in Ireland (for which information was available) was estimated at 6.34 TWh/yr, and distributed over the different wastewater treatment plants as shown in Figure 7.5. However, not all of these wastewater treatment plants are located sufficiently close to areas with a high heat density. Therefore this list is narrowed down later this Section.

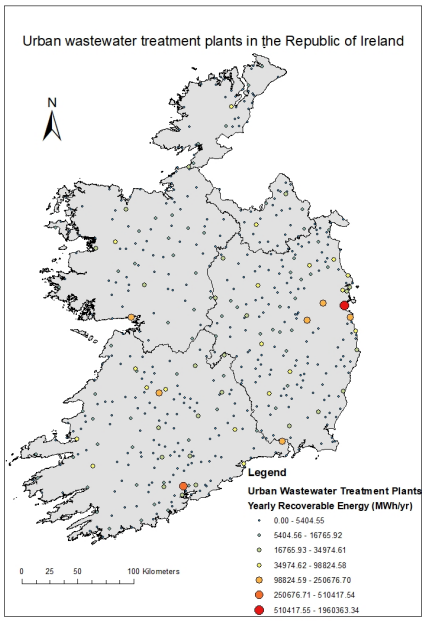


Figure 7.5.: Deliverable energy from all wastewater treatment plants in Ireland.

The largest potential can be found in the Ringsend wastewater treatment plant in the city of Dublin, with a potential of 1 960 GWh/yr. However this treatment plant is located on a finger into the Irish sea, and might not be located in close proximity to heat demand. That being said, a district heating plant is planned in the area, and heat recovery from the wastewater treatment plant can serve as a low-carbon supplement to the heating sources of the district heating network. [Flanagan, 2017]

Spatial analysis: Proximity to heat demand

The list of 479 wastewater treatment plants is then narrowed down to 40 plants located within 2 km of small areas with a heat density superior to 40 kWh/m^2. They have a combined potential of 4.5 TWh/yr, however when only the small areas with sufficient heat demand density are considered, only 236.55 GWh/yr were used. This number is thus the most conservative estimate of potential thermal energy that can be delivered, by heat recovery from wastewater treatment plants. However, when the backbone of the infrastructure for (district) heating networks is in place, the criteria could be less stringent, in these case it's an option to consider small areas with smaller heat demand density [Gartland and Bruton, 2016], and consider areas which are further away [Hao et al., 2019]. The wastewater treatment plants, and their potential for delivering thermal energy to heating networks through effluent heat recovery are shown in Figure 7.6.

One can note that, although the Ringsend wastewater treatment plant has the largest potential, it is only fifth on the ranking of exploited potential, when only small areas with sufficient heat demand density are considered, due to its location, as described above. In this scenario only 0.6% (10.8 GWh/yr) would be utilized. As mentioned earlier, this can be extended to areas with smaller heat demand density and areas which are further away, as the district heating network is already in place. [Flanagan, 2017]

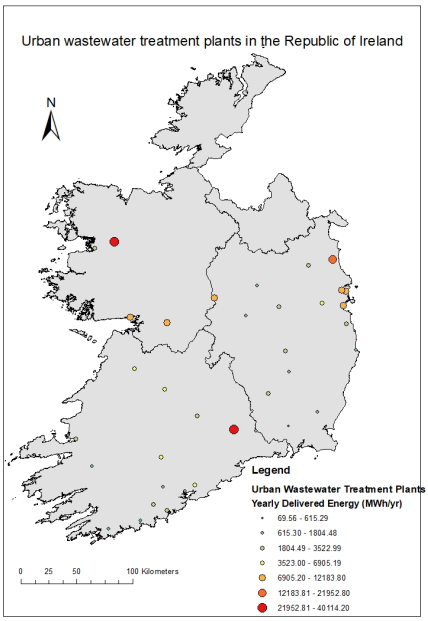


Figure 7.6.: Deliverable energy from suitable wastewater treatment plants in Ireland.

The potential embedded thermal energy, and the amount that would be recovered in this scenario is shown in Table 7.1, for the 3 largest wastewater treatment plants. One can observe that the used energy under this scenario represents only a small portion of the actual potential. These low percentages also indicate that the wastewater travels a long distance before reaching the treatment plant.

Name	**Potential Energy** (GWh/yr)	**Used Energy** (GWh/yr)	**Precentage**
Ringsend	1 960.36	10.84	0.55%
Lower Liffey Valley	1 178.91	4.02	0.34%
Galway	250.68	8.57	3.42%

Table 7.1.: Heat recovery from the three suitable WWTPs with a potential larger than 100 GWh/yr .

The other 37 wastewater treatment plants are represented in Figure 7.7.

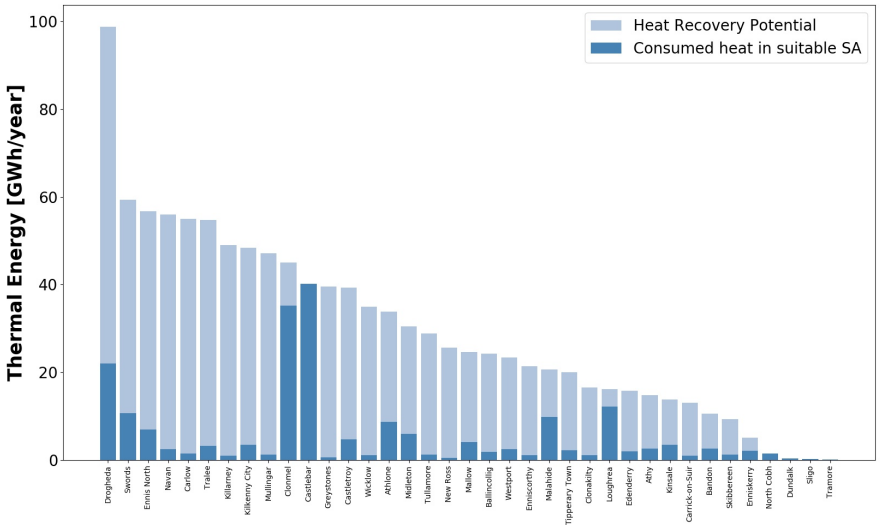


Figure 7.7.: Heat recovery from the suitable WWTPs in the Republic of Ireland.

7.2.4. Discussion

Analysis of 479 wastewater treatment plants in the Republic of Ireland, showed a total embedded energy in wastewater treatment effluent of 6.34 TWh/yr, with the largest potential (1.96 TWh/yr) in the Ringsend wastewater treatment plant. 40 wastewater treatment plants are located withing 2 km of a suitable small area with a heat demand density superior to 40 kWh/m^2, these plants have a potential of 4.5 TWh/yr. However when only the suitable small areas were considered, only 236.55 GWh/yr of consumption could be met. In this scenario, at the Ringsend wastewater treatment plant, only 0.6% (10.8 GWh/yr) was used. However, once a heating network is considered feasible (when the heat demand density superior to 40 kWh/m^2), it can be extended to regions with smaller heat demand density, and areas which are located further away. This has the potential to increase the amount of recovered heat that can be used in a sensible way.

In the example of Ringsend, a district heating network is currently planned in the region, and the recovery of the embedded energy in the effluent of the wastewater, can provide a large amount of heat, which can be used in case the district heating network is extended. A detailed study can provide the amount of heat that can be delivered to the heating network, and what the related costs are. To predict the operation of such systems and to assess the feasibility, the temporal variation of both supply and demand must be taken into account. These aspects, in combination with the spatial aspects discussed before, or discussed in Section 7.3, for the wastewater treatment in Tullamore, which is one of the 40 plants discussed earlier. Environmental and financial aspects of this case study are discussed in Section 7.4.

7.3. Integrated spatio-temporal analysis for wastewater heat recovery

The variation over a day, and over a year of the available heat in wastewater was investigated in Zurich, Switzerland [Schmid, 2008], in a valley in Austria [Kretschmer et al., 2016b], in Stockholm, Sweden [Lindstrom, 1985], in Bologna, Italy [Cipolla and Maglionico, 2013], and in Ireland [Spriet and McNabola, 2019*a*]. A review of methods to determine daily variation in heat demand for residential use is given by Fuentes et al. [2018]. The impact of these variations, and potential mismatches in supply and demand, on the operation and feasibility of such systems, was discussed by Spriet and McNabola [2019*a*] and by Wallin and Claesson [2014]. These temporal variations were identified as a significant factor in the feasibility of heat

recovery systems. Temporal mismatches reduce the amount of usable, recoverable heat, and thus have a negative effect on the feasibility of heat recovery projects.

The importance of spatial proximity of the heat recovery location to potential users was highlighted by Neugebauer et al. [2015]. The considered impacts were the amount of operating hours, and the thermal losses due to transport of the heat [Lichtenwoehrer et al., 2019]. These contributions have provided useful insight into the impact of temporal and spatial variations on the operation of heat recovery systems. However, the combination of both considerations is currently missing in literature, this section aims to bridge that gap. [1]

The focus of this research lies in combining the spatial and temporal considerations of assessing the operation and feasibility of wastewater heat recovery systems. System choices, such as questions of demand and principle technological options, have to be surveyed on the strategic level of planning [Stoeglehner, 2019]. It investigates both the spatial proximity and the temporal match between supply (recovered heat from wastewater) and demand. This is done by introducing a three-step methodology, containing an energetic, a spatio-temporal, and an integrated analysis. This allows for a comprehensive assessment of the operation of such projects, considering the exclusion of locations where heat demand is insufficient for an attractive heat recovery system, but also allowing for the identification of periods of scarcity or excess of heat. The former allows the identification of the need for additional heating systems and/or demand side management. The latter allows for the identification of potential expansion of industrial, commercial or agricultural activities in the vicinity of wastewater heat sources. This provides an additional tool for planners in assessing the feasibility of heat recovery projects, and also district heating projects. Summarizing the above, the paper provides a method to include both the spatial and temporal aspects in the assessment of the operation and feasibility of an effluent heat recovery system at a WWTP. This leads to a more detailed and comprehensive prediction of the actual recovered heat, and thus allows for a more precise prediction of the feasibility of such projects. The application on a case study in Ireland indicated the general practicability of the suggested method as well as the promising potential of wastewater heat recovery, and the role it can play to reach renewable energy and greenhouse gas reduction targets.

The graphical abstract, related to the published paper, is shown in Figure 7.8

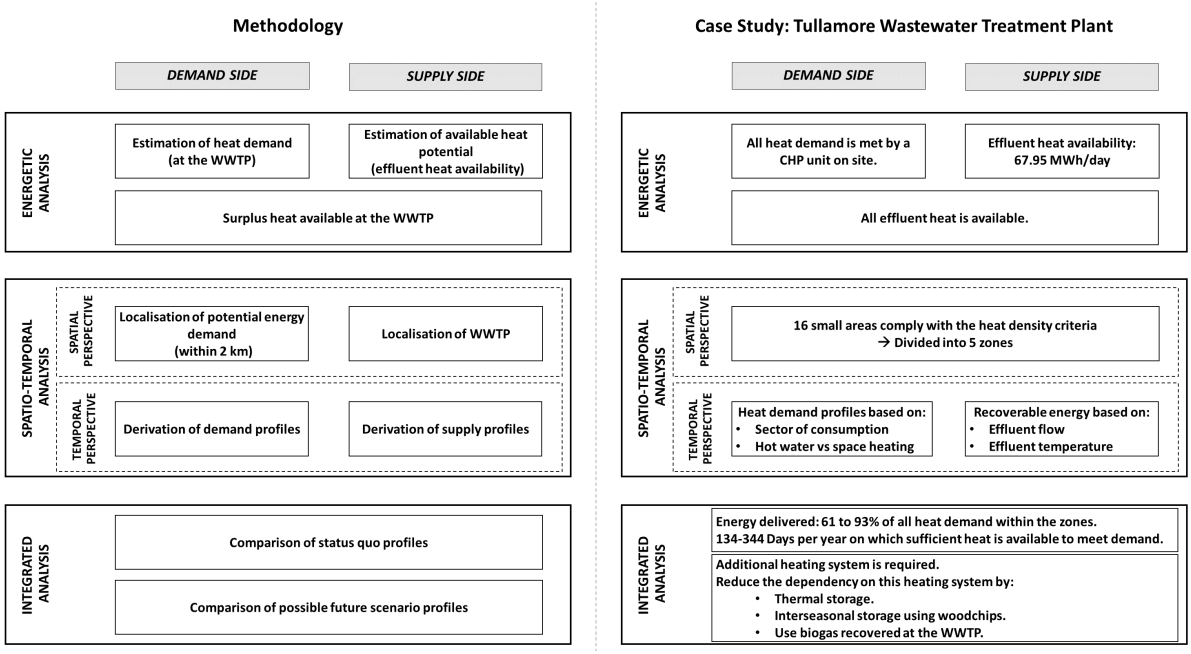


Figure 7.8.: Graphical abstract of the integrated three-step methodology.

[1] The research presented in this Section was published as a journal paper in the *Journal of cleaner production* [Spriet et al., 2020]

7.3.1. Methods and materials

Objectives of the method

The objective of the method presented in this Section is to combine both the spatial and temporal aspects of heat recovery from the effluent of wastewater treatment plants (WWTP) and heat demand in the vicinity. This is needed to accurately predict the amount of recovered heat that can be consumed in a sensible way. It studies both the proximity of the heat supply to the heat demand, and potential temporal mismatches between supply and demand.

The outcome of the study provides not only the amount of recoverable heat that is usable, taking into account the variations in supply and demand over a year, but also provides information on where demand can be met by the heat recovered from the effluent. In addition, it also identifies potential periods of scarcity, where alternative measures are needed to meet demand, such as additional heating sources or demand side management. Periods of excess can also be identified, showing the potential for thermal energy storage, or the possibility for development of additional activities during these periods of excess heat.

Methodology

The integrated method consists of three phases in the analysis, the energetic analysis at the wastewater treatment plants (see later in this Section), the spatio-temporal analysis (see later in this Section), and the integration of these methods (see later in this Section). The spatio-temporal analysis is the combination and integration of two analyses, a spatial one and a temporal analysis (both aspects discussed later in this Section). The method is summarized graphically, on the left of Figure 7.8. A detailed flow chart is given in Figures E.1 and E.2 in Appendix E.

- **Energetic analysis**

The availability of heat in the effluent of the wastewater is determined based on the daily hydraulic effluent flow ($V_{WW}\ (day)$), and the effluent temperature ($T_{ww,in}\ (day)$). In this study the minimal temperature of the wastewater (after heat recovery, $T_{WW,out}$ is assumed to be $8°C$). This assumption can be explained as follows. Webb and Walsh [2004] highlighted the vast literature available concerning (surface water) temperature influences on fish populations. The receiving water in the presented case study is the Tullamore river. In 2018 it had an annual average temperature of around $10.5°C$, the average winter temperature was around $6.1°C$ [Office of Public Works Ireland, 2019]. To (at least theoretically) account for the temperature sensitivity of fish and to minimize a potential thermal impact on the entire river ecosystem, we limited wastewater heat recovery to a level right between the annual and winter average water temperatures in our calculations (although further cooling would still be possible from a technical point of view). Where the effluent temperature was below the value of $8°C$, it was considered that the system was not operational. The embedded energy ($Q_{embedded}\ (day)$, for each day can then be calculated using Equation 7.4, where ρ_{WW} is the wastewater density, and Cp_{WW} is the specific heat of wastewater.

$$Q_{embedded}\ (day) = V_{WW}\ (day)\ \rho_{WW}\ Cp_{WW}\ (T_{ww,in}(day) - T_{WW,out)} \quad (7.4)$$

The evolution over a year of the effluent flow and temperature for the case study (see Section 3), as measured on the site, is shown in Section 7.3.2. This data was recovered from the SCADA system of the wastewater treatment plant.

The thermal energy must then be upgraded using a heat pump. The coefficient of performance ($COP\ (day)$) for a water-to-water heat pump is strongly dependent on the temperature of the heat source (the effluent water in this case). The impact of this variation on the final result is studied using the information on the COP evolution of a particular water-to-water heat pump, with a nominal power of 248 kW (largest heat pump for which the data was available), as described in its datasheet [Daikin Europe NV, n.d.]. The evolution of the COP, for different source temperatures, and a delivery temperature of $55°C$ is shown in Figure 7.9.

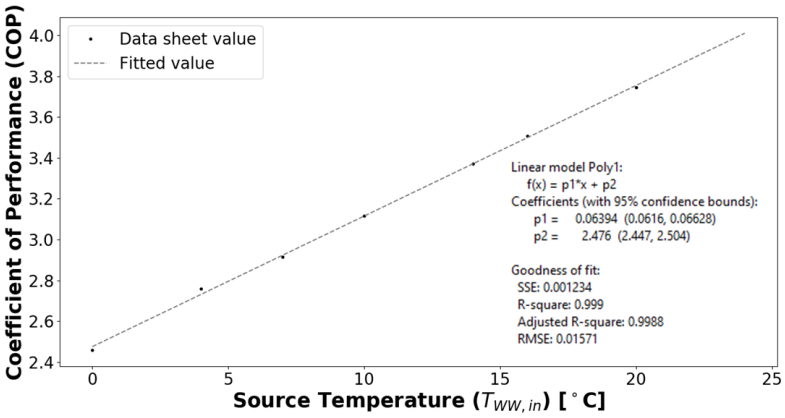


Figure 7.9.: Evolution of the COP of a water source heat pump (based on Daikin Europe NV [n.d.]).

The available energy from the wastewater source heat pump ($Q_{HP,available}\ (day)$) was then determined by Equation 7.5 [Yunus and Boles, 2007]. The required electric input ($W_{in}\ (day)$) can be found using Equation 7.6.

$$Q_{HP,available}\ (day) \ = \ \frac{COP\ (day)}{COP\ (day)\ -\ 1}\ Q_{embedded}\ (day) \tag{7.5}$$

$$W_{in}\ (day) \ = \ \frac{Q_{HP,available}\ (day)}{COP\ (day)} \tag{7.6}$$

Concerning the (internal) heat consumption at the wastewater treatment plant, Lindtner [2008] distinguishes between two different demands: (1) heat demand of the infrastructure (e. g. heating of offices, workshops) and in the case of anaerobic digestion (2) heat demand for sludge treatment (e. g. sludge heating, compensation of transmission loss). In the context of anaerobic sludge treatment, the optimal temperature for the maximal rate of reaction in a digester is $35°C$, as described by Hilkiah Igoni et al. [2008].

Measurements at the different consumption points provide the best basis to quantify on-site heat consumption. In the case of incomplete or even missing measurement data, the potential heat demand could also be calculated. According to Lindtner [2008] the heat demand of the infrastructure can be estimated at 50 to 150 $kWh/(m^2\ yr)$ (depending on the age and the fabric of the related building). In contrast, the heat demand for sludge heating primarily depends on the amount of sludge to be heated and the difference between the temperature of the raw sludge and the temperature in the digester. Whereas the heat demand for compensating transmission losses depends on the surface of the digester, the difference between ambient temperature and the digester temperature, and a material specific heat transition coefficient. For further details concerning the calculation of heat demands we refer to the quoted literature above.

To reduce operational costs of a WWTP, achieving energy neutrality is a major objective at many WWTPs around the world. Consequently, the heat available should be primarily used to meet WWTP internal demands, potential surplus quantities can then be supplied to adjacent WWTP external demand. Surplus heat available ($Q_{surplus}\ (day)$) can be calculated by subtracting the actual heat demand at the WWTP ($Q_{demand}\ (day)$) from the total heat available ($Q_{HP,available}\ (day)$ as shown in Equation 7.7.

$$Q_{surplus}\ (day) \ = \ Q_{HP,available}\ (day)\ Q_{demand}\ (day) \tag{7.7}$$

- **Spatio-temporal analysis**

Spatial perspective

Unlike combustibles such as gas, coal, and fuel oil, thermal energy cannot be transported over large distances, without major heat losses. Hence the thermal energy recovered from the effluent of the wastewater treatment plant must be distributed and consumed in the vicinity of the plant. This can be done by locating a single large consumer close to the plant, or through district heating. Because of the potential energy loss during the transportation of thermal energy, district heating is categorized as a local transportable energy source. The overall efficiency of district heating networks depends on heat demand densities. [Lichtenwoehrer et al., 2019]

In order to take this requirement into account, and to account for the financial feasibility criteria for district heating networks, the method described in this paper identifies areas which lie, at least partly, within 2 km of the wastewater treatment plant [Sandvall et al., 2016], which adhere to one of the following criteria:

- The overall heat density is larger than 40 $kWh/(m^2\ yr)$. [Gartland and Bruton, 2016]
- The linear heat density is larger than 2 $MWh/(m\ yr)$. [Erker et al., 2019]

The information available for the identified small areas is then the heat demand, divided into four categories (residential, industrial, commercial/retail and public sector/offices): the overall heat demand density in the area; the linear heat demand density in the area (along the gas lines, water mains and along the roads); and the distance from the small area to the wastewater treatment plant. The process of selecting suitable small areas based on the spatial considerations is summarized in the spatial perspective of the spatio-temporal analysis in Figure 7.8. Additional geographic characteristics, such as the static head, and distance between the treatment plant and the edge of the consumption zones (See Section 7.3.2), are also provided using the spatial considerations of the method.

Temporal perspective

Temporal matching of supply and demand has a significant impact on the operation and feasibility of drain and wastewater heat recovery projects. Temporal mismatches can greatly reduce the financial viability of these systems as described by Spriet and McNabola [2019*a*] and Wallin and Claesson [2014]. Once the spatially suitable sites have been selected (see above), these temporal aspects were studied, both for the supply (the recoverable heat from the wastewater treatment plants effluent), and the demand (consumers in the vicinity of the wastewater treatment plant) side.

On the supply side, the profile of the available heat is determined based on the evolution of both the effluent flow and temperature (the [procedure is shown on the left of Figure 7.8). The effluent temperature also defines the coefficient of performance of the heat pump. This introduces an additional variation on the available heat profile. The data, and the introduced variation over a year is described in Section 7.3.2.

The annual heat demand, divided into four categories (residential, industrial, commercial and public sector), was obtained from the spatial analysis. Each of these categories, was related to a specific yearly consumption profile, resulting in four different demand profiles, for each of the spatially suitable areas determined above. This is also shown on the left in Figure 7.8. The data and the introduced variation over a year, for both supply and demand, is described in Section 7.3.2.

- **Integrated analysis**

Supply and demand were then matched with the (district) heating set-up. In this analysis, this matching was done for every day of the year. This allowed for the identification of mismatches between heat supply and demand at certain times. At certain times of the year the available heat might exceed the heat demand, this is typically expected outside of the heating season. When the amount of recovered heat is lower than the available heat in the wastewater, due to lower demand, the system can be considered as over-dimensioned for that operation point in time, thus being inefficient. When the heat demand exceeds the available heat at the wastewater treatment plant, additional heat sources are needed, introducing additional costs.

It is important to identify the periods of the year at which these situations occur, to identify potential synergies with other systems in the vicinity, or to identify the potential for the extension of certain heat consuming activities.

Temporal matching of supply and demand allowed for the determination of the amount of actual recoverable heat, and the related fuel consumption (electricity in the case of electric heat pumps). The process used in this study to investigate these temporal variations is summarized in the bottom of Figure 7.8.

Case study

The method described above was applied to an urban wastewater treatment plant in Ireland (see below). The spatial and temporal considerations are applied to this particular wastewater treatment plant, and the surrounding areas.

- **Tullamore, Ireland wastewater treatment plant**

In the Republic of Ireland 32% of primary energy is required to produce thermal energy, which relates to 31% of the countrys total greenhouse gas emissions. Furthermore, in 2014, only 6.6% of thermal energy was delivered by renewable heating sources, and 87% of the thermal energy was delivered by oil, gas or coal [Howley et al., 2015]. For 2020, Ireland has a renewable heat target of 12% [Scheer et al., 2016] , which it has not met [Clancy, 2015].

The wastewater treatment works consists of two settling stages, with biological filters and aeration tanks in between those stages. In addition to this, the site also contains a sludge treatment facility, where biogas is recovered and used for combined heat and power (CHP) units on the site. These CHP units are used to provide part of the on-site electricity consumption and to maintain the anaerobic digesters at the desired temperature ($35 - 40°C$). These CHP units also provide on-site heat and electricity consumption. This consumption is thus monitored through the control of the CHP units. The lay-out of the plant is shown in Figure 7.10. This study investigates the possibility of pumping part of the effluent to different heat pumps, in order to provide heat for district heating in the area.

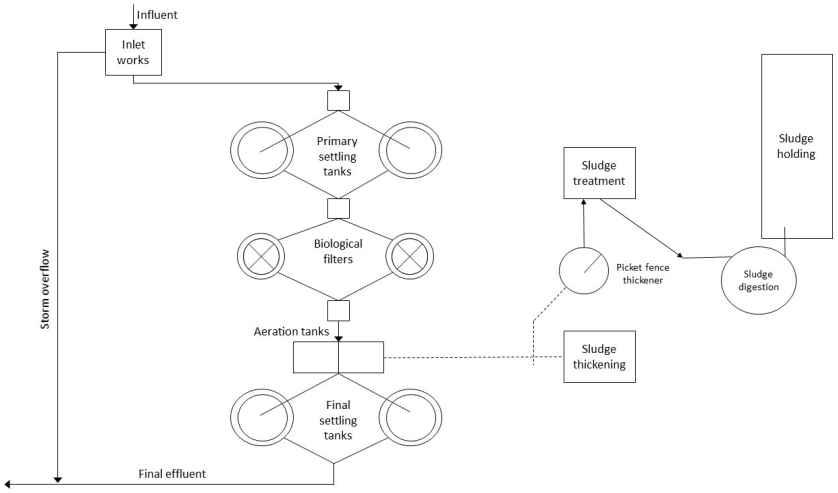


Figure 7.10.: Schematic of the Tullamore WWTP.

- **Local Heat demand**

The Sustainable Energy Authority of Ireland, used the same small areas to represent the distribution of heat demand over Ireland, divided into four categories: residential, industrial, commercial and public sector heat demand, for 2015 and a predicted demand for 2025. This database also includes the linear heat density, along gas lines, water mains and along the roads in these small areas [SEAI, 2015*c*].

The annual heat demand (Q_{annual} $(sector)$) was then distributed over the year. This was carried out by splitting the heat demand into space heating (subscript SH) and hot water heating (subscript HW) among the four sectors. The factor determining this share is denoted as α $(sector)$), with a different factor for the four different sectors. These factors are determined based on data delivered by the UKâs Department for Business, Energy and Industrial strategy [Ramboll, 2019]. The annual space heating and hot water

heating demand, was then distributed over the months (using the factor β $(sector, month)$) [Ramboll, 2019], and the space heating demand was distributed over the days depending on the heating degree days (using the factor γ $(sector, month, day)$) [MET Eireann, 2019]. This resulted in a daily heat demand for space heating ($Q_{daily,SH}$ $(sector, month, day)$), and for hot water heating ($Q_{daily,HW}$ $(sector, month, day)$). The hot water heating demands daily distribution was maintained constant over the days of the month for the industrial and public sector profiles [Ramboll, 2019], while the distribution for the residential and commercial profiles was based on the incoming fresh water temperature, as reported by Gill et al. [2016]). The method to distribute the annual data over the days of the year is represented in Equations 7.8 and 7.9.

$$Q_{daily,SH}\,(sector, month, day) = \alpha_{SH}(sector)\,\beta_{SH}(sector, month)\,\gamma_{SH}(sector, month, day)\,Q_{annual}(sector) \tag{7.8}$$

$$Q_{daily,HW}\,(sector, month, day) = (1-\alpha_{SH}(sector))\beta_{HW}(sector, month)\gamma_{HW}(sector, month, day)\,Q_{annual}(sector) \tag{7.9}$$

- **Local Heat supply**

The proposed system pumps the effluent to the heat pump, which is located within the area served by the district heating network. If the effluent can be discharged at this location, this would reduce pumping costs and material investment, and is thus the desirable option. If this is not possible, the effluent can be pumped in a loop, back to the treatment plant, and be discharged at the regular location. This set-up, rather than placing the heat pump at the treatment plant, was chosen because of the reduced heat loss. The effluent, having a lower temperature than the working fluid of the district heating system, had a smaller temperature difference with the surroundings, and thus a smaller driving force for heat losses. The heat pump then upgrades the heat to $55°C$, the required temperature for modern, 4th generation district heating [Thorsen et al., 2018]. Currently there is no district heating network at this location, this study investigated the potential of effluent heat recovery to supply heat to such a hypothetical, future network. The schematic of the system is shown in Figure 7.11.

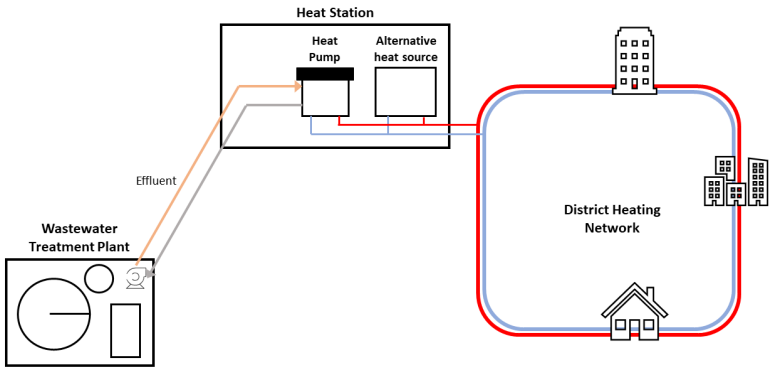


Figure 7.11.: Schematic of the system set-up.

A detailed feasibility study of district heating is not the object of this study. For this case study, the proximity of the effluent heat recovery to consumers, and its potential for meeting the heat demand of these consumers was studied. This included considering the temporal variations of both supply and demand, taking into account mismatches between these two factors, to assess the potential integration of an effluent heat recovery system into the local energy supply systems.

7.3.2. Results

The methodology described in Section 7.2.2 was applied on the urban wastewater treatment plant in Tullamore, Ireland, also described in 7.2.2.

Energetic analysis

The energetic analysis aims at determining the surplus heat available at the WWTP. Following the description in Section 7.2.2, this requires the estimation of the amount of heat embedded in the wastewater and the definition of the WWTP internal heat demand. Depending on the wastewater flow and temperature at the case study WWTP, the supply side can be summarized as follows:

The wastewater treatment plant in Tullamore, county Offaly, Ireland (see Figure 7.12) has a design person equivalent (PE) of 45 000, however the average current loading is about 16 000 PE, and the agglomeration PE is 21 571. This results in an average daily effluent hydraulic loading of 7 554 m^3/day, the daily variation over a year is discussed further in this Section. The average temperature of the effluent over the year is around 15.8°C, with a yearly variation as discussed further this Section, resulting in an average available embedded heat of around 67.95 MWh/day (24 801.75 MWh/yr).

To meet the internal energy demand (primarily for sludge treatment), the WWTP is equipped with a CHP unit (see Section 7.2.2). Although this heat demand might also be supplied by heat recovered from the effluent (making digester gas available for other purposes), this (internal) supply option was excluded as the presented research primarily highlights the potential of WWTP external heat supply. Consequently, the surplus heat available in the case study can be set equal to the total heat available in the effluent of the WWTP.

Spatio-temporal analysis

- **Spatial perspective**

  The spatial analysis, described in Section

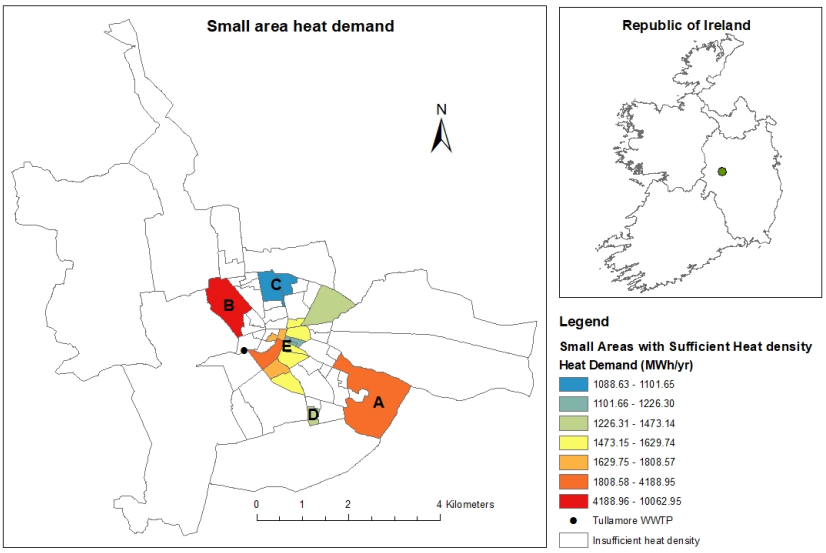


Figure 7.12.: Small areas complying with the heat density criteria in the Tullamore region.

The annual heat demand for each of these zones is summarized in Table 7.2.

In this analysis, these 5 zones were studied independently, however one can observe that, in case a district heating network is present in zone E, extending it to zones A, C and D would require less pumping distance than setting up a new district heating network in the latter zones, pumping effluent from the WWTP to a technical room in each of these zones. However, the precise lay-out and operation of the heating network is not the object of this assessment.

	Heat demand in 2015 ($MWh/year$)				
Zone	**Residential**	**Industrial**	**Commercial**	**Public sector**	**Total**
Zone A	740.62	184.14	3 110.78	0.00	4 035.54
Zone B	982.99	3 824.37	81.88	5 173.72	10 062.95
Zone C	1 965.68	0.00	224.60	0.00	2 190.28
Zone D	1 409.88	0.00	5.01	0.00	1 414.89
Zone E	11 215.85	623.57	7 491.16	314.68	19 645.26

Table 7.2.: Parameters of the five identified zones.

- **Temporal perspective**

Heat demand profile

The evolution of the heat demand (in MWh/day), in all five zones, across a full calendar year (per day) is shown in Figure 7.13. One can observe that the general trend shows a dip in consumption during summertime. One can also observe that when the residential and commercial sectors represent the bulk of the heat consumption (Zone E), the relative difference is more important than when the bulk of the heat consumption is delivered by the industrial or public sector.

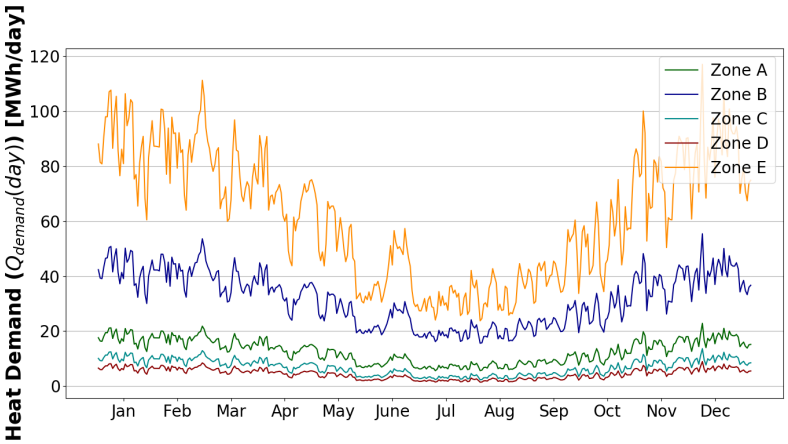


Figure 7.13.: Evolution of total heat demand in the different zones.

For each of the zones the heat demand can be broken down into space heating and hot water heating, and in the different sectors, as is shown in Figure 7.14 for zone E, over a calendar year. One can observe that the variability is largest for space heating in the commercial and domestic (residential) sector.

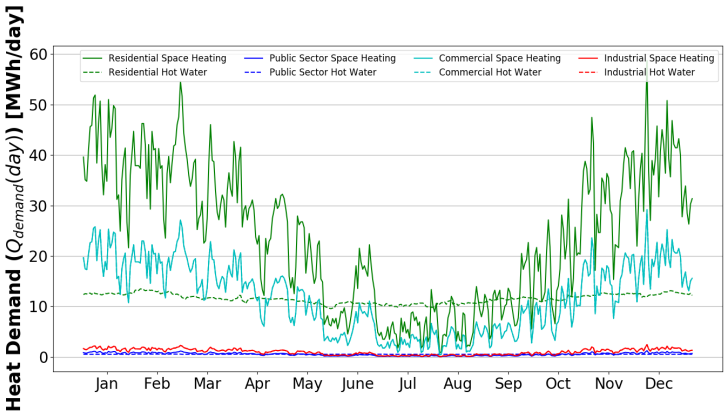


Figure 7.14.: Evolution of the heat demand per sector in zone E.

Heat Supply profile

The embedded energy in the effluent changes with varying effluent flow and temperature. It is shown for the Tullamore wastewater treatment plant in Figure 7.15 and Figure 7.16, respectively over the year 2018, and was calculated using Equation 7.4.

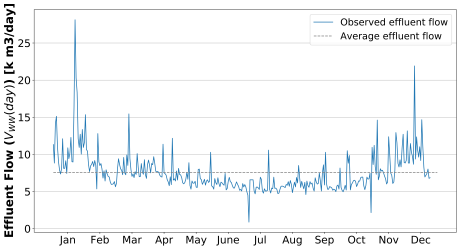


Figure 7.15.: Evolution of the effluent flow at the Tullamore WWTP in 2018.

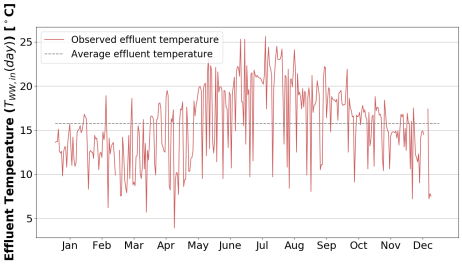


Figure 7.16.: Evolution of the effluent temperature at the Tullamore WWTP in 2018.

In order to upgrade the heat to temperatures that are sufficiently elevated for use in a heating network or heating system (55°C in this case), a heat pump was used. The heat pumps COP was determined based on the effluent temperature (see Figure 7.9). The average seasonal value was 3.48, and the total amount of exploitable heat was determined using Equation 7.5. The resulting evolution of exploitable heat over the year 2018, for a heat recovery system at the Tullamore WWTP is shown in Figure 7.17.

The recoverable energy was set to 0, assuming that the system was not operational, when the effluent temperature was below 8°C. When no data was available, no value was displayed, hence the discontinuities in Figure 7.17. In 2018 this resulted in 347 days for which operation was feasible, March and December are the months where most days of inactivity were observed, with 7 and 8 days, respectively.

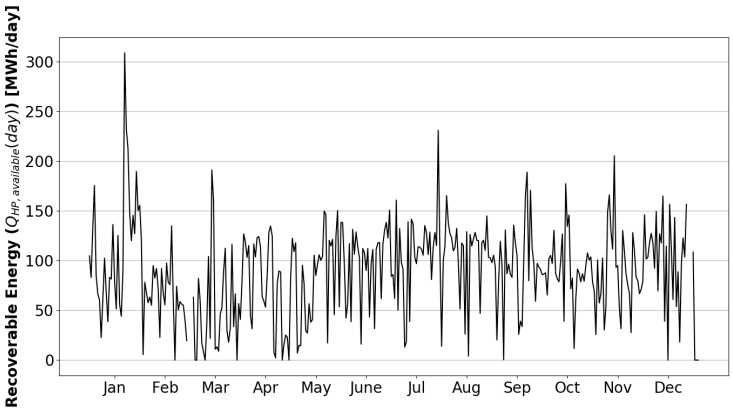


Figure 7.17.: Exploitable heat for an effluent heat recovery system at the Tullamore WWTP.

Integrated analysis

In the integrated analysis, supply and demand were then overlaid in order to estimate the amount of recovered heat that could be used in a sensible way. The summary results for all zones are shown, and a more detailed analysis, applied on Zone E is also shown below.

- **Summary statistics for all zones**

Using the analysis described in Section 7.3.1, the amount of days where the available energy from the wastewater treatment plant's effluent (Days of Excess in Figure 7.18), and the total amount of excess available energy were determined. In case the available energy is insufficient to meet demand, a negative contribution is counted. In Figure 7.18 one can observe that, although significant amounts of yearly excess energy are available for each of the zones individually, there remains 21 to 123 days on which the heat supply from the wastewater treatment plant is insufficient to meet demand in the zones, called days of excess in Figure 7.18. In the opposite case, when all zones are combined, total annual available heat is insufficient to meet demand, however, 134 days remain for which the available heat is sufficient or even exceeds demand.

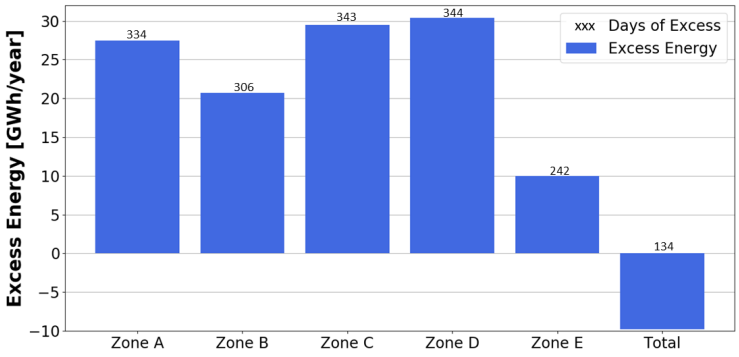


Figure 7.18.: Summary of Excess available energy at the wastewater treatment plant.

This indicates that the effluent heat recovery system can be used to meet the baseload heat demand, but must be complemented by other sources to be able to meet all demand. The amount of yearly recovered energy, used in a sensible way, when this strategy is applied is shown in Figure 7.19.

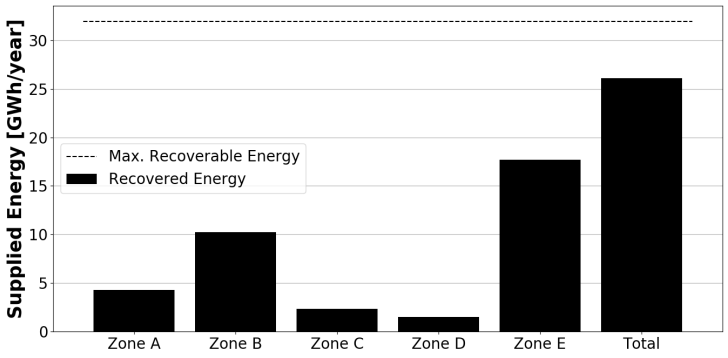


Figure 7.19.: Yearly recovered Energy at the Tullamore WWTP.

Figure 7.19 shows that even in cases where the yearly excess energy is negative, and thus on the aggregate additional heat needs to be supplied (the total of all zones), the recovered heat does not reach the full, maximal potential, because of temporal mismatches. In all cases there will be days of excess heat where additional demand can be met (in addition to the baseload mentioned earlier). The total yearly energy that was supplied by the heat recovery system, varies from around 60% (Total of all zones), to 93% (for Zone D) of all demand within the respective zones.

- **Detailed analysis of Zone E**

In Zone E an estimated 78% (17.72 GWh/yr) of all heat demand can be supplied by the effluent heat recovery system, as shown in Figure 7.19. An annual excess heat of 9.99 GWh is available at the wastewater treatment plant, however 123 days remain where the available heat is insufficient. The distribution of these days of insufficiency (when the excess is negative), over the year can be observed in Figure 7.20.

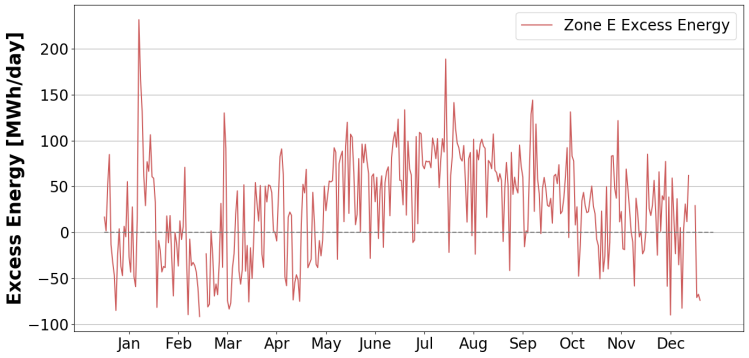


Figure 7.20.: Evolution of the excess available heat in Zone E.

In Figure 7.20, one can observe that the bulk of days requiring additional heat sources to meet demand, occur during the heating season (November-April). This is due to both the increased demand in this period (see Figure 7.13), and reduced temperature of the effluent (see Figure 7.16). However, occasional days of scarcity occur all through the year, even during summer months. This indicates that the back-up system used to provide additional heat must be available all through the year.

7.3.3. Discussion

This section introduced a novel method integrating spatial and temporal aspects of effluent heat recovery, and demonstrating the significance of both these components on the recovered thermal energy. The integrated method consists of three phases in the analysis, the energetic analysis at the wastewater treatment plants, the spatio-temporal analysis, and the integration of these methods (see Section 7.3.1). This method was applied to a case study at the wastewater treatment plant in Tullamore, Ireland.

Case study

This case study showed five different zones where the heat density was sufficient to consider integration in the effluent heat recovery system. The analysis then determined the annual heat consumption, divided into four different categories (residential, industrial, commercial and public sector), and the distribution of the heat demand over the year was then determined for each of these zones. The available heat from the wastewater heat recovery system was determined based on effluent flow and temperature, and the COP of the heat pump, based on the effluent temperature. The integrated analysis consists of overlaying these supply and demand profiles, identifying mismatches, and showing the recovered heat that can be used in a sensible way. Financial and environmental aspects are discussed in Section 7.4.

The detailed, daily breakdown of the excess heat available from the WWTPs effluent shows that days of scarcity occur mainly during the heating period (November-April), but occasional days of scarcity occur during summer months as well, mainly related to low effluent flows on these days. Consequently, a back-up heating system for wastewater heat recovery would be required for the entire period of the year. However, days of scarcity during summer could also be dealt with using solar thermal heating. So alternatives to decrease the dependency on this back-up heating system would also be available.

When excess heat is available, this can be used to increase the temperature, or flow in the district heating network. This thermally stored heat can then be used during days of scarcity, when not enough heat is available in the effluent to meet demand. However, due to heat losses, this type of thermal storage is only applicable for heat storage over a couple of days, and is thus not suited for longer periods of scarcity, such as those observed in this case study in December-March. Such systems are compared with thermal inertia storage in buildings by Romanchenko et al. [2018].

Another possibility, aimed at interseasonal storage is to use excess heat (e. g. in the summer period), to dry woodchips. A reduced moisture content reduces the cost of handling, transportation and pyrolysis in biomass boilers, and would thus improve efficiency for the use of these boilers during the period of scarcity [Haque and Somerville, 2013]. However, these seem a rather inefficient way of storing and reusing the excess heat.

In addition to these possibilities for thermal storage, excess heat could also be used to supply heat to future residential or industrial/commercial development zones, or to provide heat for new agricultural activities, namely in greenhouses settled in the vicinity of the WWTP, reducing the dependency on food imports.

However, the most obvious option to use excess heat from wastewater is to cover the WWTP internal heat demand, especially the one for sludge treatment. At the Tullamore WWTP this is done through biogas boilers at the moment. An alternative use of the available wastewater heat would result in the availability of biogas, which can be stockpiled, and used during periods of scarcity to meet demand (backup system). Furthermore, it would then also be available for WWTP external applications.

Strengths and weaknesses of the proposed method

The presented work provides a novel concept for planners and operators of energy and/or wastewater systems to assess the operation and feasibility of heat recovery at WWTPs from an integrated perspective. The methods (1) energetic component provides information on the availability of wastewater based excess heat at a WWTP. Its (2a) spatial component takes the proximity of the location of heat source (WWTP) to local heat consumers into account, and thus provides a view on the possibilities for integrating the heat recovery system into local energy supply systems. Its (2b) temporal component enables a detailed view on the potential heat supply as well as on the estimated heat demand in the intended supply areas. Finally, its

(3) integrated analysis of status quo and future supply and demand profiles gives insight into the practical feasibility of wastewater based heat supply in the vicinity of a WWTP. The spatio-temporal comparison of potential heat supply and actual heat demand reveal periods of supply shortages and oversupply. This allows to identify the need for alternative heat sources, the need for thermal storage, and indicate the type of storage needed (daily, seasonal, etc.).

When a detailed study is performed, the required pumping energy must be considered as well. This was not done in this study, as the requirements are strongly dependent on the selected lay-out, connection point and design of the heating system or network connected to the heat recovery system. An environmental impact assessment of the effect of the reduced temperature of the effluent on the recipient should also be included. The timescale at which the supply and demand profiles were matched remains a limitation of this study. The daily resolution used here, leaves the potential for mismatches in the diurnal pattern. For the day-to-day operation, diurnal patterns provide more insights, as this information, on the supply side, was not available, an additional monitoring campaign, focusing on these diurnal flow and temperature patterns is recommended in the planning phase of such projects.

Implications for theory and practice

When planning the energy transition, spatial and temporal patterns of energy demand and volatile renewable energy sources, become more important in order to balance demand and supply, and to determine grid as well as storage capacities [Ramirez Camargo and Stoeglehner, 2018]. This applies not only for the whole energy system, but also for the sustainable integration of single sources of energy, as they might realign the balance between supply and demand. In the beginning of the energy transition, renewable energies had very low shares so that their yield was always within the range of the grid capacity. The further societies proceed in the energy transition, the more important the issue of spatial and temporal patterns becomes for finding feasible solutions. Therefore, the spatial patterns of the surrounding areas of grid-bound energy supply, as well as the layout of buildings and new grid typologies become important determinants for energy transition strategies [Zach et al., 2019].

The example of wastewater energy use as presented here can increase the output of wastewater treatment plants by adding another product $\hat{a}$ heat and cold $\hat{a}$ with a moderate additional use of electricity [Neugebauer et al., 2015]. As the grids can serve as energy storage in this power to heat/cold solution for volatile renewable electricity sources, this additional technology can serve as a hub for coupling different energy grids (heat and electricity) and infrastructure systems (wastewater, energy, buildings). In line with several energy strategies that identify sector coupling as an important objective (see e.g. Lund et al. [2017]), the proposed approach will help to identify and plan for suitable areas of cities, towns and regions, where supply and demand can meet in high resolution temporal patterns as an important precondition to optimized energy provision, grid and storage capacities. As is demonstrated by this example, environmental pressures on rivers, because of warm wastewater disposal can be reduced, creating additional benefits for river ecology and nature protection [United States Environmental Protection Agency, 2014].

Therefore, it is proposed that strategies for a sustainable energy system transition take the spatial and temporal patterns of the considered area into account from the start. Methods as proposed in this article might spur further thought of academics and practitioners to develop and implement similar theoretical and methodological approaches in further cases of wastewater energy extraction or transfer this thinking to other sources of energy or other technologies. In this way highly efficient and optimized energy and resource flows can be achieved in line with cleaner production principles, reducing environmental pressures of the respective energy and infrastructure systems.

7.4. Environmental and financial aspects of effluent heat recovery

7.4.1. Introduction

The energetic analysis, discussed in Section 7.3, was complemented in this section by an analysis of the financial and environmental aspects related to recovering this heat from the effluent of the wastewater treatment plant, and whether or not this is beneficial compared to a gas fired system. The amount of recovered heat that was used in a sensible way, and the amount of required additional heat supply to meet demand, was a result of the analysis described in Section 7.3. Both the fuel consumption, and the energy required to pump the effluent towards the different consumption zones were discussed. The current gas and electricity prices in Ireland, along with the Irish Carbon Conversion factors for company reporting were used to assess the potential benefits.

7.4.2. Methods and Materials

In this analysis, the heat supply, divided between heat supplied from the wastewater heat recovery system and by the back up system (here considered to be a gas fired system), and the related fuel consumption are considered, along with the the required pumping to reach the different zones.

Effluent pumping requirements

The pumping requirements are related to the effluent being pumped from the wastewater treatment plant, to the area where the heat will be consumed (see Section 7.3.2). The wastewater is pumped towards the heating network, rather than the heating network being extended to include the wastewater treatment plant. This is done because the lower temperature of the wastewater, compared to the operational fluid of the district heating network, results in lower heat losses. These heat losses were not considered in this section. At this location the effluent serves as the heat source for a heat pump. The pumping head is divided into 2 types: the static head and the head related to friction losses.

In this study the static head (Δh_s) is defined as the altitude difference between the wastewater treatment plant, and the edge of the consumption area. This altitude difference was a result of the spatial analysis. In addition to that a safety factor of 20% is introduced, in order to account for unpredictable losses, for example due to bends, turns and changes in pipe size.

The head related to friction losses (Δh_l) is determined based on the distance between the treatment plant and the edge of the consumption area (L), which is also a result of the spatial analysis. The friction losses vary on a day by day basis, and are determined by the Darcy-Weisbach formula [Yunus and Boles, 2007], as shown in Equation 7.10, where v is the flow velocity, g is the gravitational constant and f_D the Darcy friction factor, determined as $64/Re$ with Re the Reynolds number. The diameter (D) is fixed and determined based on the average flow conditions.

$$\Delta h_l \;=\; f_D \; \frac{L}{2\,g} \; \frac{v^2}{D} \tag{7.10}$$

The pumping requirements (W_{pump}) can then be determined by Equation 7.11, where $V_{ww,required}$ is the required amount of wastewater to be pumped and η_{pump} is the efficiency of the pump.

$$W_{pump} \;=\; \frac{V_{ww,required}\;\rho_{WW}\;g\;(\Delta h_s + \Delta h_l)}{\eta_{pump}} \tag{7.11}$$

In this analysis the required amount of wastewater is determined based on the available heat in the effluent and the heat demand in the suitable areas. The assumption was that the lower value of the source temperature (at the outlet of the heat pump evaporator) remained at $8°C$, however using advanced control systems, can be used to optimize the operation of such a system, reduce the required pumping consumption, and improve the amount of recovered heat.

Levelized Cost of Energy

In order to estimate the economic potential of decentralized heat recovery systems, the Levelized Cost of Energy was used (see Section 4.3.1). The investment cost consists of the heat pump, circulation pump, and gas boiler and a 30% overhead. The cost of the heat pump is determined as a multiple of the cost of a 250 kW Heat pump [Daikin Europe NV, n.d.], depending on the number of heat pumps (n_{HP}) required to reach the desired output power (see Equation 7.12). The price of the circulation pump was determined using Equation 7.13, where $V_{ww,required}$ was expressed in m^3/s, and the total head (h_{tot}) is the sum of the static head (Δh_s) and the friction losses (Δh_l) [Novara et al., 2019]. The price of the gas boiler was determined using equation 7.14, using the per unit cost given in Sandvall et al. [2017], and the determined power of the gas boiler ($P_{gas\ boiler}$). The yearly maintenance cost was estimated at 1% of the investment cost for pumps and boilers, and 0.7% for heat pumps. [Sandvall et al., 2017].

$$I_{HP} = n_{HP}\ (32\ 174\ €) \tag{7.12}$$

$$I_{pump} = 1\ 289.92€ + V_{ww,required}\ \sqrt{h_{tot}}\ 1\ 913.91€ \tag{7.13}$$

$$I_{gas\ boiler} = 95.5\ €/kW\ P_{gas\ boiler} \tag{7.14}$$

The considered fuel costs were the prices for the Republic of Ireland, as described in Howley et al. [2015], these depend on the amount of energy consumed by the system, prices will thus vary between the different zones and scenarioś. The price categories are given in Table 7.3. The fuel costs (F_n) were calculated by multiplying fuel consumption with the unit cost of the fuel in question.

Electricity		**Gas**	
Band	Price (c€/kWh)	Band	Price (c€/kWh)
Band IA: $< 20\ MWh/yr$	23.07		
Band IB: $20\ -\ 500\ MWh/yr$	17.72	Band I1: $< 278\ MWh/yr$	5.00
Band IC: $500\ -\ 2\ 000\ MWh/yr$	14.91	Band I2: $278\ -\ 2\ 778\ MWh/yr$	4.32
Band ID: $2\ 000\ -\ 20\ 000\ MWh/yr$	11.93	Band I3: $2\ 778\ -\ 27\ 778\ MWh/yr$	3.77
Band IE: $20\ 000\ -\ 70\ 000\ MWh/yr$	11.17	Band I4: $27\ 778\ -\ 277\ 778\ MWh/yr$	2.86
Band IF: $70\ 000\ -\ 150\ 000\ MWh/yr$	10.11		

Table 7.3.: Commercial Fuel Cost in the Republic of Ireland in 2019.

Total Equivalent Warming Impact

To estimate the environmental impact of the different heating systems, the Total Equivalent Warming Impact ($TEWI$), divided by the produced heat was considered (See Section 4.3.1). The values that were employed for these calculations are summarized in Table 7.4.

Carbon conversion factors		
Electricity	K_{el}	0.4366 kg/kWh
Gas	K_{gas}	0.2047 kg/kWh
Refrigerant		
Type		R 407-C
Mass of refrigerant per heat pump	m_{refr}	16.8 kg
Global Warming Potential	GWP_{refr}	1774
Leakage rate	L	2%/yr
Recovery rate	α_{recov}	85%

Table 7.4.: Characteristics used for TEWI calculation.

7.4.3. Results

The financial and environmental analysis, described in Section 7.4.2 was then applied to the Tullamore wastewater treatment plant, the results are described below.

Effluent pumping requirements

As mentioned in Section 7.3.2, the heat recovery system requires the effluent to be pumped to the edge of these zones, where a heat pump can upgrade the heat to the temperatures required for a district heating network. The consumption of the pumps is dependent on the amount of flow (which will vary from day to day), the static head, the pumped distance, and the diameter of the pipe. The pipes are sized based on an assumed 1 m/s flow velocity in the average conditions, and 12 operating hours per day. The required average power of the pump was determined on the same basis. The resulting distances, static head, pipe diameters and average pump power are summarized in Table 7.5. The price of the pump was determined based on Novara et al. [2019].

Zone	**Distance** (m)	**Static Head** (m)	**Pipe diameter** (cm)	**Avg Pump Power** (kW)
Zone A	2 000	3.64	20	1.06
Zone B	292.5	0.17	30	0.13
Zone C	1 005.8	12.50	15	1.91
Zone D	2 000	12.96	15	1.28
Zone E	81.7	0.44	50	0.60

Table 7.5.: Piping characteristic for the five identified zones.

Levelized Cost of Energy

The levelized cost of Energy was determined using the method described in Section 7.4.2, the investment costs, estimated at the material cost and 30% overhead, are shown in Table 7.6.

	Heat Recovery system				Gas Boiler system	
	Pump	Heat Pump	Gas Boiler	Total	Gas Boiler	Total
Zone A	1 950	128 696	142 814	355 497	181 580	236 054
Zone B	1 649	321 740	345 856	870 019	440 907	573 179
Zone C	1 944	96 522	81 927	234 510	108 377	140 890
Zone D	1 721	64 348	53 312	155 195	70 884	92 149
Zone E	2 386	579 132	743 741	1 722 836	931 362	1 210 770
Total	3 373	1 126 090	1 513 115	3 435 352	1 733 110	2 253 043

Table 7.6.: Investment costs, in €, for the different zones at the Tullamore Wastewater treatment plants.

The fuel costs for each of the zones, set by their electricity and gas consumption, as determined in Section 7.3.2, are represented in Table 7.7.

	Heat Recovery system		Gas Boiler system
	Electricity price (c€/kWh)	Gas Price (c€/kWh)	Gas Price (c€/kWh)
Zone A	14.91	5.00	3.77
Zone B	11.93	4.32	3.77
Zone C	14.91	5.00	4.32
Zone D	17.72	5.00	4.32
Zone E	11.93	3.77	3.77
Total	11.93	3.77	2.86

Table 7.7.: Fuel costs, for the different zones at the Tullamore Wastewater treatment plants.

Given the data in Tables 7.6 and 7.7, a lifetime of 15 *years* and a discount rate of 7% [Rushing et al., 2013], this resulted in levelized costs as shown in Figure 7.21.

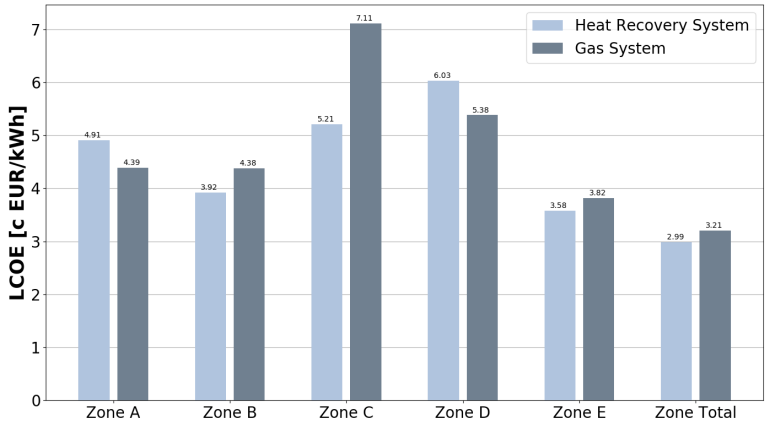


Figure 7.21.: Levelized Cost of Heating for the different zones at the Tullamore Wastewater treatment plants.

In this Figure, one can observe that the effluent heat recovery system delivers heat at a lower price cost a classic gas system, for zones B, C, E and when the heat recovery system was used as the heat source for all zones. With the lowest levelized cost (2.99 c€/kWh) observed in the scenario where the heat recovery system was used as the heat source for all zones.

Total Equivalent Warming Impact

Using the method and data described in Section 7.4.2, and a lifetime of 15 *years*, this resulted in total equivalent warming impacts per kWh, as shown in Figure 7.22.

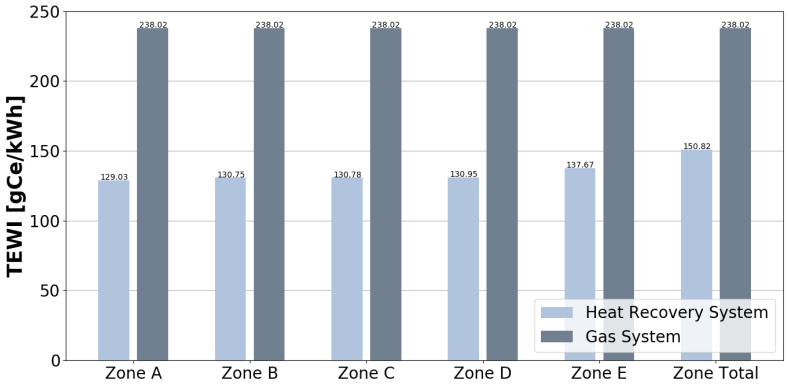


Figure 7.22.: Total Equivalent Warming Impact for the different zones at the Tullamore Wastewater treatment plants.

Again, one can observe that the Total Equivalent Warming Impact of the heat delivered by the effluent heat recovery system is lower than for a gas system. The lowest equivalent warming impact (129.03 gC_e/kWh) was observed in the scenario where the recovered heat was used for zone A.

7.4.4. Discussion

Taking into account pumping requirements and fuel consumption, both the environmental impact and the financial cost of the wastewater heat recovery system were lower than for an equivalent gas system. One can observe a variation in the levelized cost across the different scenario's (the variable being which zone is heated by the wastewater heat recovery system) for both the heat recovery system and the gas system. For the Total Equivalent Warming impact, no variation was observed for the gas system, as only the operational emissions are considered for this system [Zottl et al., 2011].

This resulted in discounted annual financial savings ranging from 47 821 to 92 732 €(for zones B, C, E and for all zones), and additional costs for zones A and D (characterised by negative savings in Table 7.8) and a yearly reduction in greenhouse gas emissions ranging from 174 to 3 741 $k\ tons\ C_e$, as shown in Table 7.8. The largest savings, both from a financial as well as an environmental point of view, were observed in the zones with the largest heat consumption. The feasibility of district heating networks in the studied zones, was taken into account by only considering zones with sufficient heat demand density (see Section 7.3.1).

	Financial savings (€)	Emission reduction ($k\ tons\ C_e/yr$)
Zone A	−24 035	505
Zone B	52 452	1 240
Zone C	47 821	270
Zone D	−10 620	174
Zone E	54 366	2 264
Total	92 732	3 741

Table 7.8.: Financial and environmental savings, for the different zones at the Tullamore Wastewater treatment plants.

The analysis performed in this chapter thus indicates that using a combination of wastewater heat recovery from the Tullamore wastewater treatment plant to heat up a potential district heating network for the discussed zones in the Tullamore Urban agglomeration, is both financially and environmentally profitable, compared to providing the heat for the same district heating network with a gas fired system, for a district heating network serving zones B, C E, individually, and for a network serving the combination of all zones. The studied zones have a heat demand density (either overall or linear) that warrants the consideration of district heating, however the district heating network itself, or it's financial viability have not been studied in this analysis (see Section 7.3.2).

7.5. Summary

In December 2018, wastewater was officially recognized by the European Union as a renewable source of energy, thus wastewater heat recovery can be included in efforts to reduce greenhouse gas emissions. Given the fact that wastewater treatment plants can generate enormous heat surpluses, this decision gives leeway to couple the wastewater infrastructure with the energy system in order to increase energy efficiency at the system level, allow for power to heat solutions in order to integrate volatile renewable electricity generation and, thus, foster a sustainable energy transition and cleaner production. Yet, the success of these system integrations depends on the availability of energy consumers in proximity of the wastewater treatment plants, and the temporal patterns of energy supply and energy demand. In this chapter the spatial proximity to heat demand is studied, for all wastewater treatment plants in Ireland (Section 7.2), an integrated spatio-temporal method is applied to a case study on the treatment plant in Tullamore, Co. Offaly (Section 7.3), and the environmental and financial aspects of this case study (Section 7.4).

In Section 7.2, analysis of 479 wastewater treatment plants in the Republic of Ireland, showed a total embedded energy in wastewater treatment effluent of 6.34 TWh/yr, with the largest potential (1.96 TWh/yr) in the Ringsend wastewater treatment plant. 40 wastewater treatment plants are located withing 2 km of a suitable small area with a heat demand density superior to 40 kWh/m^2, these plants have a potential of 4.5 TWh/yr. However, when only the suitable small areas were considered, only 236.55 GWh/yr of consumption could be met. This indicates that wastewater heat recovery from the effluent of wastewater treatment plants, as the sole heat source for a district heating network has only a limited market for financially profitable application. However, in the case of heating networks with multiple heat sources, they can provide an interesting interface between the electricity and heat networks.

So far, the importance of both temporal and spatial variations in performance of wastewater heat recovery systems have been discussed in literature, but only as separate considerations to date. In order to exhaust the potential of wastewater energy, the combination of both aspects still has to be studied sufficiently, and Section 7.3), and the corresponding paper [Spriet et al., 2020], aim at filling that gap. A three-step methodology was proposed, including an energetic analysis at the wastewater treatment plant, a spatio-temporal analysis of supply and demand in potential supply areas, and an integrated analysis, overlaying the supply and demand profiles. This allows to account for both the proximity of consumers and potential temporal mismatches between supply and demand. The methodology was applied on a case study in Ireland, being able to clearly identify potentials and pitfalls for laying out grids and dimensioning the energy generation systems. The practicability of the suggested concept was shown in this section. Investigations also resulted in 21 to 123 days on which the heat supply from the wastewater treatment plant is insufficient to meet demand in the zones due to temporal mismatches. However, the net annual excess recovered heat is positive, meaning that on an annual basis, there is more heat available than consumed. If all zones are combined the net annual excess recovered heat is negative, indicating a net need for additional heating systems, but still 124 days of excess remained, indicating that the effluent heat recovery system can be used to meet the baseload heat demand, but must be complemented by other sources.

The daily analysis show that days of heat scarcity mainly occur during the heating period (November-April), but occasional they occur during summer months as well. During these days additional heat sources are needed to bridge the gap between supply and demand. Different possibilities to decrease the dependency on the back-up heating system are proposed, including day-to-day thermal storage, drying woodchips for interseasonal storage and the development of new supply zones in the vicinity of the WWTP (mainly industrial, commercial and agricultural). Furthermore, WWTP internal use of wastewater heat to substitute digester gas-based CHP generation would make the gas available for other purposes as for instance as a backup for days of supply scarcity of for WWTP external consumption.

The presented research gives clear evidence that heat recovery from wastewater can provide valuable contribution to local energy supply. An integrated planning approach considering supply and demand from a spatial and temporal perspective is imperative to ensure the best possible activation and use of this new renewable energy source.

In Section 7.4, the financial and environmental indicators were assessed, for the case study in Tullamore, Ireland. This showed that the effluent heat recovery system was competitive from a financial point of view, and largely outperformed the classical gas system from an environmental point of view. Effluent heat recovery was concluded to be more financially competitive with increasing consumption in the supplied zone.

8. Drainwater Heat Recovery in Commercial Kitchens: Demonstrator at Penrhyn Castle

8.1. Introduction

The food and drink industry in the United Kingdom was responsible for an energy consumption of approximately 37 TWh in 2013, in combination with a water consumption varying between 347.3 and 366.4 Mm^3, of which $153.7-158.8\ Mm^3/yr$ was consumed in the hospitality and food services [Bromley-Challenor et al., 2013], as discussed in Chapter 6. Over 80% of the heat for hot water is provided by fossil fuels, both in Ireland and the UK, and only 6.2% (UK) and 6.6% (Ireland) of the heat is provided by renewable sources [Goodright, 2014; Howley et al., 2015; Spriet and McNabola, 2019*a*]. This renewable heat is mainly provided by biomass incineration. Over 95.6% of the renewable heat in the UK was provided from biogas and biomass combustion in 2016 [Waters, Liz; Hemingway, 2016]. Combustion of biomass and biogas is considered a renewable energy source, and as such has a very low carbon conversion factor, used for reporting of carbon emissions [Department for Business Energy & Industrial Strategy, 2018*a*; SEAI, 2017*b*]. However the technical emissions are much higher [Sterman et al., 2018]. Reducing the fuel consumption related to heating would thus also reduce technical GHG emissions in most cases of renewable heating.

Styles et al. [2015] provided an estimate for energy savings in the kitchen of a 100-room hotel of 3 434 kWh per year, mainly by proposing water savings measures. Given that kitchen drain water is characterized by high wastewater temperatures [Cunniffe and McNabola, 2014], direct drain water heat recovery can be employed here. This provides an interesting potential for the reduction of fuel consumption and related greenhouse gas (GHG) emissions in commercial kitchens. Commercial kitchens can be found in multiple building types, such as hotels, restaurants, pubs, cafes, fast-food outlets. This chapter aims to quantify the savings at the kitchen of a particular site, Penrhyn castle, in Wales, UK. Most commercially available drain water heat recovery systems focus on shower heat recovery, and this chapter aims at evaluatimg the design and subsequent long-term performance of this type of system in a kitchen drain water heat recovery application.

Penrhyn Castle is a country house in Llandegai, Bangor, Gwynedd, North Wales, in the form of a Norman castle, shown in Figure 8.1. It was originally a medieval fortified manor house, founded by Ednyfed Fychan. In 1438, Ioan ap Gruffudd was granted a licence to crenellate and he founded the stone castle and added a tower house. Samuel Wyatt reconstructed the property in the 1780s. The present building was created between about 1822 and 1837 to designs by Thomas Hopper who expanded and transformed the building beyond recognition. It now belongs to the National Trust and is open to the public [National Trust, 2019].

Penrhyn receives around 100,000 visitors a year, two-thirds of whom visit the house and garden, the rest the grounds only. Around 63% are National Trust members. Only 25% of the member visits are from Wales, and at present just 10% of visitors are local. 30% of visitors are on a day trip and 70% are on holiday [National Trust, 2019]. The location of the kitchen discussed here is the tea room at the castle, serving these visitors, and 32 to 45 on-site staff. As with other National Trust properties, the conditions in areas of the site are considered to be historically significant and are rigorously protected. As the site is historically and archaeologically important, any construction works may require the presence of a surveyor. During this process, any archaeological findings may mandate the postponement of the works.



Figure 8.1.: Penrhyn castle, Bangor, Wales, UK (taken by author).

This project also aims at disseminating best practices for the improvement of the sustainability of the water cycle, both in terms of water– and energy use. To disseminate the efforts in energy saving, by heat recovery from the drain water, a poster is presented to the visitors, shown in Appendix F.1.

This chapter[1] describes:

1. The heat recovery method that was used, and the data used for sizing and design.
2. The design of the experimental set-up.
3. The feasibility study for the designed heat recovery unit.
4. The installation procedure.
5. The operation of the pilot site.

8.2. Selection of the pilot site

8.2.1. The kitchen and hospitality sector

As described in Chapter 6, different feasibility studies were performed in commercial kitchens in the food and hospitality sector.

- The kitchen of a 145-bedroom hotel and resort, in county Wicklow, Ireland. The monitoring campaign and feasibility study, briefly described in Section 6.2.1, and Appendix B.1, studied a hybrid and an indirect heat recovery system (see Section 3.2.1). As can be seen in Figure 8.2, the hybrid heat recovery system was characterized by the lowest levelized cost of heating, the indirect heat recovery system (wastewater source heat pump) showed a greater levelized cost than a classical gas boiler system. This indicates that the savings of the hybrid system are mainly due to direct heat recovery.

[1] The research presented in this Section was presented as an archival paper at the *14th conference on sustainable development in energy, water and environment system 2019, Dubrovnik, Croatia*

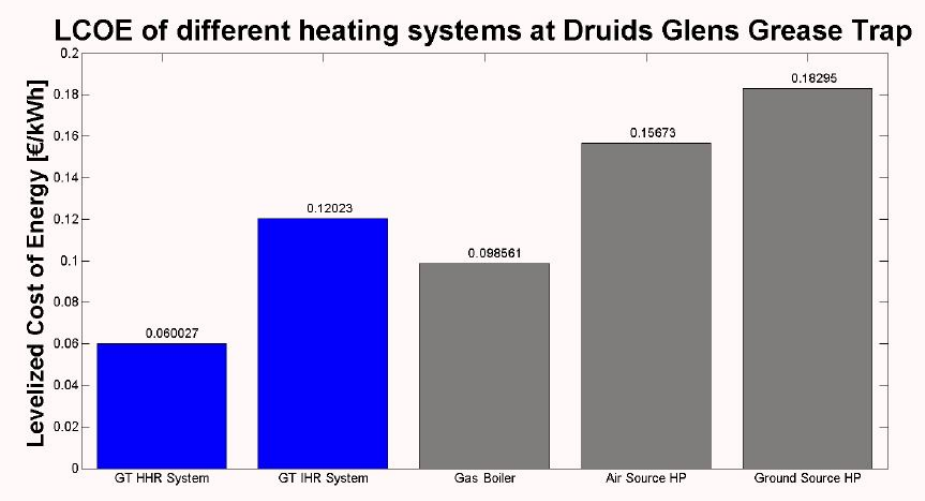


Figure 8.2.: LCOE for different heating technologies at the grease trap in Druids Glen.

- The kitchen of a 150-bedroom hotel in Dublin, Ireland.

  In this hotel in Stillorgan, Dublin a direct heat recovery system was studied for the kitchen drain water, this is described in Section 6.2.1, and Appendix B.2. This showed a payback period of less than 9 years, and over 700 $kg\ C_e/yr$ of emission reduction, as shown in Table 8.1.

System	Operating days	Energy Savings	GHG Savings	Payback period
Direct-DWHR	220 $days/yr$	3.5 MWh/yr	711.88 $kg\ C_e/yr$	8.62yrs

Table 8.1.: Payback period and emission reduction at a hotel in Dublin, Ireland.

- The kitchen of a retirement home, with 52 residents, in county Tipperary, Ireland.

  At the retirement home in Tipperary, the drain water flow from the kitchen was estimated at 782.61 l/day, this showed a payback period just under 10 years, and GHG savings of just over half a ton of C_e emissions per year, as shown in Table 8.2.

System	Operating days	Energy Savings	GHG Savings	Payback period
Direct-DWHR	365 $days/yr$	2.6 MWh/yr	542.33 $kg\ C_e/yr$	9.94 yrs

Table 8.2.: Payback period and emission reduction at a nursing home in Tipperary, Ireland.

The location of the pilot study, Penrhyn Castle, Wales, UK, was the object of a feasibility study as well. The details of the selection of the heat recovery location are described in this section, the feasibility, and operation of the pilot site is described further this chapter.

8.2.2. Penrhyn castle

In September 2016 a renewable heating system was built at Penrhyn Castle aiming at replacing the old oil fuelled heating system by a woodchip based one, which could be fed by locally harvested source. Composed of two Froling biomass boilers of 150 kW each (total 300 kWp) the system allows the supply of $50-100\%$ of the heating demand of the building according to the needs of the castle management. As well as saving money and reducing CO_2 emissions; the new heating system also reduces the risks associated with oil storage by removing four large oil tanks which were housed within the property. The new heating system of Penrhyn Castle is part of a larger project which included the installation of 2000 m^2 of solar (PV) panels, nearly 1000 LED light bulbs, and 7000 m^2 of loft insulation in previous years.

Proposed heat recovery locations

Two main options are to be considered for implementation in the present study (Figure 8.3): (i) Option-1 locating the heat exchanger inside the castle, at the kitchen drain; and (ii) Option-2 locating the heat exchanger in one of three septic settlement tanks.

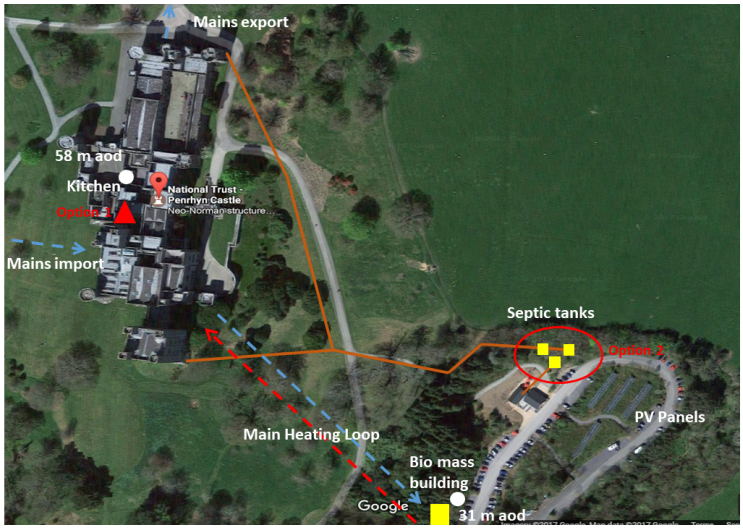


Figure 8.3.: Map of the Penrhyn grounds.

- **Option 1: Kitchen drain**

The kitchen being one of the important hot water consumers, National Trust is planning to use an additional, local heat source for the kitchen, including a buffer tank. A hybrid heat recovery system, using the kitchen drain water as a heat source will be investigated. The main heating network from the castle, heated by the Biomass boilers would provide the back up and additional peak heating. This has the advantage of a higher temperature of the drain water, and being located closer to the heat consumer, minimizing heat losses to the environment. However, it would recover heat from a small portion of the drain water, leaving some of the potential untouched, and might suffer from irregular flow.

- **Option 2: Septic tanks**

The heat exchange location for Option-2 is contemplated at the settlement tanks (v.s., Figure 8.3), where heat is first transferred by DWHR technology from the waste water to a closed loop that would transport the heat to the energy centre where there would be a second heat exchange to release the heat in the cold water before entering into the boilers. This system requires pumping and has the advantage of being independent to the singularities of the Castle setup, offering therefore higher repeatability (i.e. many NT properties include settlement or septic tanks).

The option by the settlement tanks also then incorporates the public visitor toilets which are the first port of call for the majority of the visitors and also the last place they visit before they leave. Therefore high flows potentially closer to the tanks so higher baseline water temperature incorporated making the coefficient of performance for the heat pumps better. This will offset pumping losses.

This option has the advantage of a constant water mass in the septic tanks, however it is located at significant distance from the waste heat producers, and might thus suffer from the heat losses to the environment during transportation of the drain water to the septic tanks.

Monitoring campaign

In order to collect the required temperature data for a reliable feasibility assessment of the waste water heat recovery potential of Penryhn Castle and to carry out a preliminary design of the options, a monitoring campaign has to be launched aiming at collecting temperature and flow data at specific points of the drainage network and heating pipes of Penryhn Castle (Shown in Figure 8.4). The monitoring period was carried out from March 20th 2017 to March 19th 2018. The sampling frequencies are shown in Table 8.3. the sensors specifications are attached in Appendix A.

Location	Description	Measurement	Devices	Period	Sampling
1	Kitchen drain	Flow and temperature	Flow Sensors Temperature sensors	19/06/2017 – 27/02/2018	every minute
2	Conduit Junction	Flow and temperature	Atex MSFM Multi Sensor flow monitor	27/07/2017 – 27/02/2018	every 15 min
3a	Settlement tank-1	Water temperature	Tinytag TG-4100	20/03/2017 – 19/03/2018 –	every 5 min
3b	Settlement tank-2	Water temperature	Tinytag TG-4100	20/03/2017 – 19/03/2018 –	every 5 min
3c	Settlement tank-3	Water temperature	Tinytag TG-4100	20/03/2017 – 19/03/2018 –	every 5 min

Table 8.3.: Summary table of monitoring programme at Penrhyn Castle, Wales.

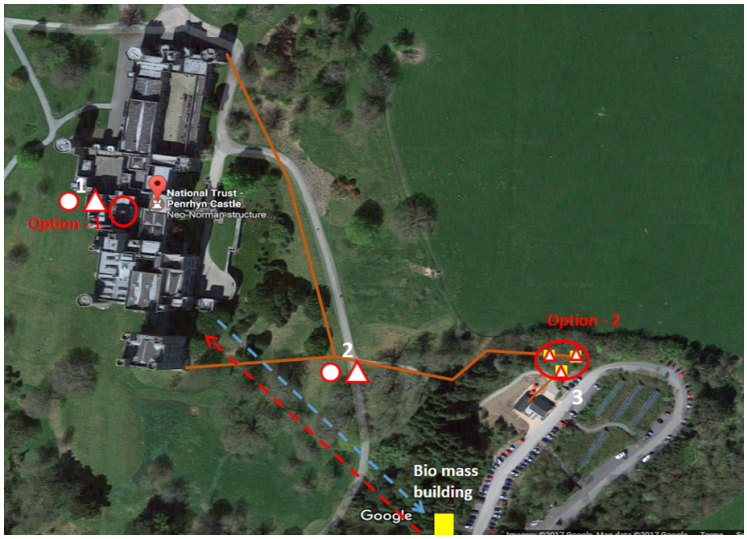


Figure 8.4.: Monitoring campaign at Penryhn Castle, Wales.

- **Option 1: Kitchen drain**

A monitoring campaign was performed at a vertical drop in the kitchen drain, this was accessible through the coal yard. The temperature was measured at the base of the vertical drain (see Figure 8.5). The drain in this picture is also the one being replaced by a heat exchanger.



Figure 8.5.: The vertical drop in the kitchen drain, as seen from the coal yard at Penrhyn castle.

The drain water temperature was measured at the kitchen drain, which resulted in measurements of temperatures of up to $55°C$, and a median value, ranging from 22 to $38°C$ during the opening hours of the kitchen, as shown in Figure 8.6. The fresh water consumption of the kitchen was monitored as well, both characteristics were measured over the period from June 2017 to January 2018.

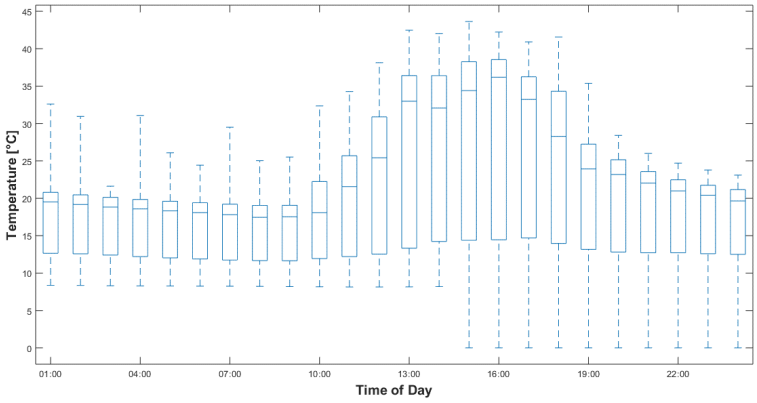


Figure 8.6.: Boxplot of the drain water temperature at the kitchen in Penrhyn castle.

The fresh water consumption was measured at this location as well. Figure 8.7 shows the evolution over a day of the cold (in blue) and hot (in orange) water consumption of the kitchen. The squares represent the mean observed values.

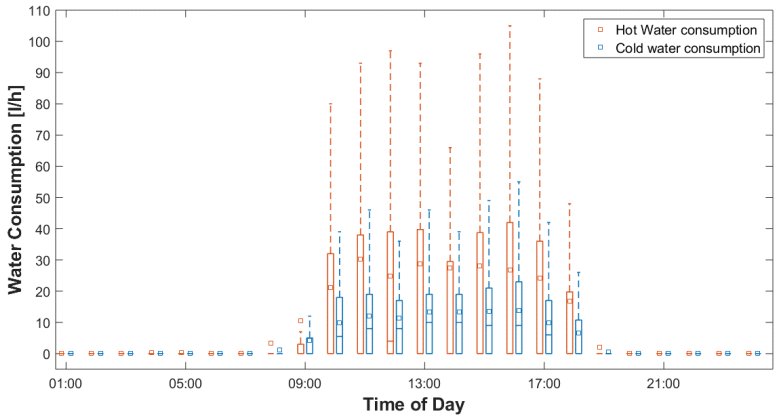


Figure 8.7.: Boxplot of the fresh water consumption at the kitchen in Penrhyn castle.

The return factor (link between water consumption and drain water flow) for the UK was estimated at 95% by Butler and Davies [2010]. However, the authors opted for a more conservative 90% for the analysis. The remaining 10% was assumed to have been dried with towels, evaporated, or left the kitchen through routes other than the drain. Another assumption that was made is that the water retention time of the kitchen appliances did not exceed one hour, resulting in the drain water exiting the kitchen within the hour after it entered.

- **Option 2: Septic tanks**

The three settlement tanks (also called septic tanks), are of the Klargester type, with two large (9 000 l) units, collecting the wastewater from the castle, and one smaller (4 500 l) unit, collecting the wastewater from the visitor toilets at the entrance.

A Klargester septic tank consists of an inner and an outer chamber. The raw wastewater flows into the inner chamber, where most of the suspended solids settle. The wastewater then flows into the outer chamber, where settling continues, and from which the wastewater flows onwards. A schematic is shown in Figure 8.8. Figure 8.9 shows the overflow protection system of the settlement tanks at Penrhyn castle, where a floating ball blocks the top opening of the inner chamber in case it gets too much water inflow.



Figure 8.8.: Schematic of a Klargester settlement tank.



Figure 8.9.: Overflow protection of the settlement tanks at Pernhyn castle, Wales.

Settlement tank – 1

The temperature profile over the period 20th of March 2017 to 04th of April 2017 is given in Figure 8.10. One should note that both temperature sensors in the outer compartment of the tank and the higher sensor in the inner compartment were not submerged, this explains the daily variations highlighted in the black box. In air these variations are observed due to the smaller thermal inertia of air compared to water. The distances shown in the legend are the height above the tank bottom.

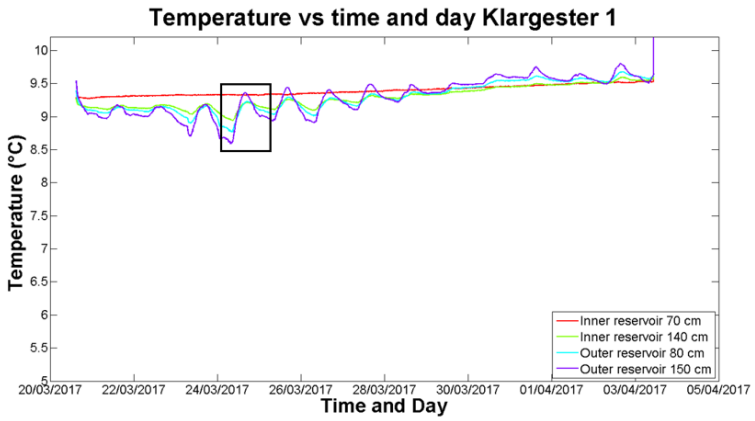


Figure 8.10.: Temperature profile in the first settlement tank at Penrhyn Castle, Wales.

One can observe that the water temperature was steadily increasing, but shows no influence of events, such as washing machines,etc. This indicated that the wastewater had lost its heat to the environment while being transported to the settlement tanks and the waste water was at the same temperature as the surrounding soil. The steady increase is due to seasonal heating of the soil and the wastewater.

The fact that three out of four sensors were not submerged at any point in the measuring period indicates that the settlement tank had reached its steady state operation state, and that the tank was half filled at this stage. This might indicate that the outlet of the outer reservoir, towards the second settlement tank is placed too low, which causes the second settlement tank to fill up first.

Settlement tank – 2

The temperature profile over the period 20th of March 2017 to 04th of April 2017 is given in Figure 8.11. Similar to the first settlement tank, the observed temperature increases steadily, due to seasonal variation in the soil temperature. The spike at the end of the monitoring campaign is due to an error at the moment of data collection.

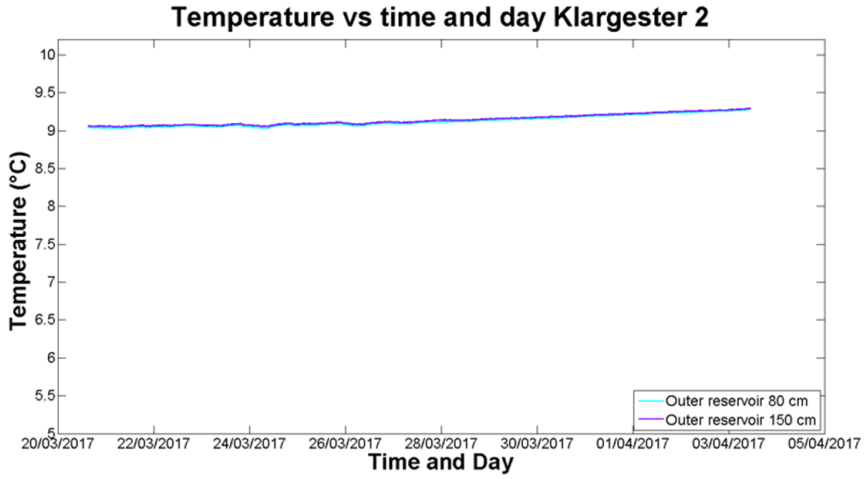


Figure 8.11.: Temperature profile in the second settlement tank at Penrhyn Castle, Wales.

Settlement tank – 3

The temperature profile over the period 20th of March 2017 to 04th of April 2017 is given in Figure 8.12. This profile shows the influence of events on the temperature of the waste water inside the settlement tank.

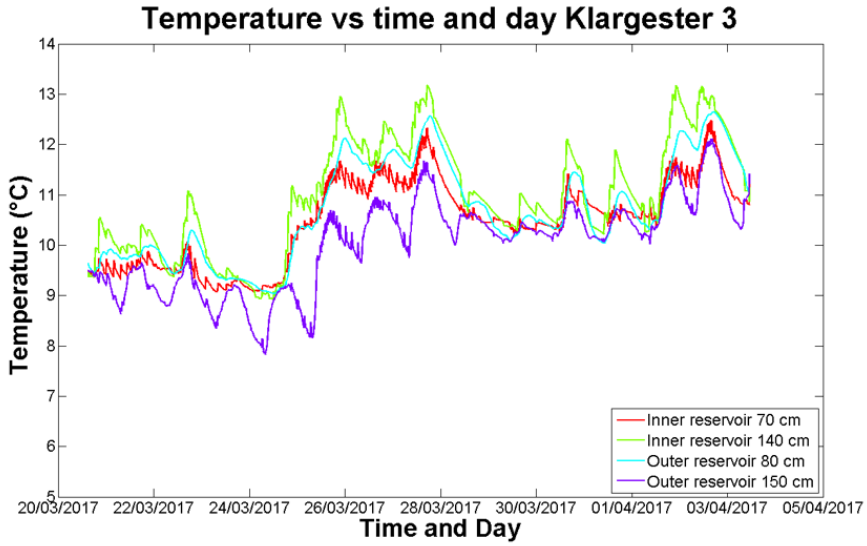


Figure 8.12.: Temperature profile in the third settlement tank at Penrhyn Castle, Wales.

In the Klargester tank models, such as the ones installed on the Penrhyn site the wastewater enters the settlement tank at the top of the inner reservoir, and exits the inner reservoir into the outer reservoir at medium height, the outlet of the outer reservoir depends on the design of the tank. In the inner tank, the results indicate that stratification occurs, as the inlet temperature (140 *cm*) is generally higher than the bottom temperature (70 *cm*). In the outer reservoir the higher temperature (150 *cm*) is generally lower than the one at the bottom (80 *cm*). Which can be explained by stratification as well. However the relationship between the temperature in the inner and outer reservoir seems less straight forward, as the bottom temperature of the outer reservoir is generally higher than the one at the bottom of the inner reservoir, this is likely due to the location of the overflow, at medium height.

The shorter distance to the production of the hot waste water results in a higher temperature than in both other settlement tanks, but also a more variable temperature profile. In Figure 8.13, the temperature profile at the inlet of the third settlement tank is shown.

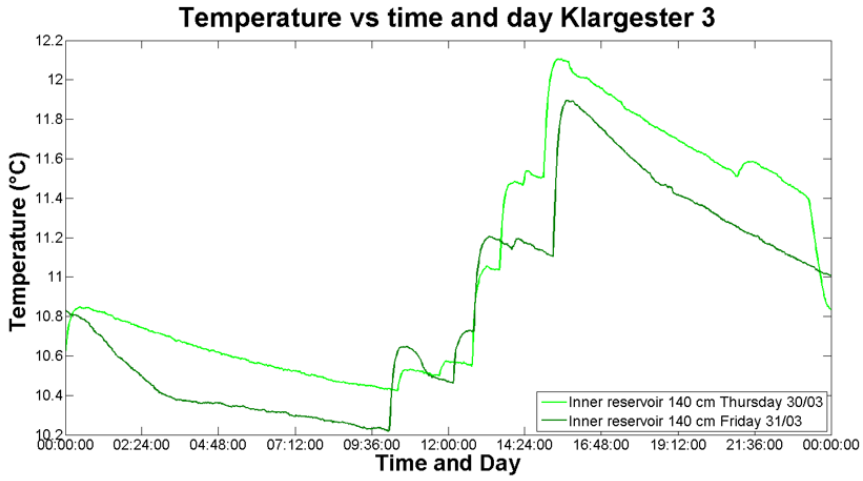


Figure 8.13.: Temperature profile at the inlet of the third settlement tank at Penrhyn Castle, Wales on March 30th and 31st.

One can observe that the temperature is decreasing during the night time and starts increasing around 10 AM, when visitors start to arrive, the decrease in temperature starts after opening hours, around 5 PM. The changes in slope are likely related to different weather conditions (eg. Rain,â¦).

8.2.3. Selection of the pilot location at Penrhyn castle

All heat embedded in the wastewater from the castle is lost to the environment during the transport of the waste water to the settlement tanks. The large settlement tanks receiving the waste water from the castle will thus not be suitable for heat recovery. Furthermore the maximal fill of the first settlement tank seems to be at approximately half its volume, which could indicate that the outflow pipe is too low in the tank, resulting in its inability to fill up.

The settlement tank collecting the waste water from the visitor centre and the toilets contains heat, and an indirect heat recovery system can be investigated, observed temperatures in the tank are expected to be too low to use direct heat recovery. It is also to be noted that a large portion of the heat is lost during night time, as a result of this phenomenon the recoverable heat will only be available during day time.

Temperature stratification can occur in the different compartments (reservoirs) of the settlement tank. The relationship between the temperature of the inner and outer reservoir is less straight forward, as the overflow between both reservoirs is located at medium height.

The monitoring of drain water temperatures at the kitchen drain showed high temperatures, with median observed temperatures up to 35°, and an average, daily flow of around 650 l during the monitoring period, June 2017 to February 2018. These conditions provide the opportunity for a direct heat recovery system. For these reasons, the first heat recovery option, at the kitchen drain, was selected as a pilot site. The designed experimental unit, and its feasibility, installation and operation are discussed in this Chapter.

8.3. Methods and Materials

8.3.1. Heat Recovery Methods

Direct drain water heat recovery

When the temperature of the drain water is sufficiently elevated, as is the case for kitchen drain water (see Section 6.2.1), it can be used as a heat source to directly preheat the mains water, using a heat exchanger (see Figure 8.14). This method requires a heat exchanger, associated pipework components and, in case the mains pressure is insufficient, a pump to circulate clean water through the heat exchanger.

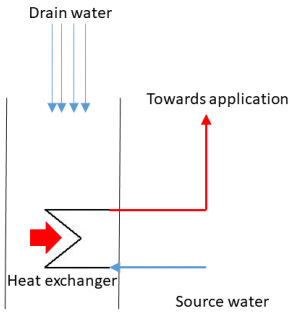


Figure 8.14.: Direct Drain Water Heat Recovery System.

By preheating the mains source water, the required heat from the conventional heating system is reduced, resulting in a decrease in fuel consumption and thus related costs and emissions.

8.3.2. Components

Heat exchanger

The heat exchanger that was considered comprised 168 cm long concentric pipes. Each pipe had a capacity of 50 l/min of drain water. In this analysis, the effectiveness of the heat exchanger was estimated at 58%. The variation of the effectiveness of the heat exchanger, with varying flows was shared by the manufacturer, and is shown in Figure 8.18. The estimated effectiveness here is a weighted average of the expected effectiveness, based on the manufacturer's information, and the flows observed in the drain of the kitchen at the tourist attraction in Wales. The heat exchanger is shown in Figure 8.15.



Figure 8.15.: The ShowerSave Q-Blue 1 heat exchanger.

Circulation pump

In case the mains pressure is insufficient, an circulation pump can be used to supplement the existing infrastructure. In the case of this project a Grundfoss Alpha 2L (see Figure 8.16) was selected. The sizing of the pump (Appendix F.2) and its data sheet (Appendix F.3) can be found in Appendix H.



Figure 8.16.: The Grundfoss Alpha 2L circulation pump.

8.3.3. Monitored data

In order to assess the possibility for drain water heat recovery, prior to system design and installation, the different system parameters (the temperatures and flow of both fresh– and drain water) had to be assessed. The different measurements and assumptions are described in Section 8.2 and this section.

Feed water temperature

The feed water temperature was measured, on a daily basis, for one year in a residence in Dublin in 2011-2012 Gill et al. [2016]. For a simulation of the operation, these measured temperatures (Figure 8.17) were used. It was assumed that, given the similarities in terms of climate between the east coast of Ireland, and the west coast of Wales, seperated by only 160 km, the feed water temperatures measured in Dublin were indicative for the ones encountered in Wales.

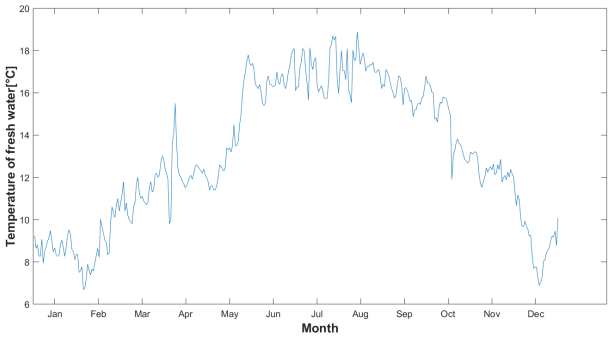


Figure 8.17.: Feed water temperature in Dublin, 2012.

Kitchen drainwater: Monitoring campaign

As mentioned in Section 8.2, the drain water temperature was measured at the kitchen drain, which resulted in measurements of temperatures of up to $55°C$, and a median value, ranging from 22 to $38°C$ during the opening hours of the kitchen, as shown in Figure 8.6. The fresh water consumption of the kitchen was monitored as well, both characteristics were measured over the period from June 2017 to January 2018. The return factor for the UK was estimated at 95% by Butler and Davies [2010]. However, the authors opted for a more conservative 90% for the analysis.

Heat exchanger effectiveness

The effectiveness of the heat exchanger depends on the clean water flow, the relation, as given by the manufacturer can be found in Figure 8.18 (see also Section 6.2.2).

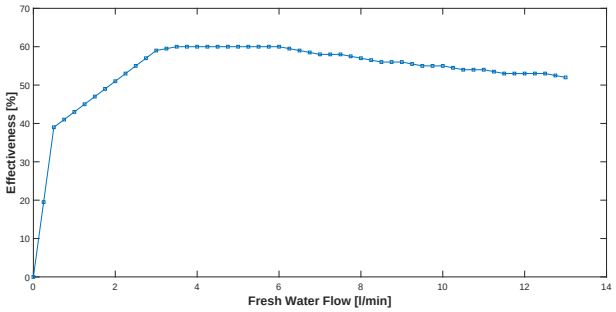


Figure 8.18.: Effectiveness of the heat exchanger.

8.4. Design of the experimental unit

This section describes the pre-analysis and design that was completed for heat recovery systems at the kitchen drain of the castle, using the performed monitoring campaign (Section 8.3.3), the current heating system (Section 8.4.1), and the proposed heat recovery systems (Section 8.4.2).

8.4.1. Current heating system

The current heating system is located in a biomass building (plant room), 250 m away from the castle, and at an elevation of about 30 m lower than the castle, as can be seen in Figure 8.3. Reducing heat consumption at the castle would also result in reduced pumping costs for the main heating loop, which improves profitability.

The property is currently heated by two boilers of 150 kW each (total 300 kWp), presented by the traditional heating system in Figure 8.19. The heat produced by the boilers is collected by a primary heating loop, with characteristics as described in Table 8.4. The temperature difference was assumed to be constant over time. The heat is then delivered to the secondary loop, also denoted as main heating loop, by a plate heat exchanger, this loop is represented by the dashed lines in Figure 8.3. A simplified schematic is shown in Figure 8.19, the detailed schematic is shown in Appendix F.5.

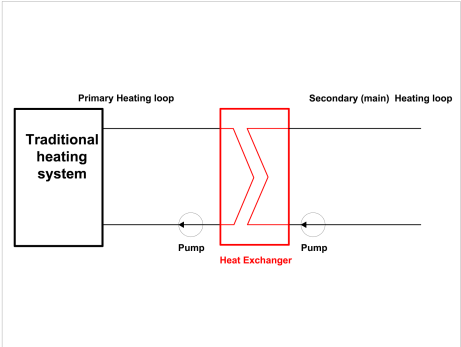


Figure 8.19.: Simplified schematic of the heating system in the plant room at Penrhyn Castle.

The hydraulic characteristics of both the primary and the secondary (main) heating loop are described in Table 8.4.

Primary heating loop		
	Pump	Grundfoss Magna 3D
	Pumping Head	3 m
	Temperature difference	30°C
Secondary heating loop		
	Pump	2 Grundfoss TPE 3
	Pumping Head	31.38 m
	Temperature difference	10°C

Table 8.4.: Hydraulic characteristics of the heating system at the plant room of Penrhyn castle.

Heat consumption inside the castle, and thus also by the kitchen discussed in this paper, is done by extracting the heat from the main heating loop, for local consumption, through heat interface units (see Figure 8.19).

8.4.2. Drainwater heat recovery system

Three different designs were made for the heat recovery system at the castle. The simplest design (Configuration 1), is a simple preheating system, similar to the system proposed in Chapter 6. However, because of the fact that only the fresh water consumption (hot and cold) of the kitchen was measured, the reduced heat recovery, due to potential temporal mismatches, could not be assessed in the design and feasibility phase of this pilot site. For that reason, a second configuration was also designed, where the fresh water, to be heated, was first collected in a buffer tank, and continuously circulated through the heat exchanger. This means that all opportunities for heat recovery (every time wastewater falls through the drain) are exploited, but requires input pumping power, also when no water is coming down the drain. The design of a third configuration is a combination of both previously mentioned configurations. The configurations are described in more detail in this section.

Configuration 1

The schematic of the direct drain water heat recovery (DWHR) system is shown in Figure 8.20. The drain water was not diverted from the main drain, but rather part of the drain was replaced by the heat exchanger. The incoming fresh water feed was preheated, before it reached the heat interface unit (ESSCO). This heat interface unit provides the interface between the fresh water and the mains heating loop and heats the water to the required $60°C$. The presence of the DWHR system results in a higher temperature for the water going into the heat interface unit. The water thus requires less energy to reach the required $60°C$.

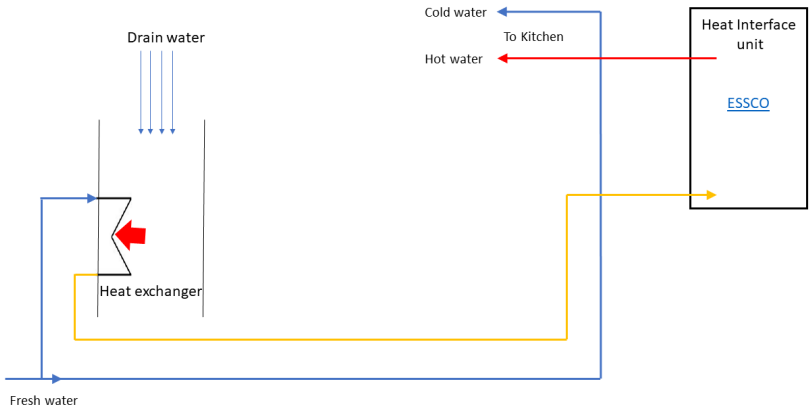


Figure 8.20.: Configuration 1 of the drain water heat recovery system at Penrhyn Castle, Wales.

Configuration 2

In order to compensate for potential temporal mismatches, configuration 2 was designed, and implemented. The incoming water was collected in a buffer vessel, from where it is recirculated through the heat exchanger until consumption in the kitchen. This resulted in continuous (recirculating) presence of fresh water in the heat exchanger, such that heat could be recovered from all wastewater going through the drain. However, this also results in circulation through the heat exchanger, when no wastewater is going through the drain pipe, and thus no heat can be recovered. In the latter case the electricity consumed to pump the water through the system doesn't result in a usefull output. Improvements can be made to the system to counteract this, for example setting the pumps in the system to a timer, or with a more sophisticated control system, only pumping the fresh water through the heat exchanger at times when wastewater is flowing through the drain. The system is summarized in Chapter 8.21.

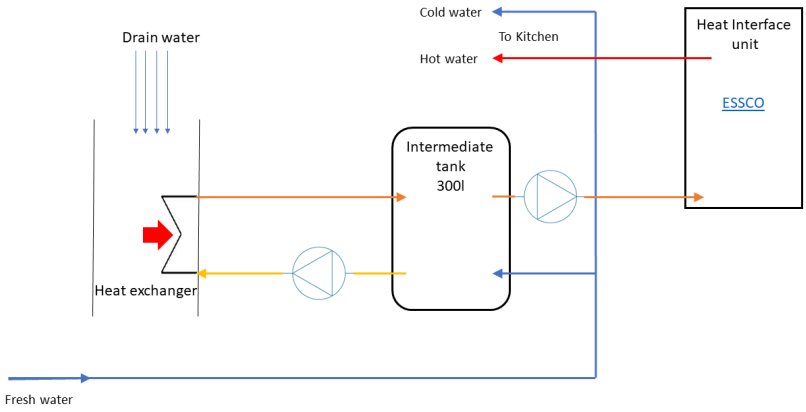


Figure 8.21.: Configuration 2 of the drain water heat recovery system at Penrhyn Castle, Wales.

Configuration 3

In configuration 3, both systems are combined, both preheating the incoming fresh water, and recirculating the fresh water from the buffer vessel. This was expected to recover the largest amount of energy, however it also has the largest material requirements and capital investment. The system is summarized in Figure 8.22.

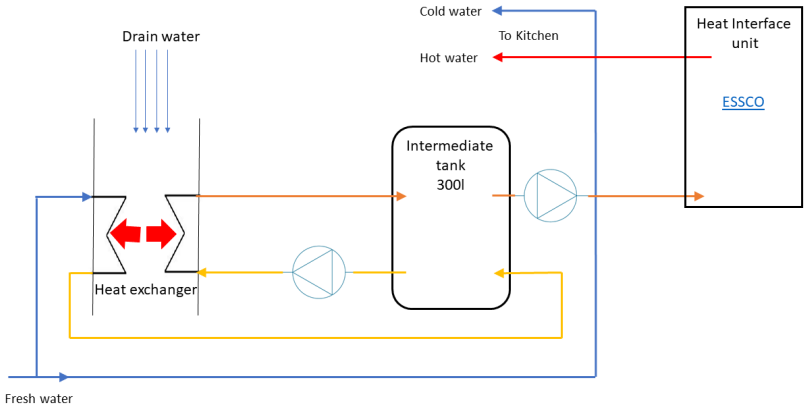


Figure 8.22.: Configuration 3 of the drain water heat recovery system at Penrhyn Castle, Wales.

8.4.3. Instrumentation

The test rig, and the different metering instruments are displayed in Appendix H. The metering scheme of the three configurations described above (Section 8.4.2) is shown in Figure 8.23. The instruments used to record the different parameters are discussed in this section, the flow meters were not described, as they were already present, and just added to the logging system. One can observe that wastewater flow was not monitored, due to space constraints. The wastewater flow is estimated based on the recovered heat in the heat exchangers, and the temperature difference of the wastewater across the heat exchanger set-up. This estimation assumes that all heat released by the wastewater was recovered by the fresh water in the heat exchangers, and not lost to the environment.

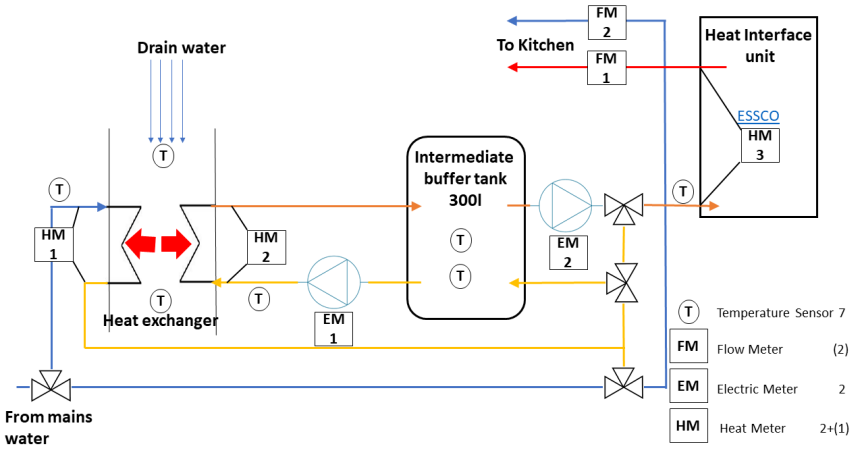


Figure 8.23.: Metering of the drain water heat recovery system at Penrhyn Castle, Wales.

Heat meters

The heat recovered from the wastewater is recorded using ITRON CF ECHO II heat meters(see Section 4.4.4). The locations where heat recovery is measured are listed below, and are shown in Figure 8.23:

- HM1: the preheating heat exchanger.
- HM 2: the reheating heat exchanger.
- HM3: The heat consumption from the heat interface unit.

Temperature sensors

The temperature sensors used in this experimental set-up are PT 100 resistance sensors (see Section 4.4.4), and are referred as T, in Figure 8.23.

8.5. Feasibility study

8.5.1. Methodology

The expected energy savings are twofold, on the one hand there is a direct reduction of heat consumption, and thus of wood pellet consumption in the biomass building (See Section 8.4.1). On the other hand, reducing the heat consumption will reduce the required flow in the primary and secondary (main) heating loop, and thus reduce the electric consumption of the pumps.

The reduction in fuel consumption is equal to the recovered heat, which was calculated using the effectiveness method [Yunus and Boles, 2007]. As described in Equation 8.1, C_{min} is the minimal heat capacity rate, Q_{max} is the maximal recoverable heat, and $Q_{recovered}$ is the recovered heat. The subscript DW stands for drain water, and FW for fresh water. The effectiveness of the heat exchanger η_{HE} depends on the fresh water flow rate ($V_{FW,hot}$) and was considered to be 58%, as per manufacturer's datasheet.

$$\begin{cases} C_{min} = min([\dot{V}\ \rho\ c_p]_{DW},\ [\dot{V}\ \rho\ c_p]_{FW,hot}) \\ Q_{max} = C_{min}\ (T_{DW,in} - T_{FW,in}) \\ Q_{recovered} = \eta_{HE}([\dot{V}_{FW,hot}) \end{cases} \tag{8.1}$$

The expected reduction in electric consumption, related to pumping in the primary and secondary heating loop (see Figure 8.19), was calculated based on the assumption that the control loop keeps the temperature drop over the loop constant, at the values shown in Table 8.4. The total heat consumption

(Q_{total}) can then be expressed as in the set of Equations 8.2, over both the primary and the secondary loop. Considering the expected recovered heat by the DWHR system, the previous total heat consumption can also be expressed as a function of the new total heat consumption ($Q_{new,\ total}$) and the recovered heat ($Q_{recovered}$).

$$\begin{cases} Q_{total} = [\dot{V}\ \rho\ c_p\ \Delta T]_{primary\ loop} \\ Q_{total} = [\dot{V}\ \rho\ c_p\ \Delta T]_{secondary\ loop}) \\ Q_{total} = Q_{new,\ total} + Q_{recovered} \end{cases} \tag{8.2}$$

Assuming that the temperature difference over the loop remains constant, and the volumetric flow ($\dot{V}$) is the control parameter, the expression can be rewritten as in the set of Equations 8.3.

$$\begin{cases} Q_{total} - Q_{new,\ total} = [(\dot{V}_{prev} - \dot{V}_{new})\ \rho\ c_p\ \Delta T]_{primary\ loop} \\ Q_{total} - Q_{new,\ total} = [(\dot{V}_{prev} - \dot{V}_{new})\ \rho\ c_p\ \Delta T]_{secondary\ loop}) \\ Q_{total} - Q_{new,\ total} = Q_{recovered} \end{cases} \tag{8.3}$$

This expression enables the calculation of the reduction in required volumetric flow in the primary and secondary loop. Using the values shown in Table 8.4, the reduction in pumping consumption (S) can be estimated as in Equation 8.4. Where η_{pump} is the pump efficiency, ρ water density, g the gravitational constant and H the pumping height.

$$\begin{cases} S_{elec,\ primary\ loop} = [\eta_{pump}\ (\dot{V}_{prev} - \dot{V}_{new})\ \rho\ g\ H]_{primary\ loop} \\ S_{elec,\ secondary\ loop} = [\eta_{pump}\ (\dot{V}_{prev} - \dot{V}_{new})\ \rho\ g\ H]_{secondary\ loop}) \end{cases} \tag{8.4}$$

8.5.2. Expected savings

The savings generated by recovering the heat from the kitchen drain, and thus reducing the heat demand at that level are twofold (see Section 8.5.1). On the one hand the required thermal energy, delivered by the biomass boilers will be reduced, and on the other a smaller volume of water needs to be pumped through the main heating loop, reducing the consumption of the pumps for the main heating loop. The estimated reductions in energy consumption, operating expenses (OPEX) and related greenhouse gas emissions, based on the observations and measurements over 228 days (the opening days reported by National trust in 2018), before a DWHR system was installed, are described in this section. The savings predicted for the particular case of Penrhyn castle, are described in the first three subsections, later the results for Configuration 1 (judged most profitable) was extended using the average fuel prices in the UK, to generalize the results for other locations, with different heating fuels.

Energy savings

The energy savings generated by reduced heat consumption are straight forward, however the calculation of the reduced pumping consumption in the main heating loop will change depending on the control strategy employed in this loop. In order to assess the reduced pumping consumption, it was assumed that the temperature drop over the entire heating loop is kept constant at $10°C$ (as measured on site on $March\ 13th$ 2018). A reduced heat consumption in the kitchen will thus result in a reduced flow in the main heating loop. A smaller temperature drop will lead to increased savings. The estimated pumping head is 31.38 m (as mentioned on the technical plate of the pump). The reduced pumping consumption of the boiler loop was estimated in the same way, assuming a temperature drop of $30°C$, and a pumping head of 3 m. (As described in 8.5.1)

The actual control system can act on both the temperature difference (by changing the temperature at the start of the loop), and by acting on the flow rate (by changing the pumping rate). The operation of the control system is known only to Dunstar (the engineering company that installed the heating loop), however the efficient operation of heating loops requires a stable return temperature, and it can thus be expected that the pumping rate is the main control parameter.

The considerations described in Section 8.5.1 result in expected savings, shown in Table 8.5. Where the total consumption is estimated based on the observed hot water flow at Penrhyn castle, the fresh water temperature as measured in Dublin on that date in 2012 (see Section 8.3), and the required $60°C$ temperature fed to the kitchen. The total electric consumption of the pumps was unknown.

	Heat Consumption (kWh_{th}/day)		**Electric pumping savings** (kWh_{el}/day)
	Main heating loop	**Savings**	
Current	23.48	–	–
Config 1	15.03	−8.45	−0.20
Config 2	16.78	−6.70	−0.09
Config 3	14.41	−9.07	−0.09

Table 8.5.: Daily energy consumption related to the kitchen at Penrhyn castle, Wales.

Note that the electric pumping consumption is related to all heat consumption on the branch of the loop on which the kitchen is installed, not only for the kitchen heat interface unit. The differences in electric pumping consumption are related to the reduction in heat consumption of the kitchen, but the absolute values are related to the heat consumption of the entire branch, which was unknown, and thus not included.

One can observe that Configuration 3 is characterized by the largest energetic savings, however the electric savings are smaller than for Configuration 1. This has an important impact on the financial and environmental considerations. For Configuration 2, one can observe that the energy savings are smaller than the for Configuration 1. This is related to two main factors:

- Heat losses (mainly overnight), from the buffer vessel. These heat losses were estimated by assuming a wall thickness (5 cm) and insulating material (heat exchange coefficient 0.02 W/mK) of the buffer vessel
- The recovered heat for configurations 1 and 3 could be reduced due to the (currently) unquantified temporal mismatch between supply (the kitchen drain) and kitchen demand.

The flow of the drain water was not directly measured, and is thus unknown. The drain water flow could not be measured due to space constraints in the drain network. In this assessment it was assumed that 90% of the ingoing flow leaves through the drain [Butler and Davies, 2010]. However, there is a significant temporal uncertainty, indeed the residence time of the water inside the kitchen and its appliances is unknown. This might reduce the heat recovery for Configurations 1 and 3, as the concurrence of drain water flow and clean water flow could be reduced.

Reduction in GHG emissions

The reduction in emissions related to the reduced consumption in the previous Section are summarized in Table 8.6. The GHG intensity of the different fuels is as stated in Department for Business Energy & Industrial Strategy [2018*a*]. It was assumed that 23.3% (As reported by National trust in 2018) of the electricity is generated by the on-site PV panels (see Section 8.2.2).

	GHG intensity reduction ($g\ C_e/kWh$)	**yearly savings** ($kg\ C_e$)
Current	–	–
Config 1	−34.3	50.27
Config 2	−25.48	37.36
Config 3	−26.3	38.57

Table 8.6.: Emission parameters related to the kitchen at Penrhyn castle, Wales.

This table shows that, from an environmental point of view, the 1st configuration is the desired option, characterised by the highest reduction in GHG intensity, and the largest yearly savings.

Reduction in operation costs

The estimated capital investment, based on supplier quotations, is summarized in Table 8.7.

		Config 1		Config 2		Config 3	
Component	**Unit cost(£)**	#	**Cost(£)**	#	**Cost(£)**	#	**Cost(£)**
ShowerSave QB16	495.6	1	495.6	1	495.6	2	991.2
Pump: Grundfos Alpha 2L	182.23	0	0	2	364.46	2	364.46
Buffer tank	400	0	0	1	400	1	400
Labour Cost	35	10	350	15	525	15	525
Additional material			100		100		100
Total			945.6		1 885.06		2 380.66

Table 8.7.: Summary of the estimated capital investment at Penrhyn castle, Wales.

The operation costs (OPEX)savings and estimated financial payback period are summarized in Table 8.8.

	OPEX(£/*day*)	**Savings (£/*day*)**	**Payback Period (*yrs*)**
Current	1.02	–	–
Config 1	0.61	−0.41	13.4
Config 2	0.74	−0.27	34.4
Config 3	0.65	−0.37	31.9

Table 8.8.: OPEX and payback period at Penrhyn castle, Wales.

One can observe that, in the case of the kitchen at Penrhyn castle, the payback periods are larger than 10 *years* for all configurations. The National Trust has favourable bio-mass and electricity prices at Penrhyn castle (see Table 8.9), partially explaining the unfavourable conditions. Another explanation lies in the amount of drainwater flow and consumption, being insufficient to overcome the capital investment, despite reduced operational costs.

Fuel	**Abbreviation**	**Price(p£/kWh)**	**C intensity ($kg\ C_e/kWh$)**
Electricity	Elec	7.00	0.28307
Bio Mass (Wood Pellets)	BMWP	4.50	0.01506

Table 8.9.: Fuel prices and carbon conversion factors for the National Trust property at Penrhyn castle.

Generalizing the results

The assessment was extrapolated to look at the applicability of this installation in other properties. In this extrapolation the savings are considered with regard to the reduction in consumption of traditional heating sources. The reduction of required pumping in the main heating loop is not considered in this extrapolation, as it might not be of relevance in many cases. Similarly, the electricity, delivered to the different sites is considered to have the same impact and costs as the general mix in the UK, as the information about on-site production is unknown. The employed fuel prices [Department for Business Energy & Industrial Strategy, 2018*b*], and Carbon-intensities [Department for Business Energy & Industrial Strategy, 2018*a*] are shown in Table 8.10.

Fuel	Abbreviation	Price($p£/kWh$)	C intensity ($kg\ C_e/kWh$)
Heavy Fuel Oil	HeFO	4.88	0.28544
Electricity	Elec	15.72	0.28307
Natural Gas	NGas	4.32	0.20437
Coal	Coal	4.98	0.36288
Bio Mass (Wood Pellets)	BMWP	4.50	0.01506

Table 8.10.: Fuel prices and carbon conversion factors in the UK.

Using the prices and carbon conversion factors, as considered in Table 8.10. This results in yearly financial savings as shown in Figure 8.24. One can observe that the payback period is below 10 years in all cases.

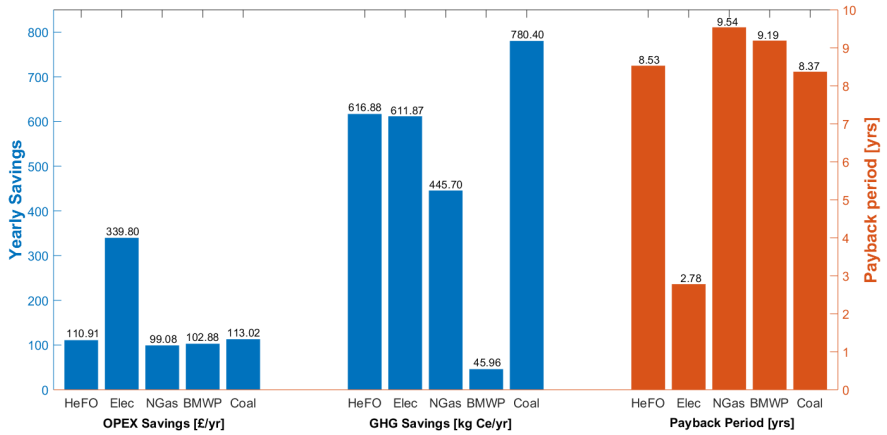


Figure 8.24.: Savings related to the DWHR system on the kitchen drain at Penrhyn castle, Wales.

Using the carbon conversion factors described in Table 8.10, this results in an expected reduction of carbon equivalent emissions as described in Figure 8.24. One can note that the savings for biomass are small due to the low carbon conversion factor, for company reporting, of biomass.

8.6. Installation procedure

8.6.1. Physical installation of the components

Penrhyn castle is a classified site, requiring all works and alterations to be performed by a certified contractor. In this case, the plumbing and piping connections were installed by ASKEW LTD. Under the contract agreement between the national Trust and the Dwr-Uisce project, the project collaborators were also certified to make alterations and corrections to the system. The installation, and hydraulic operation of the system required multiple iterations of the installation procedures, as the system needed to be adapted and fitted to the conditions at the coal yard and the kitchen drain. For this reason all steps and procedure in the installation had to be performed on-site, requiring the collaboration with certified contractors.

The logging and visualisation system (see Section 4.4.4) was provided by DETECTRONIC (see Section 4.4.4), and installed on site after the installation of the hydraulic system. Three transmitters were installed on site, 2 in the coal yard, where the kitchen drain is located (see Figure 8.25) and one in the technical room (Shown in Figure 8.26, see Appendix F.4). The technical room, with thick walls creating problems for the wireless transmission of data, for this reason, the data transmission system was moved from the technical room to the coal yard, at a later date, by extending the connection cable.

8.6.2. Commissioning

The hydraulic installation of the DWHR system was first performed using copper components (see Figure 8.25), and in a later stage insulated (see Figure 8.26). The heat exchangers, replacing the kitchen drain, are shown in Figure 8.25, the left one representing the preheating heat exchanger (see Figure 8.20), and one the right one can find the heat exchanger from the recirculation loop.

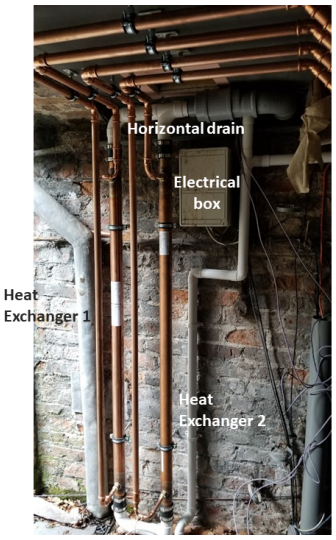


Figure 8.25.: Heat exchangers installed at the sewer drain in Pernhyn castle, Wales.

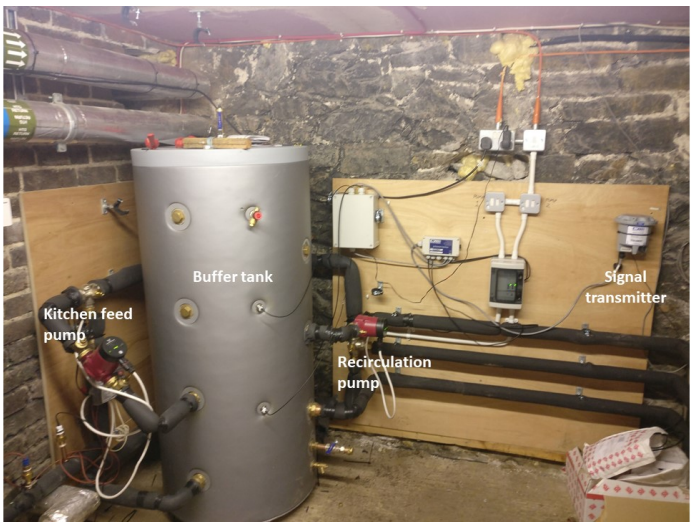


Figure 8.26.: Buffer tank installed at the sewer drain in Pernhyn castle, Wales.

As can be observed in Figure 8.25, the heat exchangers were not placed straight under the drain, but have been moved to the left, to circumvent the electrical box. This creates the need for the wastewater to travel horizontally, causing the majority of wastewater to flow through the heat exchanger on the right (heat exchanger 2, the one in the recirculation loop), this renders Configuration 1 and Configuration 3 practically unusable. The operation of the system was thus only performed under Configuration 2.

Initially, no flow was observed in the recirculation loop. A meeting with the plumbing contractor on-site resulted in multiple (four agreed, three confirmed), visits of the contractor on-site, aimed at resolving this problem. All of these meetings turned out to be unfruitful, as established remotely on the on-line platform (see Section 4.4.4). After a visit of a technical team from the project (and Trinity College itself), it was established that the issues had been caused by a closed valve. This anecdote shows the imporance of the so-called 'Gemba–walk'. In lean manufacturing the idea of Gemba is that problems are often easily spotted, and that actions like 'management by walking around', allow for the identification of potential, easy solutions. It shows how certain problems can be easily resolved by a physical presence on-site, where remote monitoring often leads to omit the simplest checks [Lean Construction, 2017].

This also shows the importance of the transition between exploratory research (such as the feasibility study, see Section 8.5), and applied, demonstrative research projects. Where sub-ideal situations and behaviours can have an equally important effect on the success of projects as the theoretical framework and concept.

8.7. Pilot site operation

The heat recovery system installed at Penrhyn castle was commissioned on January 24th 2020. As mentioned in Section 8.6.2, only configuration 2 was operational. The operation of the system was observed, and is reported here, until March 21st 2020, as all activities at Penrhyn castle ceased (for an unknown period of time) after that day, as a safety measurement during the Corona health crisis.

8.7.1. Heat recovery from the kitchen drain

During the period of operation (From January 24th 2020 until March 21st 2020), the recovered energy, and flow through the recirculation loop was measured. As the energy is logged by pulses (one pulse per 0.01 MWh), the total recovered energy is given as an interval. The drain water flow was estimated as 90% of the incoming water flow see Section 8.2.2, [Butler and Davies, 2010]). This is an over–estimation of the drain water flow, as can be seen in Figure 8.25, not all drain water from the kitchen, flows through the heat exchanger. However, this would underestimate the amount of heat recovered per m^3 of drain water and is thus an error 'on the safe side'. This means that the calculated heat recovery related to the drain water flow is lower than the actual value. This is confirmed by comparing it to the theoretical calculated value of 10.54 kWh/m^3_{WW}, assuming the average wastewater temperature observed in Section 8.2.2. The measurements are summarized in Table 8.11.

Recovered energy	$60 - 70\ kWh$
Flow in the reheating loop	$4.90\ l/min$
Estimated drain water volume	$7.77\ m^3$
Heat recovery compared to drain water flow	$7.77 - 9.01\ kWh/m^3_{WW}$
Heat recovery compared to hot water consumption	$13.64 - 16.98\ kWh/m^3_{HW}$

Table 8.11.: Measurements of the heat recovery from the kitchen drain water at Penrhyn castle, Wales.

This recovered heat increased the temperature of the incoming fresh water from an average of $11.75°C$, to an average of $17.59°C$, when entering the heat interface unit. The temperature evolution is shown in Figure 8.27. In this figure, one can observe an upward trend from February 17th, the time the kitchen effectively opened for public, rather than only internal staff use.

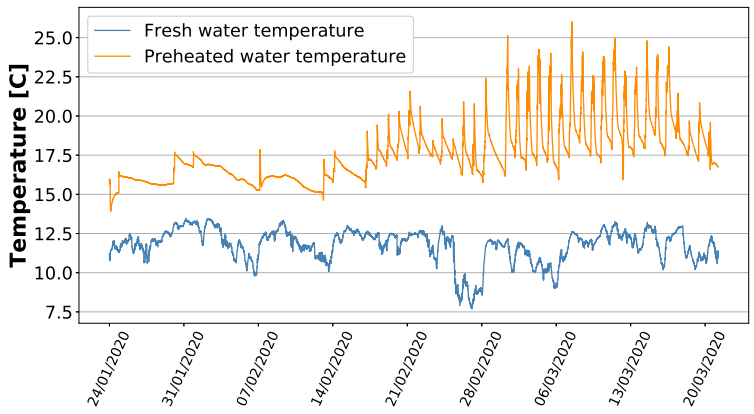


Figure 8.27.: Evolution of the fresh water temp at Penrhyn castle, Wales.

8.7.2. Energy efficiency of the kitchen's hot water

To compare the energy consumption before and after installation of the heat recovery system, the heating energy efficiency metric was used, describing the energy efficiency of delivering hot water to the kitchen. This was defined as the amount of heat required from the heat interface unit, and thus from the biomass boiler in the biomass building (Figure 8.3), per m^3 of hot water consumed by the kitchen. The energy efficiency, without the heat recovery system, was benchmarked in the period from April 12th 2019, until December 31st 2019. The energy delivered by the heat interface unit, and the volume of hot water to be heated, were measured by a heat meter (see Section 4.4.4), the volumetric consumption of hot water was also measured a second time, by a flow meter, already installed on the premises. The measurements are summarized in Table 8.12.

Reading device		**Heat meter**		**Flow meter**
		Energy (MWh)	**Volume** (m^3)	**Volume** (m^3)
Benchmark	(12/04/2019 – 31/12/2019)	$2.00 - 2.01$	32.36	32.54
Configuration 2	(24/01/2020 – 21/03/2020)	$0.07 - 0.08$	4.40	4.12

Table 8.12.: Measurements of heat consumption for hot water at Penrhyn castle, Wales.

In Table 8.12, one can observe that there is a slight difference in the observed volume of hot water consumed, when measured with the heat meter or flow meter. This results in a difference in the energy efficiency metric. This difference is larger for the observed operation of the heat recovery unit, because the total operating period, and thus the total volume, was smaller for that period. The resulting energy efficiency metric is shown in Figure 8.28, in blue for the results with the flow meter, and in orange for the results using the heat meter data. One can compare the results of the benchmark energy consumption $(61.37 - 61.70\ kWh/m^3_{HW})$ to the estimated $55.91\ kWh/m^3_{HW}$, required to raise the temperature of the incoming fresh water from the temperature, as observed on site (Section 8.7.1), to the required $60°C$.

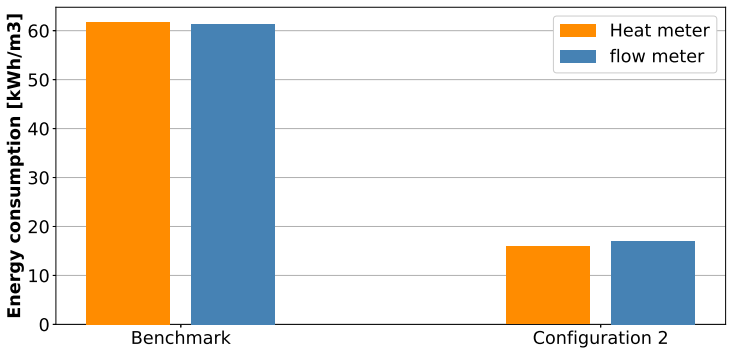


Figure 8.28.: Energy efficiency metric for hot water consumption of the kitchen at Penrhyn castle, Wales.

In Figure 8.28, one can observe that the energy efficiency metric was observed to be between 72 and 74% lower when the heat recovery system was in place. This seems a very large improvement, especially given the limited amount ($0.06 - 0.07\ MWh$) of heat recovery, discussed in Section 8.7.1. The total amount of heat added to the fresh water, through both heat recovery and the heating interface unit, during the operation period of the DWHR system, amounts to $29.55 - 36.39\ kWh/m^3_{HW}$. Comparing this to the benchmark metric, this leaves between 40.70% and 52.11%, of heat consumption unaccounted for. Given the relatively small amount of energy measured over the operation period ($6 - 7$ pulses), the measurement is very sensitive to errors. Furthermore, the kitchen served only as a staff kitchen from January 24th until February 17th. During this period, kitchen activities are expected to be different than during the tourist season, which could have an impact on the result.

Because of this discrepancy, and the fact that the benchmarked energy consumption was found to be close to the theoretical estimate, the heat recovery observation (see Section 8.7.1) was used for further calculation, and compared to the benchmarked energy consumption, rather than the energy efficiency metric.

8.7.3. Electric consumption in the recirculation loop

The heat recovery system, in configuration 2, employs two pumps, one to recirculate the preheated fresh water through the heat exchanger, and one to feed the fresh water, through the heat interface unit, to the kitchen, where it is consumed as hot water (see Figure 8.21). Both of these pumps will thus consume electricity during the operation of the system.

During the operation of the experimental heat recovery system (24/01/2020 – 21/03/2020), the recirculation pump ran continuously (24/7). This was the case because no control system was installed on the unit. A correction was applied on this value, assuming a simple, on–off system. Turning on when activities in the kitchen began (time of first water consumption, hot, or cold), and turning off when they ceased (time of last water consumption). The consumption of both pumps is summarized in Table 8.13, where the *corrected* consumption, is the consumption assuming this on–off control system. This Table also shows the relationship of this electric consumption to the amount of hot water consumed in the kitchen, called consumption density in this Table.

	Recirculation pump	**Feed pump**
Total consumption (24/01/2020 – 21/03/2020)	$157.6\ kWh$	$0.1\ kWh$
Corrected consumption (24/01/2020 – 21/03/2020)	$26.78\ kWh$	$0.1\ kWh$
Total consumption density	$35.82 - 38.23\ kWh/m^3_{HW}$	
Corrected consumption density	$6.09 - 6.50\ kWh/m^3_{HW}$	

Table 8.13.: Measurements of electric consumption of the pumps at Penrhyn castle, Wales.

In this Table, one can observe that the consumption of the feed pump is insignificant ($0.1\ kWh$). This can be explained by the oversized recirculation pump, being able to provide sufficient power to supply the kitchen from the buffer tank, and recirculating the fresh water through the heat exchanger.

8.7.4. Yearly savings and financial viability

Energy savings

The recorded operation does not cover a full year, as the logging system was installed from April 12th 2019, and running until March 21st 2020. During this period the heat recovery system operated from January 24th until March 21st 2020. 22 days are missing for observations of the kitchen over a full year, the heat recovery system only operated for 2 months, meaning 10 months are missing for the operation of the heat recovery system itself. On these 22 days, the kitchen is expected to be open[2]. In this section the operation of the kitchen during is extrapolated, based on the data gathered during the rest of the year, slightly underestimating the water consumption, but equally underestimating the heat recovery.

[2]As affirmed by Jane Davies of National Trust by email on 04/03/2020

Due to the COVID-19 pandemic, the castle has closed at the end of March 2020 and the 2020 tourist season is likely to be severely impacted. The resulting hot water consumption at the castle in 2020 is therefore not expected to be a true reflection of seasonal performance. A full picture can not be obtained until the end of 2021.

Figure 8.29, shows the total consumption of the hot water delivery to the kitchen, in terms of heat supplied by the alternative heating system (in the case of Penrhyn castle, the biomass boiler), but also by the heat recovery system (as a negative value, since this is a reduction in consumption), and the consumption of the related pumps. Because the operation of a main heating loop is not common to all kitchen hot water provision systems, and its consumption was not monitored, the pumping savings from the main boiler loop were not considered (using the same assumptions as in Section 8.5.2). In this Figure, the current system (without heat recovery) was compared to configuration 2 (as installed), and a corrected configuration 2 (See Section 8.7.3, above).

In this Figure, one can observe that the heat consumption, and heat recovery are significantly lower than the estimated values in Section 8.5.2. This is because the average water consumption of the kitchen per operation day was only 293.05 l/day, well below the 652.5 l/day observed during the monitoring period (June 2017–February 2018), for the feasibility study (see Section 8.3.3).

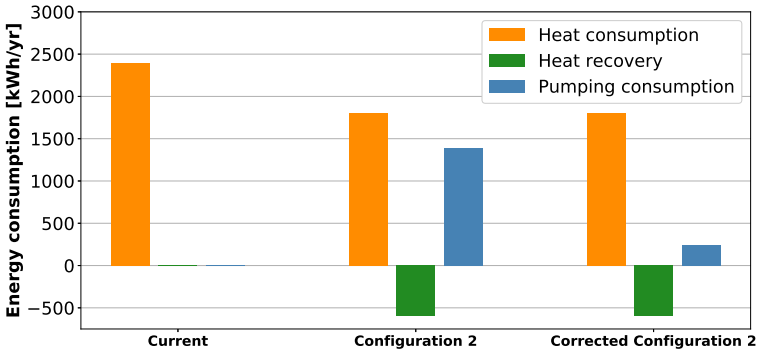


Figure 8.29.: Energy consumption of the kitchen at Penrhyn castle, Wales.

Financial and environmental savings

The reduction in operation expenses, and in heating related GHG emissions was calculated based on the fuel costs, and carbon intensity, as described in Table 8.10. The results, for the corrected configuration 2 are shown in Figure 8.30. In this figure, the same abbreviations are used as in Table 8.10. Other results are not shown, as the corrected configuration 2 produced most energetic savings. The payback period was not shown here, as no financial savings were obtained for any of the fuels except for electric heating.

One can observe that in this case, no reduction in operating expenses was achieved, but reduction in GHG gas emission was achieved for all fuel types, except for biomass. As discussed in Section 8.5.2, the technical emissions from biomass are larger than the conversion factor used by UK government. The technical reduction in GHG emissions is similar to the one obtained for coal [Gunn et al., 2012]. For a financially attractive system (with a payback period below 10 years), the water consumption of the kitchen would need to be about nine times as large as the one observed at Penrhyn castle.

Configuration 2 is thus not financially viable, this was also predicted in Section 8.5.2. However the operational savings and reduction in GHG emissions were lower than predicted, mainly because the water consumption of the kitchen, and thus the related drain water and recoverable heat, were lower than observed during the feasibility period. During the period of the feasibility study (June 2017–February 2018), the kitchen consumed around 652.5 l/day, and the predicted heat recovery was about 6.70 kWh/day (this relates to about 14.68 kWh/m^3_{HW}). During the observed operation (April 2019– March 2020), the kitchen's water consumption was around 293.05 l/day, showing a heat recovery of about 2.80 $-$ 3.48 kWh/day.

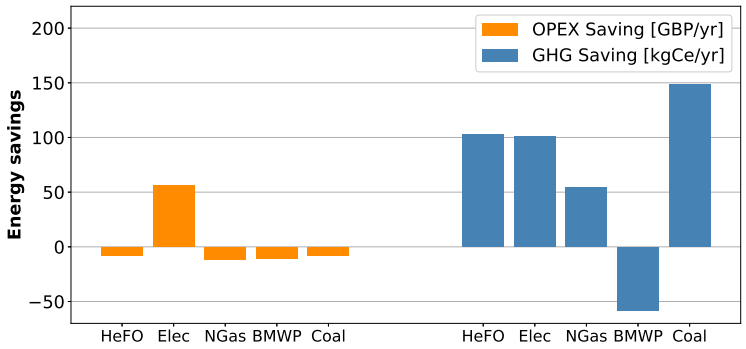


Figure 8.30.: Yearly savings of the corrected operation of configuration 2 at Penrhyn Castle, Wales.

However, as shown in Table 8.11, the amount of heat recovered, compared to the hot water consumption ($13.64 - 16.98\ kWh/m^3_{HW}$) was as predicted in the feasibility study. On a day during the peak tourist season (water consumption 1 200 l/day, given the heat recovery as observed in the period January 2020–March 2020, the heat recovery is expected to be in the interval $11.46 - 14.26\ kWh$ per day.

8.8. Summary

Drain water temperature, and clean water consumption, both hot and cold, were measured on the kitchen drain at Penrhyn castle, Wales over the period from *June* 2017 to *January* 2018. This showed temperature peaks of up to $55°C$, and a median value, ranging from 22 to $38°C$ during the opening hours of the kitchen. This shows a large potential of embedded energy flushed through the kitchen drain.

A drain water heat recovery system on the kitchen drain was proposed and installed on the site. The concept of the system was to be able to switch between three configurations, configuration 1, where the water is simply preheated, configuration 2, where the fresh water is recirculated from a buffer tank, through the heat exchanger, and configuration 3, where both these systems are combined. The savings realized by this system were twofold, on the one hand it reduces the fuel consumption related to the hot water heating. On the other hand, reduced heat demand reduces the required flow in the main heating loop on the grounds, resulting in reduced pumping costs.

Configuration 1 was deemed to be most profitable, its expected yearly savings were around 2.1 MWh of heat and around 50 kWh of electricity, resulting in a reduction in related GHG emission ranging from 45 to 780 $kg\ C_e/yr$, and a payback period ranging from 2.8 to 9.5 years, both depending on the current heating fuel on the grounds.

These theoretical results are subject to some uncertainties, one being the assumption that the temperature difference over the primary and secondary circuit is kept constant over time, meaning that the control loop only acts on the flow rate, and thus the electric consumption of the pumps. An increased temperature drop would result in a reduction in flow rate, and thus increased savings.

Further uncertainty lies in the temporal concurrence of the drain water flow and fresh water flow, the system was assessed on an hourly basis, but there could still be a temporal mismatch between the drain water flow and fresh water flow within this timestep. There was no real data available regarding this issue, as only the fresh water could be measured. This would reduce the amount of recovered heat. To counter this, a system which recirculates the fresh water through the heat exchanger can be designed, however this would introduce extra pumping costs, so a trade-off should be made.

The installed system aims at investigating the evolution of the system operation over time, given the difficult circumstances of working with kitchen drain water. It also aims at investigating temporal mismatches between drain water heat availability and heat demand in the kitchen.

At Penrhyn castle, with general fuel prices, the financial payback for configuration 1, was shorter than the targeted 10 years, in all cases. Furthermore, the carbon conversion factor for wood pellets in the UK is small, this is because biomass emissions, are considered to be biogenic, and thus non-fossil. This results in reduced GHG savings, however the technical carbon intensity of burning wood is similar to the carbon intensity of coal (even slightly higher due to lower efficiency of the burners) [Sterman et al., 2018]. Gunn et al. [2012] present the opinion that this difference is an inappropriate conceptual basis to assess GHG emissions. For completeness, using the Carbon conversion factor of coal (see Table 8.10) the yearly reduction of Carbon equivalent emissions would increase to 780.40 $kg\ C_e/year$.

The installed system at Penrhyn castle could only operate in one of the proposed configurations, configuration 2, and showed a reduced heat demand from the biomass boiler of about 594 kWh per year. This is significantly lower than the predicted recovery, due to the lower water consumption of the kitchen during this operation period than at the time of the feasibility study (293.05 l/day vs 652.5 l/day). This configuration of the heat recovery system was not financially profitable, although it provided a reduction in technical GHG emissions ranging from 50 to 150 kg/yr.

Configuration 1, where the incoming fresh water is simply preheated, was the simplest solution, and was deemed the most profitable. This is mainly due to its smaller capital investment, and the fact that no additional pumping is required.

9. Centralized drainwater Heat Recovery: Demonstrator in the meat processing industry

9.1. Introduction

Feasibility studies at Pepsico, Co. Cork (see Appendix B.5), and the ABP facility in Clones, Co. Monaghan (see Appendix B.4), showed a profitable potential for heat recovery at industrial wastewater treatment facilities. These feasibility studies showed that large volumes of wastewater were available, resulting in favourable conditions for indirect heat recovery. Furthermore, measurements of the inlet temperature, showed temperatures as high as $30 - 40°C$, favourable for direct heat recovery systems as well. Under these conditions, a combined, direct and hybrid, experimental heat recovery unit could be considered for energy recovery from industrial wastewater.

After a call through Enterprise Ireland, the meat processing company, ABP food group, expressed interest in hosting an experimental, pilot unit. ABP has undertaken multiple projects to reduce its carbon footprint, as their project, featured in the 'Green Business Resource Efficiency – Case Studies', a publication by the Environmental Protection Agency (EPA), of Ireland. [ABP Food Group, 2014*b*] The project described in this article consisted of implementing a waste hierarchy, reducing the amount of produced waste by 330 $tons/yr$, and the emissions by 9 $tons C_e/yr$. This resulted in a potential cost saving of around 10 000€$/yr$. Similarly, a water savings project across all ABP plants reduced their water consumption by 70 000 m^3/yr, and added a cost saving of around 150 000 €$/yr$ [ABP Food Group, 2014*a*].

The environmental department of ABP is located at the meat processing plant in Cahir, co. Tipperary. The presence of the department and its members, allowed for the experimental unit to be facilitated. The experimental heat recovery unit, described in this section, was thus installed at the wastewater treatment works of the facilities in Cahir.

This chapter[1] describes:

1. The heat recovery methods that were used, and the data used for sizing and design.
2. The design of the experimental set-up.
3. The feasibility study for the designed heat recovery unit.
4. The construction of the experimental unit.
5. The installation procedure.
6. The operation of the pilot site.
7. Suggested alterations to the heat recovery system.
8. The extrapolation of these findings to a full heat recovery system, for the full extent of wastewater from the activities on site.

[1]The research presented in this Section was submitted and accepted as an extended abstract at the *6th International Association for Hydro-Environment Engineering and Research (IAHR) conference, Warsaw, Poland, June 2020*

9.2. Selection of the pilot site

9.2.1. Industrial wastewater treatment systems

Large industrial facilities and factories, consuming large amounts of water, are characterised by large wastewater quantities. These facilities often have their own, on-site wastewater treatment system, tailored to the particular loading and pollutants in the wastewater of the site-specific process. In terms of heat recovery from the wastewater, these on-site, industrial wastewater treatment plants, present promising conditions, as they indicate the presence of large volumes of wastewater, close to a large water and (heating) energy consumer. A call for interested parties was launched through Enterprise Ireland, and yielded two interested parties: Pepsico, and ABP Food Group.

One of the main challenges for interaction with these type of large companies. is confidentiality. Both Pepsico and ABP, requested non-disclosure agreements highlighting the importance of this concern.

PEPSICO, Co. Cork

The feasibility study at Pepsico studied two different possibilities for heat recovery:

1. The CIP drain The Clean in Place (CIP) drain, accepting drain water from different processes showed temperature peaks of up to $70°C$, with a regular pattern, but a large spread in temperatures (ranging from 20 to $70°C$). A direct heat recovery system was proposed, because the drain and water feed ran next to each other the implementation of such a system is simple from a practical point of view (see Figure 9.1). Because the flow pattern was not available, the feasibility could not be assessed.



Figure 9.1.: CIP drain at the Pepsico facility in Cork.

‘

2. The wastewater treatment plant The operational data of the wastewater treatment plant was taken from the SCADA data analysis system, and allowed access to daily wastewater flow volumes. The temperature was measured using temperature sensors (see Appendix A). The proposed indirect heating system required additional pumping of a heat carrier, feeding the heat pump, from the factory to the wastewater treatment system and back. Heat recovery at this location was characterised by a large investment, but a payback period below 4 years (see Table 9.1, where $TEWI$ is the total equivalent warming impact, $CAPEX$ the capital expenditure, $LCOE$ the levelized cost of energy, see Section 7.4.2). This would reduce GHG emission by 88 $ton\ C_e$ per year.

System	Operation	TEWI	CAPEX	LCOE	Payback period
With circulation	250 $days/yr$	123.2 $g\ C_e/kWh$	147 700 €	0.045€/kWh	3.65 yrs

Table 9.1.: Results of the feasibility study at PEPSICO, Cork.

ABP Food Group, Co. Monaghan

The firs feasibility study at ABP FOOD GROUP was completed for their site in Clones, Co. Monaghan. This study investigated heat recovery at different locations in the wastewater treatment system.

1. The Outlet of the DAF unit At the outlet of the Dissolved Air Flotation (DAF) unit, a direct (D−DWHR) and a hybrid (H−DWHR) heat recovery system were studied. For the direct heat recovery system, three different possibilities for the heat exchanger were considered. The first two being replacing the vertical outlet pipe by a Co Flo system (see Chapter 8), with 34 and 16 pipes respectively. The third one being a heat exchanger integrated into the DAF unit. This resulted in a reduction in GHG emissions ranging from 17 to 207 $ton\ C_e$ per year. The results are summarized in Table 9.2. Details can be found in Appendix B.4.

System	Operation	TEWI	CAPEX	LCOE	Payback period
D-DWHR (34 pipes)	200 $days/yr$		23 090 €	0.012€/kWh	1.32 yrs
D-DWHR (16 pipes)	200 $days/yr$		16 160 €	0.038€/kWh	4.31 yrs
D-DWHR (integrated)	200 $days/yr$		24 355 €	0.014€/kWh	1.60 yrs
H-DWHR	200 $days/yr$	70.5 $g\ C_e/kWh$	130 130 €	0.031€/kWh	2.55 yrs

Table 9.2.: Results of the feasibility study at the DAF unit at ABP, Monaghan.

2. The outlet of the wastewater treatment works.

   At the outlet an indirect wastewater heat recovery system was considered, heating the water up to $45°C$, and reduce heating related emissions by up to 96 $ton\ C_e$ per year. The detailed results are summarized in Table 9.3. More details of the study can be found in Appendix B.4.

System	Operation	TEWI	CAPEX	LCOE	Payback period
I-DWHR	250 $days/yr$	110.7 $g\ C_e/kWh$	109 140 €	0.048€/kWh	4.57 yrs

Table 9.3.: Results of the feasibility study at the outlet at ABP, Monaghan.

ABP Food Group, Co. Tipperary

ABP FOOD GROUP accepted to host an experimental heat recovery system, however the offices of their environmental department are located at their facilities in Cahir, Co. Tipperary. Furthermore, Clones, Co, Monaghan was outside of the project area (see Section 1.3). For this reason the experimental rig was delivered and installed at the ABP facilities in Cahir. There, the wastewater treatment system is located at a larger distance from the heating system, however the presence of the staff on-site allows to react quicker to unforeseen circumstances. The feasibility study for the Cahir site is described in this section, along with the design, construction and operation of the experimental set-up.

9.2.2. Selection of the pilot location at ABP Food Group, Co. Tipperary

The aforementioned feasibility studies clearly showed that the amount of recoverable heat, and thus the feasibility, was increased when the heat recovery location was moved upstream in the treatment works. Meaning that the largest amount of recoverable heat and thus the most gains were estimated at the inlet of the treatment system. However the amount of suspended solids, and thus risks of fouling of the heat exchanger also increases when moving upstream.

Therefore, the experimental set-up was designed to be moveable, along the wastewater treatment system, aiming to investigate heat recovery at the different locations, and making the trade-off between higher temperatures at the inlet and the higher concentration of pollutants and suspended solids, and its effect on fouling.

9.3. Methods and Materials

9.3.1. Heat Recovery Methods

Two different heat recovery methods are studied. A direct method, preheating the mains water before it enters the conventional, heavy fuel heating systems, and a hybrid method, where the mains water is first preheated, and then heated to the required temperature by a heat pump, which is using the drain water as a heat source.

Direct drain water heat recovery

When the temperature of the drain water is sufficiently elevated, it can be used as a heat source to directly preheat the mains water, using a heat exchanger (see Figure 9.2). This method requires a heat exchanger, associated pipework components and, in case the mains pressure is insufficient, a pump to circulate clean water through the heat exchanger.

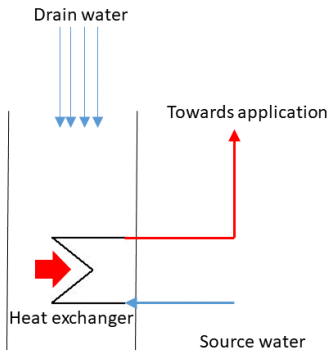


Figure 9.2.: Direct Drain Water Heat Recovery System.

By preheating the mains source water, the required heat from the conventional heating system is reduced, resulting in a decrease in fuel consumption and thus related costs and emissions.

Hybrid drain water heat recovery

Hybrid drain water heat recovery (Hybrid-DWHR) is used to indicate the combination of direct DWHR (see above) and indirect heat recovery, which means the heat from the drain water is used as a heat source for a heat pump (see Figure 9.3).

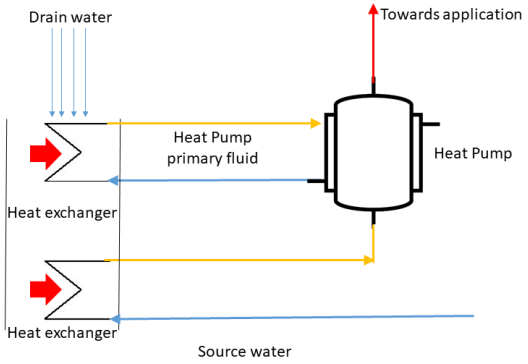


Figure 9.3.: Hybrid Drain Water Heat Recovery System.

The advantage of using a heat pump, as compared to traditional heating sources lies in the fact that it is considered a renewable heat source, and enables the reduction of heating related greenhouse gas emission and costs, depending on its coefficient of performance (COP). Wastewater, being generally warmer than the ground or air (the traditional heat sources for a heat pump), allows for the reduction of the required temperature lift (this is the temperature difference between source temperature and required hot water temperature). A smaller temperature lift increases the COP of the heat pump, and thus reduces electric consumption, and related costs and emissions (see Section 5.4).

By bypassing the heat exchanger on the source water, an indirect heat recovery system can also be tested using this set-up.

9.3.2. Components

Heat Exchanger

The proposed heat exchanger is the ShowerSave Coflo system [Building Products Distributors Limited., n.d.], for commercial scale projects, combining multiple Recoh-vert 16 heat exchangers (Figure 9.4). These heat exchangers consist of 2 concentric pipes, where the wastewater flows in the central pipe, and the clean water in the outer one.

A Co Flo system with 10 pipes would be able to recover the heat from max. 30 m^3/h of drain water. In this case 6 pipes will be used for the direct DWHR system, 1 for the direct component of the hybrid DWHR system, and 3 for the indirect component of the DWHR system. The required available head space is about 2.5 m for this system, the available head from the outlet of the different tanks in the wastewater treatment system, such as the DAF unit, aeration tanks, etc. If this head is not available on site, a smaller (and thus less efficient) system can be used requiring 2.1 m of head or 1.65 m. The heat exchangers were chosen such that they could accommodate a wastewater flow ranging from the design flow ($5 - -10$ m^3/h) to the expected, total wastewater flow (29 m^3/h).

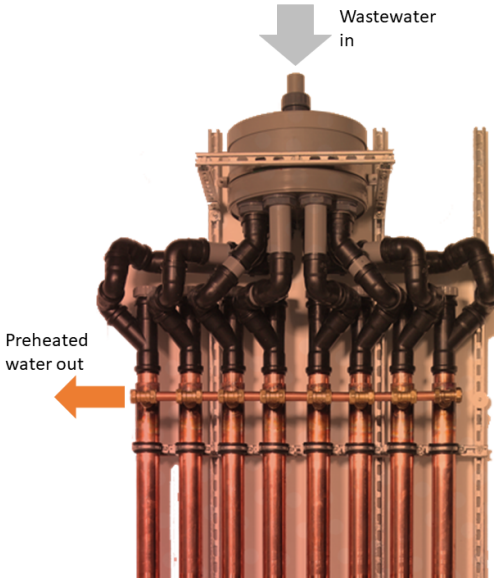


Figure 9.4.: Co Flo heat exchanger.

Heat pump

The heat pump used in this test rig was a NIBE F1145 ground source heat pump, intended for the heating of small houses, smaller multi-occupancy houses and industrial premises. Its intended heat sources are ground, bedrock, lakes or groundwater, the latter requiring an intervening heat exchanger. In this test rig, the configuration for groundwater was set-up, using the 3 Co Flo heating pipes for the indirect component of the DWHR system as the intervening heat exchanger.

The heat pump is used to heat the water to $45°C$, the nominal characteristics in these operating conditions are given in Table 9.4.

Heat output	3.98 kW
Electrical input	1.21 kW
COP	3.29
Refrigerant Type	$R407C$
Refrigerant mass	1.4 kg
Global Warming Potential Refrigerant	1774 $kg\ C_e/kg$

Table 9.4.: NIBE F1145 output data, according to EN 14511 at 0/45.

9.3.3. Measured Data

The wastewater treatment system at the ABP in Cahir treats the wastewater from both Munster Proteins and the ABP meat processing plant. Munster Proteins represents the rendering and by-products division of ABP, storing processed animal protein rendering fat oils, and producing fertilisers. The meat processing plant (ABP Cahir), runs through the full beef processing chain. Animals are brought in to the slaughter house, and packaged products leave the facility to be delivered to retail businesses.

The effluent from both plants is introduced in a balance tank, from which it runs into the Disolved Air Flotation (DAF) Unit, after whcih the effluent flow to an anoxic tank, and the sludge is separated to be used as landspread. Munster Proteins also has a condensate outflow, running into a set of balancing tanks, which end up in the anoxic tank . Through an intermediate ('Blue') tank, the water runs through the clarifiers. In these clarifiers, a part of the flow is recirculated to the anoxic tank, the overflow flows out as effluent of the treatment system, and the sludge is recirculated to the DAF sludge collection tank (in practice, a lorry in this case). The schematic of the treatment system is shown in Figure 9.5.

The idea of the experimental unit, presented in this chapter, was to make a trade-off between, the higher temperature of the wastewater upstream (close to the inlet), and the reduced amount of pollutants and suspended solids (reducing the risk of fouling), downstream. For this reason, the designed experimental unit was moveable, and able to be placed at different locations along the wastewater treatment process.

The wastewater temperature was measured for 11 days at 3 different locations in the wastewater treatment system (see Figure 9.5). These were at the Inlet screen ($T1$), the condensate flow from Munster Proteins ($T2$), and the effluent discharge to the River Suir ($T3$). The drain water flow of condensate from Munster Proteins was measured hourly, and the total discharge was measured daily, the influent flow at the screen was not monitored.

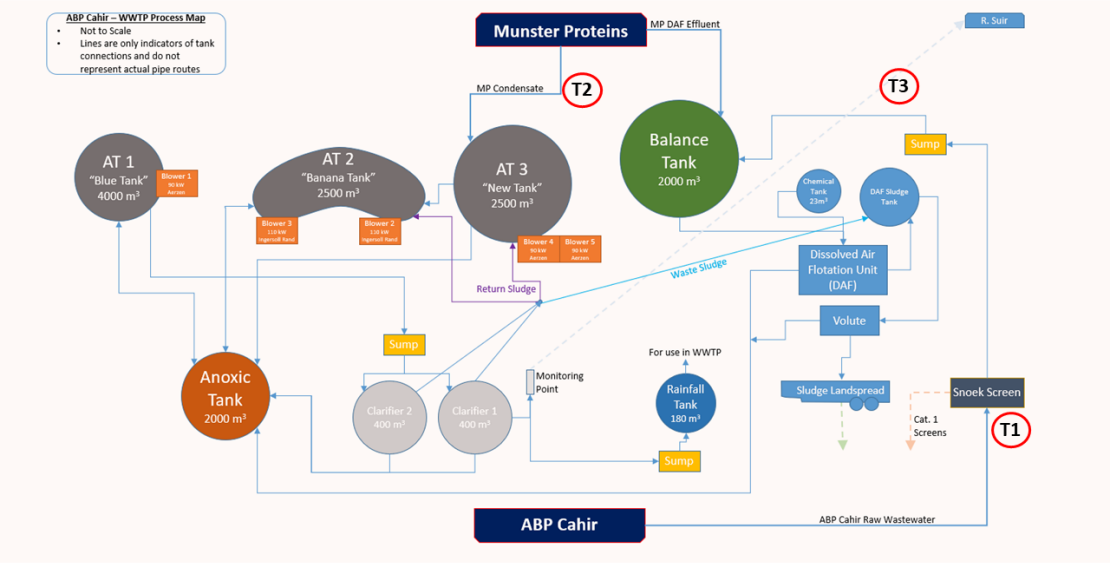


Figure 9.5.: Schematic of the WWTS at ABP, Cahir.

Because the available temperature data and flow data were only coinciding for 3 days, average values were used for the temperature at the different locations. For the case of this test rig, it was assumed that a fixed flow rate is diverted from the wastewater treatment system. The average values of the measured data, and the diverted flow rate at each of the locations are discussed in this section.

Inlet to screen

The temperature measured at the inlet screen is relatively stable, around $21.5 - 22°C$ (blue in Figure 9.6), the flow diverted from the wastewater, was assumed to be 15 m^3/h.

Condensate

The average condensate temperature shows more variation, peaking at around $32°C$ at midday, and dropping to as low as $24°C$ around 6-7 AM (Orange in Figure 9.6). The flow observations have shown that a diversion of 15 m^3/h is not realistic, therefore a diversion of 5 m^3/h was assumed.

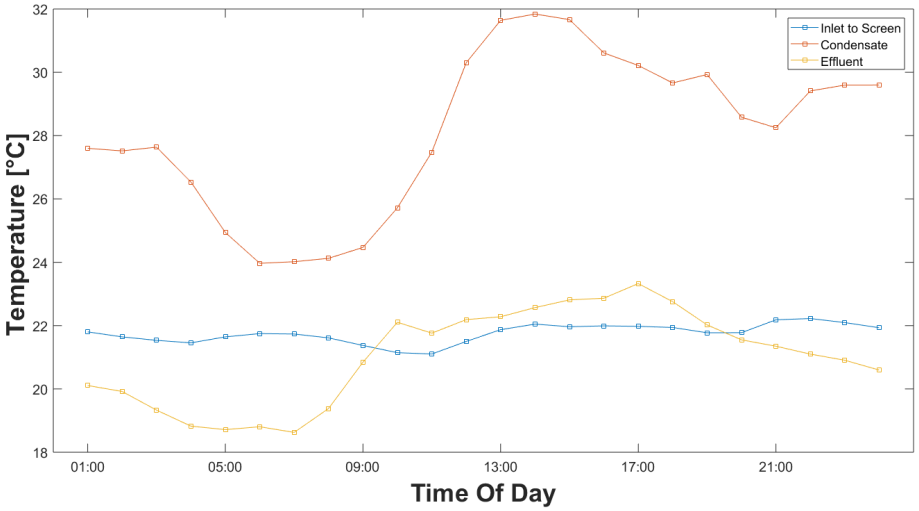


Figure 9.6.: Average temperature profile at the WWTS of ABP, Cahir.

Effluent

The effluent temperature varied between 19 and 22°C (Yellow on Figure 9.6), and a diversion of 15 m^3/h was assumed.

Fresh water and glycerol temperature

The fresh water temperature was measured in Dublin in 2012. For a simulation of the operation over a whole year, these measured temperatures (see Section 8.3.3) were used. It was assumed that the primary working fluid of the heat pump (glycerol) operates at the same temperature

9.4. Design of the experimental unit

9.4.1. The current heating system

Currently, the heat required for the operations at the ABP meet processing plant in Cahir, Co. Tipperary is provided by a gas boiler system. The facilities in Clones, Co. Monaghan are supplied by a fuel oil system. The ABP facilities consume heat at three different temperatures, supplied by three closed heating loops: 45, 60 and 90°C.

9.4.2. Working principle of the experimental unit

To be able to study the operation of the heat recovery system at different locations in the wastewater treatment system, the experimental unit was designed to be moveable, with a simple forklift. The idea being for it to be placed at different locations, in order to make a trade-off between increased wastewater temperature, and increased concentration of suspended solids.

The test rig incorporates both the direct and the hybrid heat recovery system in a single moveable set-up. A single Co Flo heat exchanger was used, with different connections for the different DWHR systems. The rig requires:

- a connection to pressurized clean feed water
- a connection to a diversion of the waste water
- an electric connection for the heat pump (single-phase)

The principle scheme can be found in Figure 9.7. A more detailed schematic can be found in Appendix H.1. One can observe that the hybrid set up slightly differs from the configurations described in Section 9.3.1. The hybrid set up in Section 9.3.1 uses a configuration in series, whereas the direct and indirect part of the hybrid heat recovery system are parallel in the test set up.

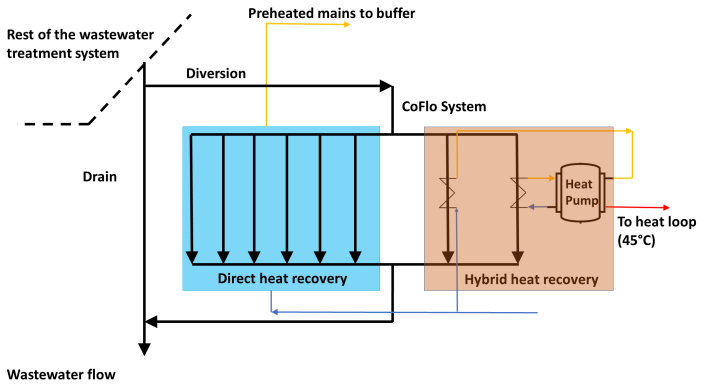


Figure 9.7.: Principle scheme of the test rig.

The design flow rates, on the clean fluid side of the heat exchanger, are summarized in Table 9.5.

	Number of Pipes	Flow per pipe
Direct heat recovery		
Fresh water	6	8 l/min
Direct heat recovery		
Fresh water	1	8 l/min
Glycolated water	3	6 l/min

Table 9.5.: Test rig design, clean fluid flows, ABP, Cahir.

The pressured drop, assuming 1 (DN 25) connections for each QB1-16 pipe is estimated at 0.15 bar on the fresh water side, and 0.53 bar for the glycerol circuit.

9.4.3. Instrumentation

The test rig, and the different metering instruments are displayed in Appendix H. The instruments used to record the different parameters are discussed.

Heat meters

The heat recovered from the wastewater is recorded using Itron CF Echo II heat meters (see Section 4.4.4). The locations where heat recovery is measured are listed below, and are shown in Figure 9.8:

- The direct heat recovery component of the test rig.
- The preheating component of the test rig.
- The glycerol circuit which serves as heat source for the heat pump.
- The heat delivered by the heat pump.

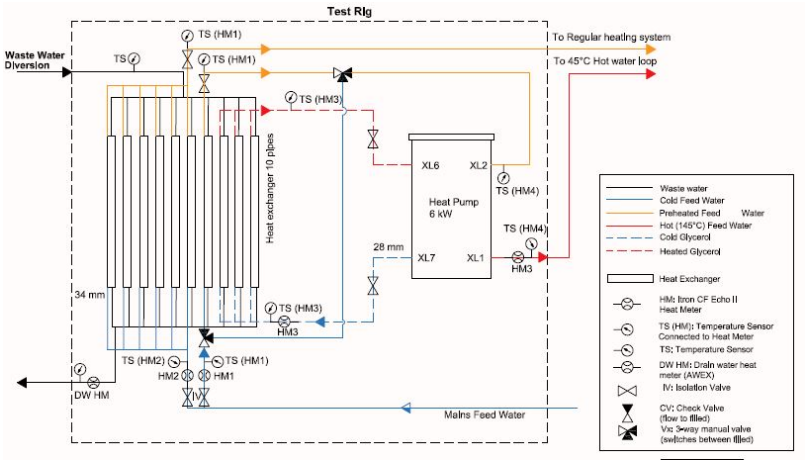


Figure 9.8.: Schematic of the experimental unit at ABP, Cahir.

Temperature sensors

The temperature sensors used in this experimental set-up are PT 100 resistance sensors (see Section 4.4.4), and are referred as T, in Figure 9.8.

Wastewater flow meter

A combined meter measuring both wastewater flow and wastewater temperature was installed on the test rig, measuring the wastewater flow through the rig, and the temperature when it leaves the rig. This was done with a MCERTS Multi Sensor Flow Meter (See Section 4.4.4).

9.5. Feasibility study

An initial feasibility was performed for the ABP meat processing facilities in Clones, Co. Monaghan, Ireland. However, for practical reasons the pilot demonstration site was moved to Cahir, co. Tipperary, Ireland. The feasibility study for the ABP facilities in Clones can be found in Appendix B.4.

The operation of this test rig was simulated at the three locations where the temperature was measured (see Section 9.3.3). It was assumed that the test rig operates 250 days per year, and the test rig operates from 8 AM to 5 PM. The reduced fuel consumption, reduced operating expenses (OPEX), reduced greenhouse gas emissions and the payback period are estimated, and reported in this section. The employed fuel prices [SEAI, 2017a], and carbon conversion factors [SEAI, 2017b] are summarized in Table 9.6.

Fuel	**Price** ($c€/kWh$)	**C intensity** ($kg\ C_e/kWh$)
Heavy Fuel Oil	7.47	0.2639
Electricity (Band IC)	13.99	0.4828
Natural Gas (Band I2)	4.80	0.2047
Coal	4.65	0.3406
Bio Mass (Wood Pellets)	5.57	0.01506

Table 9.6.: Financial and Environmental parameters.

9.5.1. Estimated cost of the experimental unit

The estimated costs for a commercial installation of the described heat recovery unit are summarized in Table 9.7. This data was also used for the comparison of the different systems in Sections 9.5.4 and 9.5.5.

Materials	
Co flo Heat Exchanger (10 pipes)	4 750€
Heat Pump (5 kW)	6 263€
Extra piping and connections	200€
Labour (3x15 hrs) (incl. VAT)	1 800€
VAT	2 202€
Contractor overhead (20%)	3 043€
Total	18 258€

Table 9.7.: Cost Estimate for the experimental unit.

9.5.2. Energy savings

The energy savings, and the electric consumption related to the heat pump of the hybrid heat recovery system are summarized in Figure 9.9. One can observe that the condensate provides the maximal recoverable heat, and that the inlet and effluent provide similar amounts of recoverable heat.

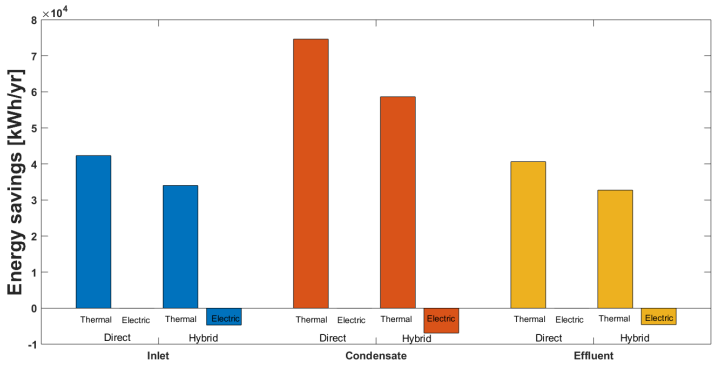


Figure 9.9.: Energetic savings for the different locations at the ABP plant in Cahir.

9.5.3. Greenhouse gas emission savings

Inlet to screen

The reduced GHG emissions, compared to the different possible heating fuels, are summarized in Figure 9.10. One can observe that the hybrid heat recovery would not reduce related emissions compared to a biomass boiler, when the current conversion factors are used. However, the technical reduction in emissions would be similar to the one shown for coal (see Section 8.8) [Sterman et al., 2018]. Given the current GHG intensity of electricity, the potential for reduced is highest when replacing (resistive) electric heating. The comparison between the hybrid and direct system is made in Section 9.5.5.

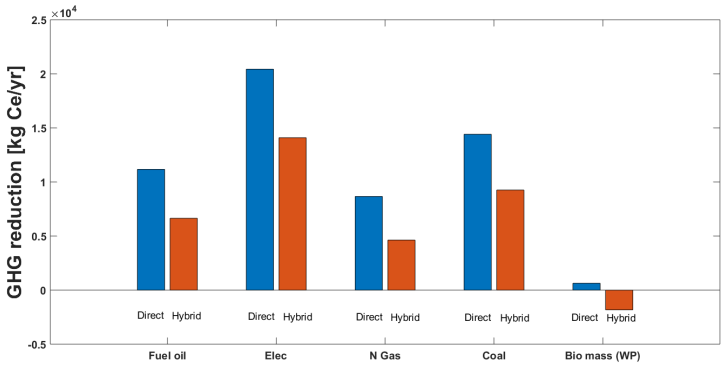


Figure 9.10.: GHG reduction at the inlet.

Condensate

The reduced GHG emissions, compared to the different possible heating fuels, are summarized in Figure 9.11. One can observe that the hybrid heat recovery would not reduce related emissions compared to a biomass boiler, when the current conversion factors are used. One can also observe that the savings potential is about 50% higher compared to the inlet of the effluent from the meat processing plant.

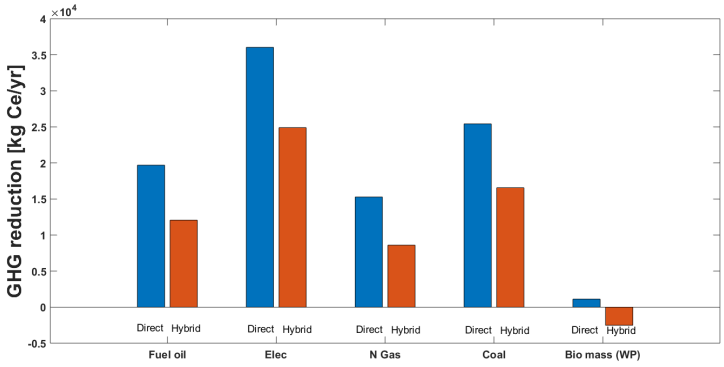


Figure 9.11.: GHG reduction at the condensate.

Effluent

The reduced heat and reduced GHG emissions, compared to the different possible heating fuels, are summarized in Figure 9.12. One can observe that the hybrid heat recovery would not reduce related emissions compared to a biomass boiler, when the current conversion factors are used. Compared to the inlet, the reduction in GHG emissions reaches similar values.

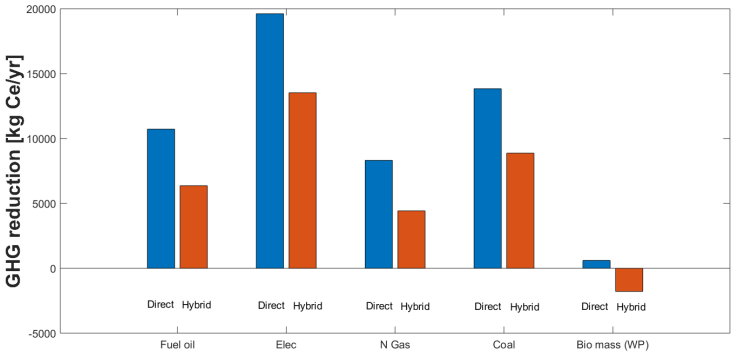


Figure 9.12.: GHG reduction at the effluent.

9.5.4. Financial savings

The reduced OPEX and the payback is discussed in this section. In general, both heat recovery systems are not financially attractive compared to coal, and the hybrid heat recovery system has a payback period exceeding 10 *years* when compared to natural gas or biomass heating, at both the inlet screen and the effluent. Compared to the current heat source, fuel oil, the payback period of the combined system is 3.6 *years*. The comparison between the hybrid and direct system is made in Section 9.5.5.

Inlet to screen

The OPEX savings (Figure 9.13) and payback period (Table 9.8) are summarized below. One can observe that the system is not financially attractive when compared to coal, and the hybrid system is unattractive when compared to natural gas and biomass. The hybrid system includes capital expenditure for a heat pump, and additional operational expenditure through the cost of the electricity consumed by the heat pump's compressor.

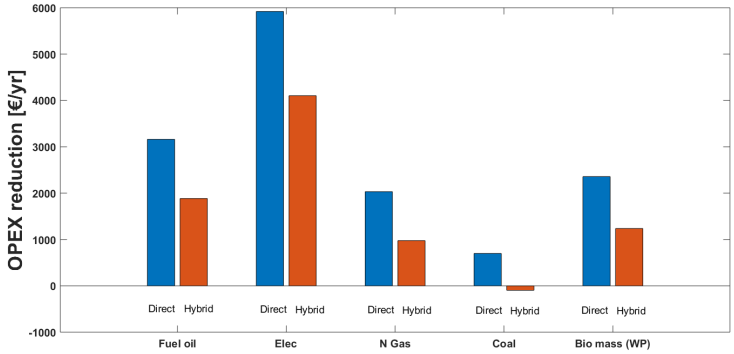


Figure 9.13.: OPEX reduction at the inlet.

	Payback period (yrs)				
	Fuel oil	**Elec**	**N Gas**	**Coal**	**Biomass**
Direct	2.06	1.10	3.20	9.31	2.76
Hybrid	7.51	3.45	14.51	*none*	11.44
Total	3.62	1.82	6.07	30.32	5.08

Table 9.8.: Financial results for DWHR at the inlet screen, ABP, Cahir.

Condensate

The OPEX savings (Figure 9.14) and payback period (Table 9.9) are summarized below. One can observe that the system is not financially attractive when compared to coal but it has a payback below 4 *years* in all other cases. Similar to the observations for the reduction in GHG emissions, the OPEX savings are about 50% higher than at the inlet.

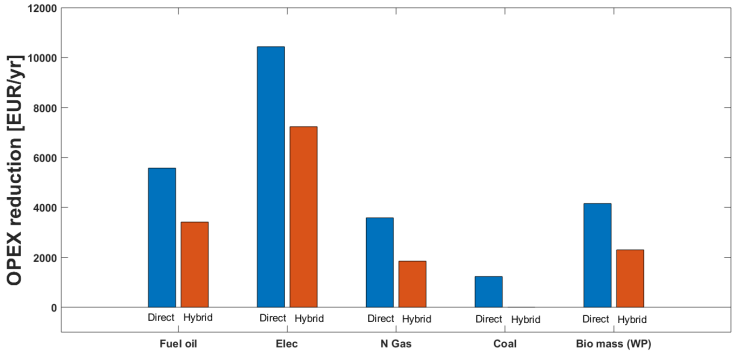


Figure 9.14.: OPEX reduction at the Condensate, ABP, Cahir.

	Payback period (yrs)				
Fuel oil	**Elec**	**N Gas**	**Coal**	**Biomass**	
Direct	1.17	0.62	1.82	5.28	1.56
Hybrid	4.15	1.96	7.66	*none*	6.16
Total	2.03	1.03	3.36	14.81	2.83

Table 9.9.: Financial results for DWHR at the Condensate, ABP, Cahir.

Effluent

The OPEX savings (Figure 9.15) and payback period (Table 9.10) are summarized below. One can observe that the system is not financially attractive when compared to coal, and the hybrid system is unattractive when compared to natural and biomass. OPEX and pauback periods are similar to the ones observed at the inlet. This finding, when backed up by the results of the practical operation, could indicate that the reduced yield of heat recovery at the outlet, compared to the inlet is relatively small. It is thus highly likely that the benefit of operating with purified water offsets this small drop in heat yield.

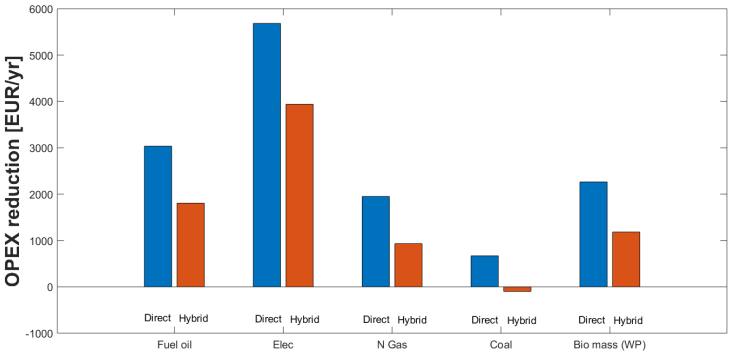


Figure 9.15.: OPEX reduction at the Effluent, ABP, Cahir.

	Payback period (yrs)				
	Fuel oil	**Elec**	**N Gas**	**Coal**	**Biomass**
Direct	2.14	1.14	3.34	9.70	2.87
Hybrid	7.84	3.59	15.19	*none*	11.96
Total	3.77	1.90	6.34	31.96	5.30

Table 9.10.: Financial results for DWHR at the Effluent, ABP, Cahir.

9.5.5. Comparing the direct and hybrid system

The comparison within the test rig, between the direct heat recovery unit, and the hybrid heat recovery unit, is not straight forward from the results described above, as both parts of the test rig provide a different amount of heat. This is due to design choices which were selected based on convenience rather than a techno-economic trade -off. In order to determine the most suitable heat recovery system for the 3 locations of interest, the Levelized Cost of Energy (LCOE) and the Total Equivalent Warming Impact (TEWI), to heat the water to $45°C$ were calculated for both systems. Both of these values calculate a cost (financial for the former, environmental for the later) per produced heat unit, considering the capital investment, emissions from the refrigerant of the heat pump, and other costs which are not incorporated in the OPEX savings are reduced GHG emissions.

Inlet to screen

The LCOE and TEWI at the inlet screen, calculated over 15 operating years are summarized in Table 9.11. One can observe that the hybrid heat recovery is financially attractive in case the alternative heating system is running on heavy fuel oil, or electric heating. Its GHG emissions are lower in all cases, except when compared to wood pellets (biomass).

	LCOE ($c€/kWh$)					**TEWI** ($g\ C_e/kWh$)				
	Fuel oil	**Elec**	**N Gas**	**Coal**	**Biomass**	**Fuel oil**	**Elec**	**N Gas**	**Coal**	**Biomass**
Direct	7.40	13.84	4.77	1.65	5.53	260.67	477.64	202.19	336.96	14.90
Hybrid	7.33	7.33	7.33	7.33	7.33	68.65	68.65	68.65	68.65	68.65

Table 9.11.: Comparison of heat recovery systems at the inlet screen, ABP, Cahir.

Condensate

The LCOE and TEWI at the condensate, calculated over 15 operating years are summarized in Table 9.12. One can observe that the hybrid heat recovery is financially attractive in all cases, except when the alternative heating system is running on natural gas or coal. Its GHG emissions are lower in all cases, except when compared to wood pellets (bio mass).

	LCOE ($c€/kWh$)					**TEWI** ($g\ C_e/kWh$)				
	Fuel oil	**Elec**	**N Gas**	**Coal**	**Biomass**	**Fuel oil**	**Elec**	**N Gas**	**Coal**	**Biomass**
Direct	7.31	13.67	4.71	1.64	5.46	257.32	470.76	199.60	332.11	14.68
Hybrid	4.78	4.78	4.78	4.78	4.78	57.98	57.98	57.98	57.98	57.98

Table 9.12.: Comparison of heat recovery systems at the condensate, ABP, Cahir.

Effluent

The LCOE and TEWI at the inlet screen, calculated over 15 operating years are summarized in Table 9.13. One can observe that the hybrid heat recovery is financially attractive in case the alternative heating system is running on heavy fuel oil, or electric heating. Its GHG emissions are lower in all cases, except when compared to wood pellets (biomass).

	LCOE ($c€/kWh$)					**TEWI** ($g\ C_e/kWh$)				
	Fuel oil	**Elec**	**N Gas**	**Coal**	**Biomass**	**Fuel oil**	**Elec**	**N Gas**	**Coal**	**Biomass**
Direct	7.41	13.85	4.77	1.65	5.53	260.82	477.16	202.31	336.62	14.88
Hybrid	7.57	7.57	7.57	7.57	7.57	69.43	69.43	69.43	69.43	69.43

Table 9.13.: Comparison of heat recovery systems at the effluent, ABP, Cahir.

9.5.6. Discussion

The proposed test rig contains both a direct and an indirect DWHR system. It requires a connection to the drain water, pressurized mains fresh water and an electric connection for the heat pump. The required head is around 2.1 m, but this can be reduced to 1.8 m. The capital investment is just over 18 000 €and the expected payback at Cahir, is between 2 and 3.8 $years$. The system could save up to 35 $tons$ in Carbon equivalent emissions, each year.

The heat exchangers to be used is a Co Flo system, splitting the wastewater stream in 10 pipes. Four of these pipes serve as the heat exchangers in the hybrid DWHR system, three serve to heat the glycolated water (primary fluid of the heat pump), one will serve to preheat the mains feed water. A 5 kW heat pump will complete the system. The remaining pipes are part of the direct DWHR system, which can be operated in parallel with the hybrid DWHR system.

The test rig is moveable, and is to be plugged in at different locations in the wastewater treatment system, in order to study its operation at different temperatures and degrees of contamination. The fouling and required maintenance are to be monitored closely.

The operation of the heat recovery system on the test rig depends on the location of the system. Its financial viability, and the related reduction in greenhouse gas depend on the fuel used in the regular heating system. The choice between either the direct, or the hybrid heat recovery also strongly depends on the location and the fuel used.

From an energy savings point of view (Section 9.5.2), the condensate from Munster Proteins provides the largest potential for heat recovery. The potential at the inlet and effluent is similar, however the effluent would be desirable in this case, as the clean effluent will provide less issues with fouling and material build-up.

From the point of view of emissions (Section 9.5.3), the system will reduce the GHG emissions related to heating in all cases, except if the heating fuel is bio mass (wood pellets). This is due to the conversion factor for biomass, used in legislation, which is close to zero. Evolution in other countries (Belgium, Germany, etc.), indicate that the conversion factor for biomass could increase over the coming years, however this depends on policy choices.

Compared to coal as the regular heating system, the heat recovery system is not financially attractive, however coal is likely to be the most polluting traditional heating fuel (at the moment this is electric heating, but with the increasing share of renewables in the electric mix, the impact decreases, and could drop below the level of coal, as it did in the UK this year). At the inlet and effluent, the payback period compared to natural gas and bio mass exceeds 10 *years*. This is still below the expected life time of the heat recovery system, however the uncertainty on long term price and conversion factor prediction is large.

At the inlet and effluent, the direct heat recovery system seems to be the most attractive solution from a financial point of view, except in case of electric heating. At the condensate the hybrid system is financially attractive, except when compared to natural gas and coal heating systems.

From an environmental point of view the hybrid heat recovery system is most attractive, except when compared to a bio mass heating system.

9.6. Construction of the experimental unit

The experimental unit was constructed in several phases:

- Construction of the heat exchanger arrangement
- Hydraulic arrangement and rig construction
- Installation of the logging system

Some were performed in-house, others were completed by contractors. This Section details the different steps in the construction of the test rig.

9.6.1. Heat exchanger arrangement

The arrangement (as described in Section 9.4) of the different (10) heat exchangers was performed by Q-Blue (Figure 9.16), in the Netherlands. The wastewater is introduced in a distributor at the top, from where it is distributed over the different heat exchange pipes (see Figure 9.17).



Figure 9.16.: Heat exchanger arrangement.

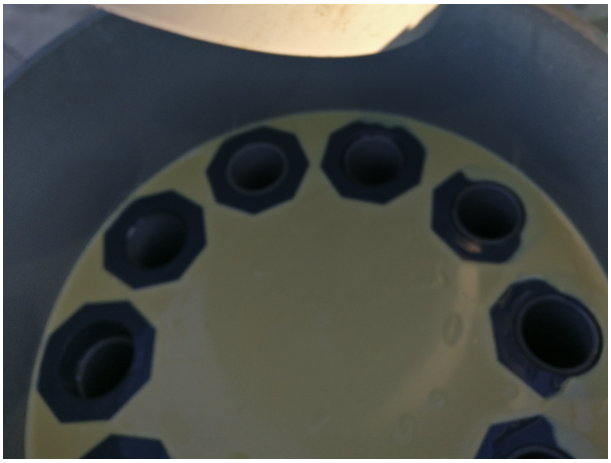


Figure 9.17.: Distributor of the heat exchanger arrangement, ABP, Cahir.

9.6.2. Hydraulic arrangement and rig construction

The hydraulic arrangement was then completed in-house at the Civil Engineering department of Trinity College, Dublin. The metering equipment (see Section 9.4), and the heat pump was connected (see Figure 9.18). Additionally, stairs, with platform, were attached to the test rig to facilitate cleaning and maintenance, as can be seen in Figure 9.19



Figure 9.18.: Connection of the heat pump to the test rig.



Figure 9.19.: Stairs on the experimental unit.

The pipe draining the wastewater from the test rig was also extended, in order to place the wastewater flow meter, as is shown in Figure 9.20. The wastewater flow meter was placed in a wider pipe (diameter 150 mm) to improve precision.



Figure 9.20.: The experimental test rig, with extended drain pipe.

9.6.3. Installation of the logging system

The logging system was provided by DETECTRONIC, and consists of two components, the hardware component, logging the data and transmitting it to the software component, where data can be stored and displayed.

The hardware component consists of a recorder (square component in Figure 9.21), which records the signal from the meters, and a transmitter (cylindrical component in Figure 9.21) sending the data to the online platform.

After measurement the data is recorded (logged) and made available on an online platform. Pulses, representing the electric or thermal energy, or the volumetric flow, are counted during the logging interval (15 minutes in the cases represented in this thesis), and the temperature signal is measured at the end of each interval, by the data logger (the square box on Figure 9.21). These recorded values are then sent to the online platform (see Figure 9.22) by the transmitter (the cylinder on Figure 9.21), and converted to the physical units.



Figure 9.21.: The data logger and transmitter.

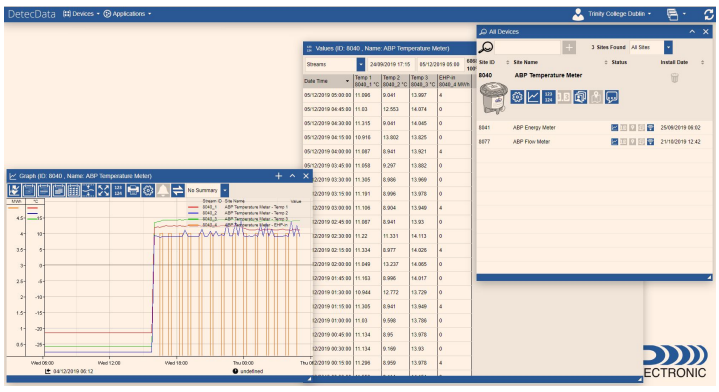


Figure 9.22.: The online data platform.

9.7. Installation and commissioning of the experimental unit

9.7.1. Installation

The moveable experimental set-up was first installed at the effluent, to verify its operation. As the effluent is essentially clean water, the effect of fouling on the performance of the system is not a factor on the timescale of this project. The set-up was placed on a platform (as can be seen in Figure 9.23), to facilitate the discharge of the effluent, after use in the experimental set-up. During the testing phase of this experimental set up, the wastewater was pumped into the set-up using a submersible pump (see Figure 9.24).



Figure 9.23.: Experimental set-up, placed on a platform at the effluent of the WWTP at ABP, Cahir.

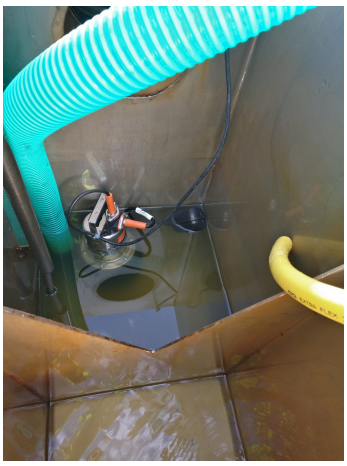


Figure 9.24.: Submersible pump placed in the effluent flow at ABP, Cahir.

9.7.2. Commissioning and verifying the operation

At the request of ABP, the experimental set-up could only be operated during night time, when the effluent of the wastewater treatment plant was discharged into the river Suir. The set-up thus had to be equipped with an additional, timed solenoid valve, opening and closing at the required, set times. During the delay this incurred, sporadic operational runs were performed, of a qualitative rather than quantitative nature.

Commissioning

After the qualitative operational runs, a single night of operation was performed at the effluent, to verify the operation of the experimental set-up, before moving it to the inlet of the wastewater treatment plant. Operation occurred during the night of December 4th, 2019, the observed values are summarized in Table 9.14, where negative values show energy consumption rather than recovery.

These savings, although significant, have the disadvantage of occurring through the night. As consumption occurs during the day, this temporal mismatch of heat recovery and heat consumption would reduce the amount of heat that could be used in a practical manner. Furthermore, earlier in the heat recovery system much larger quantities of heat are available.

One can observe that, in the direct system the recovered heat is significantly higher than the expected value. The hybrid system, however, is slightly underperforming compared to expectations. The improved performance of the direct heat recovery system could be due, to an underestimation of the flow rate, or a larger efficiency than advertised. The reduced performance of the heat pump can be due to an error made in the prediction, as this is done based on an average of a set of heat pumps (See Section 5.4.2).

Operating time				$16.5hrs$
Average effluent temperature				$13.41°C$
	Observations		**Expected values**	
	Energy(kWh)	**Volume** (m^3)	**Energy**(kWh)	**Volume** (m^3)
Direct DWHR system				
Heat Recovery	250	47	191.52	
Hybrid DWHR system				
Preheating	90	27	94.79	
Supplied heat (heat pump)	59.4	27	62.85	
Consumed electricity (heat pump)	-17	$(COP = 3.49)$	-14.98	$(COP = 4.20)$

Table 9.14.: Commissioning of the experimental set-up, ABP, Cahir.

Adaptations

These operational runs, performed for commissioning and verification also showed some potential threats to the operation. Some adaptations were made or are suggested, and they are listed in this Section.

- The submersible pump

The submersible pump, pumping the wastewater into the test rig, was expected to clog during operation with the highly loaded wastewater at the inlet. The pump was replaced by a different model, the GOVOX 204 model, the data sheet can be found in Appendix H.3.

- Operation of the heat pump

When not enough heat is available in the heat exchangers, serving as heat source for the heat pump, the protection measures of the heat pump are triggered, requiring a manual reset. To avoid this, an additional protection measure should be installed, turning the heat pump of when the wastewater flow through the heat exchangers is too small. An additional help can be the insulation of the heat exchangers.

- Measuring the fresh water flow through the heat pump

The fresh water flow, heated by the heat pump to 45° was around 0.120 m^3/h, in order to stay within the power limitations of the heat pump. This relatively low flow is within the limitations of the heat meters (see Section 9.4.3), however, discrepancies were observed between the actual flow and the measured value. To ascertain this, and compensate for the error, an additional flow meter was installed, its datasheet can be found in Appendix H.4.

9.8. Experimental Operation

After commissioning of the experimental unit at the outlet of the wastewater treatment system, the unit was moved to the inlet sump (See Figure 9.5).

9.8.1. Operation at the inlet of the wastewater treatment system

From the inlet sump, the raw wastewater was pumped into the experimental unit. At this location the wastewater is highly loaded in solids, with a suspended solids concentration of $2000 - 4000\ mg/l$[2]. After usage by the unit, the wastewater flowed back out into the inlet sump. This set-up is shown in Figure 9.25.

[2]As affirmed by ABP in an email on Decmeber 18th 2019

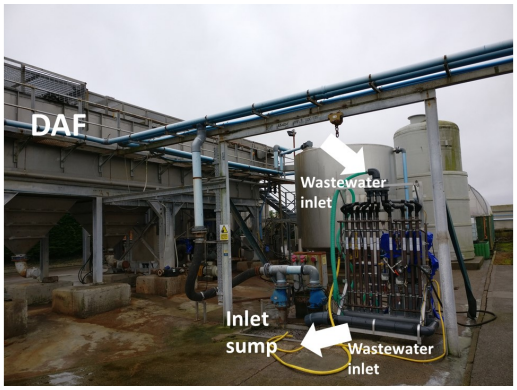


Figure 9.25.: The experimental unit, set up at the inlet sump.

Direct heat recovery system

At the inlet of the wastewater treatment system, the direct heat recovery system operated over five days. This short operating period was due to repeated blocking of the wastewater submersible pump (see further this section). The first stretch of operation was completed between January 15th and 17th 2020, after which the pump blocked. The pump was then replaced by a larger model (See Section 9.7.2, and further this section), this larger model operated on January 29th and 30th. The average power of recovered heat, operating time, and temperature of the wastewater is shown in Figure 9.26. In this figure, one can clearly observe the decrease in heat recovery power over time, indicating the gradual clogging of the pipe, and thus a reduction in wastewater flow through the experimental unit.

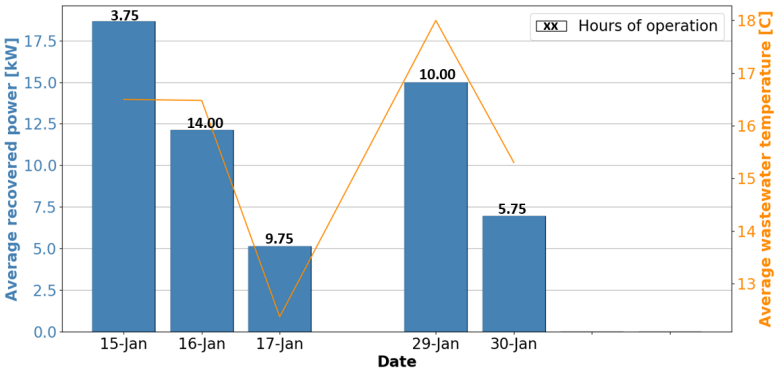


Figure 9.26.: Operation of the direct heat recovery system at the inlet.

Assuming 10 hours of operation per day, 250 days per year, and natural gas heating on site, the maximal heat recovery (18.67 kW), results in a heat recovery of 46 MWh/yr and a corresponding reduction of 8.02 *tons* C_e per year, and a cost saving of 1 880.4€per year. This is similar to the predicted value in Figure 9.9. However, the long term operation of such a system could not be verified by the research presented here.

In Table 9.15, one can observe that in all cases, except for January 30th, the experimentally recovered energy, exceeded the predicted recovered energy. This can be explained by a conservative estimation of the heat exchanger's effectiveness, especially at the start of its lifetime, this effect is expected to be flattened out over the lifetime of the heat exchanger. The different behaviour for January 30th could be explained by the fact that the pump issue was only noticed later, causing a period where the unit stayed in operation, but no wastewater was circulating through the unit, making heat recovery impossible.

		Fresh water		Recovered Energy (kWh)	
Date	**Operation time (hrs)**	**Volume (m^3)**	**Flow rate (m^3/h)**	**Observed**	**Expected**
15 January 2020	3.75	6.5	1.70	70	37.13
16 January 2020	14.00	19.5	1.43	170	111.19
17 January 2020	9.75	11.7	1.20	50	34.35
29 January 2020	10.00	14.3	1.39	150	96.11
30 January 2020	5.75	9.8	1.76	40	48.11

Table 9.15.: Operation of the direct heat recovery system at the inlet, ABP, Cahir.

In Table 9.15, one can also observe that the flow rate ($Flow/OperationTime$), through the experimental unit is not constant. This is due to the influence of the water height in the rain water tank. This water height is dependant on other consumption, rainfall, etc. The flow rate through the experimental number was thus not controlled.

Hybrid heat recovery system

The heat pump, and by extension the hybrid heat recovery system, could not be operated, because of a temperature limiter alarm (52, see Figure 9.27). This required a manual reset, which was not completed before the occurrence of other issues (see next Section).

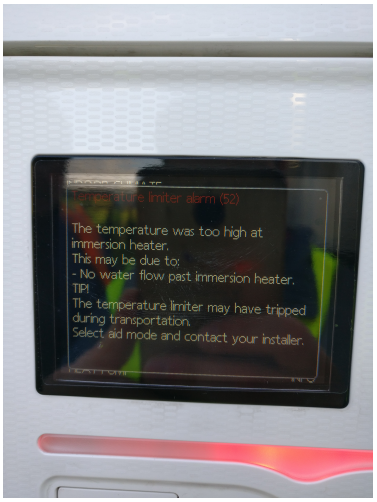


Figure 9.27.: The temperature limiter alarm of the heat pump.

Clogging of the submersible wastewater pump

The large suspended solids concentration caused material accumulation on the components of the pump. This caused a decrease in the pump flow (represented by decreasing flow velocity in Figure 9.28) and ultimately blockages of the submersible pump.

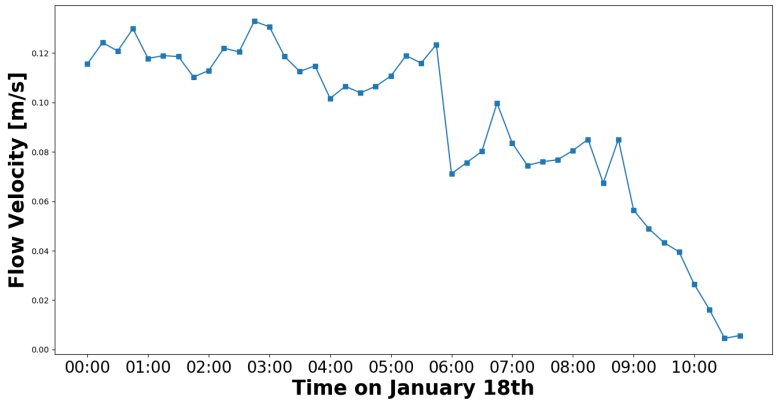


Figure 9.28.: The decreasing flow velocity at the inlet on January 18th 2020.

The blockages in the submersible pumps led to the replacement of the initially installed pump (Figure 9.29). But also the larger replacement model clogged in a short time span (see Figure 9.30). The blockages were mainly due to grass from the stomachs of cows, getting tangled in the impeller of the pump.



Figure 9.29.: Clogging of the Savy 300 pump at the inlet at ABP, Cahir.



Figure 9.30.: Clogging of the GOVOX 204 pump at the inlet at ABP, Cahir.

For this reason, the pump was then moved to the outlet of the Dissolved Air Flotation (DAF) unit (See Figure 9.5).

9.8.2. Operation at the outlet of the DAF unit

The submersible pump was thus moved to the outlet of the DAF unit (the elevated unit, on the left in Figure 9.25). DAF units are water treatment processes aiming at clarifying the wastewater by the removal of suspended matter, such as oil and solids. This results in outgoing wastewater which has a lower suspended solids concentration, and thus less risk of clogging of the pump. The pump was placed just before the outlet wedge of the DAF unit (see Figure 9.31), and its power supply was connected to the power switch of the DAF unit (see Figure 9.32). This way the pump is turned off, once the DAF unit is switched off, avoiding that the pump will run dry. The wastewater, after running through the experimental unit, is discharged in the inlet sump (see Figure 9.25).

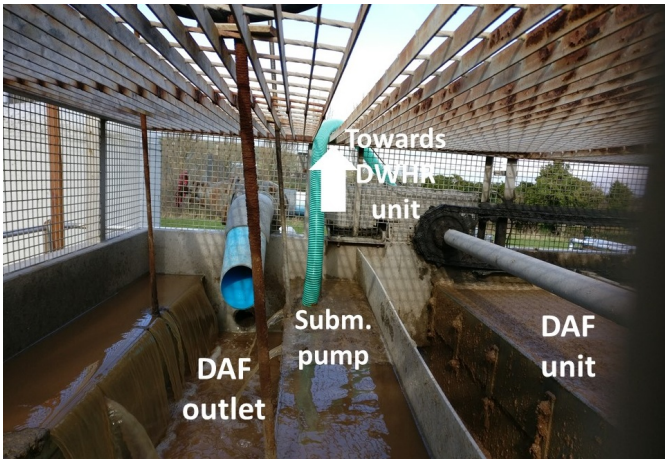


Figure 9.31.: Submersible pump, placed at the outlet wedge of the DAF unit, ABP, Cahir.



Figure 9.32.: Power supply of the submersible pump, connected to the power switch of the DAF unit, ABP, Cahir.

Direct heat recovery system

The direct heat recovery system was operated over five days, starting on Monday February 24th 2020, around 1.30pm, until Friday February 28th around 1pm. During this period, the power of recovered heat varied between 8.4 and 10 kW, on Friday, the power was lower, but this was because of continued circulation of the fresh water, when the submersible pump was switched off. The daily average temperature of the wastewater varied around 17°, during the operation of the experimental unit. The operational data is shown in Figure 9.33.

Comparing this Figure 9.33, to the results at the inlet (Figure 9.26), shows that, at the start, the recovered heating power is significantly higher at the inlet. However, at the inlet, the power dropped dramatically over three days, due to clogging of the pump, whereas the power at the DAF unit remained relatively constant. In case a larger submersible pump is used (or no pump is required, see Section 9.8.3), a similar pattern can be expected, over a longer period of time, for the fouling of the heat exchanger. The operating time, fresh water volume, flow rate and recovered energy are shown in Table 9.16.

Assuming 10 hours of operation per day, 250 days per year, and natural gas heating on site, the average heat recovery (8.85 kW) would result in a reduction in energy consumption of 22 125 kWh per year, meaning that this experimental unit alone would save the equivalent of the heat consumption of an entire household. It would also save the corresponding 4.53 $tons\ C_e$ of emissions per year, and introduce a cost saving of 1 062.0€per year. This test unit only recovers the heat from a small part of the wastewater flow, scaling it up could increase these numbers significantly. A more detailed picture of the financial and environmental benefits is shown in Section 9.10.3.

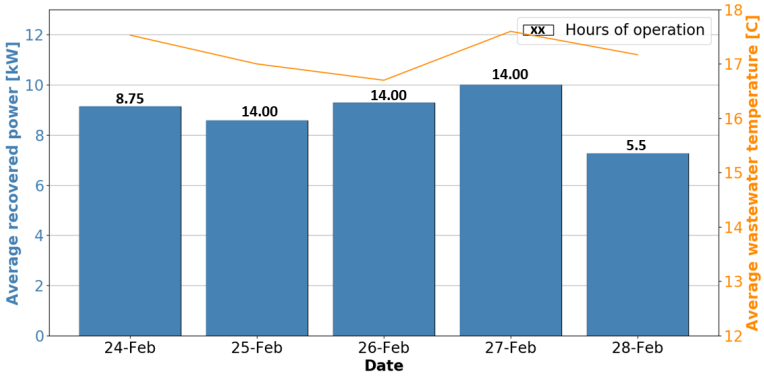


Figure 9.33.: Operation of the direct heat recovery system at the DAF unit.

Date	Operation time (hrs)	Fresh water Volume (m^3)	Fresh water Flow rate (m^3/h)	Recovered Energy (kWh) Observed	Recovered Energy (kWh) Expected
24 February 2020	8.75	13.1	1.50	80	83.89
25 February 2020	14.00	21.5	1.54	120	130.05
26 February 2020	14.00	22.2	1.59	130	129.84
27 February 2020	14.00	22.7	1.62	140	146.41
28 February 2020	5.50	8.7	1.58	40	53.60

Table 9.16.: Operation of the direct heat recovery system at the DAF, ABP, Cahir.

As discussed in Section 9.8.3, the operation at the DAF was halted after one week. This was due to an increased chemical demand, related to the configuration of this experimental unit (see Figure 9.37, Section 9.8.3). The operation was later restarted, using a different, in–line configuration (see Figure 9.38, Section 9.8.3).

In this configuration, the wastewater was pumped out of the DAF, into the test rig, situated as shown in Figure 9.25, and back up the DAF unit. This changes the operation of the wastewater network, from an open, non–pressurized system, to a pressurized system. To account for this additional pressure, the lid was screwed on, as can be seen in Figure 9.34.



Figure 9.34.: Lid of the experimental unit, secured with additional screws, at ABP, Cahir.

When operating the experimental unit, however, the different joints and connections in the wastewater network could not withstand the increased pressure (see Figures 9.35 and 9.36), and operation was halted once more. Significant changes are thus required to the heat recovery unit, and thus also the commercial units on which this experimental system is based, to be able to operate under pressurized conditions.



Figure 9.35.: Disconnected pipe of a single heat exchanger.



Figure 9.36.: Disconnected wastewater collector.

Due to the COVID-19 pandemic, access to the premises of ABP in Cahir was suspended for external contractors and visitors at the end of March 2020. In addition to this, no non–essential travel could be undertaken. Due to the restrictions, these issues could not be fixed, as would be the case under normal circumstances, hence additional data could not be collected during the PhD project.

Hybrid heat recovery system

The hybrid heat recovery system ran from Monday February 24th until Thursday February 27th 2020. The heat pump displayed an alarm, and thus a shut down of operation. Presumably, the fresh water flow rate increased (see Section 9.8.1), exceeding the power limitations of the heat pump. The rated power of the heat pump was 5 kW, as an example, assuming an incoming water temperature of 10°C, this allows for a maximal fresh water flow of 2.05 l/min. Once this flow was exceeded for a significant period, the outlet temperature (with target temperature at 45°C starts dropping, as will the temperature of the brine exiting the evaporator, due to the fact that the power requirement exceeds the limitations of the heat pump. If this occurs gradually, the heat pump's control system will pick this up, send an alarm signal and perform an emergency shut down. If this happens abruptly (due to a very high flow rate), the electric demand of the heat pump will increase drastically, as the heat pump causing the fuses to trip.

To avoid this, the incoming fresh water flow of the heat pump should be controlled, and maintained under the maximal fresh water flow at all time. For reasons described in Section 9.7.2, the operational parameters of the hybrid heat recovery system could not be monitored.

9.8.3. Challenges regarding the experimental unit

Submersible pump

The submersible pump, used to pump the wastewater into the experimental unit, blocked multiple times during the operation at the inlet (see Section 9.8.1). This resulted in short operating periods for the heat recovery system. As the blocking of the submersible pump was the bottleneck for the operation of this experimental unit, the long term operation of the designed heat recovery system could not be tested to its limits. The boundary conditions, in this case the auxiliary equipment (submersible pump), failed before the system could be pushed to its limits, leaving the test runs inconclusive with regard to the question of whether fouling of the heat recovery unit would create a significant problem.

Due to the COVID-19 pandemic, access to the premises of ABP in Cahir was suspended for external contractors and visitors at the end of March 2020. This prevented alterations and improvements addressing this challenge.

Forward Feed of the DAF effluent

As described in Section 9.8.2, the operation of the experimental unit at the DAF unit, required the pumping of the wastewater from the outlet of the DAF unit, through the experimental unit, back into the inlet sump. This introduced an additional feedback (recirculation) loop, into the wastewater treatment system, as shown in Figure 9.37. This additional inflow into the inlet sump, requires an increased outflow of this sump (up to 35 m^2, and thus of the DAF unit, the avoid overflowing of the sump. This increased forward feed, requires increased chemical dosing, the particular experimental set-up thus pressured the operation of the wastewater treatment system. For this reason the operation of the experimental set-up was halted after February 28th.

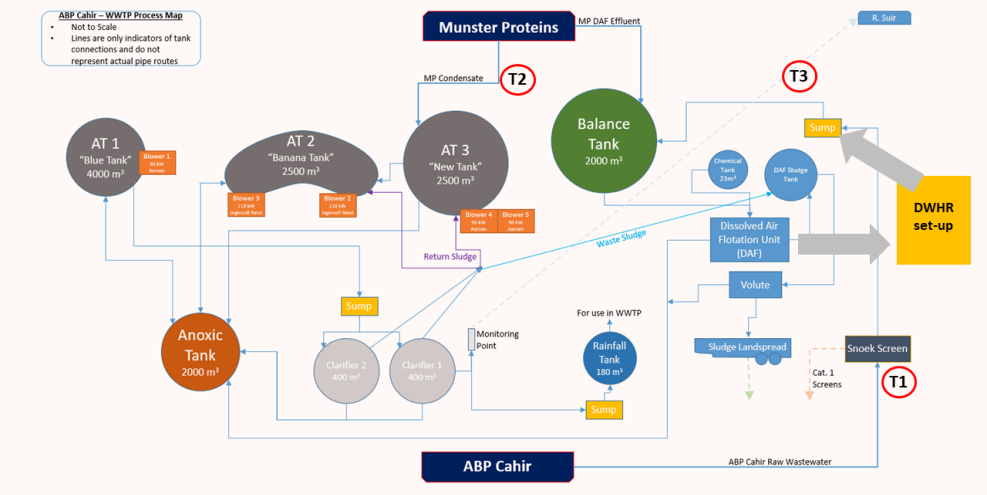


Figure 9.37.: Feedback loop introduced by the experimental set-up at the DAF at ABP, Cahir.

In a full, permanent installation of a heat recovery system at the DAF outlet, the heat recovery unit would be installed in line with the DAF unit (see Figure 9.38). Such a system could also utilise the available vertical drop (see Figure 9.25), for introducing the wastewater in hte heat recovery system. This practical, permanent set-up would thus eliminate two important challenges, encountered in the operation of this experimental set-up.

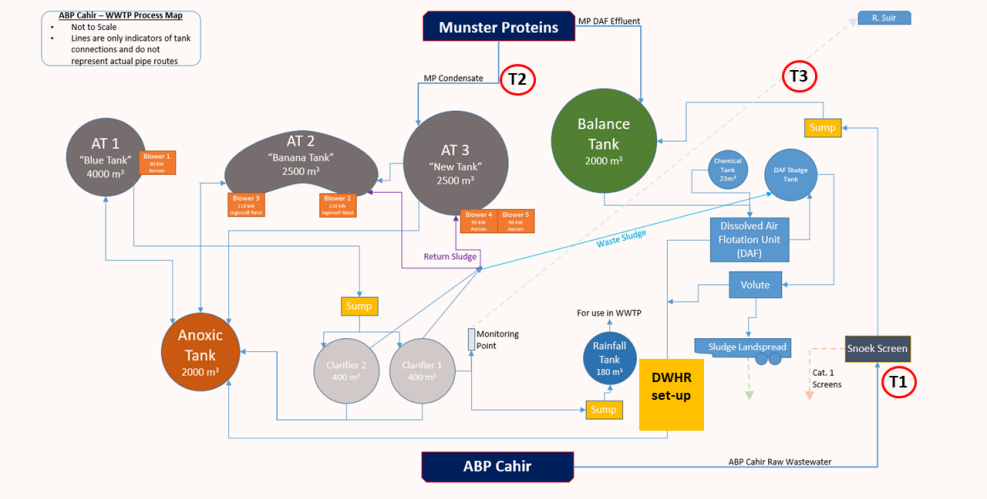


Figure 9.38.: In-line DWHR set-up at the DAF at ABP, Cahir.

This in-line configuration was tested with the experimental unit (as mentioned in Section 9.8.2). However, because true in-line operation, replacing the connection between the DAF unit and the anoxic tank (see Figure 9.38) by the heat exchanger was not permitted during this test phase, the set-up was installed parallel to the aforementioned connection. This still involved pumping the wastewater from the DAF outlet to the experimental unit, and back up into the DAF outlet. This altered the hydraulic properties of the wastewater network from a free–flowing, non pressurized system, into a pressurized system. This additional pressure caused the lid of the experimental unit to lift off (see Figure 9.34). To counteract this, additional screws were placed to keep the lid from lifting off.

Organisational challenges

Another important challenge was the organisation and communication with and within ABP. This manifested itself in two separate instances:

- Operation and commissioning at the outlet of the wastewater treatment system.
- Operation at the outlet of the DAF unit.

The design of the experimental unit, and the planning of the experimental campaign was agreed upon by the environmental department of ABF FOOD GROUP, however, some unexpected circumstances remained, requiring adaptations to the system.

When installing the experimental set-up at the outlet of the wastewater treatment system, the site operator of the site indicated that the effluent from the wastewater treatment only flows at night. The experimental set-up, at that point designed for $24h$ operation, would thus continue its fresh water consumption, at times where no wastewater flowed through the experimental set-up, and thus no heat could be recovered. This would cause the waste of a large volume of unused fresh water (in this case rain water). To counteract this, a timed valve was installed. However, at the start the experimental set-up was started manually during the afternoon, and shut off manually the next morning.

The operation of the experimental set-up at the DAF unit, introduced a feedback loop (as described in Section 9.8.2). The operation at the DAF unit was originally agreed upon by the environmental department, however, the site operator mentioned that this would require additional chemical dosing, due to the increased forward feed. This resulted in only one week of operation at this particular location.

Both of these challenges could have been anticipated and or prevented by a more efficient communication, and earlier involvement of the site operator. This shows the importance of involvement of all different actors and stakeholders in the planning of the project.

9.9. Effluent heat recovery

The effluent of the wastewater treatment system at ABP, Cahir, is clean water, discharged in the river Suir. In this case, rather than transferring the embedded heat in this effluent water to an intermediary heat carrier (the brine in this case), the effluent could be used directly as the heat source for the evaporator of the heat pump. This would reduce the material requirements, as no heat exchangers are required. The principle of this change is shown in Figure 9.39.

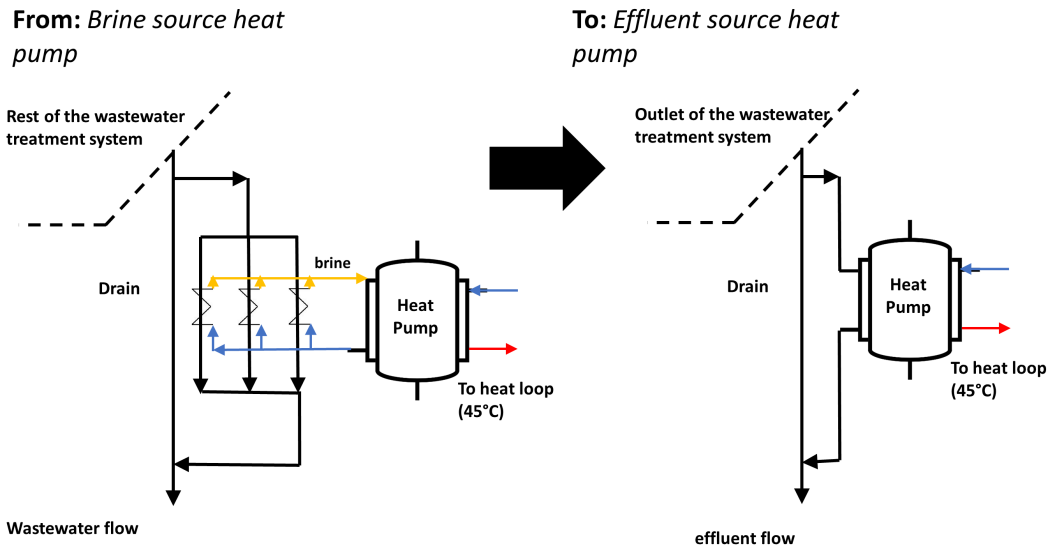


Figure 9.39.: Moving from a brine to an effluent source heat pump.

9.9.1. Effluent temperature

The temperature of the effluent was monitored at ABP Cahir, over the same period as the operation of the experimental unit. The comparison between the effluent temperature, and the temperature of the brine, when entering the evaporator of the heat pump, is shown in Figure 9.40.

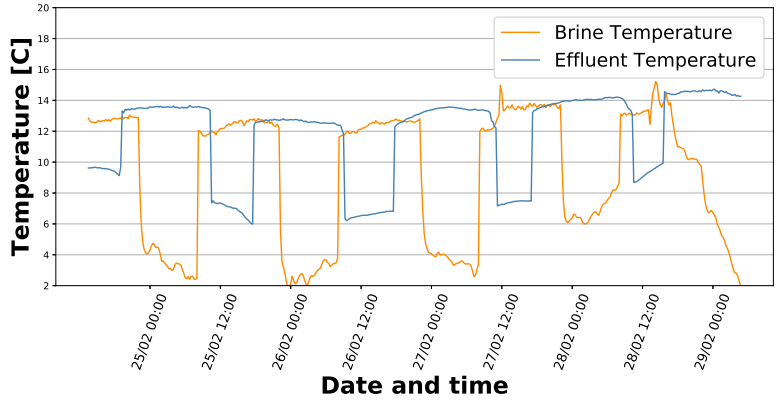


Figure 9.40.: Comparison of the brine and effluent temperature at ABP, Cahir.

Using the COP prediction method, described in Section 5.4.2, for the brine source heat pump, as used in the experimental unit. And the data from Daikin Europe NV [n.d.], for a similar size (5 kW) water source heat pump, this resulted in the evolution of the respective COPs, as shown in Figure 9.41.

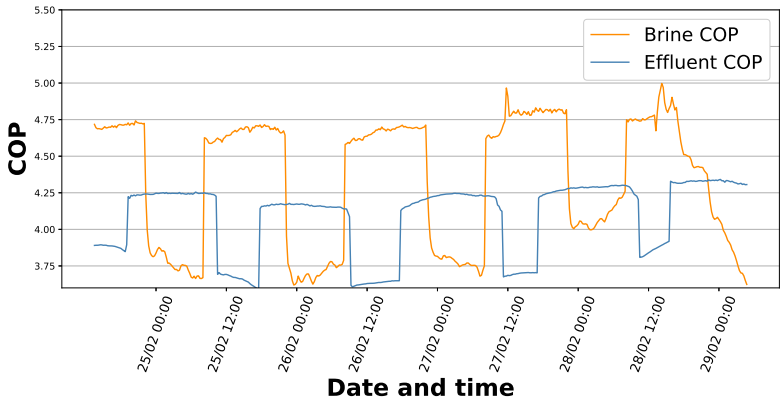


Figure 9.41.: Comparison of the brine and effluent system COP at ABP, Cahir.

In Figures 9.40 and 9.41, one can observe that the period for which the COP is greatest for the effluent is during night time, as the effluent was discharged during night time. This can be counteracted by circulating the effluent through the heat pump from the final effluent clarifiers.

9.9.2. Comparison between the brine and effluent source system

In this comparison, only the indirect heat recovery system was compared, as the direct components would be identical for both systems. Comparisons are made based on the system size as in the experimental unit. For the comparison the same methods as in Section 5.4.3 were used, the LCOE and TEWI.

The financial comparison is based on an LCOE, over 15 years, similar to Section 9.5.5. It is assumed that, as the effluent source system has less components, less time is required for installation, and thus the labour cost is reduced. The heat recovery system, using the brine as a heat carrier, uses more components, and deals with more polluted wastewater, for this reason it is assumed that more maintenance is required, and thus less operating days can be achieved. An overview of the capital investment, and the operating days is given in Table 9.17.

System	Brine Source	Effluent source
Materials		
Co flo Heat Exchanger (3 pipes)	1 425€	–
Heat Pump (5 kW)	6 263€	5 731€
Extra piping and connections	100€	100€
Labour (incl. VAT)	1 200€(3x10 hrs)	800€(2x10 hrs)
VAT	1 557.6€	1 326.2€
Contractor overhead (20%)	2 109.12€	1 751.44€
Total	12 654.72€	10 508€

Table 9.17.: Comparison of the capital investment for both systems.

The environmental comparison was based on TEWI per produced unit of energy. The comparison of the operational parameters and LCOE and TEWI is shown in Table 9.18. As the estimation of the COP was based on four days in February, likely to be colder than the average day over a year, the LCOE and TEWI are likely overestimated, as the COP is expected to be greater during other periods of the year.

System	Brine Source	Effluent source
Operating days	200	250
Average source temperature	12.47°C	13.51°C
Average COP (corrected)	4.68 (3.88)	4.24
LCOE (c€)	16.84 (17.46)	12.50
TEWI ($g\ C_e$)	113.28 (134.55)	120.96

Table 9.18.: Comparison of the operational parameters for both systems.

This comparison indicates that the effluent source heat pump delivers the heating energy at a lower cost (lower LCOE) than the brine source heat pump. In terms of environmental impact (represented by the TEWI) there is more ambiguity in the results, as the brine source heat pump was characterised by a higher theoretical COP, and thus a lower TEWI. However, when a correction was applied, scaling the theoretical COP with the same factor as the ratio between the theoretical and observed COP (see Table 9.14), the effluent source heat pump performs better.

9.10. Yearly savings of the recommended DWHR system

In this section, recommendations are made for the direct and indirect heat recovery systems, and estimates of savings are made over a longer term.

9.10.1. Recommended direct heat recovery system

The suspended solids at the inlet prevented long–term operation of the experimental unit at the inlet. This location was thus not considered for the recommendations, as the results were inconclusive. This location has a significant heat potential, up to 18.67 kW, as discussed in Section 9.8.1, but the impact of the suspended solids in the wastewater on the operation of the heat recovery system remains to be investigated. The outlet of the DAF unit, however, has the additional advantage of an approximate vertical drop of around 3 m being available. This makes it a natural fit for placing the heat exchangers, which require a head space of around 2.1 m. This is also sufficiently early in the chain of the wastewater treatment system to allow for the presence of process heat from the meat processing plant, as indicated by an average wastewater temperature (after heat recovery) of about 17.2°C. The experimental operation showed an average heat recovery power at this location of about 8.85 kW, lower than the available power at the inlet (as expected), however the wastewater at this location has a lower concentration of suspended solids, expected to improve the long–term operation.

The operation at the outlet of the DAF unit showed that, when the wastewater circuit of the heat recovery unit is pressurized, ie. by pumping the wastewater through the heat recovery unit, and back out to the DAF unit, significant changes were required to the heat recovery unit. For this reason, a gravitational wastewater circuit, utilising the vertical drop already present at the DAF outlet, is recommended. At the DAF unit, placing the heat recovery system in line with the DAF unit's drain would achieve the discussed conditions.

9.10.2. Recommended indirect heat recovery system

The temperature of the brine (the heat carrier used in this application), when entering the evaporator of the heat pump, was smaller than temperature of the effluent of the wastewater treatment system, as is shown in Table 9.18. This is not reflected in the COP, due to the difference in performance curves of the considered brine vs. effluent source heat pump. Due to reduced cost, and a less complex system, allowing for more operating days, the overall cost of heat provided through an effluent source heat pump, rather than a brine source heat pump (which was proposed in the experimental unit described in Section 9.4) was expected to be lower.

It is thus recommended to install an effluent source heat pump at the outlet of the wastewater treatment system, rather than installing a brine source heat pump, regardless of the location of its heat source.

9.10.3. Yearly savings and financial viability of the recommended system

The recommended system consists of:

- A direct heat recovery system, located at the DAF outlet.
- An indirect heat recovery system: using an effluent source heat pump, at the outlet of the wastewater treatment system.

To estimate the performance of such a system, the experimental results were used for the direct heat recovery system. For the indirect heat recovery system, a simulation was performed based on the technical data of the heat pump [Daikin Europe NV, n.d.].

The operation of the recommended system, was assessed based on an operation period of 10 hours (8AM – 18PM), and 250 days per year. The cost of the different fuels is given in Table 9.6. For each of the systems the NPV (see Section 6.2.1) was calculated over 15 years, compared to the different fuels mentioned in Table 9.6. The environmental discussion was based on carbon emission savings per year.

The recommended system, studied in this Section, was assumed to have the same size as the experimental unit, discussed in Section 9.4.

Direct heat recovery system

The investment for the direct heat recovery system, consisting of 6 heat exchanger pipes, is summarized in Table 9.19.

This resulted in an evolution of the NPV as shown in Figure 9.42. This shows a payback period ranging from 2.5 *years* (when complementing electric heating) to 9 *years* (when complementing a coal–fired heating system).

Materials	
Co flo Heat Exchanger (10 pipes)	4 750€
Extra piping and connections	200€
Labour (2x15 hrs) (incl. VAT)	1 200€
VAT	610€
Contractor overhead (20%)	3 043€
Total	6 318€

Table 9.19.: Cost Estimate for the recommended direct heat recovery unit.

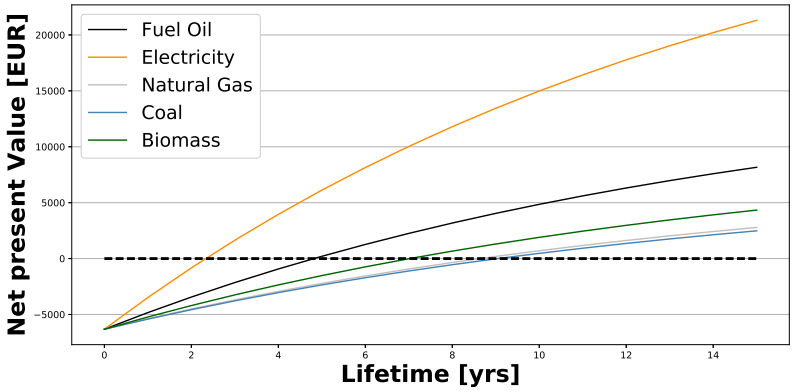


Figure 9.42.: Evolution of the NPV over time for the recommended direct heat recovery unit.

The yearly reduction in heating related GHG emissions, based on the experimental results is shown in Table 9.20. In this table, one can observe that the extrapolated yearly savings are smaller than the predicted savings in Section 9.5.3. This can be explained by three factors, i) Moving the heat recovery unit to the DAF unit, rather than the location described in Section 9.5.3 entails a reduction of wastewater temperature, ii) the wastewater flow through the experimental unit was smaller than estimated and iii) the observed temperatures during operation of the heat recovery unit were smaller than the temperatures used during the pre–feasibility phase.

	Fuel Oil	**Electricity**	**Natural Gas**	**Coal**	**Biomass**
Yearly GHG reduction ($ton\ C_e/yr$)	5.84	10.69	4.53	7.54	0.33

Table 9.20.: Reduction in yearly GHG emissions for the recommended direct heat recovery unit.

Indirect heat recovery system

The investment for the recommended indirect heat recovery system was summarized in Table 9.17, the total cost was estimated at 10 508€. Figure 9.43 shows the evolution of the NPV, compared to different heating fuels. As mentioned in Section 9.9.2, this is likely an underestimation, as the NPV over a whole year is expected to be larger than the one for the observed days in February. Here, one can observe that, except for when compared to electric heating, the payback period of the system is larger than 15 *years* in all cases.

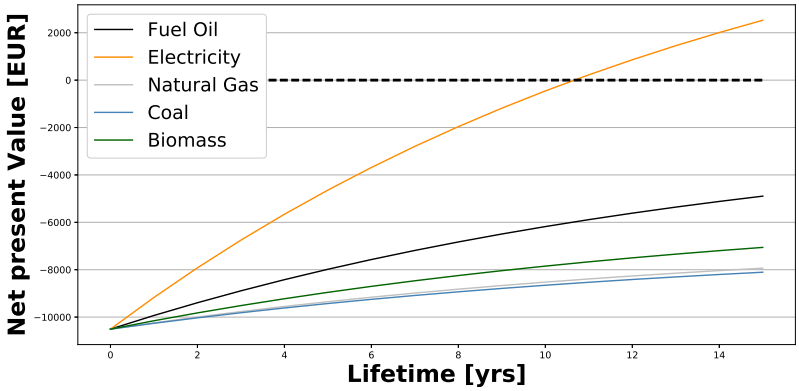


Figure 9.43.: Evolution of the NPV over time for the recommended indirect heat recovery unit.

The yearly reduction in heating related GHG emissions, based on the experimental results is shown in Table 9.21. Again, one can observe that the extrapolated yearly savings are smaller than the predicted savings in Section 9.5.3. The reduction in GHG emissions compared to biomass, shown here, is negative, meaning that this would increase GHG emissions. As mentioned in Section 8.8, this is due to a policy choice in terms of reporting of GHG emissions, in terms of technical ereduction in GHG emissions it is similar to coal [Gunn et al., 2012].

	Fuel Oil	**Electricity**	**Natural Gas**	**Coal**	**Biomass**
Yearly GHG reduction ($ton\ C_e/yr$)	1.87	4.61	1.14	2.83	−1.23

Table 9.21.: Reduction in yearly GHG emissions for the recommended indirect heat recovery unit.

The indirect heat recovery system, recommended here, was not financially profitable, compared to classical, fossil fuel heating systems. However, in case these fossil fuel systems would be phased out in future policies, as is mentioned for example, in the UK's 'Clean Growth Strategy'[HM Government, 2018], or when low–cost electricity is available on–site (for example, thanks to on–site renewable production), the effluent source heat pump could become competitive.

When increasing the size of the heat pump, an increased amount of heat can be recovered, which could improve the profitability of the effluent source heat pump. The largest available water source heat pump in Daikin Europe NV [n.d.], is 248 kW. When reducing the temperature of the effluent by $6°C$ [Somogyi et al., 2018], this would require an effluent volume of 356.69 m^3, well below the minimal effluent at ABP Cahir of 500 m^3 per day[3], and thus achievable.

The capital cost of this heat pump is 32 174€(see Section 7.4.2), using the same characteristics as in Table 9.17, this results in a total capital expenditure of 47 435€. This resulted in the evolution of the NPV as shown in Figure 9.44. In this figure, one can observe a payback period ranging from 1 $year$ (when replacing electric heating) and 8 $years$ (when replacing a coal–fired system).

[3]As affirmed by Fergus Halligan of ABP

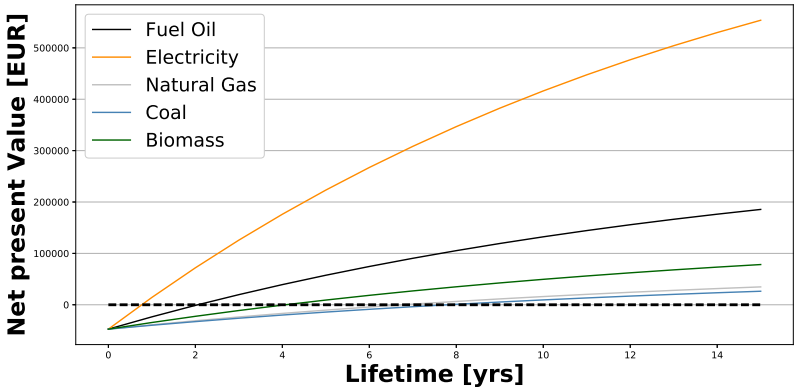


Figure 9.44.: Evolution of the NPV over time for a 248 kW indirect heat recovery unit.

One can observe that economies of scale clearly apply here. Where the experimental unit, with a smaller size (5 kW) was not financially viable, the larger system proves to be profitable, compared to all considered fuel alternatives.

The yearly GHG reduction in case of a 248 kW effluent source heat pump is shown in Table 9.22. Again, the same asterisk can be placed by the negative savings compared to a biomass system.

	Fuel Oil	**Electricity**	**Natural Gas**	**Coal**	**Biomass**
Yearly GHG reduction ($ton\ C_e/yr$)	93.06	228.74	56.32	140.57	−61.26

Table 9.22.: Reduction in yearly GHG emissions for a 248 kW indirect heat recovery unit.

9.11. Summary

The monitoring campaign at the ABP meat processing plant in Cahir, Co. Tipperary showed a temperature ranging from 18 (at the outlet) to 32°C (the condensate inlet from Munster Proteins), showing promise for both direct and indirect heat recovery systems.

A moveable experimental unit was designed, combining both a direct and a hybrid heat recovery system. The idea for this experimental unit was to be able to test the system at different locations in the wastewater treatment works. The feasibility study for this heat recovery system, showed a potential heat recovery ranging from 80 to 130 $MWh/year$. The estimated payback period at the test site in Ireland was predicted to be between 2 and 15 $years$, depending on the heating fuel it is replacing. The system could save up to 35 $tons$ in carbon equivalent emissions, each year. When comparing the direct and hybrid heat recovery systems, it was concluded that, from an environmental perspective, the hybrid system was the favoured system. However, from a financial perspective there was more ambiguity to the results.

The experimental unit was assembled in house at the Civil, Structural and Environmental Engineering Department of Trinity College Dublin, and Delivered to the ABP premises in December 2019. The first operational tests were performed on the effluent of the treatment works, where the direct heat recovery system recovered 250 kWh, the preheating system, part of the hybrid heat recovery system supplied 90 kWh, whereas the heat pump delivered 59.4 kWh, at a COP of 3.49. These savings, although significant, have the disadvantage of occurring through the night. As consumption occurs during the day, this temporal mismatch of heat recovery and heat consumption would reduce the amount of heat that could be used in a practical manner. Furthermore, earlier in the treatment works, much larger quantities of heat are available.

The operation of the experimental unit at the inlet, showed some operational challenges. As the wastewater at the inlet was highly loaded in suspended solids, causing the submersible pumps, charged with pumping the wastewater into the unit, clogged up after a short (a few days) operation time. The power of the direct heat recover showed a clear decline, from around 18 kW on day 1 to 5 kW on day 3, due to reduced wastewater flow through the system. Assuming 10 hours of operation per day, at maximum heat recovery capacity, 250 days per year, and natural gas heating on site, this would result in the reduction of 8.02 $tons\ C_e$ per year, and a cost saving of 1 880.4€per year. However, the long term operation of such a system could not be verified by the research presented here. In future work, this system should be tested, over a longer period of time. This requires the use of a larger pump, to avoid clogging.

To avoid clogging of the pump, the experimental unit was moved to the DAF outlet, where it operated for 5 days, and the temperature of the wastewater varied around $17°C$. The observed average heat recovery varied around $120 - 140\ kWh/day$, at 8.5 kW. Extrapolating these experimental results observed at ABP, Cahir, indicated a payback period ranging from 2.5 to 9 $years$, and emission savings of up to 10.69 $ton\ C_e/yr$.

After 5 days, the operation was interrupted because the set-up of the experimental unit required an additional forward feed in the wastewater treatment system, requiring higher chemical dosing, and thus increased operation costs. An attempt at in–line set up of the experimental unit resulted in a pressurized system, for which the unit was not designed, and which thus required significant alterations. Applying these alterations was hindered by the emergence COVID 19 pandemic. The hybrid system could not be studied, as due to flow variations in the fresh water unit, the power requirement repeatedly exceeded the heat pump's operational limits, causing repeated safety shut–downs of the heat pump.

An effluent heat source heat pump was proposed to counteract this problem, showing a lower cost of heating than the brine source heat pump of the hybrid heat recovery unit. The recommended system was thus as follows:

- A direct heat recovery system, located at the DAF outlet.
- An indirect heat recovery system: using an effluent source heat pump, at the outlet of the wastewater treatment system.

Extrapolating the experimental results observed at ABP, Cahir, indicated a payback period ranging from 2.5 to 9 $years$, and emission savings of up to 10.69 $ton\ C_e/yr$, for the direct heat recovery system. The effluent source heat pump didn't prove to be financially profitable, compared to classical, fossil fuel heating systems. A possibility to improve financial competitiveness, is scaling up the system. At ABP, Cahir, a 248 kW system was largely within the possibilities, and would be financially attractive, compared to all considered fuel alternatives. In addition to this, in case these fossil fuel systems would be phased out in future policies, as is mentioned for example, in the UK's 'Clean Growth Strategy'[HM Government, 2018], or when low–cost electricity is available on–site (for example, thanks to on–site renewable production), the competitiveness of the effluent source heat pump is increased.

In short, when compared to natural gas boiler (the current heating source), the experimental direct heat recovery system, installed at the DAF outlet would reduce GHG emissions with 4.53 $ton\ C_e$ per year, and have a payback period just under 9 years. The effluent source heat pump of 5 kW is not financially profitable, however a 248 kW system, well within reach at ABP, Cahir, would have a payback period of around 5.5 years, and would reduce GHG emissions by 40.91% compared to the gas boiler, equivalent to 56.32 $ton\ C_e$ per year.

10. Prototype development: Heat recovery from grease interceptors

10.1. Introduction

In previous chapters (6 and 8), the potential for heat recovery from kitchen waste water was highlighted. However, these chapters also showed the drawbacks of the current state of the market for heat recovery devices. The available devices require a significant (between 1.5 and 2.1 m) vertical drop, which might not be available at all locations with potential. Furthermore, the analysis showed that the current market–ready systems are not cost effective for the food–outlets which are on the lower–end of the spectrum of water consumption in the hospitality sector.

In the UK and Ireland, the installation of grease interceptors is mandatory for all commercial, hot–food outlets [Irish Government, 2010; HM Government, 2000]. This introduces a volume of (almost) standing water inside the technical rooms of these outlets, to which a heat recovery unit could be added, without additional space constraints, and by keeping the additional cost (for the food outlet), to a minimum.

The prototype described in this chapter thus aims to recover heat from these grease interceptors, by integrating a heat exchanger into the grease interceptor. Ideally, this is done during the manufacturing phase, eliminating the need for additional contracting hours.

This heat recovery unit reduces the remaining required heat, to be provided by a traditional heating system, and thus reduces the fuel consumption, connected with heating up the incoming cold water supplies(as this is passed through the integrated grease interceptor heat exchanger) of the latter. This, in turn, reduces heating fuel–related costs, and related greenhouse gas (GHG) emissions.

In this research, the concept was first tested through experimental investigation in lab conditions. Afterwards a numerical model was created, in order to simulate different conditions and designs. This chapter describes the different steps and thought processes to come to the design of the prototype, and discusses challenges and possibilities for future development. It starts with the steps in the design thinking process, leading to the testing of a first prototype, then continues with the description of the tests performed on this prototype. It also describes the numerical simulations, their challenges, and the proposed alternative designs for such a heat recovery unit. Finally, it discusses future steps in the evolution of this concept to a market–ready product.

10.2. Design thinking

The design thinking process, described in Section 4.5, consists of five steps, summarized in Figure 10.1. The thought process during these different phases is described in this section.

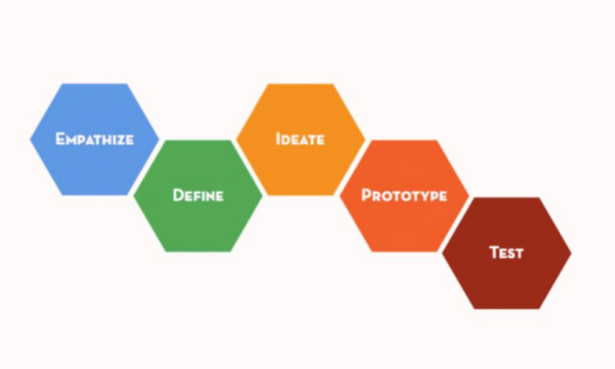


Figure 10.1.: The five phases in design thinking [Rodgers, 2017].

10.2.1. Empathize

As described in Chapter 2, the disruption of the climate, as one of the planetary boundaries, is reaching alarming levels. The human influence on climate change, amongst others, through the emission of greenhouse gases (GHG), is widely accepted. The production of thermal energy (heating and cooling) was responsible for around 50% of the final energy consumption in the EU, 75% of this energy was produced by GHG-intensive fossil fuels. [Commision, 2016] The production of heat is thus an important area of improvement, in order to reduce the greenhouse gas emissions related to human activities, in an effort to combat anthropogenic climate change. The designed prototype aims to reduce the fuel consumption, and thus the related greenhouse gas emissions, of producing hot water.

Recent climate protests, and the development of the European Green Deal [European Commision, 2019], show the importance of mitigating the changing climate.

10.2.2. Define

Chapter 6 showed a large potential for drain water heat recovery in commercial kitchens, however, two different limitations for the deployment of existing commercial heat recovery systems were identified:

- The studied systems require the presence of a vertical drop of around 2 m, space which is not always available, and/or might require the use of pumping systems, which also require an energy input.
- At low flow rates, the studied systems are not financially profitable, but can still provide a reduction in related greenhouse gas emissions.

In Chapter 6, the analysis for the United Kingdom, showed that each year, around 160 GWh of available heat, is not recoverable in a financially attractive way, given the currently available commercial systems. This corresponds to around 44 $k\ tons\ C_e$ each year. This is due to the lower water consumption in 104 879 food outlets. In addition to these outlets, there is an unknown amount of outlets where the proposed system of Chapter 6 is financially feasible, but space constraints make installation of the system in question not practical. The prototype developed in this chapter is looking to fill this gap in the market, providing a low cost solution for which space constraints are not the limiting factor.

10.2.3. Ideate

Monitoring campaigns, already described in Chapter 6, and reported in Appendix B, showed very high temperatures in kitchen drains (with peaks up to $55°C$). Other than the drain, the temperature sensors for these monitoring campaigns were often placed in the grease interceptors (traps) of the kitchen, mandatory equipment in hot food commercial kitchens [Irish Government, 2010; HM Government, 2000].

These grease interceptors hold the kitchen drain water, in order for the heavier components to sink, and the fat, oil and grease (FOG) to float, resulting in pretreated drain water entering the general drainage or sewer system, this is done to avoid fatberg formation (see Section 10.3.2). The concept of the prototype introduced in this chapter, is to utilise the presence of these mandatory grease interceptors, to provide a drain water heat recovery solution, without additional space requirements. Furthermore, as the purchase of the equipment, and the presence of qualified personnel, is already required, the aim is to provide this system with minimal additional cost.

10.2.4. Prototype and Testing

This chapter shows the design and testing of a prototype of a DWHR system, integrated into a grease interceptor. The prototype was tested in laboratory conditions, the results of these tests were used to validate a numerical model, which could, in turn, be used to simulate the performance of alternative designs. These alternative designs open the path towards increasing the Technology Readiness Level (TRL), which could be further extended into a commercial product.

10.3. Methods and Materials

10.3.1. Objectives

The objective of the analysis and experiments was to evaluate the performance of a drain water heat recovery (DWHR) device, designed specifically for kitchen drain water. The DWHR device (also referred to as heat exchanger), is integrated into the grease trap, which is required for drainage systems in hot food commercial kitchens [Irish Government, 2010; HM Government, 2000]. This is done to reduce capital investment and installation cost of the device, and to reduce space requirements, both of which had been identified as reasons for reduced penetration of DWHR devices in the market of UK's commercial kitchens [Spriet and McNabola, 2019*b*]. This would result in a heat recovery device, which could be provide financially attractive heat recovery for kitchens with low water consumption, a gap in the market as identified by Spriet and McNabola [2019*b*] (see also Chapter 6).

The performance of this DWHR unit was investigated experimentally, in steady state, at different conditions. The results of these experiments were then used to validate computational fluid dynamics simulations, so the design can be altered for improved performance.

10.3.2. Grease interceptors

The problem

Sewer overflows are a common occurrence in many cities and countries. The untreated wastewater, spreading due to these overflows, contaminates the environment, water, and the living space in general. These overflows thus cause a threat to human health, create water issues and may damage property. An estimated 47% of all sewer blockages (causing 48% of all overflows) can be contributed to the accumulation of fat oil and grease. Water UK, the association of water and wastewater utilities in the United Kingdom, reports about 366 000 blockages in sewers each year, they claim 70% of those are caused by FOGs and fatberg formation [British Water, 2014]. Blockages caused by FOG occur because of the solidification of these components at lower temperatures, creating so-called fatbergs, which can form barriers in the run of sewers and drainage systems, causing overflow. [Sorensen, 2009; Long et al., 2012] To reduce this risk, the installation of grease interception systems has been made mandatory in the UK and Ireland. [Irish Government, 2010; HM Government, 2000]

Fat, oils and greases also increase the production of bio-gas, as mentioned in Section 3.1.2, kitchen wastewater can be viewed as a resource, both thermally and chemically. Long et al. [2012] indicated that FOGs can be more easily recovered before mixing with raw sewage. The FOG, removed by the grease interceptor, can be collected, and treated in anaerobic digesters, generating bio-gas (see Section 2.4.2).

Different types of grease interceptors

Grease interceptors are device engineered to separate fat, oil and grease (FOG) from the wastewater stream, in order to avoid that these components reach the urban wastewater drainage and sewage networks. Generally, grease interceptors will hold these components until the interceptor is cleaned out, meaning that these waste components are collected. Three different types of fat, oil and grease treatment methods are generally distinguished, Passive grease interceptors, bacteria dosing systems, and mechanical grease interceptors. [Kenny et al., 2011] These different types can be combined for improved FOG removal. [British Water, 2014]

- **Passive grease interceptors**

Passive grease interceptors collect the grease as it is rising up in stagnant water, due to the difference in density. Heavier solid materials will sink to the bottom of the passive interceptor, as shown in Figure 10.2. All passive interceptors work on the principle of slowing down the water flow. The efficiency of the unit is determined by the size and the flow rate going through it. The FOG is kept in the unit by baffles, covering the inlet and outlet of the tank, preventing it from flowing out of the grease separator, while food solids remain on the bottom. [British Water, 2014]

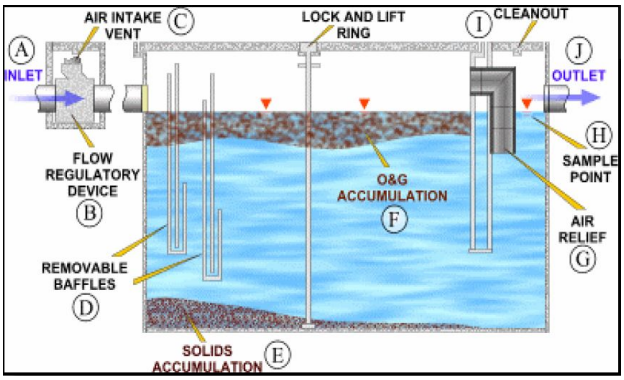


Figure 10.2.: Example of a passive grease interceptor [Dempsey and Rowe, n.d.].

- **Mechanical grease interceptors**

Mechanical grease interceptors, also called Grease Removal Units (GRU) are grease interception units that empty themselves autonomously. Generally this self-emptying is achieved by mechanically skimming the top layer of FOG of the interceptor, into a separate container, as shown in Figure 10.3. This allows for smaller units, compared to passive systems, but requires the use of an additional container, and additional energy consumption.[British Water, 2014]

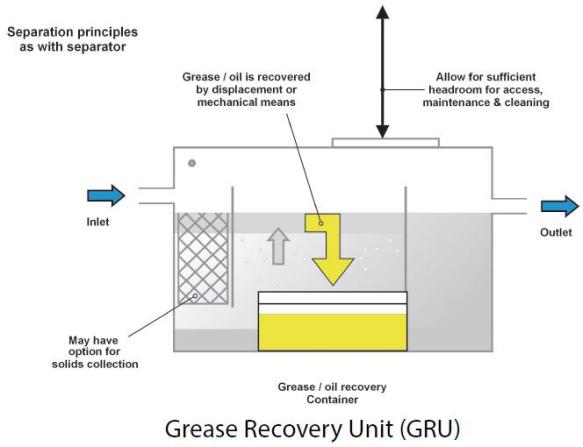


Figure 10.3.: Example of a mechanical grease interceptor [British Water, 2014].

- **Bacteria dosing systems**

In case the passive or mechanical interception units are insufficient, bacteria dosing can be used to improve the FOG removal efficiency of the unit. These systems use micro-organism metabolism to remove the FOGs, generally using cultures to biologically neutralize FOG build-up in the drainage or sewage system. The operation of these bacteria is usually dependant on the pH, the temperature, the presence of oxygen in the wastewater, detergent levels, the natural levels of the organisms in the wastewater, and, often most importantly, time. By increasing the community of the micro-organisms in the wastewater the biological degradation of FOGs over time is increased or accelerated, resulting in FOG decomposing in simpler compounds which can pass through the drainage and sewage systems. [British Water, 2014] A schematic example of a bacteria dosing system is shown in Figure 10.4.

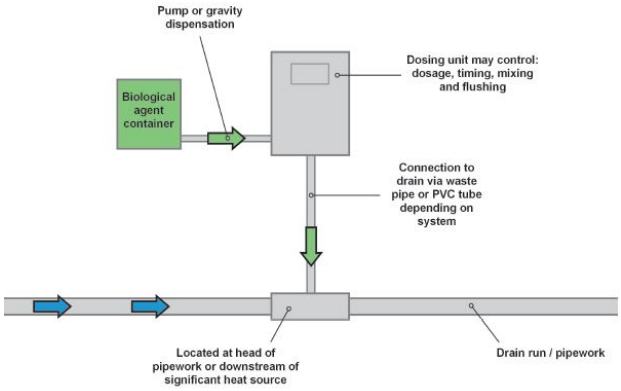


Figure 10.4.: Example of a bacteria dosing system [British Water, 2014].

The effect of temperature

Gallimore et al. [2011] show a decrease in FOG removal efficiency with increased temperature, because of increased breakage of FOG globules at the elevated temperature. This was experimentally tested on both mechanical and passive interceptors, more specifically a passive and an active internal flow-based grease interceptors and a retention-based grease interceptor. For the passive internal flow-based interceptor, the FOG removal efficiency decreased from 82% at $21°C$ to 38% at $38°C$ at a flow rate of 19 l/min.

The FOG removal efficiency thus increases with decreased temperature (and thus increased heat recovery). This results in a greater amount of FOG, recovered from the grease trap, and thus more bio-gas production in anaerobic digesters. Therefore the development of an integrated heat recovery unit and grease interceptor would result in a double benefit. It generates both improved FOG removal as well as reduced energy consumption connected with hot water activities.

10.3.3. Experimental lab set-up

Drain water heat recovery device

The drain water heat recovery device was integrated with a passive grease interceptor (but the concept can be integrated with a mechanical grease interceptor as well). In the prototype, the heat exchanger was attached to the baffle wall. This was the result of a compromise between ease of access, and the higher temperatures close to the inlet of the grease trap. The prototype consists of a serpentine of six copper pipes, through which the fresh water flows in series. The drawing of the grease trap with heat exchanger, and an image of the actual experimental set-up are shown in Figure 10.5 and Figure 10.6. The total heat exchange area of the prototype is around 0.8 m^2.

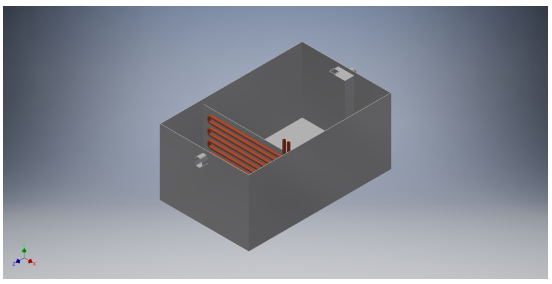


Figure 10.5.: Drawing of the grease trap with prototype DWHR device.



Figure 10.6.: Picture of the prototype DWHR device.

Source data

The temperature of the drain water was measured in four different, large-scale or commercial kitchens, as described by Spriet and McNabola [2019*b*], and in Chapter 6, the feasibility studies, performed at these commercial kitchens, can be found in Appendix B :

- The kitchen of the tea rooms of a tourist attraction, welcoming 100 000 visitors a year, in Wales.
- The kitchen of a 145-bedroom hotel and resort, in county Wicklow, Ireland.
- The kitchen of a 150-bedroom hotel in Dublin, Ireland.
- The kitchen of a retirement home, with 52 residents, in county Tipperary, Ireland

The resulting profile can be found in Figure 10.7. Based on this profile, the device was tested for drain water temperatures of 30 and $40°C$, and for drain water flows of 2 and 4 l/min.

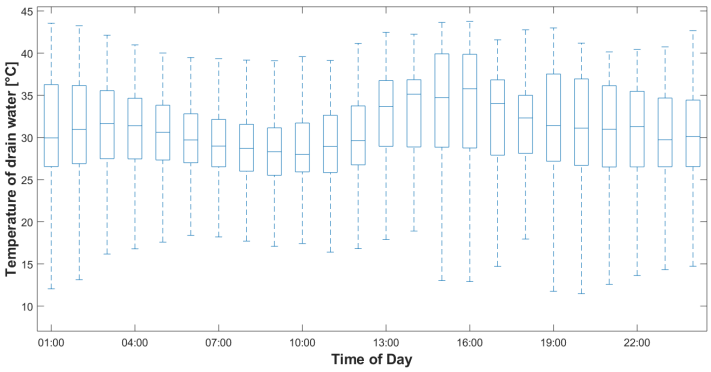


Figure 10.7.: Boxplot of the temperature profile at the observed kitchens.

Experimental set-up

The set-up consists of a warm water reservoir, simulating the kitchen drain water, it includes two heating elements to heat the water to the desired temperature. Once the desired temperature was reached, the water flowed into the grease trap, with integrated DWHR device, where it stayed for the residence time. Upon exiting the grease trap the warm water is recovered and recirculated (Figure 10.8 and Figure 10.9 show a schematic and a picture of the set-up, respectively). The recirculated water dropped into the reservoir from the top, aiding in the mixing of cold (incoming) water, and hot water (which was already present in the reservoir). This was only possible because the performance was evaluated using clean water to simulate the drain water. Further expansion of the set-up could include the introduction of fats, oil and grease (FOG) into the simulated drain water to evaluate the impact of heat recovery on the FOG removal efficiency.

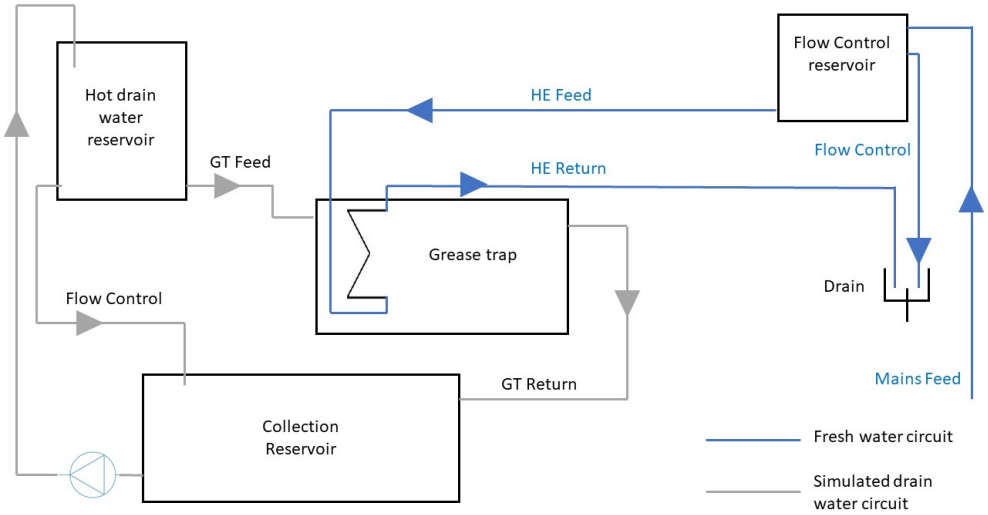


Figure 10.8.: Schematic of the experimental set-up.

The clean water, circulating in the DWHR device was running straight from the mains fresh water, through a flow control reservoir, damping the variation in mains pressure, and returned to the drain. The fresh water flow was measured at the inlet of the heat exchanger, using a magnetic–inductive flow meter (the first page of the instruction manual is shown in Appendix A.2). The inlet and outlet (to the heat exchanger) temperature of the fresh water were measured as well, using type K thermocouples.

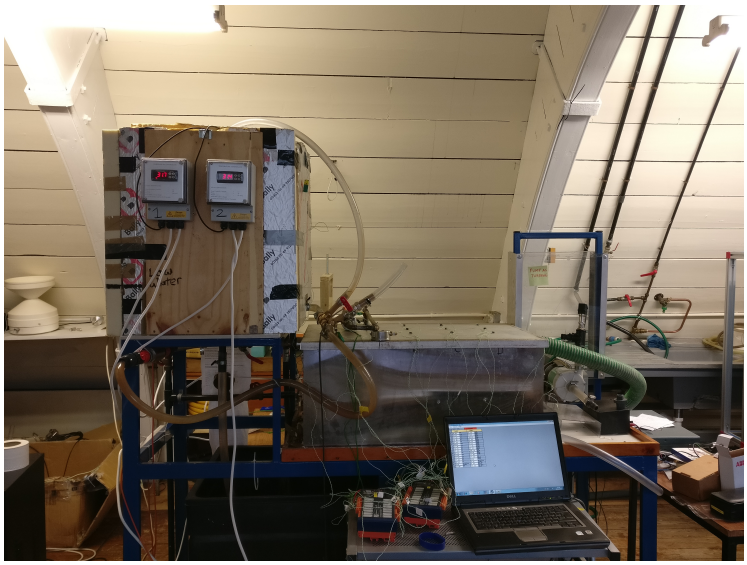


Figure 10.9.: Picture of the experimental set-up.

The simulated drain water flow was measured at the inlet of the grease trap, the temperature was measured in the reservoir, at the inlet and outlet of the grease trap, and at different locations and depths in the grease trap (schematic and picture in Figure 10.10 and Figure 10.11, respectively).

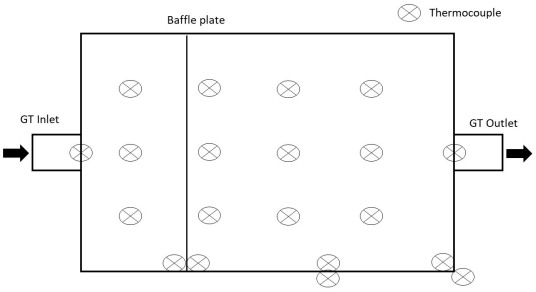


Figure 10.10.: Schematic of the measuring grid in the grease trap.

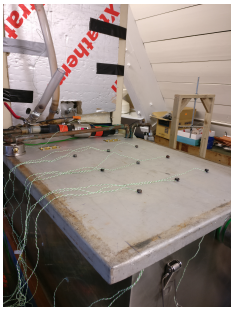


Figure 10.11.: Picture of the measuring grid in the grease trap.

Data measuring and logging

The temperature was measured using type K thermocouples. Thermocouples are electric measuring devices, consisting of an electrical junction of two different conductors (usually through welding). They produce a temperature dependent voltage as a result of the thermoelectric effect, which can then be converted to the measured temperature. A type K thermocouple consist of a Chromel–Alumel junction. The conversion was built in to the logger software, and verified with the temperature measurement of a water–ice mixture ($0°C$) and the measurement of boiling water ($100°C$).

The flow was measured using a magnetic–inductive flow meter. This flow meter sent an analogue output to the data logger (a current between 4 and 20 mA), which was then converted to a flow reading.

The calibration of this conversion factor was done by comparing with another, already calibrated flow meter. The calibration is shown in Figure 10.12. This calibration was later verified, as can be seen in Figure 10.13. Where the 95% confidencee interval of the slope includes 1 (meaning that it the true mean value of this slope is, with 95% confidence, not significantly different from 1), and the confidence interval of the intercept contains 0, confirming the calibration set in Figure 10.13.

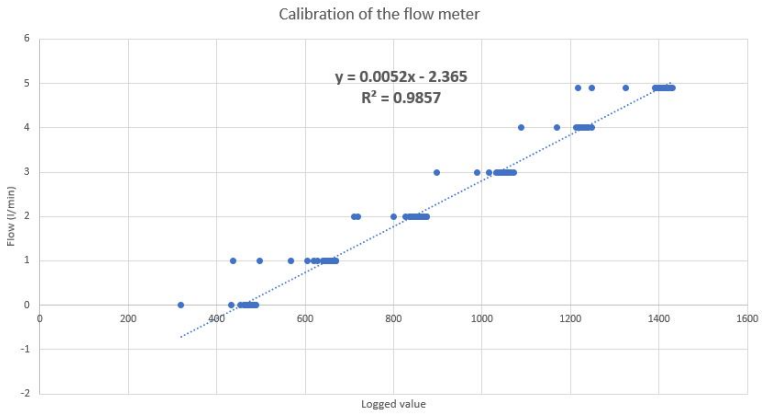


Figure 10.12.: Calibration curve of the flow meter.

Linear model Poly1:
f(x) = p1*x + p2
Coefficients (with 95% confidence bounds):
p1 = 1.004 (0.994, 1.015)
p2 = -0.02132 (-0.05125, 0.008609)

Goodness of fit:
SSE: 6.665
R-square: 0.9921
Adjusted R-square: 0.992
RMSE: 0.1503

Figure 10.13.: Verification of the flow meter calibration.

The measurement were logged in 1 s intervals, using a DATASCAN 7220 datalogger, and its corresponding RS RECORDER software, on a laptop (see Figure 10.9). The data was then exported to a CSV format, and loaded into PYTHON for post processing and comparison.

Experimental runs

Sixteen different experimental runs were performed, with different 'wastewater'and fresh water conditions. These conditions are summarized in Table 10.1, the temperature of the fresh water was not controlled, but was the temperature of the mains feed water in the hydraulics lab of the department of civil, structural and environmental engineering.

The temperature of the wastewater was set by two temperature controllers in the hot drain water reservoir (upper left in Figures 10.8 and 10.9). These controllers consists of a binary (on/off) controller, and an electrical, resistive heating element. The controller turns the current through the resistive element on or off, depending on the measured temperature in the reservoir, and the relationship of this temperature to the set point. The first page of the operation manual of these temperature controllers is shown in Appendix A.3.

The experiments ran over several hours, in order to reach the steady state operating conditions. These were defined as the situation where the temperature of the wastewater exiting the grease trap does not show any significant trend, the details of the definition of the steady state are discussed in Appendix G.1.

Wastewater		Fresh Water
Temperature	Flow	Flow
$30°C$	2 l/min	1 l/min
		3 l/min
		5 l/min
		6 l/min
	4 l/min	1 l/min
		3 l/min
		5 l/min
		6 l/min
$40°C$	2 l/min	1 l/min
		3 l/min
		5 l/min
		6 l/min
	4 l/min	1 l/min
		3 l/min
		5 l/min
		6 l/min

Table 10.1.: Approximate settings of the experimental runs, simulated during the validation process.

10.3.4. Numerical simulations

The numerical model, being a Computational Fluid Dynamics (CFD) model was simulated using the ANSYS Fluent software. As can be seen in Figure 10.14, this numerical simulation consists of four steps, described below.

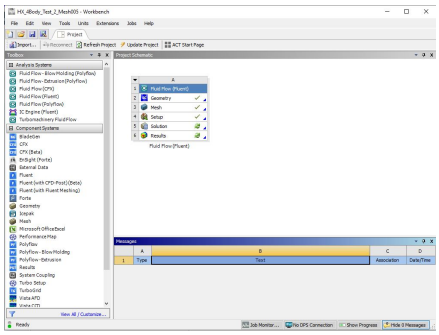


Figure 10.14.: Five steps in the fluent workbench.

- Building the geometry.
- Meshing (Discretizing) the geometry.
- Setting-up and solving the simulation.
- Analysing the simulation results.

Geometry

The geometery of the protoype was drawn in a commercial Computer Aided Design (CAD) application called Autodesk Inventor. This software was specifically developed for 3D mechanical design, simulation, visualization, and documentation. It allows for the design and drawing of different components of the system, and to assemble them into one integrated system (see Figure 10.15). This assembled system, or one of its components can be imported in the Fluent workflow.

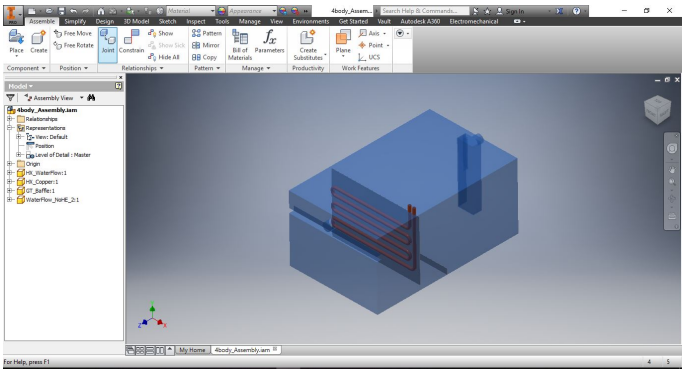


Figure 10.15.: A preview of the Autodesk Inventor software.

Meshing

The imported geometry is then subdivided into discrete cells, for which the different variables of interest are determined by the simulation. This set of discrete cells is called the mesh, finer mesh size (or cell size) increases the amount of cells required to cover the entire simulated system. This increases the precision of the calculations and results, but also the required computational time. An example of a mesh, in the ANSYS meshing software can be found in Figure 10.16.

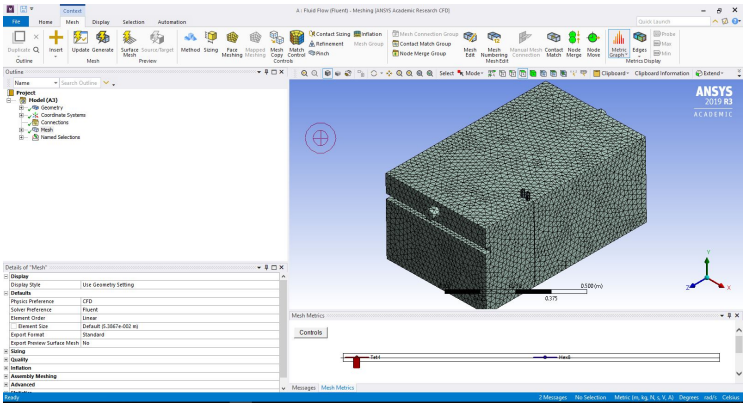


Figure 10.16.: A preview of the ANSYS meshing software.

Dividing a continuous domain (whether it being a running fluid or a solid material) into discrete cells introduces a discretization error in the results, quantifying this error can be done by the Grid Convergence Index (GCI) method [Celik et al., 2008], which is further explained in Section 10.6.2.

Meshing can be done in the built-in meshing software, common to all ANSYS applications.

Simulation set-up

The set-up and solving of the relevant equations is done in ANSYS FLUENT. This is a software used to model flow, turbulence, heat transfer, and reactions for industrial applications. In this set-up, the different equations to be solved need to be set up, along with the material properties, boundary conditions, etc. A more detailed overview is given in Section 10.6.2. The fluent module, for the problem set-up is shown in Figure 10.17.

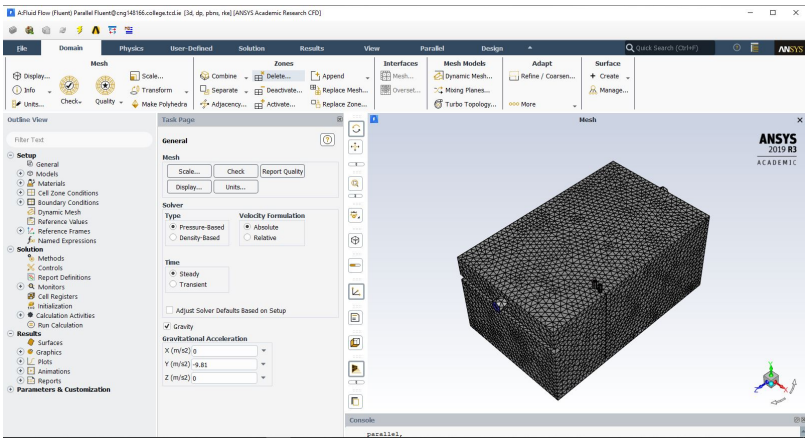


Figure 10.17.: A preview of the ANSYS FLUENT solver.

Solving the simulation

The governing equations (see Section 10.6.2) of the numerical model are solved by an iterative process, terminating the iterations once the scaled residuals drop below a certain tolerance ($1E-6$ for the energy equation, $1E-3$ for all other equation parameters). The scaled residual is defined as the local imbalance of a conserved variable in a control volume. [ANSYS, 2019] An example of decreasing residuals is shown in Figure 10.18.

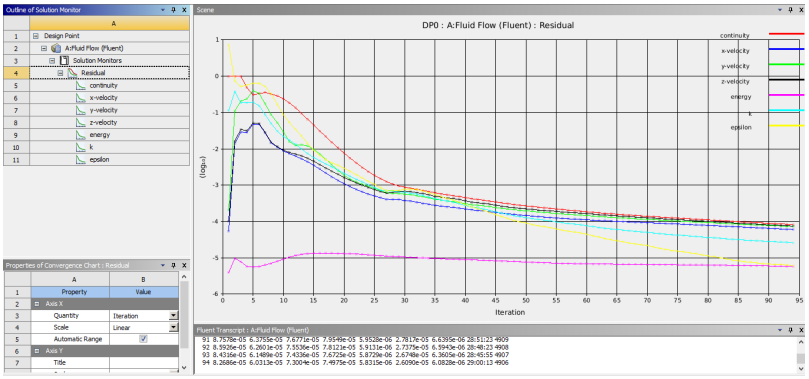


Figure 10.18.: Example of residual evolution over the different iteration.

In the pressure-based solver of ANSYS FLUENT (the one used in the simulations described in this chapter), two algorithms are available:

1. A segregated algorithm. In this segregated algorithm the governing equations for the solution variables are solved sequentially. This algorithm is memory efficient, since only one equation needs to be stored in the memory at the time. However the convergence of the solution is slower.
2. A coupled algorithm This algorithm solves a coupled system of equations. This improves the convergence, but requires more memory.

The solver algorithms are summarized in Figure 10.19 [ANSYS, 2019].

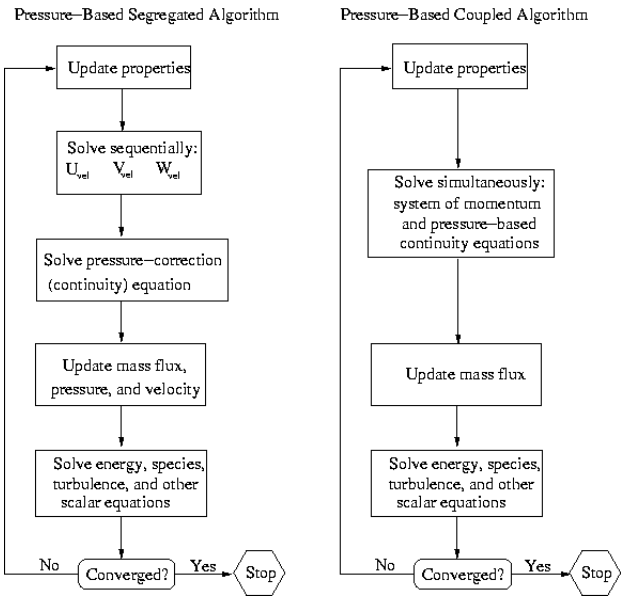


Figure 10.19.: Overview of the Pressure-Based Solution Methods [ANSYS, 2019].

Simulation results

The results can be viewed among singular points, along streamlines, in planes,... in the general software ANSYS CFD-Post. A preview of this can be found in Figure 10.20.

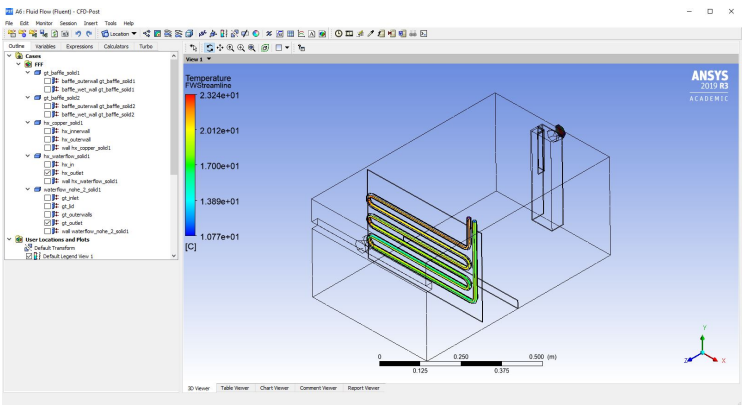


Figure 10.20.: A preview of the ANSYS CFD-Post application.

10.4. Experimental results

The device was tested under different drain water and fresh water flow conditions, with the drain water temperature set at 30 and 40°C, the drain water flow at 2 and 4 l/min. The fresh water flow was set to 0, 1, 3, 5 and 6 l/min, its temperature was the mains fresh water temperature at Trinity College, Dublin, Ireland at the time of the tests, in January and February 2019.

Evolution of the effectiveness

At low fresh water flow (1 l/min) the heat exchanger's effectiveness reached a median value as high as 56% at a drain water flow of 4 l/min and 40°C, as can be seen in Figure 10.21. At a drain water flow of 4 l/min the effectiveness reaches a lowest point of around 23%. At 30°C the effectiveness reached a maximum of 58% for a drain water flow of 4 l/min, and a minimum around 21%.

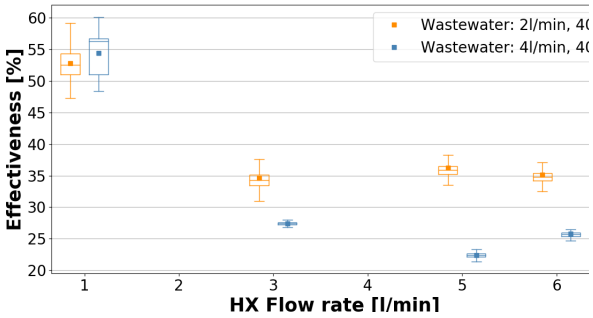


Figure 10.21.: Effectiveness of the heat exchanger at 40°C drain water.

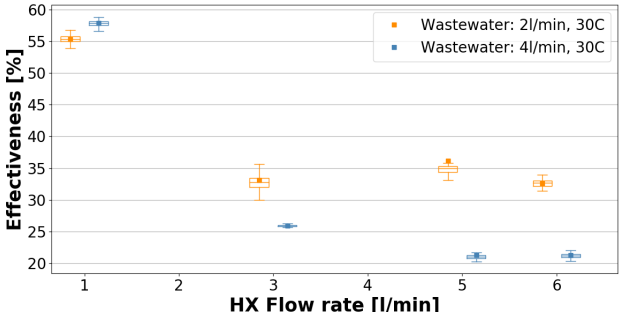


Figure 10.22.: Effectiveness of the heat exchanger at 30°C drain water.

This could, mistakenly, lead to the conclusion that the lower flow values (for both fresh and drain water), are desired for optimal heat recovery, and thus an increased chance for profitability of the system. Figures 10.23 and 10.24, however, show that the amount of heat recovered, expressed by the power in this figure, is larger at the larger drain water flows (for both fresh and drain water). One can observe that a maximum is reached at a fresh water flow of 5 l/min, increasing the fresh water flow further leads to a stagnation or even decrease in recovered heat.

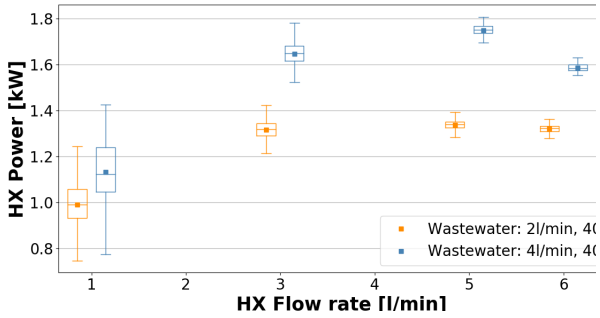


Figure 10.23.: Recovered heating power of the heat exchanger at 40°C drain water.

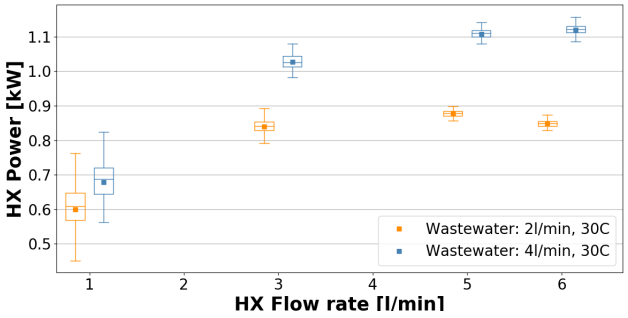


Figure 10.24.: Recovered heating power of the heat exchanger at 30°C drain water.

The recovered heating power for this prototype ranges from 1 to 1.8 kW at 40°C and from 0.6 to 1.1 kW at 30°C. The CFD simulation, discussed in Section 10.6 shows the potential heat recovery for optimized heat exchangers (see Section 10.7), with larger exchange surfaces.

Evolution of the temperature

An important aspect of recovering heat from grease traps is to reduce the temperature inside this grease trap. High temperatures in grease traps are identified by installers[1] as the main challenge regarding their operation, and reduced temperature improves the fat, oil and grease (FOG) removal efficiency [Gallimore et al., 2011]. Figure 10.25 shows the evolution of the temperature at the center plane (The plane along the flow direction, connecting the inlet and outlet of the grease interceptor) of the grease trap. It shows a significant drop, from the set 40.25°C to around 35.5°C at a fresh water flow of 6 l/min, for a drain water flow of 2 l/min, as shown in Figure 10.25.

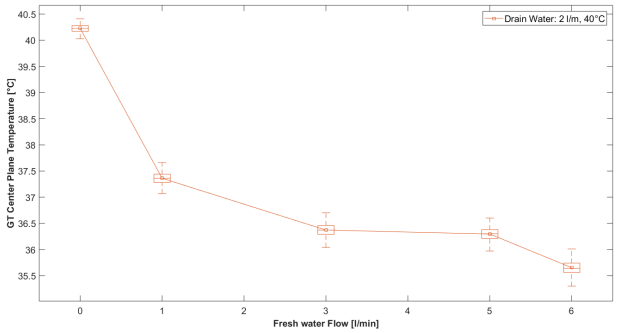


Figure 10.25.: Temperature in the center plane of the grease trap.

10.5. Viability of the prototype

The objective of this prototype was to construct a heat recovery device, reducing the space constraints and costs that are currently associated with drain water heat recovery systems in commercial kitchens (see Chapters 6 and 8). The prototype discussed in the previous sections reduces space constraints, but what with the related costs? And how would this heat recovery unit position itself in the market?

These questions are researched in this section, for two different situations:

1. The prototype, in its current form.
2. The prototype, when integrated into the manufacturing process of grease interceptors (further denoted as *commercialised prototype*).

10.5.1. The current prototype

Manufacturing costs

The manufacturing costs, as encountered during the actual, in-house construction of the prototype, are listed in Table 10.2, a contractor overhead of 30% was added. These costs are then used to estimate a cost per exchange area (proportional to the power) of the device, and to estimate costs for different sizes. The cost per m^2 of the device is around 204.81 €/m^2. The cost of the full unit (163.85€) equates to 152.17£.

[1] As mentioned by Steven Carter of SUPERDRAIN in an interview on February 1st 2019

	Unit cost (€)	units	Total cost (€)
Labour			25.03
Material and fittings	40	2 hrs	80
Copper pipe (400 mm)	2.24	7	15.68
Copper pipe (100 mm)	0.56	1	0.56
90° bends	0.63	14	8.79
Overhead (30%)			31.51
VAT (20%)			27.31
Total			163.85

Table 10.2.: Breakdown of the construction costs of the prototype DWHR device.

Financial viability

As discussed in Sections 6.2.1 and 6.2.3, the system is considered financially viable if the Net Present Value (NPV) over 5 (Figure 10.26) or 10 $years$ (Figure 10.27) is greater than zero (0). The evolution of the NPV of the current prototype, with daily water consumption is shown in Figure 10.27. One can observe that the threshold values, in terms of daily water consumption of the kitchen, for viability, are significantly lower than for the commercial system, discussed in Section 6.2.3. The threshold value for replacing electric heating lies between 95 (for an NPV over 10 years) and 150 l/day (for an NPV over 5 years), whereas the threshold value for fuel oil, natural gas and biomass is comprised between $300 - 335$ l/day (for an NPV over 10 years) and $490 - 555$ l/day (for an NPV over 5 years).

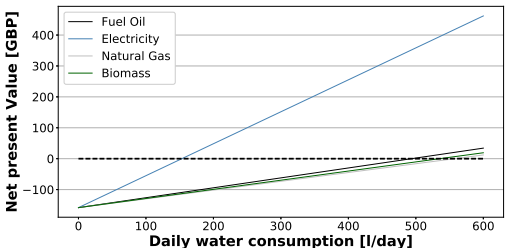


Figure 10.26.: Evolution of the NPV over 5 years for the current prototype.

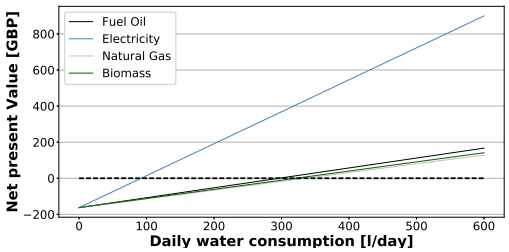


Figure 10.27.: Evolution of the NPV over 10 years for the current prototype.

Market position

To assess the position of this prototype in the market the NPV over 10 years is compared to the NPV of the commercially available system, discussed in Section 6.2.3. This NPV is calculated using the price of the general fuel mix, $6.13p£/kWh$. The results for the current prototype are shown in Table 10.3[2]. The Carbon NPV is not discussed, as the emissions related to the production of this prototype was not studied. The NPV values in bold are more profitable than the equivalent, commercially available system. One can observe that for the larger outlets, the NPV remains constant, this is because, the heat recovery capacity of the prototype is limited. In practice, larger outlets will have larger grease interceptors, and can thus have larger heat exchangers, however this alternative design is not the object of this analysis. First steps towards an improved, alternative design are discussed in Section 10.7.

[2]This data is divided into four categories: Cat I up to 10 000 meals per year, Cat II 10 000 – 29 000 meals per year, Cat III 30 000 – 100 000 meals per year, and cat IV more than 100 000 meals per year

Table 10.3.: NPV for the current prototype.

	Cat I ***NPV*** (£)	**Cat II** ***NPV*** (£)	**Cat III** ***NPV*** (£)	**Cat IV** ***NPV*** (£)
Restaurants	**342.57**	**806.79**	806.79	806.79
QSR	**73.25**	**487.59**	806.79	806.79
Pubs	**73.25**	**487.59**	806.79	806.79
Hotels	**238.98**	**806.79**	806.79	806.79
Leisure	**73.25**	**487.59**	806.79	806.79
Staff Catering	**207.91**	**806.79**	806.79	806.79
Health Care	**342.57**	**806.79**	806.79	806.79
Education	**207.91**	**806.79**	806.79	806.79
Services	**342.57**	**806.79**	806.79	806.79

This results in a total amount of potential customers in the UK, for whom the current prototype would be a profitable heat recovery option. These customers, and the potential revenue generated by selling the prototype for a price as discussed in Table 10.2, are divided in customers without competition (customers where the system discussed in Chapter 6 is not profitable), and with competition (where the the system discussed in Chapter 6, but the NPV is lower than the one for the current prototype.

Table 10.4.: Potential customers for the current prototype.

	Outlets	**Estimated revenue (£)**
Without competition	93 292	15 285 894.24
With competition	58 268	9 531 479.44
Total	151 560	24 817 373.64

One can observe that a considerable additional revenue , to the sale of grease interceptors, can be generated in this way. However, as grease interceptors typically have a long lifetime, this revenue should be spread over a long period, making this business unsuitable as a sole revenue center.

10.5.2. The commercialised prototype

The commercialised prototype, considered in this section, was assumed to have the same heat recovery characteristics as the actual prototype, described above. However, it was assumed that this prototype was already included in the manufacturing of the grease interceptor, and thus required no additional intervention for installation.

Manufacturing costs

The manufacturing costs were thus estimated on the same basis as the current prototype (see Table 10.2, however excluding the labour labour costs. This results in an estimated manufacturing cost of the unit (to be added to the price of the grease interceptor) of 39.05€, this equates to 36.27£.

Financial viability

The evolution of the NPV of the commercialised prototype, with daily water consumption is shown in Figure 10.29. One can observe that the threshold values, in terms of daily water consumption of the kitchen, for viability, are even lower than for the current prototype, discussed above, around 25 l/day (for an NPV of 10 years) and around 35 l/day (for an NPV of 5 years) for electric heating, and ranging between $70-80$ l/day (for an NPV of 10 years) and $115 \ -135$ l/day for fuel oil, natural gas and biomass.

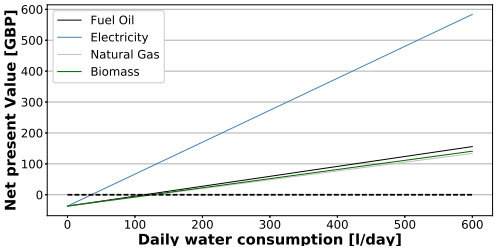


Figure 10.28.: Evolution of the NPV over 5 years for the commercialised prototype.

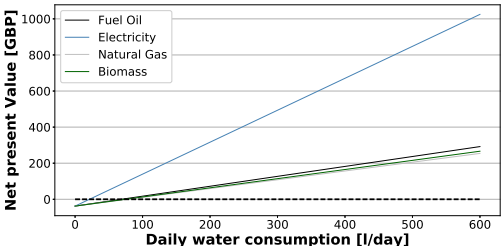


Figure 10.29.: Evolution of the NPV over 10 years for the commercialised prototype.

Market position

The NPV values for the commercialised prototype are shown in Table 10.6[3]. One can observe that profitability occurs in the same instances as for the current system. However the NPV for the outlet is larger, due to the lower investment cost.

Table 10.5.: NPV for the commercialised prototype.

	Cat I ***NPV*** (£)	**Cat II** ***NPV*** (£)	**Cat III** ***NPV*** (£)	**Cat IV** ***NPV*** (£)
Restaurants	**479.11**	**943.32**	943.32	943.32
QSR	**209.79**	**624.13**	943.32	943.32
Pubs	**209.79**	**624.13**	943.32	943.32
Hotels	**375.52**	**943.32**	943.32	943.32
Leisure	**209.79**	**624.13**	943.32	943.32
Staff Catering	**344.45**	**943.32**	943.32	943.32
Health Care	**479.11**	**943.32**	943.32	943.32
Education	**344.45**	**943.32**	943.32	943.32
Services	**479.11**	**943.32**	943.32	943.32

Similarly, Table 10.6 shows the same amount of customers in the UK, however, the profit for the manufacturer of the heat exchanger is smaller due to the smaller retail price. This indicates that a significant additional profit margin is available.

Table 10.6.: Potential customers for the commercialised prototype.

	Outlets	**Estimated revenue (£)**
Without competition	93 292	3 383 700.84
With competition	58 268	2 113 380.36
Total	151 560	5 497.081.2

[3]This data is divided into four categories: Cat I up to 10 000 meals per year, Cat II 10 000 – 29 000 meals per year, Cat III 30 000 – 100 000 meals per year, and cat IV more than 100 000 meals per year

10.6. Validation of the numerical model

10.6.1. Objectives of the numerical model

The objective of generating a verified and validated numerical model of the prototype was to allow the comparison and testing of different designs, without having to spend the resources to physically build the altered design. The model, once validated through comparison with the experimental results, could then be applied to predict the operation of altered and improved design, facilitating design choices.

10.6.2. Computational Fluid Dynamics

The numerical model, and simulation consists of multiple steps:

- Building the geometry model of the that is to be simulated.
- Discretizing (meshing) this geometry domain, in several cells and nodes, where the parameters of interest are calculated.
- Setting up the simulation model.
- Simulating the operation.
- Comparing and post-processing the results of the simulation.

These steps, and the way they were achieved in this research are described in this section. The model was run for all different sets of parameters, performed in the experimental runs, as summarized in Table 10.1. The results of the simulations were compared to the experimental results, in order to validate the model.

Geometry model

Two different geometries were used in this analysis:

- The full geometry, modelling the full system.
- The sliced geometry, modelling the zone around the heat exchanger.

The sliced geometry was introduced to reduce the cell count, and to allow for a finer mesh, increasing precision, and reducing calculation time.

- **Full geometry**

The geometric model was built in Autodesk Inventor, and consists of four different compenents:

- The wastewater body.
- The fresh water body.
- The heat exchanger, copper solid body.
- The solid, stainless steel baffles of the grease interceptor.

Notably the exterior walls and lid of the heat exchangers were not included in these components, these were set as boundary conditions. This geometry is shown in Figure 10.15.

- **Sliced geometry**

A second geometry was simulated, where a slice was cut out of the full geometry, allowing for a finer mesh in the zone of interest, namely around the heat exchanger. The same four bodies as in the full geometry were used.A picture of the sliced geometry is shown in Figure 10.30.

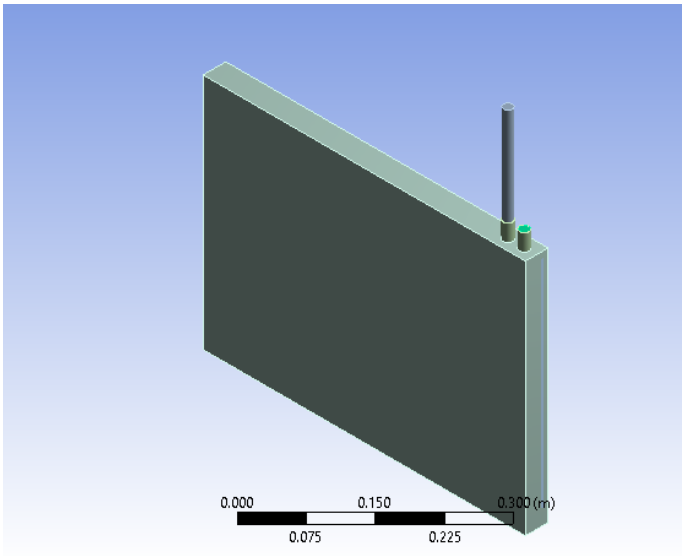


Figure 10.30.: Sliced geometry for the CFD simulation.

Meshing

- **Full geometry**

In this simulation, different mesh sizes were selected, a finer one, covering the wastewater body, around the heat exchanger, and the fresh water flowing through the heat exchanger. A second, coarser mesh, covered the other part of the wastewater body, both at the inlet and at the rear. This was done because the zone of interest is the fresh water flowing through the heat exchanger. The heat exchanger outlet, and the outlet of the grease interceptor were extended, in order to counteract the potential effects of backflow on the resulting values. An image of the mesh is shown in Figure 10.31.

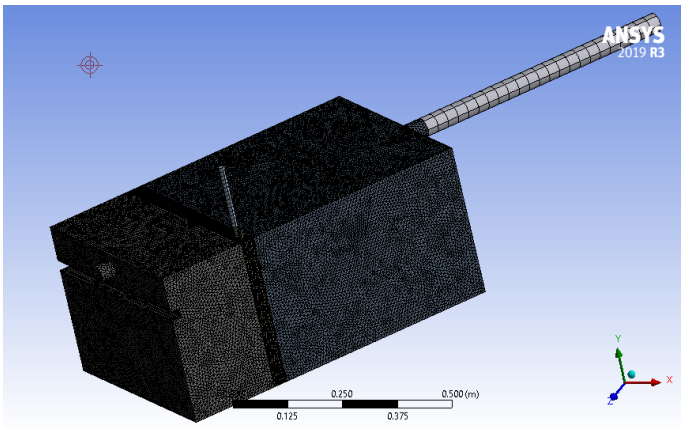


Figure 10.31.: The employed mesh for the CFD simulations of the full geometry.

The characteristics of the final mesh are summarized in Table 10.7. In this table **Skewness** is a function of the ratio of internal angles against a 'perfect angle ', typically the maximal allowed skewness value is 0.95. Similarly the orthogonal quality relates to how close the angles between adjacent element faces are to an optimal angle, typically the minimal required orthogonal quality is 0.01 [ANSYS, 2019].

Number of nodes		5 552 330	
Number of elements		3 912 886	
	min	avg	max
Skewness	$1.3E-10$	0.21	0.92
Orthogonal quality	0.08	0.79	1

Table 10.7.: Main characteristics of the employed mesh.

- **Sliced geometry**

For the sliced geometry, a finer mesh was applied to the simulation region. To this finer mesh, an inflation layer was added, in the fresh water body. This means that a smaller cell size (thus a finer mesh) was applied on the contact wall of the fresh water body with the copper of the heat exchanger. This smaller cell size was 0.05 mm, and was gradually increased when moving away from the wall, by a growth rate of 1.2, for a depth of 10 cells. The inflation layer is shown in Figure 10.32.

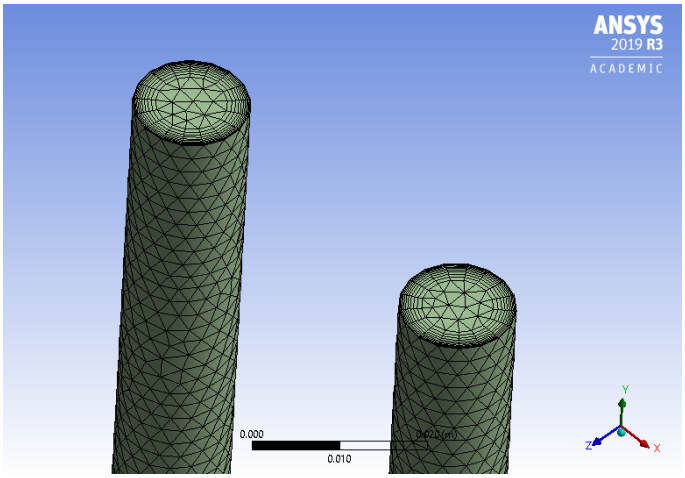


Figure 10.32.: Example of an inflation layer.

The characteristics of the final mesh are summarized in Table 10.8.

Number of nodes		5 775 812	
Number of elements		3 195 164	
	min	avg	max
Skewness	$1.3E-10$	0.21	0.89
Orthogonal quality	0.11	0.79	1

Table 10.8.: Main characteristics of the employed mesh for the sliced geometry.

Setting up the model

The different equations to be solved were set-up in the ANSYS Fluent solver, and an overview of the equations, and the selected parameters is given in this section.

- **Energy model**

The employed energy model in FLUENT was the same for both geometries.

In order to determine the temperature of the fluids involved, after heat exchange, the energy equation is solved by the ANSYS FLUENT SOLVER, and shown in Equation 10.1. In this equation ρ is the density, H is the enthalpy, $\vec{v}$ the velocity, k the conduction coefficient, T the temperature and S a source term.

$$\frac{d}{dt}(\rho\, H) \;+\; \nabla \;\cdot\; (\rho\, \vec{v}\, H) \;=\; \nabla \;\cdot\; (k\, \nabla T) \;+\; S \tag{10.1}$$

- **Viscous model**

As can be seen in Figure 10.33, the flow through the main wastewater body of the grease trap is laminar for all the simulated cases, whereas the flow through the heat exchanger is turbulent in most cases (except for the lowest flow rate, around 1 l/min). To address this the flow is modelled as a turbulent flow, for both the full and the sliced geometry, and the wastewater bodies in the grease interceptor (grease trap) were set as a *laminar zone*.

	Grease trap				Heat Exchanger		
Flow	Velocity	T in	T out	Reynolds	Velocity	Tin	Reynolds
1.99	0.000179	35.38	34.81	18.08631	0.118173	10.77	1513.733
2.01	0.000181	33.53	33.07	18.26808	0.36255	9.07	4644.076
1.95	0.000176	32.55	32.28	17.72277	0.603485	8.98	7730.328
2.02	0.000182	32.4	32.36	18.35897	0.723953	8.76	9273.455
4.03	0.000363	37.53	36.47	36.62705	0.122762	9.74	1572.519
4.04	0.000364	36.06	35.59	36.71793	0.351077	8.77	4497.111
4.02	0.000362	35.61	35	36.53616	0.603485	8.83	7730.328
3.57	0.000322	33.4	32.8	32.44629	0.721658	8.38	9244.062
2.059208	0.000186	28.38	27.97	18.71531	0.094965	10.13	1216.446
1.954441	0.000176	26.3	26.05	17.76313	0.336624	9.01	4311.98
1.907037	0.000172	25.75	26.2	17.33229	0.597239	8.77	7650.315
1.974545	0.000178	25.73	25.85	17.94584	0.707595	8.72	9063.919
3.982796	0.000359	29.18	28.3	36.19803	0.101035	10.16	1294.205
3.986944	0.000359	27.94	27.3	36.23573	0.335811	8.92	4301.566
3.884731	0.00035	27.63	27.74	35.30676	0.59311	8.7	7597.428
3.971923	0.000358	27.52	27.18	36.09921	0.706495	8.91	9049.825

Laminar
Turbulent

Figure 10.33.: Summary of the flow conditions in the different flow bodies.

Three basic approaches can be used to calculate turbulent flow in FLUENT:

1. Direct Numerical Simulation (DNS)
2. Large Eddy Simulation (LES)
3. Reynolds Averaged Navier-Stokes Simulation (RANS)

In the case of this heat exchange problem, RANS turbulence models were used, with a different approach close to the walls compared to far away from the walls [ANSYS, 2019].

- Away from the walls a realizable k–ϵ model was used.
- Close to the walls an SST k–Ω model was used.

Both turbulence models are described in the section, along with their respective approach for the modelling of walls. Near walls, the gradient of the solutions are very high, resulting in the risk of inaccurate solutions. The approach for wall modelling is thus important for accurate results. A parameter to judge the applicability of wall functions is the dimensionless wall distance ($y+$) described in Equation 10.2. This can also be interpreted as a local Reynolds number, meaning that it describes the importance of viscous and turbulent processes. In this equation, u_r is the friction velocity, y is the absolute distance from the wall, and ν is the kinematic viscosity of the fluid.

$$y+ \ = \ \frac{y \ u_r}{\nu} \tag{10.2}$$

Near the wall, on can distinguish between three different wall regions and layers, as shown in Figure 10.34:

1. The viscous sublayer ($y+ < 5$) In this layer, the fluid is dominated by the viscous effect.
2. The buffer layer ($5 < y+ < 30$) The buffer layer is the transition region between the viscosity-dominated region and turbulence-dominated part of the flow. The velocity profile is not well defined, this layer should be avoided for the numerical simulations.
3. The logarithmic layer ($y+ > 30$)

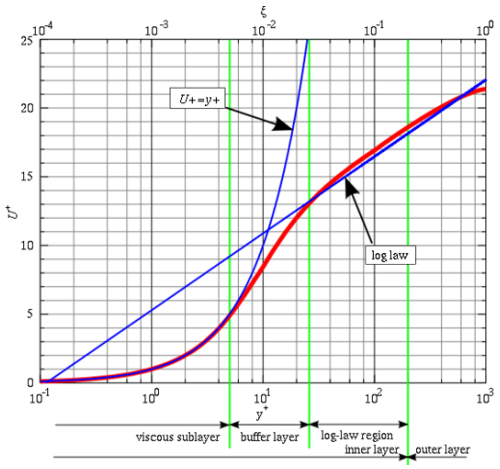


Figure 10.34.: The law of the wall [Simscale, 2018].

Away from the walls: Realizable k–ϵ model

The viscous model allows to set parameters for inviscid, laminar, and turbulent flow. In this case the 'Realizable k–ϵ'turbulence model was selected. The realizable k–ϵ model gives a general description of the turbulence through two transport equations. The first equation, for turbulent kinetic energy (k), is solved for k, and is shown in Equation 10.3. In this equation u_i, is the velocity component in direction i, G_k represents the generation of turbulence kinetic energy due to the mean velocity gradients, G_b is the generation of turbulence kinetic energy due to buoyancy and μ_t represents the eddy viscosity, and Y_m represents the contribution of the fluctuating dilatation in compressible turbulence to the overall dissipation rate. S_k is a source term. [Launder and Spalding, 1974; ANSYS, 2019]

$$\frac{d}{dt}(\rho \ k) \ + \ \frac{d}{dx_i}(\rho \ k \ u_i) \ = \ \frac{d}{dx_i}[\mu + \frac{\mu_t}{\sigma_k} \ \frac{d}{dx_j}(k)] \ + \ G_k \ + G_b \ - \ \rho \ \epsilon \ - Y_M \ + S_k \tag{10.3}$$

The equation for dissipation (ϵ), is shown in Equation 10.4, where S_ϵ is a source term, and $S = \sqrt{2 \ S_{ij} \ S_{ij}}$. In these equations $C_{1,\epsilon)}$, $C_{2,\epsilon)}$, $C_{3,\epsilon)}$ σ_k and σ_ϵ are model constants.[Launder and Spalding, 1974; ANSYS, 2019]

$$\frac{d}{dt}(\epsilon\, k) + \frac{d}{dx_i}(\rho\, \epsilon\, u_i) = \frac{d}{dx_i}[\mu + \frac{\mu_t}{\sigma_\epsilon}\frac{d}{dx_j}(\epsilon)] + \rho\, C_{1,\epsilon}\, S\, \epsilon - \rho\, C_{2,\epsilon}\frac{\epsilon^2}{k + \sqrt{\nu\, \epsilon}} + C_{1,\epsilon}\frac{\epsilon}{k}\, C_{3,\epsilon}\, G_b + S_\epsilon \quad (10.4)$$

These equations can be summarized as: the rate of change for k or *epsilon* + the transport of k or *epsilon* by convection = transport of k or *epsilon* by diffusion + Rate of production of k or *epsilon* - rate of destruction of k or *epsilon*.

Close to the walls: SST k–Ω model

The shear-stress transport (SST) k–Ω model uses a blending function, designed to be 1 in the near wall region, where the equations for the k–Ω model are used, and 0 away from the surface, which activates the k–ϵ model. The equations are shown in Equations 10.5 and 10.6. Similar to the k–ϵ model hese equations can be summarized as: the rate of change for k or Ω + the transport of k or Ω by convection = transport of k or Ω by diffusion + Rate of production of k or Ω - rate of destruction of k or Ω.

$$\frac{d}{dt}(\rho\, k) + \frac{d}{dx_i}(\rho\, k\, u_i) = \frac{d}{dx_j}[\Gamma_k\, \frac{d}{dx_j}(k)] + G_k - Y_k - + S_k \quad (10.5)$$

$$\frac{d}{dt}(\rho\, \omega) + \frac{d}{dx_i}(\rho\, \omega\, u_i) = \frac{d}{dx_j}[\Gamma_\omega\, \frac{d}{dx_j}(\omega)] + G_\omega - Y_\omega - + D_\omega + S_\omega \quad (10.6)$$

In these equations G are generation terms, Γ represents the diffusivity, Y the dissipation, D is a cross-diffusion term, and S is a source term.

Wall modelling approach: modelling the viscous sublayer

With the k–Ω model, the viscous sublayer is resolved, meaning that the $y+$ value of the first cell should be smaller than 5 (preferably $y+ \approx 1$), and a growth rate no larger than 1.2. The principal is shown in Figure 10.35 [ANSYS, 2019].

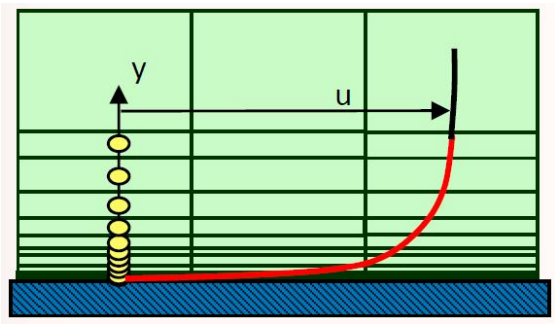


Figure 10.35.: Viscous sublayer resolving approach used to resolve boundary layer[ANSYS, 2019].

Simulation: Boundary conditions

The conditions at the in- and outlet of both the grease interceptor and the different baffles and walls, are set by introducing boundary conditions. The different boundary conditions are set as described in this section.

- **Inlets**

Full geometry

Both the inlet of the grease interceptor, and the inlet of the heat exchanger, have been set as a velocity inlet, to which a thermal component is added, related to the solving of the energy equation. The average inlet velocity was used, observed during the steady state of the respective experimental runs. Similarly, in the thermal part of the inlet flow definition, the temperature was set to the average temperature during the steady state of the respective environmental runs. The set points of the different parameters, as set in the simulation runs used for validation, are summarized in Table 10.9, where the temperatures are the inlet temperatures.

Wastewater			**Fresh Water**		
Temperature ($°C$)	**Flow** (l/min)	**Velocity** (m/s)	**Temperature** ($°C$)	**Flow** (l/min)	**Velocity** (m/s)
28.97	2.06	0.0216	10.13	0.83	0.0950
27.77	1.95	0.0205	9.01	2.93	0.3366
27.31	1.91	0.0200	8.77	5.21	0.5972
27.64	1.97	0.0207	8.72	6.17	0.7076
29.33	3.98	0.0417	10.16	0.88	0.1010
28.38	3.99	0.0418	8.92	2.93	0.3358
28.03	3.88	0.0407	8.70	5.17	0.5931
27.99	3.97	0.0416	8.91	6.16	0.7065
37.08	1.99	0.0209	10.77	1.03	0.1182
36.38	2.01	0.0211	9.07	3.16	0.3626
36.30	1.95	0.0204	8.98	5.26	0.6035
35.61	2.02	0.0212	8.76	6.31	0.7240
38.00	4.03	0.0422	9.74	1.07	0.1182
36.99	4.04	0.0423	8.77	3.06	0.3626
36.73	4.02	0.0421	8.83	5.26	0.6035
34.72	3.57	0.0374	8.38	6.29	0.7217

Table 10.9.: Specific set points of the simulation runs, during the validation process.

Sliced geometry

Similarly, for the sliced geometery, the inlet velocity of the wastewater body was adjusted for the larger cross section. The temperature at the inlet was set to the temperature at the first row of sensors (see Figure 10.10). These adjusted values are shown in Table 10.10.

Wastewater			Fresh Water		
Temperature ($°C$)	**Flow** (l/min)	**Velocity** (m/s)	**Temperature** ($°C$)	**Flow** (l/min)	**Velocity** (m/s)
28.38	2.06	0.000186	10.13	0.83	0.0950
26.30	1.95	0.000176	9.01	2.93	0.3366
25.75	1.91	0.000172	8.77	5.21	0.5972
25.73	1.97	0.000178	8.72	6.17	0.7076
29.18	3.98	0.000359	10.16	0.88	0.1010
27.94	3.99	0.000359	8.92	2.93	0.3358
27.63	3.88	0.000350	8.70	5.17	0.5931
27.52	3.97	0.000358	8.91	6.16	0.7065
35.38	1.99	0.000179	10.77	1.03	0.1182
33.53	2.01	0.000181	9.07	3.16	0.3626
32.55	1.95	0.000176	8.98	5.26	0.6035
32.40	2.02	0.000182	8.76	6.31	0.7240
37.53	4.03	0.000363	9.74	1.07	0.1182
36.06	4.04	0.000364	8.77	3.06	0.3626
35.61	4.02	0.000362	8.83	5.26	0.6035
33.40	3.57	0.000322	8.38	6.29	0.7217

Table 10.10.: Specific set points of the simulation runs, during the validation process, using the sliced geometry.

- **Outlets**

All outlets (both the outlet of the grease interceptor, and of the heat exchanger) were set as pressure outlet with the external pressure being atmospheric pressure. The backflow temperature was set to the temperature of the surroundings during the lab experiments ($18°C$).

- **Walls**

Three different types of walls can be identified:

1. **The outer walls and lid of the grease interceptor**.

   The outer walls are set as stationary walls, allowing no flow through them. Their thermal behaviour is set by a fixed outer temperature. The temperature of the environment was set to the temperature of the surroundings during the lab experiments ($18°C$), and the heat exchange coefficient was set to a typical value for the specific material, as shown in Table 10.11. The thickness was set to 2.5 mm.

Grease interceptor lid	
Material	Aluminium
Heat exchange coefficient	
Grease interceptor side walls	
Material	Stainless steel
Heat exchange coefficient	

Table 10.11.: The heat exchange characteristics of the specific materials of the outer walls of the heat exchanger.

2. **The inner walls of the grease interceptor (baffles).**

   The baffles, inside the grease interceptor, were set as stationary walls, their thermal behaviour was set through the interface between the fluid (wastewater), and the solid (the steel baffle). This is explained in the next section.

3. **The walls of the heat exchanger.**

   The heat exchanger walls, were considered to be an interface, on both sides of the heat exchanger, as is explained in the next section.

- **Interfaces**

  Two types of interfaces are distinguished in this simulation:

1. **The interface between fluids and solids.**

   The interface between fluids and solids was set to a coupled wall function, meaning that the thermal behaviour is determined by system coupling, and the characteristics of the modeled solid. In this case a 'shadow wall'is created to ensure that each side of the wall is a distinct zone. This is shown for the heat exchanger in Figure 10.36.

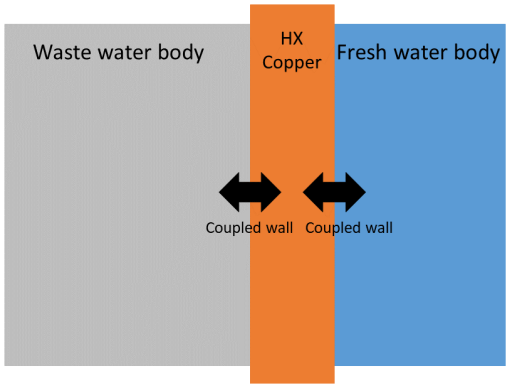


Figure 10.36.: The coupled walls for the heat exchanger fluid-solid interfaces.

2. **The interface between the coarse and the fine mesh.**

   The interface between the fine and the coarse mesh was ensured by a matching interface, ensuring that, at the contact surface the parameters are continuous.

Post-processing

During the validation phase of the project, the post-processing was used for three purposes:

1. **Verification of the dimensionless wall distance ($y+$).**

   The first step in the post-processing is to verify that the values for the dimensionless wall distance ($y+$) was within the acceptable parameters for the selected modelling method of the wall (see earlier this Section). This verification is done for the highest flow velocities hence the case where the wastewater flow is 4 l/min and the fresh water flow is 6 l/min. The $y+$ values were highest on the wall between the heat exchanger and the fresh water.

2. **The verification of the mesh independence, through the grid convergence index.**

   The grid convergence index (GCI) is a method of quantifying and reporting the discretization error for CFD simulations. When the calculated GCI is below the set tolerance, the simulation is said to be independent from the mesh size, meaning that a finer mesh will not result in significant change in the result of the simulation [Celik et al., 2008]. The GCI is calculated in five steps:

   a) Defining the mesh size. The mesh size (h) is defined as in Equation 10.7, where ΔV_i is the volume of the ith cell and N is the total number of cells.

$$h = [\frac{1}{N}\sum_{i=1}^{N}(\Delta V_i)]^{1/3} \tag{10.7}$$

b) Selecting three significantly different sets of mesh sizes, and run simulations, determining the results for key variables. The variables ϕ are considered (in this case the outlet temperature of both the grease interceptor, and the heat exchanger), the grid refinement factor is defined as $r = h_{coarse}/h_{fine}$.

c) Calculating the apparent order (p). The apparent order (p) is calculated using Equation 10.8, when a constant r is chosen. Where $\epsilon_{32} = \phi_3 - \phi_2$

$$p = \frac{1}{ln(r_{21})}|ln|\epsilon_{32}/\epsilon_{21}|| \tag{10.8}$$

d) Calculating the extrapolated values.

The extrapolated value can be calculated using Equation 10.9.

$$\phi_{ext}^{21} = (r_{21}^p\phi_1 - \phi_2))/(r_{21}^p - 1) \tag{10.9}$$

e) Calculating and reporting the error estimates.

The error estimates to be reported are the approximate relative error (Equation 10.10), the extrapolated relative error (Equation 10.11), and the grid convergence index (GCI, Equation 10.12).

$$e_a^{21} = |\frac{\phi_1 - \phi_2}{\phi_1}| \tag{10.10}$$

$$e_{ext}^{21} = |\frac{\phi_{ext}^{12} - \phi_1}{\phi_{ext}^{12}}| \tag{10.11}$$

$$GCI^{21} = \frac{1.25\ e_a^{21}}{r_{21}^p - 1} \tag{10.12}$$

Full geometry

For the full geometry, the error estimates were calculated along three different lines in the wastewater body, with 30 verification points on each line, and two lines across the outlets, for both the grease interceptor and the heat exchanger, with 10 verification points on each line, as shown in Figure 10.37.

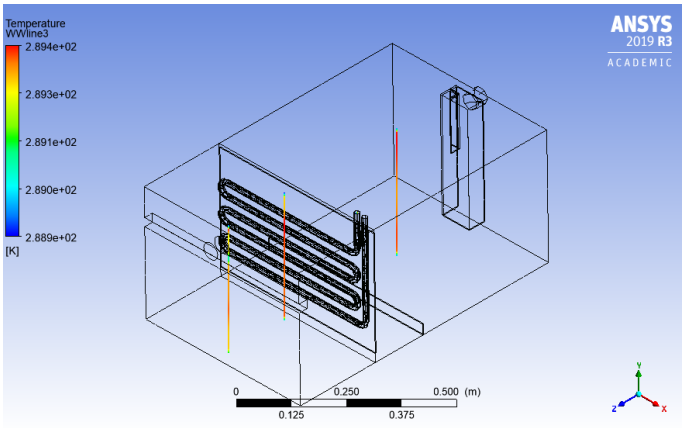


Figure 10.37.: Location of the verification control lines.

Sliced geometry

The verification of the GCI for the sliced geometry was done across four lines, containing 20 points each, in the wastewater body, and across two lines, containing 10 points each in the fresh water body, as shown in Figure 10.38.

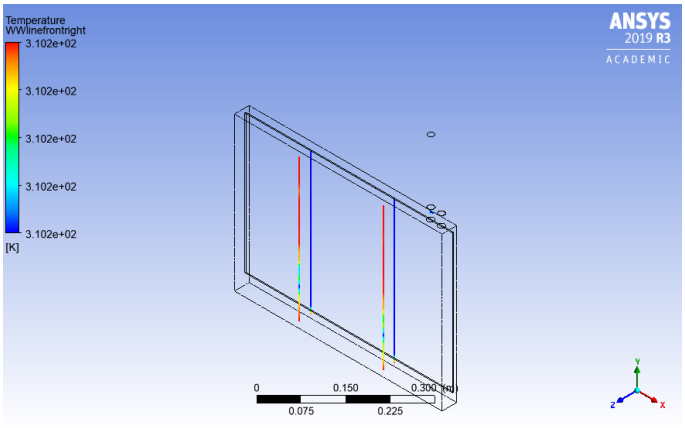


Figure 10.38.: Location of the verification control lines in the sliced geometry.

3. **The validation of the numerical model, through comparison with experimental results.**

   The model was validated by comparing the simulation results to the spread as observed during the steady state of the experimental runs. When the simulation results fall within the experimental spread, they are considered validated. The key variables considered were the outlet temperature of the grease interceptor and of the heat exchanger.

10.6.3. Simulation results and discussion

Dimensionless wall distance ($y+$)

As can be seen in Figure 10.39, the maximal dimensionless wall distance was 2.37, well below the limit of the viscous sublayer (5). Additionally, the recommended value for simulation ($y+ \approx 1$), was reached for the bulk of the cells on the wall layer, as shown for the highest fresh water flow rate (6 l/min) in Figure 10.39.

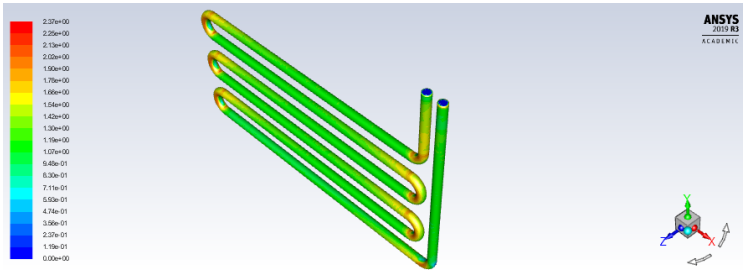


Figure 10.39.: Dimensionless wall distance at the wall of the fresh water, for a fresh water flow rate of 6 l/min.

Mesh independence

The mesh is considered to be independent when the grid convergence index was found below the set tolerance (5%) in this case). The verification for both the full and the sliced geometry is discussed in this section.

- **Full geometry**

  The verification of the mesh independence was done for the mesh zones of interest:

1. The finely meshed zone around the heat exchanger.

   The grid convergence index was calculated along a line at the outlet of the heat exchanger, as mentioned in section 10.6.2. They are shown in Figure 10.40. One can observe that these GCIs are well below the tolerance, however to comply with the requirements of Skewness and orthogonal quality, the mesh size (see Section 10.6.2) was set to 3.5 mm. An inflation layer was set up at the wall between the fresh water and copper of the heat exchanger (See Figure 10.32).

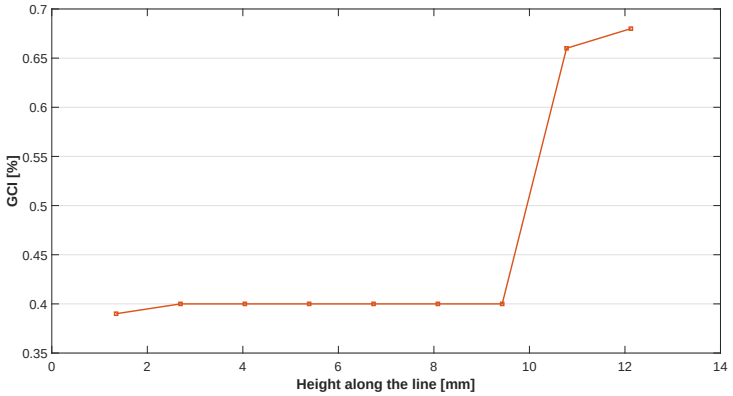


Figure 10.40.: GCI for the fine mesh.

2. The more coarsely meshed zone in the rest of the wastewater body.

   The grid convergence index was calculated along three lines in the wastewater body, as mentioned in section 10.6.2. They are shown in Figure 10.41. One can observe that these GCIs are well below the tolerance, however to comply with the requirements of Skewness and orthogonal quality, the mesh size (see Section 10.6.2) was set to 7.5 mm.

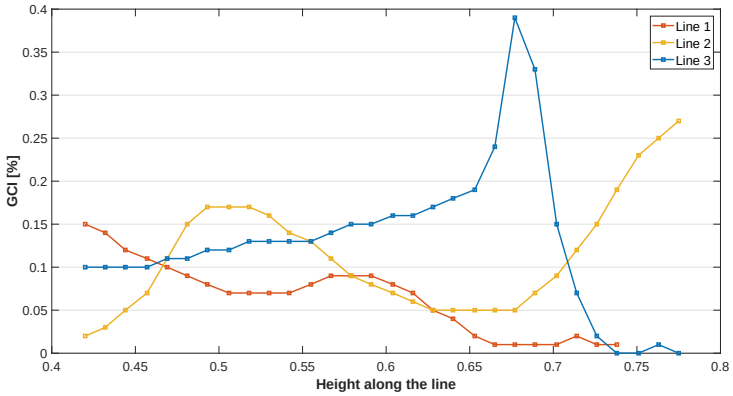


Figure 10.41.: GCI for the coarser mesh.

- **Sliced geometry**

In the sliced geometry, the grid independence was measured along four lines in the wastewater body, and along two lines at the outlet of the heat exchanger (see Figure 10.38):

1. Grid convergence index in the wastewater body.

   In the wastewater body, the observed GCI was below 0.5% at all locations, as shown in Figure 10.42.

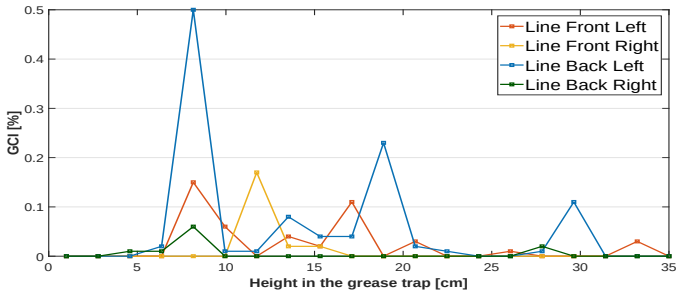


Figure 10.42.: GCI in the wastewater body.

2. Grid convergence index at the heat exchanger outlet.

   At the heat exchanger outlet, the observed GCI reached a maximum of 3.8% across the diameter, as shown in Figure 10.43.

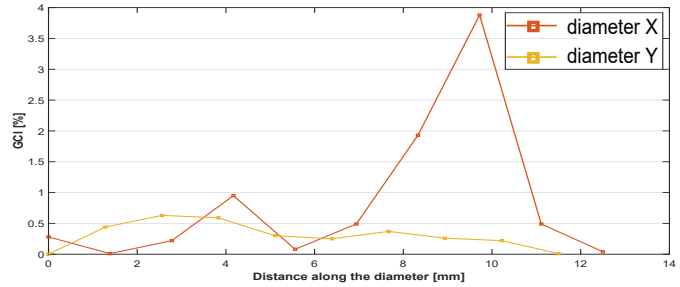


Figure 10.43.: GCI at the heat exchanger outlet.

Model validation

- **Comparing the full geometry with the sliced geometry**

Both the full and sliced geometry were simulated resulting in a relative difference ranging from 1.6 to 8.2% (in $°C$, in K this difference ranged from 0.1 to 0.4%), and an absolute difference ranging from 0.06 to 1.28$°C$. As shown in Figures 10.44 and 10.45. In these figures, one can also observe that the difference is larger at lower flow rates.

The difference between these two models was deemed small enough to consider simulation of both geometries as equivalent. For reasons of improved precision and reduced cell count, in future analysis, the sliced geometry was used.

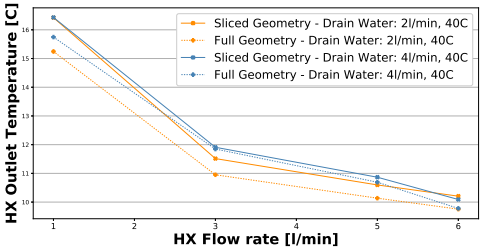


Figure 10.44.: Comparison of simulated results for the full and sliced geometry for a wastewater flow at $40°C$.

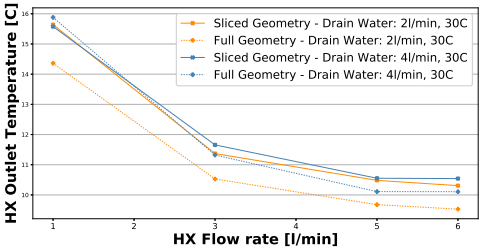


Figure 10.45.: Comparison of simulated results for the full and sliced geometry for a wastewater flow at $30°C$.

- **Comparing the sliced geometry with the experimental results**

The validation step in the model development consisted of comparing the results of the simulation to the results of the experimental analysis. This is done through the comparison of the variable of interest, which is the Outlet temperature of the heat exchanger in this case. In Figures 10.46 (for $40°C$) and 10.47 (for $30°C$), one can observe that simulated results fall out of the spread of experimental results. The difference was large at small fresh water flow rates ($25-34\%$ at a fresh water flow rate of 1 l/min), than at great fresh water flow rates ($3.6-17\%$ at a fresh water flow rate of 6 l/min). The error is also smaller at a lower wastewater temperature. This means that the simulation was not validated, and can not be used for quantitative analysis.

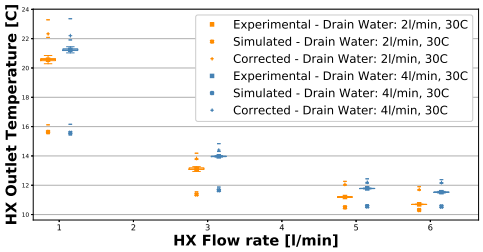


Figure 10.46.: Comparison of simulated and experimental results for a wastewater flow at $40°C$.

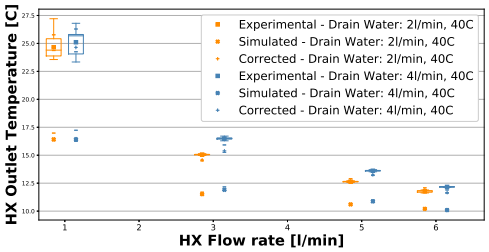


Figure 10.47.: Comparison of simulated and experimental results for a wastewater flow at $30°C$.

As can be seen in Figure 10.48, the relationship between experimental and simulated temperature (for all simulation-experiment pairs) was close to linear ($R^2 = 0.9782$). However, applying this correction to the simulated temperature did not result in a validated model, as can be seen in Figures 10.46 and 10.47.

The validation step in the process showed that the model was not equivalent to the experimental (real world) result. The simulation model, in the current state, does not result in reliable real world values. The hypothesis being that this is due to the difficulty of simulating both laminar and turbulent flow. However, the model was still used to make qualitative comparisons, when comparing the prototype to new designs, or different operating conditions. This was done using the same set-up of the simulation model.

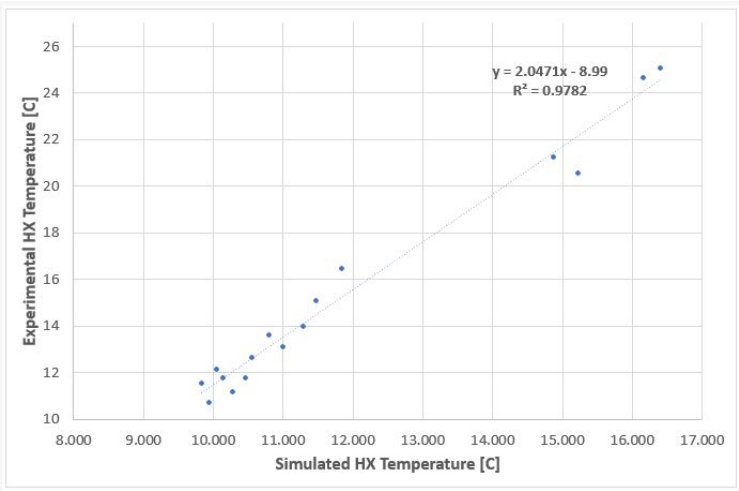


Figure 10.48.: Approximate linear relationship between the experimental and simulated outlet temperature of the heat exchanger.

10.7. Design of the heat recovery unit

Two different analysis were performed in the further evolution of the prototype:

1. Emulating the FOG mix.
2. Simulating the changed design.

In a first further step, the changed thermal characteristics of mixture of water, fat, oil and grease (FOG) were emulated, by changing the fluid characteristics, this is described in Section 10.7.1. In a second step, two options for an alternative design of the heat exchanger were studied, as discussed in 10.7.2.

These changes can only be compared qualitatively, as the numerical model was not validated. They serve as a stepping stone towards further development of the prototype, further improving the Technology Readiness Level (TRL), towards a commercially applicable product.

10.7.1. FOG simulation

The experiments, and the validation simulations were performed with fresh water, and the related thermal characteristics. In the practical case of an operational grease interceptor, the interceptor is filled with drain water from a kitchen application. Drain water from kitchens is heavily loaded in fat, oil and grease (FOG), the simulations described in this section, aim at showing the effect of these added components.

Emulating the FOG mix

The FOG mix was emulated by representing the wastewater as perfect mixture of water and vegetable oil. The characteristics were calculated based on Equation 10.13, where ϕ is the characteristic, and m is the mass of FOG or water (w), respectively.

$$\phi_{mix} = \frac{m_{FOG} + m_w}{\frac{m_{FOG}}{\phi_{FOG}} + \frac{m_w}{\phi_w}} \tag{10.13}$$

The characteristics of the mixture were determined based on a concentration of vegetable oil of 1250 mg/l [Gallimore et al., 2011]. The characteristics for water, vegetable oil, and the mix are shown in Table 10.12.

	Density $\rho\ (kg/m^3)$	**Specific heat** $C_p\ (kJ/kgK)$	**Kinematic viscosity** $\nu\ (kg/ms)$	**Thermal conductivity** $\lambda\ (W/mK)$
Water	998.2	4.18	0.001003	0.6
Vegetable oil	920	1.67	0.034	0.16
FOG mix	953.07	2.28	0.00218	0.237

Table 10.12.: Thermal characteristics of the fluids.

Limitations of the approach

This approach represents the mixture of water and fat, oil and grease as a perfect mixture, when it is, in fact, an emulsion. The FOG matter is suspended in the water, and the objective of grease interceptors is to break this emulsion, and create a stratified system, where FOG floats on top of the water body.

This emulsion could show Non-Newtonian behaviour, meaning that it does not follow Newton's law of viscosity [Cengel Yunus, 2006]. This law is implicitly incorporated in the model set-up of the CFD simulation. The temperature and flow evolution in the wastewater body could thus be different than simulated with CFD, and this would, in turn, impact the recovered heat. A detailed study of Non-Newtonian fluid simulations should be performed in future work.

Effect on heat recovery

Figures 10.49 (for $40°C$) and 10.50 (for $30°C$) shows a slightly increased outlet temperature when working with the FOG emulation fluid. Meaning that working with actual wastewater should, slightly, improve the effectiveness.

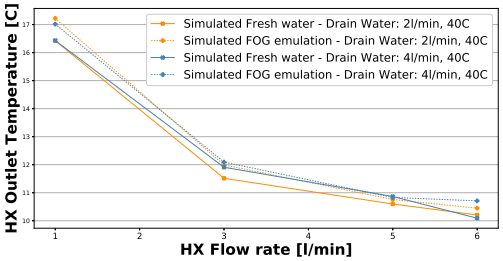


Figure 10.49.: Comparison between the outlet temperature of the heat exchanger for clean water, and the FOG emulation fluid at $40°C$.

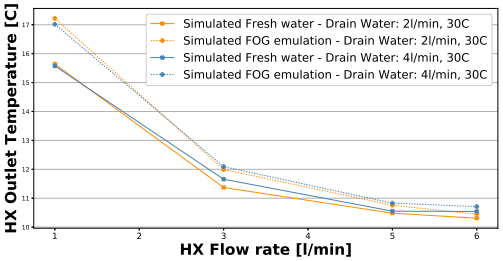


Figure 10.50.: Comparison between the outlet temperature of the heat exchanger for clean water, and the FOG emulation fluid at $30°C$.

In the further development, this simulation should be modified to incorporate the Non-Newtonion behaviour of the emulsion. The effect of the separation of water and FOGs on the performance of the heat recovery system should be studied. In addition to this, the effect of heat recovery on the separation of water and FOGs should also be studied.

10.7.2. Heat exchanger integrated in the baffle

In this section, an alternative design for the heat exchanger is discussed. The idea behind this different design was to integrate the heat exchanger into the baffle of the grease trap. This allows for additional space saving, and, compared to the experimental unit, described in Section 10.3.3, a reduced risk of material deposition (fouling), and thus a reduced risk of reduction of the efficiency over time.

Heat exchanger design

The baffle, with integrated heat exchanger, consists of a baffle with thickness of 15 mm, with an integrated, 10-pipe heat exchanger of diameter 13.5 mm. A rendering of the heat exchanger, integrated in the grease interceptor, is shown in Figure 10.52. The technical drawing of the system is shown in Figure 10.52.

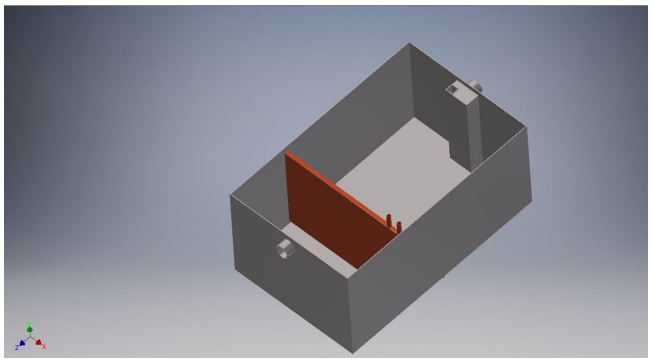


Figure 10.51.: Rendering of the heat exchanger, integrated into the baffle of the grease interceptor.

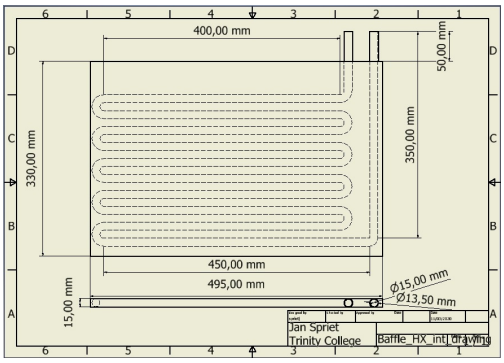


Figure 10.52.: Technical drawing of the heat exchanger, integrated into the baffle of the grease interceptor.

This design has an outer surface of the baffle, in contact with the wastewater of 0.34 m^2 and a heat exchange surface of 0.21 m^2, about 50% larger than the tested prototype. One can also observe that this design would use a much larger amount of copper. Because copper is more expensive than, for example, stainless steel (the material of the grease interceptor), a financial optimum should be found, balancing the additional heat recovery by using more copper, to the additional cost.

Effect on heat recovery

In Figures 10.53 (for 40°C) and 10.54 (for 30°C), one can observe that the outlet temperature of the heat exchanger, and thus the recovered heat, was increased by this changed design. This was mainly observed at higher fresh water flows. This could prove to be a great advantage, for an unregulated system, where the incoming fresh water would be directed through the heat exchanger without a flow control system, as the flow rate could show a great variation in this case.

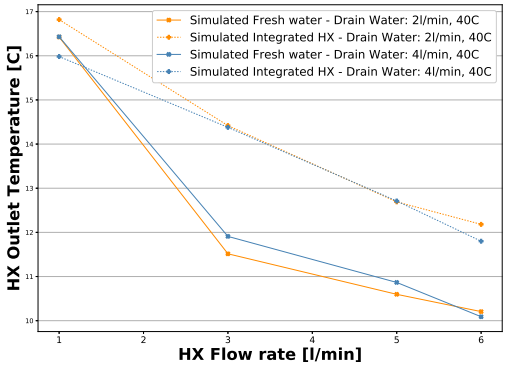


Figure 10.53.: Comparison between the outlet temperature of the heat exchanger for the initial, and improved design at 40°C.

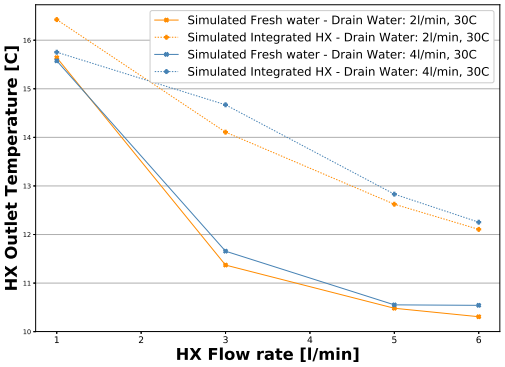


Figure 10.54.: Comparison between the outlet temperature of the heat exchanger for the initial, and improved design at 30°C.

10.8. Summary

10.8.1. Discussion

Chapter 6 showed a large potential for drain water heat recovery in commercial kitchens, however, two different limitations for the deployment of existing commercial heat recovery systems were identified:

- The studied systems require the presence of a vertical drop of around 2 m, space which is not always available, and/or might require the use of pumping systems, which also require an energy input.
- At low flow rates, the studied systems are not financially profitable, but can still provide a reduction in related greenhouse gas emissions.

The aim of this prototype was thus to fill this gap in the market, providing a low cost solution for which space constraints are not the limiting factor.

Grease interceptors, devices designed for primary treatment of wastewater from kitchens, separating fat, oil and grease (FOG) out of the wastewater, are mandatory, both in the UK and Ireland for commercial kitchens. This provides the opportunity to integrate a heat recovery device, into this mandatory piece of equipment, reducing space constraints, and cost requirements.

In this chapter a prototype for a heat recovery device, integrated into the grease interceptor was constructed, and tested in controlled, lab conditions. This showed an effectiveness ranging between 23 and 58%, and a recovered heating power varying from 0.6 up to 1.8 kW, depending on the conditions of the wastewater and fresh water flow. Additionally, this heat recovery reduced the temperature of the grease trap, which has positive effects on the FOG removal efficiency. Additional removal of FOG, means that more FOG is trapped in the grease trap, this has the drawback of an increased emptying frequency, however, it has the advantage that, when the removed FOG is treated in anaerobic digesters, additional bio–gas can be recovered. This is another example of the opportunity to utilise waste and wastewater as resource, rather than an end -(waste) product. In the UK this type of heat recovery system, has about 151 560 potential customers, food outlets for which this heat recovery solution is the most profitable option.

In addition to this, a numerical model of the prototype was developed, and simulated using Computational Fluid Dynamics (CFD). This model could not be validated, so only qualitative, rather than quantitative conclusions could be drawn. The prototype was simulated, replacing the pure water, as used during the experiments, by an emulated FOG mixture, representing the kitchen wastewater. This showed an increased heat recovery when the prototype was used with the emulated FOG mixture. However, kitchen wastewater, with suspended FOG, behaves as an emulsion, this represent limitations as to the simulation, which represented the wastewater as a perfect mixture. Further research is required to study the impact of the emulsion behaviour of the wastewater.

In a second step, an alternative design, integrating the heat exchanger into the baffle of the grease interceptor was simulated. This showed a greater amount of heat recovered, when using the alternative design. In addition to this, this baffle – integrated design should reduce the accumulation of bio–materials on the heat exchanger, and thus decrease the risk of fouling. Quantifying these advantages is required in future steps of the prototype development, as is the impact of replacing the stainless steel baffle by a copper system, both in terms of operation and in terms of cost.

A proposal for future development of the prototype is outlined in the next section.

10.8.2. Future work

This chapter describes the first steps in the design of an innovative, heat recovery unit, integrated in grease interceptors for kitchen wastewater. To develop this prototype further, a few key steps are required, firstly in terms of the numerical model:

- Create a validated numerical model of the prototype, tested in lab conditions (see Section 10.3.3).
- Create a model for the emulsion and separation behaviour of the wastewater (the FOG – water mix).

Based on these validated models, the prototype can then evolve further. Below a non–comprehensive list of future research axis are listed:

- Determining the material. Copper, used in the prototype described in this chapter, has good heat (and electric) conduction characteristics, however it is more expensive than for example stainless steel. Furthermore, research is being conducted into thermo–conductive plastics, which could ease the manufacturing of these heat exchangers.
- Determining the mechanical and structural requirements. Depending on the selected material, different requirements will occur for the minimum thickness of the heat exchanger, to be able to withstand the water pressure in the system. Reducing the thickness of the heat exchanger, increases the overall heat transfer (for a fixed material), and thus the amount of required heat. In addition to this, it reduce the amount of material required, and thus the raw material cost.
- Determining the optimal location(s). Based on the selected material(s) an optimal location for the heat exchanger should be selected. In this chapter, heat recovery was only considered at the baffle of the grease interceptor. However, heat exchanger can be installed at all walls of the grease interceptor, increasing the amount of recovered heat, but also increasing the raw-material use.
- Applying a full life-cycle analysis on the prototype design. This life cycle analysis (LCA) allows for the trade-off between environmental impacts made at the manufacturing and installation phase of the heat recovery unit's lifetime on the one hand, and the reduced impact due to reduced fuel consumption (induced by the recovered heat) on the other hand.

These research axes contribute to the definition of an optimal design of the heat exchange unit. This optimal design can be found from a financial perspective, trading–off the cost of additional material, to the benefit of reduced heating costs, through reduced fuel consumption. Alternatively, this optimum can also be found from the perspective of a specific environmental indicator (in this thesis the indicator was mainly GHG emissions, in LCA software often represented by the Global Warming Potential (GWP)), trading off the additional impact of materials, to the reduced impact of reduced fuel consumption.

This optimum design can then be simulated dynamically, through actual kitchen wastewater flow and temperature profiles, to study its transient behaviour. Additionally, a renewed iteration of the prototype can be manufactured, for testing at a pilot site, and/or a living lab.

The information gathered from these experimental tests can then be used to further develop the business case and pricing for this product.

11. Discussion, conclusions and perspectives

11.1. Discussion

In this thesis, the sectoral potential for drain– and wastewater was studied, through three exploitation strategies. At first the potential for heat recovery from individual domestic residences, as, in the EU, 91% of heating is provided in an individual (non district heating) manner (Chapter 5). Later, in Chapter 6 the potential for drain water heat recovery from commercial kitchens was studied. And lastly, in Chapter 7, the potential for indirect heat recovery from the effluent of licensed wastewater treatment plants was studied.

To illustrate how these systems operate, and how they differ between the various sectors, two demonstration sites were installed. The first one, recovering heat from a commercial kitchen at Penrhyn castle, Wales (Chapter 8). A second one, recovering heat from the licensed wastewater treatment system at the ABP meat processing plant in Cahir ,Co. Tipperary, Ireland (Chapter 9.

Lastly, in Chapter 10, a prototype was introduced, integrating heat recovery in the operation of grease interceptor. This aimed at addressing a gap in the market, where current commercial systems were not profitable.

The novelty of this thesis, lies in the application of temporal considerations in considering the feasibility of heat recovery systems, highlighting the importance of mismatches in supply and demand over time. In addition to that, it studies the application of existing commercial systems, in markets and sectors that are currently untouched. Furthermore, it propose a prototype to complement the existing gamma of commercial drain water heat recovery devices.

11.1.1. Exploitation Strategies

In order to study, and optimise the optimal location of heat recovery, within (waste)water networks three different heat recovery locations were considered:

1. DWHR in a domestic setting.
2. DWHR in a commercial kitchen setting.
3. DWHR from the effluent of wastewater treatment plants.

DWHR in a domestic setting

Currently, domestic wastewater accounts for a flow of about 1.42 m^3/day, yearly this accounts for about 4.79 TWH of embedded energy being flushed through the drain, corresponding to about 1.24 $M\ tonsC_e$ emissions, and a cost of 397 $M€$. In addition to this, recovering (all) this heat would increase the share of renewable heat in Ireland's thermal energy mix to $17.4 - 18.4\%$, well above the 12% target for 2020. This thesis described a probabilistic method, for studying the interaction of this heat recovery with the wastewater system.

Temporal mismatches between heat provided by a drain water heat recovery system, and heat consumption are, although often disregarded in literature, a crucial factor in assessing the feasibility of the former. Generally, the only available information for residences is the average monthly consumption. This analysis described a probabilistic method to assess the temporal, daily evolution of DHW and SH demand, and the availability of waste heat in domestic drain water, using observations from 113 residences in the UK. The operation of the drain water heat recovery systems was then predicted to assess the concurrence between the availability of waste heat in drain water, and the heat demand. The temporal aspect impacts the financial viability, and related emission reductions of such systems

The method was applied to assess the feasibility of having drain water source heat pumps, as a means to indirectly recover the waste heat in drain water, for a hypothetical average Irish residence. When using a drain water heat recovery system, a back-up heating system remains necessary. It is generally required right after the consumption peaks, when the accumulated recovered heat is depleted to meet the peak in demand. The share of heat demand that can be met by the DWHR system varies between 8% and 42%. Using a hot water reservoir of 300l can reduce the amount of recovered heat that is unused from 75% without a reservoir to less than 1%, with a reservoir. This shows a mismatch between heat demand and the availability of heat in the wastewater.

Using the DWHR system greenhouse gas emissions related to domestic hot water and space heating can be reduced by 7.6% to 22%. However, this increases heating costs by a factor ranging from 120% to 130%. At current traditional heating prices, the DWHR system for a single residence is not financially competitive with traditional systems, due to its high capital investment.

Policy makers should consider the financial incentivization of domestic DWHR systems to enable the GHG savings of up to 22% to be achieved. Financial incentives which could cover the additional 630€to 680€per year in heating costs, could be an attractive government level investment in GHG reductions, depending on the eventual cost of exceeding reduction targets.

Different choices in exploitation strategy exist, and could counteract this increased cost:

- Moving upstream, where temperatures (and thus energy density) are higher, however the total energy volume is smaller.
- Move downstream, where a larger volume is available, however temperatures will be lower.
- Using hybrid–source heat pumps. This means that a traditional air or ground source heat pump is complemented with a heat recovery from drain- or wastewater, to boost the performance.

DWHR in a commercial kitchen setting

The feasibility of applying commercially available heat exchangers to commercial kitchens was assessed based on financial and environmental criteria, both are a NPV calculated over 10 $years$. The financial criterion showed feasibility threshold values for the water consumption, varying with the heating fuel used in the kitchen. The environmental criterion yielded a feasible solution in all studied cases.

The financial criterion was then applied to estimate the total profitable potential for drain water heat recovery in the hospitality and food service sector in the UK. The fuel price was assumed as the price of the heating mix for hot water heating (6.13 $p£/kWh$) the same method was used for the carbon conversion factor (0.2773 $kg\ C_e/kWh$). Using the aforementioned Monte Carlo method, the study showed a financially attractive drain water heat recovery potential of around 1.24 TWh/yr which could result in a reduction in the global warming potential of the sector of 344 $k\ tons\ C_e/yr$. The outlet type with highest recovery potential was found in kitchens in the Health Care sector. However, in kitchens with low water consumption, unexploited heat recovery potential remains, which should be recovered by other methods.

The installation of the proposed system in all financially feasible outlets in the sector would require an estimated investment of around 101.2 $M£$, which results in an investment cost of around 2.94 $p£/kg\ C_{e,saved}$ over a 10 $year$ lifetime. This ratio is several orders of magnitude smaller than the cost of replacing all current heating systems by heat pumps, it can thus be considered low hanging fruit on the pathway to a less-carbon intensive hot water production in the sector.

Commercially available drain water heat recovery systems could, when installed, exploit around 88% of current potential in drain water heat in commercial kitchens (1.40 TWh/yr) in a manner that is financially profitable. However, this analysis assumes the availability of a 2 m vertical drop in the kitchen drain, required to install the heat exchanger, and thus achieve optimal effectiveness. In case this head is not available, the heat recovery potential would be untapped, as in approximately 160 GWh, in kitchens where the hot water consumption is too small for financial profitability. This corresponds to a reduction in GHG emissions of 44 $k\ tons\ C_e/yr$ and leaves a gap in the market for inexpensive DWHR devices, which could exploit this potential at lower efficiencies.

DWHR from the effluent of wastewater treatment plants

Wastewater treatment plants (WWTP) can generate enormous heat surpluses, and provide the possibility to couple the wastewater infrastructure with the energy system, increasing the energy efficiency at the system level, allowing for power to heat solutions in order to integrate volatile renewable electricity generation and, thus, foster a sustainable energy transition. Yet, the success of these system integrations depends on the availability of energy consumers in proximity of the wastewater treatment plants, and the temporal patterns of energy supply and energy demand. In this analysis the spatial proximity to heat demand was studied, for all wastewater treatment plants in Ireland, an integrated spatio-temporal method was applied to a case study on the treatment plant in Tullamore, Ireland, and the environmental and financial aspects were assessed.

The analysis of 479 WWTPs in the Republic of Ireland, showed a total embedded energy in wastewater treatment effluent of 6.34 TWh/yr, with the largest potential (1.96 TWh/yr) in the Ringsend WWTP. 40 WWTPs are located withing 2 km of a suitable small area with a heat demand density superior to 40 kWh/m^2, these plants have a potential of 4.5 TWh/yr. However, when only the suitable small areas were considered, only 236.55 GWh/yr of consumption could be met. This indicates that wastewater heat recovery from the effluent of WWTPs, as the sole heat source for a district heating network has only a limited market for financially profitable application. However, in the case of heating networks with multiple heat sources, they can provide an interesting interface between the electricity and heat networks.

A three-step methodology was proposed, including an energetic analysis at the WWTP, a spatio-temporal analysis of supply and demand in potential supply areas, and an integrated analysis, overlaying the supply and demand profiles. This allows to account for both the proximity of consumers and potential temporal mismatches between supply and demand. The methodology was applied on a case study in Ireland. The practicability of the suggested concept was shown in this section. Investigations also resulted in 21 to 123 days on which the heat supply from the WWTP is insufficient to meet demand in the zones due to temporal mismatches. However, the net annual excess recovered heat is positive, meaning that on an annual basis, there is more heat available than consumed. If all zones are combined the net annual excess recovered heat is negative, indicating a net need for additional heating systems, but still 124 days of excess remained, indicating that the effluent heat recovery system can be used to meet the baseload heat demand, but must be complemented by other sources.

The daily analysis show that days of heat scarcity mainly occur during the heating period (November-April), but occasional they occur during summer months as well. During these days additional heat sources are needed to bridge the gap between supply and demand. Different possibilities to decrease the dependency on the back-up heating system are proposed, including day-to-day thermal storage, drying woodchips for interseasonal storage and the development of new supply zones in the vicinity of the WWTP (mainly industrial, commercial and agricultural). Furthermore, WWTP internal use of wastewater heat to substitute digester gas-based CHP generation would make the gas available for other purposes as for instance as a backup for days of supply scarcity of for WWTP external consumption.

The financial and environmental indicators were also assessed, for the case study in Tullamore, Ireland. This showed that the effluent heat recovery system was competitive from a financial point of view, and largely outperformed the classical gas system from an environmental point of view. Effluent heat recovery was concluded to be financially competitive with increasing consumption in the supplied zone.

11.1.2. Design methodologies: Demonstration sites

The heat recovery system for two demonstration sites (also referred to as pilot sites) was designed, constructed and installed, as a way to illustrate how the systems, assessed during the exploitation strategies, operate in a live setting.

Demonstrator at a commercial kitchen

A drain water heat recovery system on the kitchen drain was proposed and installed on the site. The concept of the system was to be able to switch between three configurations, configuration 1, where the water is simply preheated, configuration 2, where the fresh water is recirculated from a buffer tank, through the heat exchanger, and configuration 3, where both these systems are combined. The savings realized by this system were twofold, on the one hand it reduces the fuel consumption related to the hot water heating. On the other hand, reduced heat demand reduces the required flow in the main heating loop on the grounds, resulting in reduced pumping costs.

At Penrhyn castle, configuration 1 was deemed to be most profitable, its expected yearly savings were around 2.1 MWh of heat and around 50 kWh of electricity, resulting in a reduction in related GHG emission ranging from 45 to 780 $kg\ C_e/yr$, and a payback period ranging from 2.8 to 9.5 years, both depending on the current heating fuel on the grounds. Furthermore, the carbon conversion factor for wood pellets in the UK is small, this is because biomass emissions, are considered to be biogenic, and thus non-fossil. This results in reduced GHG savings, however the technical carbon intensity of burning wood is similar to the carbon intensity of coal (even slightly higher due to lower efficiency of the burners) [Sterman et al., 2018]. Gunn et al. [2012] present the opinion that this difference is an inappropriate conceptual basis to assess GHG emissions. For completeness, using the Carbon conversion factor of coal (see Table 8.10) the yearly reduction of Carbon equivalent emissions would increase to 780.40 $kg\ C_e/year$.

These theoretical results are subject to some uncertainties, one being the assumption that the temperature difference over the primary and secondary circuit is kept constant over time, meaning that the control loop only acts on the flow rate, and thus the electric consumption of the pumps. An increased temperature drop would result in a reduction in flow rate, and thus increased savings. Further uncertainty lies in the temporal concurrence of the drain water flow and fresh water flow, the system was assessed on an hourly basis, but there could still be a temporal mismatch between the drain water flow and fresh water flow within this timestep. There was no real data available regarding this issue, as only the fresh water could be measured. This would reduce the amount of recovered heat. Configurations 2 and 3 were designed to counter this.

At Penrhyn castle, the installed system could only operate in one of the proposed configurations, configuration 2. This was due to the presence of of an electric box straight under the drain, which had to be circumvented. Because of this diversion, the wastewater travelling horizontally could not reach the preheating heat exchanger, and thus only the reheating loop could be tested. This configuration showed a reduced heat demand from the biomass boiler of about 594 kWh per year. This is significantly lower than the predicted recovery, due to the lower water consumption of the kitchen during this operation period than at the time of the feasibility study (293.05 l/day vs 652.5 l/day). This configuration of the heat recovery system was not financially profitable (payback period larger than 10 years), at the observed flow rates, neither in the feasibility study, nor in the experimental observation, although it provided a reduction in technical GHG emissions ranging from 50 to 150 kg/yr.

Configuration 1, where the incoming fresh water is simply preheated, was the simplest solution, and was deemed the most profitable. This is mainly due to its smaller capital investment, and the fact that no additional pumping is required.

Due to the COVID-19 pandemic, the castle has closed at the end of March 2020 and the 2020 tourist season is likely to be severely impacted. The resulting hot water consumption at the castle in 2020 is therefore not expected to be a true reflection of seasonal performance. A full picture can not be obtained until the end of 2021.

Demonstrator in the meat processing industry

A moveable experimental unit was designed, combining both a direct and a hybrid heat recovery system. The idea for this experimental unit was to be able to test the system at different locations in the wastewater treatment works. The feasibility study for this heat recovery system, showed a potential heat recovery ranging from 80 to 130 $MWh/year$. The estimated payback period at the test site in Ireland was predicted to be between 2 and 15 $years$, depending on the heating fuel it is replacing. The system could save up to 35 $tons$ in carbon equivalent emissions, each year. When comparing the direct and hybrid heat recovery systems, it was concluded that, from an environmental perspective, the hybrid system was the favoured system. However, from a financial perspective there was more ambiguity to the results.

The experimental unit was assembled in house at the Civil, Structural and Environmental Engineering Department of Trinity College Dublin, and it was delivered to the ABP premises in December 2019. The first operational tests were performed on the effluent of the treatment works, where the direct heat recovery system recovered 250 kWh, the preheating system, part of the hybrid heat recovery system supplied 90 kWh, whereas the heat pump delivered 59.4 kWh, at a COP of 3.49. These savings, although significant, have the disadvantage of occurring through the night. As consumption occurs during the day, this temporal mismatch of heat recovery and heat consumption would reduce the amount of heat that could be used in a practical manner. Furthermore, earlier in the treatment works much larger quantities of heat are available.

To avoid clogging of the pump, at the highly loaded inlet, the experimental unit was moved to the DAF outlet, where it operated for 5 days, with an average heat recovery of around $120 - 140$ kWh/day, at 8.5 kW. This means that this experimental unit alone would save the equivalent of the heat consumption of an entire household. Extrapolating these experimental results, indicated a payback period ranging from 2.5 to 9 $years$, and emission savings of up to 10.69 $ton\ C_e/yr$. After 5 days, the operation was interrupted because the set-up of the experimental unit required an additional forward feed in the wastewater treatment system, requiring higher chemical dosing, and thus increased operation costs. An attempt at in–line set up of the experimental unit resulted in a pressurized system, for which the unit was not designed, and which thus required significant alterations. The hybrid system could not be studied, because, due to flow variations in the fresh water circuit, the power requirement repeatedly exceeded the heat pump's operational limits, causing repeated safety shut–downs of the heat pump.

An effluent heat source heat pump was proposed to counteract this problem, showing a lower cost of heating than the brine source heat pump of the hybrid heat recovery unit. The recommended system consisted of a direct heat recovery system, located at the DAF outlet and an indirect heat recovery system, using an effluent source heat pump, at the outlet of the wastewater treatment system.

Extrapolating the experimental results observed at ABP, Cahir, indicated a payback period ranging from 2.5 to 9 $years$, and emission savings of up to 10.69 $ton\ C_e/yr$, for a direct heat recovery system. A 5 kW effluent source heat pump didn't prove to be financially profitable, compared to classical, fossil fuel heating systems. A possibility to improve financial competitiveness, is scaling up the system. At ABP, Cahir, a 248 kW system was largely within the possibilities, and would be financially attractive, compared to all considered fuel alternatives. In addition to this, in case these fossil fuel systems would be phased out in future policies, as is mentioned for example, in the UK's 'Clean Growth Strategy'[HM Government, 2018], or when low–cost electricity is available on–site (for example, thanks to on–site renewable production), the competitiveness of the effluent source heat pump is improved.

In short, when compared to natural gas boiler (the current heating source), the experimental direct heat recovery system, installed at the DAF outlet would reduce GHG emissions with 4.53 $ton\ C_e$ per year, and have a payback period just under 9 years. The effluent source heat pump of 5 kW is not financially profitable, however a 248 kW system, well within reach at ABP, Cahir, would have a payback period of around 5.5 years, and would reduce GHG emissions by 40.91% compared to the gas boiler, equivalent to 56.32 $ton\ C_e$ per year.

11.1.3. Prototype development

The study of exploiting strategies showed a large potential for drain water heat recovery in commercial kitchens, however, two different limitations for the deployment of existing commercial heat recovery systems were identified: i) the space requirements , ii) untapped potential at low flow rates.

The aim of this prototype was thus to fill this gap in the market, providing a low cost solution for which space constraints are not the limiting factor. Grease interceptors, devices designed for primary treatment of wastewater from kitchens, separating fat, oil and grease (FOG) out of the wastewater, are mandatory, both in the UK and Ireland for commercial kitchens.

A prototype for a heat recovery device, integrated into the grease interceptor was constructed, and tested in lab conditions. This showed an effectiveness ranging between 23 and 58%, and a recovered heating power between 0.6 and 1.8 kW, depending on the conditions of the wastewater and fresh water flow. Additionally, this heat recovery reduced the temperature of the grease trap, which has positive effects on the FOG removal efficiency. Additional removal of FOG, means that more FOG is trapped in the grease trap, this has the drawback of an increased emptying frequency, however, it has the advantage that, when the removed FOG is treated in anaerobic digesters, more bio–gas can be recovered, an opportunity to utilise waste and wastewater as resource, rather than an end –(waste) product. In the UK this type of heat recovery system, has about 151 560 potential customers, food outlets for which this heat recovery solution is the most profitable option.

In addition to this, a numerical model of the prototype was developed, and simulated using Computational Fluid Dynamics (CFD). This model could not be validated, so only qualitative, rather than quantitative conclusions could be drawn. Additionally, kitchen wastewater, with suspended FOG, behaves as an emulsion, this represent limitations as to the simulation, which represented the wastewater as a perfect mixture. Further research is required to study the impact of the emulsion behaviour of the wastewater.

In a second step, an alternative design, integrating the heat exchanger into the baffle of the grease interceptor was simulated. The baffle–integrated design should reduce the accumulation of bio–materials on the heat exchanger, and thus decrease the risk of fouling. Quantifying these advantages is required in future steps of the prototype development, as is the impact of replacing the stainless steel baffle by a copper system, both in terms of operation and in terms of cost.

11.2. Future work and perspectives

Exploitation strategies

In terms of DWHR in a domestic setting, the possibility of hybrid source heat pumps, combining wastewater as a source, with a traditional source (such as the air, or the soil, through brine as a heat carrier), remains a field of study that could be exploited. Especially in remote areas, where wastewater holding tanks are available under the form of on–site wastewater treatment systems. Should the sources of such a system be installed in parallel or series? Does the additional gains in efficiency (and thus increased COP) outweigh the complexity of such a hybrid system? Is it practically exploitable?

The sectoral potential assessment in the food and hospitality sector does not provide certainty on the temporal aspect of the availability of heat, this could introduce temporal mismatches, which could, in turn, reduce the profitability of such systems. A thorough, on–site study of such temporal mismatches would provide insight on their impact and importance. Furthermore, the study assumes the required space is available, but no information is available on how realistic this assumption is.

The sectoral assessment of DWHR from the effluent of licensed wastewater treatment plants assumes the deployment of 4th generation district heating systems, at low temperature, and with multiple heat sources. However, how are these low temperature heating networks implemented in practice? Furthermore, a heat pump requires steady operating conditions, in order to optimize efficiency, how would this be achieved, and what would an interaction with other heating systems look like? A district heating network, fed by a heat pump, could serve as an interface between the electric and the heating energy network. But the practical operation of such an interaction remains to be studied.

Demonstration sites

The demonstration system at Penrhyn castle should be monitored over a longer period of time, looking at the long–term effects of fouling on the operation of the system. Switching the system configuration one, which was deemed more advantageous should also be done, in order to verify the operation of a simplified system.

At ABP, abstraction should be made of issues, and one should determine whether they are related to the experimental nature of the unit, or whether they would translate into a fully integrated heat recovery systems. In order to do this, a longer observation period is required.

Additionally, swimming pools provide good conditions for effluent source heat pumps, as they have a relatively low temperature demand (below $40°C$), and high temperatures of the spillage from the pool itself (generally around $27°C$), this low temperature lift, could provide interesting conditions for indirect DWHR systems. However this was not studied, for lack of data.

Prototype development

Lastly, this thesis described the first steps in the design of an innovative, heat recovery unit, integrated in grease interceptors for kitchen wastewater. To develop this prototype further, a few key steps are required, firstly in terms of creating a validated numerical model, both for the prototype, and for the emulsive behaviour of the wastewater (the FOG – water mix).

Based on these validated models, the prototype can then evolve further. Below a non–comprehensive list of future research axis are listed:

- Selecting a suitable, optimal material for the heat exchanger.
- Determining the mechanical and structural requirements.
- Determining the optimal location(s) in the grease interceptor.
- Applying a full life-cycle analysis on the prototype design.

These research axes contribute to the definition of an optimal design of the heat exchange unit. This optimal design can be found from a financial perspective, trading–off the cost of additional material, to the benefit of reduced heating costs, through reduced fuel consumption. Alternatively, this optimum can also be found from the perspective of a specific environmental indicator (in this thesis the indicator was mainly GHG emissions, in LCA software often represented by the Global Warming Potential (GWP)), trading off the additional impact of materials, to the reduced impact of reduced fuel consumption.

11.3. Research purpose

The answers to the research questions are summarized as follows:

1. *How can DWHR contribute to the current heating mix, and to reaching emission reduction and renewable heating targets?*

   DWHR can contribute to the reduction of emissions in two ways: (i) by reducing the fuel demand of traditional heating systems. (ii) by providing a high–temperature heat source for heat pumps, providing an additional renewable heating alternative, with low carbon intensity (depending on the heating mix). The former can be achieved by direct heat recovery at locations where high temperature wastewater is available (such as kitchens, shower systems, lavatories, etc.), but where the wastewater flow is intermittent, and less predictable. This heat recovery method is characterised by a low capital investment, but requires an additional heating source. The total amount of recovered energy is low, however it is performed at low cost. This results in a limited impact on the total carbon budget of a nation, even when applied nation–wide, but provides the reduction in GHG emissions at a cost that is several orders of magnitude smaller than switching entire energy systems. The latter is usually performed through indirect and/or hybrid heat recovery, in places where a large, steady flow of wastewater is available. These are often found in large sewer collectors or wastewater treatment plants. They present the additional challenge that these are often located at a distance from the

consumer, and require a means of transporting the heat to the consumer. This can be achieved, for example through heating networks. Providing heat in this way can significantly change the energy landscape and mix of a region, and thus have a great effect on GHG reduction targets. This has the added benefit of providing an interface between the electric and heating energy system, through the use of a heat pump, and could thus also be used to attenuate electricity production peaks, caused by the intermittent character of renewable electricity sources such as solar and wind.

2. *How do different situations in different sectors affect the design of DWHR systems? How can DWHR be implemented?*

   As mentioned above, temperature and flow have an important impact on the selection and design of a DWHR system. High temperature, intermittent flow lends itself to direct heat recovery, whereas constant, large flow is more suited for indirect or hybrid heat recovery. The amount of pollutants in the wastewater also affects the design of DWHR systems. Wastewater with a high concentration of suspended solids may not be suited for DWHR systems, or be required to go through primary treatment before heat recovery can be attempted. As these solids clog heat exchangers and other auxiliary equipment. On the other end of the spectrum, fully treated wastewater can still be a valuable source of heat. Contradictory to the widespread belief that the wastewater looses all (or most) of its heat through the treatment process, the temperature of the wastewater leaving the treatment plant still has a significantly higher temperature than the ground or surrounding air during heating season. This was observed in the Tullamore municipal wastewater treatment plant, but also in the industrial wastewater treatment plants of ABP food and Pepsico. The effluent of wastewater treatment plants can be used directly in a water–source heat pump, eliminating the need for intermediary heat carriers. Indirect or hybrid DWHR from the inlet of wastewater treatment plants requires the use of an intermediary heat carrier, to transfer the heat from the wastewater to the heat pump, in order to fully separate the wastewater and heating system. This requires the use of an additional heat exchanger, and thus introduces an additional temperature drop. This added complexity and heat loss could offset the advantage of the higher temperature observed at the inlet of the treatment system, compared to the outlet.

3. *How can the current set of commercially available DWHR system be complemented or extended?*

   Current DWHR systems often require a significant vertical drop, as the effectiveness of the commonly used double-walled heat exchanger is much higher in vertical systems. In a society where space constraints become more and more of a factor, this could prove to be an important bottleneck. To counteract this, the research presented in this thesis looks at integrating the DWHR system in existing, often mandatory, equipment. This could reduce additional space constraints to a minimum, but also reduce installation costs, as qualified personnel can install both systems at once. This thesis focused on integrating DWHR systems into grease interceptors for kitchen wastewater, but the same thought process could also be applied to other equipment, such as septic tanks, DAF units, etc.

11.4. Conclusion: The place of DWHR in the future heating landscape

Heat recovery from drain and wastewater can find its place in the future energy landscape in three different ways, under three different operating conditions.

1. *As an energy efficiency measure.*
   This form represents the use of direct DWHR, to preheat the incoming wastewater, resulting in a reduced heat and fuel consumption of traditional heating systems. This form is particularly suited for locations with high temperatures, but with sporadic or small flow. It is characterised by a low investment cost, but also by relatively small amounts of recovered energy. This makes it particularly suitable for new installations (eg. in new buildings or commercial kitchens), where it can be installed at a minimal added cost, but less so for retrofitting, as these marginal gains may be deemed unworthy of the trouble.

2. *As an efficiency boost for individual heat pump systems.*
   This second form, represents the recovery of heat for individual residences, and could be particularly beneficial for systems in remote areas with low population density. It consists of using the wastewater as an additional heat source for a traditional (air–source or ground–source) heat pump system. As the wastewater has a higher temperature than these traditional sources during most of the heating season, but (for an individual residence), does not contain sufficient energy to meet all heating demand in this building, it could be used as a booster for the temperature of the heat carrier (often brine in ground source heat pumping systems). This boost in temperature would induce a boost in COP of the heat pump.
3. *As the heat source for heating networks.*
   This last form requires the availability of large volumes of wastewater, usually in centralized locations, such as large sewer collectors or wastewater treatment plants. It uses an indirect heat recovery system to provide heat to a network using heat pumps. For this form to be profitable, large quantities of wastewater are necessary to provide economies of scale. However, the centralized locations where these quantities are available are often located at a distance from consumers. Heating networks are thus required for the distribution of the heat to consumers. This can be under the form of district heating, but also the heating network in a factory or industrial plant.

   In addition to this, a wastewater source heat pump could provide for a highly efficient interface between the electric and the heating network. This provides the option for increased flexibility of both networks, required with the growing importance of intermittent renewable source, such as PV and wind, but also solar-thermal heat.

Bibliography

ABP Food Group [2014*a*], 'ABP Food Group is doing more with less and saving on water bills!', *Green Business Resource Efficiency – Case Studies* pp. 30–31.
URL: *greenbusiness.ie*

ABP Food Group [2014*b*], 'ABP Food Group make "Zero Waste to Landfill" possible and reduce carbon footprint', *Green Business Resource Efficiency – Case Studies* pp. 28–29.
URL: *www.greenbusiness.ie*

Alekseiko, L. N., Slesarenko, V. V. and Yudakov, A. A. [2014], 'Combination of wastewater treatment plants and heat pumps', *Pacific Science Review* **16**(1), 36–39.
URL: *https://www.sciencedirect.com/science/article/pii/S1229545014000084*

Alfa Lavel [2020], 'WideGap plate heat exchangers'.
URL: *https://www.alfalaval.com/microsites/gphe/types/widegap/*

Alnahhal, S. and Spremberg, E. [2016], 'Contribution to Exemplary In-House Wastewater Heat Recovery in Berlin, Germany', *Procedia CIRP* **40**, 35–40.
URL: *http://dx.doi.org/10.1016/j.procir.2016.01.046*

Alter, L. [2010], Lessons From The UK Heat Pump Study: Insulate First And Know What You Are Getting.

Amador, J. A. and Loomis, G. W. [2019], *Soil-based Wastewater Treatment*, American Society of Agronomy; Soil Science Society of America; Crop Science Society of America, Kingston, Rhode Island, USA.

ANSYS [2019], ANSYS FLUENT Theory Guide, Technical report.

Backman, P. [2018], The Foodservice Market, Technical report, Peter Backman FS limited, London.

Baek, N. C., Shin, U. C. and Yoon, J. H. [2005], 'A study on the design and analysis of a heat pump heating system using wastewater as a heat source', *Solar Energy* **78**(3), 427–440.
URL: *http://www.sciencedirect.com/science/article/pii/S0038092X04002014*

Barbier, S. [2015], Systems â Theoretical Principles for Heating and Sanitary Warm Water (in Dutch), *in* 'Passive and Low-energy Buildings'.

Beentjes, I., Manouchehri, R. and Collins, M. R. [2014], 'An investigation of drain-side wetting on the performance of falling film drain water heat recovery systems', *Energy and Buildings* **82**, 660–667.
URL: *http://dx.doi.org/10.1016/j.enbuild.2014.07.069*

BEIS [2019], The UK National Energy and Climate Plan (NECP), Technical Report January.
URL: *https://assets.publishing.service.gov.uk/government/uploads/system/uploads/attachment_data/file/774235/*

Bertrand, A., Aggoune, R. and Maréchal, F. [2017], 'In-building waste water heat recovery: An urban-scale method for the characterisation of water streams and the assessment of energy savings and costs', *Applied Energy* **192**, 110–125.
URL: *https://www.sciencedirect.com/science/article/abs/pii/S0306261917301137*

Brennan, D. P. and Cagney, D. [2015], Ireland\'s Response to the EU\'s 2030 Energy and Climate Change Targets, Technical report, PPAN.

British Water [2014], FOOD SERVICE INDUSTRY FATS OILS AND GREASE - CODE OF PRACTICE, Technical report.
URL: *https://www.brent.gov.uk/media/16413926/fat-oils-and-grease-cop-2.pdf*

Bromley-Challenor, K., Kowalski, M., Barnard, R. and Lynn, S. [2013], 'Water use in the UK food and drink industry. Technical report. Project code: PAD 101 202', (February).

Building Products Distributors Limited. [n.d.], ShowerSave Recent Projects - CoFlo, Technical report, Antrim.

Butler, D. and Davies, J. W. [2010], *Urban Drainage*, 3rd editio edn, Spon Press, London and New York.
URL: *http://www.kuliah.ftsl.itb.ac.id/wp-content/uploads/2016/10/Urban-Drainage-3rd-Edition.pdf*

CCC [2018], Reducing UK emissions - 2018 Progress Report to Parliament - Committee on Climate Change, Technical Report June.

CCC [n.d.], 'Carbon budgets: how we monitor emissions targets'.
URL: *https://www.theccc.org.uk/tackling-climate-change/reducing-carbon-emissions/carbon-budgets-and-targets/*

Celik, I. B., Ghia, U., Roache, P. J., Freitas, C. J., Coleman, H. and Raad, P. E. [2008], 'Procedure for estimation and reporting of uncertainty due to discretization in CFD applications', *Journal of Fluids Engineering, Transactions of the ASME* **130**(7), 0780011–0780014.

Cengel Yunus [2006], *Heat and Mass Transfer*, McGraw Hill.

Chae, K.-J. and Kang, J. [2013], 'Estimating the energy independence of a municipal wastewater treatment plant incorporating green energy resources', *Energy Conversion and Management* **75**, 664–672.
URL: *http://www.sciencedirect.com/science/article/pii/S0196890413004871*

Chao, S., Yiqiang, J., Yang, Y. and Shiming, D. [2012], 'Experimental performance evaluation of a novel dry-expansion evaporator with defouling function in a wastewater source heat pump', *Applied Energy* **95**, 202–209.
URL: *http://www.sciencedirect.com/science/article/pii/S0306261912001249*

Chao, S., Yiqiang, J., Yang, Y., Shiming, D. and Xinlei, W. [2013], 'A field study of a wastewater source heat pump for domestic hot water heating', *Building Services Engineering Research and Technology* **34**(4), 433–448.
URL: *http://dx.doi.org/10.1177/0143624412463571*

Chen, H., Li, D. and Dai, X. [2006], Economic Analysis of a Waste Water Resource Heat Pump Air-Conditioning System in North China, *in* 'Renewable Energy Resources and a Greener Future', Vol. III of *2*.

Chenghu, Z., Zhaoyi, Z. and Dexing, S. [2011], Design Generalization of Urban Sewage Source Heat Pump Heating and Air Conditioning Engineering, *in* '2011 Third International Conference on Measuring Technology and Mechatronics Automation', Vol. 1, pp. 926–929.

Cipolla, S. S. and Maglionico, M. [2013], 'Heat recovery from urban wastewater: analysis of the variability of flow rate and temperature in the sewer of Bologna, Italy', *Conference of the Italian Thermal Machines Engineering Association* pp. 288–297.

Clancy, M. [2015], Renewable Heat in Ireland to 2020, Technical report, Sustainable Energy Authority in Ireland.

Commision, E. [2016], An EU Strategy on Heating and Cooling, Technical report, European Commision.

Coskun, S., Motorcu, A. R., Yamankaradeniz, N. and Pulat, E. [2012], 'Evaluation of control parameters effects on system performance with Taguchi method in waste heat recovery application using mechanical heat pump', *International Journal of Refrigeration* **35**(4), 795–809.
URL: *http://www.sciencedirect.com/science/article/pii/S0140700711003094*

Cunniffe, J. and McNabola, A. [2014], Drain Water Heat REcovery From A Single Domestic household, Technical report, Trinity College Dublin; The Unitveristy of Dublin.

Daikin Europe NV [n.d.], Daikin Chillers Technical Data, Technical report, Oostende, Belgium.
URL: *http://daikinvrv.hu/uploads/downloads/ewwp-kbw1n-mernokipdf*

David, A., Mathiesen, B. V., Averfalk, H., Werner, S. and Lund, H. [2017], 'Heat Roadmap Europe: Large-Scale Electric Heat Pumps in District Heating Systems', *Energies* **10**(4), 578.
URL: *http://www.mdpi.com/1996-1073/10/4/578*

Davis, M. L. [2011], *Water and Wastewater Engineering*, internatio edn, McGraw Hill, New York, USA.

De Paepe, M., Theuns, E., Lenaers, S. and Van Loon, J. [2003], 'Heat recovery system for dishwashers', *Applied Thermal Engineering* **23**(6), 743–756.
URL: *https://www.sciencedirect.com/science/article/pii/S1359431103000164*

Dempsey, S. and Rowe, S. [n.d.], Fats, Oil, & Grease (FOG) Pretreatment Systems, *in* 'Town of Hingham - Health and sewer deparment'.

Department for Business Energy & Industrial Strategy [2018*a*], 'Government emission conversion factors for greenhouse gas company reporting'.
URL: *https://www.gov.uk/government/collections/government-conversion-factors-for-company-*

reporting#conversion-factors-2018

Department for Business Energy & Industrial Strategy [2018*b*], 'International domestic energy prices'.
URL: *https://www.gov.uk/government/statistical-data-sets/international-domestic-energy-prices*

Di Lucia, L. and Ericsson, K. [2014], 'Low-carbon district heating in Sweden - Examining a successful energy transition', *Energy Research and Social Science* .

Dong, J., Zhang, Z., Yao, Y., Jiang, Y. and Lei, B. [2015], 'Experimental performance evaluation of a novel heat pump water heater assisted with shower drain water', *Applied Energy* **154**, 842–850.
URL: *http://dx.doi.org/10.1016/j.apenergy.2015.05.044*

Donnelly, M. [2018], Why the public sector must lead in energy efficiency - An EU perspective, *in* 'Public Sector Energy Efficiency', Dublin, Ireland.

Dumas, M. [2014], Récupération de la chaleur des eaux d'égouts, *in* 'L'actualité 2014 des énergies renouvelables et du stockage énergétique'.

Dürrenmatt, D. J. and Wanner, O. [2014], 'A mathematical model to predict the effect of heat recovery on the wastewater temperature in sewers', *Water Research* **48**, 548–558.
URL: *http://www.sciencedirect.com/science/article/pii/S0043135413007951*

Elías-Maxil, J. A., van der Hoek, J. P., Hofman, J. and Rietveld, L. [2014], 'Energy in the urban water cycle: Actions to reduce the total expenditure of fossil fuels with emphasis on heat reclamation from urban water', *Renewable and Sustainable Energy Reviews* **30**, 808–820.
URL: *http://www.sciencedirect.com/science/article/pii/S1364032113007065*

Energy Monitoring Company and Energy Savings Trust [2011], Measurement of Domestic Hot Water Consumption in Dwellings, Technical report, Sustainable Energy Policy Division of the Department for Environment, Food and Rural Affairs (Defra), London, UK.

Environmental Protection Agency [2018], Waste Water Discharge Licensing Application Guidance Note, Technical report.
URL: *www.epa.ie*

Erker, S., Lichtenwoehrer, P., Zach, F. and Stoeglehner, G. [2019], 'Interdisciplinary decision support model for grid-bound heat supply systems in urban areas', *Energy, Sustainability and Society* **9**(1).

Eslami-nejad, P. and Bernier, M. [2009], IMPACT OF GREY WATER HEAT RECOVERY ON THE ELECTRICAL DEMAND OF DOMESTIC HOT WATER HEATERS, *in* 'Eleventh International IBPSA Conference', Glasgow, UK, pp. 681–687.

EU2015.LV [2015], Intended Nationally Determined Contribution of the EU and its Member States, Technical report, SUBMISSION BY LATVIA AND THE EUROPEAN COMMISSION ON BEHALF OF THE EUROPEAN UNION AND ITS MEMBER STATES.

Europeam Environmental Agency [2018], 'Heating and Cooling Degree Days'.
URL: *https://www.eea.europa.eu/data-and-maps/indicators/heating-degree-days-2/assessment*

European Commision [2019], 'The European Green Deal'.
URL: *https://ec.europa.eu/info/sites/info/files/european-green-deal-communication_en.pdf*

European Commission [2016], An EU Strategy on Heating and Cooling, Technical report, European Commission, Brussels, Belgium.
URL: *https://ec.europa.eu/energy/sites/ener/files/documents/1_EN_ACT_part1_v14.pdf*

European Council [2014], Conclusions on 2030 Climate and Energy Policy Framework, Technical Report October 2014, Brussels.
URL: *http://scholar.google.com/scholar?hl=en&btnG=Search&q=intitle:No+Title#0*

European Parliament; Council of the European Union [2018], 'DIRECTIVE (EU) 2018/2001 OF THE EUROPEAN PARLIAMENT AND OF THE COUNCIL of 11 December 2018 on the promotion of the use of energy from renewable sources (recast)'.
URL: *https://eur-lex.europa.eu/legal-content/EN/TXT/?uri=uriserv:OJ.L_.2018.328.01.0082.01.ENG*

Eurostat [2017], 'Final Energy Connsumption by Sector', European Commision.
URL: *http://ec.europa.eu/eurostat/web/products-datasets/-/tsdpc320*

Fernández-Arévalo, T., Lizarralde, I., Fdz-Polanco, F., Pérez-Elvira, S. I., Garrido, J. M., Puig, S., Poch,

M., Grau, P. and Ayesa, E. [2017], 'Quantitative assessment of energy and resource recovery in wastewater treatment plants based on plant-wide simulations', *Water Research* **118**, 272–288.

Flanagan, J. W. [2017], Dublin District Heating System Environment SPC Update, Technical Report November, Environment & Transportation Department, Dublin City Council, Technical Support Division,, Dublin, Ireland.
URL: *http://www.dublincity.ie/ddhs*

Fox, J. T., Zook, A. N., Freiss, J., Appel, B., Appel, J., Ozsuer, C. and Sarac, M. [2019], 'Thermal conversion of blended food production waste and municipal sewage sludge to recoverable products', *Journal of Cleaner Production* **220**, 57–64.
URL: *https://doi.org/10.1016/j.jclepro.2019.02.055*

Frijns, J., Hofman, J. and Nederlof, M. [2013], 'The potential of (waste)water as energy carrier', *Energy Conversion and Management* **65**, 357–363.
URL: *http://www.sciencedirect.com/science/article/pii/S0196890412003512*

Friotherm, A. G. [2005], 'Energy from sewage water â District heating and district cooling in Sandvika, with 2 Unitop 28C heat pump units', Zürcherstrasse 12 · P.O.Box 414 - CH-8400 Winterthur · Switzerland.

Fuentes, E., Arce, L. and Salom, J. [2018], 'A review of domestic hot water consumption profiles for application in systems and buildings energy performance analysis'.

Gallimore, E., Aziz, T. N., Movahed, Z. and Ducoste, J. [2011], 'Assessment of Internal and External Grease Interceptor Performance for Removal of FoodâBased Fats, Oil, and Grease from Food Service Establishments', *Water Environment Research* **83**(September), 882–892.

Gartland, D. and Bruton, T. B. [2016], A Guide to District Heating in Ireland, Technical report, SEAI, Dublin, IE.
URL: *https://www.seai.ie/resources/publications/2016_RDD_79._Guide_District_Heating_Irl_-_CODEMA.pdf*

Gill, L. [2015], Chapter 5 Type 1 Treatment Options, pp. 1–35.

Gill, L., Dubber, D., O'Flaherty, V., Keggan, M., Kilroy, K., Curneen, S., Misstear, B., Johnston, P., Pilla, F., McCarthy, T., Qazi, N. and Smyth, D. [2015], *Assessmeent of disposal options for treated waste water from single houses in low pereability soils*, Environmental Protection Agency, Dublin, Ireland.
URL: *https://www.epa.ie/pubs/reports/research/biodiversity/EPA RR 188 web final.pdf*

Gill, L., Mac Mahon, J. and Ryan, K. [2016], 'The performance of an evacuated tube solar hot water system in a domestic house throughout a year in a northern maritime climate (Dublin)', *Solar Energy* **137**, 261–272.
URL: *https://www.sciencedirect.com/science/article/pii/S0038092X16303103*

González Hidalgo, I., Magnaga, D., Bidoglio, G. and Peteves, S. [2019], *Policy Report Water Energy Nexus in Europe*, European Commision, Brussels, Belgium.
URL: *https://www.eaufrance.fr/sites/default/files/2019-06/water-energy-nexus-in-europe-european-commission-2019.pdf*

González, L. M. L., Tabarés, J. L. M., Alvarez, M. G. and Viar, P. F. [2001], 'Feasibility study for the installation of HVAC for a spa by means of energy recovery from thermal waterâPart I: Analysis of conditions', *Renewable Energy* **23**(1), 123–134.
URL: *http://www.sciencedirect.com/science/article/pii/S0960148100001610*

Goodright, V. [2014], Estimates of heat use in the United Kingdom in 2013, Technical Report December, Department of Energy and Climate Change.
URL: *www.gov.uk/government/collections/energy-consumption-in-the-uk*

Gray, N. [2017], *Water Science & Technology*, fourth edi edn, Taylor & Francis, Dublin, Ireland.

Gu, Y., Li, Y., Li, X., Luo, P., Wang, H., Wang, X., Wu, J. and Li, F. [2017], 'Energy Self-sufficient Wastewater Treatment Plants: Feasibilities and Challenges', *Energy Procedia* **105**, 3741–3751.
URL: *http://www.sciencedirect.com/science/article/pii/S1876610217309530*

Gunn, J. S., Ganz, D. J. and Keeton, W. S. [2012], 'Biogenic vs. geologic carbon emissions and forest biomass energy production', *GCB Bioenergy* **4**(3), 239–242.

Hao, X., Li, J., van Loosdrecht, M. C., Han, J. and Liu, R. [2019], 'Energy recovery from wastewater:

Heat over organics', *Water Research* (June).
URL: *https://linkinghub.elsevier.com/retrieve/pii/S0043135419305044*

Haque, N. and Somerville, M. [2013], 'Techno-economic and environmental evaluation of biomass dryer', *Procedia Engineering* **56**, 650–655.

Hawley, C. and Fenner, R. [2012], 'The potential for thermal energy recovery from wastewater treatment works in southern England', *Journal of Water and Climate Change* **3**(4), 287–299.

Hilkiah Igoni, A., Ayotamuno, M. J., Eze, C. L., Ogaji, S. O. and Probert, S. D. [2008], 'Designs of anaerobic digesters for producing biogas from municipal solid-waste', *Applied Energy* **85**(6), 430–438.

HM Government [2000], 'Building Regulations UK 2010 - Drainage and waste disposal - Approved Document H'.
URL: *https://assets.publishing.service.gov.uk/government/uploads/system/uploads/attachment_data/file/442889*

HM Government [2018], The Clean Growth Strategy Leading the way to a low carbon future, Technical report, London.
URL: *https://www.gov.uk/government/publications/clean-growth-strategy*

Howley, M., Holland, M. and Dineen, D. D. [2015], Energy in Ireland Key Statistics 2015, Technical report, Sustainable Energy Authority of Ireland.

HSE/HPSC [2009], Legionella Prevention and Control, Technical report, Dublin, Ireland.
URL: *https://www.hpsc.ie/a-z/respiratory/legionellosis/guidance/nationalguidelinesforthecontroloflegionellosisin 5 Legionella Prevention and Control.pdf*

Hua, L. [2005], HEAT EXCHANGER DEVELOPMENT FOR WASTE WATER HEAT RECOVERY, Master's thesis, UNIVERSITY OF CANTERBURY.

IEA [2017], Tracking Clean Energy Progress 2017, Technical report, International Energy Agency.

IEA and IRENA [2017], Perspectives for the Energy Transition, Technical report, International Energy Agency and International Renewable Energy Agency.

Ip, K., She, K. and Adeyeye, K. [2018], 'Life-cycle impacts of shower water waste heat recovery: case study of an installation at a university sport facility in the UK', *Environmental Science and Pollution Research* **25**(20), 19247–19258.
URL: *https://doi.org/10.1007/s11356-017-0409-0*

Irish Government [2010], *Building Regulations 2010: Drainage and wastewater disposal*, Dublin, IE.
URL: *https://www.housing.gov.ie/sites/default/files/migrated-files/en/Publications/DevelopmentandHousing/Bu*

Itron [2014], MOUNTING AND OPERATING INSTRUCTIONS CF Echo II, Technical report.

Jantrania, A. R. and Gross, M. A. [2006], *Advanced onsite wastewater systems technologies*, Taylor & Francis, Boca Raton, Fl, USA.

Kahraman, A. and Celebi, A. [2009], 'Investigation of the Performance of a Heat Pump Using Waste Water as a Heat Source', *Energies* **2**(3), 697–713.
URL: *http://www.mdpi.com/1996-1073/2/3/697*

Kenny, L., Geelan, D. and Clohosy, E. [2011], Guidelines to Management of Fats, Oils & Grease in Food Service Establishments, Technical report, Musgrave Wholesale Partners, ARAMARK Food Services, BWG Foods.

Kimmels, A. [2011], Shower Heat Recovery, Overview of Commercially Available DWHR Systems, Technical Report April, Meander Heat Recovery.

Knappe, J. [2018], The influence of a growing microbial biomat on water retention and pollutant attenuation in soil treatment units receiving domestic effluent, PhD thesis, University of Limerick.

Knappe, J., Somlai, C., Fowler, A. C. and Gill, L. W. [2020], 'The influence of pre-treatment on biomat development in soil treatment units', *Journal of Contaminant Hydrology* **232**, 103654.
URL: *http://www.sciencedirect.com/science/article/pii/S0169772220300206*

Kollmann, R., Neugebauer, G., Kretschmer, F., Truger, B., Kindermann, H., Stoeglehner, G., Ertl, T. and Narodoslawsky, M. [2017], 'Renewable energy from wastewater - Practical aspects of integrating a wastewater treatment plant into local energy supply concepts', *Journal of Cleaner Production* **155**, 119–129.

Kretschmer, F., Neugebauer, G., Kollmann, R., Eder, M., Zach, F., Zottl, A., Narodoslawsky, M., Stoeglehner, G. and Ertl, T. [2016a], 'Resource recovery from wastewater in Austria: Wastewater treatment plants as regional energy cells', *Journal of Water Reuse and Desalination* **6**(3), 421–429.

Kretschmer, F., Neugebauer, G., Stoeglehner, G. and Ertl, T. [2018], 'Participation as a key aspect for establishing wastewater as a source of renewable energy', *Energies* **11**(11).

Kretschmer, F., Simperler, L. and Ertl, T. [2016b], 'Analysing wastewater temperature development in a sewer system as a basis for the evaluation of wastewater heat recovery potentials', *Energy and Buildings* **128**, 639–648.
URL: *http://dx.doi.org/10.1016/j.enbuild.2016.07.024*

Kretschmer, F., Weissenbacher, N. and Ertl, T. [2015], 'Integration of Wastewater Treatment Plants into Regional Energy Supply Concepts', *Sustainable Sanitation Practice* (22).

Launder, B. and Spalding, D. [1974], 'The numerical computation of turbulent flows', *Computer Methods in Applied Mechanics and Engineering* **3**(2), 269–289.
URL: *https://www.sciencedirect.com/science/article/pii/0045782574900292?via%3Dihub*

Lean Construction [2017], Gemba walks for construction, *in* '19th LCI Congress - October 16-20', Anaheim, California.

Leuenberger, M. [2006], 'Chauffer et rafraîchir grâce aux eaux usées'.

Li, F., Zheng, G. and Tian, Z. [2013], 'Optimal operation strategy of the hybrid heating system composed of centrifugal heat pumps and gas boilers', *Energy and Buildings* **58**, 27–36.
URL: *http://www.sciencedirect.com/science/article/pii/S0378778812005555*

Li, H., Russell, N., Sharifi, V. and Swithenbank, J. [2011], 'Techno-economic feasibility of absorption heat pumps using wastewater as the heating source for desalination', *Desalination* **281**, 118–127.
URL: *http://www.sciencedirect.com/science/article/pii/S0011916411006631*

Li, X. and Li, Y. [2010], Second Law-Based Thermodynamic Analysis of a Heat Pump System Utilizing Sewage Source, *in* '2010 4th International Conference on Bioinformatics and Biomedical Engineering', pp. 1–4.

Lichtenwoehrer, P., Erker, S., Zach, F. and Stoeglehner, G. [2019], 'Future compatibility of district heating in urban areas - A case study analysis in the context of integrated spatial and energy planning', *Energy, Sustainability and Society* **9**(1).

Lindstrom, H. O. [1985], 'Experience with a 3.3 MW heat pump using sewage water as a heat source', *Symposium on The Large Scale Application of Heat Pumps* .

Lindtner, S. [2008], Leitfaden für die Erstellung eines Energiekonzeptes kommunaler Kläranlagen (Guideline for the development of an energy concept for municipal wastewater treatment plants), Technical Report April, Austrian Federal Ministry of Agriculture and Forestry, Environment and Water Management, Vienna, Austria.
URL: *http://www.umweltfoerderung.at/uploads/energieleitfaden_endversion.pdf*

Liu, L., Fu, L. and Jiang, Y. [2010], 'Application of an exhaust heat recovery system for domestic hot water', *Energy* **35**(3), 1476–1481.
URL: *http://www.sciencedirect.com/science/article/pii/S0360544209005246*

Liu, L., Fu, L. and Zhang, S. [2014], 'The design and analysis of two exhaust heat recovery systems for public shower facilities', *Applied Energy* **132**, 267–275.
URL: *http://www.sciencedirect.com/science/article/pii/S0306261914006801*

Liu, X., Lau, S.-K. and Li, H. [2014b], 'Optimization and analysis of a multi-functional heat pump system with air source and gray water source in heating mode', *Energy and Buildings* **69**, 1–13.
URL: *http://www.sciencedirect.com/science/article/pii/S037877881300621X*

Liu, X., Ni, L., Lau, S.-K. and Li, H. [2013*a*], 'Performance analysis of a multi-functional heat pump system in cooling mode', *Applied Thermal Engineering* **59**(1), 253–266.
URL: *http://www.sciencedirect.com/science/article/pii/S1359431113003955*

Liu, X., Ni, L., Lau, S.-K. and Li, H. [2013*b*], 'Performance analysis of a multi-functional Heat pump system in heating mode', *Applied Thermal Engineering* **51**(1), 698–710.
URL: *http://www.sciencedirect.com/science/article/pii/S1359431112005662*

Liu, Z., Ma, L. and Zhang, J. [2014a], 'Application of a heat pump system using untreated urban sewage as a heat source', *Applied Thermal Engineering* **62**(2), 747–757.
URL: *http://www.sciencedirect.com/science/article/pii/S1359431113006091*

Long, J. H., Aziz, T. N., Reyes, F. L. L. and Ducoste, J. J. [2012], 'Anaerobic co-digestion of fat, oil, and grease (FOG): A review of gas production and process limitations', *Process Safety and Environmental Protection* **90**(3), 231–245.
URL: *http://dx.doi.org/10.1016/j.psep.2011.10.001*

Lund, H., Østergaard, P. A., Connolly, D. and Mathiesen, B. V. [2017], 'Smart energy and smart energy systems', *Energy* **137**, 556–565.
URL: *https://www.sciencedirect.com/science/article/pii/S0360544217308812*

Lund, R., Østergaard, D. S., Yang, X. and Mathiesen, B. V. [2017b], 'Comparison of low-temperature district heating concepts in a long-term energy system perspective', *International Journal of Sustainable Energy Planning and Management* **12**, 5–18.

Ma, L., Zhen, X. and Zhang, J. [2017], 'The Performance Simulation Analysis of the Sewage-source Heat Pump Heater Unit Dealing with Large Temperature Difference', *Procedia Engineering* **205**, 1769–1776.
URL: *https://doi.org/10.1016/j.proeng.2017.10.028*

Manouchehri, R. and Collins, M. R. [2016], 'An experimental analysis of the impact of temperature on falling film drain water heat recovery system effectiveness', *Energy and Buildings* **130**(April), 1–7.
URL: *http://dx.doi.org/10.1016/j.enbuild.2016.08.031*

McNabola, A. and Shields, K. [2013], 'Efficient drain water heat recovery in horizontal domestic shower drains', *Energy and Buildings* **59**, 44–49.
URL: *http://www.sciencedirect.com/science/article/pii/S0378778812006755*

McQuiston, F. C., Parker, J. D. and Spitler, J. D. [2005], *Heating, ventilating, and air conditioning*, sixth edit edn, John Wiley & Sons, Inc., Danvers, MA, USA.

Meggers, F. [2008], 'Exergy Optimized Wastewater Heat Recovery: Minimizing Losses and Maximizing Performance', *Proceedings of the Eighth International Conference for Enhanced Building Operations, .*

Meggers, F. and Leibundgut, H. [2011], 'The potential of wastewater heat and exergy: Decentralized high-temperature recovery with a heat pump', *Energy and Buildings* **433**, 879–886.

MET Eireann [2019], 'Degree Days'.

Mo, W. and Zhang, Q. [2013], 'Energyânutrientsâwater nexus: Integrated resource recovery in municipal wastewater treatment plants', *Journal of Environmental Management* **127**, 255–267.
URL: *http://www.sciencedirect.com/science/article/pii/S0301479713003277*

Müller, E. A. and Schmid, F. [2005], Heizen mit und Kühlen Abwasser (Heating and cooling with wastewater), Technical report, Institut Energie in Infrastrukturanlagen Bundesverband Wärmepumpe, Munchen, Germany.

National Trust [2019], 'Penrhyn Castle and Garden'.
URL: *https://www.nationaltrust.org.uk/penrhyn-castle*

Neugebauer, G., Kretschmer, F., Kollmann, R., Narodoslawsky, M., Ertl, T. and Stoeglehner, G. [2015], 'Mapping Thermal Energy Resource Potentials from Wastewater Treatment Plants', *Sustainability* **7**(10), 12988–13010.
URL: *http://www.mdpi.com/2071-1050/7/10/12988*

Ni, L., Lau, S. K., Li, H., Zhang, T., Stansbury, J. S., Shi, J. and Neal, J. [2012], 'Feasibility study of a localized residential grey water energy-recovery system', *Applied Thermal Engineering* **39**, 53–62.
URL: *http://www.sciencedirect.com/science/article/pii/S1359431112000403*

Niemela, M. and Saarela, R. [2014], 'The wastewater utilization in Kakola heat pump plant'.
URL: *http://www.districtenergyaward.org/wp-content/uploads/2012/10/New_scheme_Finland_Turku.pdf*

Ninikas, K., Hytiris, N., Emmanuel, R. and Aaen, B. [2019], 'Recovery and Valorisation of Energy from Wastewater Using a Water Source Heat Pump at the Glasgow Subway: Potential for Similar Underground Environments', *Resources* **8**(4), 169.
URL: *https://www.mdpi.com/2079-9276/8/4/169*

Novara, D., Carravetta, A., McNabola, A. and Ramos, H. M. [2019], 'Cost Model for Pumps as Turbines in Run-of-River and In-Pipe Microhydropower Applications', *Journal of Water Resources Planning and Management* **145**(5), 04019012.
URL: *http://ascelibrary.org/doi/10.1061/%28ASCE%29WR.1943-5452.0001063*

Office of Public Works Ireland [2019], 'Realtime Water Level'.
URL: *http://waterlevel.ie/*

Oh, S., Cho, Y. and Yun, R. [2014], 'Raw-water source heat pump for a vertical water treatment building', *Energy and Buildings* **68**, 321–328.
URL: *http://www.sciencedirect.com/science/article/pii/S0378778813005860*

Pachauri, R. K., Meyer, L. and Team, C. W. [2015], Climate Change 2014 - Synthesis Report, Technical report, The Intergovernmental Panel on Climate Change, Geneva, Switzerland.

Pillai, G. G., Putrus, G. A. and Pearsall, N. M. [2014], 'Generation of synthetic benchmark electrical load profiles using publicly available load and weather data', *International Journal of Electrical Power & Energy Systems* **61**, 1–10.
URL: *https://www.sciencedirect.com/science/article/pii/S0142061514001070*

Postrioti, L., Baldinelli, G., Bianchi, F., Buitoni, G., Di Maria, F. and Asdrubali, F. [2016], 'An experimental setup for the analysis of an energy recovery system from wastewater for heat pumps in civil buildings', *Applied Thermal Engineering* **102**, 961–971.
URL: *http://dx.doi.org/10.1016/j.applthermaleng.2016.04.016*

Qian, J. [2011], Optimization design of urban sewage source heat pump system with freezing latent heat collection, *in* '2011 International Conference on Mechatronic Science, Electric Engineering and Computer (MEC)', pp. 636–639.

Qian, J., Zhang, J. and Sun, D. [2009], Form and Applicability of a New Urban Sewage Source Heat Pump System with Freezing Latent Heat Collection, *in* '2009 International Conference on Energy and Environment Technology', Vol. 2, pp. 578–581.

Qu, Y. X., Feng, Y. and Liu, H. [2011], 'Study on the Growth Characteristics of Fouling in Sewage Source Heat Pump Systems', *Advanced Materials Research* **374-377**, 86–89.
URL: *https://www.scientific.net/AMR.374-377.86*

Ramadan, M., Lemenand, T. and Khaled, M. [2016], 'Recovering heat from hot drain waterâExperimental evaluation, parametric analysis and new calculation procedure', *Energy and Buildings* **128**, 575–582.
URL: *http://dx.doi.org/10.1016/j.enbuild.2016.07.017*

Ramboll [2019], Alternative heat solutions converting a town to low carbon heating, Technical Report February, Department for Business, Energy and Industrial strategy, UK Government, London, UK.
URL: *www.ramboll.co.uk/energy https://www.gov.uk/government/publications/alternative-heat-solutions-converting-a-town-to-low-carbon-heating*

Ramirez Camargo, L. and Stoeglehner, G. [2018], 'Spatiotemporal modelling for integrated spatial and energy planning', *Energy, Sustainability and Society* **8**(1), 1–29.

Rockström, J., Steffen, W., Noone, K., Persson, Å., Chapin, F. S. I. I. I., Lambin, E., Lenton, T. M., Scheffer, M., Folke, C., Schellnhuber, H. J., Nykvist, B., de Wit, C. A., Hughes, T., van der Leeuw, S., Rodhe, H., Sörlin, S., Snyder, P. K., Costanza, R., Svedin, U., Falkenmark, M., Karlberg, L., Corell, R. W., Fabry, V. J., Hansen, J., Walker, B., Liverman, D., Richardson, K., Crutzen, P. and Foley, J. [2009], 'Planetary Boundaries: Exploring the Safe Operating Space for Humanity', *Ecology and Society* .

Rodgers, D. [2017], Introduction to Design Thinking, *in* 'The innovation academy', Dar Es Salaam, Tanzania.

Romanchenko, D., Kensby, J., Odenberger, M. and Johnsson, F. [2018], 'Thermal energy storage in district heating: Centralised storage vs. storage in thermal inertia of buildings', *Energy Conversion and Management* **162**(January), 26–38.
URL: *https://doi.org/10.1016/j.enconman.2018.01.068*

Rubinstein, R. Y. T. and Kroese, D. P. U. o. Q. [2017], *Simulation and the Monte Carlo Method*, 3rd editio edn, John Wiley & Sons, Inc., Hoboken, New Jersey.
URL: *https://books.google.ie/books?hl=en&lr=&id=r2VODQAAQBAJ&oi=fnd&pg=PR1&dq=monte+carlo+method&ots=14U*

b4b&sig=PACf1xf_943aiuB_HHzU7ADSprU&redir_esc=y#v=onepage&q=monte carlo method&f=false

Rushing, A. S., Kneifel, j. D. and Lippiatt, B. C. [2013], Energy Price Indices and Discount Factors for Life-Cycle Cost Analysis - 2013, Technical report, U.S. Department of Commerce, Washington DC. USA.

Sandvall, A. F., Ahlgren, E. O. and Ekvall, T. [2016], ECONOMICALLY OPTIMAL HEAT SUPPLY TO LOW ENERGY BUILDING AREAS, *in* 'The 15th International Symposium on District Heating and Cooling September 4-7, 2016, Seoul, Republic of Korea (South Korea).', Seoul, South Korea, pp. 235–243.
URL: *https://www.iea-dhc.org/fileadmin/public_documents/Proceedings_of_the_15th_IS_on_DHC2016_Final_Copy*

Sandvall, A. F., Ahlgren, E. O. and Ekvall, T. [2017], 'Cost-efficiency of urban heating strategies â Modelling scale effects of low-energy building heat supply', *Energy Strategy Reviews* **18**, 212–223.
URL: *https://www.sciencedirect.com/science/article/pii/S2211467X17300615*

Scheer, J., Clancy, M. and Gaffney, F. [2016], Ireland\'s Energy Targets - Progress, Ambition & Impacts, Technical report, Sustainable Energy Authority of ireland.

Schmid, F. [2008], 'SEWAGE WATER: INTERESTING HEAT SOURCE FOR HEAT PUMPS AND CHILLERS', *9th International IEA Heat Pump Conference* **1**, 1–12.

Scottish Water [2017], 'Recovering Heat from Waste Water'.
URL: *http://www.scottishwater.co.uk/business/horizons/heat-recovery/heat-recovery*

SEAI [2014], A Guide to Building Energy Rating for Homeowners, Technical report.
URL: *http://www.seai.ie/Your_Building/BER/Your_Guide_to_Building_Energy_Rating.pdf*

SEAI [2015*a*], 'Achieving Ireland's 2020 Renewable Heat Target'.

SEAI [2015*b*], Energy in Ireland 1990 â 2014. Sustainable Energy Authority of Ireland (SEAI), Technical report.
URL: *http://www.seai.ie/Publications/Statistics_Publications/Energy_in_Ireland/*

SEAI [2015*c*], 'Heat Map'.
URL: *http://maps.seai.ie/giswiki/maps/heat-map/*

SEAI [2017*a*], Domestic Fuels: Energy Costs comparisons, Technical Report Jan.
URL: *http://www.seai.ie/Publications/Statistics_Publications/Fuel_Cost_Comparison/Commercial_Fuel_Cost_Co*

SEAI [2017*b*], 'What are the carbon emission factors used?'.
URL: *https://www.seai.ie/your_business/public_sector/FAQ/energy_reporting_overview/what_are_the_carbon_emis*

SEAI [2018], 'DEAP Resources'.
URL: *https://www.seai.ie/energy-in-business/ber-assessor-support/deap/*

SEAI [2019*a*], Commercial / Industrial Fuels Comparison of Energy Costs, Technical Report January 2019, SEAI, Dublin, Ireland.
URL: *https://www.seai.ie/resources/publications/Commercial-Fuel-Cost-Comparison.pdf*

SEAI [2019*b*], 'Conversion Factors'.
URL: *https://www.seai.ie/resources/seai-statistics/conversion-factors/*

SEAI [2019*c*], Energy in Ireland Energy in Ireland-Key Statistics, Technical report, Sustainable Energy Authority of Ireland, Dublin, Ireland.
URL: *https://www.seai.ie/data-and-insights/seai-statistics/key-publications/energy-in-ireland/*

SEAI [2020], 'Ireland's Energy Targets'.
URL: *https://www.seai.ie/about/irelands-energy-targets/*

Shen, C., Yang, L., Wang, X., Jiang, Y. and Yao, Y. [2014], 'An experimental and numerical study of a de-fouling evaporator used in a wastewater source heat pump', *Applied Thermal Engineering* **70**(1), 501–509.
URL: *http://www.sciencedirect.com/science/article/pii/S1359431114004165*

Simperler, L. [2015], IMPACT OF THERMAL USE OF WASTEWATER IN A SEWER ON THE INLET TEMPERATURE OF A WASTEWATER TREATMENT PLANT, PhD thesis.

Simscale [2018], 'What is y+(yplus)?'.
URL: *https://www.simscale.com/forum/t/what-is-y-yplus/82394/2*

Slyś, D. and Kordana, S. [2014], 'Financial analysis of the implementation of a Drain Water Heat Recovery

unit in residential housing', *Energy and Buildings* **71**, 1–11.
URL: *http://www.sciencedirect.com/science/article/pii/S0378778813008062*

Słyś, D., Pochwat, K. and Czarniecki, D. [2020], 'An Analysis of Waste Heat Recovery from Wastewater on Livestock and Agriculture Farms', *Resources* **9**(1), 3.
URL: *https://www.mdpi.com/2079-9276/9/1/3*

SMET, P. D. E. [2016], 2 years of experience in riothermia for social residences, *in* 'Micro- heating networks'.

Somogyi, V., Sebestyén, V. and Domokos, E. [2018a], 'Assessment of wastewater heat potential for district heating in Hungary', *Energy* **163**, 712–721.

Somogyi, V., Sebestyén, V., Kovács, Z., Hargitai, R. H. and Domokos, E. [2018], 'Enhanced pollution removal with heat reclamation in a small hungarian wastewater treatment plant', *Journal of Sustainable Development of Energy, Water and Environment Systems* **6**(3), 494–504.

Song, Y., Yao, Y., Ma, Z. and Na, W. [2006], Study of Performance of Heat Pump Usage in Sewage Treatment and Fouling Impact on System, *in* 'China Renewable Energy Resources and a Greener Future'.

Sorensen, K. [2009], Oil and Grease Removal technologies, *in* 'EPA Region 8 conference', Bismarck, UT, USA.

Spriet, J. and Hendrick, P. [2017], 'Wastewater as a heat source for individual residence heating: A techno-economic feasibility study in the brussels capital region', *Journal of Sustainable Development of Energy, Water and Environment Systems* **5**(3).

Spriet, J. and McNabola, A. [2019*a*], 'Decentralized drain water heat recovery: A probabilistic method for prediction of wastewater and heating system interaction', *Energy and Buildings* **183**, 684–696.
URL: *https://www.sciencedirect.com/science/article/pii/S037877881832200X?utm_campaign=STMJ_75273_AUTH_SERV_PPU*
1899763637&SIS_ID=-1&dgcid=STMJ_75273_AUTH_SERV_PPUB&CMX_ID=&utm_in=DM424764&utm_source=AC_30

Spriet, J. and McNabola, A. [2019*b*], 'Decentralized drain water heat recovery from commercial kitchens in the hospitality sector', *Energy and Buildings* **194**, 247–259.

Spriet, J., McNabola, A., Neugebauer, G., Stoeglehner, G., Ertl, T. and Kretschmer, F. [2020], 'Spatial and temporal considerations in the performance of wastewater heat recovery systems', *Journal of Cleaner Production* **247**, 119583.
URL: *https://www.sciencedirect.com/science/article/pii/S0959652619344531*

Stec, A. and Kordana, S. [2015], 'Analysis of profitability of rainwater harvesting, gray water recycling and drain water heat recovery systems', *Resources, Conservation and Recycling* **105**, 84–94.

Steffen, W., Richardson, K., Rockström, J., Cornell, S. E., Fetzer, I., Bennett, E. M., Biggs, R., Carpenter, S. R., de Vries, W., de Wit, C. A., Folke, C., Gerten, D., Heinke, J., Mace, G. M., Persson, L. M., Ramanathan, V., Reyers, B. and Sörlin, S. [2015], 'Planetary boundaries: Guiding human development on a changing planet', *Science* **347**(6223).
URL: *http://science.sciencemag.org/content/347/6223/1259855*

Sterman, J. D., Siegel, L. and Rooney-Varga, J. N. [2018], 'Does replacing coal with wood lower CO 2 emissions? Dynamic lifecycle analysis of wood bioenergy', *Environmental Research Letters* **13**(1), 15007.
URL: *http://stacks.iop.org/1748-9326/13/i=1/a=015007*

Stillwell, A. S., Hoppock, D. C. and Webber, M. E. [2010], 'Energy recovery from wastewater treatment plants in the United States: A case study of the energy-water nexus', *Sustainability* **2**(4), 945–962.

Stoeglehner, G. [2019], 'Strategicnessâthe core issue of environmental planning and assessment of the 21st century', *Impact Assessment and Project Appraisal* **00**(00), 1–5.
URL: *https://doi.org/10.1080/14615517.2019.1678969*

Styles, D., Schoenberger, H. and Galvez-Martos, J. L. [2015], 'Water management in the European hospitality sector: Best practice, performance benchmarks and improvement potential', *Tourism Management* **46**, 187–202.
URL: *https://www.sciencedirect.com/science/article/pii/S026151771400137X*

Taal, M., Bulatov, I., Klemeš, J. and StehlÄ±Ìk, *P.*[2003], '*Costestimationandenergypriceforecastsforeconomicevaluationofre*
−1835.
URL:*https://www.sciencedirect.com/science/article/pii/S1359431103001364*

Tanha, K., Fung, A. S. and Kumar, R. [2015], 'Performance of two domestic solar water heaters with drain water heat recovery units: Simulation and experimental investigation', *Applied Thermal Engineering* **90**, 444–459.

Templeton, M. R. and Butler, D. [2011], *Introduction to Wastewater Treatment*, Ventus Publishing.

Thorsen, J. E., Lund, H. and Mathiesen, B. V. [2018], 'Progression of District Heating â 1st to 4th generation'.
URL: *https://vbn.aau.dk/ws/portalfiles/portal/280710833/1_4GDH_progression_revised_May2018.pdf*

Torras, S., Oliet, C., Rigola, J. and Oliva, A. [2016], 'Drain water heat recovery storage-type unit for residential housing', *Applied Thermal Engineering* **103**, 670–683.
URL: *http://dx.doi.org/10.1016/j.applthermaleng.2016.04.086*

UNFCCC [2016], 'A Guide to the UNFCCC and its Processes', internet.
URL: *http://bigpicture.unfccc.int/#content-the-paris-agreemen*

United Nations [2018], '68% of the world population projected to live in urban areas by 2050, says UN'.
URL: *https://www.un.org/development/desa/en/news/population/2018-revision-of-world-urbanization-prospects.html*

United States Environmental Protection Agency [2014], *Being Prepared for Climate Change. A Workbook for Developing Risk-Based Adaptation Plans.*
URL: *https://www.epa.gov/sites/production/files/2015-01/documents/cre_2014workbook_appendix_f_508.pdf*

van der Hoek, J. P. [2011], 'Energy from the water cycle: a promising combination to operate climate neutral', *Water Practice and Technology* **6**(2).
URL: *http://wpt.iwaponline.com/content/6/2/wpt2011019*

van der Hoek, J. P., de Fooij, H. and Struker, A. [2016], 'Wastewater as a resource: Strategies to recover resources from Amsterdam's wastewater', *Resources, Conservation and Recycling* **113**, 53–64.
URL: *https://www.sciencedirect.com/science/article/pii/S0921344916301227?via%3Dihub*

Wallin, J. and Claesson, J. [2014], 'Analyzing the efficiency of a heat pump assisted drain water heat recovery system that uses a vertical inline heat exchanger', *Sustainable Energy Technologies and Assessments* **8**, 109–119.
URL: *http://www.sciencedirect.com/science/article/pii/S2213138814000733*

Wang, H., Wang, Q. and Chen, G. [2013], 'Experimental performance analysis of an improved multifunctional heat pump system', *Energy and Buildings* **62**, 581–589.
URL: *http://www.sciencedirect.com/science/article/pii/S037877881300217X*

Wang, Z. [2017], Trade-offs in Levelized Cost of Heat among different domestic heating technologies, *in* 'All Energy Conference', Glasgow, UK.

Wanner, O., Panagiotidis, V., Clavadetscher, P. and Siegrist, H. [2005], 'Effect of heat recovery from raw wastewater on nitrification and nitrogen removal in activated sludge plants', *Water Research* **39**(19), 4725–4734.
URL: *http://www.sciencedirect.com/science/article/pii/S0043135405005403*

Waters, Liz; Hemingway, J. [2016], Energy Trends: June 2017, special feature article - Renewable energy in 2016, Technical report, Department for Business, Energy & Industrial Strategy, London,UK.
URL: *https://www.gov.uk/government/uploads/system/uploads/attachment_data/file/622815/Renewable_energy_i*

Webb, B. and Walsh, A. [2004], 'Changing UK river temperatures and their impact on fish populations', *Hydrology: Science and Practice for the 21st Century. Volume II.* **II**, 177–191.
URL: *http://hdl.handle.net/10036/41373*

Welsh Government [2019], 'Wales accepts Committee on Climate Change 95% emissions reduction target'.
URL: *https://gov.wales/wales-accepts-committee-climate-change-95-emissions-reduction-target*

Wong, L. T., Mui, K. W. and Guan, Y. [2010], 'Shower water heat recovery in high-rise residential buildings of Hong Kong', *Applied Energy* **87**(2), 703–709.
URL: *http://www.sciencedirect.com/science/article/pii/S0306261909003225*

Xiao-Yan, L. and Hai-Tao, L. [2005], 'Study on reutilization of low level heat energy from muncipal Wastewater of China', *International conference on environmental science and technology* .

Xiao-Yan, L. and Tao, L. H. [2005], Study on Reutilization of Heat Energy from Municipal Wastewater, *in* 'Proceedings of the 9th International Conference on Environmental Science and Technology'.

Yaxiu, G., Huqiu, D., Yu, G. and Huanjuan, Z. [2011], The potential of urban wastewater heat: The feasibility analysis of using wastewater source heat pump, *in* '2011 International Symposium on Water Resource and Environmental Protection', Vol. 2, pp. 1481–1484.

Yunus, C. and Boles, M. A. [2007], *Thermodynamics: An engineering approach*, 6th edn, McGraw Hill.

Zach, F., Erker, S. and Stoeglehner, G. [2019], 'Factors influencing the environmental and economic feasibility of district heating systems - A perspective from integrated spatial and energy planning', *Energy, Sustainability and Society* **9**(1).

Zaloum, C., Lafrance, M. and Gusdorf, J. [2007], Drain Water Heat Recovery Characterization and Modeling, Technical report, DRAFTSustainable Buildings and Communities Natural Resources Canada, Ottawa.

Zhang, M. y., Sun, L. y., Jiang, Y. q. and Yao, Y. [2010], Comprehensive Evaluation of Sewage Source Heat Pump System Applied in Shanghai, *in* '2010 International Conference on E-Product E-Service and E-Entertainment', pp. 1–4.

Zhao, X. L., Fu, L., Zhang, S. G., Jiang, Y. and Lai, Z. L. [2010], 'Study of the performance of an urban original source heat pump system', *Energy Conversion and Management* **51**(4), 765–770.
URL: *http://www.sciencedirect.com/science/article/pii/S0196890409004415*

Zhi-Feng, C. [2011], Application prospect of plastic heat exchanger in sewage source heat pump systems, *in* 'MSIE 2011', pp. 1184–1187.

Zhou, W. Z. and Li, J. X. [2004], Sewage Heat Source Pump System's Application Examples and Prospect Analysis in China, *in* 'International Refrigeration and Air Conditioning Conference'.

Žižlavský, O. [2014], 'Net Present Value Approach: Method for Economic Assessment of Innovation Projects', *Procedia - Social and Behavioral Sciences* **156**, 506–512.
URL: *https://www.sciencedirect.com/science/article/pii/S1877042814060509*

Zottl, A., Lindahl, M., Nordman, R., Rivière, P. and Miara, M. [2011], SEasonal PErformance factor and MOnitoring for heat pump systems in the building sector SEPEMO-Build Evaluation method for comparison of heat pump systems with conventional heating systems D4.3. Concept for evaluation of CO2-reduction potential, Technical report.

A. Data sheets of sensors

A.1. TinyTag temperature logger

gemini DATA LOGGERS

Tinytag

DATA SHEET

Tinytag Aquatic 2 (-40 to +70°C)

TG-4100

Issue 8
8th January 2016
E&OE

Designed with long term immersion in mind, this unit is waterproof to a depth of 500m making it ideal for environmental monitoring in rivers and oceans. The high visibility yellow case has an attachment point that can be used to secure the logger in position.

The lid can be removed to enable user replacement of the battery.

Data is downloaded to the computer via a USB or serial download pad. This 'wireless connection' eliminates the need for sockets with waterproof caps which can easily be lost or forgotten.

Popular Applications

- Environmental monitoring
  - Fisheries
  - Aquaculture
  - Rivers
- Food Processing



Features

- Submersible temperature recorder
- Waterproof to 500m
- 32,000 reading capacity
- User-programmable logging interval
- 2 user-programmable alarms
- Delayed and trigger start options
- 3 stop options
- User-replaceable battery
- Low battery warning

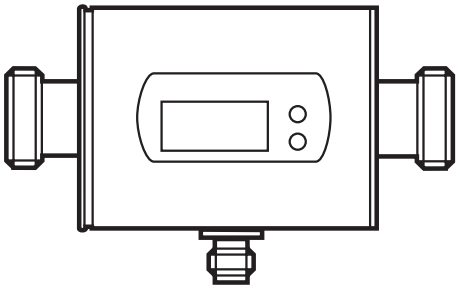


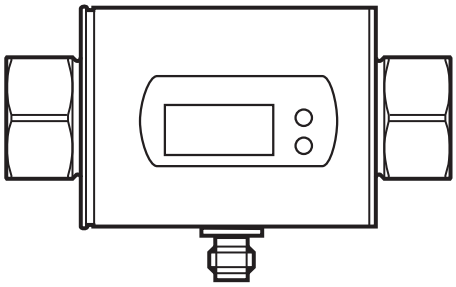
A.2. Magnetic-inductive flow meter

Operating instructions
Magnetic-inductive flow meter

SM4x00
SM6x00
SM7x00
SM8x00
SM6x01
SM7x01
SM8x01

UK





80224865 / 00 02 / 2018

A.3. Temperature controller

IMPACT
IMPACT
IMPACT

Thermostat - Digital Display
CN060/2

Impact Test Equipment Ltd
www.impact-test.co.uk & www.impact-test.com

User Guide
User Guide
User Guide

B. Non financial support scheme: Feasibility studies

B.1. Druids Glen: Hotel and Leisure center

Trinity College Dublin
Coláiste na Tríonóide, Baile Átha Cliath
The University of Dublin

Dŵr Uisce
Energy Recovery in Water Services
Adennill Ynni yn y Diwydiant Dŵr

Prifysgol Bangor University

Monitoring campaign at Druids Glen Hotel and Resort:
Potential for heat recovery from drain water

Feasibility study
October 2017

Cronfa Datblygu Rhanbarthol Ewrop
European Regional Development Fund

Ireland's European Structural and Investment Funds Programmes 2014-2020
Co-funded by the Irish Government and the European Union

Tionól Réigiúnach an Deiscirt
Southern Regional Assembly

EU Funds: Ireland Wales Programme 2014-2020

Table of Contents

1. Introduction 1
2. Objectives 1
3. Monitoring points 1
   3.1 Shower drain 2
   3.2 Kitchen grease trap 2
4. Observations 3
   4.1 Shower drain 3
   4.2 Kitchen grease trap 3
5. Results and Discussion 3
   5.1 Shower drain 4
   5.2 Kitchen grease trap 6
6. Conclusion 8

Appendix A: Instrumentation 11
   Technical specifications of temperature sensor (Tinytag TG-4100): 11

1. Introduction

The aim of this monitoring campaign was to assess the feasibility of implementing a waste water heat recovery system at Druids Glen Hotel & Resort, whereby waste heat from waste water flows in the facility would be recovered and transferred to the existing heating system. This has the potential to reduce the gas consumption of the existing boilers, and generate financial and environmental savings for the resort. The proposal is based on the Drain Water Heat Recovery concept (DWHR), which consists of a heat exchanger placed in the waste water drain, connected to a heat pump. The novelty of the present approach is the projection of the idea to an entire building, concentrating the heat transfer from a tank or manhole. Two different potential installation options are presented for further assessments on their heat exchange potentials.

This proposal forms part of the Dŵr Uisce project (*www.dwr-uisce.eu*), which aims at improving the energy efficiency of the distribution of water resources by quantifying and demonstrating the potential of integrated smart and low-carbon technology. In this context the Druids Glen Hotel and Resort offers a unique opportunity to investigate the potential of waste water heat recovery technology in the hospitality sector. This technology can help towards improving environmental, energetic and financial performance of the facilities.

2. Objectives

The primary objectives of this project include:

- Assessing the potential to improve the energy efficiency of Druids Glen Hotel and Resort water heating activities through DWHR.
- Assessing the potential to reduce operating costs, both financial and environmental of water and space heating at the Druids Glen Hotel and Resort.
- To facilitate awareness raising, public and industry engagement in the concept of DWHR

In order to reach and quantify these primary objectives, the embedded energy in the wastewater on the property must be measured and quantified. This requires the following measurements or estimations, at the locations that are proposed in this document

- Wastewater temperature.
- Wastewater flow.

3. Monitoring points

Two different monitoring points have been used, one of them located at the drain pipe from the swimming pool and golf club showers (16 showers total) and the swimming pool spill-over drain (location 1 on Figure 1). The other one was located at the grease trap of the drain coming from the kitchen, which is located in the technical room, where the boilers for the hot water network are located as well (Location 2 on Figure 1).

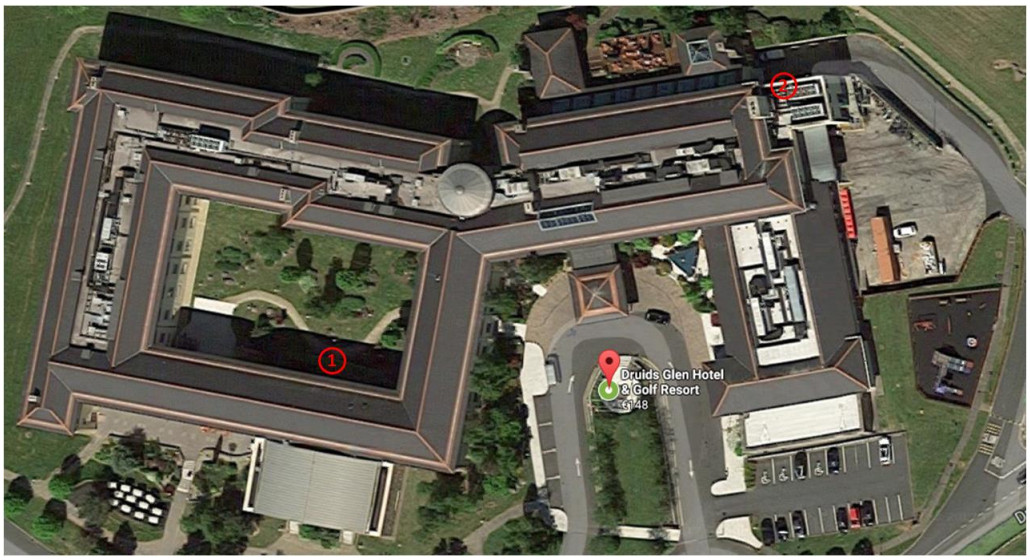


Figure 1. Druids Glen Hotel and Resort

3.1 Shower drain

The temperature of the drain water from the showers of the swimming pool (10 showers) and the golf club (6 showers), along with the spill-over water of the swimming pool was measured using a TinyTag temperature logger (see Appendix A), placed in the sewer drains. The flow was estimated assuming a certain number of showers, with a given shower length and flow rate, as summarized in Table 1. The average flow rate is then used for calculations.

Table 1. Assumption for flow calculation at the shower drains

Number of events per day	175
Shower flow rate	10 l/min [1]
Shower duration	4 min
Shower operating period	6 AM – 10 PM

3.2 Kitchen grease trap

The second monitoring point is located at the outlet of the grease trap, installed in the technical building. The temperature at the outlet was measured, and the embedded energy was estimated using the volume of the grease trap (1.5 m^3). In order to estimate the embedded energy of the incoming drain water, the flow is required, and it was estimated at an average of two thirds of the maximum allowable flow. This maximum flow was calculated based on the legal minimum required retention time for grease traps. These assumptions are summarized in Table 2.

Table 2. Assumptions for flow calculation at the grease trap

Volume of the grease trap	1.5 m^3
Minimum required retention time	30 min
Estimated flow	2 m^3/h

4. Observations

The observed embedded energy was calculated assuming a minimum temperature of the drain water of $10°C$, the embedded energy is thus the energy available when cooling down the drain water to $10°C$. In winter, the mains water temperature can drop as low as $5°C$, allowing for a reasonable cushion between the hot wastewater temperature and the cold mains temperature.

4.1 Shower drain

The boxplot of the embedded energy in the shower drain, per unit of flow (m^3/h), over the measuring period 18/08/2017 – 09/09/2017 is given in Figure 2. The observed temperatures are too low to directly preheat the mains water, thus the only possibility here is to use the embedded heat as a heat source for a heat pump.

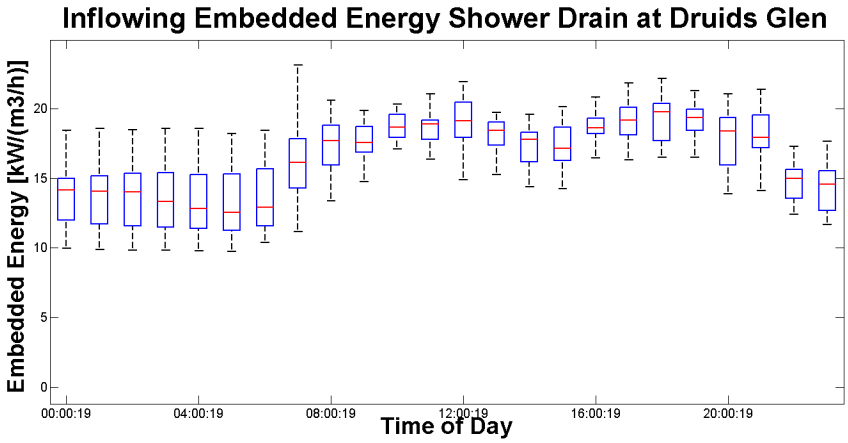


Figure 2. Embedded energy at the shower drain in Druids Glen

4.2 Kitchen grease trap

The energy embedded in the water body inside the grease trap, at different times of the day is shown in the boxplot in Figure 3. In this case temperatures are relatively high, and thus the embedded heat can be used for both preheating the mains water, and as a heat source for a heat pump.

5. Results and Discussion

Based on the embedded energy observed, and described in Section 4, a heat recovery system was selected and roughly designed, in order to estimate the Levelized Cost of Energy, and Total Equivalent Warming Impact [2] of such an installation. The first indicates a cost per produced kWh of heat, taking into account the capital investment, operating and maintenance costs, whereas the latter is indication for the related greenhouse gas emissions.

For all calculations a lifetime of $15\ years$, at 300 operating days per year was assumed, along with an electricity price of $0.22\ €/kWh$ [3]. The required size of the components is calculated using the Logarithmic Mean Temperature Difference Method [4], and the price using the Vatavuk method [5].

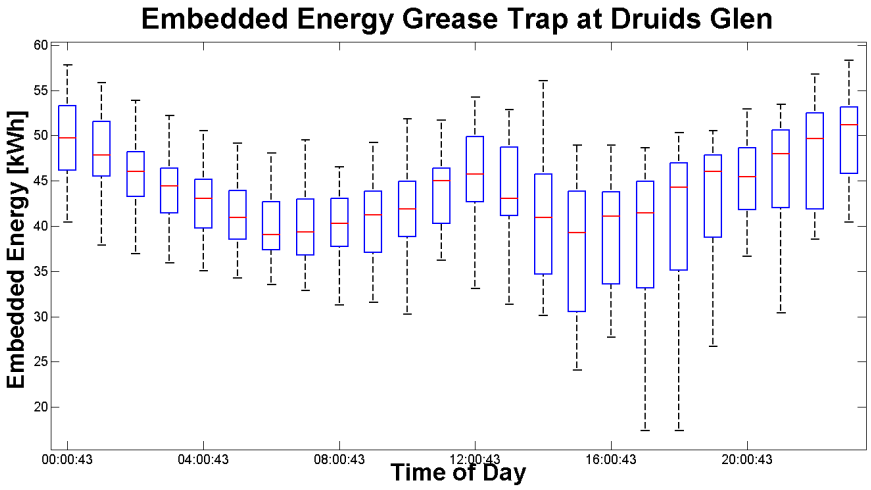


Figure 3. Embedded energy at the grease trap in Druids Glen

5.1 Shower drain

The observed temperature at the shower drain only allows for the heat to be used as a heat source for a heat pump, this type of heat recovery is denoted as indirect, and summarized in Figure 4.

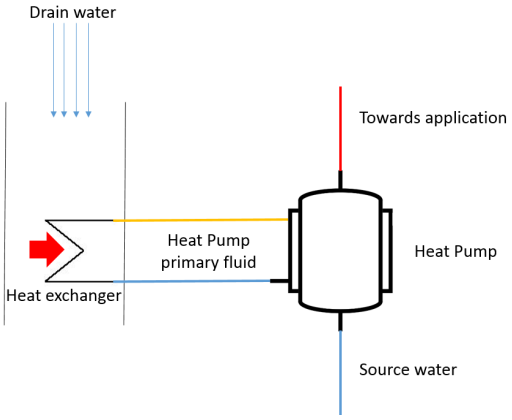


Figure 4. Indirect Drain Water Heat Recovery System

The main characteristics of the rough design of the system are summarized in Table 3.

Table 3. Main characteristics of the heat recovery system

	Direct	Indirect
Recovered Heating Power	\	$2.75\ kW$
Available Heating Power (Heat Pump)	\	$3.54\ kW$
Coefficient of Performance	\	4.45
Daily Operating Time	\	$6\ hrs$

The sizing of the different components in this heat recovery system, and their price is summarized in Table 4.

Table 4. Main components of the Heat Recovery System

	Direct	Indirect
Heat Exchanger Size	\	$0.73\ m^2$
Heat Exchanger Price	\	$775\ €$
Heat pump price	\	$6\ 650\ €$

Using the component prices as described in Table 4, the Levelized Cost of Energy can be calculated, and be compared to the values of classic heating systems as described in [6]. The results are summarized in Figure 5.

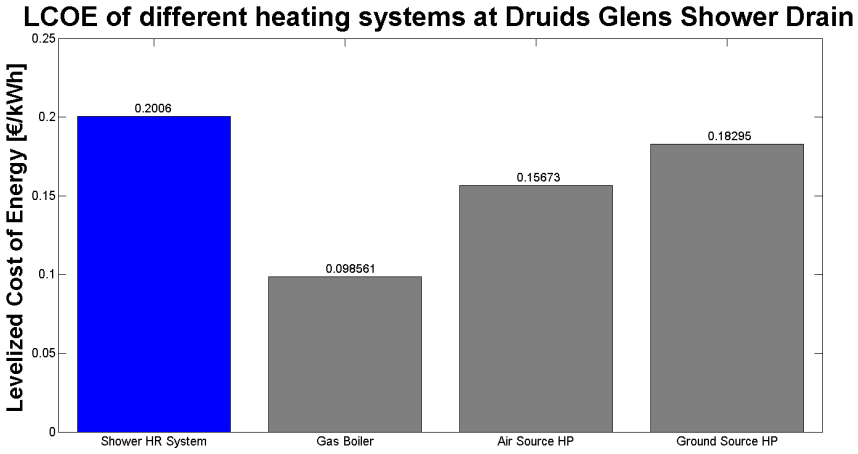


Figure 5. LCOE for different heating technologies at the shower drain in Druids Glen

In this Figure one can observe that the shower heat recovery system has the highest Levelized Cost of Energy, and is thus not cost-effective compared to its competitors, given the assumed flow rates. This is largely due to the increased capital cost, which will take up a higher share of the Levelized Cost of Energy.

Similarly the Total Equivalent Warming Impact per produced kWh can be estimated, using the emission factors as described in [7], the efficiency of the gas boiler is assumed to be 90%. The results are summarized in Figure 6.

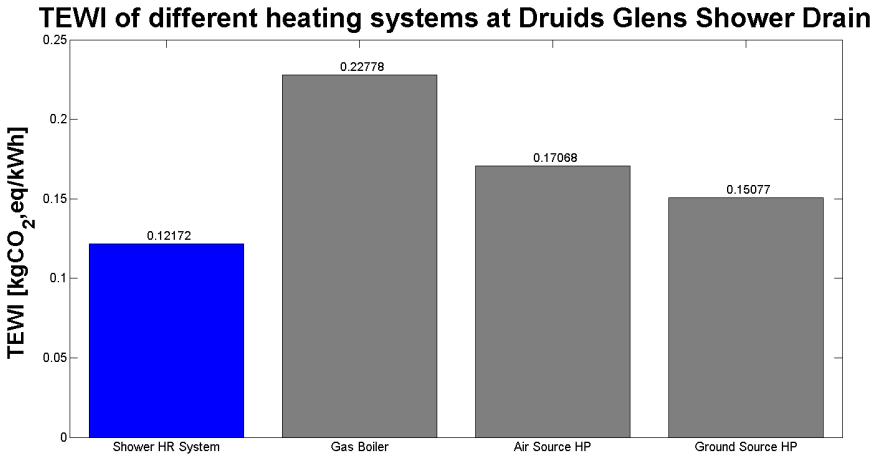


Figure 6. TEWI of different heating technologies at the shower drain in Druids Glen

This figure shows that the greenhouse gas emissions related to heat production through the heat recovery system are lower than the ones related to production through classical heating systems, thanks to an improved coefficient of performance.

Compared to a classic gas boiler system, the shower heat recovery system would introduce an estimated increased cost of 651.03 € per year, but an estimated reduction in greenhouse gas emissions of $676.94\ kg\ CO_{2,eq}$ per year.

5.2 Kitchen grease trap

The observed temperature at the kitchen grease trap allows for the heat to be used both to directly preheat the mains water, and as a heat source for a heat pump, this type of heat recovery is denoted as hybrid, and is a combination of a direct and an indirect heating system. The system is summarized in Figure 7.

The main characteristics of the rough design of the system are summarized in Table 5Table 3.

Table 5. Main characteristics of the heat recovery system

	Direct	Indirect
Recovered Heating Power	$4.29\ kW$	$2.90\ kW$
Available Heating Power (Heat Pump)	\	$3.74\ kW$
Coefficient of Performance	\	4.45
Daily Operating Time	$12\ hrs$	$12\ hrs$

The sizing of the different components in this heat recovery system, and their price is summarized in Table 6.

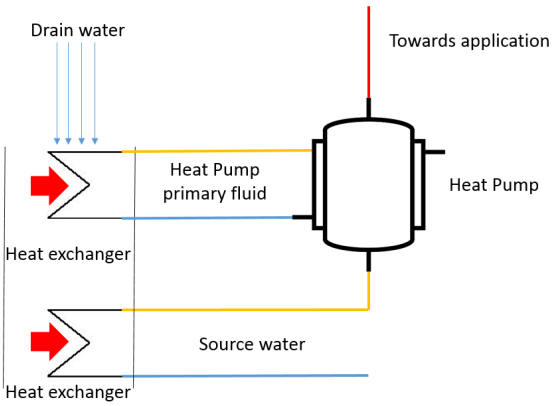


Figure 7. Hybrid Drain Water Heat Recovery System

Table 6. Main components of the heat recovery system

	Direct	Indirect
Heat Exchanger Size	1.05 m^2	0.40 m^2
Heat Exchanger Price	900 €	585 €
Heat pump price	\	6 740 €

Using the component prices as described in Table 6Table 4, the Levelized Cost of Energy can be calculated, and be compared to the values of classic heating systems as described in [6]. The results are summarized in Figure 8, where GT HHR stands for the Grease Trap Hybrid Heat Recovery, and GT IHR for Grease Trap Indirect Heat Recovery.

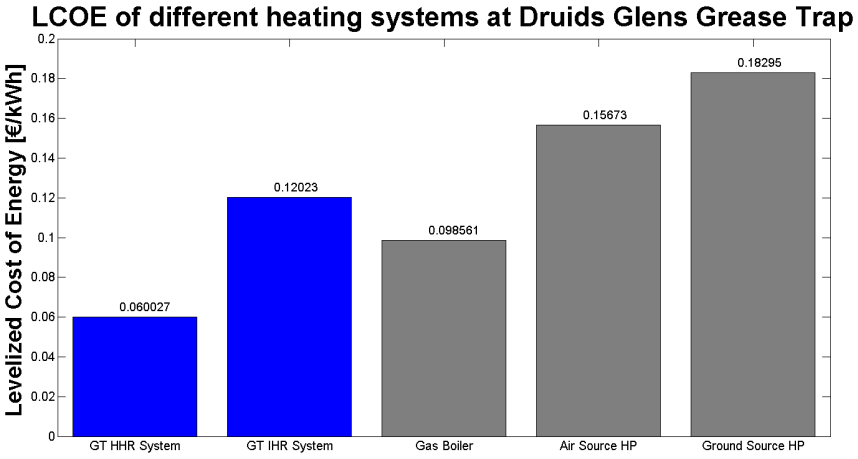


Figure 8. LCOE for different heating technologies at the grease trap in Druids Glen

In this Figure one can observe that the hybrid heat recovery system provides the heat at the lowest cost, however, the unit cost of the indirect part of the system is still higher than for a classic gas boiler system. The hybrid heat recovery system would provide an estimated decrease in heating spending of 1 110 € per year, compared to the gas heating, however a system combining direct heat

recovery with gas boiler heating would provide an estimated decrease in heating spending of $1\,400$ € per year, compared to the gas heating.

The LCOE of the indirect part of the heat recovery system, is significantly lower than the one for the shower heat recovery system, this is due to two main factors. On the one hand the embedded energy is larger, such that the lower fuel cost of heat production can make up for the increased capital cost. On the other hand the component price is lower due to higher drain water temperatures.

Similarly the Total Equivalent Warming Impact per produced kWh can be estimated, using the emission factors as described in [7], the efficiency of the gas boiler is assumed to be 90%. The results are summarized in Figure 9.

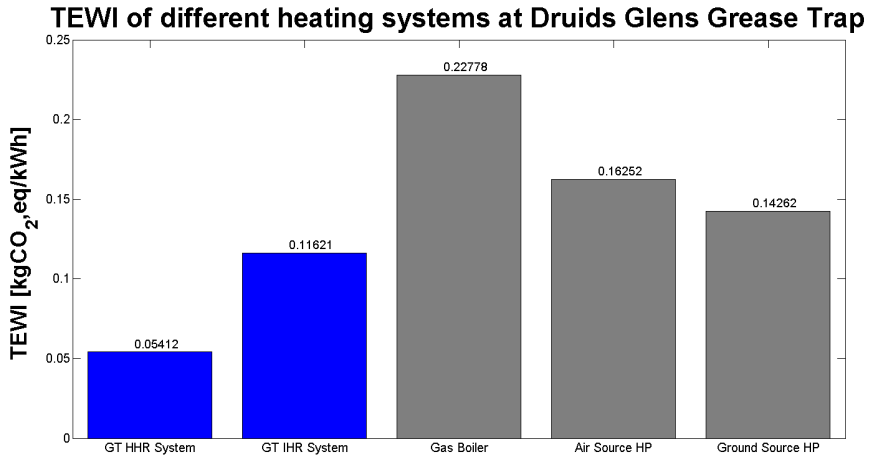


Figure 9. TEWI of different heating technologies at the grease trap in Druids Glen

This figure shows that the greenhouse gas emissions related to heat production through the hybrid heat recovery system are lower than the ones related to production through classical heating systems, thanks to an improved coefficient of performance.

Compared to a classic gas boiler system, the hybrid heat recovery system would introduce an estimated reduction in greenhouse gas emissions of $5\,000\ kg\ CO_{2,eq}$ per year, compared to a classic gas boiler system, a system combining direct heat recovery with gas boiler heating would introduce an estimated reduction in greenhouse gas emissions of $3\,500\ kg\ CO_{2,eq}$ per year.

6. Conclusion

The drain water at both measuring locations (shower drain and kitchen grease trap) in the Druids Glen hotel and resort contains a minimum of $10\ kW/(m^3/h)$ of embedded energy, both are

potential sites for drain water heat recovery. However, the proposed heat recovery system at the shower drain is not cost-effective compared to its competitors. It does have a potential for reducing the heating related greenhouse gas emissions by $676.94\ kg\ CO_{2,eq}$ per year and considerable more environmentally friendly than alternative techniques as a result..

The proposed hybrid heat recovery system at the kitchen grease trap is competitive compared to the classic heating system, but a combination of direct heat recovery with a gas boiler would be even more so, they represent estimated annual savings, compared to a classic gas system of $1\ 110$ € and $1\ 400$ €, respectively. The hybrid heat recovery system has a higher estimated GHG savings potential, $5\ 000\ kg\ CO_{2,eq}$ compared to $3\ 500\ kg\ CO_{2,eq}$, annually.

The opportunities for drain water heat recovery at Druids Glen Hotel & Resort are potentially useful candidates for a pilot demonstration of this technology supported by the Dwr Uisce Project. We are keen to explore the possibilities of installing such a pilot plant at the hotel further.

Bibliography

[1] D. Styles, H. Schoenberger and J. L. Galvez-Martos, “Water management in the European hospitality sector: Best practice, performance benchmarks and improvement potential,” *Tourism Management,* vol. 46, pp. 187-202, 2015.

[2] A. Zottl, M. Lindahl, R. Nordman, P. Rivière and M. Miara, “Evaluation method for comparison of heat pump systems with conventional heating systems,” Intelligent Energy Europe, 2011.

[3] SEAI, “Domestic Fuels- Comparison of Energy Costs,” Sustainable Energy Authority of Ireland, Dublin, 2017.

[4] Y. Cengel and M. A. Boles, Thermodynamics: An engineering approach, McGraw Hill, 2007.

[5] M. Taal, I. Bulatov, J. Klemes and P. Stehlik, “Cost estimation and energy price forecasts for economic evaluation of retrofit projects,” *Applied Thermal Engineering,* no. 23, pp. 1819-1835, 2003.

[6] Z. Wang, “Trade-offs in Levelized Cost of Herat among different domestic heating technologies,” in *All-Energy conference*, Glasgow, UK, 2017.

[7] SEAI, “What are the carbon emission factrs used?,” Sustainable Energy Authority Ireland, Dublin, Ireland, 2017.

Appendix A: Instrumentation

Technical specifications of temperature sensor (Tinytag TG-4100):

Gemini DATA LOGGERS

Tinytag Aquatic 2 (-40 to +70°C)
TG-4100
Issue 8 : 8th January 2016 (E&OE)



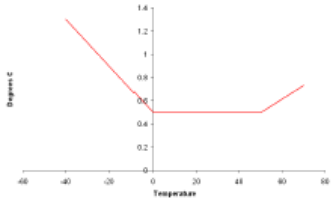
Features

Total Reading Capacity	32,000 readings
Memory type	Non Volatile
Trigger Start	Magnetic Switch
Delayed Start	Relative / Absolute (up to 45 days)
Stop Options	When full After n Readings Never (overwrite oldest data)
Reading Types	Actual, Min, Max
Logging Interval	1 sec to 10 days
Offload	While stopped or when logging in minutes mode
Alarms	2 fully programmable; latchable

Reading Specification

Reading Range	-40°C to +70°C (-40°F to +158°F)
Sensor Type	10K NTC Thermistor (Internally mounted)
Response Time	<20mins to 90% FSD in moving water
Reading Resolution	0.01°C or better

Reading Accuracy



Physical Specification

IP Rating	IP68 water proof (see notes)
Operational Range*	-40°C to +70°C (-40°F to +158°F)
Case Dimensions	
Diameter	51mm / 2.01"
Height	50mm / 1.97"
Weight	90g / 3.17oz

*The Operational Range indicates the physical limits to which the unit can be exposed, not the reading range over which it will record.

Calibration

This unit is configured to meet Gemini's quoted specification during its manufacture.

We recommend that the calibration of this unit should be checked annually against a calibrated reference meter.

A certificate of calibration, traceable to a national standard, can be supplied for an additional charge either at the point of purchase, or if the unit is returned for a service calibration.

Notes

This unit should only be opened when a battery replacement is required.

Battery Type	Renata CR2450N
Replacement Interval	Annually*

*If deployed for long periods, the logger's battery should be replaced annually to prevent the loss of data during a recording run. If the logger is being used frequently, the battery should be changed when prompted by a low battery warning from the Tinytag Explorer software.

Before replacing the battery the data logger must be stopped.

Data stored on the logger will be retained after a battery is replaced.

Please refer to the service kit instruction sheet for battery replacement instructions.

If used at low temperatures the data logger should be allowed to warm to room temperature before it is opened to avoid condensation forming inside the unit.

The IP68 rating is valid only when the unit's lid is securely fitted and is valid to a depth of 500m (1640ft).

The gasket fitted in this unit must be replaced every time it is opened.

The position of the unit's trigger start switch is indicated by the - - - marking on its base. The switch itself is positioned on the side of the unit, just above the base-lid join, on the edge indicated. When a magnet is held in the correct location, the status LED will light until the magnet is removed.

LED Flash Patterns

When logging, a status LED is visible through the base of the unit. The flash patterns of this indicator are as follows:

Flash Pattern	Indication
1 flash every 4 seconds	Logging
1 flash every 8 seconds	Waiting to Log (trigger or delayed start set)
A double flash every 4 seconds	Alarm limit breached

Approvals

Gemini Data Loggers (UK) Ltd. operates a Business Management System which conforms to ISO 9001 and ISO 14001.

CE

Required and Related Products

To use this data logger you will require a copy of the following software:

SWCD-0040: Tinytag Explorer software

and an

ACS-3030: USB Inductive Pad

These items can be purchased together in a discounted pack:

SWPK-3-USB Tinytag Explorer and Inductive Pad Pack.

Further Related Products

SER-9525: Tinytag Aquatic 2 Service Kit

data sheet

www.tinytag.info sales@tinytag.info

B.2. Talbot Hotel Stillorgan

Trinity College Dublin
Coláiste na Tríonóide, Baile Átha Cliath
The University of Dublin

Dŵr Uisce
Energy Recovery in Water Services
Adennill Ynni yn y Diwydiant Dŵr

PRIFYSGOL BANGOR UNIVERSITY

Monitoring campaign at Talbot Hotel, Stillorgan: Potential for heat recovery from waste water

TALBOT HOTEL
STILLORGAN

Feasibility study
April 2018

Cronfa Datblygu Rhanbarthol Ewrop
European Regional Development Fund

Ireland's European Structural and Investment Funds Programmes 2014-2020
Co-funded by the Irish Government and the European Union

Tionól Réigiúnach an Deiscirt
Southern Regional Assembly

EU Funds: Ireland Wales Programme 2014-2020



Table of Contents

1. Introduction 1
2. Objectives 1
3. Monitoring points 1
4. Observations 2
4.1 Flow through the grease trap 2
4.2 Temperature in the grease trap 3
5. Results and Discussion 4
5.1 Direct Drain Water Heat Recovery 4
6. Conclusion 5
Bibliography 5
Appendix A: Instrumentation 6
Technical specifications of temperature sensor (Tinytag TG-4100): 6

1. Introduction

The aim of this monitoring campaign was to assess the feasibility of implementing a waste water heat recovery system in the commercial activities at Talbot Hotel in Stillorgan, Dublin, whereby waste heat from the kitchen drain would be recovered and transferred to the existing heating system. This has the potential to reduce the gas consumption of the existing boilers and generate financial and environmental savings for the company. The proposal is based on the Drain Water Heat Recovery concept (DWHR), which consists of a heat exchanger placed in the waste water drain.

This assessment forms part of the Dŵr Uisce project (*www.dwr-uisce.eu*), which aims at improving the energy efficiency of the distribution of water resources by quantifying and demonstrating the potential of integrated smart and low-carbon technology. In this context the commercial hot-water activities at Talbot Hotel Stillorgan offers an opportunity to investigate the potential of waste water heat recovery technology in the hospitality sector. This technology can help towards improving environmental, energetic and financial performance of the hotel facilities.

2. Objectives

The primary objectives of this project include:

- Assessing the potential to improve the energy efficiency of water heating activities in the Talbot hotel, Stillorgan, through DWHR.
- To facilitate awareness raising, public and industry engagement in the concept of DWHR

In order to reach and quantify these primary objectives, the embedded energy in the wastewater on the property must be measured and quantified. This requires the following measurements or estimations, at the locations that are proposed in this document

- Wastewater temperature.
- Wastewater flow.

3. Monitoring points

Only one possible monitoring point was identified at the hotel, the kitchen grease trap. This grease trap is installed under the above ground parking of the hotel, as shown in Figure 1.

The temperature in the grease trap is high enough to consider Direct Drain Water Heat Recovery (D-DWHR), as shown in Figure 2. A potential hybrid heat recovery system (combining the direct heat recovery system with a heat pump) is not discussed in the report, as the system proved to be financially unattractive (the payback period was larger than the lifetime of the system).

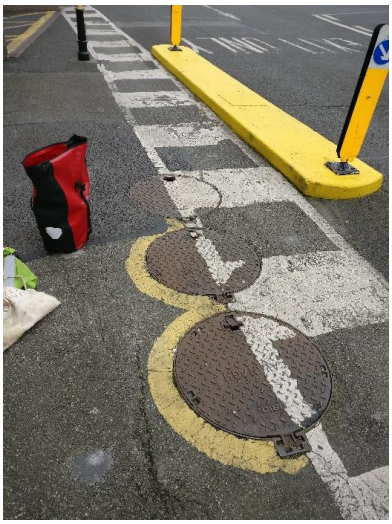


Figure 1. Manholes leading to the grease trap

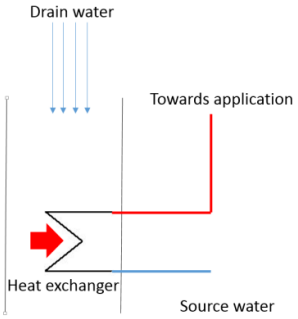


Figure 2. Direct Drain Water Heat Recovery

4. Observations

4.1 Flow through the grease trap

The water consumption of the kitchen, which flows to the grease trap is not available. The flow through the grease trap is estimated based on the information regarding the total water consumption of the hotel, the gas consumption of the kitchen and the total gas consumption. It is assumed that the share of the kitchen's consumption, as compared to the total consumption is the same for gas and water (ranging between 7 and 9%, with an exceptional peak of 11% in August), and that 80% of the consumed water will leave the kitchen as wastewater. This results in a total monthly flow as shown in Figure 3.

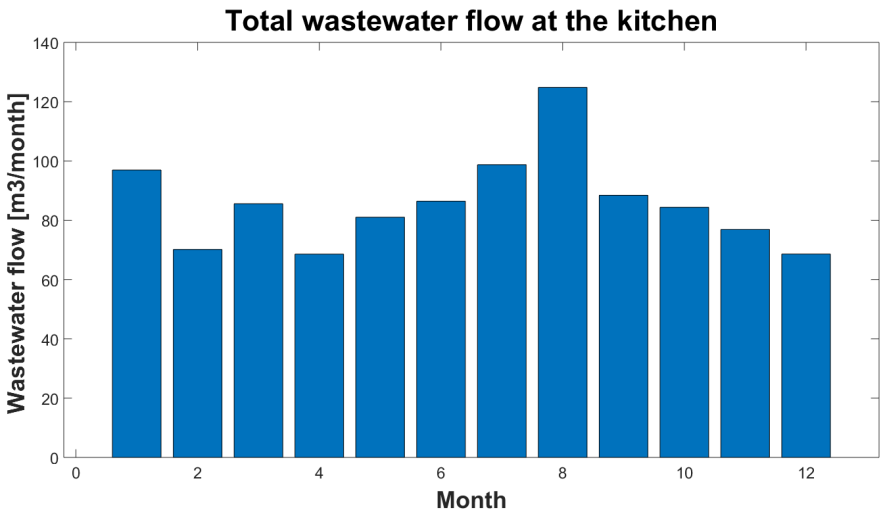


Figure 3. Estimated wastewater flow from the kitchen

4.2 Temperature in the grease trap

The observed temperatures are shown in Figure 4.

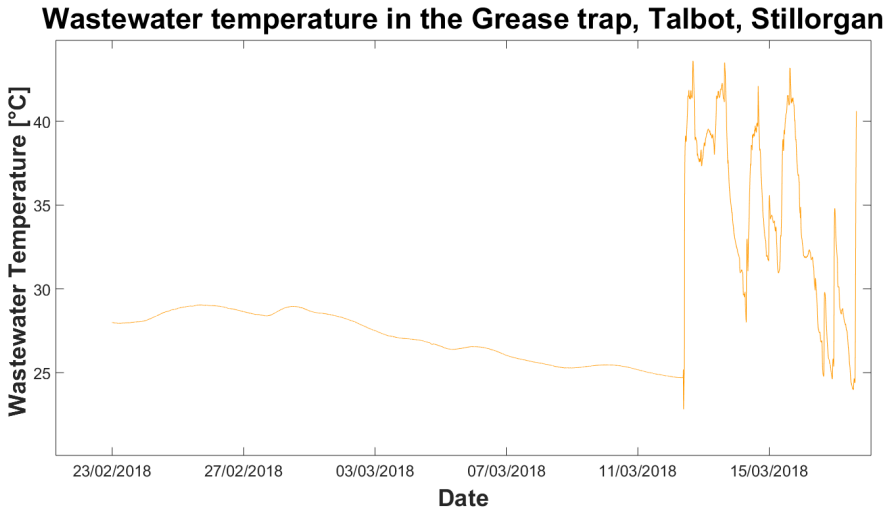


Figure 4. Temperature at the Grease trap, Talbot Hotel, Stillorgan

A remarkable shift can be observed around March 12th, this shift is due to the change in position of the temperature sensor. At that time, the grease trap was emptied, and the sensor was moved from the middle manhole to the first (inlet), the manholes are shown in Figure 1. One can observe that

the temperature is higher, but much less stable in the inlet region of the grease trap. The calculations in this report will thus provide a lower estimate of the recoverable heat.

5. Results and Discussion

Based on the observations, described in Section 4, a heat recovery system was selected and roughly designed, in order to estimate payback period and total saved greenhouse gas emissions of such an installation.

For the calculations an electricity price of $0.12\ €/kWh$, and a gas price of $0.0334\ €/kWh$ (as given in the documentation provided by Talbot Hotel) were used [1]. The required size of the components was calculated using the Logarithmic Mean Temperature Difference Method [2], and the price using the Vatavuk method [3].

5.1 Direct Drain Water Heat Recovery

The wastewater flow data was only available in monthly values, it is therefore not possible to assess whether the wastewater flow and fresh water flow will occur at the same moment. To address this issue, one possibility is to use a custom-made heat exchanger, placed in the grease trap, which circumvents this problem. However, this would require the fresh water to be pumped through this heat exchanger, in this case this would reduce cost and emission savings.

The feasibility of a horizontal Direct-DWHR system, installed on the drain pipes connecting the kitchen to the grease trap is thus assessed. The analysis is using the effectiveness data from the ShowerSave Linear Drain system, which is commercially available. A horizontal system is required, because the kitchen is situated at the same elevation as the grease trap. A concurrence rate of 80% is assumed, meaning that in 80% of cases there will be concurrence between wastewater flow and fresh water flow. A breakdown of the estimated capital investment is given in Table 1.

Table 1. Breakdown of cost for the D-DWHR system

Fuel Prices	
Electricity	$0.12\ €/kWh$
Current heating fuel	$0.0334€/kWh$
Capital Investment	$1\,000\ €$
Direct Component	
Heat Exchanger	$500\ €$
Plumbing	$500\ €$

Using these estimates, the payback period is calculated. The total yearly GHG savings are calculated as well, the carbon intensities employed are as mentioned in [4].

Table 2. Simulation results

System	Operating days	GHG savings $kg\ C_e/yr$	Investment	Payback Period
D-DWHR	220	711.88	$1\,000\ €$	$8.62\ yrs$

The Direct-DWHR system would save about $3.5\ MWh$ of heavy fuel from being burnt, per year, resulting in a cost reduction of about 116 €, and $711.88\ kg\ CO_{2,eq}$ of emission reduction. These values are rather conservative. The proposed heat recovery system is situated upstream the grease trap, and temperatures are thus expected to be higher than the ones observed in the grease trap, and employed in this analysis. This is confirmed by experiences in other locations.

Some uncertainty on the effectiveness of the horizontal Direct-DWHR system remains, as the ShowerSave Linear Drain system was designed for use in combination with showers. The characteristics of this system might not directly translate to its performance in case it is used in combination with a kitchen drain.

6. Conclusion

At the Talbot Hotel in Stillorgan, a horizontal, Direct-DWHR system is considered. It could be installed on the horizontal drain connecting the kitchen drain with the grease trap. The expected payback period of such a system is a little under $9\ years$, furthermore, some uncertainty remains regarding the effectiveness of the horizontal DWHR system, as the employed values relate to a system design for use in combination with showers. The system would save about $700\ kg\ C_e$ per year.

Bibliography

[1] SEAI, “Domestic Fuels- Comparison of Energy Costs,” Sustainable Energy Authority of Ireland, Dublin, 2017.

[2] Y. Cengel and M. A. Boles, Thermodynamics: An engineering approach, McGraw Hill, 2007.

[3] M. Taal, I. Bulatov, J. Klemes and P. Stehlik, “Cost estimation and energy price forecasts for economic evaluation of retrofit projects,” *Applied Thermal Engineering,* no. 23, pp. 1819-1835, 2003.

[4] SEAI, “What are the carbon emission factrs used?,” Sustainable Energy Authority Ireland, Dublin, Ireland, 2017.

[5] A. Zottl, M. Lindahl, R. Nordman, P. Rivière and M. Miara, “Evaluation method for comparison of heat pump systems with conventional heating systems,” Intelligent Energy Europe, 2011.

Appendix A: Instrumentation

Technical specifications of temperature sensor (Tinytag TG-4100):

Gemini DATA LOGGERS

Tinytag Aquatic 2 (-40 to +70°C)
TG-4100
Issue 8 : 8th January 2016 (E&OE)



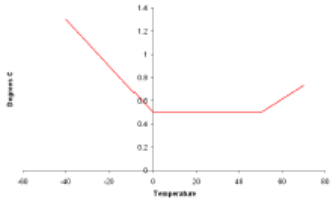
Features

Total Reading Capacity	32,000 readings
Memory type	Non Volatile
Trigger Start	Magnetic Switch
Delayed Start	Relative / Absolute (up to 45 days)
Stop Options	When full After n Readings Never (overwrite oldest data)
Reading Types	Actual, Min, Max
Logging Interval	1 sec to 10 days
Offload	While stopped or when logging in minutes mode
Alarms	2 fully programmable; latchable

Reading Specification

Reading Range	-40°C to +70°C (-40°F to +158°F)
Sensor Type	10K NTC Thermistor (Internally mounted)
Response Time	<20mins to 90% FSD in moving water
Reading Resolution	0.01°C or better

Reading Accuracy



Physical Specification

IP Rating	IP68 water proof (see notes)
Operational Range*	-40°C to +70°C (-40°F to +158°F)
Case Dimensions	
Diameter	51mm / 2.01"
Height	50mm / 1.97"
Weight	90g / 3.17oz

*The Operational Range indicates the physical limits to which the unit can be exposed, not the reading range over which it will record.

Calibration

This unit is configured to meet Gemini's quoted specification during its manufacture.

We recommend that the calibration of this unit should be checked annually against a calibrated reference meter.

A certificate of calibration, traceable to a national standard, can be supplied for an additional charge either at the point of purchase, or if the unit is returned for a service calibration.

Notes

This unit should only be opened when a battery replacement is required.

Battery Type	Renata CR2450N
Replacement Interval	Annually*

*If deployed for long periods, the logger's battery should be replaced annually to prevent the loss of data during a recording run. If the logger is being used frequently, the battery should be changed when prompted by a low battery warning from the Tinytag Explorer software.

Before replacing the battery the data logger must be stopped.

Data stored on the logger will be retained after a battery is replaced.

Please refer to the service kit instruction sheet for battery replacement instructions.

If used at low temperatures the data logger should be allowed to warm to room temperature before it is opened to avoid condensation forming inside the unit.

The IP68 rating is valid only when the unit's lid is securely fitted and is valid to a depth of 500m (1640ft).

The gasket fitted in this unit must be replaced every time it is opened.

The position of the unit's trigger start switch is indicated by the - - - marking on its base. The switch itself is positioned on the side of the unit, just above the base-lid join, on the edge indicated. When a magnet is held in the correct location, the status LED will light until the magnet is removed.

LED Flash Patterns

When logging, a status LED is visible through the base of the unit. The flash patterns of this indicator are as follows:

Flash Pattern	Indication
1 flash every 4 seconds	Logging
1 flash every 8 seconds	Waiting to Log (trigger or delayed start set)
A double flash every 4 seconds	Alarm limit breached

Approvals

Gemini Data Loggers (UK) Ltd. operates a Business Management System which conforms to ISO 9001 and ISO 14001.

CE

Required and Related Products

To use this data logger you will require a copy of the following software:

SWCD-0040: Tinytag Explorer software

and an

ACS-3030: USB Inductive Pad

These items can be purchased together in a discounted pack:

SWPK-3-USB Tinytag Explorer and Inductive Pad Pack.

Further Related Products

SER-9525: Tinytag Aquatic 2 Service Kit

data sheet

www.tinytag.info sales@tinytag.info

B.3. Ashlawn Nursing Home

Trinity College Dublin
Coláiste na Trionóide, Baile Átha Cliath
The University of Dublin

Dŵr Uisce
Energy Recovery in Water Services
Adennill Ynni yn y Diwydiant Dŵr

Prifysgol Bangor University

Monitoring campaign at Ashlawn Nursing Home, Tipperary: Potential for heat recovery from waste water

Ashlawn House
NURSING HOME

Feasibility study
August 2018

Cronfa Datblygu Rhanbarthol Ewrop
European Regional Development Fund

Ireland's European Structural and Investment Funds Programmes 2014-2020
Co-funded by the Irish Government and the European Union

Tionól Réigiúnach an Deiscirt
Southern Regional Assembly

EU Funds: Ireland Wales Programme 2014-2020



Table of Contents

1. Introduction 1
2. Objectives 1
3. Monitoring points 1
4. Observations & Estimates 3
4.1 Grease Trap 3
4.2 Septic tank 4
5. Results and Discussion 5
5.1 Grease trap 5
5.2 Septic Tank 5
6. Conclusion 6
Bibliography 6
Appendix A: Instrumentation 7
Technical specifications of temperature sensor (Tinytag TG-4100): 7

1. Introduction

The aim of this monitoring campaign was to assess the feasibility of implementing a waste water heat recovery system in the different waste water streams at the Nursing home in Ashlawn, Tipperary, whereby waste heat from the drain would be recovered and used to preheat the mains water. This has the potential to reduce the gas consumption of the existing boilers and generate financial and environmental savings for the company. The proposal is based on the Drain Water Heat Recovery concept (DWHR), which consists of a heat exchanger placed in the waste water drain.

This assessment forms part of the Dŵr Uisce project (*www.dwr-uisce.eu*), which aims at improving the energy efficiency of the distribution of water resources by quantifying and demonstrating the potential of integrated smart and low-carbon technology. In this context the commercial activity at Ashlawn Nursing Home offers a unique opportunity to investigate the potential of waste water heat recovery technology in the elderly care sector. This technology can help towards improving environmental, energetic and financial performance of the facilities.

2. Objectives

The primary objectives of this project include:

- Assessing the potential to improve the energy efficiency of water heating activities in the nursing home in Ashlawn, Tipperary, through DWHR.
- To facilitate awareness raising, public and industry engagement in the concept of DWHR

In order to reach and quantify these primary objectives, the embedded energy in the wastewater on the property must be measured and quantified. This requires the following measurements or estimations, at the locations that are proposed in this document

- Wastewater temperature.
- Wastewater flow.

3. Monitoring points

Two different, potential locations for drain water heat recovery have been identified. The first one being the grease trap, where the drain water from the kitchen is collected before streaming on to the septic tank. The septic tank is the second location being considered. TinyTag temperature sensors (see Appendix A) have been used.

The temperature in the grease trap is expected to be high enough to consider Direct Drain Water Heat Recovery (D-DWHR), as shown in Figure 2. A potential indirect heat recovery system (using the drain water as a heat source for a heat pump) is discussed to recover heat from the septic tank, see Figure 1.



Figure 1. Septic tank at the Ashlawn nursing home

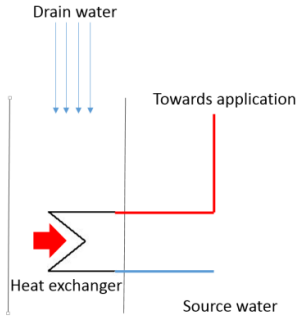


Figure 2. Direct Drain Water Heat Recovery

The temperature of the drain water in the septic tank is expected to be too low for a direct heat recovery system. This heat could be used as the heat source for a heat pump, the technique is called Indirect Drain Water Heat Recovery (I-DWHR), and is summarized in Figure 3.

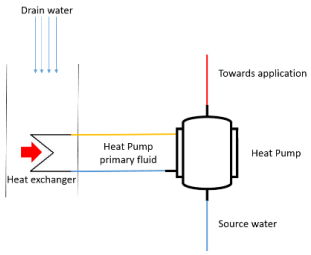


Figure 3. Indirect Drain Water Heat Recovery

4. Observations & Estimates

Temperatures have been measured at both locations, but the flow could not be measured. Flow was estimated based on the total yearly flow data provided, and the average flow profile in a residence in the UK, as given in [1]. The average flow value was multiplied with average synthetic load profile (percentage of the flow at that point in time, compared to the total daily flow), as shown in Figure 4.

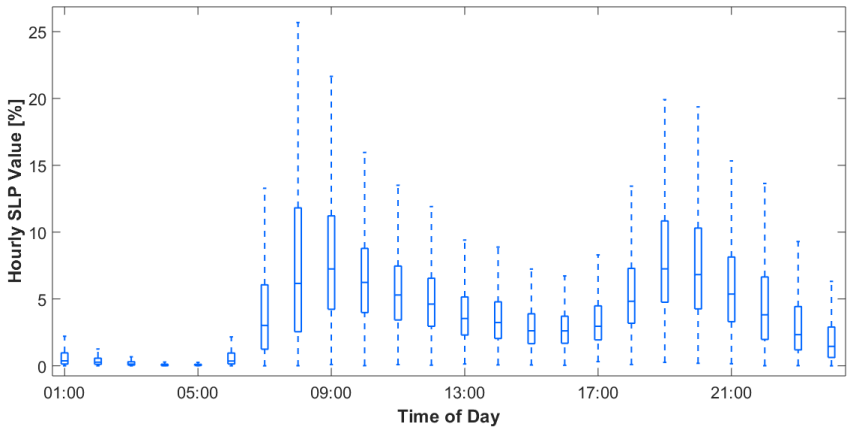


Figure 4. Synthetic Load Profile for the drain water in a residence.

4.1 Grease Trap

The temperature in the grease trap was measured over a three-week period, the measurements are shown in Figure 5, with peaks up to $45°C$.

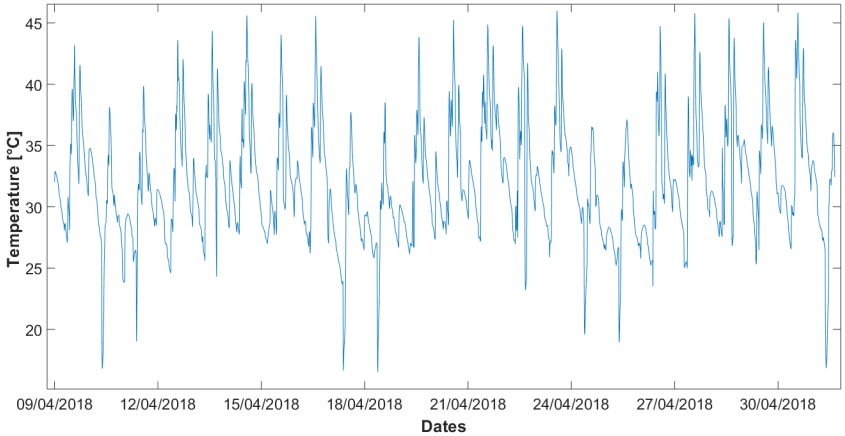


Figure 5. Temperature Evolution in the grease trap of the Ashlawn nursing home

The total daily flow was estimated based on the total annual water consumption, assuming that 90% of this flow will result in drain water, considering the other 10% to be evaporated, spilled, or lost through other mechanisms. The flow through the grease trap is assumed to be the total flow ($1\,600\ m^3/year$), minus water consumption for showers, toilets, and drinking, and clothes washing. The total drain water flow for the kitchen is estimated in Table 1. This value is then multiplied with the Synthetic Load profile (Figure 4), to obtain a daily profile.

Table 1. Kitchen drain flow estimates.

Shower flow estimate	$2\,496\ l/day$
Number of inhabitants	52
Shower time	$6\ min/inhabitant$
Shower flow rate	$8\ l/min$
Number of staff at the premises	10
Drinking water estimate	$124\ l/day$
Drinking water per person	$2\ l/person$
Toilet flow estimate	$744\ l/day$
Flush volume	$2 * 6l/person$
Water consumption for Clothes washing	$150\ l/day$
Total kitchen drain flow estimate	$782.61\ l/day$

4.2 Septic tank

The temperature in the first chamber of the septic tank was measured over the same period as in the grease trap, as can be seen in Figure 6, the temperature in the septic tank is much lower than in the grease trap. One can clearly observe daily patterns, and an increasing trend, related to increasing outside temperature.

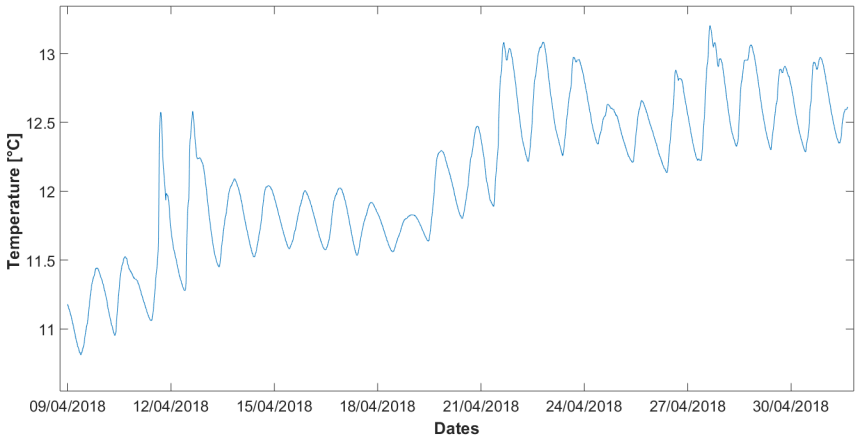


Figure 6. Temperature in the septic tank at the Ashlawn Nursing Home

The flow is estimated as 90% of the total water consumption, or $3.5\ m^3/day$, and its profile is obtained by multiplying this value with the Synthetic Load profile (Figure 4).

5. Results and Discussion

Based on the observations, described in Section 4, a heat recovery system was selected and roughly designed, in order to estimate payback period and total saved greenhouse gas emissions of such an installation.

For the calculations an electricity price of $0.12\ €/kWh$, and a gas price of $0.045\ €/kWh$ were assumed [2]. The required size of the components was calculated using the Logarithmic Mean Temperature Difference Method [3], and the price using the Vatavuk method [4].

5.1 Grease trap

The feasibility of horizontal Direct-DWHR systems, installed in the grease trap was assessed. The analysis was conducted using a system effectiveness of 50%. A breakdown of the estimated capital investment is given in Table 2.

Table 2. Breakdown of cost for the D-DWHR system

Fuel Prices	
Electricity	$0.12\ €/kWh$
Current heating fuel	$0.045\ €/kWh$
Capital Investment	$1\,075\ €$
Direct Component	
Heat Exchanger	$375\ €$
Circulation pump	$400\ €$
Plumbing	$300\ €$

Using these estimates, the payback period was calculated. The total yearly GHG savings were calculated as well. The carbon intensities employed were mentioned in [4]. The savings are compared to a gas boiler system. The results are summarized in Table 3.

Table 3. Simulation results

System	Operating days	Energy savings kWh/yr	GHG savings $kg\ C_e/yr$	Investment	Payback Period
D-DWHR	365	2 644	542.33	1 075 €	9.94 yrs

The Direct-DWHR system would save about $2.6\ MWh$ of gas from being burnt, per year, resulting in a cost reduction of about $119\ €$, and $542.33\ kg\ CO_{2,eq}$ of emission reduction.

5.2 Septic Tank

The feasibility of an Indirect DWHR system was assessed, with a heat exchanger installed in the septic tank, recovering the heat which will serve as the heat source for the heat pump. A breakdown of the estimated capital investment is given in Table 4.

Table 4. Breakdown of cost for the I-DWHR system

Fuel Prices	
Electricity	0.12 €$/kWh$
Current heating fuel	0.045 €$/kWh$
Capital Investment	11 610 €
Indirect Component	
Heat Exchanger	1 505 €
Heat Pump	7 105 €
Circulation pump	500 €
Plumbing	2 500 €

It is assumed that the heat pump will deliver heat at a temperature of 45°C, this will result in a COP varying between 4.5 and 4.8 depending on the temperature in the septic tank. Using these estimates, the payback period was calculated. The yearly GHG savings were calculated as well. The carbon intensities employed are as mentioned in [4]. The results are summarized in Table 5.

Table 5. Septic tank DWHR simulation results

System	Operating days	GHG savings $kg\ C_e/yr$	Investment	Payback Period
I-DWHR	365	3 560.3	11 610 €	16.79 yrs

6. Conclusion

Two different locations for heat recovery have been considered, although both of them would entail energy and greenhouse gas savings, their financial payback periods (around 10 and 17 $years$), are relatively long compared to the lifetime of the heat recovery system (20 $years$), and they would thus not be considered economically viable. The Direct-DWHR system at the grease trap and the Indirect-DWHR system at the septic tank could result in yearly GHG emission reductions of 542.33 and $3\ 560.3\ kg\ C_e/yr$, respectively.

Bibliography

[1] J. Cunniffe and A. McNabola, “Drain Water Heat REcovery From A Single Domestic household,” 2014.

[2] SEAI, “Domestic Fuels- Comparison of Energy Costs,” Sustainable Energy Authority of Ireland, Dublin, 2017.

[3] Y. Cengel and M. A. Boles, Thermodynamics: An engineering approach, McGraw Hill, 2007.

[4] M. Taal, I. Bulatov, J. Klemes and P. Stehlik, “Cost estimation and energy price forecasts for economic evaluation of retrofit projects,” *Applied Thermal Engineering,* no. 23, pp. 1819-1835, 2003.

[5] SEAI, “What are the carbon emission factrs used?,” Sustainable Energy Authority Ireland, Dublin, Ireland, 2017.

[6] A. Zottl, M. Lindahl, R. Nordman, P. Rivière and M. Miara, “Evaluation method for comparison of heat pump systems with conventional heating systems,” Intelligent Energy Europe, 2011.

Appendix A: Instrumentation

Technical specifications of temperature sensor (Tinytag TG-4100):

Gemini DATA LOGGERS

Tinytag Aquatic 2 (-40 to +70°C)
TG-4100
Issue 8 : 8th January 2016 (E&OE)



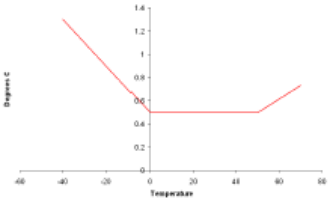
Features

Total Reading Capacity	32,000 readings
Memory type	Non Volatile
Trigger Start	Magnetic Switch
Delayed Start	Relative / Absolute (up to 45 days)
Stop Options	When full After n Readings Never (overwrite oldest data)
Reading Types	Actual, Min, Max
Logging Interval	1 sec to 10 days
Offload	While stopped or when logging in minutes mode
Alarms	2 fully programmable; latchable

Reading Specification

Reading Range	-40°C to +70°C (-40°F to +158°F)
Sensor Type	10K NTC Thermistor (Internally mounted)
Response Time	<20mins to 90% FSD in moving water
Reading Resolution	0.01°C or better

Reading Accuracy



Physical Specification

IP Rating	IP68 water proof (see notes)
Operational Range*	-40°C to +70°C (-40°F to +158°F)
Case Dimensions	
Diameter	51mm / 2.01"
Height	50mm / 1.97"
Weight	90g / 3.17oz

*The Operational Range indicates the physical limits to which the unit can be exposed, not the reading range over which it will record.

Calibration

This unit is configured to meet Gemini's quoted specification during its manufacture.

We recommend that the calibration of this unit should be checked annually against a calibrated reference meter.

A certificate of calibration, traceable to a national standard, can be supplied for an additional charge either at the point of purchase, or if the unit is returned for a service calibration.

Notes

This unit should only be opened when a battery replacement is required.

Battery Type	Renata CR2450N
Replacement Interval	Annually*

*If deployed for long periods, the logger's battery should be replaced annually to prevent the loss of data during a recording run. If the logger is being used frequently, the battery should be changed when prompted by a low battery warning from the Tinytag Explorer software.

Before replacing the battery the data logger must be stopped.

Data stored on the logger will be retained after a battery is replaced.

Please refer to the service kit instruction sheet for battery replacement instructions.

If used at low temperatures the data logger should be allowed to warm to room temperature before it is opened to avoid condensation forming inside the unit.

The IP68 rating is valid only when the unit's lid is securely fitted and is valid to a depth of 500m (1640ft).

The gasket fitted in this unit must be replaced every time it is opened.

The position of the unit's trigger start switch is indicated by the - - - marking on its base. The switch itself is positioned on the side of the unit, just above the base-lid join, on the edge indicated. When a magnet is held in the correct location, the status LED will light until the magnet is removed.

LED Flash Patterns

When logging, a status LED is visible through the base of the unit. The flash patterns of this indicator are as follows:

Flash Pattern	Indication
1 flash every 4 seconds	Logging
1 flash every 8 seconds	Waiting to Log (trigger or delayed start set)
A double flash every 4 seconds	Alarm limit breached

Approvals

Gemini Data Loggers (UK) Ltd. operates a Business Management System which conforms to ISO 9001 and ISO 14001.

CE

Required and Related Products

To use this data logger you will require a copy of the following software:

SWCD-0040: Tinytag Explorer software

and an

ACS-3030: USB Inductive Pad

These items can be purchased together in a discounted pack:

SWPK-3-USB Tinytag Explorer and Inductive Pad Pack.

Further Related Products

SER-9525: Tinytag Aquatic 2 Service Kit

data sheet

www.tinytag.info sales@tinytag.info

B.4. ABP meat processing plant, Clones

Trinity College Dublin
Coláiste na Trionóide, Baile Átha Cliath
The University of Dublin

Dŵr Uisce
Energy Recovery in Water Services
Adennill Ynni yn y Diwydiant Dŵr

Prifysgol Bangor University

Monitoring campaign at ABP, Clones:
Potential for heat recovery from waste water

abp Food Group

Feasibility study
April 2018

Cronfa Datblygu Rhanbarthol Ewrop
European Regional Development Fund

Ireland's European Structural and Investment Funds Programmes 2014-2020
Co-funded by the Irish Government and the European Union

Tionól Réigiúnach an Deiscirt
Southern Regional Assembly

EU Funds: Ireland Wales Programme 2014-2020



Table of Contents

1. Introduction 1
2. Objectives 1
3. Monitoring points 1
3.1 WWTP Inlet 1
3.2 DAF outlet 2
3.3 WWTP outlet 2
4. Observations 3
4.1 Flow through the system 3
4.2 Temperatures throughout the WWTP 4
5. Results and Discussion 5
5.1 Hybrid Drain Water Heat Recovery at the DAF unit 5
5.1 Direct Drain Water Heat Recovery at the WWTP outlet 7
6. Conclusion 9
Bibliography 9
Appendix A: Instrumentation 10
Technical specifications of temperature sensor (Tinytag TG-4100): 10

1. Introduction

The aim of this monitoring campaign was to assess the feasibility of implementing a waste water heat recovery system in the industrial process at the ABPs meat processing facilities, whereby waste heat from the process would be recovered and transferred to the existing heating system. This has the potential to reduce the heavy fuel oil consumption of the existing boilers and generate financial and environmental savings for the company. The proposal is based on the Drain Water Heat Recovery concept (DWHR), which consists of a heat exchanger placed in the waste water drain, and, if necessary, a heat pump.

This assessment forms part of the Dŵr Uisce project (*www.dwr-uisce.eu*), which aims at improving the energy efficiency of the distribution of water resources by quantifying and demonstrating the potential of integrated smart and low-carbon technology. In this context the industrial process at ABP offers a unique opportunity to investigate the potential of waste water heat recovery technology in the food processing sector. This technology can help towards improving environmental, energetic and financial performance of the facilities.

2. Objectives

The primary objectives of this project include:

- Assessing the potential to improve the energy efficiency of water heating activities in the process at ABP meat processing facilities, through DWHR.
- To facilitate awareness raising, public and industry engagement in the concept of DWHR

In order to reach and quantify these primary objectives, the embedded energy in the wastewater on the property must be measured and quantified. This requires the following measurements or estimations, at the locations that are proposed in this document

- Wastewater temperature.
- Wastewater flow.

3. Monitoring points

After visiting the site, three monitoring points were identified. The inlet of the wastewater treatment plant (WWTP), the outlet of the Dissolved Air Flotation (DAF) unit, and the outlet of the total treatment plant were equipped with temperature loggers (Appendix A). The flow at these locations was estimated based on information provided by ABP.

3.1 WWTP Inlet

The wastewater at the inlet of the wastewater treatment plant is too rich in nutrients to have a reasonable DWHR system. A DWHR system in this part of the wastewater chain would have serious fouling issues, increasing the risk of blockages of the system. The data is used, however, as a baseline for comparison and understanding of the processes further in the wastewater treatment system.

3.2 DAF outlet

As Figure 1 shows, the wastewater leaving the DAF is still rich in nutrients, however the large vertical drop upon leaving the DAF unit reduces fouling issues, while providing an opportunity for a more efficient, vertical heat exchanger.



Figure 1. Wastewater leaving the DAF unit

At this location a hybrid drain water heat recovery can be considered, as shown in Figure 2. The direct heat recovery system, which consist of preheating the mains water is generally feasible at high wastewater temperatures, whereas indirect heat recovery, using a heat pump, is generally reserved for locations with large flows. In this case one can expect that both these conditions are met.

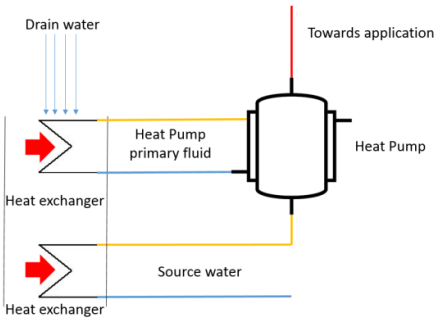


Figure 2. Hybrid drain water heat recovery system

3.3 WWTP outlet

The outlet of the WWTP provides the advantage of clean water, and thus less fouling issues. Additionally, the wastewater can be cooled down to a lower temperature, compared to other

locations in the treatment system, providing a greater heat recovery potential. This is due to the fact that no further treatment will be performed, downstream of the DWHR system. A lower temperature can thus not affect the treatment process. However the wastewater will have cooled down through heat losses while traveling through the treatment system, and thus only indirect heat recovery, using the wastewater as a heat source for a heat pump is considered, shown schematically in Figure 3.

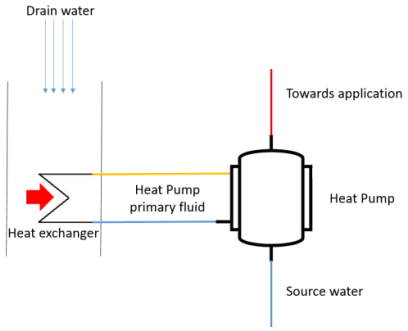


Figure 3. Indirect Drain Water Heat Recovery System

4. Observations

4.1 Flow through the system

The flow through the system is estimated based on information shared by ABP, the daily flow profile, Monday through Friday is as given in Figure 4. It is assumed that the flow is the same in all nodes of the system.

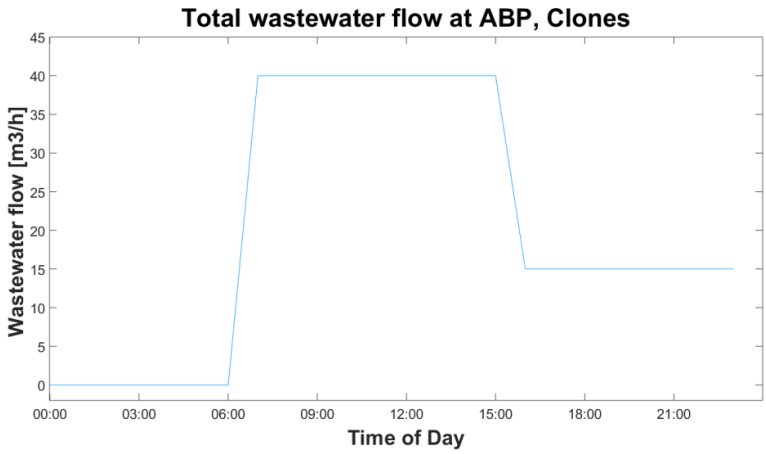


Figure 4. Evolution of the wastewater flow over a day.

4.2 Temperatures throughout the WWTP

The temperature evolution and the inlet of the wastewater system (in red), at the outlet of the DAF unit (in orange), and at the outlet of the WWTP (in blue) are shown in Figure 5.

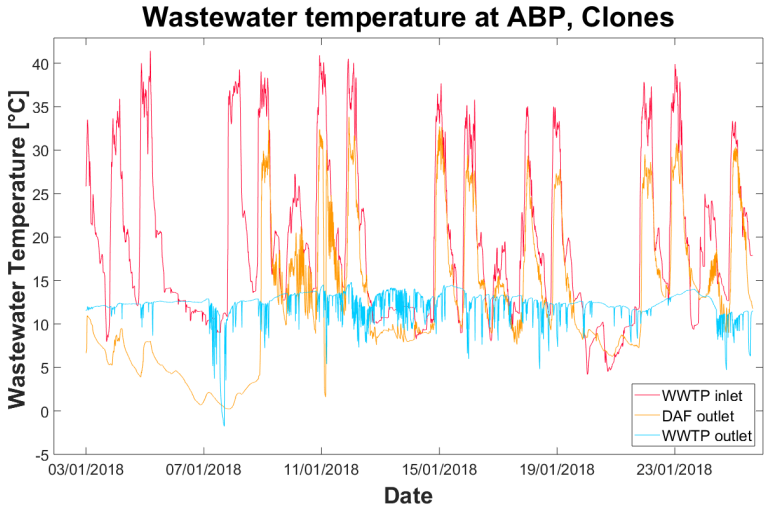


Figure 5. Temperatures at different nodes in the WWTP

This graph shows several remarkable observations regarding the wastewater temperature. First of all, we can observe that the outlet temperature during daytime in weekends often exceeds the inlet, and DAF temperatures. This is likely due to a small amount of wastewater still leaving the treatment system, whereas no wastewater is flowing at the inlet and DAF nodes.

Secondly one can observe that the wastewater temperature is dropping during night time (most notably at the outlet of the WWTP). This is caused by colder surrounding temperature, and the reduced flow at night time.

Thirdly the DAF temperature observations are not behaving as expected before January 10th, the temperature difference with the WWTP inlet is significantly larger, and the temperature is lower than the WWTP outlet. During the visit of the plant, at the end of December, problems were occurring at the DAF unit, it's thus believed that the temperatures at the DAF units are influenced by these issues, and that these were resolved on January 10th. The analysis related to heat recovery at the DAF node is thus performed based on the observations after January 10th.

To avoid the adverse effect of night time drops and drops during the weekend, it is assumed that the DWHR system will be operated during weekdays, and during business hours (9AM to 5 PM).

5. Results and Discussion

Based on the observations, described in Section 4, a heat recovery system was selected and roughly designed, in order to estimate the Levelized Cost of Energy, payback period and Total Equivalent Warming Impact [1] of such an installation. The first indicates a cost per produced kWh of heat, taking into account the capital investment, operating and maintenance costs, whereas the latter is an indication of the related greenhouse gas emissions.

For the calculations an electricity price of $0.12\ €/kWh$, and a price of heavy fuel oil of $0.067\ €/kWh$ [2] was assumed. The required size of the components was calculated using the Logarithmic Mean Temperature Difference Method [3], and the price using the Vatavuk method [4].

5.1 Hybrid Drain Water Heat Recovery at the DAF unit

Hybrid DWHR (H-DWHR) consists of a direct component, and an indirect component, each of these components can also be implemented separately. In this section, the results for both the direct, and hybrid systems are given.

The feasibility of the direct component (D-DWHR) is assessed using the effectiveness data from the ShowerSave CoFlo system, which is commercially available. The indirect components feasibility is assessed through regression on the data of several heat pumps, and their catalogue prices. The design parameters for the system are summarized in Table 1.

Table 1. Design parameters for the H-DWHR system at the DAF unit

Direct Component	
Heat Exchanger	
ShowerSave CoFlo	$34\ pipes$
ShowerSave CoFlo	$16\ pipes$
Indirect Component	
Heat Exchanger	
Rated Power	$245\ kW$
Required Exchange Area	$265\ m^2$
Heat Pump	
Rated Power	$327\ kW$
Seasonal COP	4.77

In this table one can observe the large number of CoFlo pipes required, which is impractical. The calculation was performed employing the dimensions of the commercially available CoFlo pipes, because their performance under different operating circumstances is well known. During a meeting ShowerSave representatives mentioned that the company is expanding its catalogue for industrial applications, and it's expected that larger diameter pipes are/will be available. Their performance evolution is unknown to the authors of this report, and was thus assumed to be similar to the system described here. Other heat exchange distributors could have similar heat exchangers with large diameter pipes.

As a comparison, a DWHR system where 16 CoFlo pipes are installed (the largest known installation has 16 pipes), is also considered. The wastewater flow through a CoFlo pipe is $8l/min$, the remaining flow bypasses the DWHR system. Similarly, a direct, horizontal heat exchanger, placed on the floor of the DAF unit is analysed as well. The effectiveness of this heat exchanger is assumed to be 30%.

In case the solution with 34 CoFlo pipes is not achievable, both systems mentioned above can be used as the direct component, to recover part of the embedded energy.

A breakdown of the estimated capital investment is given in Table 2.

Table 2. Breakdown of cost for the H-DWHR system

Fuel Prices	
Electricity	0.12 €/kWh
Current heating fuel	0.067€/kWh
Capital Investment	130 130 €
Direct Component	
Heat Exchanger (34 pipes)	13 090 €
Heat Exchanger (16 pipes)	6 160 €
Horizontal DAF heat exchanger	14 355 €
Indirect Component	
Heat Exchanger	9 867 €
Heat Pump	72 172 €
Plumbing	25 000 €

Using these estimates, the financial parameters are calculated, such as the payback period and the Levelized Cost of Energy. Similarly, the Total Equivalent Warming Impact (TEWI) per produced unit of Heat is calculated, as a comparison the value for heavy fuel oil 274 $g\ C_e/kWh$, as mentioned in [5].

It's assumed that the heat pump produces hot water at $45°C$. The results are summarized in Table 3.

Table 3. Simulation results

System	Operating days	TEWI $g\ C_e/kWh$	Investment	LCOE €/kWh	Payback Period
D-DWHR (34 pipes)	200		23 090 €	0.012	1.32 yrs
D-DWHR (16 pipes)	200		16 160 €	0.038	4.31 yrs
D-DWHR (DAF)	200		24 355 €	0.014	1.60yrs
H-DWHR	200	70.5	130 130 €	0.031	2.55 yrs

The Direct-DWHR system with 34 CoFlo pipes would save about 260 MWh of heavy fuel from being burnt, yearly, resulting in a cost reduction of about 17 000 €, and 72 $tons\ CO_{2,eq}$ of emission reduction.

The Direct-DWHR system with 16 CoFlo pipes would save about 61 MWh of heavy fuel from being burnt, yearly, resulting in a cost reduction of about 4 115 €, and 17 $tons\ CO_{2,eq}$ of emission reduction. The Direct, horizontal-DWHR system on the floor of the DAF unit would save about 135 MWh of heavy fuel from being burnt, yearly, resulting in a cost reduction of about 9 000 €, and 37 $tons\ CO_{2,eq}$ of emission reduction.

The Hybrid DWHR system would save about 1 GWh of heavy fuel from being burnt, resulting in a cost reduction of about 68 000 € per year, and 207 $tons\ CO_{2,eq}$ of emission reduction.

The large required heat exchange surface for the indirect component of the system could pose problems, as the required space might not be available. One possibility is to use the walls of the DAF unit to install such a heat exchanger and have a reduced size heat exchanger and heat pump, resulting in reduced savings.

Another work around could be to install a Direct-DWHR system at the DAF unit, and install an Indirect-DWHR system at the WWTP outlet (see Section 5.2). This would circumvent the fouling problem in this heat exchanger as well. And would be the simplest installation from a technical point of view, as no alterations to the DAF unit are required.

As mentioned earlier, the vertical drop present at the outlet of the DAF unit, provides a good opportunity for the installation of a heat exchanger, the orientation of the pipe will also reduce the fouling issue, and provide an easy solution for cleaning (see Figure **6**). However, the small diameters of the pipes, and the collection after the wastewater flow is split in the different pipes could result in solids build-up and thus fouling of the heat exchanger. This remains to be discussed with the manufacturer.

5.2 Direct Drain Water Heat Recovery at the WWTP outlet

The design of the Indirect-DWHR system considered at the WWTP outlet is identical to the direct component of the Hybrid-DHWR system considered at the DAF unit (Section 5.1).The design parameters for this system are summarised in Table 4.



Figure 6. Example of a CoFlo system with 16 pipes.

Table 4. Design parameters for the I-DWHR

Heat exchanger	
Rated Power	$251\ kW$
Required Exchange Area	$280\ m^2$
Heat pump	
Rated Power	$335\ kW$
Seasonal COP	4.43

A breakdown of the estimated capital investment is given in Table 5.

Table 5. Breakdown of cost for the I-DWHR system

Fuel Prices	
Electricity	$0.12\ €/kWh$
Current heating fuel	$0.067€/kWh$
Capital Investment	109 140 €
Heat Exchanger	10 088 €
Heat Pump	74 055 €
Plumbing	25 000 €

It's assumed that the heat pump produces hot water at $45°C$. The results are summarized Table 6.

Table 6. Simulation results

System	Operating days	TEWI $g\ C_e/kWh$	Investment	LCOE $€/kWh$	Payback Period
I-DWHR	250	110.7	109 140 €	0.048	4.57 yrs

The Direct-DWHR system would save about 590 MWh of heavy fuel from being burnt, yearly, resulting in a cost reduction of about 39 500 €, and 96 $tons\ CO_{2,eq}$ of emission reduction.

One can observe that 50 more operation days are considered, compared to Hybrid-DHWR system considered at the DAF unit (Section 5.1). This is done to take additional cleaning requirements into account due to fouling, similarly the estimated lifetime here is 20 $years$ compared to 15 in Section 5.1.

6. Conclusion

An Indirect-DWHR system located at the DAF-unit would result in the largest reduction in heavy fuel consumption on the site. However, the payback period for the Direct-DWHR system on that same location is shorter.

The vertical drop from the DAF outlet to the rest of the wastewater treatment system provides a good opportunity for a Direct-DWHR system, adding the heat exchanger for the indirect component of the Hybrid-DWHR system might prove to be complicated due to space constraints.

Technically the simplest solution is the installation of a Direct-DWHR system at the DAF unit, and an Indirect-DWHR system at the outlet of the WWTP. This would result in a slightly longer payback period, but would avoid fouling problems on the heat exchanger, by utilising the cleaner effluent.

Installing either of the systems would result in fuel savings between 850 and $1000\ MWh$, with a related annual cost reduction ranging from $56\ 500$ € and $68\ 200$ €, and $167 - 207\ tons\ CO_{2,eq}$. The Payback period ranges from 2.55 to 4.57 years.

The direct component of this system would require 34 CoFlo pipes to be installed in parallel, which seems rather impractical. As a comparison a system with 16 CoFlo pipes is also analysed. This would reduce the savings mentioned above by $200\ MWh$, about $13\ 000$ € and $55\ tons\ CO_{2,eq}$, per year. The Payback period is increased as well.

Replacing the 34 CoFlo pipes by a horizontal heat exchanger, with an effectiveness of 30%, placed on the floor of the DAF unit, would result in reducing the savings mentioned above by $125\ MWh$, about $8\ 000$ € and $35\ tons\ CO_{2,eq}$, per year.

Bibliography

[1] A. Zottl, M. Lindahl, R. Nordman, P. Rivière and M. Miara, “Evaluation method for comparison of heat pump systems with conventional heating systems,” Intelligent Energy Europe, 2011.

[2] SEAI, “Domestic Fuels- Comparison of Energy Costs,” Sustainable Energy Authority of Ireland, Dublin, 2017.

[3] Y. Cengel and M. A. Boles, Thermodynamics: An engineering approach, McGraw Hill, 2007.

[4] M. Taal, I. Bulatov, J. Klemes and P. Stehlik, “Cost estimation and energy price forecasts for economic evaluation of retrofit projects,” *Applied Thermal Engineering,* no. 23, pp. 1819-1835,

[5] SEAI, “What are the carbon emission factrs used?,” Sustainable Energy Authority Ireland, Dublin, Ireland, 2017.

Appendix A: Instrumentation

Technical specifications of temperature sensor (Tinytag TG-4100):

Gemini DATA LOGGERS

Tinytag Aquatic 2 (-40 to +70°C)
TG-4100
Issue 8 : 8th January 2016 (E&OE)



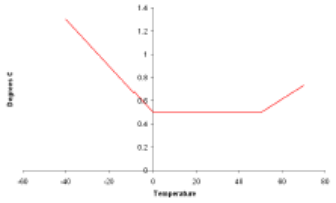
Features

Total Reading Capacity	32,000 readings
Memory type	Non Volatile
Trigger Start	Magnetic Switch
Delayed Start	Relative / Absolute (up to 45 days)
Stop Options	When full After n Readings Never (overwrite oldest data)
Reading Types	Actual, Min, Max
Logging Interval	1 sec to 10 days
Offload	While stopped or when logging in minutes mode
Alarms	2 fully programmable; latchable

Reading Specification

Reading Range	-40°C to +70°C (-40°F to +158°F)
Sensor Type	10K NTC Thermistor (Internally mounted)
Response Time	<20mins to 90% FSD in moving water
Reading Resolution	0.01°C or better

Reading Accuracy



Physical Specification

IP Rating	IP68 water proof (see notes)
Operational Range*	-40°C to +70°C (-40°F to +158°F)
Case Dimensions	
Diameter	51mm / 2.01"
Height	50mm / 1.97"
Weight	90g / 3.17oz

*The Operational Range indicates the physical limits to which the unit can be exposed, not the reading range over which it will record.

Calibration

This unit is configured to meet Gemini's quoted specification during its manufacture.

We recommend that the calibration of this unit should be checked annually against a calibrated reference meter.

A certificate of calibration, traceable to a national standard, can be supplied for an additional charge either at the point of purchase, or if the unit is returned for a service calibration.

Notes

This unit should only be opened when a battery replacement is required.

Battery Type	Renata CR2450N
Replacement Interval	Annually*

*If deployed for long periods, the logger's battery should be replaced annually to prevent the loss of data during a recording run. If the logger is being used frequently, the battery should be changed when prompted by a low battery warning from the Tinytag Explorer software.

Before replacing the battery the data logger must be stopped.

Data stored on the logger will be retained after a battery is replaced.

Please refer to the service kit instruction sheet for battery replacement instructions.

If used at low temperatures the data logger should be allowed to warm to room temperature before it is opened to avoid condensation forming inside the unit.

The IP68 rating is valid only when the unit's lid is securely fitted and is valid to a depth of 500m (1640ft).

The gasket fitted in this unit must be replaced every time it is opened.

The position of the unit's trigger start switch is indicated by the - - - marking on its base. The switch itself is positioned on the side of the unit, just above the base-lid join, on the edge indicated. When a magnet is held in the correct location, the status LED will light until the magnet is removed.

LED Flash Patterns

When logging, a status LED is visible through the base of the unit. The flash patterns of this indicator are as follows:

Flash Pattern	Indication
1 flash every 4 seconds	Logging
1 flash every 8 seconds	Waiting to Log (trigger or delayed start set)
A double flash every 4 seconds	Alarm limit breached

Approvals

Gemini Data Loggers (UK) Ltd. operates a Business Management System which conforms to ISO 9001 and ISO 14001.

CE

Required and Related Products

To use this data logger you will require a copy of the following software:

SWCD-0040: Tinytag Explorer software

and an

ACS-3030: USB Inductive Pad

These items can be purchased together in a discounted pack:

SWPK-3-USB Tinytag Explorer and Inductive Pad Pack.

Further Related Products

SER-9525: Tinytag Aquatic 2 Service Kit

data sheet

www.tinytag.info sales@tinytag.info

B.5. PEPSICO, Cork

Trinity College Dublin
Coláiste na Trionóide, Baile Átha Cliath
The University of Dublin

Dŵr Uisce
Energy Recovery in Water Services
Adennill Ynni yn y Diwydiant Dŵr

Prifysgol Bangor University

Monitoring campaign at Pepsi Co., Cork: Potential for heat recovery from waste water

PEPSICO

Feasibility study
March 2018

Cronfa Datblygu Rhanbarthol Ewrop
European Regional Development Fund

Ireland's European Structural and Investment Funds Programmes 2014-2020
Co-funded by the Irish Government and the European Union

Tionól Réigiúnach an Deiscirt
Southern Regional Assembly

EU Funds: Ireland Wales Programme 2014-2020



Table of Contents

1. Introduction 1
2. Objectives 1
3. Monitoring points 1
3.1 CIP-drain 1
3.2 Inlet of the wastewater treatment plant 2
4. Observations 2
4.1 CIP-drain 2
4.2 Inlet of the wastewater treatment plant 3
5. Results and Discussion 4
5.1 CIP-drain 4
5.2 Inlet of the wastewater treatment plant 5
6. Conclusion 7
Bibliography 7
Appendix A: Instrumentation 8
Technical specifications of temperature sensor (Tinytag TG-4100): 8

1. Introduction

The aim of this monitoring campaign was to assess the feasibility of implementing a waste water heat recovery system in the industrial process at the Pepsi facility in county Cork, whereby waste heat from the process would be recovered and transferred to the existing heating system. This has the potential to reduce the gas consumption of the existing boilers and generate financial and environmental savings for the company. The proposal is based on the Drain Water Heat Recovery concept (DWHR), which consists of a heat exchanger placed in the waste water drain, and, if necessary, a heat pump.

This assessment forms part of the Dŵr Uisce project (*www.dwr-uisce.eu*), which aims at improving the energy efficiency of the distribution of water resources by quantifying and demonstrating the potential of integrated smart and low-carbon technology. In this context the industrial process at PepsiCo offers a unique opportunity to investigate the potential of waste water heat recovery technology in the food processing sector. This technology can help towards improving environmental, energetic and financial performance of the facilities.

2. Objectives

The primary objectives of this project include:

- Assessing the potential to improve the energy efficiency of water heating activities in the process at PepsiCo., county Cork, through DWHR.
- To facilitate awareness raising, public and industry engagement in the concept of DWHR

In order to reach and quantify these primary objectives, the embedded energy in the wastewater on the property must be measured and quantified. This requires the following measurements or estimations, at the locations that are proposed in this document

- Wastewater temperature.
- Wastewater flow.

3. Monitoring points

After visiting the site, two monitoring points were identified. The drain of the Cleaning in Place (CIP) water and the inlet of the wastewater treatment plant (WWTP) were equipped with temperature loggers (Appendix A). The flow at these locations was recovered from the SCADA control system of the site.

3.1 CIP-drain

The CIP drain is shown in Figure 1, the temperature logger was placed under the grid shown in this figure. The flow needs to be recovered from the SCADA system, where the flow through the cleaning loop is recorded, the information on whether or not the valve to the drain is opened allows for the calculation of the flow at this location.



Figure 1. CIP drain at the PEPSICO facility in Cork

3.2 Inlet of the wastewater treatment plant

The overall wastewater temperature was measured at the inlet sump of the wastewater treatment plant. The flow was obtained from the control system of the treatment plant. This wastewater treatment plant is situated at the edge of the property, which introduces the inconvenience that the heat must be transported to the boiler room.

4. Observations

4.1 CIP-drain

The temperatures observed at the CIP-drain are shown in Figure 2. One can observe peaks up to $70°C$, but that the temperature profile is highly variable, and follows a regular pattern. One can also clearly distinguish the down time during the weekend.

The flow data for the CIP-drain was not available when this report was drafted.

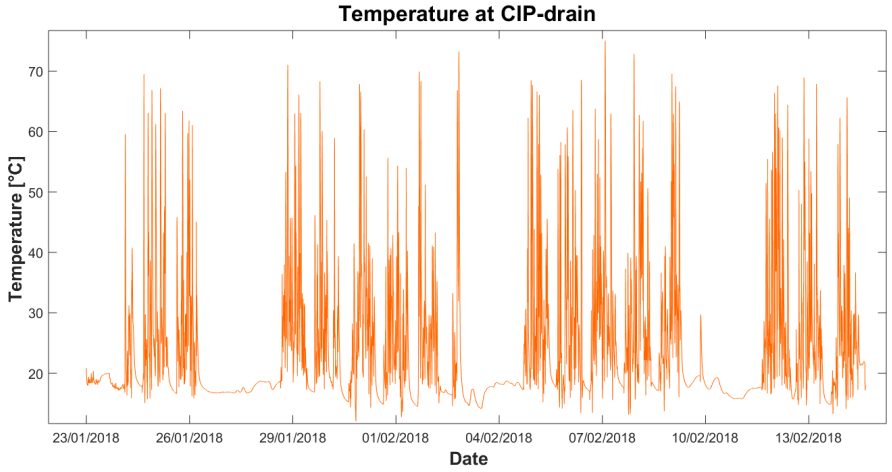


Figure 2. Evolution of the temperature at the CIP drain during the monitoring period

4.2 Inlet of the wastewater treatment plant

Similarly, the temperature of the wastewater in the inlet sump is shown in Figure 3. In this figure one can observe peaks of over $30°C$, and the lack of activity during the weekend.

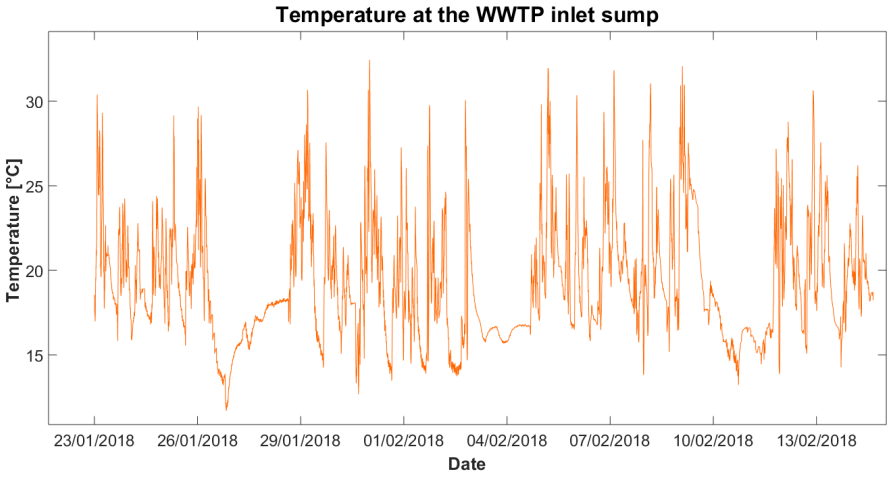


Figure 3. Evolution of the temperature at the WWTP inlet sump during the monitoring period

The flow observations were only available on a daily basis, the observations are shown in Figure 4. Because these values are only available daily, the mean temperature during working hours (9 AM to 5PM) was used for the calculations.

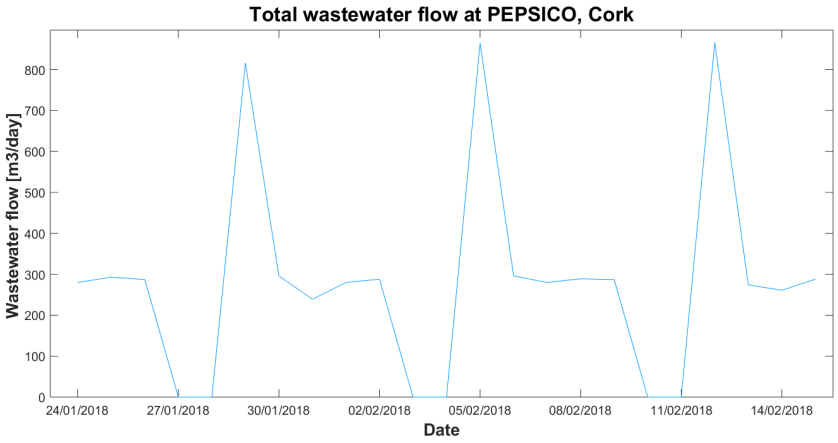


Figure 4. Evolution of the wastewater flow during the monitoring period

5. Results and Discussion

Based on the embedded energy observed, and described in Section 4, a heat recovery system was selected and roughly designed, in order to estimate the Levelized Cost of Energy, and Total Equivalent Warming Impact [1] of such an installation. The first indicates a cost per produced kWh of heat, taking into account the capital investment, operating and maintenance costs, whereas the latter is an indication of the related greenhouse gas emissions.

For all calculations a lifetime of $15\ years$, at 250 operating days per year was assumed, along with an electricity price of $0.12\ €/kWh$ [2]. The required size of the components was calculated using the Logarithmic Mean Temperature Difference Method [3], and the price using the Vatavuk method [4].

5.1 CIP-drain

Because the flow data is not available for the CIP drain is not possible to give reasonable estimations for the investment and a payback period for a heat recovery system on this part of the process.

The temperatures observed at the CIP-drain were very high, suggesting the possibility to use a Direct Drain Water Heat Recovery (D-DWHR) device at this location. When using D-DWHR the heat from the drain water is recovered through a heat exchanger, heating up the fluid that is used in the process (here the CIP water). This will lead to an increased temperature of this fluid when entering its traditional heating source (here the heat exchangers with the main heating loop), reducing the energy consumption. The technique is summarised in Figure 5.

D-DWHR has the advantage of a small capital investment, the only cost is the purchase of the heat exchanger and the plumbing to connect it. Furthermore, the current lay-out at the facility, where the drain pipe runs parallel to the water to be heated, right before the current heating source (the heat exchangers), allows for an integration of D-DWHR with little to no changes in the lay-out of the plant.

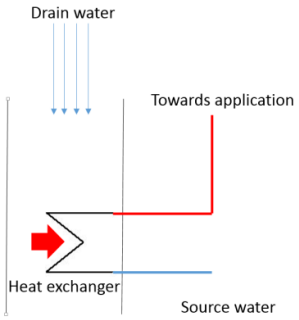


Figure 5. Direct Drain Water Heat Recovery

5.2 Inlet of the wastewater treatment plant

The inlet of the wastewater treatment plant is characterised by a lower temperature than the CIP drain, and is located further away from the heat consumption. Therefor it's not suited for D-DWHR, however the large flows associated with this location make it suited for Indirect Drain Water Heat Recovery (I-DWHR). In this case the wastewater is used as the heat source for a heat pump (see Figure 6). Because the temperature of the wastewater is generally higher than ground and air temperature the Coefficient of Performance of the heat pump will be higher than for traditional heat pump systems.

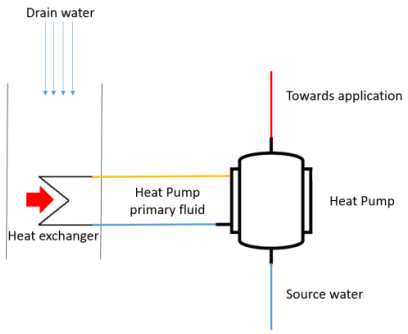


Figure 6. Indirect Drain Water Heat Recovery

The design parameters for this system are summarised in Table 1.

Table 1. Design parameters for the I-DWHR

Heat exchanger	
Rated Power	367 kW
Heat pump	
Rated Power	480 kW
Seasonal COP	4.24
Primary fluid circulation pump	
Estimated pumping head	30 m

In order to transport the heat from the WWTP to its application, the primary fluid of the heat pump is circulated from the boiler room (where is assumed the heat pump would be installed). Because there is no detailed hydraulic design of this circuit, it's difficult to estimate pumping energy consumption. This analysis is performed in two different ways, once ignoring the pumping consumption, and a second iteration using the estimated pumping head shown in Table 1.

The assumptions and estimations for component and fuel prices are given in Table 2. They are estimated based on available literature and catalogue prices.

Table 2. Price estimations for the I-DWHR system

Fuel Prices		
Electricity		$0.12\ €/kWh$
Current heating fuel		$0.067€/kWh$
Capital Investment	**Total**	147 700 €
Heat exchanger		9 500 €
Heat pump		108 200 €
Circulation pump		5 000 €
Plumbing		25 000 €

Using these estimates, the financial parameters are calculated, such as the payback period and the Levelized Cost of Energy. Similarly, the Total Equivalent Warming Impact (TEWI) per produced unit of Heat is calculated, as a comparison the value for gas is $205\ g\ C_e/kWh$, and for heavy fuel oil $274\ g\ C_e/kWh$, as mentioned in [5].

It is assumed that the heat pump produces hot water at $55°C$.

The results are summarized in Table 3.

Table 3. Simulation results

System	Operating days	TEWI $g\ C_e/kWh$	Investment	LCOE $€/kWh$	Payback Period
No circulation	250	117.1	142 700 €	0.043	3.39 yrs
With circulation	250	123.2	147 700 €	0.045	3.65 yrs

As expected including the circulation pump increases the cost, payback period, and environmental impact of the system. There is a large uncertainty on the required pumping head, and this might further impact on these factors. However, there is still significant margin compared to the values for gas and heavy fuel oil.

Compared to a gas system the I-DWHR system, taking into account the circulation pump, would reduce heat related GHG emissions by 88 $tons\ CO_{2,eq}$ and reduce costs by 24 875 €, annually (when discounting the investment cost over 15 years).

6. Conclusion

Installing an I-DWHR on the WWTP inlet requires a large investment (estimated at $147\,700$ €), however the payback period for this investment is estimated at less than $4\ years$. However, a large amount of uncertainty remains regarding the amount of energy required to circulate the primary fluid of the heat pump. This is due to the fact that the plant lay-out and topography is poorly known to the authors of this report.

Assuming a required pumping head of $30\ m$, this system would save about $88\ tons\ CO_{2,eq}$ and reduce costs by $24\,875$ €, annually, compared to a classic gas fired system.

Due to its high wastewater temperature (peaks up to $70°C$), and a favourable plant lay-out at this location, the CIP-drain seems to be a good location for a D-DWHR system, which is characterised by much lower investment costs than I-DWHR systems. However, the analysis can only be completed with the availability of flow data for that location.

Bibliography

[1] A. Zottl, M. Lindahl, R. Nordman, P. Rivière and M. Miara, "Evaluation method for comparison of heat pump systems with conventional heating systems," Intelligent Energy Europe, 2011.

[2] SEAI, "Domestic Fuels- Comparison of Energy Costs," Sustainable Energy Authority of Ireland, Dublin, 2017.

[3] Y. Cengel and M. A. Boles, Thermodynamics: An engineering approach, McGraw Hill, 2007.

[4] M. Taal, I. Bulatov, J. Klemes and P. Stehlik, "Cost estimation and energy price forecasts for economic evaluation of retrofit projects," *Applied Thermal Engineering,* no. 23, pp. 1819-1835, 2003.

[5] SEAI, "What are the carbon emission factrs used?," Sustainable Energy Authority Ireland, Dublin, Ireland, 2017.

Appendix A: Instrumentation

Technical specifications of temperature sensor (Tinytag TG-4100):

Gemini DATA LOGGERS

Tinytag Aquatic 2 (-40 to +70°C)
TG-4100
Issue 8 : 8th January 2016 (E&OE)



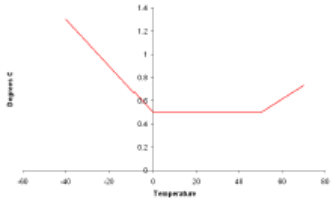
Features

Total Reading Capacity	32,000 readings
Memory type	Non Volatile
Trigger Start	Magnetic Switch
Delayed Start	Relative / Absolute (up to 45 days)
Stop Options	When full After n Readings Never (overwrite oldest data)
Reading Types	Actual, Min, Max
Logging Interval	1 sec to 10 days
Offload	While stopped or when logging in minutes mode
Alarms	2 fully programmable; latchable

Reading Specification

Reading Range	-40°C to +70°C (-40°F to +158°F)
Sensor Type	10K NTC Thermistor (Internally mounted)
Response Time	<20mins to 90% FSD in moving water
Reading Resolution	0.01°C or better

Reading Accuracy



Physical Specification

IP Rating	IP68 water proof (see notes)
Operational Range*	-40°C to +70°C (-40°F to +158°F)
Case Dimensions	
Diameter	51mm / 2.01"
Height	50mm / 1.97"
Weight	90g / 3.17oz

*The Operational Range indicates the physical limits to which the unit can be exposed, not the reading range over which it will record.

Calibration

This unit is configured to meet Gemini's quoted specification during its manufacture.

We recommend that the calibration of this unit should be checked annually against a calibrated reference meter.

A certificate of calibration, traceable to a national standard, can be supplied for an additional charge either at the point of purchase, or if the unit is returned for a service calibration.

Notes

This unit should only be opened when a battery replacement is required.

Battery Type	Renata CR2450N
Replacement Interval	Annually*

*If deployed for long periods, the logger's battery should be replaced annually to prevent the loss of data during a recording run. If the logger is being used frequently, the battery should be changed when prompted by a low battery warning from the Tinytag Explorer software.

Before replacing the battery the data logger must be stopped.

Data stored on the logger will be retained after a battery is replaced.

Please refer to the service kit instruction sheet for battery replacement instructions.

If used at low temperatures the data logger should be allowed to warm to room temperature before it is opened to avoid condensation forming inside the unit.

The IP68 rating is valid only when the unit's lid is securely fitted and is valid to a depth of 500m (1640ft).

The gasket fitted in this unit must be replaced every time it is opened.

The position of the unit's trigger start switch is indicated by the - - - marking on its base. The switch itself is positioned on the side of the unit, just above the base-lid join, on the edge indicated. When a magnet is held in the correct location, the status LED will light until the magnet is removed.

LED Flash Patterns

When logging, a status LED is visible through the base of the unit. The flash patterns of this indicator are as follows:

Flash Pattern	Indication
1 flash every 4 seconds	Logging
1 flash every 8 seconds	Waiting to Log (trigger or delayed start set)
A double flash every 4 seconds	Alarm limit breached

Approvals

Gemini Data Loggers (UK) Ltd. operates a Business Management System which conforms to ISO 9001 and ISO 14001.

CE

Required and Related Products

To use this data logger you will require a copy of the following software:

SWCD-0040: Tinytag Explorer software

and an

ACS-3030: USB Inductive Pad

These items can be purchased together in a discounted pack:

SWPK-3-USB Tinytag Explorer and Inductive Pad Pack.

Further Related Products

SER-9525: Tinytag Aquatic 2 Service Kit

data sheet

www.tinytag.info sales@tinytag.info

C. Appendices related to decentralized drain water heat recovery in a domestic setting (Chapter 5)

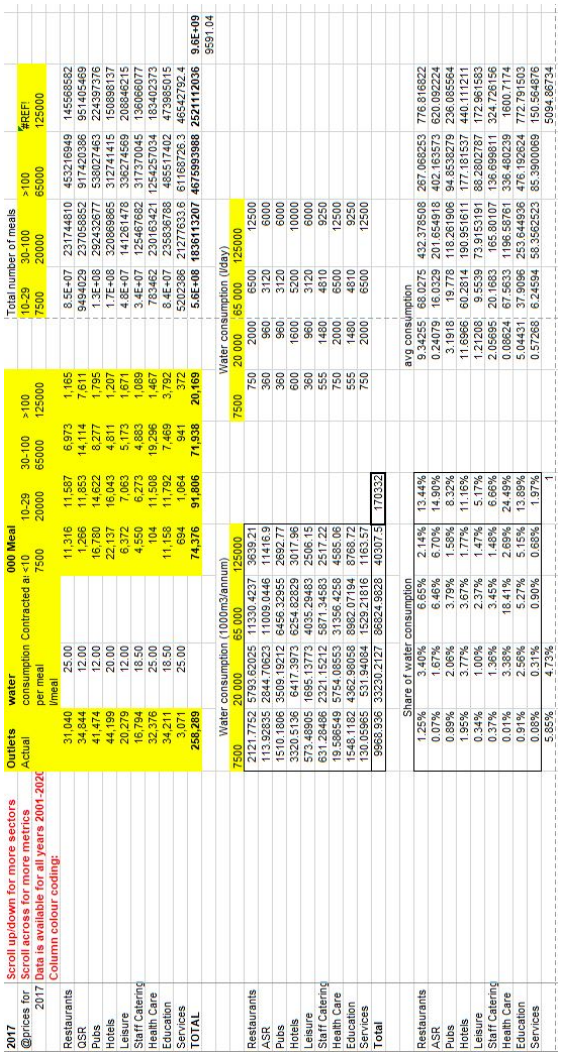
C.1. List of heat pumps

Table C.1.: List of heat pumps

Model	**Nominal Power** (kW)	**Price (excl. VAT, €)**
Vitocal 200 G - BWC.A06	5.76	5 542
Vitocal 200 G - BWC.A08	7.63	6 004
Vitocal 300 G - BWC.A06	5.69	6 068
Vitocal 300 G - BWC.A08	7.64	6 716
Vitocal 222 G - BWC.A06	5.90	7 978
Vitocal 222 G - BWC.A08	7.70	8 441
Vitocal 242 G - BWC.A06	5.90	8 886
Vitocal 242 G - BWC.A08	7.70	9 348
Stiebel - Eltron WPC 05 S GB	5.88	9 313
Stiebel - Eltron WPC 07 S GB	7.61	9 904
Stiebel - Eltron WPF 05 S	5.80	7 250
Stiebel - Eltron WPF 07 S	7.80	7 450
Roth Terracompact E 6kW	5.70	–
Roth Terracompact E 8kW	8.90	–
Weishaupt WWP S 6 ID	6.10	–
Weishaupt WWP S 8 ID	8.10	–
Ochsner GMSW 6 +	5.80	6 812
Ochsner GMSW 8 +	7.50	7 882
HelioTherm HP05 S 07W	6.03	–
HelioTherm HP07 S 08W	7.13	–
Dimplex SIH 6ME	6.00	5 473
Dimplex SIH 9ME	8.90	6 500
Envision NSKW 06	5.80	–
Envision NSKW 08	8.30	–
MasterTherm AQ22I	4.38	–
MasterTherm AQ22ZI	7.80	–
Alpha Innotec WZSV62 - 3M	3.32	8 000
Alpha Innotec WZSV92 - 3M	4.00	8 350

D. Appendices related to decentralized drain water heat recovery in commercial kitchens (Chapter 6)

D.1. Commercial kitchens in the United Kingdom



2017	Scroll up/down for more sectors	Outlets	water	000 Meal					Total number of meals				
@prices for 2017	Scroll across for more metrics	Actual	consumption Contracted a:	<10	10-29	30-100	>100		10-29	30-100	>100	#REF!	
	Data is available for all years 2001-2026		per meal	7500	20000	65000	125000		7500	20000	65000	125000	
	Column colour coding:		l/meal										
Restaurants		31,040	25.00	11,316	11,587	6,973	1,165		8.5E+07	2317448 10	453216949	145568582	
QSR		34,844	12.00	1,266	11,853	14,114	7,611		9494029	2370588 52	917420386	951405469	
Pubs		41,474	12.00	16,780	14,622	8,277	1,795		1.3E+08	2924326 77	538027463	224397376	
Hotels		44,199	20.00	22,137	16,043	4,811	1,207		1.7E+08	3208696 85	312741415	150898137	
Leisure		20,279	12.00	6,372	7,063	5,173	1,671		4.8E+07	1412614 78	336274569	208846215	
Staff Catering		16,794	18.50	4,550	6,273	4,883	1,089		3.4E+07	1254678 82	317370045	136066077	
Health Care		32,376	25.00	104	11,508	19,296	1,467		783462	2301634 21	1254257034	183402373	
Education		34,211	18.50	11,158	11,792	7,469	3,792		8.4E+07	2358367 88	485517402	473985015	
Services		3,071	25.00		694	1,064	941	372	5202386	2127763 36	61168726 3	46542792 4	
TOTAL		258,289		74,376	91,806	71,938	20,169		5.6E+08	1836113207	4675993988	2521112036	9.6E+09
													9591.04
			Water consumption (1000m3/annum)						Water consumption (l/day)				
		7500	20 000	65 000	125000			7500	750	2000	6500	12500	
Restaurants		2121.7752	5793.62025	11330.4237	3639.21				360	960	3120	6000	
ASR		113.92835	2844.70623	11009.0446	11416.9				360	960	3120	6000	
Pubs		1510.1806	3509.19212	6456.32955	2692.77				360	960	3120	6000	
Hotels		3320.5136	6417.3973	6254.82829	3017.96				600	1600	5200	10000	
Leisure		573.48905	1695.13773	4035.29483	2506.15				360	960	3120	6000	
Staff Catering		631.28486	2221.15212	5871.34583	2517.22				555	1480	4810	9250	
Health Care		19.586549	5754.08553	31356.4258	4585.06				750	2000	6500	12500	
Education		1548.1182	4362.98058	8982.07194	8768.72				555	1480	4810	9250	
Services		130.05965	531.94084	1529.21816	1163.57				750	2000	6500	12500	
Total		9968.936	33230.2127	86824.9828	40307.5	170332							
			Share of water consumption						avg consumption				
Restaurants		1.25%	3.40%	6.65%	2.14%	13.44%			9.34255	68.0275	432.378598	267.068253	776.816822
ASR		0.07%	1.67%	6.46%	6.70%	14.99%			0.24079	16.0329	201.654918	402.163573	620.092224
Pubs		0.89%	2.06%	3.79%	1.58%	18.32%			3.1918	19.7736	118.264806	94.8538279	236.085564
Hotels		1.95%	3.77%	3.67%	1.77%	11.15%			11.6966	69.2814	190.951611	177.161537	447.011211
Leisure		0.34%	1.00%	2.37%	1.47%	5.17%			1.21208	9.5539	73.9153191	88.2802787	172.961583
Staff Catering		0.37%	1.36%	3.45%	1.48%	6.68%			2.05955	20.1683	165.80107	136.699611	324.726156
Health Care		0.01%	3.38%	18.41%	2.69%	24.49%			0.08624	67.5633	1196.58781	336.480239	1600.7774
Education		0.91%	2.56%	5.27%	5.15%	13.89%			5.04431	37.9096	253.644938	478.192624	772.791503
Services		0.08%	0.31%	0.90%	0.68%	1.97%			0.57268	6.24584	58.3662523	85.3900069	150.584876
		5.85%	4.75%			1							5094.66734

E. Appendices related to the spatio-temporal analysis (Chapter 7)

E.1. Flow chart of the integrated method

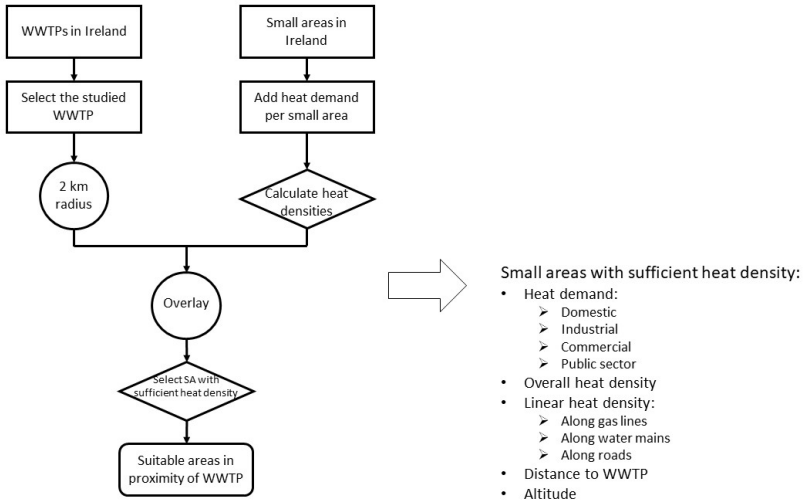


Figure E.1.: Flow chart of the spatial analysis in the integrated methodology.

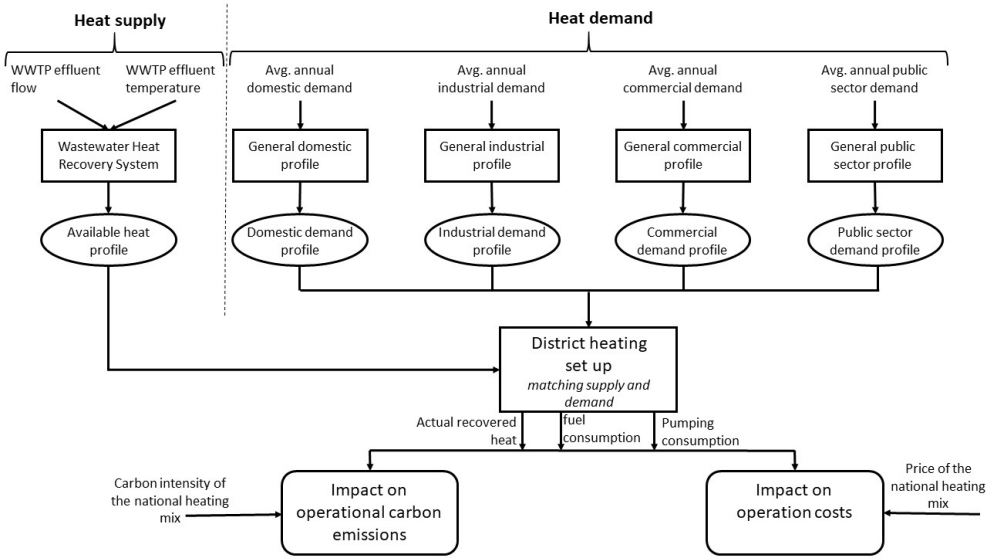


Figure E.2.: Flow chart of the temporal analysis in the integrated methodology.

F. Appendices related to Penrhyn castle

F.1. Poster of the Demonstrator at Penrhyn castle

Trinity College Dublin
Coláiste na Tríonóide, Baile Átha Cliath
The University of Dublin

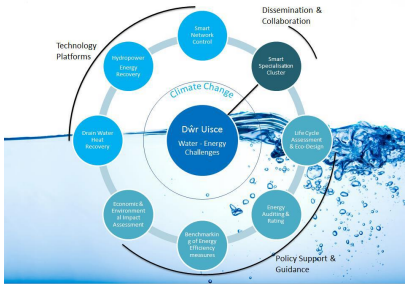
Dŵr Uisce
Energy Recovery in Water Services
Adennill Ynni yn y Diwydiant Dŵr

PRIFYSGOL BANGOR UNIVERSITY

Ymddiriedolaeth Genedlaethol
National Trust

Heat recovery from the kitchen drain at Penrhyn Castle

The Dŵr-Uisce project

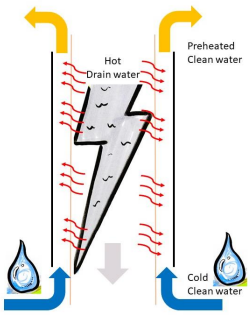


Distributing our Water Resources: Utilising Integrated, Smart and low-Carbon Energy

The Dŵr-Uisce project is a multi-disciplinary research project aiming at improving the long-term sustainability of water supply, treatment and end-use in Ireland and Wales .

The heat recovery system

The Heat Exchanger



The heat exchanger consists of 2 concentric pipes.

The hot drain water flows through the inner pipe.

The clean water forms a film around the drain water pipe.

The hot drain water yields its heat to the clean water flowing around it.

This reduces the energy required to heat up the clean water for kitchen applications.

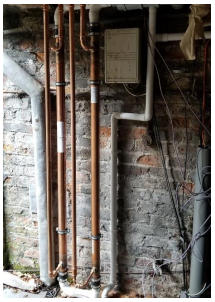
The Heat Recovery System

3 different configurations are tested.

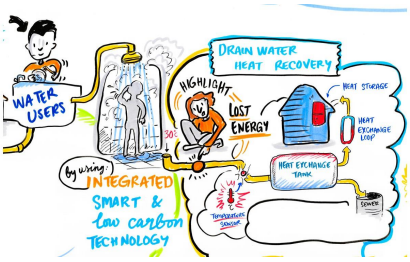
They use a different arrangements of heat exchangers and a buffer tank.

The performance of the system is continuously monitored.

The goal is to maximize heat recovery, and reduce fuel consumption.



Heat in kitchen drain water



- Kitchen drain water is hot (up to 55°C)
- This is due to :
  - Dishwashing
  - Cooking
  - Hot beverages
- Drain water is a large source of energy loss in buildings.

→ This system recovers the heat that is flushed through the drain, and reduces the castles fuel consumption.

Benefits



The fuel consumption of the kitchen is reduced.

The pumping costs, from the main boiler house are reduced.

→ The castle reduces its greenhouse gas emissions!

In short

The National Trust and the Dŵr-Uisce project collaborate to reduce the greenhouse gas emissions of Penrhyn castle! They do this by recovering heat from the hot drain water being flushed down the kitchen drains. This heat is used to preheat the clean water that is used in the kitchen.

This system reduces the fuel consumption at the boiler house, and reduces the pumping power needed to transfer the heat to the castle.

The Dŵr Uisce project is aimed at improving the long-term sustainability of water supply, treatment and end-use in Ireland and Wales. The present research has been supported by the ERDF Interreg Ireland-Wales Programme 2014-2020.

www.dwr-uisce.eu @Dwr_uisce *sprietj@tcd.ie*

F.2. Sizing of the circulation pump at Penrhyn castle

General characteristics

g	9.81		

Pipe Characteristics

diameter	1.00	inch	
	2.54	cm	
Length	6	m	*Estimated length from the resrvoir to drain (back and forth)*
f	0.053792		Darcy friction factor

Fluid Characteristics

nu	1.05E-06	m2/s	kinematic viscosity of the fluid
Re	1189.774		<2000 --> Laminar

Flow Rate

6	l/min
0.1	l/s

Flow Velocity

0.049338131	m/s
4.933813103	cm/s

Differential head	**amount**	**Coefficient**	**head loss (m)**	
suction head			0	*circulation pump, arriving at the starting point*
static head			0	*circulation pump, arriving at the starting point*
90° bend	7	0.3	0.000260547	
ShowerSave Inlet	1	1	0.00012407	
ShowerSave Outlet	1	0.2	2.4814E-05	
ShowerSave Pressure drop	1		1.529051988	*As given by the Showersave calculation sheet*
Pipe friction losses			0.00157652	
Total Head			**1.531037939**	**m**
Differential pressure			**0.150194822**	**bar**

Pump

		Grundfoss	ALPHA2 L 15-50 130		19.30%
Hydraulic Power	1.501948 W	Grundfoss	Alpha 3 25-30 130		22.60%
Efficiency	0.231	Grundfoss	Alpha 3 25-80 180		23.10%
Absorbed electric power	6.50194 W	Ecocirc	15-3	nob setting	11%

F.3. Data sheet of the circulation pump at Penrhyn castle

GRUNDFOS **DATA BOOKLET**

ALPHA2 L

Circulator pumps

50 Hz



be
think
innovate

GRUNDFOS

Table of contents

1. Product introduction **3**
Type key . . . 3
Performance range . . . 3

2. Applications **4**
Pumped liquids . . . 4
Control of heating systems . . . 4
Advantages of pump control . . . 5

3. Construction **6**
Sectional drawing . . . 6
Material specification . . . 6
Motor and control box . . . 7

4. Installation and startup **8**
Installation . . . 8
Electrical data . . . 8
Startup . . . 8
Liquid temperature . . . 8
System pressure . . . 8
Inlet pressure . . . 8
Setting the pump . . . 8
Change of pump performance . . . 9

5. Guide to performance curves **10**
Energy labelling . . . 10
Curve conditions . . . 10

6. Performance curves and technical data **11**
ALPHA2 L 15-40, 20-40 (N), 25-40 (N), 32-40 . . . 11
ALPHA2 L 20-45 N . . . 12
ALPHA2 L 15-50, 20-50 N, 25-50 (N), 32-50 . . . 13
ALPHA2 L 15-60, 20-60, 25-60, 32-60 . . . 14

7. Accessories **15**
Insulating kits . . . 15
ALPHA plugs . . . 15
Union and valve kits . . . 16

8. Product range **17**
ALPHA2 L, United Kingdom . . . 17
ALPHA2 L, Russia . . . 17

9. Grundfos Product Center **18**

1. Product introduction

Grundfos ALPHA2 L is a complete range of circulator pumps with the following features:

- integrated differential-pressure control enabling adjustment of pump performance to the actual system requirement
- motor based on permanent-magnet/compact-rotor technology.

The pumps are energy-optimised and comply with the requirements of the EuP directive.



Fig. 1 EuP ready

The installation of one of these pumps will reduce power consumption considerably, reduce noise from thermostatic valves and similar fittings and improve the control of the system.

The Grundfos ALPHA2 L range offers a host of advantages:

Energy savings

High-efficient permanent-magnet motors.

Flexibility

Suitable for installation in existing systems.

Comfort

Low-noise operation.

Safety

Built-in electrical and thermal protection of the pump.

User friendliness

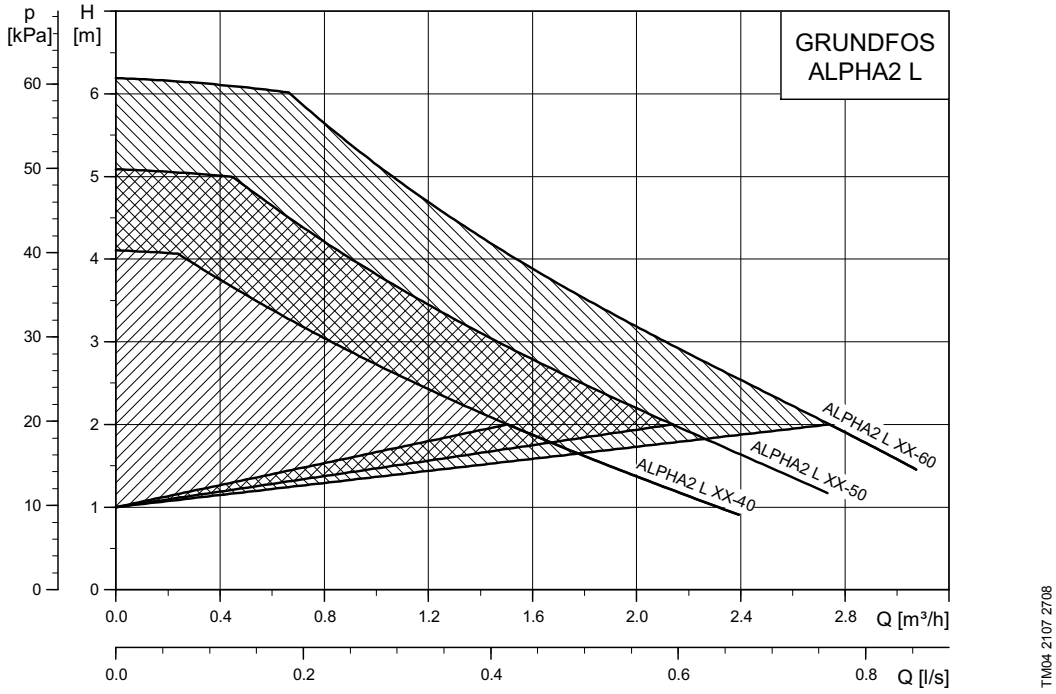
Simple setting and operation.

Type key

Example	ALPHA2 L	15 -	50	130
Pump range				
Nominal diameter (DN) of suction and discharge ports [mm] (15 = 1"*, 20 = 1 1/4", 25 = 1 1/2", 32 = 2")				
Maximum head [dm]				
[ ]: Cast-iron pump housing				
Port-to-port length [mm]				

* Exception: UK version, size 15 = 1 1/2".

Performance range



TM04 2107 2708

Fig. 2 Performance range

2. Applications

Grundfos ALPHA2 L is designed for circulating liquids in heating systems.

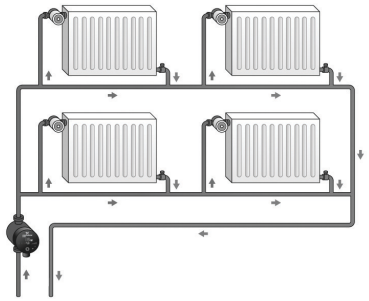
The pumps are suitable for the following systems:

- Systems with constant or variable flows where it is desirable to optimise the pump duty point.
- Systems with variable flow-pipe temperature.

Grundfos ALPHA2 L is especially suitable for the following:

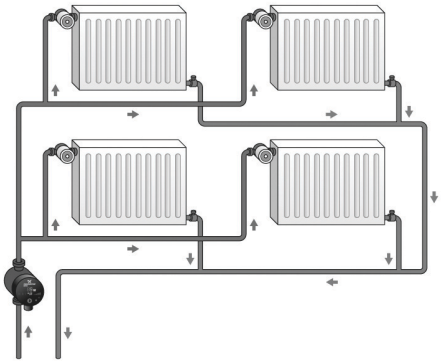
- Installation in existing systems where the differential pressure of the pump is too high during periods of reduced flow demand.
- Installation in new systems for automatic adjustment of the performance to flow demands without the use of bypass valves or similar expensive components.

Examples of systems



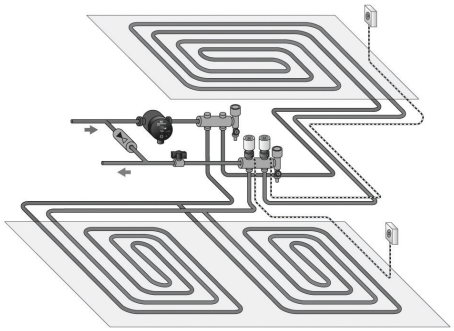
TM03 3988 4507

Fig. 3 One-pipe heating system



TM03 9889 4507

Fig. 4 Two-pipe heating system



TM03 9890 4507

Fig. 5 Underfloor heating system

Pumped liquids

The pump is suitable for clean, thin, non-aggressive and non-explosive liquids, not containing solid particles, fibres or mineral oil.

The pump must not be used for the transfer of flammable liquids, such as diesel oil, petrol and similar liquids.

Control of heating systems

The heating required in a building varies greatly during the day due to changing outdoor temperatures, solar radiation and heat emanating from human beings, electric appliances, etc.

Add to this that the need for heating may vary from one section of the building to another and that the thermostatic valves of some radiators may be turned down by the users.

These circumstances will cause an uncontrolled pump to produce a too high differential pressure when the heating demand is low.

Possible consequences:

- too high energy consumption
- irregular control of the system
- noise in thermostatic valves and similar fittings.

Grundfos ALPHA2 L automatically controls the differential pressure by adjusting the pump performance to the actual heating demand, without the use of external components.

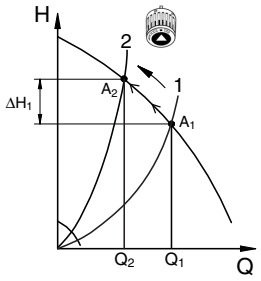
Advantages of pump control

In Grundfos ALPHA2 L, control is effected by adapting the differential pressure to the flow (proportional- and constant-pressure control).

Contrary to an uncontrolled pump, the proportional-pressure-controlled ALPHA2 L pump reduces the differential pressure in case of falling heating demand.

If the heating demand falls, for instance due to solar radiation, the radiator valves will close, and, for the uncontrolled pump, the flow resistance of the system will rise for instance from A_1 to A_2.

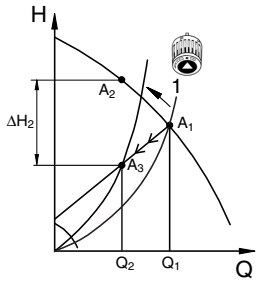
In a heating system with an uncontrolled pump, this situation will cause a pressure rise in the system by ΔH_1.



TM01 9119 5002

Fig. 6 Uncontrolled pump

In a system with a Grundfos ALPHA2 L pump, the pressure will be reduced by ΔH_2.



TM01 9120 5002

Fig. 7 Pump in proportional-pressure control mode

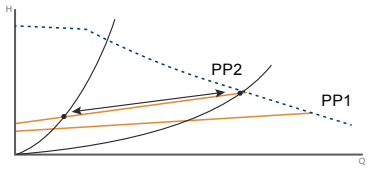
In a system with an uncontrolled pump, a pressure rise will often cause flow-generated noise in the thermostatic valves. This noise will be reduced considerably with the Grundfos ALPHA2 L.

The pump has the following control modes

- Proportional-pressure control
- Constant-pressure control
- Constant-curve control.

Proportional-pressure control

Proportional-pressure control adjusts the pump performance to the actual heat demand in the system, but the pump performance follows the selected performance curve, PP1 or PP2. See fig. 8 where PP2 has been selected. See *Change of pump performance* for further information.

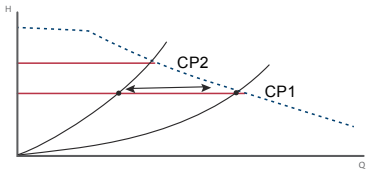


TM061833 3114

Fig. 8 Three proportional-pressure curves/settings

Constant-pressure control

Constant-pressure control adjusts the pump performance to the actual heat demand in the system, but the pump performance follows the selected performance curve, CP1 or CP2. See fig. 9 where CP1 has been selected. See *Change of pump performance* for further information.



TM06 1832 3114

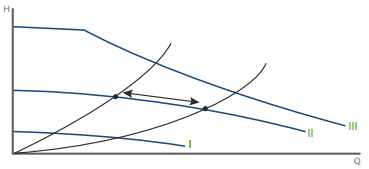
Fig. 9 Three constant-pressure curves/settings

The selection of the right constant-pressure setting depends on the characteristics of the heating system in question and the actual heat demand.

Constant-curve control

At constant-curve/constant-speed operation, the pump runs at a constant speed, independent of the actual flow demand in the system. The pump performance follows the selected performance curve, I, II or III.

See fig. 10 where II has been selected. See *Change of pump performance* for further information.



TM05 3068 0912

Fig. 10 Three constant-curve/constant-speed settings

3. Construction

Grundfos ALPHA2 L is designed for long and trouble-free operation due to the canned-rotor type, i.e. pump and motor form an integral unit without shaft seal and with only two gaskets for sealing. The bearings are lubricated by the pumped liquid. These constructions ensure maintenance-free operation.

The pumps are characterised by the following:

- Permanent-magnet/compact-stator motor which contribute to high efficiency and high starting torque.
- Ceramic shaft and radial bearings which contribute to long life.
- Carbon thrust bearing which contributes to long life.
- Stainless-steel rotor can, bearing plate and rotor cladding which contribute to corrosion-free long life.
- Composite impeller which contributes to corrosion-free long life.
- Automatic air venting which contributes to easy commissioning.
- Compact design featuring pump head with integrated control box and control panel which fit into most common installation.

Sectional drawing

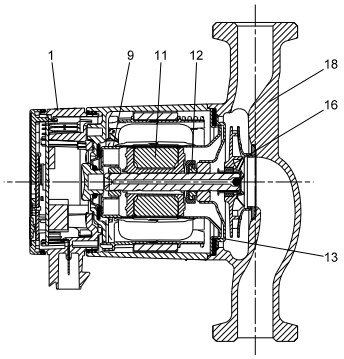


Fig. 11 Position numbers

Material specification

Pos.	Description	Material	EN	AISI/ ASTM
1	Controller complete	Composite, PC		
9	Rotor can	Stainless steel	1.4301	304
	Radial bearing	Ceramics		
11	Shaft	Ceramics		
	Rotor cladding	Stainless steel	1.4301	304
12	Thrust bearing	Carbon		
	Thrust bearing retainer	EPDM rubber		
13	Bearing plate	Stainless steel	1.4301	304
16	Impeller	Composite, PP or PES		
18	Pump housing	Cast iron	EN-JL 1020	A48-25
	Gaskets	EPDM rubber		

Motor and control box

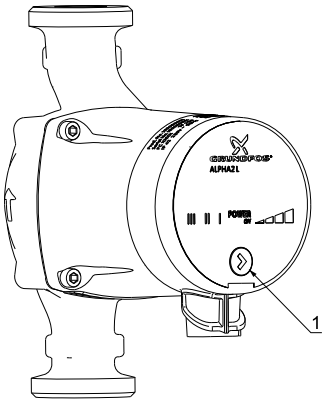
The motor is a 4-pole synchronous permanent-magnet motor.

The pump controller is incorporated in the control box, which is fitted to the stator housing with screws.

Control panel

The control panel is located on the front and is connected to the stator via a terminal plug. The control panel has a push-button (pos. 1) for selection of pump setting and seven light fields for indication of the selected pump setting. See fig. 12.

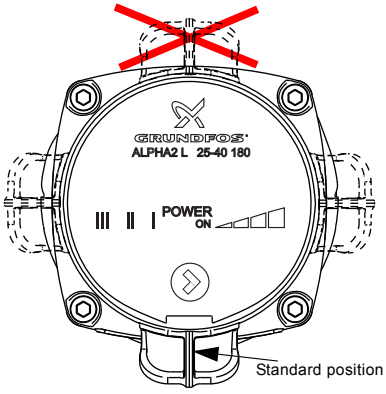
The "POWER ON" light field indicates that the power supply has been switched on. When the "POWER ON" light field is on and shows "- -", a fault preventing the pump from operating properly (for example seizing-up) has occurred.



TM04 2539 2608

Fig. 12 Push-button position

Control box positions



TM04 2538 2608

Fig. 13 Possible control box positions

ALPHA cable with plug

The plug incorporates cable relief and a locking function for securing the supply cable connection.



TM05 3073 0612

Fig. 14 ALPHA plug with cable relief and angled ALPHA plug with fixed cable

Stainless-steel versions N

The pump housing of the stainless-steel versions is painted in red colour. The stainless-steel versions can be identified by the N in the type key or by the silver ring around the display. See fig. 15.



GF-350

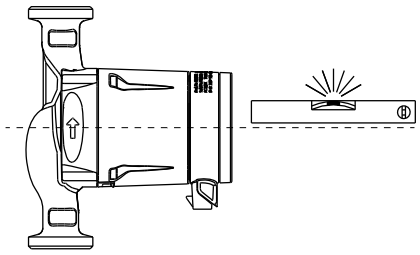
Fig. 15 Stainless-steel version N

4. Installation and startup

Installation

In most cases, the installation of the Grundfos ALPHA2 L is reduced to the mechanical installation and the connection to the power supply.

The pump must always be installed with horizontal motor shaft.



TM03 8501 1707

Fig. 16 Horizontal motor shaft

Electrical data

Supply voltage	1 x 230 V - 10 %/+ 10 %, 50/60 Hz, PE
Motor protection	The pump requires no external motor protection.
Enclosure class	IP42
Insulation class	F
Relative air humidity	Maximum 95 %
Ambient temperature	0-40 °C
Temperature class	TF110 to CEN 335-2-51
EMC (electromagnetic compatibility)	EN 55014-1:2006 and EN 55014-2:1997
Sound pressure level	≤ 43 dB(A)

Startup

The pump must not be started until the system has been filled with liquid and vented. Furthermore, the required minimum inlet pressure must be available at the pump inlet. The system cannot be vented through the pump.

The pump is self-venting and does not require venting before startup.

Liquid temperature

To avoid condensation in the control box and stator, the liquid temperature must always be higher than the ambient temperature. See table below.

Ambient temperature [°C]	Liquid temperature	
	Minimum [°C]	Maximum [°C]
0	2	110
10	10	110
20	20	110
30	30	110
35	35	90
40	40	70

System pressure

PN 10: Maximum 1.0 MPa (10 bar).

Inlet pressure

To avoid cavitation noise and damage to the pump, the following minimum pressures are required at the pump suction port.

Liquid temperature		
75 °C	**90 °C**	**110 °C**
0.5 m head	2.8 m head	10.8 m head

Setting the pump

Using the push-button on the control box, the electronically controlled pump can be set to the following:

- two constant-pressure curves
- two proportional-pressure curves
- three fixed-speed curves.

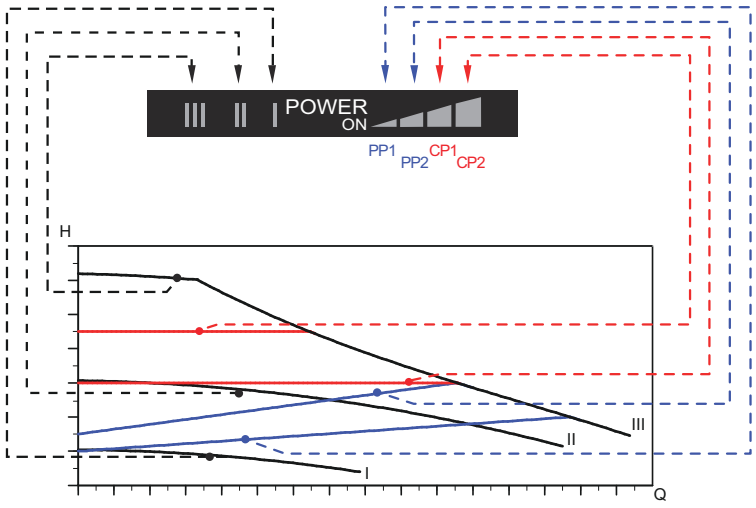
Factory setting

The pump has been factory-set to proportional-pressure curve (PP2). See fig. 17.

This setting is suitable for the majority of all single-family houses.

Change of pump performance

The pump performance (flow and head) can be changed by pressing the control box push-button as indicated in fig. 17 and the table below.



TM04 2532 2608

Fig. 17 Pump setting in relation to performance

Setting	Pump curve	Function
PP1	Lowest proportional-pressure curve	The duty point of the pump will move up or down on the lowest proportional-pressure curve, depending on the heat demand in the system. See fig. 17. The head (pressure) is reduced at falling heat demand and increased at rising heat demand.
PP2	Highest proportional-pressure curve	The duty point of the pump will move up or down on the highest proportional-pressure curve, depending on the heat demand in the system. See fig. 17. The head (pressure) is reduced at falling heat demand and increased at rising heat demand.
CP1	Lowest constant-pressure curve	The duty point of the pump will move out or in on the lowest constant-pressure curve, depending on the heat demand in the system. See fig. 17. The head (pressure) is kept constant, irrespective of the heat demand.
CP2	Highest constant-pressure curve	The duty point of the pump will move out or in on the highest constant-pressure curve, depending on the heat demand in the system. See fig. 17. The head (pressure) is kept constant, irrespective of the heat demand.
III	Speed III	The pump runs at a constant speed and consequently on a constant curve. In speed III, the pump is set to run on the maximum curve under all operating conditions. See fig. 17. Quick venting of the pump can be obtained by setting the pump to speed III for a short period.
II	Speed II	The pump runs at a constant speed and consequently on a constant curve. In speed II, the pump is set to run on the intermediate curve under all operating conditions. See fig. 17.
I	Speed I	The pump runs at a constant speed and consequently on a constant curve. In speed I, the pump is set to run on the minimum curve under all operating conditions. See fig. 17.

5. Guide to performance curves

Energy labelling

The Grundfos ALPHA2 L is energy-optimised and complies with the EuP Directive (Commission Regulation (EC) No 641/2009) which has been effective since 1 January 2013.

For more information about the new energy directive, please visit:

Energy.grundfos.com

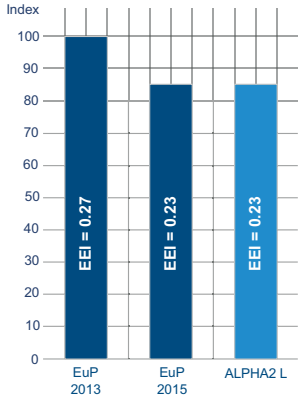
TM05 2683 0412

Curve conditions

The guidelines below apply to the performance curves on the following pages:

- Test liquid: airless water.
- The curves apply to a density of ρ = 983.2 kg/m^3 and a liquid temperature of 60 °C.
- All curves show average values and should not be used as guarantee curves. If a specific minimum performance is required, individual measurements must be made.
- The curves for speeds I, II and III are marked.
- The curves apply to a kinematic viscosity of υ = 0.474 mm^2/s (0.474 cSt).
- The conversion between head H [m] and pressure ρ [kPa] has been made for water with a density of ρ = 1000 kg/m^3. For liquids with other densities, for example hot water, the discharge pressure is proportional to the density.

The EEI values for Grundfos ALPHA2 L pumps are far below the EuP 2013 value and comply with the requirements for 2015. See fig. 18.



TM05 7835 1613

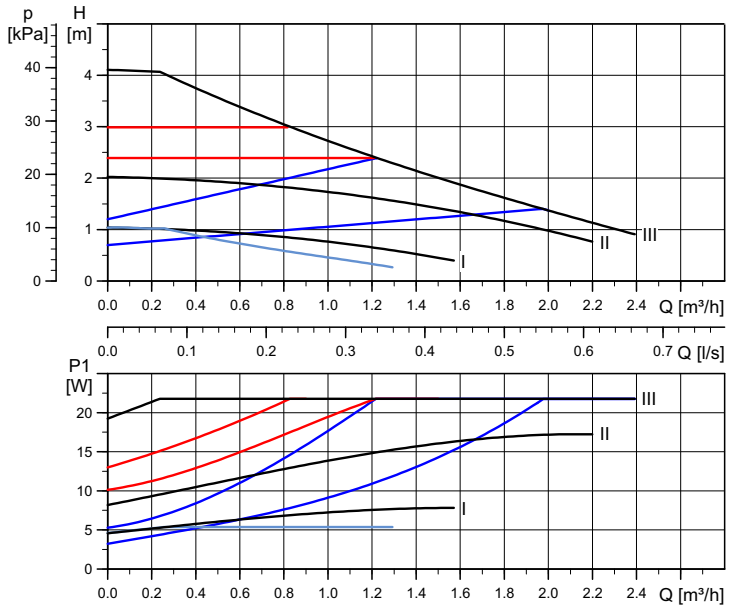
Fig. 18 EEI limits and the current positioning of the ALPHA2 L

With an energy efficiency index (EEI) at the EuP 2015 requirement level, you can achieve considerable energy savings compared to a typical circulator pump and thus a remarkably fast return on investment.

6. Performance curves and technical data

ALPHA2 L 15-40, 20-40 (N), 25-40 (N), 32-40

1 x 230 V, 50/60 Hz

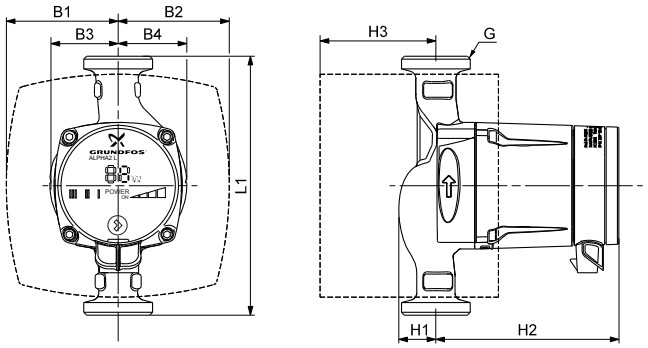


TM04 2110 2614 - TM03 0868 0705

Speed	P1 [W]	$I_{1/1}$ [A]
Min.	5	0.05
Max.	22	0.19

The pump incorporates overload protection.

Connections: See *Insulating kits*, page 15.
System pressure: Maximum 1.0 MPa (10 bar).
Liquid temperature: 2-110 °C (TF 110).

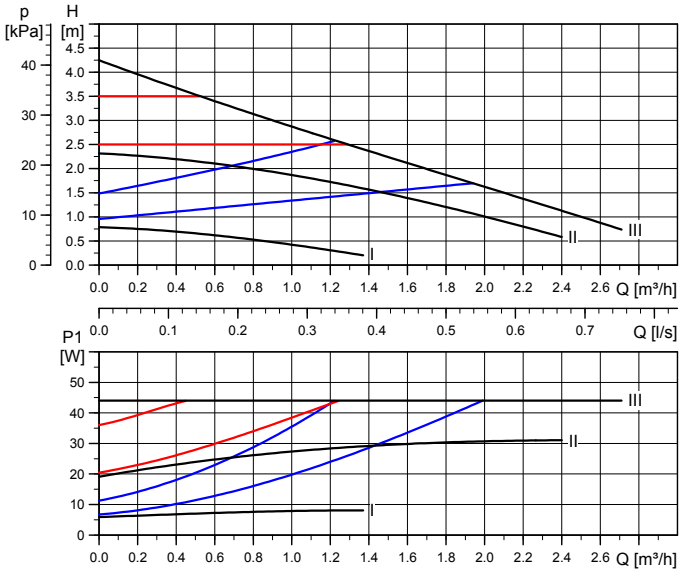


TM05 8040 1813

Pump type	EEI <	Dimensions [mm]									Weights [kg]		Ship. vol. [m³]
		L1	B1	B2	B3	B4	H1	H2	H3	G	Net	Gross	
ALPHA2 L 15-40	0.23	130	78	78	46	49	27	129	58	1	1.9	2.1	0.00383
ALPHA2 L 20-40	0.23	130	78	78	46	49	27	129	58	1 1/2	1.9	2.1	0.00383
ALPHA2 L 20-40 N	0.23	150	78	78	46	49	27	129	58	1 1/4	2.4	2.6	0.00383
ALPHA2 L 25-40	0.23	130	78	78	46	49	27	129	79	1 1/2	1.9	2.1	0.00383
ALPHA2 L 25-40 (N)	0.23	180	78	78	47	48	26	127	81	1 1/2	2.1	2.3	0.00383
ALPHA2 L 25-40 A	0.23	180	63	93	32	65	50	135	82	1 1/2	3.1	3.3	0.00383
ALPHA2 L 32-40	0.23	180	78	78	47	65	26	127	81	2	2.1	2.3	0.00383
ALPHA2 L 32-40	0.23	180	78	78	47	48	26	127	81	2	2.1	2.3	0.00383

ALPHA2 L 20-45 N

1 x 230 V, 50 Hz

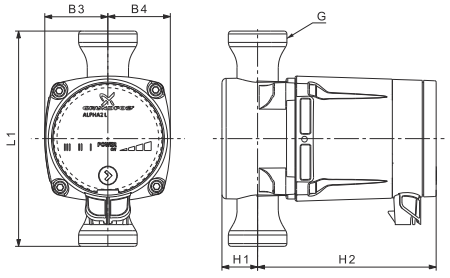


TM05 2213 4611

Speed	P1 [W]	$I_{1/1}$ [A]
Min.	7	0.07
Max.	45	0.34

The pump incorporates overload protection.

System pressure: Maximum 1.0 MPa (10 bar).
Liquid temperature: 2-110 °C (TF 110).

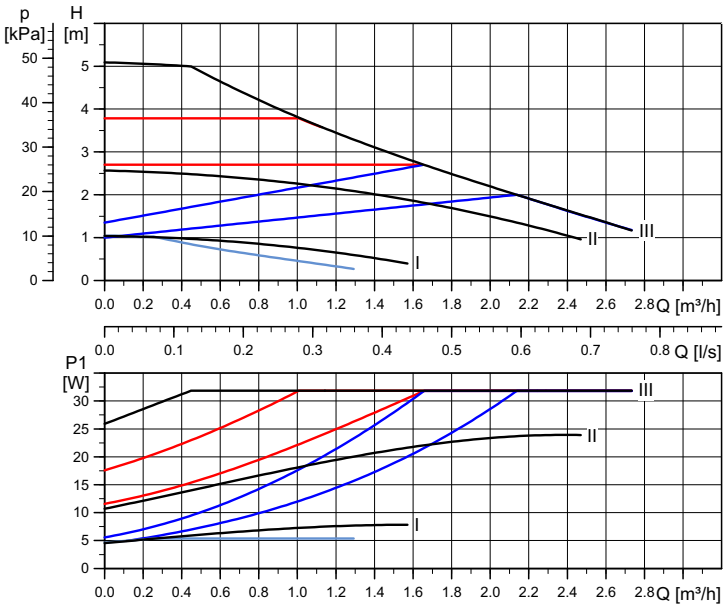


TM05 2201 4611

Pump type	Dimensions [mm]						Weights [kg]		Ship. vol. [m^3]
	L1	B3	B4	H1	H2	G	Net	Gross	
ALPHA2 L 20-45 N	150	43	43	27	127	1 1/4	1.8	2.0	0.00383

ALPHA2 L 15-50, 20-50 N, 25-50 (N), 32-50

1 x 230 V, 50/60 Hz

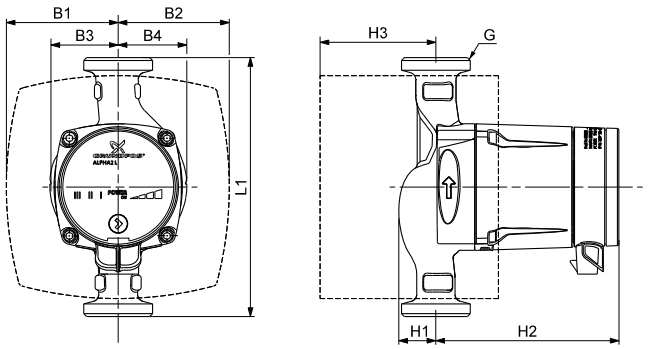


TM04 2109 2614 - TM03 0868 0705

Speed	P1 [W]	$I_{1/1}$ [A]
Min.	5	0.05
Max.	32	0.27

The pump incorporates overload protection.

Connections: See *Insulating kits*, page 15.
System pressure: Maximum 10 bar.
Liquid temperature: 2-110 °C (TF 110).

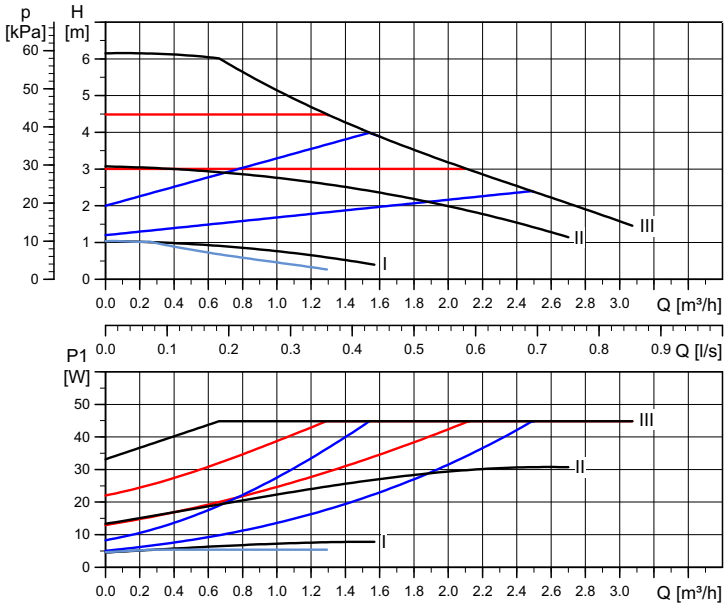


TM04 2533 2608

Pump type	EEI <	Dimensions [mm]									Weights [kg]		Ship. vol. [m³]
		L1	B1	B2	B3	B4	H1	H2	H3	G	Net	Gross	
ALPHA2 L 15-50	0.23	130	78	78	46	49	27	129	58	1 1/2	2.0	2.2	0.00383
ALPHA2 L 20-50	0.23	130	78	78	46	49	27	129	58	1 1/2	1.9	2.1	0.00383
ALPHA2 L 20-50 N	0.23	150	78	78	46	49	27	129	58	1 1/4	2.4	2.6	0.00383
ALPHA2 L 25-50	0.23	130	78	78	46	49	27	129	79	1 1/2	1.9	2.1	0.00383
ALPHA2 L 25-50 (N)	0.23	180	78	78	47	65	26	127	81	2	2.1	2.3	0.00383
ALPHA2 L 32-50	0.23	180	78	78	47	65	26	127	81	2	2.1	2.3	0.00383

ALPHA2 L 15-60, 20-60, 25-60, 32-60

1 x 230 V, 50/60 Hz

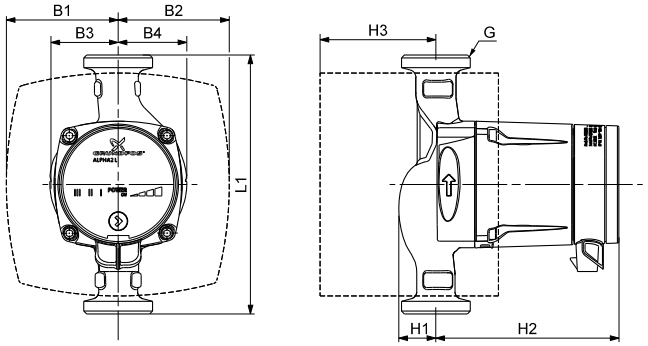


TM04 2108 2614 - TM03 0868 0705

Speed	P1 [W]	$I_{1/1}$ [A]
Min.	5	0.05
Max.	45	0.38

The pump incorporates overload protection.

Connections: See *Insulating kits*, page 15.
System pressure: Maximum 10 bar.
Liquid temperature: 2-110 °C (TF 110).



TM04 2533 2608

Pump type	EEI <	Dimensions [mm]									Weights [kg]		Ship. vol. [m³]
		L1	B1	B2	B3	B4	H1	H2	H3	G	Net	Gross	
ALPHA2 L 15-60	0.23	130	78	78	46	49	27	129	58	1 1/2	1.9	2.1	0.00383
ALPHA2 L 20-60	0.23	130	78	78	46	49	27	129	58	1 1/2	1.9	2.1	0.00383
ALPHA2 L 20-60 N	0.23	150	78	78	46	49	27	129	58	1 1/4	2.4	2.6	0.00383
ALPHA2 L 25-60	0.23	180	78	77	47	48	26	127	81	1 1/2	2.1	2.3	0.00383
ALPHA2 L 25-60 (N)	0.23	180	78	78	47	65	26	127	81	2	2.1	2.3	0.00383
ALPHA2 L 25-60 A	0.23	180	63	93	32	65	50	135	82	1 1/2	3.1	3.3	0.00383
ALPHA2 L 32-60	0.23	180	78	77	47	48	26	127	81	2	2.1	2.3	0.00383

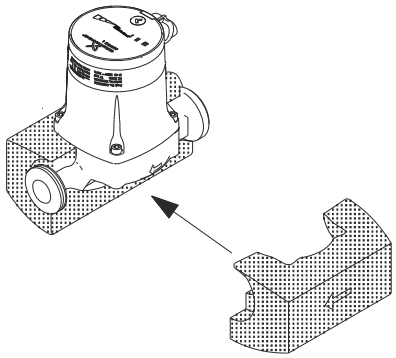
7. Accessories

Insulating kits

Grundfos ALPHA2 L pumps can be fitted with two insulating shells.

The insulation thickness of the insulating shells corresponds to the nominal diameter of the pump.

The insulating kit, which is tailored to the individual pump type, encloses the entire pump housing. The two insulating shells are easy to fit around the pump.



TM04 2806 3208

Fig. 19 Insulating shells

Pump type	Product number
Insulating shells (not available for ALPHA2 L 20-45)	505821

ALPHA plugs



TM05 3073 0612

Fig. 20 ALPHA plugs

Pos.	Description	Product number
1	ALPHA plug, standard plug connection	98284561
2	ALPHA angle plug, standard angle plug connection	98610291
3	ALPHA plug, 90 ° bend, including 4 m cable	96884669

Grundfos offers a special cable with an active built-in NTC protection circuit which will reduce possible inrush currents. To be used in case of e.g poor quality of relay components which are sensitive to inrush current.

Union and valve kits

ALPHAx	Connection	Product numbers, unions														
		Rp			R		★ Rp			★ mm		mm				
		3/4	1	1 1/4	1	1 1/4	3/4	1	1 1/4	∅22	∅28	∅15	∅18	∅22	∅28	∅42
15-xx*	G 1	•														
15-xx N*		•														
25-xx	G 1 1/2	529921	529922	529821	529925	529924										
25-xx N		529971	529972				519805	519806	519807	519808	519809		529977	529978	529979	
32-xx	G 2		509921	509922												
32-xx N				509971											•	529995

* When ordering UK versions, use product numbers for 25-xx (G 1 1/2).
• Available on request.
★ Fittings including isolating valve.

Thread types

G-threads have a cylindrical form in accordance with the EN-ISO 228-1 standard.

R-threads have a conical form in accordance with the ISO 7-1 standard.

In the case of a thread of size 1 1/2", for example, the threads are specified as G1 1/2 or R1 1/2. Male G-threads (cylindrical) can only be screwed into female G-threads. Male R-threads (conical) can be screwed into female G-threads or R-threads. See fig. 21.

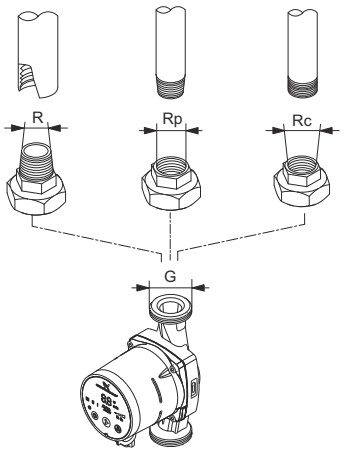


Fig. 21 G-thread and R-thread

8. Product range

ALPHA2 L, international

Note: Click on the product number and go directly to the performance curve in Grundfos Product Center.

Pump type	Port-to-port length [mm]	Connection	Voltage [V] 50 Hz	Product number	Product number stainless steel	Data sheet Page
ALPHA2 L 15-40	130	G 1	230	95047560		11
ALPHA2 L 15-50	130			98288721		13
ALPHA2 L 15-60	130			96984037		14
ALPHA2 L 20-40	130	G 1 1/4		98288722		11
ALPHA2 L 20-40 N	150				98288708	11
ALPHA2 L 20-45 N	150				98094952	12
ALPHA2 L 20-50	130			98288723		13
ALPHA2 L 20-50 N	150				98290112	13
ALPHA2 L 20-60	130			98288724		13
ALPHA2 L 20-60 N	150				98288709	14
ALPHA2 L 25-40	130	G 1 1/2		95047561		11
ALPHA2 L 25-40 (N)	180			95047562	98288702	11
ALPHA2 L 25-40 A	180			98288725		11
ALPHA2 L 25-50	130			98288726		13
ALPHA2 L 25-50 (N)	180			98124072	98288705	13
ALPHA2 L 25-60	130			95047563		14
ALPHA2 L 25-60 (N)	180			95047564	95047506	14
ALPHA2 L 25-60 A	180			98288728		14
ALPHA2 L 32-40	180	G 2		95047565		11
ALPHA2 L 32-50	180			98288729		13
ALPHA2 L 32-60	180			95047566		14

ALPHA2 L, United Kingdom

Note: Click on the product number and go directly to the performance curve in Grundfos Product Center.

Pump type	Port-to-port length [mm]	Connection	Voltage [V] 50 Hz	Product number	Data sheet Page
ALPHA2 L 15-50	130	G 1 1/2	230	95047567	12
ALPHA2 L 15-60				95047568	14

ALPHA2 L, Russia

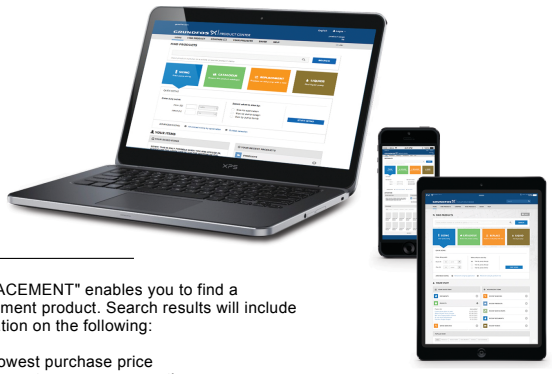
Note: Click on the product number and go directly to the performance curve in Grundfos Product Center.

Pump type	Port-to-port length [mm]	Connection	Voltage [V] 50 Hz	Product number	Data sheet Page
ALPHA2 L 25-40	180	G 1 1/2	230	98257789	11
ALPHA2 L 25-60				98286490	14
ALPHA2 L 32-40		G 2		98286501	11
ALPHA2 L 32-60				98286503	14

9. Grundfos Product Center

Online search and sizing tool to help you make the right choice.

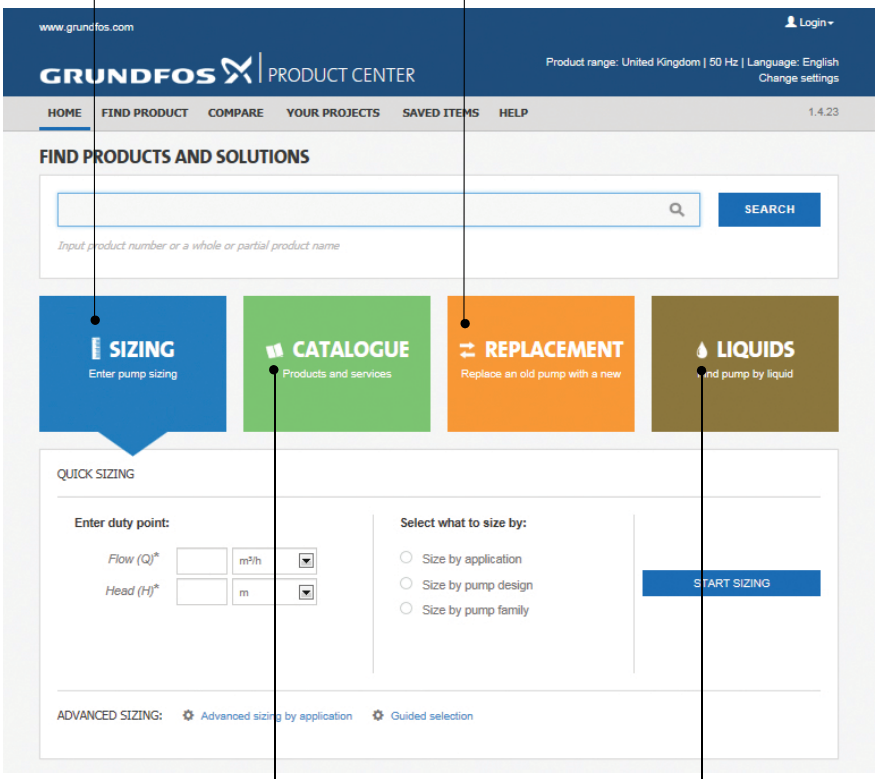
http://product-selection.grundfos.com



"SIZING" enables you to size a pump based on entered data and selection choices.

"REPLACEMENT" enables you to find a replacement product. Search results will include information on the following:

- the lowest purchase price
- the lowest energy consumption
- the lowest total life cycle cost.



"CATALOGUE" gives you access to the Grundfos product catalogue.

"LIQUIDS" enables you to find pumps designed for aggressive, flammable or other special liquids.

All the information you need in one place

Performance curves, technical specifications, pictures, dimensional drawings, motor curves, wiring diagrams, spare parts, service kits, 3D drawings, documents, system parts. The Product Center displays any recent and saved items - including complete projects - right on the main page.

Downloads

On the product pages, you can download installation and operating instructions, data booklets, service instructions, etc. in PDF format.

Subject to alterations.

be think innovate

The name Grundfos, the Grundfos logo, and **be think innovate** are registered trademarks owned by Grundfos Holding A/S or Grundfos A/S, Denmark. All rights reserved worldwide.

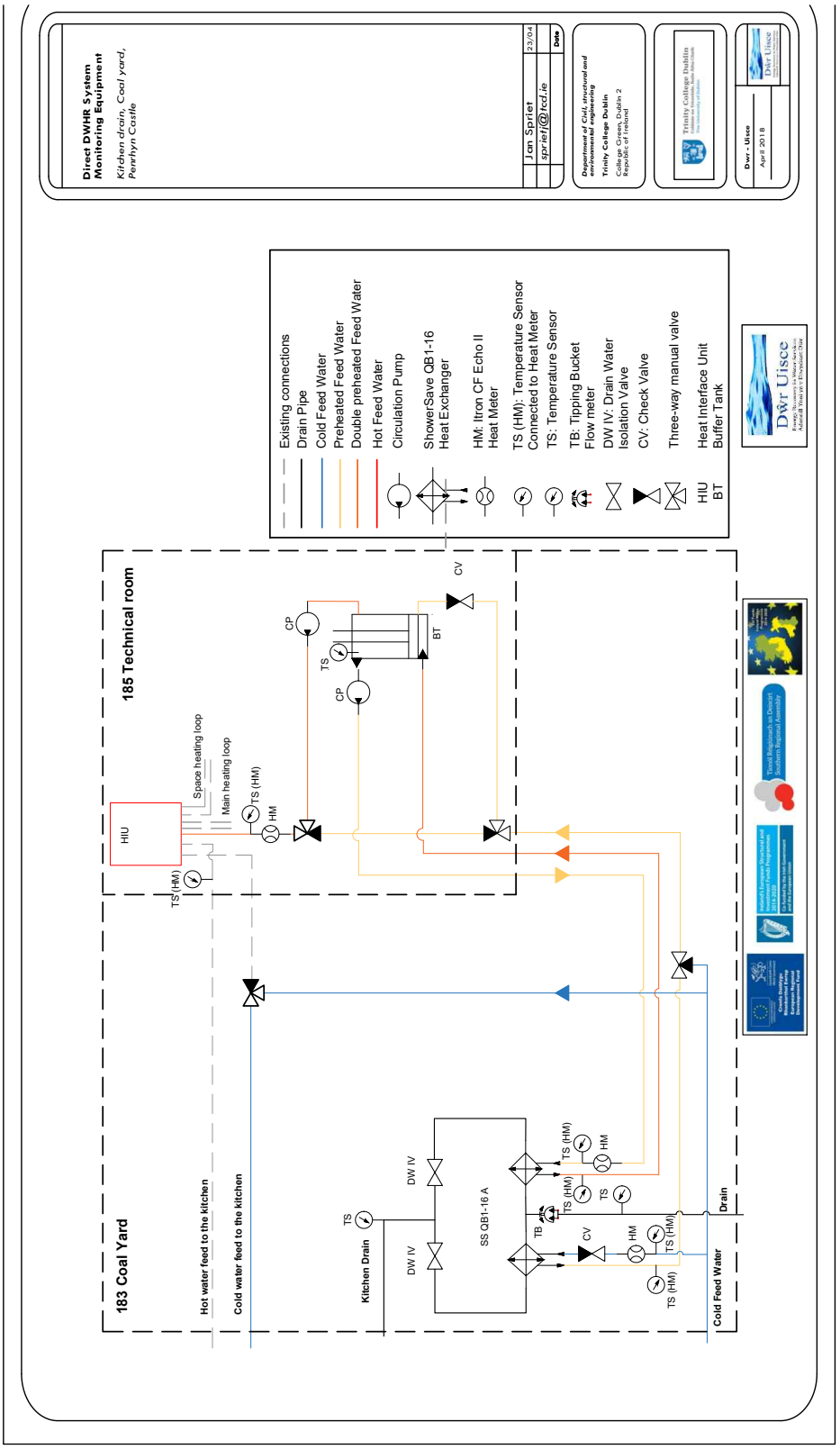
© Copyright Grundfos Holding A/S

98505141 0915
ECM: 1167282

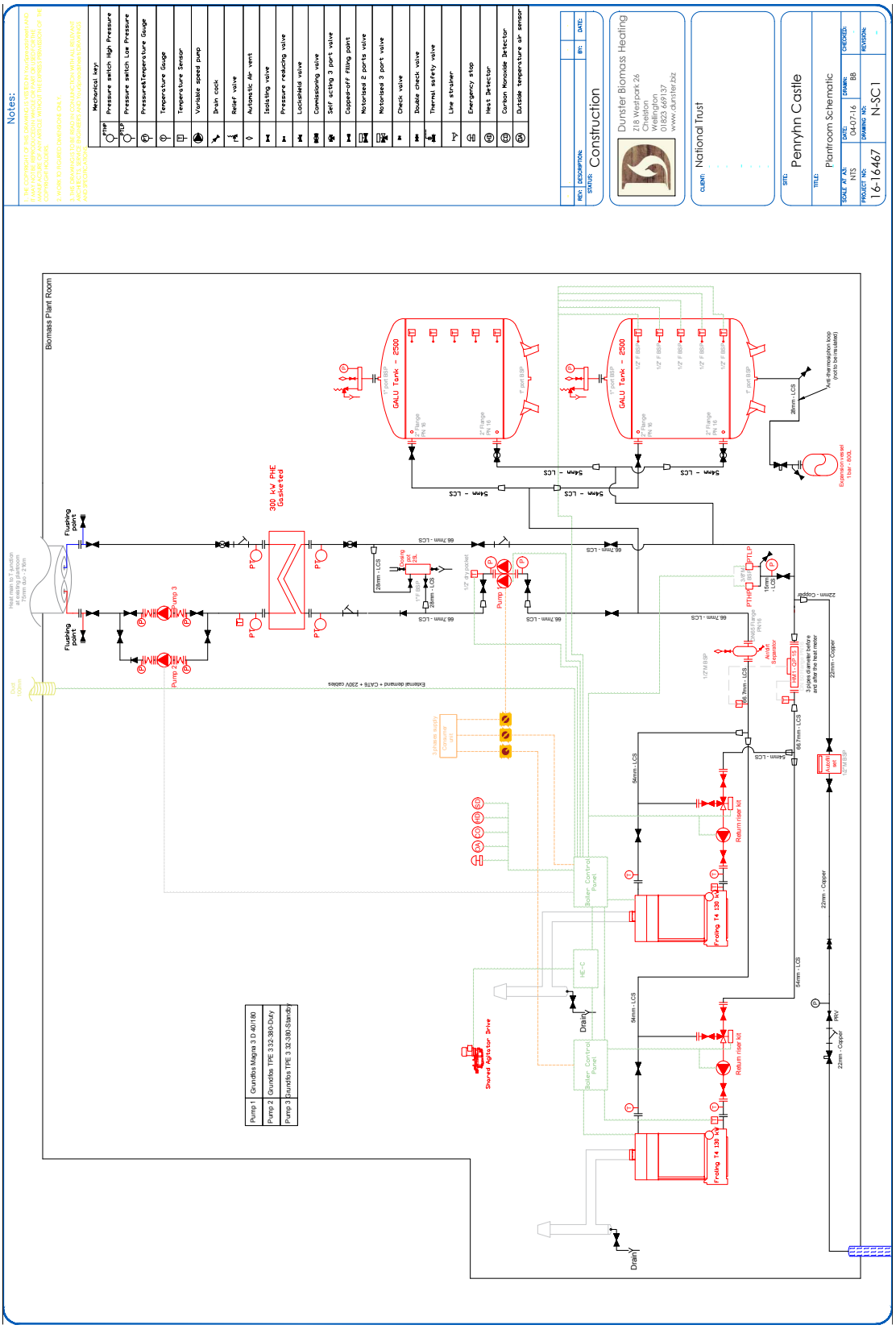
GRUNDFOS A/S
DK-8850 Bjerringbro . Denmark
Telephone: +45 87 50 14 00
www.grundfos.com

GRUNDFOS

F.4. Detailed schematic of the Demonstrator at Penrhyn castle



F.5. Schematic of the heating system in the plant room



G. Characterization of the experimental set-up

The operation of different components of the experimental set-up, and the definition of different operating conditions are described in this Appendix.

G.1. Definition of the steady state condition

The steady state condition is defined as the operating state within which the effluent temperature of the grease trap, the flow into the grease trap and the flow through the heat exchanger don't show a significant trend. This means that all variation is due to chance, noise, measuring errors,... but no structural change is present. This is studied by fitting a linear curve on the effluent temperature, the trend is considered to be negligible when the difference between the true mean of the slope of this linear fit and 0 is not statistically significant, with 95% confidence. Meaning that the 95% confidence interval contains the value 0. This is shown in Figure G.1, for the evolution at an incoming drain water flow of 4 l/min at a temperature of $40°C$, the flow through the heat exchanger was 3 l/min.

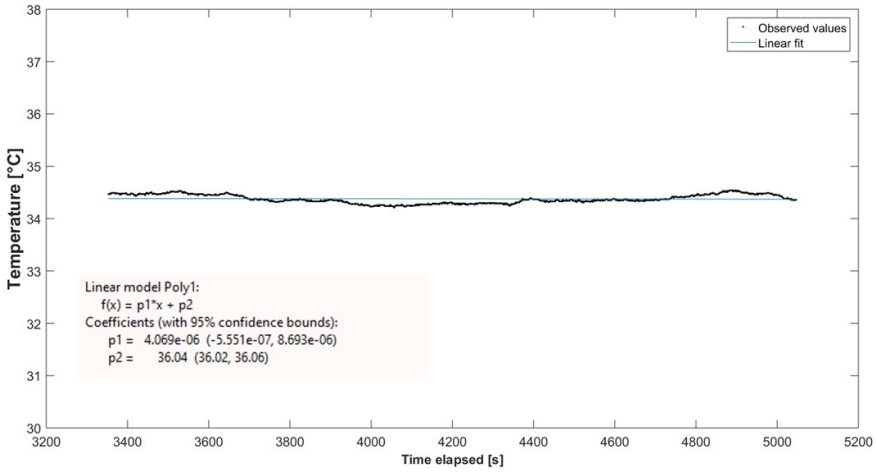


Figure G.1.: Effluent temperature and fit in steady state.

The recovered heat, absorbed by the fresh water for the experiment with a flow through the grease trap of 2 l/min at $40°C$, and a flow through the heat exchanger of 3 l/min is shown in Figure G.2. One can observe that although a seemingly gaussian curve can be observed around the average, some outliers can be observed at lower heat recovery values. This is confirmed by the probability plot (also called p-plot) in Figure G.3, as this plot doesn't follow the linear curve, indicating deviation from the normal distribution.

To remedy the situation, the outliers, lying outside the interval $[\mu - 3\sigma,\ \mu + 3\sigma]$ were removed from the steady state dataset. This resulted in the histogram, for the recovered heat, as shown in Figure G.4, and a probability plot as shown in Figure G.5. This prabibility plot shows an almost linear characteristic. The Anderson-Darling normality test, however showed a p-value of $2.94E-6 < 0.05$, indicating that the null-hypothesis (normally distributed data) should be rejected. However, as the probability plot shows almost

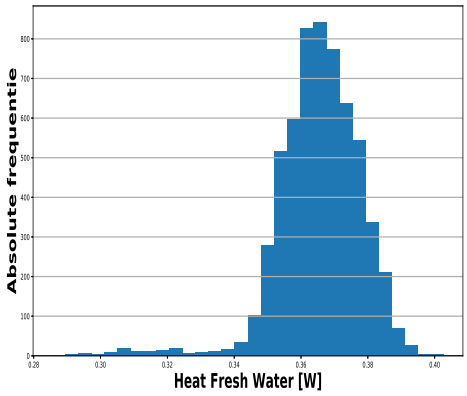


Figure G.2.: Histogram of the observed recovered heat during steady state.

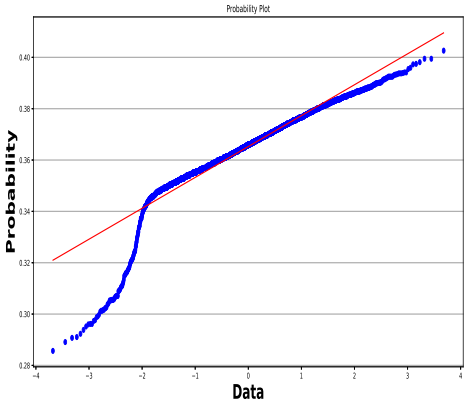


Figure G.3.: Probability plot f the observed recovered heat during steady state.

linear behaviour, the 95% confidence interval for normally distributed data was used for the validation of the CFD simulation results.

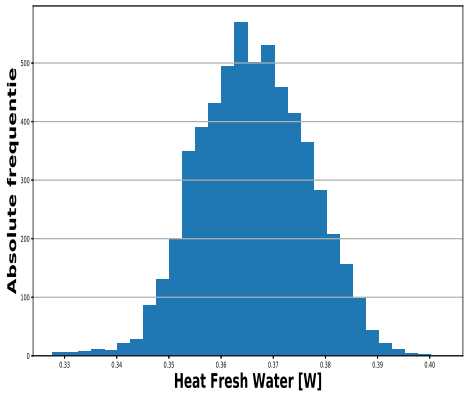


Figure G.4.: Histogram of the treated recovered heat during steady state.

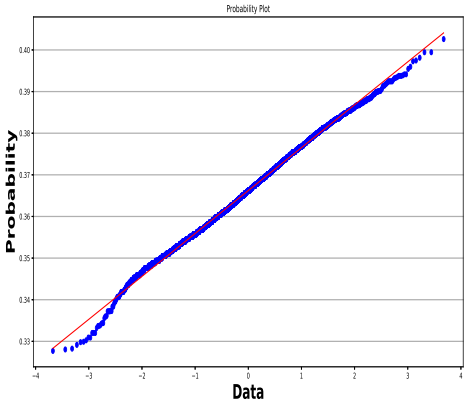


Figure G.5.: Probability plot of the treated recovered heat during steady state.

G.2. Flow Control

The flow control is obtained by keeping a constant level in the feeding reservoirs, both in the Hot drain water reservoir, and the Flow Control reservoir (see Figure G.6).

The constant level is obtained by an overflow system, as shown in Figure G.7.

The verification of the constant flow is done in a similar manner as the determination of the steady state. It was verified that the true mean of the trend on the flow value was statistically equal to 0, with 95% confidence. Figure G.8 and G.9 show the steady state flow of the simulated drain water and through the heat exchanger for the same test conditions as described in Section G.1.

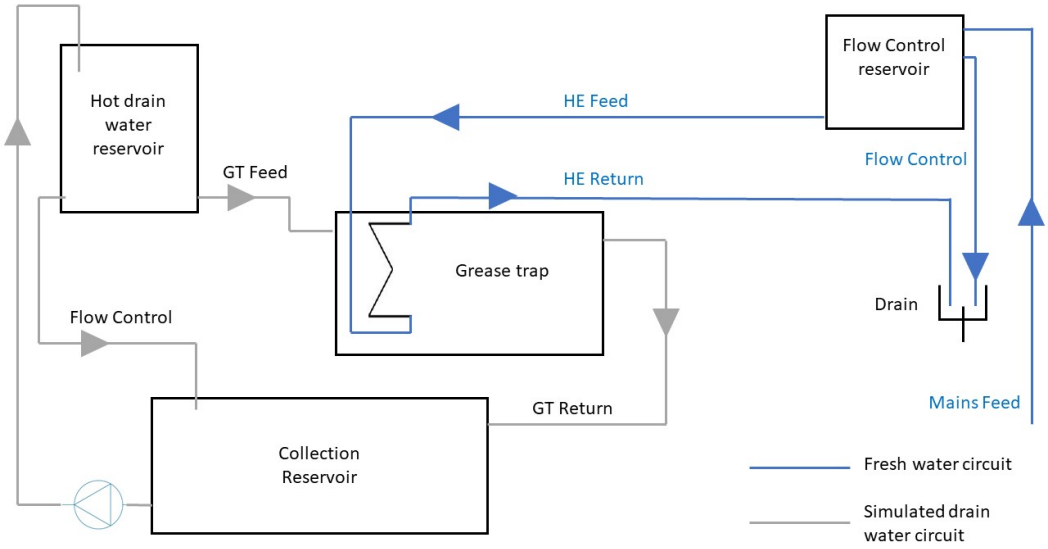


Figure G.6.: Schematic of the experimental set-up.

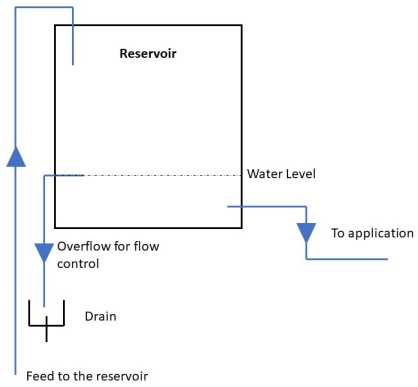


Figure G.7.: Schematic of the overflow system.

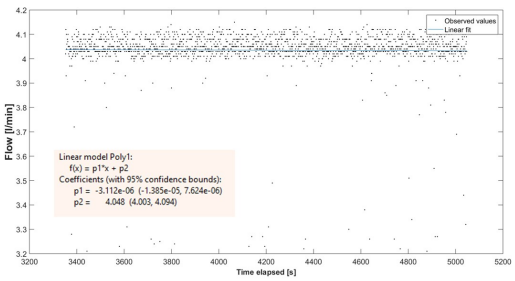


Figure G.8.: Simulated drain water flow in steady state.

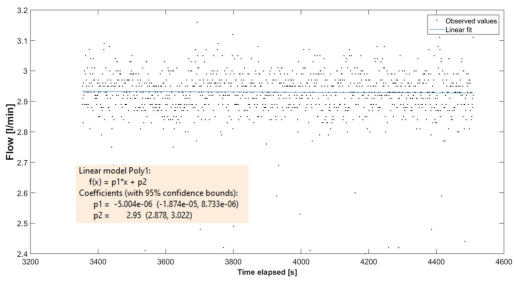


Figure G.9.: Heat exchanger flow in steady state.

G.3. Temperature Equivalence of the fresh water flow control system

When the fresh water passes through a flow control reservoir, before entering the heat exchanger, there is a possibility that the surrounding temperature influences the temperature of the feed water. To verify

this the temperature is measured for one hour, when fed straight from the mains into the heat exchanger, and when fed through the flow control reservoir. Figure G.10 shows the boxplots from both situations, the expected values (center of the box), fall within the 95% confidence intervals (whiskers) of each other, meaning that the results are not statistically different. One can observe that the uncertainty on the system with flow control is much smaller (the whisker is smaller), this is due to the damping effect of the reservoir on temperature variations on the main water feed.

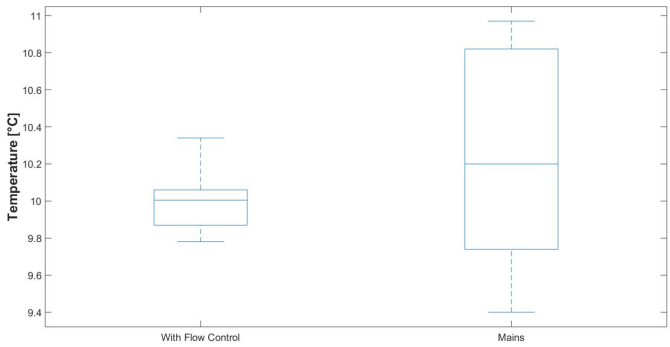
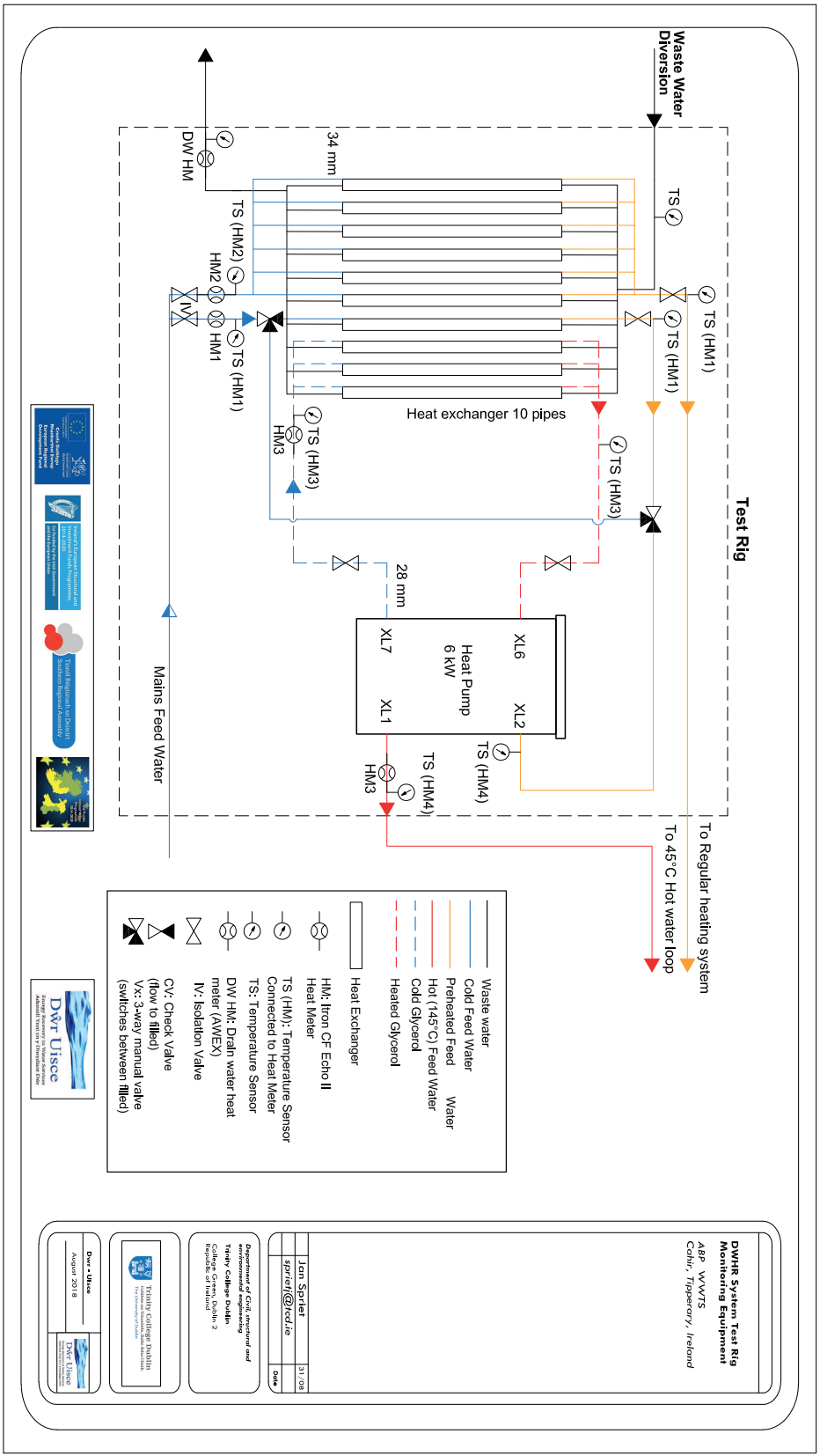


Figure G.10.: Boxplot of the feed water temperature for both configurations.

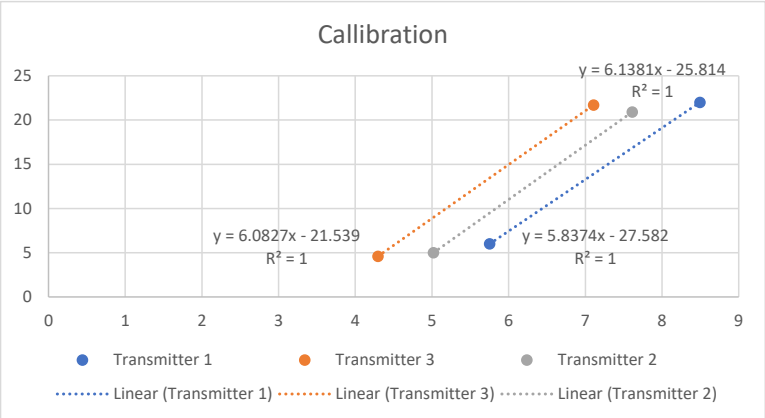
H. Appendices related to ABP, Cahir

H.1. Schematic of the ABP test rig



H.2. Calibration of the temperature sensors

					Current (mA)	
					4	20
Resistance	996					
Transmitter 1		5.8374	-27.582		-4.2324	89.166
Temperature	Voltage	Current		Channel		
6	5.73	5.753012				
22	8.46	8.493976				
28.573788	9.62	9.658635	*Verification*			
Transmitter 2		6.1381	-25.814		-1.2616	96.948
Temperature	Voltage	Current		Channel		
5	5	5.02008				
20.9	7.58	7.610442				
30.82168173	9.19	9.226908	*Verification*			
Transmitter 3		6.0827	-21.539		2.7918	100.115
Temperature	Voltage	Current		Channel		
4.6	4.28	4.297189				
21.7	7.08	7.108434				
31.34873293	8.66	8.694779	*Verification*			



H.3. Datasheet of the submersible pump

PRORIL

50 Hz

GOVOX Series, these vortex pumps feature a less impeller wear and longer pump life by a vortex flow that allows fibrous materials and solid matters to be pumped out without obstruction.



Sewage Pump

GOVOX 204

Vortex Pump

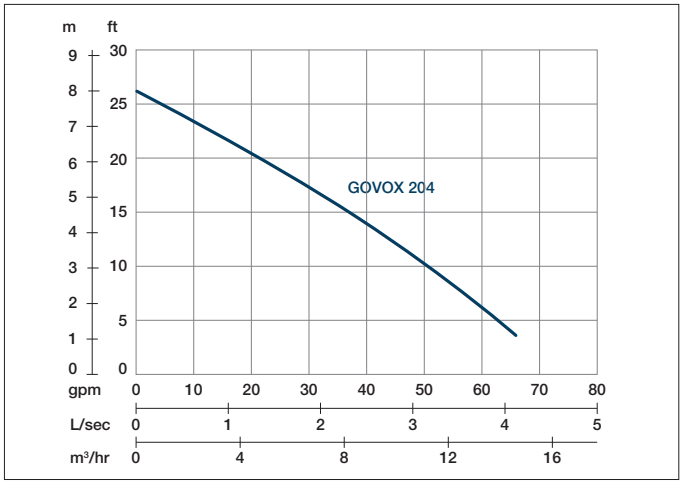
PRORIL

GOVOX 204

Vortex Pump

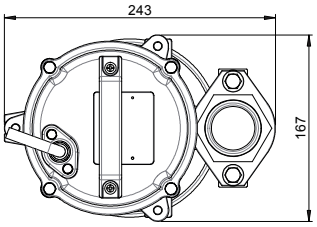
50 Hz

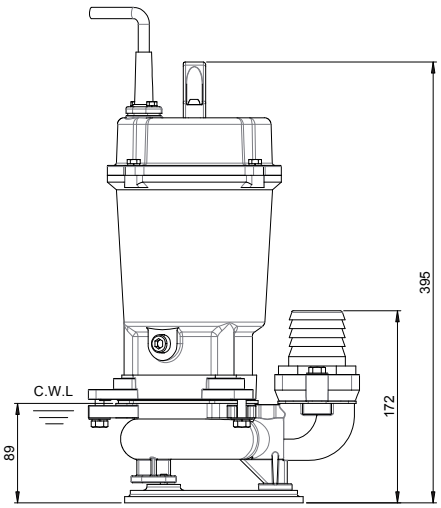




Shaft Speed : 2850 rpm | Solid Passage : 32 mm | Outlet : 50mm, 2in

OUTPUT	HEAD	FLOW
0.4 kW	Rated : 5m, 16ft	Rated : 2 l/s, 32 gpm
0.5 HP	Max : 8m, 26ft	Max : 4.2 l/s, 66 gpm





Weight : 13.5kg / 30 lbs

Pump Type		Electric Submersible Pumps
		1-Phase, 3-Phase
Motor	Type	Induction Motor
	Poles	2 Pole
	Insulation	Class F
	Protector	Circle Thermal Protector
	Starter	1-Phase • Capacitor-Run
Lubricant		Food Grade (ISO VG32)
Impeller Type		Vortex
Shaft Seal		Double Mechanical Seal
		Silicon Carbide VS Ceramic / Carbon
Bearings		C3 Shielded ball bearings
Cable		H07RNF
		Length: 10m (33ft) or longer upon request.
Materials	Pump Casing	Gray Iron
	Impeller	Gray Iron
	Motor Frame	Gray Iron
	Motor Shaft	Stainless Steel
Max. Liquid Temperature		104°F (40°C)
Max. Submersion Depth		66ft (20m)
pH Range		pH 5 - pH 8
Acessories		GRL-02

H.4. Datasheet of the additional flow meter

ENGLISH

Datasheet

Stock No: 257-149

RS Pro Liquid Acetal Copolymer 4.5 → 16 V dc Sensor/Switch without Indicator, 20bar Pressure



Liquid Flow Sensors

Two flow transducers manufactured in acetal copolymer with brass compression fittings at both ends to fit 15mm diameter pipe connections.

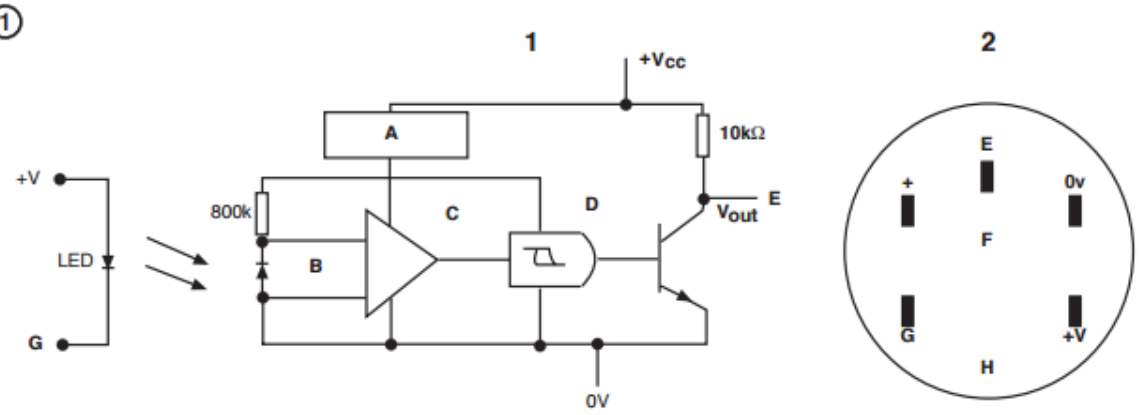
- Provides a pulsed output proportional to flow rate
- LED and photodetector are separated by a turbine mounted on sapphire bearings
- LED requires an external current limiting resistor (dependent on supply voltage)
- Suitable for use with mains and heating system waters etc.
- Rise/fall times 60/6ns
- Output voltage 200mV (low); V_{CC} (high)
- Diode: Forward current 10mA, Power dissipation 100mW

Note

Not suitable for use with strong mineral acids/solutions, strong or searching solvents.

ENGLISH

①



GB

1. Electrical (with logic hip detector)
A. Voltage regulator
B. Photo diode
C. Amplifier
D. Schmitt trigger
2. Electrical connection
E. Output
F. Photodetector
G. Cathode
H. Diode

D

1. Elektrische Bauteile (mit Detektorlogik)
A. Spannungsregler
B. Fotodiode
C. Verstärker
D. Schmitt-Trigger
2. Elektrische Anschlüsse
E. Ausgang
F. Fotodetektor
G. Kathode
H. Diode

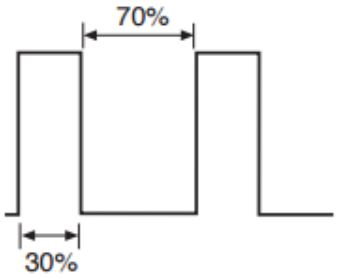
E

1. Sistema Eléctrico (con detector de chip lógico)
A. Regulador de tensión
B. Fotodiodo
C. Amplificador
D. Disparador de Schmitt
2. Conexión eléctrica
E. Salida
F. Fotodetector
G. Cátodo
H. Diodo

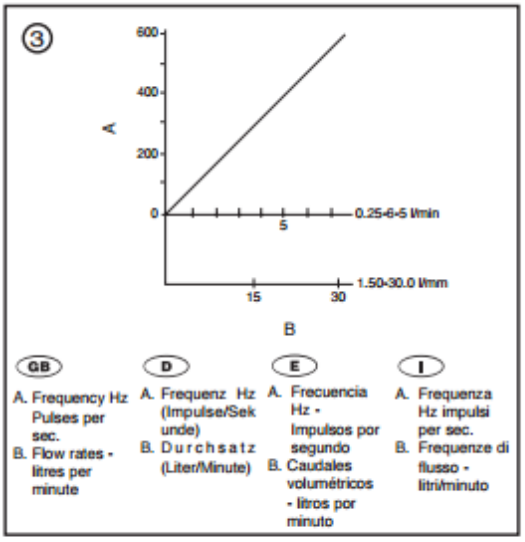
I

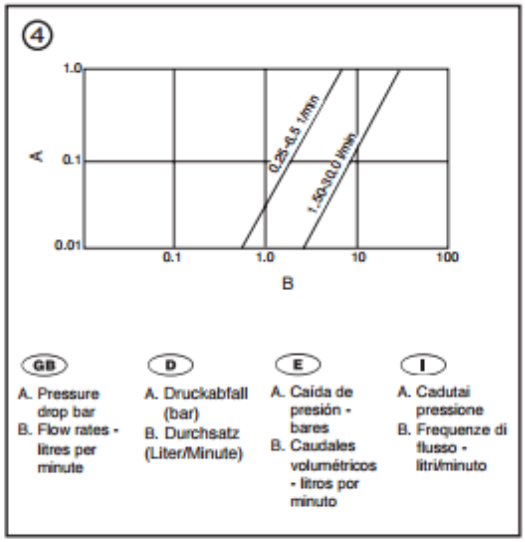
1. Elettrico (con rilevazione logica chip)
A. Regolatore di tensione
B. Fotodiodo
C. Amplificatore
D. Trigger Schmitt
2. Collegamento elettrico
E. Uscita
F. Fotorivelatore
G. Catodo
H. Diodo

②



ENGLISH





GB **RS Stock No.**

257-133 and 257-149

General

These flow transducers have been designed for use with mains and heating system waters. Subject to customer evaluation, it may also be possible to use them with demineralised water, neutral or dilute alkaline solutions, hydrocarbon or mild oxy-hydrocardon solvents (including light fuel oils and spirits) and dilute, weak organic acids depending on concentration. (generally up to 5% at ambient temperature is acceptable) and temperature.
It is not possible to use these flow transducers with strong mineral acids or acid solutions at any temperature or dilution, nor with strong or searching solvents (e.g. methylene chloride, acetone, alcohols, chloroform).

Installation

Before installation check the free running of the sensor by blowing through it. DO NOT USE AN AIR LINE. Ideally the flowsensor should be installed with the arrow on the turbine housing pointing vertically upwards. The unit may, however, be installed in any attitude providing the pipes are full of liquid. Pockets of vapour or bubbles of air will affect some of the light and so alter the number of pulses recorded from the sensor. On the lower flow model these bubbles may take some time to clear because of the low fluid velocities inside the chamber. A large back pressure will reduce any tendency the liquid has to form vapour pockets. As the detection system is optical it is undesirable to install the flow sensor near a strong light source or in direct sunlight, as this may 'swamp' the detection system.

Pumps

All pumps cause pulsations in the fluid, centrifugal pumps have probably the lowest disturbance, and reciprocating pumps the largest. With a centrifugal pump the pulsations reduce after a fairly short pipe run so if the flow sensor is positioned as far from the pump as possible, the effects will be minimised. With reciprocating pumps more positive isolation is desirable and a pulse damper or accumulator is probably required. If pulsations cannot be removed the unit must be recalibrated over the desired flow range.

Considerations

All flow sensors should only be installed with the following in mind: bends, valves, flow regulators, tee junctions and other fittings which cause the flow to travel faster at one side of the pipe relative to the other. This asymmetry in the flow can seriously affect the calibration and the disturbance should be as far removed from the sensor as possible and if at all practical, put after the flow sensor. Recalibration on site will, of course, remove any doubt about the installation. In all cases an 80 mesh filter should be fitted upstream of the flow sensor.

Viscosity

Viscosity effects:- all turbine transducers are affected by viscosity and where possible the viscosity (temperature) of the liquid should be kept fairly constant. Viscous drag causes the turbine to be slowed down quicker at the lower flows, as viscosity increases so does the threshold to operation. If the fluid is lubricating and a higher pressure drop is acceptable, the turbine can be run at up to 50% over range with no detrimental effects.

Electronic

Inside the housing is an infra-red light emitting diode. The LED is directed at the receiver which has a built-in voltage regulator, photo diode, amplifier, schmitt trigger and output stage. Every turbine blade passage blocks the light beam and so reduces the level of the output signal to typically 200mV (maximum 400mV). The 'unblocked' level is the supply voltage and the output is tied to this through a 10k resistor. The output rise and fall times are typically 60ns and 6ns respectively. At the maximum continuous operating temperature (70°C) the power dissipation of the detector output stage is 2.5mW, care must therefore be taken not to overload the output. At ambient temperatures the unit can dissipate up to 250mW.
The power to the LED is dependent on supply current, and this MUST be limited with a series resistor and potentiometer. Current required is subject to optical density of medium being measured. Maximum recommended current = 30mA.

ENGLISH

Diode

Absolute Maximum Ratings

Reverse voltage @ 25°C free air temperature	3.0V
Continuous forward current at (or below) 25°C free air temperature	60mA
Recommended current	30mA
Operating free air temperature range	-40°C to 70°C
Storage temperature range	-40°C to 70°C
Lead temperature 1.6mm from case for 5 sec.	260°C
Power dissipation	100mW

Photodetector

(Typical)

Max. dissipation	250mW @ 25°C
Operating supply voltage	4.5 to 16Vd.c. supply (Vcc)
Output low	6mA
Supply current	7mA
Output high	0.4mA
Supply current	5mA
Output voltage low	0.2V
Output voltage high	Vcc
Rise time	60ns
Fall time	6ns

Note: At the maximum continuous operating temperature (70°C) the power dissipation of the detector output stage is 2.5mW. Care must therefore be taken not to overload the output.

The pulses from the sensor when viewed on an oscilloscope should look like the central drawing in Figure 2. If the LED current is too high, an increase in ambient light levels could cause the signal to stay high. A 50-50 mark space ratio is not possible as the blades are thinner than the spaces.

Figures 3 and 4 show results of flowtransducers calibrated on a gravimetric flow rig. The differential pressure is set using a rising mercury manometer. Water temperature 8°C

Colour Code	Grey Body (RS stock no. 257-149)	Beige Body (RS stock no. 257-133)
Flow Range	0.25-6.5 l/m	1.50-30.0 l/m
Linearity at FSD Frequency	±1.0%	±1.5%
Approximate Full Scale At Full Scale	500Hz	600Hz
Approximate Pulses per Litre	4600 pulses/litre	1200 pulses/litre

Standard materials of construction

Body	-	Acetal copolymer
Retaining Cap	-	Acetal copolymer
Rotor	-	Acetal copolymer
Rotor housing	-	Clear nylon
Spindle	-	Stainless steel
Bearings	-	Sapphire
'O' Ring	-	Nitrile rubber

Standard connections

15mm Cu x 15mm Cu (compression fittings)

Operation pressure

Max. 300lbs/sq ins

Dimensions mm

Length	=	89 (over fittings)
Height	=	51
Breadth	=	37

RS Components shall not be liable for any liability or loss of any nature (howsoever caused and whether or not due to RS Components' negligence) which may result from the use of any information provided in RS technical literature.